Appendix 1:
Description of the Tanner Crab Stock Assessment Model, Version 2

William T. Stockhausen
Alaska Fisheries Science Center
September 2020

Introduction

The "TCSAM02" (Tanner Crab Stock Assessment Model, version 2) modeling framework was developed "from scratch" to eliminate many of the constraints imposed on potential future assessment models by TCSAM2013, the previous assessment model framework (Stockhausen, 2016). Like TCSAM2013, TCSAM02 uses AD Model Builder libraries as the basis for model optimization using a maximum likelihood (or Bayesian) approach. The model code for TCSAM02 is available on GitHub (the 2020 assessment model code is available at "202009CPTVersion"). TCSAM02 was first used for the Tanner crab assessment in 2017 (Stockhausen, 2017) and will be used until a transition is made to Gmacs (the Generalized Model for Alaska Crab Stocks). Gmacs is intended to be used for all crab stock assessments conducted for the North Pacific Fisheries Management Council (NPFMC), including both lithodid (king crab) and *Chionoecetes* (Tanner and snow crab) stocks, while TCSAM02 is specific to *Chionoecetes* biology (i.e., terminal molt).

TCSAM02 is referred to here as a "modeling framework" because, somewhat similar to Stock Synthesis (Methot and Wetzel, 2013), model structure and parameters are defined "on-the-fly" using control files—rather than editing and re-compiling the underlying code. In particular, the number of fisheries and surveys, as well as their associated data types (abundance, biomass, and /or size compositions) and the number and types of time blocks defined for every model parameter, are defined using control files in TCSAM02 and have not been pre-determined. Priors can be placed on any model parameter. New data types (e.g., growth data) can also be included in the model optimization that could not be fit with TCSAM2013. Additionally, status determination and OFL calculations can be done directly within a TCSAM02 model run, rather having to run a separate "projection model".

Several new features have been added to TCSAM02 since the 2019 assessment. These include:

1. the ability to programmatically specify a retrospective model run (i.e., running the model with a specified number of the most recent years of data and associated parameters excluded from the model fit and estimation)
2. an option to estimate selectivity/availability curves based on cubic splines
3. an option to apply selectivity (catchability) and/or availability curves estimated outside the model to survey or fishery data
4. an option to apply prior probabilities determined outside the model to selectivity (catchability) and/or availability curves estimated inside the model
5. an option to estimate "additional uncertainty" parameters associated with a survey

Model Description

A. General population dynamics

TCSAM02 is a stage/size-based population dynamics model. Population abundance at the start (July 1) of year *y* in the model, $n_{y,x,m,s,z}$, is characterized by sex *x* (male, female), maturity state *m* (immature, mature), shell condition *s* (new shell, old shell), and size *z* (carapace width, CW). Changes in abundance due to natural mortality, molting and growth, maturation, shell aging, fishing mortality and recruitment are tracked on an annual basis. Because the principal crab fisheries occur during the winter, the model year runs from July 1 to June 30 of the following calendar year.

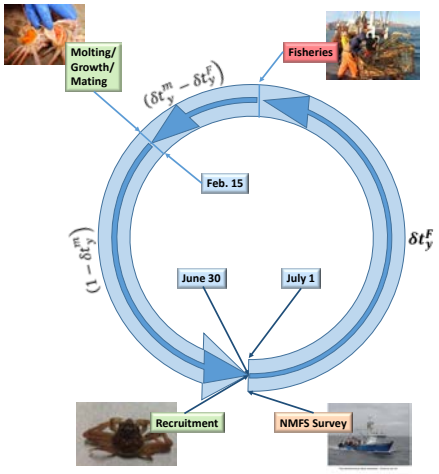

Fig. 1. Timing of annual events in TCSAM02 when fisheries occur before molting/growth/mating.

The order of calculation steps to project population abundance from year *y* to *y*+1 depends on the assumed timing of the fisheries (δt_y^F) relative to molting/growth/mating (δt_y^m) in year *y*. The steps when the fisheries occur before molting/growth/mating ($\delta t_y^F \leq \delta t_y^m$) are outlined below first (Steps A1.1-A1.4), followed by the steps when molting/growth/mating occurs after the fisheries ($\delta t_y^m < \delta t_y^F$; Steps A2.1-A2.4).

A1. Calculation sequence when $\delta t_y^F \leq \delta t_y^m$

Step A1.1: Survival prior to fisheries

Natural mortality is applied to the population from the start of the model year (July 1) until just prior to prosecution of pulse fisheries for year *y* at δt_y^F. The numbers surviving to δt_y^F in year *y* are given by:

$n^1_{y,x,m,s,z} = e^{-M_{y,x,m,s,z} \cdot \delta t_y^F} \cdot n_{y,x,m,s,z}$	A1.1

where *M* represents the annual rate of natural mortality in year *y* on crab classified as *x*, *m*, *s*, *z*.

Step A1.2: Prosecution of the fisheries

The directed and bycatch fisheries are modeled as simultaneous pulse fisheries occurring at δt_y^F in year *y*. The numbers that remain after the fisheries are prosecuted are given by:

$n^2_{y,x,m,s,z} = e^{-F^T_{y,x,m,s,z}} \cdot n^1_{y,x,m,s,z}$	A1.2

where $F^T_{y,x,m,s,z}$ represents the total fishing mortality (over all fisheries) on crab classified as *x*, *m*, *s*, *z* in year *y*.

Step A1.3: Survival after fisheries to time of molting/growth/mating

Natural mortality is again applied to the population from just after the fisheries to the time just before molting/growth/mating occurs for year *y* at δt_y^m (generally Feb. 15). The numbers surviving to δt_y^m in year *y* are given by:

$n^3_{y,x,m,s,z} = e^{-M_{y,x,m,s,z} \cdot (\delta t_y^m - \delta t_y^F)} \cdot n^2_{y,x,m,s,z}$	A1.3

where, as above, *M* represents the annual rate of natural mortality in year *y* on crab classified as *x*, *m*, *s*, *z*.

Step A1.4: Molting, growth, and maturation
The changes in population structure due to molting, growth and maturation of immature (new shell) crab, as well as the change in shell condition for mature new shell (MAT, NS) crab to mature old shell (MAT, OS) crab due to aging, are given by:

$n^4_{y,x,MAT,NS,z} = \phi_{y,x,z} \cdot \sum_{z'} \Theta_{y,x,z,z'} \cdot n^3_{y,x,IMM,NS,z'}$	A1.4a
$n^4_{y,x,IMM,NS,z} = (1 - \phi_{y,x,z}) \cdot \sum_{z'} \Theta_{y,x,z,z'} \cdot n^3_{y,x,IMM,NS,z'}$	A1.4b
$n^4_{y,x,MAT,OS,z} = n^3_{y,x,MAT,OS,z} + n^3_{y,x,MAT,NS,z}$	A1.4c

where $\Theta_{y,x,z,z'}$ is the growth transition matrix in year *y* for an immature new shell (IMM, NS) crab of sex *x* and pre-molt size *z'* to post-molt size *z* and $\phi_{y,x,z}$ is the probability that a just-molted crab of sex *x* and post-molt size *z* has undergone its terminal molt to maturity (MAT). All crab that molted remain new shell (NS) crab. Additionally, all mature crab that underwent terminal molt to maturity the previous year are assumed to change shell condition from new shell to old shell (A1.4c). Note that the numbers of immature old shell (IMM, OS) crab are identically zero in the current model because immature crab are assumed to molt each year until they undergo the terminal molt to maturity; consequently, the "missing" equation for *m=IMM*, *s=OS* is unnecessary.

Step A1.5: Survival to end of year, recruitment, and update to start of next year
Finally, the population abundance at the start of year *y*+1, due to natural mortality on crab from just after the time of molting/growth/mating in year *y* until the end of the model year (June 30) and recruitment ($R_{y,x,z}$) at the end of year *y* of immature new shell (IMM, NS) crab by sex *x* and size *z*, is given by:

$n_{y+1,x,m,s,z} = \begin{cases} e^{-M_{y,x,IMM,NS,z} \cdot (1-\delta t^m_y)} \cdot n^4_{y,x,IMM,NS,z} + R_{y,x,z} & m = IMM, s = NS \\ e^{-M_{y,x,m,s,z} \cdot (1-\delta t^m_y)} \cdot n^4_{y,x,m,s,z} & otherwise \end{cases}$	A1.5

A2. Calculation sequence when $\delta t^m_y < \delta t^F_y$

Step A2.1: Survival prior to molting/growth/mating
As in the previous sequence, natural mortality is first applied to the population from the start of the model year (July 1), but this time until just prior to molting/growth/mating in year *y* at δt^m_y (generally Feb. 15). The numbers surviving at δt^m_y in year *y* are given by:

$n^1_{y,x,m,s,z} = e^{-M_{y,x,m,s,z} \cdot \delta t^m_y} \cdot n_{y,x,m,s,z}$	A2.1

where *M* represents the annual rate of natural mortality in year *y* on crab classified as *x*, *m*, *s*, *z*.

Step A2.2: Molting, growth, and maturation
The changes in population structure due to molting, growth and maturation of immature new shell (IMM, NS) crab, as well as the change in shell condition for mature new shell (MAT, NS) crab to mature old shell (MAT, OS) crab due to aging, are given by:

$n^2_{y,x,MAT,NS,z} = \phi_{y,x,z} \cdot \sum_{z'} \Theta_{y,x,z,z'} \cdot n^1_{y,x,IMM,NS,z'}$	A2.2a
$n^2_{y,x,IMM,NS,z} = (1 - \phi_{y,x,z}) \cdot \sum_{z'} \Theta_{y,x,z,z'} \cdot n^1_{y,x,IMM,NS,z'}$	A2.2b
$n^2_{y,x,MAT,OS,z} = n^1_{y,x,MAT,OS,z} + n^1_{y,x,MAT,NS,z}$	A2.2c

where $\Theta_{y,x,z,z'}$ is the growth transition matrix in year *y* for an immature new shell (IMM, NS) crab of sex *x* and pre-molt size *z'* to post-molt size *z* and $\phi_{y,x,z}$ is the probability that a just-molted crab of sex *x* and post-molt size *z* has undergone its terminal molt to maturity. Additionally, mature new shell (MAT, NS) crab that underwent their terminal molt to maturity the previous year are assumed to change shell condition from new shell to old shell (A2.2c). Again, the numbers of immature old shell crab are identically zero because immature crab are assumed to molt each year until they undergo the terminal molt to maturity.

Step A2.3: Survival after molting/growth/mating to prosecution of fisheries
Natural mortality is again applied to the population from just after molting/growth/mating to the time at which the fisheries occur for year *y* (at δt^F_y). The numbers surviving at δt^F_y in year *y* are then given by:

$n^3_{y,x,m,s,z} = e^{-M_{y,x,m,s,z} \cdot (\delta t^F_y - \delta t^m_y)} \cdot n^2_{y,x,m,s,z}$	A2.3

where, as above, *M* represents the annual rate of natural mortality in year *y* on crab classified as *x*, *m*, *s*, *z*.

Step A2.4: Prosecution of the fisheries
The directed fishery and bycatch fisheries are modeled as pulse fisheries occurring at δt^F_y in year *y*. The numbers that remain after the fisheries are prosecuted are given by:

$n^4_{y,x,m,s,z} = e^{-F^T_{y,x,m,s,z}} \cdot n^3_{y,x,m,s,z}$	A2.4

where $F^T_{y,x,m,s,z}$ represents the total fishing mortality (over all fisheries) on crab classified as *x*, *m*, *s*, *z* in year *y*.

Step A2.5: Survival to end of year, recruitment, and update to start of next year
Finally, population abundance at the start of year *y*+1 due to natural mortality on crab from just after prosecution of the fisheries in year *y* until the end of the model year (June 30) and recruitment of immature new (IMM, NS) shell crab at the end of year *y* ($R_{y,x,z}$) and are given by:

$n_{y+1,x,m,s,z} = \begin{cases} e^{-M_{y,x,IMM,NS,z} \cdot (1 - \delta t^F_y)} \cdot n^4_{y,x,IMM,NS,z} + R_{y,x,z} & m = IMM, s = NS \\ e^{-M_{y,x,m,s,z} \cdot (1 - \delta t^F_y)} \cdot n^4_{y,x,m,s,z} & otherwise \end{cases}$	A2.5

B. Parameter specification

Because parameterization of many model processes (e.g., natural mortality, fishing mortality) in TCSAM02 is fairly flexible, it is worthwhile discussing how model processes and their associated parameters are configured in TCSAM02 before discussing details of the model processes themselves. Each type of model process has a set of (potentially estimable) model parameters and other information associated with it, but different "elements" of a model process can be defined that apply, for example, to different segments of the population and/or during different time blocks. In turn, several "elements" of a model parameter associated with a model process may also be defined (and applied to different elements of the process). At least one combination of model parameters and other information associated with a model process must be defined—i.e., one process element must be defined.

Model processes and parameters are configured in a "ModelParametersInfo" file, one of the three control files required for a model run (the others are the "ModelConfiguration" file and the "ModelOptions" file). As an example of the model processes and parameter specification syntax, Text Box 1 presents the part of a "ModelParametersInfo" file concerned with specifying fishing processes in the directed Tanner crab fishery.

In Text Box 1, the keyword "fisheries" identifies the model process in question. The first section, following the "PARAMETER_COMBINATIONS" keyword (up to the first set of triple blue dots), specifies the indices associated with fishing process parameters (pHM, pLnC, pDC1, pDC2, pDC3, pDC4, pDevsLnC, pLnEffX, pLgtRet), selectivity and retention functions (idxSelFcn, idxRetFcn), and effort averaging time period (effAvgID) that apply to a single fishing process element. In this example, the indices for the selectivity and retention functions, as well as those for the effort averaging time period, constitute the "other information" specified for each fishing process element. Each fishing process element in turn applies to a specific fishery (FISHERY=1 indicates the directed fishery, in this case), time block (specified by YEAR_BLOCK), and components of the model population (specified by SEX, MATURITY STATE, and SHELL CONDITION). Using indices to identify which parameters and selectivity and retention functions apply to a given combination of fishery/time block/sex/maturity state/shell condition allows one to "share" individual parameters and selectivity and retention functions across different fishery/time block/sex/maturity state/shell condition combinations.

The second section (following the "PARAMETERS" keyword) determines the characteristics for each of the fishing process parameters, organized by parameter name (note: the parameters associated with the different selectivity and retention functions are specified in a different section of the ModelParametersInfo file). Here, each parameter name corresponds to an ADMB "param_init_bounded_number_vector" in the model code—the exception being pDevsLnC, which corresponds to an ADMB "param_init_bounded_vector_vector".

Each row under a "non-devs" parameter name in the fisheries section (e.g., pLnC) specifies the index used to associate an element of the parameter with the fishing processes defined in the PARAMETER_COMBINATIONS section, as well as characteristics of the element in the associated ADMB number_vector (upper and lower bounds, initial value, and initial estimation phase), various flags for initialization ("jitter", "resample"), definition of an associated prior probability distribution, and a label. Each row under a "devs" parameter name (e.g., pDevsLnC) specifies much the same information for the associated ADMB devs vector, with the "read" flag replacing the "initial value" entry. If "read?" is TRUE, then a vector of initial values is read from the file after all "info" rows for the devs parameter have

been read. The “jitter” flag (if set to TRUE) provides the ability to change the initial value for an element of a non-devs parameter using a randomly selected value based on the element’s upper and lower bounds. For a devs parameter, an element with jitter set to TRUE is initialized using a vector of randomly-generated numbers (subject to being a devs vector within the upper and lower bounds). The “resample” flag was intended to specify an alternative method to providing randomly-generated initial values (based on an element’s prior probability distribution, rather than its upper and lower bounds), but this has not yet been fully implemented.

Some model processes apply only to specific segments of the population (e.g., growth only applies to immature, new shell crab). In general, though, a model process element can be defined to apply to any segment of the population (by specifying SEX, MATURITY STATE, and SHELL CONDITION appropriately) and range of years (by specifying YEAR_BLOCK). In turn, an element of a parameter may be “shared” across multiple processes by specifying the element’s index in multiple rows of a PARAMETERS_COMBINATION block.

```
#-------------------------------
# Fishery parameters
#-------------------------------
fisheries #process name
PARAMETER_COMBINATIONS
42  #number of rows defining parameter combinations for all fisheries
#Directed Tanner Crab Fishery (TCF)
#                                    |MATURITY|SHELL|                                  |pDevs| pLn | pLgt| idx  | idx  |  eff  |
#id  FISHERY  YEAR_BLOCK             SEX    | STATE  |COND |  pHM  pLnC pDC1 pDC2 pDC3 pDC4 | LnC | EffX| Ret |SelFcn|RetFcn| AvgID | label
1       1     [-1:1964]             MALE      ALL    ALL     1    1    0     0    0    0      0      0    0     9       5       0    TCF:_M_T1
2       1     [1965:1984;1987:1990] MALE      ALL    ALL     1    2    0     0    0    0      1      0    0     9       5       0    TCF:_M_T2
3       1     [1991:1996]           MALE      ALL    ALL     1    2    0     0    0    0      1      0    0    10       6       0    TCF:_M_T3
4       1     [2005:2009]           MALE      ALL    ALL     1    2    0     0    0    0      1      0    1    11       7       0    TCF:_M_T4
5       1     [2013:-1]             MALE      ALL    ALL     1    2    0     0    0    0      1      0    1    12       8       0    TCF:_M_T5
6       1     [-1:1964]             FEMALE    ALL    ALL     1    1    0     1    0    0      0      0    0    13       0       0    TCF:_F_T1
7       1     [1965:1984;1987:1996] FEMALE    ALL    ALL     1    2    0     1    0    0      1      0    0    13       0       0    TCF:_F_T2
8       1     [2005:2009;2013:-1]   FEMALE    ALL    ALL     1    2    0     1    0    0      1      0    0    14       0       0    TCF:_F_T3
…
PARAMETERS
pHM #handling mortality (0-1)
3   #number of parameters
#   |   limits    |       | initial | start |         |-       priors          -|
#id |lower   upper|jitter?| value   | phase |resample?| wgt| type| params| consts| label
1      0       1    OFF     0.321      -1       OFF      1   none   none    none    handling_mortality_for_crab_pot_fisheries
…
pLnC #base (ln-scale) capture rate (mature males)
9    #number of parameters
#   |   limits    |       |  initial   | start |         |-       priors          -|
#id |lower   upper|jitter?|   value    | phase |resample?| wgt| type| params| consts| label
 1    -15     15     OFF   -2.995732274    -1      OFF      1   none  none    none      TCF:_base_capture_rate,_pre-1965_(=0.05)
 2    -15     15     ON    -1.164816291     1      OFF      1   none  none    none      TCF:_base_capture_rate,_1965+
…
pDC1 #main temporal ln-scale capture rate offset
0    #number of parameters
pDC2 #ln-scale capture rate offset for female crabs
6    #number of parameters
#   |   limits    |       |  initial   | start |         |-       priors           -|
#id |lower  upper |jitter?|   value    | phase |resample?|  wgt  type  params  consts| label
1    -5.0    5.0     ON    -2.058610432    1      OFF       1.0  none   none    none   TCF:_female_offset
…
pDevsLnC #annual ln-scale capture rate deviations
6        #number of parameter vectors
#   | index  |            index                  |      |   limits    |       |initial |start |        |-      priors               -|
#id |  type  |            block                  | read? |lower   upper | jitter?| value  |phase |resample?|  wgt | type | params | consts |label
 1     YEAR   [1965:1984;1987:1996;2005:2009;2013:-1]  FALSE   -15     15       ON       0       1      OFF       2.0  normal    0 1     none    TCF:_T2345
…
```

Text Box 1. Abbreviated example of process and parameter specifications in a “ModelParametersInfo” file for fishing mortality in TCSAM02. Only parameter combinations and parameters relevant to the directed fishery are shown. Input values are in black text, comments are in green, triple blue dots indicate additional input lines not shown.

C. Model processes: natural mortality

The natural mortality rate applied to crab of sex *x*, maturity state *m*, shell condition *s*, and size *z* in year *y*, $M_{y,x,m,s,z}$, can be specified using one of two parameterizations. The first parameterization option uses a ln-scale parameterization with an option to include an inverse- size dependence using Lorenzen's approach:

$lnM_{y,x,m,s} = \mu^0_{y,x,m,s} + \sum_{i=1}^{4} \delta\mu^i_{y,x,m,s}$	C.1a
$M_{y,x,m,s,z} = \begin{cases} \exp(lnM_{y,x,m,s}) & if\ Lorenzen\ option\ is\ not\ selected \\ \exp(lnM_{y,x,m,s}) \cdot \frac{z_{base}}{z} & if\ Lorenzen\ option\ is\ selected \end{cases}$	C.1b C.1c

where the μ^0 and the $\delta\mu^i$'s are (potentially) estimable parameters defined for time block *T*, sex *S* (MALE, FEMALE, or ANY), maturity *M* (IMMATURE, MATURE, or ANY), and shell condition *S* (NEWSHELL, OLDSHELL, or ANY), and {*y*,*x*,*m*,*s*} falls into the set {*T*,*X*,*M*,*S*}. In Eq. C.1c, z_{base} denotes the specified reference size (mm CW) for the inverse-size dependence.

The second parameterization option uses an arithmetic parameterization in order to provide backward compatibility with the 2016 assessment model based on TCSAM2013. In TCSAM2013, the natural mortality rate $M_{y,x,m,s,z}$ was parameterized using:

$M_{y,x,m=IMM,s,z} = M^{base} \cdot \delta M_{IMM}$	C.2a
$M_{y,x,m=MAT,s,z} = \begin{cases} M^{base} \cdot \delta M_{x,MAT} & otherwise \\ M^{base} \cdot \delta M_{x,MAT} \cdot \delta M^T_{x,MAT} & 1980 \le y \le 1984 \end{cases}$	C.2b

where M^{base} was a fixed value (0.23 yr^{-1}), δM_{IMM} was a multiplicative factor applied for all immature crab, the $\delta M_{x,MAT}$ were sex-specific multiplicative factors for mature crab, and the $\delta M^T_{x,MAT}$ were additional sex-specific multiplicative factors for mature crab during the 1980-1984 time block (which has been identified as a period of enhanced natural mortality on mature crab, the mechanisms for which are not understood). While it would be possible to replicate Eq.s C.2a and C.2b using ln-scale parameters, TCSAM2013 also placed informative arithmetic-scale priors on some of these parameters—and this could not be duplicated on the ln-scale. Consequently, the second option uses the following parameterization, where the parameters (and associated priors) are defined on the arithmetic-scale:

$lnM_{y,x,m,s} = \ln[\mu^0_{y,x,m,s}] + \sum_{i=1}^{4} \ln[\delta\mu^i_{y,x,m,s}]$	C.3a

A system of equations identical to C.2a-b can be achieved under the following assignments:

$\mu^0_{\{y,x,m,s\} \in \{T=ALL,X=ALL,M=ALL,S=ALL\}} = M^{base}$	C.4a
$\delta\mu^1_{\{y,x,m,s\} \in \{T=ALL,X=ALL,M=IMM,S=ALL\}} = \delta M_{IMM}$	C.4e
$\delta\mu^1_{\{y,x,m,s\} \in \{T=ALL,X=x,M=MAT,S=ALL\}} = \delta M_{x,MAT}$	C.4f
$\delta\mu^2_{\{y,x,m,s\} \in \{T=1980-1984,X=x,M=MAT,S=ALL\}} = \delta M^T_{x,MAT}$	C.4g

where unassigned $\delta\mu^{i}_{y,x,m,s}$ are set equal to 1. Pending further model testing using alternative model configurations, the TCSAM2013 option is standard.

It is worth noting explicitly that, given the number of potential parameters above that could be used, extreme care must be taken when defining a model to achieve a set of parameters that are not confounded and are, at least potentially, estimable.

D. Model processes: growth

Because Tanner crab are assumed to undergo a terminal molt to maturity, in TCSAM02 only immature crab experience growth. Annual growth of immature crab is implemented as using two options, the first based on a formulation used in Gmacs and the second (mainly for purposes of backward compatibility) based on that used in TCSAM2013. In TCSAM02, growth can vary by time block and sex, so it is expressed by sex-specific transition matrices for time block *t*, $\Theta_{t,x,z,z'}$, that specify the probability that crab of sex *x* in pre-molt size bin z' grow to post-molt size bin *z* at molting.

In the Gmacs-like approach (the standard approach as of May, 2017), the sex-specific growth matrices are given by:

$\Theta_{t,x,z,z'} = c_{t,x,z'} \cdot \int_{z-bin/2}^{z+bin/2} \Gamma\left(\frac{z'' - \bar{z}_{t,x,z'}}{\beta_{t,x}}\right) dz''$	Sex-specific (*x*) transition matrix for growth from pre-molt z' to post-molt *z*, with $z \geq z'$	D.1a
$c_{t,x,z'} = \left[\int_{z'}^{\infty} \Gamma\left(\frac{z'' - \bar{z}_{t,x,z'}}{\beta_{t,x}}\right) dz''\right]^{-1}$	Normalization constant so $1 = \sum_{z} \Theta_{t,x,z,z'}$	D.1b
$\bar{z}_{t,x,z'} = e^{a_{t,x}} \cdot {z'}^{b_{t,x}}$	Mean size after molt, given pre-molt size z'	D.1c

where the integral represents a cumulative gamma distribution across the post-molt (*z*) size bin. This approach may have better numerical stability properties than the TCSAM2013 approach below.

The TCSAM2013 approach is an approximation to the Gmacs approach, where the sex-specific growth matrices $\Theta_{t,x,z,z'}$ are given by

$\Theta_{t,x,z,z'} = c_{t,x,z'} \cdot {\Delta_{z,z'}}^{\alpha_{t,x,z'}-1} \cdot e^{-\frac{\Delta_{z,z'}}{\beta_{t,x}}}$	Sex-specific (*x*) transition matrix for growth from pre-molt z' to post-molt *z*, with $z \geq z'$	D.2a
$c_{t,x,z'} = \left[\sum_{z'} {\Delta_{z,z'}}^{\alpha_{t,x,z'}-1} \cdot e^{-\frac{\Delta_{z,z'}}{\beta_{t,x}}}\right]^{-1}$	Normalization constant so $1 = \sum_{z} \Theta_{t,x,z,z'}$	D.2b
$\Delta_{z,z'} = z - z'$	Actual growth increment	D.2c
$\alpha_{t,x,z'} = \left[\bar{z}_{t,x,z'} - z'\right]/\beta_{t,x}$	Mean molt increment, scaled by $\beta_{t,x}$	D.2d
$\bar{z}_{t,x,z'} = e^{a_{t,x}} \cdot {z'}^{b_{t,x}}$	Mean size after molt, given pre-molt size z'	D.2e

In both approaches, the $a_{t,x}$, $b_{t,x}$, and $\beta_{t,x}$ are arithmetic-scale parameters with imposed bounds. $\Theta_{t,x,z,z'}$ is used to update the numbers-at-size for immature crab, $n_{y,x,z}$, from pre-molt size z' to post-molt size *z* using:

$n^{+}_{y,x,z} = \sum_{z'} \Theta_{t,x,z,z'} \cdot n_{y,x,z'}$	numbers at size of immature crab after growth	D.3

where *y* falls within time block *t* (see also Eq.s A1.4a-b and A2.2a-b).

Priors using normal distributions are imposed on $a_{t,x}$ and $b_{t,x}$ in TCSAM2013, with the values of the hyper-parameters hard-wired in the model code. While priors may be defined for the associated parameters here, these are identified by the user in the model input files and are not hard-wired in the model code.

E. Model processes: maturity (terminal molt)

Maturation of immature crab in TCSAM02 is based on a similar approach to that taken in TCSAM2013, except that the sex- and size-specific probabilities of terminal molt for immature crab, $\phi_{t,x,z}$ (where size *z* is post-molt size), can vary by time block. After molting and growth, the numbers of (new shell) crab at post-molt size *z* remaining immature, $n^{+}_{y,x,IMM,NS,z}$, and those maturing, $n^{+}_{x,MAT,NS,z}$, are given by:

$n^{+}_{y,x,IMM,NS,z} = \left(1-\phi_{t,x,z}\right) \cdot n_{y,x,IMM,NS,z}$	crab remaining immature	E.1a
$n^{+}_{y,x,MAT,NS,z} = \phi_{t,x,z} \cdot n_{y,x,IMM,NS,z}$	crab maturing (terminal molt)	E.1b

where *y* falls in time block *t* and $n_{y,x,IMM,NS,z}$ is the number of immature, new shell crab of sex *x* at post-molt size *z*.

The sex- and size-specific probabilities of terminal molt, $\phi_{t,x,z}$, are related to logit-scale model parameters $p^{mat}_{t,x,z}$ by:

$\phi_{t,FEM,z} = \begin{cases} \dfrac{1}{1+e^{p^{mat}_{t,FEM,z}}} & z \le z^{mat}_{t,FEM} \\ 1 & z > z^{mat}_{t,FEM} \end{cases}$	female probabilities of maturing at post-molt size *z*	E.2a
$\phi_{t,MALE,z} = \begin{cases} \dfrac{1}{1+e^{p^{mat}_{t,MALE,z}}} & z \le z^{mat}_{t,MALE} \\ 1 & z > z^{mat}_{t,MALE} \end{cases}$	male probabilities of maturing at post-molt size *z*	E.2b

where the $z^{mat}_{t,x}$ are constants specifying the minimum pre-molt size at which to assume all immature crab will mature upon molting. The $z^{mat}_{t,x}$ are used here pedagogically; in actuality, the user specifies the *number* of logit-scale parameters to estimate (one per size bin starting with the first bin) for each sex, and this determines the $z^{mat}_{t,x}$ used above. This parameterization is similar to that implemented in TCSAM2013 for the 2016 assessment model.

Second difference penalties are applied to the parameter estimates in TCSAM2013's objective function to promote relatively smooth changes in these parameters with size. Similar penalties (smoothness, non-decreasing) can be applied in TCSAM02.

F. Model processes: recruitment

Recruitment in TCSAM02 consists of immature new shell crab entering the population at the end of the model year (June 30). Recruitment in TCSAM02 has a similar functional form to that used in TCSAM2013, except that the sex ratio at recruitment is not fixed at 1:1 and multiple time blocks can be specified. In TCSAM2013, two time blocks were defined: "historical" (model start to 1974) and "current" (1975-present), with "current" recruitment starting in the first year of NMFS survey data. In TCSAM02, recruitment in year *y* of immature new shell crab of sex *x* at size *z* is specified as

$R_{y,x,z} = \dot{R}_y \cdot \ddot{R}_{y,x} \cdot \ddot{\ddot{R}}_{y,z}$	recruitment of immature, new shell crab by sex and size bin	F.1

where $\dot{R}_y$ represents total recruitment in year *y* and $\ddot{R}_{y,x}$ represents the fraction of sex *x* crab recruiting, and $\ddot{\ddot{R}}_{y,z}$is the size distribution of recruits, which is assumed identical for males and females.

Total recruitment in year *y*, $\dot{R}_y$, is parameterized as

$\dot{R}_y = e^{pLnR_t + \delta R_{t,y}} \quad y \in t$	total recruitment in year *y*	F.2

where *y* falls within time block *t*, $pLnR_t$ is the ln-scale mean recruitment parameter for *t*, and $\delta R_{t,y}$is an element of a "devs" parameter vector for *t* (constrained such that the elements of the vector sum to zero over the time block).

The fraction of crab recruiting as sex *x* in year *y* in time block *t* is parameterized using the logistic model

$\ddot{R}_{y,x} = \begin{cases} \dfrac{1}{1 + e^{pLgtRx_t}} & x = MALE \\ 1 - \ddot{R}_{y,MALE} & x = FEMALE \end{cases} \quad y \in t$	sex-specific fraction recruiting in year *y*	F.3

where $pLgtRx_t$ is a logit-scale parameter determining the sex ratio in time block *t*.

The size distribution for recruits in time block *t*, $\ddot{\ddot{R}}_{t,z}$, is assumed to be a gamma distribution and is parameterized as

$\ddot{\ddot{R}}_{t,z} = c^{-1} \cdot \Delta_z^{\frac{\alpha_t}{\beta_t}-1} \cdot e^{-\frac{\Delta_z}{\beta_t}}$	size distribution of recruiting crab	F.4
$c_t = \sum_z \Delta_z^{\frac{\alpha_t}{\beta_t}-1} \cdot e^{-\frac{\Delta_z}{\beta_t}}$	normalization constant so that $1 = \sum_z \ddot{\ddot{R}}_{t,z}$	F.5
$\Delta_z = z + \delta z/2 - z_{min}$	offset from minimum size bin	F.6
$\alpha_t = e^{pLnRa_t}$	gamma distribution location parameter	F.7
$\beta_t = e^{pLnRb_t}$	gamma distribution shape parameter	F.8

where $pLnRa_t$ and $pLnRb_t$ are the ln-scale location and shape parameters and the constant δz is the size bin spacing.

A final time-blocked parameter, $pLnRCV_t$, is associated with the recruitment process representing the ln-scale coefficient of variation (cv) in recruitment variability in time block *t*. These parameters are used to apply priors on the recruitment "devs" in the model likelihood function.

G. Selectivity and retention functions

Selectivity and retention functions in TCSAM02 are specified independently from the fisheries and surveys to which they are subsequently applied. This allows a single selectivity function to be "shared" among multiple fisheries and/or surveys, as well as among multiple time block/sex/maturity state/shell condition categories, if so desired.

Currently, the following functions are available for use as selectivity or retention curves in a model:

$S_z = \left\{1 + e^{-\beta \cdot (z - z_{50})}\right\}^{-1}$	standard logistic	G.1
$S_z = \left\{1 + e^{-\beta \cdot (z - \exp(lnZ_{50}))}\right\}^{-1}$	logistic w/ alternative parameterization	G.2
$S_z = \left\{1 + e^{-\ln(19) \cdot \frac{(z - z_{50})}{\Delta z_{95-50}}}\right\}^{-1}$	logistic w/ alternative parameterization	G.3
$S_z = \left\{1 + e^{-\ln(19) \cdot \frac{(z - z_{50})}{\exp(ln\Delta z_{95-50})}}\right\}^{-1}$	logistic w/ alternative parameterization	G.4
$S_z = \left\{1 + e^{-\ln(19) \cdot \frac{(z - \exp(lnZ_{50}))}{\exp(ln\Delta z_{95-50})}}\right\}^{-1}$	logistic w/ alternative parameterization	G.5
$S_z = \frac{1}{1 + e^{-\beta_a \cdot (z - z_{a50})}} \cdot \frac{1}{1 + e^{\beta_d \cdot (z - z_{d50})}}$	double logistic	G.6
$S_z = \frac{1}{1 + e^{-\ln(19) \cdot \frac{(z - z_{a50})}{\Delta z_{a(95-50)}}}} \cdot \frac{1}{1 + e^{\ln(19) \cdot \frac{(z - z_{d50})}{\Delta z_{d(95-50)}}}}$	double logistic with alt. parameterization	G.7
$S_z = \frac{1}{1 + e^{-\ln(19) \cdot \frac{(z - z_{a50})}{\exp(ln\Delta z_{a(95-50)})}}} \cdot \frac{1}{1 + e^{\ln(19) \cdot \frac{(z - z_{d50})}{\exp(ln\Delta z_{d(95-50)})}}}$ $where\ z_{d50} = [z_{a50} + \exp(ln\Delta z_{a(95-50)}) + \exp(ln\Delta z_{d(95-50)})]$	double logistic with alt. parameterization	G.8
$S_z = \frac{1}{1 + e^{-\ln(19) \cdot \frac{(z - \exp(lnz_{a50}))}{\exp(ln\Delta z_{a(95-50)})}}} \cdot \frac{1}{1 + e^{\ln(19) \cdot \frac{(z - z_{d50})}{\exp(ln\Delta z_{d(95-50)})}}}$ $where\ z_{d50} = [\exp(lnz_{a50}) + \exp(ln\Delta z_{a(95-50)}) + \exp(ln\Delta z_{d(95-50)})]$	double logistic with alt. parameterization	G.9
$S_z = \frac{1}{1 + e^{-\beta_a \cdot (z - z_{a50})}} \cdot \frac{1}{1 + e^{\beta_d \cdot (z - [z_{a50} + \exp(lnZ_{d50-a50})])}}$	double logistic with alt. parameterization	G.10

A double normal selectivity function (requiring 6 parameters to specify) has also been implemented as an alternative to the double logistic functions. In the above functions, all symbols (e.g., β, z_{50}, Δz_{95-50}) represent parameter values, except "z" which represents crab size.

Selectivity parameters are defined independently of the functions themselves, and subsequently assigned. It is thus possible to "share" parameters across multiple functions. The "parameters" used in selectivity functions are further divided into mean parameters across a time block and annual deviations within a time block. To accommodate the 6-parameter double normal equation, six "mean" parameter sets (*pS1*, *pS2*,…, *pS6*) and six associated sets of "devs" parameter vectors (*pDevsS1*, *pDevsS2*,…, *pDevsS6*) are defined to specify the parameterization of individual selectivity/retention functions. Thus, for example, z_{50} in eq. F1 is actually expressed as $z_{50,y} = \bar{z}_{50} + \delta z_{50,y}$ in terms of model parameters *pS1* and *pDevsS1*$_y$, where $\bar{z}_{50} = pS1$ is the mean size-at-50%-selected over the time period and $\delta z_{50,y} = pDevsS1_y$ is the annual deviation.

Finally, three different options to normalize individual selectivity curves are provided: 1) no normalization, 2) specifying a fully-selected size, and 3) re-scaling such that the maximum value of the

re-scaled function is 1. A normalization option must be specified in the model input files for each defined selectivity/retention curve.

H. Fisheries

Unlike TCSAM2013, which explicitly models 4 fisheries that catch Tanner crab (one as a directed fishery, three as bycatch), there is no constraint in TCSAM02 on the number of fisheries that can be incorporated in the model. All fisheries are modeled as "pulse" fisheries occurring at the same time.

TCSAM02 uses the Gmacs approach to modeling fishing mortality (also implemented in TCSAM2013). The total (retained + discards) fishing mortality rate, $F_{f,y,x,m,s,z}$, in fishery *f* during year *y* on crab in state *x*, *m*, *s*, and *z* (i.e., sex, maturity state, shell condition, and size) is related to the associated fishery capture rate $\phi_{f,y,x,m,s,z}$ by

$F_{f,y,x,m,s,z} = \left[h_{f,t} \cdot \left(1 - \rho_{f,y,x,m,s,z}\right) + \rho_{f,y,x,m,s,z}\right] \cdot \phi_{f,y,x,m,s,z}$	fishing mortality rate	H.1

where $h_{f,t}$ is the handling (discard) mortality for fishery *f* in time block t (which includes year *y*) and $\rho_{f,y,x,m,s,z}$ is the fraction of crabs in state *x*, *m*, *s*, *z* that were caught and retained (i.e., the retention function). The retention function is assumed to be identically 0 for females in a directed fishery and for both sexes in a bycatch fishery.

In TCSAM2013, the same retention function (in each of two time blocks) was applied to male crab regardless of maturity state or shell condition. Additionally, full retention of large males was assumed, such that the retention function essentially reached 1 at large sizes. In TCSAM02, different retention functions can be applied based on maturity state and/or shell condition, and "max retention" is now an (potentially) estimable logit-scale parameter. Thus, in TCSAM02, the retention function $\rho_{f,y,x,m,s,z}$ is given by

$\rho_{f,y,x,m,s,z} = \frac{1}{1 + e^{\rho_{f,t,x,m,s}}} \cdot R_{f,y,x,m,s,z}$	retention function	H.2

where *f* corresponds to the directed fishery, *y* is in time block *t*, *x*=MALE, $\rho_{f,t,x,m,s}$ is the corresponding logit-scale "max retention" parameter, and $R_{f,y,x,m,s,z}$ is the associated selectivity/retention curve.

If $n_{y,x,m,s,z}$ is the number of crab classified as *x*, *m*, *s*, *z* in year *y* just prior to the prosecution of the fisheries, then

$c_{f,y,x,m,s,z} = \frac{\phi_{f,y,x,m,s,z}}{F^T_{y,x,m,s,z}} \cdot \left[1 - e^{-F^T_{y,x,m,s,z}}\right] \cdot n_{y,x,m,s,z}$	number of crab captured	H.3

is the number of crab classified in that state that were *captured* by fishery *f*, where $F^T_{y,x,m,s,z} = \sum_f F_{f,y,x,m,s,z}$ represents the total (across all fisheries) fishing mortality on those crab. The number of crab retained in fishery *f* classified as *x*, *m*, *s*, *z* in year *y* is given by

$r_{f,y,x,m,s,z} = \frac{\rho_{f,y,x,m,s,z} \cdot \phi_{f,y,x,m,s,z}}{F^T_{y,x,m,s,z}} \cdot \left[1 - e^{-F^T_{y,x,m,s,z}}\right] \cdot n_{y,x,m,s,z}$	number of retained crab	H.4

while the number of discarded crab, $d_{f,y,x,m,s,z}$, is given by

$d_{f,y,x,m,s,z} = \frac{(1-\rho_{f,y,x,m,s,z}) \cdot \phi_{f,y,x,m,s,z}}{F^T_{y,x,m,s,z}} \cdot \left[1 - e^{-F^T_{y,x,m,s,z}}\right] \cdot n_{y,x,m,s,z}$	number of discarded crab	H.5

and the discard mortality, $dm_{f,y,x,m,s,z}$, is

$dm_{f,y,x,m,s,z} = \frac{h_{f,y} \cdot (1-\rho_{f,y,x,m,s,z}) \cdot \phi_{f,y,x,m,s,z}}{F^T_{y,x,m,s,z}} \cdot \left[1 - e^{-F^T_{y,x,m,s,z}}\right] \cdot n_{y,x,m,s,z}$	discard mortality (numbers)	H.6

The capture rate $\phi_{f,y,x,m,s,z}$ (*not* the fishing mortality rate $F_{f,y,x,m,s,z}$) is modeled as a function separable into separate year and size components such that

$\phi_{f,y,x,m,s,z} = \phi_{f,y,x,m,s} \cdot S_{f,y,x,m,s,z}$	fishing capture rate	H.7

where $\phi_{f,y,x,m,s}$ is the fully-selected capture rate in year *y* and $S_{f,y,x,m,s,z}$ is the size-specific selectivity.

The fully-selected capture rate $\phi_{f,y,x,m,s}$ for *y* in time block *t* is parameterized in the following manner:

$\phi_{f,y,x,m,s} = \exp\left(\overline{lnC}_{f,t,x,m,s} + pDevsC_{f,y,x,m,s}\right)$	H.8

where the $pDevsC_{f,y,x,m,s}$ are elements for year *y* in time block *t* of a "devs" vectors representing annual variations from the ln-scale mean fully-selected capture rate $\overline{lnC}_{f,t,x,m,s}$. The latter is expressed in terms of model parameters as

$\overline{lnC}_{f,t,x,m,s} = pLnC_{f,t,x,m,s} + \sum_{i=1}^{4} \delta C^i_{f,t,x,m,s}$	H.9

where the $pLnC_{f,t,x,m,s}$ is the mean ln-scale capture rate (e.g., for mature males) and the $\delta C^i_{f,t,x,m,s}$ are ln-scale offsets.

I. Surveys

If $n_{y,x,m,s,z}$ is the number of crab classified as *x*, *m*, *s*, *z* in year *y* just prior to the prosecution of a survey, then the survey abundance, $a_{v,y,x,m,s,z}$, of crab classified in that state by survey *v* is given by

$a_{v,y,x,m,s,z} = q_{v,y,x,m,s,z} \cdot n_{y,x,m,s,z}$	survey abundance	I.1

where $q_{v,y,x,m,s,z}$ is the size-specific survey catchability on this component of the population.

The survey catchability $q_{v,y,x,m,s,z}$ is decomposed in the usual fashion into separate time block and size components such that, for *y* in time block *t*:

$q_{v,y,x,m,s,z} = q_{v,t,x,m,s} \cdot S_{v,t,x,m,s,z} \cdot A_{v,t,x,m,s,z}$	survey catchability	I.2

where $q_{v,t,x,m,s}$ is the fully-selected catchability in time block *t*, $S_{v,t,x,m,s,z}$ is the size-specific survey selectivity, and $A_{v,t,x,m,s,z}$ is the size-specific availability of the population to the survey. If the survey covers the complete stock area (as the standard NMFS EBS bottom trawl is assumed to do for Tanner

crab), then $A_{v,t,x,m,s,z} \equiv 1$. However, if the survey does not cover the complete stock, as is the case with the BSFRF/NMFS side-by-side catchability studies, then $A_{v,t,x,m,s,z}$ needs to be estimated or assumed.

The fully-selected catchability $q_{v,t,x,m,s}$ is parameterized in a fashion similar to that for fully-selected fishery capture rates (except that annual "devs" are not included) in the following manner:

$q_{v,t,x,m,s} = \exp\left(pLnQ_{v,t,x,m,s} + \sum_{i=1}^{4} \delta Q^{i}_{v,t,x,m,s}\right)$	I.3

where the $pLnQ_{v,t,x,m,s}$ is the mean ln-scale catchability (e.g., for mature males) and the $\delta Q^{i}_{v,t,x,m,s}$ are ln-scale offsets.

J. Model fitting: objective function equations

The TCSAM02 model is fit by minimizing an objective function, $\mathscr{O}$, with additive components consisting of: 1) negative log-likelihood functions based on specified prior probability distributions associated with user-specified model parameters, and 2) several negative log-likelihood functions based on input data components, of the form:

$\mathscr{O} = -2\sum_{p} \lambda_p \cdot \ln(\wp_p) - 2\sum_{l} \lambda_l \cdot \ln(\mathcal{L}_l)$	model objective function	J.1

where $\wp_p$ represents the *p*th prior probability function, $\mathcal{L}_l$ represents the *l*th likelihood function, and the λ's represent user-adjustable weights for each component.

Prior Probability Functions

Prior probability functions can be associated with each model parameter or parameter vector by the user in the model input files (see Section L below for examples on specifying priors).

Likelihood Functions

The likelihood components included in the model's objective function are based on normalized size frequencies and time series of abundance or biomass from fishery or survey data. Survey data optionally consists of abundance and/or biomass time series for males, females, and/or all crab (with associated survey cv's), as well as size frequencies by sex, maturity state, and shell condition. Fishery data consists of similar data types for optional retained, discard, and total catch components.

Size frequency components

Likelihood components involving size frequencies are based on multinomial sampling:

$\ln(\mathcal{L}) = \sum_{y} n_{y,c} \cdot \sum_{z} \{p^{obs}_{y,c,z} \cdot \ln(p^{mod}_{y,c,z} + \delta) - p^{obs}_{y,c,z} \cdot \ln(p^{obs}_{y,c,z} + \delta)\}$	multinomial log-likelihood	J.2

where the *y*'s are years for which data exists, "*c*" indicates the population component classifiers (i.e., sex, maturity state, shell condition) the size frequency refers to, $n_{y,c}$ is the classifier-specific effective sample size for year y, $p^{obs}_{y,c,z}$ is the observed size composition in size bin *z* (i.e., the size frequency normalized to sum to 1 across size bins for each year), $p^{mod}_{y,c,z}$ is the corresponding model-estimated size composition, and δ is a small constant. The manner in which the observed and estimated size frequencies for each data component are aggregated (e.g., over shell condition) prior to normalization is specified by the user in the model input files. Data can be entered in input files at less-aggregated levels of than will be used in the model; it will be aggregated in the model to the requested level before fitting occurs.

Aggregated abundance/biomass components

Likelihood components involving aggregated (over size, at least) abundance and or biomass time series can be computed using one of three potential likelihood functions: the normal, the lognormal, and the "norm2". The likelihood function used for each data component is user-specified in the model input files.

The ln-scale normal likelihood function is

$\ln(\mathcal{L}^N)_c = -\frac{1}{2}\sum_y \left\{ \frac{\left[a_{y,c}^{obs} - a_{y,c}^{mod}\right]^2}{\sigma_{y,c}^2} \right\}$	normal log-likelihood	J.3

where $a_{y,c}^{obs}$ is the observed abundance/biomass value in year *y* for aggregation level *c*, $a_{y,c}^{mod}$ is the associated model estimate, and $\sigma_{y,c}^2$ is the variance associated with the observation.

The ln-scale lognormal likelihood function is

$\ln(\mathcal{L}^{LN})_c = -\frac{1}{2}\sum_y \left\{ \frac{\left[ln\left(a_{y,c}^{obs}+\delta\right) - ln\left(a_{y,c}^{mod}+\delta\right)\right]^2}{\sigma_{y,c}^2} \right\}$	lognormal log-likelihood	J.4

where $a_{y,c}^{obs}$ is the observed abundance/biomass value in year *y* for aggregation level *c*, $a_{y,c}^{mod}$ is the associated model estimate, and $\sigma_{y,c}^2$ is the ln-scale variance associated with the observation.

For consistency with TCSAM2013, a third type, the "norm2", may also be specified

$\ln(\mathcal{L}^{N2})_x = -\frac{1}{2}\sum_y \left[a_{y,x}^{obs} - a_{y,x}^{mod}\right]^2$	"norm2" log-likelihood	J.5

This is equivalent to specifying a normal log-likelihood with $\sigma_{y,x}^2 \equiv 1.0$. This is the standard likelihood function applied in TCSAM2013 to fishery catch time series.

Growth data

Growth (molt increment) data can be fit as part of a TCSAM02 model. Multiple datasets can be fit at the same time. The likelihood for each dataset (L_d) is based on the same gamma distribution used in the growth model:

$L_d = -\sum_{i \in d} ln\left\{ \Gamma\left(\frac{\tilde{z}_i - \bar{z}_{y_i,x_i,z_i}}{\beta_{y_i,x_i}} \right) \right\}$	gamma log-likelihood	J.6

where z_i and $\tilde{z}_i$ are the pre-molt and post-molt sizes for individual *i* (of sex x_i collected in year y_i) in dataset *d*, respectively, $\bar{z}_{y_i,x_i,z_i}$ is the predicted mean post-molt size for individual *i*, and β_{y_i,x_i} is the scale factor for the gamma distribution corresponding to individual *i*.

Maturity ogive data

Annual maturity ogive data, the observed proportions-at-size of mature crab in a given year, can also be fit as part of a TCSAM02 model. This data consists of proportions of mature crab observed within a size bin, as well as the total number of observations for that size bin. The proportions are assumed to represent the fraction of new shell mature crab (i.e., having gone through terminal molt within the previous growth season) to all new shell crab within the size bin in that year. Multiple datasets can be fit at the same time. The likelihood for each observation is based on a binomial distribution with sample size equal to the

number of observations within the corresponding size bin, so the likelihood for each dataset (L_m) is given by:

$L_m = \sum_{y,z} n_{y,z} \cdot \{p_{y,z}^{obs} \cdot \ln(p_{y,z}^{mod} + \delta) + (1 - p_{y,z}^{obs}) \cdot \ln(1 - p_{y,z}^{mod} + \delta)\}$	binomial log-likelihood	J.7

where *y* is a year, *z* is a size bin, $n_{y,z}$ is the total number of classified crab in size bin *z* in year *y*, $p_{y,z}^{obs}$ is the observed ratio of mature, new shell males to total new shell males in size bin z in year y, $p_{y,z}^{obs}$ is the corresponding model-predicted ratio, and δ is a small constant to prevent trying to calculate ln(0).

Effort data

In both TCSAM2013 and TCSAM02, fishery-specific effort data is used to predict annual fully-selected fishery capture rates for Tanner crab bycatch in the snow crab and Bristol Bay red king crab fisheries in the period before at-sea observer data is available (i.e., prior to 1991), based on the assumed relationship

$$F_{f,y} = q_f \cdot E_{f,y}$$

where $F_{f,y}$ is the fully-selected capture rate in fishery *f* in year *y*, q_f is the estimated catchability in fishery f, and $E_{f,y}$ is the reported annual, fishery-specific effort (in pots). In TCAM2013, the fishery *q*'s are estimated directly from the ratio of fishery mean *F* to mean *E* over the time period (t_f) when at-sea observer data is available from which to estimate the $F_{f,y}$'s as parameters:

$$q_f = \frac{\sum_{y \in t_f} F_{f,y}}{\sum_{y \in t_f} E_{f,y}}.$$

Note that, in this formulation, the fishery *q*'s are not parameters (i.e., estimated via maximizing the likelihood) in the model. In TCSAM2013, the time period over which *q* is estimated for each fishery is hard-wired. This approach is also available as an option in TCSAM02, although different time periods for the averaging can be specified in the model options file.

A second approach to effort extrapolation in which the fishery *q*'s are fully-fledged parameters estimated as part of maximizing the likelihood is provided in TCSAM02 as an option, as well. In this case, the effort data is assumed to have a lognormal error distribution and the following negative log-likelihood components are included in the overall model objective function:

$$L_f = \sum_y \frac{\left(\ln(E_{f,y} + \delta) - \ln\left(\frac{F_{f,y}}{q_f} + \delta\right)\right)^2}{2 \cdot \sigma_f^2}$$

where σ_f^2 is the assumed ln-scale variance associated with the effort data and δ is a small value so that the arguments of the ln functions do not go to zero.

Aggregation fitting levels

A number of different ways to aggregate input data and model estimates prior to fitting likelihood functions have been implemented in TCSAM02. These include:

Abundance/Biomass by	Size Conpositions by	extended by
total	total	x
x		x, m
x, mature only	x	--
x, m		m
x, s		s
x, m, s	x, m	--
		s
	x, s	
	x, m, s	

where *x*, *m*, *s* refer to sex, maturity state and shell condition and missing levels are aggregated over. For size compositions that are "extended by" *x*, *m*, *s*, or {*x*, *m*}, this involves appending the size compositions corresponding to each combination of "extended by" factor levels, renormalizing the extended composition to sum to 1, and then fitting the extended composition using a multinomial likelihood.

K. Devs vectors

For TCSAM02 to accommodate arbitrary numbers of fisheries and time blocks, it is necessary to be able to define arbitrary numbers of "devs" vectors. This is currently not possible using the ADMB C++ libraries, so TCSAM02 uses an alternative implementation of devs vectors from that implemented in ADMB. For the 2017 assessment, an *n*-element "devs" vector was implemented using an *n*-element bounded parameter vector. with the final element of the "devs" vector defined as $-\sum_{n-1} v_i$, where v_i was the ith value of the parameter (or devs) vector, so that the sum over all elements of the devs vector was identically 0. Penalties were placed on the final element of the devs vector to ensure it was bounded in the same manner as the parameter vector. However, this approach was problematic when initializing the model with the values for the *n*-1 elements that defined the n-element devs vector, the value of the n-th element ($-\sum_{n-1} v_i$) was not guaranteed to satisfy the bounds placed on the vector. Thus, this approach was revised to allow specification of all n element values (the $v_n = -\sum_{n-1} v_i$ constraint was removed) while the likelihood penalty was changed to ensure the sum of the elements was 0. The new approach also has the advantage that it more closely follows the one used in ADMB to define "devs" vectors. Test runs with both approaches showed no effect on convergence to the MLE solution.

L. Priors for model parameters

A prior probability distribution can be specified for any element of model parameter. The following distributions are available for use as priors:

indicator	**parameters**	**constants**	**description**
none	none	none	no prior applied
ar1_normal	μ, σ	none	random walk with normal deviates
cauchy	x_0, γ	none	Cauchy pdf
chisquare	υ	none	χ^2 pdf
constant	min, max	none	uniform pdf
exponential	λ	none	exponential pdf
gamma	r, μ	none	gamma pdf
invchisquare	υ	none	inverse χ^2 pdf

invgamma	r, μ	none	inverse gamma pdf
invgaussian	μ, λ	none	inverse Gaussian pdf
lognormal	median, CV	none	lognormal pdf
logscale_normal	median, CV	none	normal pdf on ln-scale
normal	μ, σ	none	normal pdf
scaled_invchisquare	υ, s	none	inverse χ^2 scaled pdf
scaledCV_invchisquare	υ, CV	none	inverse χ^2 pdf, scaled by CV
t	υ	none	t distribution
truncated_normal	μ, σ	min, max	truncated normal pdf

M. Parameters and other information determined outside the model

Several nominal model parameters are not estimated in the model, rather they are fixed to values determined outside the model. These include Tanner crab handling mortality rates for discards in the crab fisheries (32.1%), the groundfish trawl fisheries (80%), and the groundfish pot fisheries (50%), as well the base rate for natural mortality (0.23 yr^{-1}). Sex- and maturity-state-specific parameters for individual weight-at-size have also been determined outside the model, based on fits to data collected on the NMFS EBS bottom trawl survey (Daly et al., 2016). Weight-at-size, $w_{x,m,z}$, is given by

$$w_{x,m,z} = a_{x,m} \cdot z^{b_{x,m}}$$

where

sex	**maturity state**	$a_{x,m}$	$b_{x,m}$
male	all states	0.000270	3.022134
female	immature	0.000562	2.816928
	mature	0.000441	2.898686

and size is in mm CW and weight is in kg.

N. OFL calculations and stock status determination

Overfishing level (OFL) calculations and stock status determination for Tanner crab are based on Tier 3 considerations for crab stocks as defined by the North Pacific Fishery Management Council (NPFMC; NPFMC 2016). Tier 3 considerations require life history information such as natural mortality rates, growth, and maturity but use proxies based on a spawner-per-recruit approach for F_{MSY}, B_{MSY}, and MSY because there is no reliable stock-recruit relationship. Equilibrium recruitment is assumed to be equal to the average recruitment over a selected time period (1982-present for Tanner crab). For Tier 3 stocks, the proxy for B_{MSY} is defined as 35% of longterm (equilibrium) mature male biomass (MMB) for the unfished stock (B_0). The proxy F_{MSY} for Tier 3 stocks is then the directed fishing mortality rate that results in $B_{35\%}$ (i.e., $F_{35\%}$), while the MSY proxy is the longterm total (retained plus discard) catch mortality resulting from fishing at F_{MSY}. The OFL calculation for the upcoming year is based on a sloping

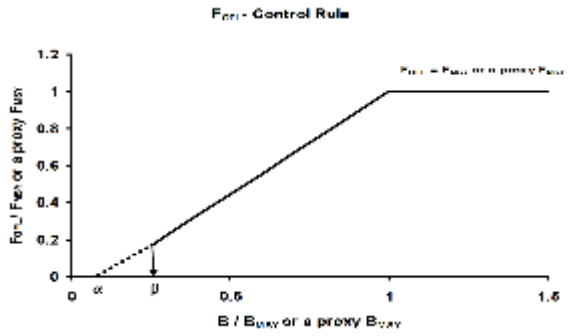

Fig. 2. The F_{OFL} harvest control rule.

harvest control rule for F_{OFL} (Fig. 2), the directed fishing mortality rate that results in the OFL. If the "current" MMB (projected to Feb. 15 of the upcoming year under the F_{OFL}) is above B_{MSY} ($B_{35\%}$), then $F_{OFL}=F_{MSY}=F_{35\%}$. If the current MMB is between $\beta \cdot B_{MSY}$ and B_{MSY}, then F_{OFL} is determined from the slope of the control rule. In either of these cases, the OFL is simply the projected total catch mortality under directed fishing at F_{OFL}. If current MMB is less than $\beta \cdot B_{MSY}$, then no directed fishing is allowed ($F_{OFL}=0$) and the OFL is set to provide for stock rebuilding with bycatch in non-directed fisheries. Note that if current MMB is less than B_{MSY}, then the process of determining F_{OFL} is generally an iterative one.

Stock status is determined by comparing "current" MMB with the Minimum Stock Size Threshold (MSST), which is defined as $0.5xB_{MSY}$: if "current" MMB is below the MSST, then the stock is overfished—otherwise, it is not overfished.

N.1 Equilibrium conditions

Both OFL calculations and stock status determination utilize equilibrium considerations, both equilibrium under unfished conditions (to determine B_0 and $B_{35\%}$) and under fished conditions (to determine $F_{35\%}$). For Tier 3 stocks, because there is no reliable stock-recruit relationship, analytical solutions can be found for equilibrium conditions for any fishing mortality conditions. These solutions are described below (the notation differs somewhat from that used in previous sections).

N.1.1 Population states

The Tanner crab population on July 1 can be characterized by abundance-at-size in four population states:

in– immature new shell crab
io– immature old shell crab
mn – mature new shell crab
mo – mature old shell crab

where each of these states represents a vector of abundance-at-size (i.e., a vector subscripted by size).

N.1.2 Population processes

The following processes then describe the dynamics of the population over a year:

S_1 – survival from start of year to time of molting/growth of immature crab, possibly including fishing mortality (a diagonal matrix)
S_2 – survival after time of molting/growth of immature crab to end of year, possibly including fishing mortality (a diagonal matrix)
Φ – probability of an immature crab molting (pr(molt|*z*), where *z* is pre-molt size; a diagonal matrix) (pr(molt|*z*) is assumed to be 1 in TCSAM02).
Θ – probability that a molt was terminal (pr(molt to maturity|*z*, molt), where *z* is post-molt size; a diagonal matrix)
T – size transition matrix (a non-diagonal matrix)
1 – identity matrix
R –number of recruits by size (a vector)

The matrices above are doubly–subscripted, and *R* is singly-subscripted, by size. Additionally, the matrices above (except for the identity matrix) can also be subscripted by population state (*in*, *io*, *mn*, *mo*) for generality. For example, survival of immature crab may differ between those that molted and those that skipped.

N.1.3 Population dynamics

The following equations then describe the development of the population from the beginning of one year to the beginning of the next:

$$in^{+} = R + S_{2in} \cdot \{(1 - \Theta_{in}) \cdot T_{in} \cdot \Phi_{in} \cdot S_{1in} \cdot in + T_{io} \cdot (1 - \Theta_{io}) \cdot \Phi_{io} \cdot S_{1io} \cdot io\} \quad \text{(N.1)}$$
$$io^{+} = S_{2io} \cdot \{(1 - \Phi_{in}) \cdot S_{1in} \cdot in + (1 - \Phi_{io}) \cdot S_{1io} \cdot io\} \quad \text{(N.2)}$$
$$mn^{+} = S_{2mn} \cdot \{\Theta_{in} \cdot T_{in} \cdot \Phi_{in} \cdot S_{1in} \cdot in + \Theta_{io} \cdot T_{io} \cdot \Phi_{io} \cdot S_{1io} \cdot io\} \quad \text{(N.3)}$$
$$mo^{+} = S_{2mo} \cdot \{S_{1mn} \cdot mn + S_{1mo} \cdot mo\} \quad \text{(N.4)}$$

where "+" indicates year+1 and all recruits (*R*) are assumed to be new shell.

N.1.4 Equilibrium equations

The equations reflecting equilibrium conditions (i.e., $in^{+} = in$, etc.) are simply:

$$in = R + S_{2in} \cdot \{(1 - \Theta_{in}) \cdot T_{in} \cdot \Phi_{in} \cdot S_{1in} \cdot in + (1 - \Theta_{io}) \cdot T_{io} \cdot \Phi_{io} \cdot S_{1io} \cdot io\} \quad \text{(N.5)}$$
$$io = S_{2io} \cdot \{(1 - \Phi_{in}) \cdot S_{1in} \cdot in + (1 - \Phi_{io}) \cdot S_{1io} \cdot io\} \quad \text{(N.6)}$$
$$mn = S_{2mn} \cdot \{\Theta_{in} \cdot T_{in} \cdot \Phi_{in} \cdot S_{1in} \cdot in + \Theta_{io} \cdot T_{io} \cdot \Phi_{io} \cdot S_{1io} \cdot io\} \quad \text{(N.7)}$$
$$mo = S_{2mo} \cdot \{S_{1mn} \cdot mn + S_{1mo} \cdot mo\} \quad \text{(N.8)}$$

where *R* above is now the equilibrium (longterm average) number of recruits-at-size vector.

N.1.5 Equilibrium solution

The equilibrium solution can be obtained by rewriting the above equilibrium equations as:

$$in = R + A \cdot in + B \cdot io \quad \text{(N.9)}$$
$$io = C \cdot in + D \cdot io \quad \text{(N.10)}$$
$$mn = E \cdot in + F \cdot io \quad \text{(N.11)}$$
$$mo = G \cdot mn + H \cdot mo \quad \text{(N.12)}$$

where *A*, *B*, *C*, *D*, *E*, *F*, *G*, and *H* are square matrices. Solving for *io* in terms of *in* in eq. 10, one obtains

$$io = \{1 - D\}^{-1} \cdot C \cdot in \quad \text{(N.13)}$$

Plugging eq. 13 into 9 and solving for *in* yields

$$in = \{1 - A - B \cdot [1 - D]^{-1} \cdot C\}^{-1} \cdot R \quad \text{(N.14)}$$

Equations 13 for *io* and 14 for *in* can simply be plugged into eq. 11 to yield *mn:*

$$mn = E \cdot in + F \cdot io \quad \text{(N.15)}$$

while eq. 12 can then be solved for *mo*, yielding:

$$mo = \{1 - H\}^{-1} \cdot G \cdot mn \quad \text{(N.16)}$$

where (for completeness):

$$A = S_{2in} \cdot (1 - \Theta_{in}) \cdot T_{in} \cdot \Phi_{in} \cdot S_{1in} \quad \text{(N.17)}$$
$$B = S_{2in} \cdot (1 - \Theta_{io}) \cdot T_{io} \cdot \Phi_{io} \cdot S_{1io} \quad \text{(N.18)}$$
$$C = S_{2io} \cdot (1 - \Phi_{in}) \cdot S_{1in} \quad \text{(N.19)}$$
$$D = S_{2io} \cdot (1 - \Phi_{io}) \cdot S_{1io} \quad \text{(N.20)}$$
$$E = S_{2mn} \cdot \Theta_{in} \cdot T_{in} \cdot \Phi_{in} \cdot S_{1in} \quad \text{(N.21)}$$

$$F = S_{2mn} \cdot \Theta_{io} \cdot T_{io} \cdot \Phi_{io} \cdot S_{1io} \quad \text{(N.22)}$$
$$G = S_{2mo} \cdot S_{1mn} \quad \text{(N.23)}$$
$$H = S_{2mo} \cdot S_{1mo} \quad \text{(N.24)}$$

Note that Θ, the size-specific conditional probability of a molt being the terminal molt-to-maturity, is defined above on the basis of post-molt, not pre-molt, size. This implies that whether or not a molt is terminal depends on the size a crab grows into, not the size it at which it molted. An alternative approach would be to assume that the conditional probability of terminal molt is determined by pre-molt size. This would result in an alternative set of equations, but these can be easily obtained from the ones above by simply reversing the order of the terms involving T and Θ (e.g., the term $(1 - \Theta_{in}) \cdot T_{in}$ becomes $T_{in} \cdot (1 - \Theta_{in})$).

N.2 OFL calculations

Because a number of the calculations involved in determining the OFL are iterative in nature, the OFL calculations do not involve automatically-differentiated (AD) variables. Additionally, they are only done after model convergence or when evaluating an MCMC chain. The steps involved in calculating the OFL are outlined as follows:

1. The initial population numbers-at-sex/maturity state/shell condition/size for the upcoming year are copied to a non-AD array.
2. Mean recruitment is estimated over a pre-determined time frame (currently 1982-present).
3. The arrays associated with all population rates in the final year are copied to non-AD arrays for use in the upcoming year.
4. Calculate the average selectivity and retention functions for all fisheries over the most recent 5-year period.
5. Determine the average maximum capture rates for all fisheries over the most recent 5-year period.
6. Using the equilibrium equations, calculate B_0 for unfished stock ($B35\% = 0.35*B_0$).
7. Using the equilibrium equations, iterate on the maximum capture rate for males in the directed fishery to find the one ($F_{35\%}$) that results in the equilibrium MMB = $B_{35\%}$.
8. Calculate "current" MMB under directed fishing at $F=F_{35\%}$ by projecting initial population (1) to Feb. 15.
    a. If current MMB > $B_{35\%}$, $F_{OFL} = F_{35\%}$. The associated total catch mortality is OFL.
    b. Otherwise
        i. set directed F based on the harvest control rule and the ratio of the calculated current MMB to $B_{35\%}$
        ii. recalculate current MMB
        iii. iterate i-iii until current MMB doesn't change between iterations. Then $F_{OFL} = F\ (< F_{35\%})$ and the OFL is the associated total (retained plus discard) catch mortality.

References

Fournier, D.A., H.J. Skaug, J. Ancheta, J. Ianelli, A. Magnusson, M.N. Maunder, A. Nielsen, and J. Sibert. 2012. AD Model Builder: using automatic differentiation for statistical inference of highly parameterized complex nonlinear models. Optim. Methods Softw. 27:233-249.

Methot, R.D. and C.R. Wetzel. 2013. Stock synthesis: A biological and statistical framework for fish stock assessment and fishery management. Fish. Res. 142: 86-99.

NPFMC. 2016. Introduction. In: Stock Assessment and Fishery Evaluation Report for the King and Tanner Crab Fisheries of the Bering Sea and Aleutian Islands: 2016 Crab SAFE. North Pacific Fishery Management Council. Anchorage, AK. pp. 1-40.

Rugolo, L.J. and B.J. Turnock. 2011. Length-Based Stock Assessment Model of eastern Bering Sea Tanner Crab. Report to Subgroup of NPFMC Crab Plan Team. 61p.

Rugolo, L.J. and B.J. Turnock. 2012a. Length-Based Stock Assessment Model of eastern Bering Sea Tanner Crab. Report to Subgroup of NPFMC Crab Plan Team. 69p.

Rugolo L,J. and B.J. Turnock. 2012b. 2012 Stock Assessment and Fishery Evaluation Report for the Tanner Crab Fisheries of the Bering Sea and Aleutian Islands Regions. In: Stock Assessment and Fishery Evaluation Report for the King and Tanner Crab Fisheries of the Bering Sea and Aleutian Islands: 2012 Crab SAFE. North Pacific Fishery Management Council. Anchorage, AK. pp. 267-416.

Stockhausen, W.T., B.J. Turnock and L. Rugolo. 2013. 2013 Stock Assessment and Fishery Evaluation Report for the Tanner Crab Fisheries of the Bering Sea and Aleutian Islands Regions. In: Stock Assessment and Fishery Evaluation Report for the King and Tanner Crab Fisheries of the Bering Sea and Aleutian Islands: 2013 Crab SAFE. North Pacific Fishery Management Council. Anchorage, AK. pp. 342-449.

Stockhausen, W.T. 2014. 2014 Stock Assessment and Fishery Evaluation Report for the Tanner Crab Fisheries of the Bering Sea and Aleutian Islands Regions. In: Stock Assessment and Fishery Evaluation Report for the King and Tanner Crab Fisheries of the Bering Sea and Aleutian Islands: 2014 Crab SAFE. North Pacific Fishery Management Council. Anchorage, AK. pp. 324-545.

Stockhausen, W.T. 2015. 2015 Stock Assessment and Fishery Evaluation Report for the Tanner Crab Fisheries of the Bering Sea and Aleutian Islands Regions. In: Stock Assessment and Fishery Evaluation Report for the King and Tanner Crab Fisheries of the Bering Sea and Aleutian Islands: 2015 Crab SAFE. North Pacific Fishery Management Council. Anchorage, AK. pp. 293-440.

Stockhausen, W.T. 2016. 2016 Stock Assessment and Fishery Evaluation Report for the Tanner Crab Fisheries of the Bering Sea and Aleutian Islands Regions. In: Stock Assessment and Fishery Evaluation Report for the King and Tanner Crab Fisheries of the Bering Sea and Aleutian Islands: 2016 Crab SAFE. North Pacific Fishery Management Council. Anchorage, AK. pp. 251-446.

Appendix 2:
Assessment Model Sensitivity to a Missing Terminal Year Survey

William T. Stockhausen
Alaska Fisheries Science Center
September 2020

1.0 Introduction

The 2020 NMFS Eastern Bering Sea shelf bottom trawl survey was cancelled due to concerns related to the Covid-19 pandemic. The survey had been conducted annually since 1975 and represents the primary source of fishery-independent data for the Tanner crab assessment. As such, the loss of the 2020 survey might be expected to have a substantial impact on the uncertainty associated with estimates of stock size and management-related quantities estimated by the Tanner crab assessment model. Consequently, the CPT and SSC requested that assessment authors conduct analyses to assess the additional uncertainty the loss of a survey in the terminal year of the assessment would have on estimates from the assessment model. This appendix presents the results of those analyses for Tanner crab.

2.0 Methods

The CPT requested that the likely uncertainty associated with the absence of a survey in the terminal year of the assessment be evaluated using two methods: 1) a retrospective analysis and 2) a sensitivity study using simulated survey data for 2020.

2.1 Retrospective analysis

A standard retrospective analysis consists of sequentially dropping the most recent year from the assessment and re-evaluating the estimates from the assessment model, repeating the process for a period of several years. Each year that is dropped from the assessment is referred to as a "peel", as are the results from the model run with data up to the "peeled" year. Large differences or trends in differences between estimates of a model quantity from the assessment and the peels can indicate underlying structural problems in the assessment model or conflicting information in the data.

The analysis the CPT requested consisted of comparing the results from each model run in a standard retrospective analysis using the accepted 2019 assessment model with a corresponding model run with the terminal year survey dropped from the model. The emphasis is not on the retrospective patterns (i.e., what happens when you sequentially remove each year of data) but on the differences between quantities from the model run that includes the terminal year survey and that which drops it. Here, I quantified the relative error (ε_y) in several management-related quantities (B_{MSY}, terminal year MMB, OFL, and the stock status) in terminal year *y* between the run with the terminal year survey (v_y) and the run with it dropped ($\tilde{v}_y$), where for each year for a given quantity

$$\varepsilon_y = 100 * \frac{\tilde{v}_y - v_y}{v_y}$$

The mean size of the errors across years (terminal years 2010-2019) for a given quantity was characterized using the relative root-mean-square error, ρ:

$$\rho = \sqrt{\frac{1}{10}\sum_{y=2010}^{2019} \varepsilon_y^2}$$

2.2 Simulation sensitivity analysis

The simulation sensitivity analysis the CPT requested was based on simulating NMFS survey data for 2020 under "reasonable" excursions from the assessment model estimates for 2020 and re-running the model while including the simulated 2020 survey data as "real". This method evaluates the impact of different hypothetical 2020 survey outcomes, and is based on a SSC recommendation in its June 2020 minutes. The method is as follows:

1. For the survey time series fit in proposed base model for this year, calculate the multiplicative residuals, $\tilde{v}_y/v_y$, where v_y is the observed survey biomass, and $\tilde{v}_y$ is the predicted survey biomass after fitting the model.
2. Obtain the 25th and the 75th percentiles of the multiplicative residuals.
3. Obtain the predicted survey values for 2020 from the base model run.
4. Multiply the predicted survey values for 2020 by the 25th and 75th percentile of the multiplicative residual to create low and high survey observations for 2020.
5. Assume a CV equal to the median survey CV and fit these values in two model runs.
6. Compare the differences in management-related quantities such as OFL and MMB among the three model runs.

The rationale for the 25th and 75th percentiles is that they are a typical high and low value for the survey. Large changes in management quantities such as OFL and MMB indicate high sensitivity.

The base model (19.03) fits survey biomass time series for all males, immature females, and mature females. The procedure described above was thus followed to generate bracketing simulated 2020 survey biomass data for these population components. The base model was then run for the two bracketing 2020 surveys and the remaining data, and the sensitivity of average recruitment, BMSY, terminal year MMB, OFL, and projected MMB to the bracketing 2020 survey data was examined.

3.0 Results

3.1 Retrospective analysis

The retrospective patterns for estimated recruitment and MMB are shown for the 2019 assessment in Figure 3.1.1. The corresponding patterns for estimated recruitment and MMB when the terminal year survey is missing are shown in Figure 3.1.2. The missing terminal year survey appears to affect the overall scale of the retrospective patterns in MMB somewhat, but not the pattern of interannual changes. In contrast, whether or not the terminal year survey is missing has a dramatic effect on the estimate of terminal year recruitment in several years. This, in turn, has a dramatic effect on the value of average recruitment (Figure 3.1.3) and associated management-related quantities such as B_{MSY}, because the averaging time period used in the Tanner crab assessment is 1982 to the terminal year and quantities like B_{MSY} scale with average recruitment.

However, using the averaging time period 1982 to (terminal year – 1) ameliorates the change in average recruitment due to a missing terminal year survey, as well as other management-related quantities (Figure 3.1.4[.1.2.6…]). In general, relative differences between management quantities calculated from models with and without a terminal year survey are small (Table 3.1.1), with root mean square relative errors on the order of 3%, with a maximum relative error of 7.26% in the 2016 estimate of average recruitment.

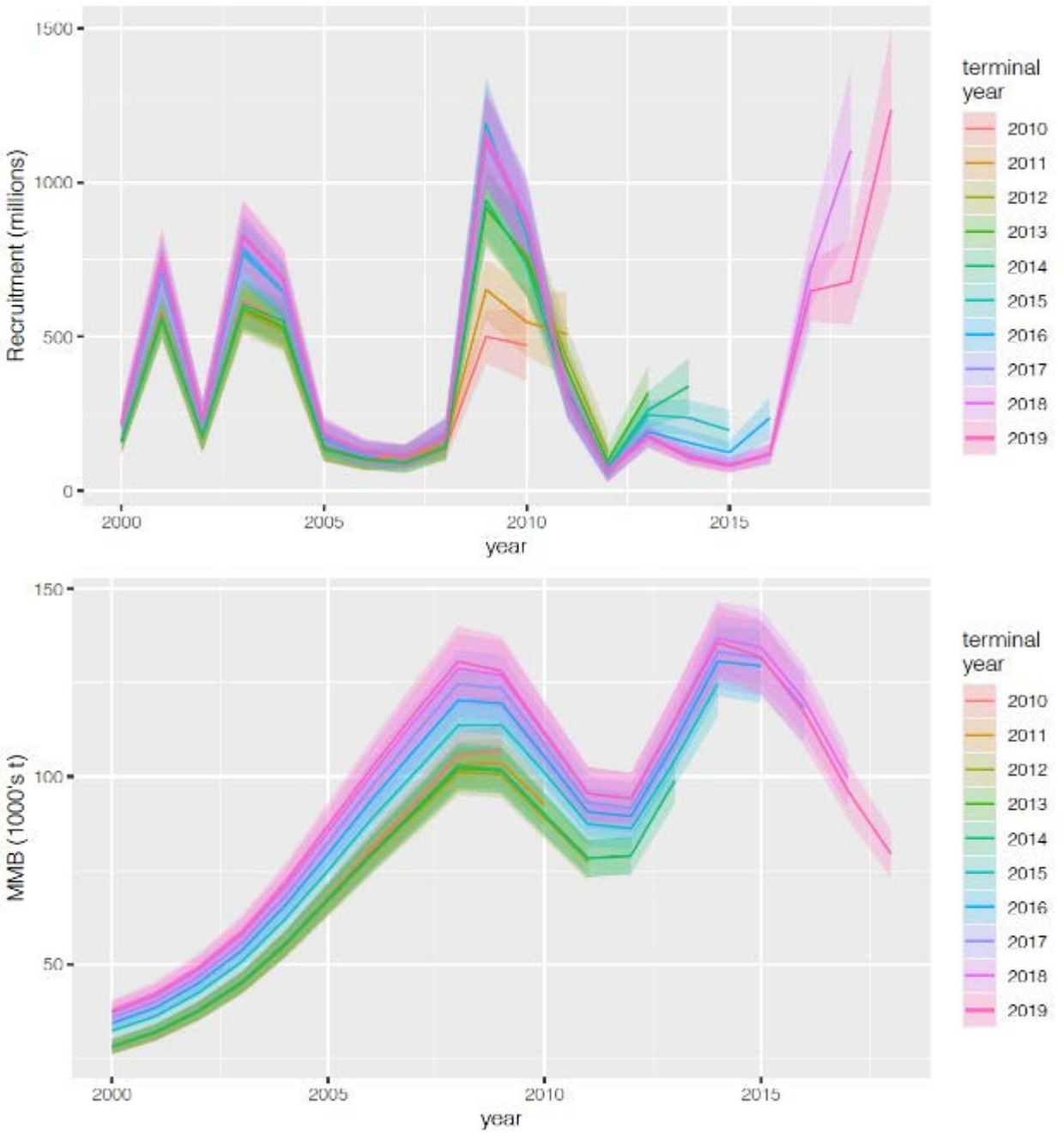

Fig. 3.1.1. 10-year retrospective patterns for the 2019 assessment model (19.03) in estimated recruitment (upper graph) and mature male biomass (MMB; lower graph). Shaded areas represent +/- 1 standard deviation of the estimate. All peels include the terminal year survey.

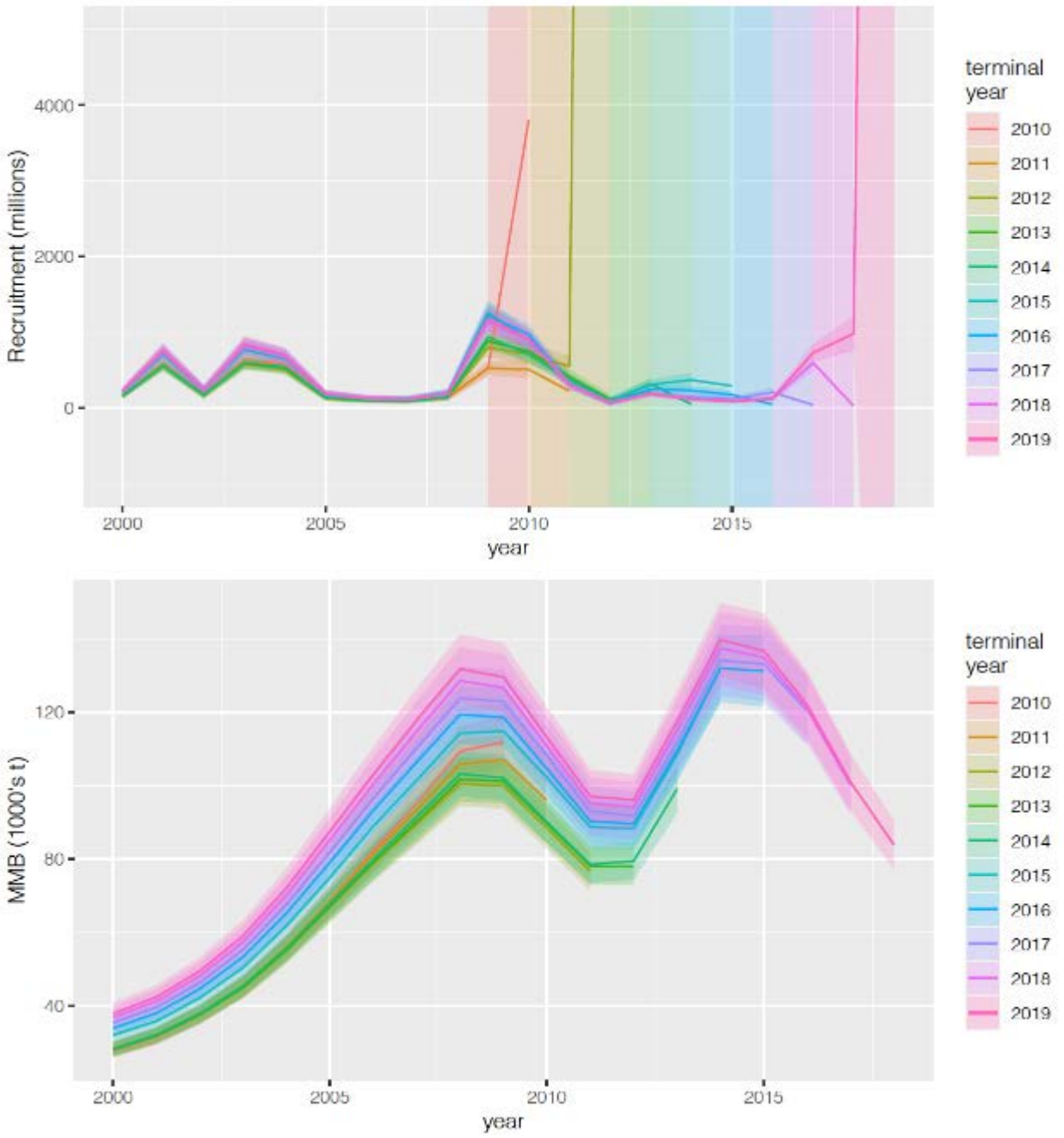

Fig. 3.1.2. 10-year retrospective patterns in estimated recruitment (upper graph) and mature male biomass (MMB; lower graph) for the 2019 assessment model (19.03) with missing terminal year survey. Shaded areas represent +/- 1 standard deviation of the estimate (note that the standard deviations for recruitment in the terminal year for the 2010, 2012, and 2019 peels are larger than the axis scaling). All peels exclude the corresponding terminal year survey.

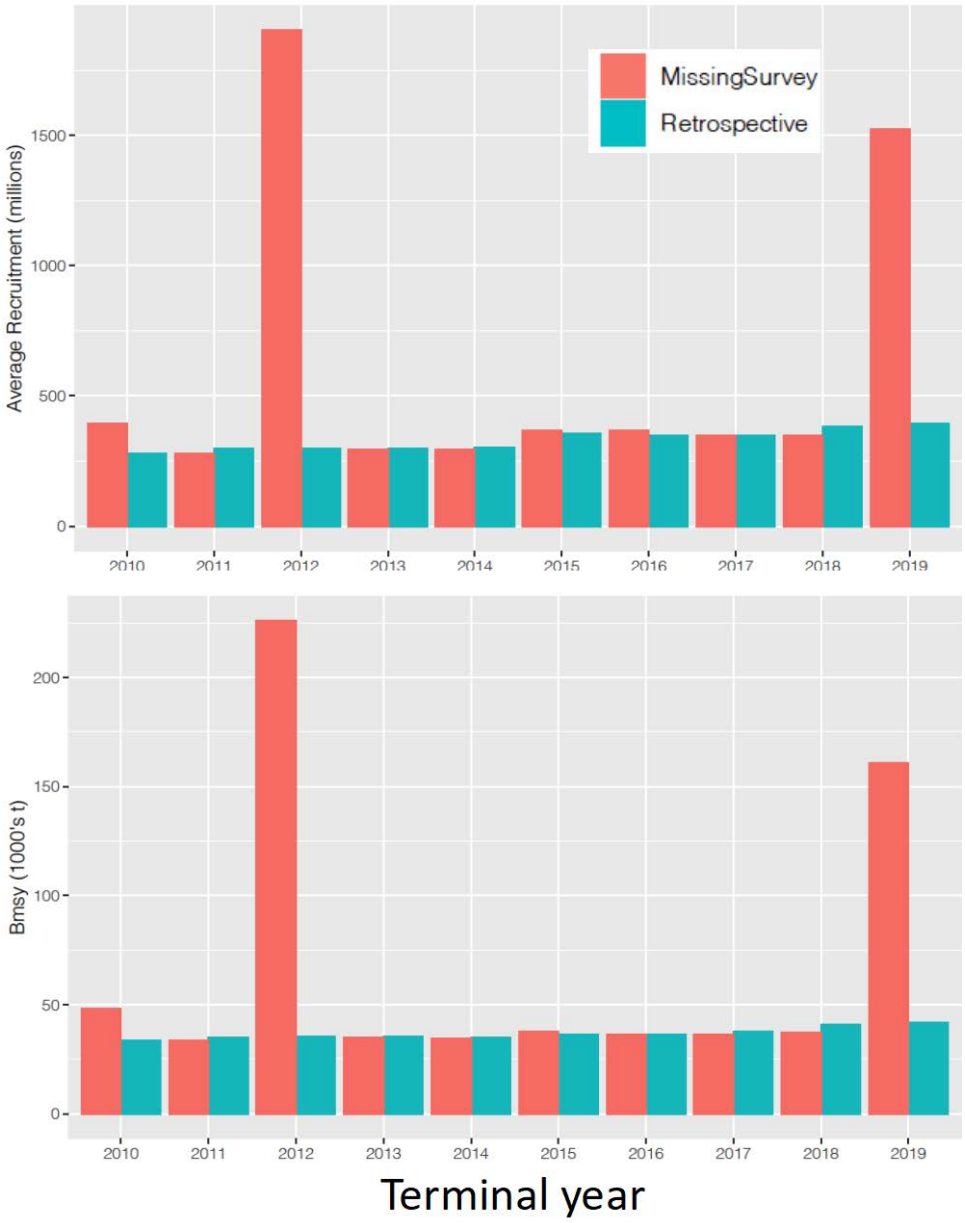

Fig. 3.1.3. Comparison, by terminal year, of estimated average recruitment and the associated B_{MSY} for the models with ("Retrospective") and without ("MissingSurvey") a terminal year survey. Average recruitment here is based on the standard time period used in the Tanner crab assessment, which is 1982 to the terminal year.

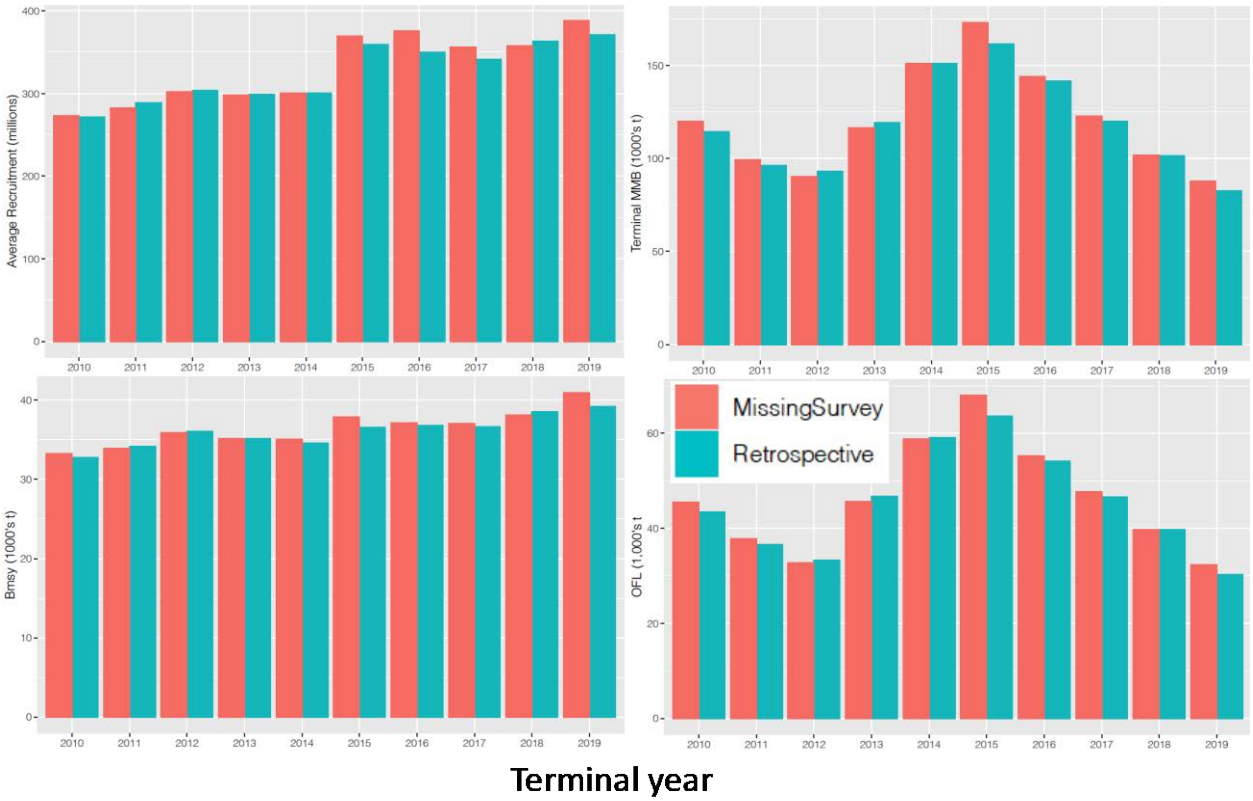

Fig. 3.1.4. Comparison, by terminal year, of estimated average recruitment (upper left), BMSY (lower left), terminal year MMB (upper right) and OFL (lower right) for the models with ("Retrospective") and without ("MissingSurvey") a terminal year survey. The terminal year recruitment estimate was excluded from the averaging period.

Table 3.1.1. Relative difference between retrospective peel with and without a terminal year survey. RMS: root mean square of relative differences. The period 1982 to (terminal year-1) is used to calculate average recruitment.

year	% Difference			
	average recruitment	Bmsy	Terminal MMB	OFL
2010	-0.43	-1.50	-4.78	-4.71
2011	2.24	0.66	-3.23	-3.41
2012	0.52	0.47	2.96	1.69
2013	0.30	-0.03	2.16	2.10
2014	-0.10	-1.61	-0.11	0.34
2015	-2.77	-3.56	-7.00	-6.83
2016	-7.26	-1.01	-1.82	-1.87
2017	-4.34	-1.04	-2.21	-2.35
2018	1.35	0.98	-0.43	-0.30
2019	-4.62	-4.34	-6.26	-6.84
RMS	3.29	2.00	3.79	3.79

3.2 Simulation sensitivity analysis

The base model (19.03) fits to male, immature female, and mature female survey biomass time series are shown in Figure 3.2.1. The resulting multiplicative differences are shown in Figure 3.2.2. Values for the 25% and 75% multiplicative quantiles for simulated survey biomass and the cv's used for the simulated survey data in the two bracketing model runs are given in the following table:

Table 3.2.1. 25% and 75% multiplicative quantiles used to determine the simulated survey biomass data, as well as the assumed cv's.

population category		multiplier		CV's
sex	maturity	25%	75%	
males	all	0.8103	1.2972	0.138
females	immature	0.6239	1.2772	0.206
	mature	0.7467	1.4653	0.216

Model fits from runs with the simulated 2020 surveys are compared with the base model run (without 2020 survey data) in Figure 3.2.3. Note that the base model run does not fit the observed survey biomass values for 2019 very well, and that it predicts overall increases in survey biomass for 2020 for all three stock components (ie., males, immature and mature females). The models with the simulated 2020 survey data fit the data reasonably well (i.e., they fall within the 80% confidence intervals) for males and immature females, but not for mature females. The model estimates for the latter quantity are almost the same for all three models, despite large differences in "observed" mature female survey biomass in 2020. At the scales used in the graphs, differences in the model predictions of the survey biomass time series among the three model runs can be traced back as far as 2014 for males and mature females. These are related to differences in estimated recruitment among the three models (Figure 3.2.4). While estimated recruitments for the terminal year vary widely, as one would expect given the differences in data for 2020, smaller differences among the estimates can be traced back to 2013 (entering the population in 2014), with estimates from SimSurvey75Q and SimSurvey25Q consistently higher and lower, respectively, than the base model without a 2020 survey.

Management-related quantities from the bracketing simulations and the base model are documented in Table 3.2.2 and illustrated in Figure 3.2.5. Differences among the models are primarily driven by the different estimates of average recruitment (the terminal year estimate of recruitment was dropped from the averaging period), with differences ranging up to 20% for equilibrium-related abundance/biomass quantities (average recruitment, B_{100} and B_{MSY}, and MSY). The differences in terminal year MMB are fairly small (<5%). One "twist" to the results here is that the OFL for both models with simulated 2020 surveys is less than the base case, with differences < 3%. This is due to the sloping control rule coming into effect for SimSurvey75Q (status<1), reducing F_{OFL} relative to F_{MSY}.

Table 3.2.2. Summary of management-related quantities from the simulation sensitivity model runs. "Status" is the ratio of projected MMB to B_{MSY}; the "kink" in the OFL control rule occurs where status=1.

management quantities	units	case			% difference from base	
		SimSurvey25Q	19.03_2020	SimSurvey75Q	SimSurvey25Q	SimSurvey75Q
average recruitment	millions	383.96	369.79	440.37	3.8	19.1
B100	1000's t	115.39	110.95	132.64	4.0	19.6
Bmsy	1000's t	40.39	38.83	46.42	4.0	19.6
terminal MMB	1000's t	77.76	75.43	79.15	3.1	4.9
Fmsy	per year	1.14	1.14	1.14	-0.1	-0.2
MSY	1000's t	18.90	18.20	21.70	3.9	19.2
Fofl	per year	1.11	1.11	1.01	-0.4	-9.5
OFL	1000's t	26.15	25.54	25.04	2.4	-2.0
projected MMB	1000's t	39.38	37.98	41.62	3.7	9.6
status	--	0.98	0.98	0.90	-0.3	-8.3

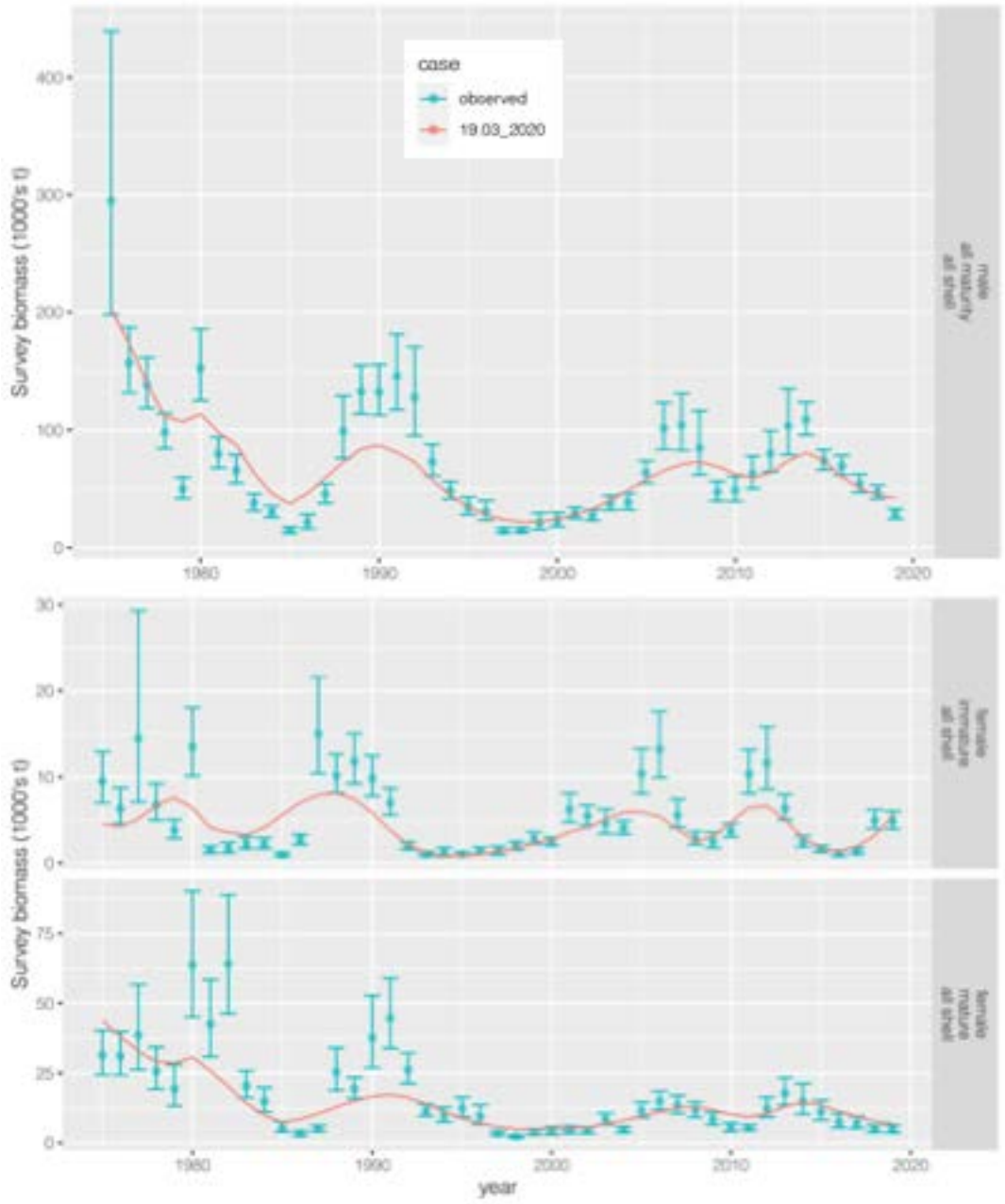

Fig. 3.2.1. Observed and predicted survey biomass time series for Model 19.03_2020 by population category. The graphs do not show the predicted 2020 survey biomass.

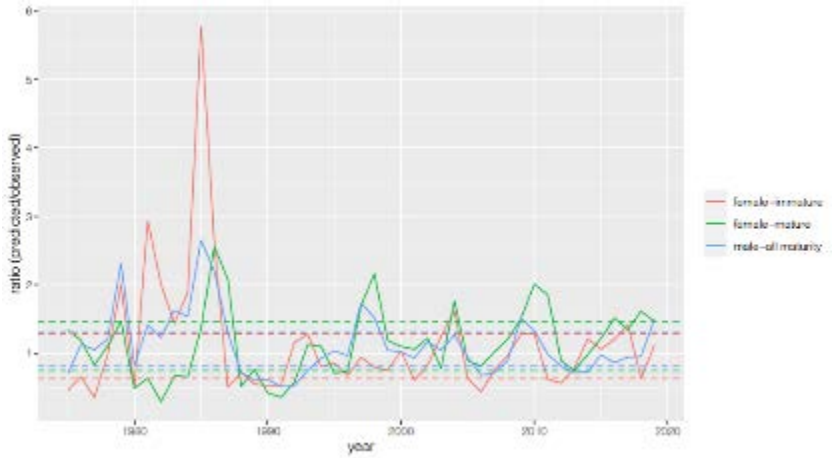

Fig. 3.2.2. Ratios (solid lines) of predicted to observed survey biomass values. Upper and lower dashed lines are 75% and 25% quantile values for the ratios. Colors indicate population category.

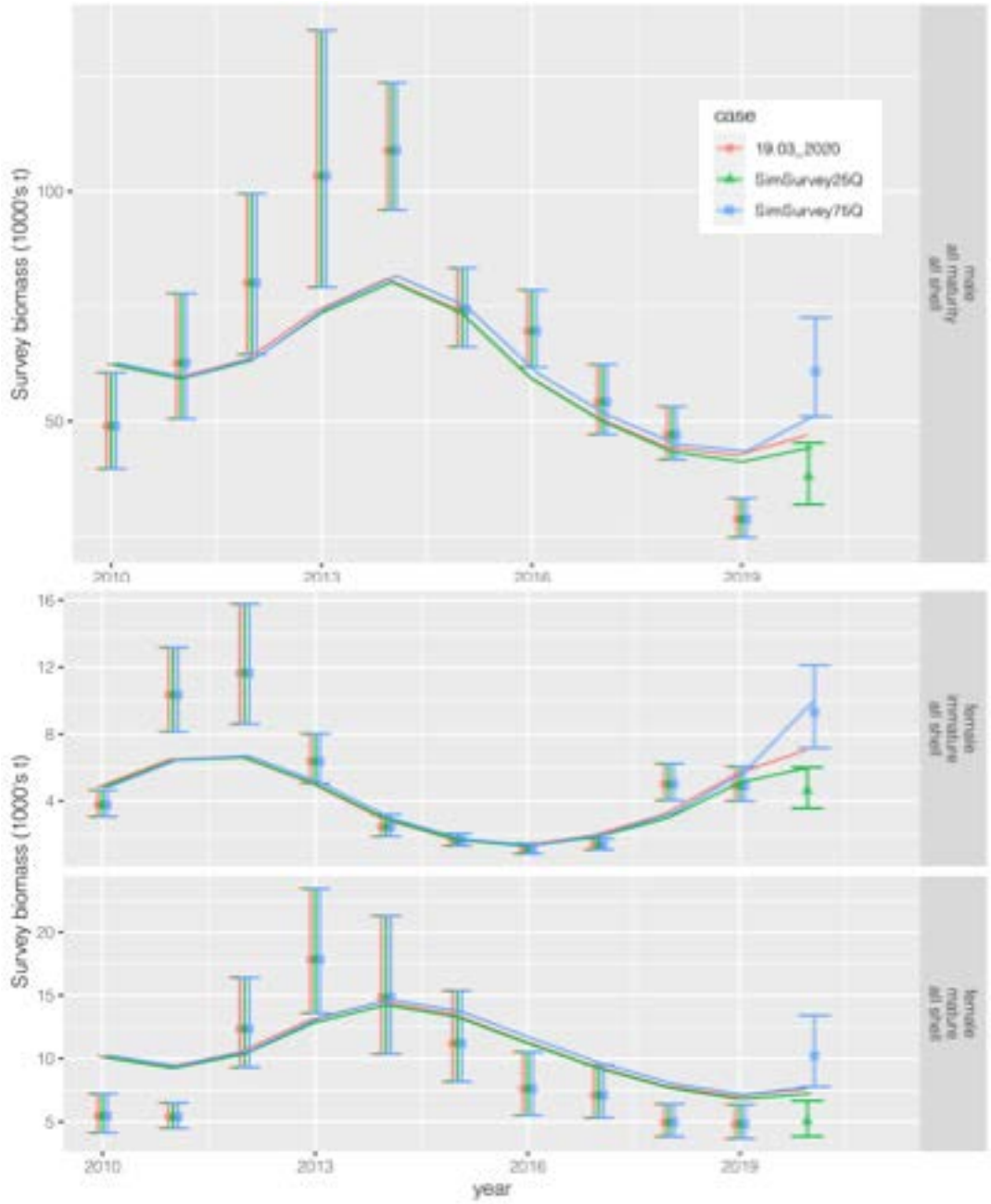

Fig. 3.2.3. Model fits (2000-2020; lines) to actual survey biomass data (1975-2019, all models; symbols) and simulated 2020 survey data (SimSurvey25Q and SimSurvey75Q models; symbols). SimSurveyQ25: simulated 2020 survey biomass data using the 25% multiplicative error quantile. SimSurveyQ75: simulated 2020 survey biomass data using the 75% multiplicative error quantile. Error bars indicate 80% confidence intervals.

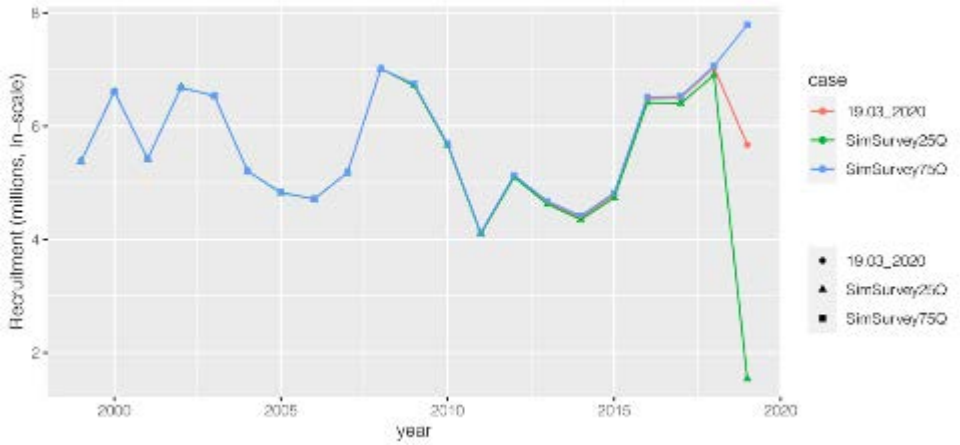

Figure 3.2.4. Comparison of estimated recruitment time series (only final 20 years shown) from the simulation sensitivity runs. The values are plotted on the natural log scale. Note that year indexing here is such that recruitment in year *y* enters the population in year *y*+1.

Fig. 3.2.5. Comparison of management-related quantities from the simulation sensitivity model runs. 19.03_2020: base model with 2020 data (no survey). SimSurveyQ25: simulated 2020 survey biomass data using the 25% multiplicative error quantile. SimSurveyQ75: simulated 2020 survey biomass data using the 75% multiplicative error quantile.

4.0 Discussion

Results from both the retrospective and simulation sensitivity analyses suggest that the principal effect on the Tanner crab assessment due to the missing 2020 NMFS EBS bottom trawl survey is the effect on estimated recruitment in the terminal year (i.e., recruits entering the population in 2020). The potential for vastly different estimates of terminal year recruitment is evident from both sets of analyses (see Figures 3.1.2, 3.1.3, and 3.2.4), and the estimated errors associated with these estimates reflect this uncertainty (Figure 3.1.2). However, errors in OFL related to the missing 2020 NMFS EBS bottom trawl survey will be relatively small, on the order of a few percent, if the period for determining average recruitment (used to scale B_{MSY}) is changed by dropping the (highly uncertain) estimate of recruitment in the terminal year. This is primarily because few recruitment-sized crab are taken as bycatch in the fisheries that capture Tanner crab and thus recruits contribute very little to the OFL. A secondary factor is that, in the current Tanner crab assessment model, terminal year recruitment has no effect on terminal year MMB (all recruits are immature) or projected MMB (very few males undergo the molt to maturity in the year following recruitment, and those that do are small and weigh much less than larger males). However, the missing survey and associated effects on the estimate of terminal year recruitment will play an increasingly important role in projecting the population forward in time beyond a single year, as the SSC has requested, as the estimated terminal year recruitment propagates into larger size classes in the population.

For this assessment, it is clear that management-related quantities need to be based on a recruitment-averaging period from which the terminal year is dropped. The BBRKC and snow crab assessments do not include the terminal year estimate of recruitment in the averaging periods used in those assessments, so this change has the added effect of bringing the Tanner crab assessment more in line with other Tier 3 assessments.

Appendix 3:
Estimating the Availability of Tanner Crab in the BSFRF Side-by-Side Studies

William T. Stockhausen
Alaska Fisheries Science Center
September 2020

Introduction

The NMFS eastern Bering Sea shelf (EBS) summer bottom trawl survey provides annual indices of the sex/size-specific abundance of Tanner crab (and other crab and groundfish stocks) on the shelf that are critical to estimating population size and productivity in the Tanner crab assessment model to provide annual advice to fishery managers on the maximum level of fishery catches that can be sustainably taken from the stock. However, these indices are relative, rather than absolute, estimates of abundance because the bottom trawl sampling gear the survey uses does not catch all Tanner crab in its path during a tow, and it catches relatively fewer small crab than large crab. Smaller crab, for example, may pass under the sampling gear or through the net mesh before entering the cod end. These indices can generally give useful information on the relative size of interannual fluctuations in different stock components, but it is necessary for them to be "scaled up" to absolute estimates of stock size in order to determine stock productivity and what a suitable catch limit should be.

In an integrated stock assessment, the assessment model typically estimates the so-called "catchability" of the survey simultaneous with estimating changes in stock abundance over time by incorporating additional information on natural mortality rates, growth, and fishery catches. As used here, "survey catchability" refers to the ratio of the numbers in a sex/size class seen in the survey, $N_{y,x,z}^{survey}$, to those in the stock, $N_{y,x,z}^{stock}$, in year *y*, where *x*, *z* denotes the sex/size class. Thus,

$$N_{y,x,z}^{survey} = C_{y,x,z}^{survey} \cdot N_{y,x,z}^{stock} \quad (1)$$

where $C_{y,x,z}^{survey}$ denotes survey catchability. In practice, survey catchability is assumed to be the same from year-to-year unless survey practices (e.g., gear, area surveyed, sampling protocols) have changed, so catchability will be denoted C_z^{survey}, where the *x* is now implied. Conceptually, then, the assessment model adjusts estimates of survey catchability, natural and fishing mortality rates, growth, and annual recruitment (the addition of new individuals to the stock) to determine the stock's population trajectory over time ($N_{y,x,z}^{stock}$) and find the best fit to the observed survey indices and fishery catches. In this framework, the mortality due to fishing is generally the only data that provides information on an absolute, rather than relative, scale. When fishing mortality is small, as it has been for Tanner crab since the mid-1990's, it can be difficult for the assessment model to unambiguously determine survey catchability and thus the absolute scale of the stock.

In order to better characterize the catchability of the NMFS survey, the Bering Sea Research Foundation (BSFRF) conducted annual paired tow experiments in coordination with the NMFS survey from 2013-2018 in which BSFRF tows were conducted "side-by-side" (SBS) with NMFS tows at standard survey stations. The BSFRF tows were conducted using a modified nephrops bottom trawl that (assumedly) captured all crab in its path. As such, the catchability for the BSFRF survey, C_z^{BSFRF}, was assumed to be 1

for all crab sex/size classes and it thus provided estimates of absolute stock size within the areas in which the SBS tows were conducted.

If the annual SBS studies had encompassed the entire stock, the resulting indices of abundance would have been absolute estimates of stock size. However, the studies were conducted within smaller areas that differed each year (Figure 1). As a consequence, the "availability" of crab to the SBS studies needs to be taken into account in order for these to provide information on absolute stock size. Here, "availability" as it pertains to a survey refers to the fraction of individuals in the surveyed population that are available to be captured in a survey (i.e., the fraction that could conceivably be caught). Availability is considered to be 1 when the survey area encompasses the entire population/stock area and no individuals occupy refuge habitats that cannot be surveyed (e.g., untrawlable rocky bottom). When a survey area does not encompass the entire population/stock area, then availability is less than 1. In addition, availability will be different for different components (e.g., males/females or small/large individuals) of a surveyed stock if the spatial distributions of the stock components are different. Availability may also change with time if the survey is conducted multiple times using different areas or if the spatial distribution of the stock changes. If availability is not considered to be 1 for a survey, it can incorporated into Eq. 1 in the form

$$N_z^{survey} = A_z^{survey} \cdot C_z^{survey} \cdot N_z^{stock} \tag{2}$$

where *A* represents sex/size-specific availability.

Using Eq. 2, relationships can be derived between the estimated annual survey abundances in the complete NMFS survey, in that part of the NMFS survey at which the SBS tows occurred, and in the BSFRF SBS survey. Availability in the NMFS EBS bottom trawl survey is considered to be 1 for all Tanner crab in the EBS stock. Because the SBS selectivity studies were conducted on smaller areas than the full survey, availability to the NMFS and BSFRF gear in these studies must be less than or equal to 1. The BSFRF gear is assumed to catch all crab within the footprint of a tow (i.e., it is non-selective and provides an estimate of absolute abundance), so the following relationships are assumed to hold:

$$N_z^{NMFS\,EBS} = 1 \cdot C_z^{NMFS} \cdot N_z^{EBS} \tag{3}$$

$$N_z^{NMFS\,SBS} = A_z^{SBS} \cdot C_z^{NMFS} \cdot N_z^{EBS} \tag{4}$$

$$N_z^{BSFRF\,SBS} = A_z^{SBS} \cdot 1 \cdot N_z^{EBS} \tag{5}$$

where A_z^{SBS} is the availability of crab in the SBS study area the assumptions $A_z^{EBS} \equiv 1$ and $C_z^{BSFRF} \equiv 1$ have been substituted into Eq.s 4 and 5.

Scenario M19F04 from last year's assessment (Stockhausen, 2019) included the 2013-2017 NMFS SBS and BSFRF SBS abundance indices in the model optimization in addition to the NMFS EBS survey indices and estimated both the NMFS survey catchability (C_z^{NMFS}) and the annual size-specific availability for the corresponding SBS study area (A_z^{SBS})—the former assuming a logistic form for survey catchability and the latter using a non-parametric, "smoothed" approach that placed fewer constraints on the shapes of the size-specific availability curves. The results were was not particularly satisfying (Stockhausen, 2019); it was felt that the redundancy expressed in Eq.s 3-5 potentially led to confounded parameter estimates that negated the information on absolute scale the SBFRF data. It was suggested that the annual availability curves did not need to be estimated inside the model, but could be determined empirically outside the model by noting that dividing Eq. 4 by Eq. 3 yields:

$$A_z^{SBS} = \frac{N_z^{NMFS\,SBS}}{N_z^{NMFS\,EBS}} \tag{6}$$

which allows one to estimate annual SBS availabilities outside the assessment model using the ratios of size compositions from the NMFS survey within the SBS to those from the full EBS.

Methods

Size compositions were calculated using the standard NMFS EBS shelf survey stratified, area-swept expansions to estimate annual survey abundance by sex and 5-mm CW size class for the entire EBS from the NMFS surveys in 2013-2017. Size compositions were then calculated using non-stratified, area-swept expansions of the data from NMSF survey stations at which SBS tows were conducted for each year. The expansions for the SBS areas were not stratified using the NMFS EBS shelf survey strata because this tended to overweight data from strata which included only one or two SBS stations.

Annual estimates of sex/size-specific availability were then calculated using Eq. 6. These estimates were then fit by generalized additive models using R (R Core Team, 2020) and the mgcv package (Wood, 2011; Wood, 2017). The sex-specific estimated availability for each year was fit using mgcv's gam function, assuming a normal error distribution with a log link function and using a cubic spline smoothing term across size. The cubic splines were penalized using the conventional cubic spline penalty and the degree of smoothing was determined automatically.

Results

The NMFS SBS and EBS size compositions, and resulting "raw" empirical availability curves, from the 2013-2017 SBS selectivity studies are shown in Figures 2 and 3 below. Availability was generally small (< 0.25) for female Tanner crab smaller than 80 mm CW and increased with size in 2013-2015 when the study areas were in the inner and middle shelf domains near Bristol Bay. When the study area shifted west to the Pribilof Islands in 2017, availability increased for small females but decreased for large females. Availabilities for male Tanner crab showed similar patterns for small crab (< 100 mm), but availability tended to decrease with size for the largest males (> 150 mm CW), except in 2016. Clearly, though, the patterns are different between the sexes and on an annual basis.

The smooth fits determined by the GAM analysis are shown in the upper plots in Figures 4 and 5 for females and males, respectively. Residuals from the fits are plotted against fitted values and in histograms in the lower plots of Figures 4 and 5.

The values for the smooth fits at the mid-points of each model size bin were used in Scenario 20.07 to define the availability curves necessary to include the BSFRF SBS data in the model fitting procedure without having to include the NMFS SBS data, as well.

Acknowledgments

The author would like to thank Scott Goodman and Madi Shipley at Natural Resources Consulting, Inc. for providing the BSFRF SBS data used in the assessment.

Literature Cited

R Core Team (2020). R: A language and environment for statistical computing. R Foundation for Statistical Computing, Vienna, Austria. URL https://www.R-project.org/.

Stockhausen, W. 2019. 2019 Stock Assessment and Fishery Evaluation Report for the Tanner Crab Fisheries of the Bering Sea and Aleutian Islands Regions. In: Stock Assessment and Fishery Evaluation Report for the King and Tanner Crab Fisheries of the Bering Sea and Aleutian Islands: 2019 Final Crab SAFE. North Pacific Fishery Management Council. Anchorage, AK.

Wood, S.N. 2011. Fast stable restricted maximum likelihood and marginal likelihood estimation of semiparametric generalized linear models. Journal of the Royal Statistical Society (B). 73(1):3-36.

Wood, S.N. 2017. Generalized Additive Models: An Introduction with R (2nd edition). Chapman and Hall/CRC.

Figures

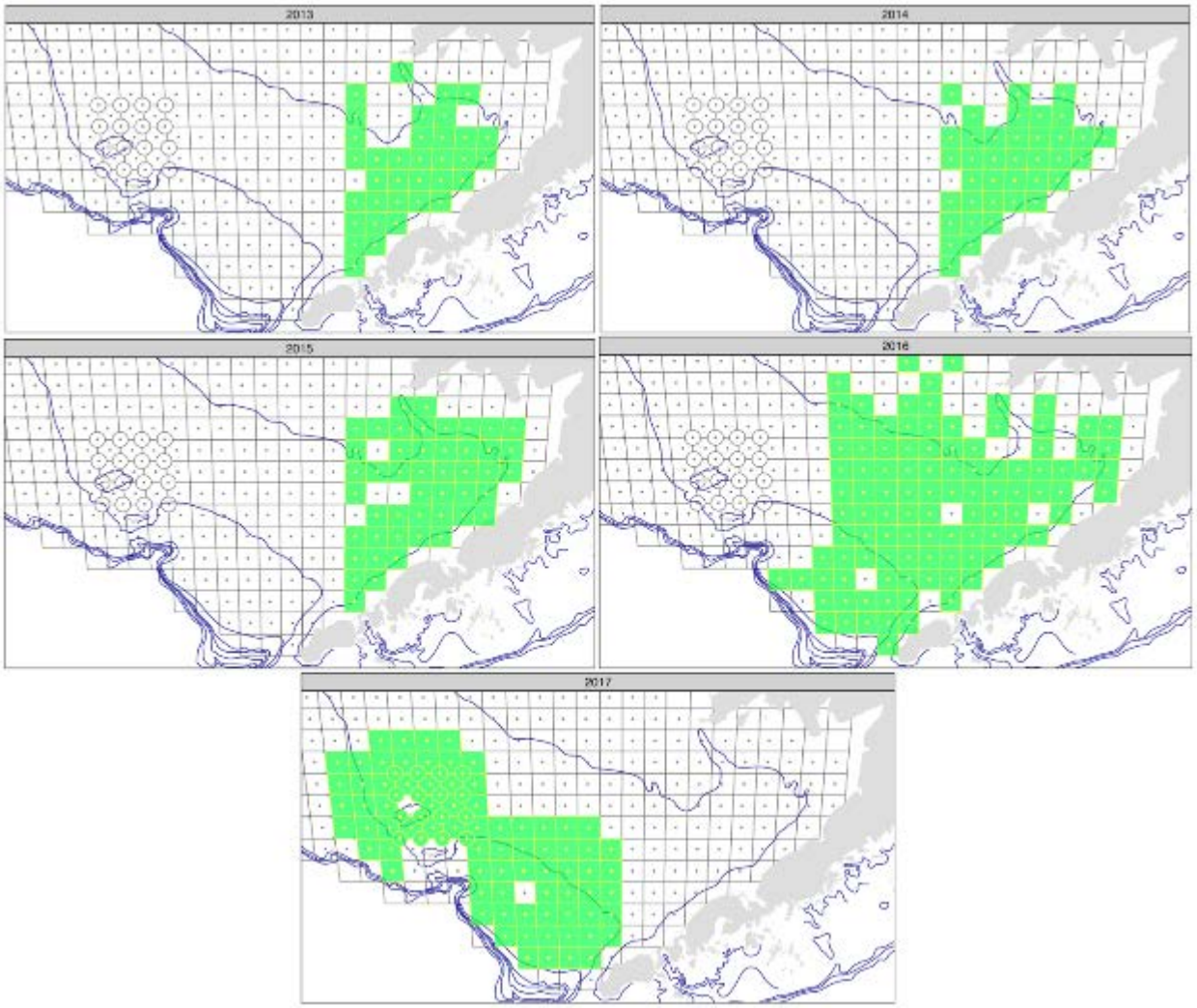

Figure 1. Spatial footprints (stations occupied in green) during the BSFRF-NMFS cooperative side-by-side (SBS) catchability studies in 2013-2017. Squares and circles represent stations in the standard NMFS EBS bottom trawl survey (which extends beyond the area shown in the maps).

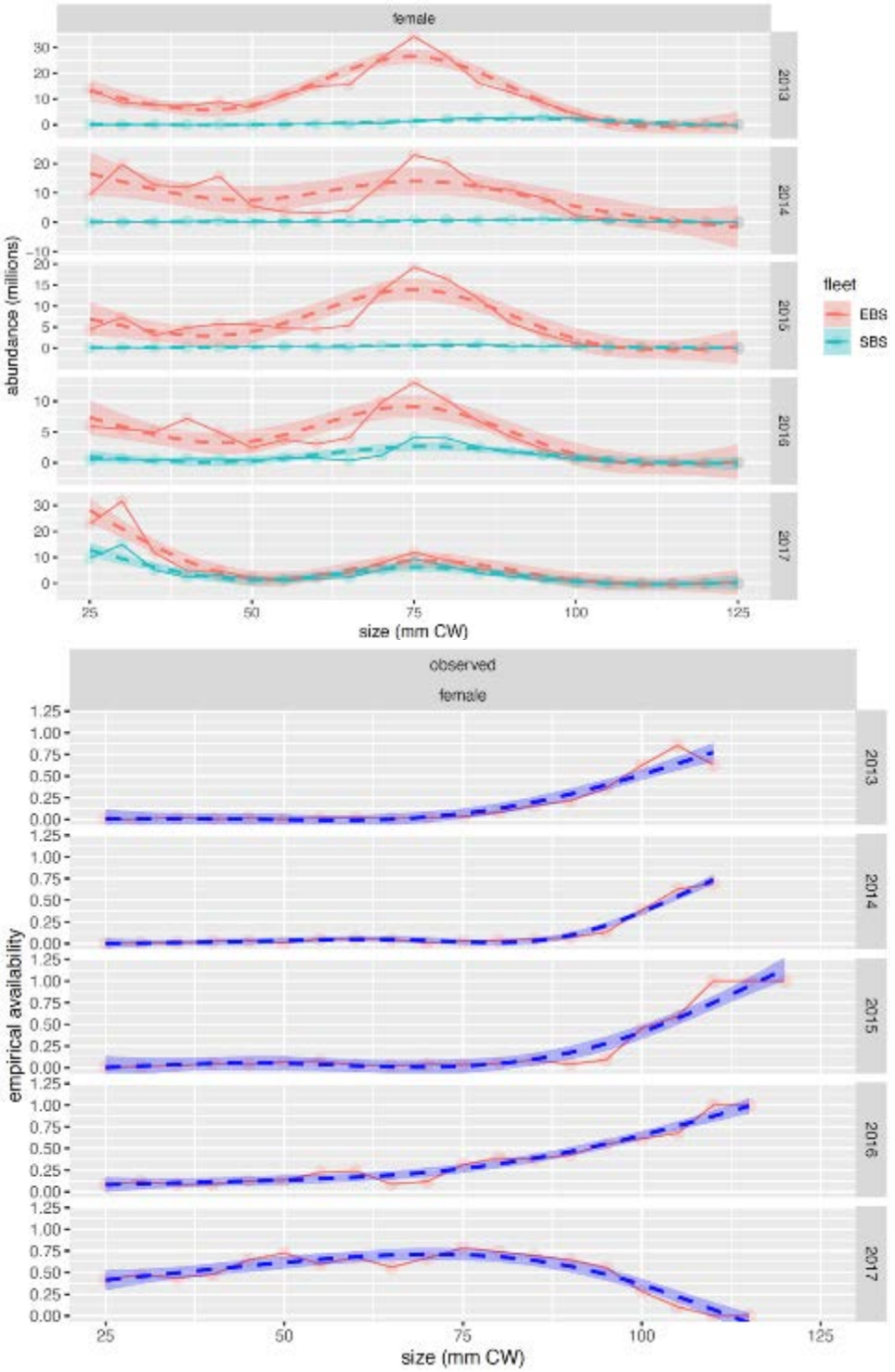

Figure 2. Upper plot: NMFS bottom trawl survey size compositions for female Tanner crab from the EBS (orange) and SBS (green) survey areas for 2013-2017. Solid lines and dots are "raw" estimates, dashed lines are smoothed fits using cubic splines. Lower plot: empirical availability curves calculated using Equation 6. Red lines and dots: "raw" curves, dashed lines and fills: smoothed fits.

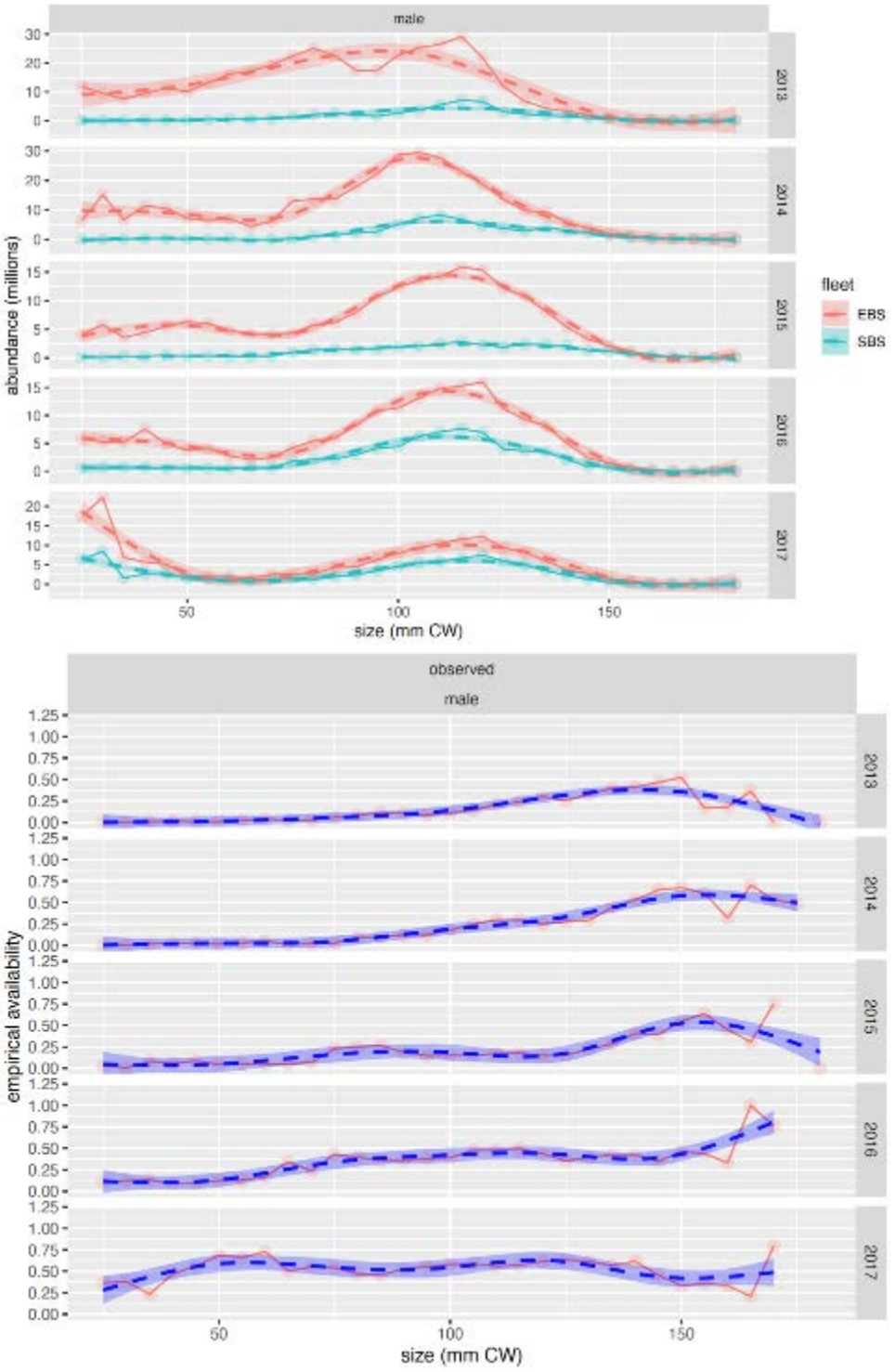

Figure 3. Upper plot: NMFS bottom trawl survey size compositions for male Tanner crab from the EBS (orange) and SBS (green) survey areas for 2013-2017. Solid lines and dots are "raw" estimates, dashed lines are smoothed fits using cubic splines. Lower plot: empirical availability curves calculated using Equation 6. Red lines and dots: "raw" curves, dashed lines and fills: smoothed fits.

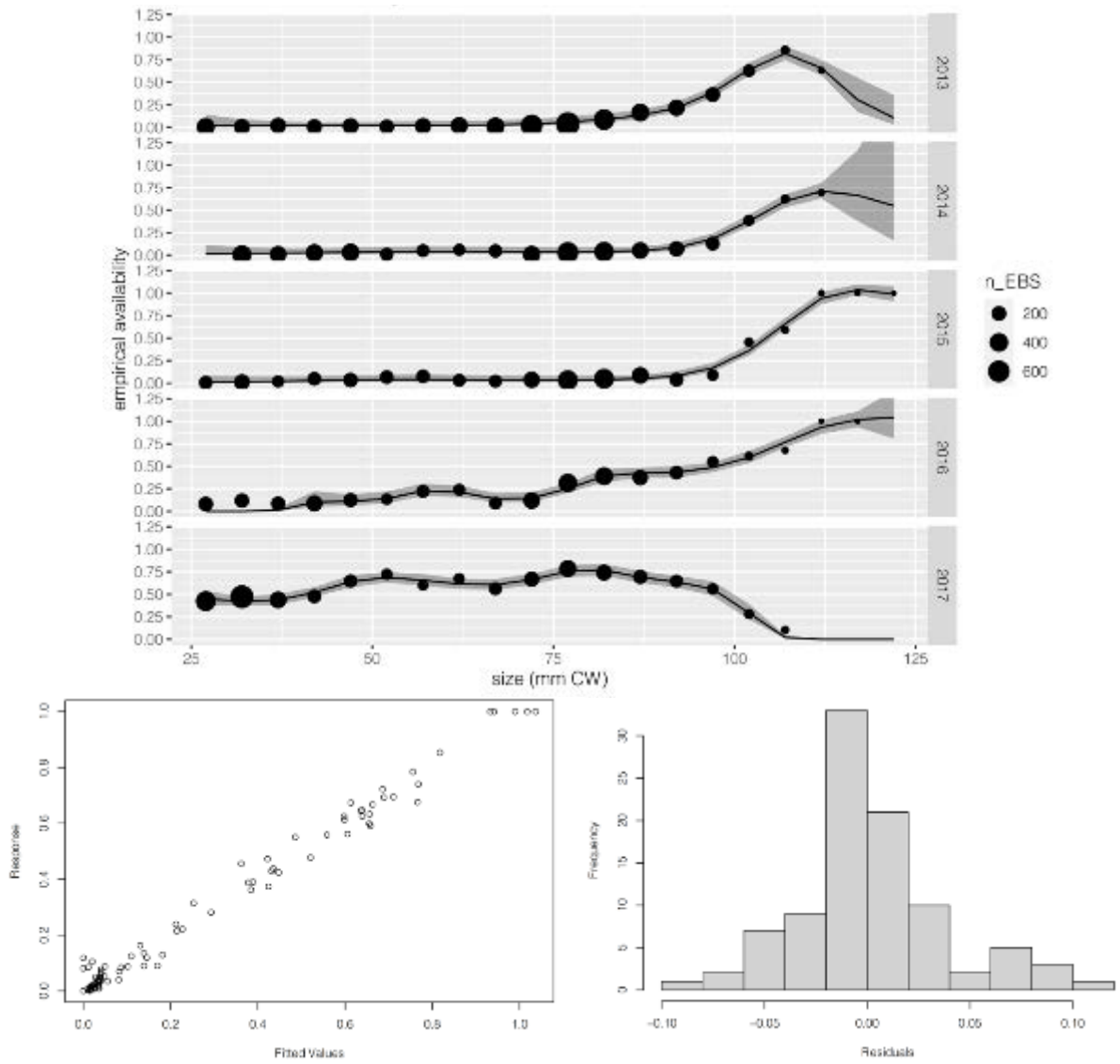

Figure 4. Upper: Empirical availability for females in the SBS study areas, by year. Upper: empirical values (points; size relative number of individuals sampled in the full survey) and the "best"-fitting GAM, by year, using cubic splines (lines; shading indicates 95% confidence intervals). Lower: diagnostic checks with response variables plotted against fitted values (left) and a histogram of residuals (right).

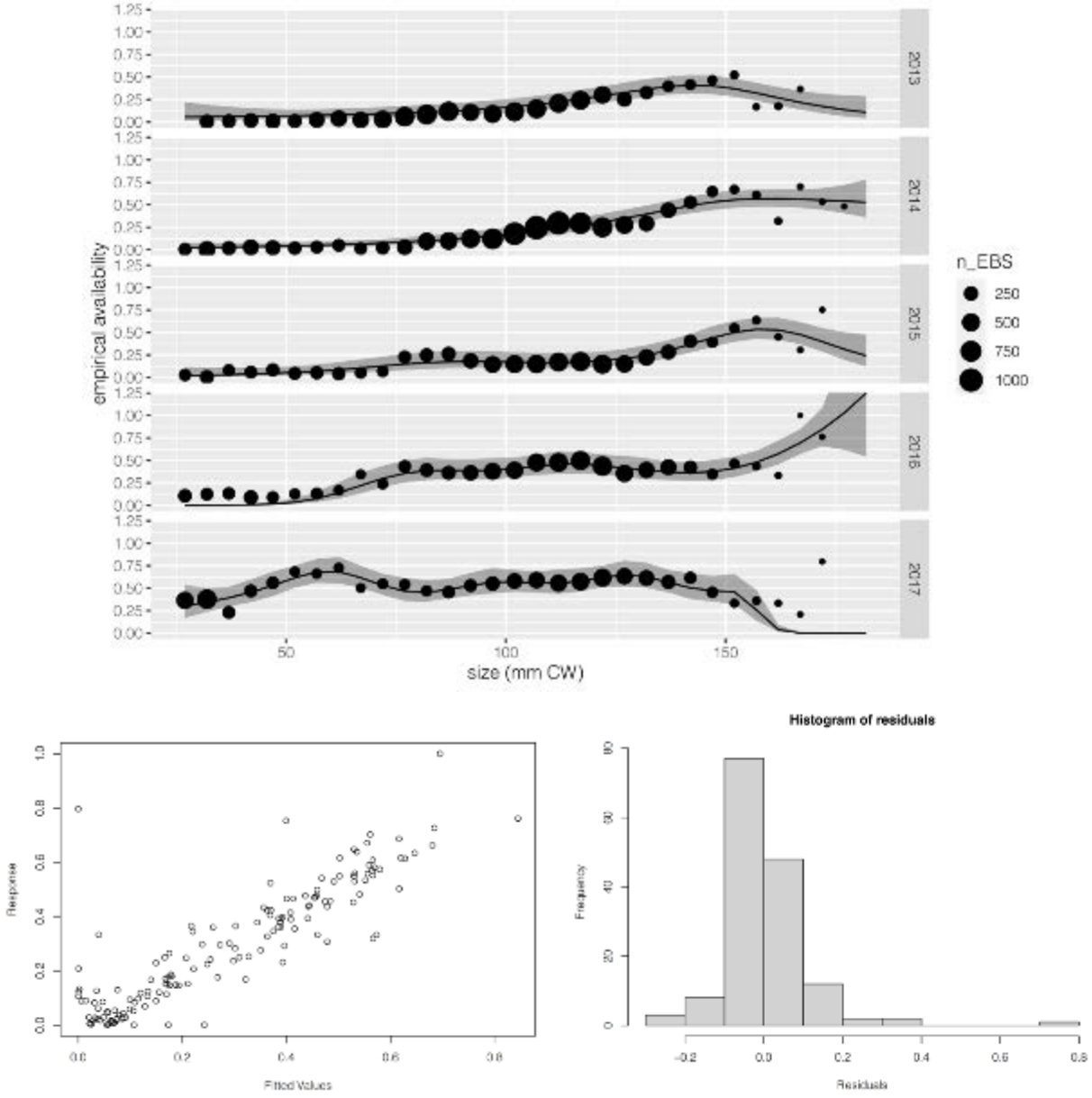

Figure 5. Upper: Empirical availability for males in the SBS study areas, by year. Upper: empirical values (points; size relative number of individuals sampled in the full survey) and the "best"-fitting GAM, by year, using cubic splines (lines; shading indicates 95% confidence intervals). Lower: diagnostic checks with response variables plotted against fitted values (left) and a histogram of residuals (right).

Appendix 4:
Estimated Survey Catchability for Tanner Crab in the Eastern Bering Sea Survey using Side-by-Side Gear Comparisons

William T. Stockhausen
Alaska Fisheries Science Center
September 2020

Introduction

The NMFS eastern Bering Sea shelf (EBS) summer bottom trawl survey provides annual indices of the sex/size-specific abundance of Tanner crab (and other crab and groundfish stocks) on the shelf that are critical to estimating population size and productivity in the Tanner crab assessment model to provide annual advice to fishery managers on the maximum level of fishery catches that can be sustainably taken from the stock. However, these indices are relative, rather than absolute, estimates of abundance because the bottom trawl sampling gear the survey uses does not catch all Tanner crab in its path during a tow, and it catches relatively fewer small crab than large crab. Smaller crab, for example, may pass under the sampling gear or through the net mesh before entering the cod end. These indices can generally give useful information on the relative size of interannual fluctuations in different stock components, but it is necessary for them to be "scaled up" to absolute estimates of stock size in order to determine stock productivity and what a suitable catch limit should be.

In an integrated stock assessment, the assessment model typically estimates the so-called "catchability" of the survey simultaneous with estimating changes in stock abundance over time by incorporating additional information on natural mortality rates, growth, and fishery catches. As used here, "survey catchability" refers to the ratio of the numbers in a sex/size class seen in the survey, $N_{y,x,z}^{survey}$, to those in the stock, $N_{y,x,z}^{stock}$, in year *y*, where *x*, *z* denotes the sex/size class. Thus,

$$N_{y,x,z}^{survey} = C_{y,x,z}^{survey} \cdot N_{y,x,z}^{stock} \quad (1)$$

where $C_{y,x,z}^{survey}$ denotes survey catchability. In practice, survey catchability is assumed to be the same from year-to-year unless survey practices (e.g., gear, area surveyed, sampling protocols) have changed, so catchability will be denoted C_z^{survey}, where the *x* is now implied. Conceptually, then, the assessment model adjusts estimates of survey catchability, natural and fishing mortality rates, growth, and annual recruitment (the addition of new individuals to the stock) to determine the stock's population trajectory over time ($N_{y,x,z}^{stock}$) and find the best fit to the observed survey indices and fishery catches. In this framework, the mortality due to fishing is generally the only data that provides information on an absolute, rather than relative, scale. When fishing mortality is small, as it has been for Tanner crab since the mid-1990's, it can be difficult for the assessment model to unambiguously determine survey catchability and thus the absolute scale of the stock.

In order to better characterize the catchability of the NMFS survey, the Bering Sea Research Foundation (BSFRF) conducted annual paired tow experiments in coordination with the NMFS survey from 2013-2018 in which BSFRF tows were conducted "side-by-side" (SBS) with NMFS tows at standard survey

stations. The data from these SBS paired tows are used here to estimate sex- and size- specific catchability curves for the NMFS survey outside the assessment model. These curves are then used in Scenario 20.10 in this assessment in lieu of estimating the curves within the assessment.

Methods

Data

The BSFRF SBS study data for 2013-2017 was provided by Scott Goodman and Madi Shipley at NRC, Inc. Corresponding NMFS hauls were identified using common dates and station id's. Individual crab observations were binned by sex using 5-mm CW bins on a haul-by-haul basis, then expanded to the appropriate SBS area using standard area-swept expansions that also took sampling fractions into account.

Direct estimation of survey catchability

As used herein, "survey catchability" refers to the fraction of individuals in a population that are available to be captured in a survey or by a fishing fleet (i.e., the fraction that could conceivably be caught). In the case of surveys, availability is considered to be 1 when the survey area encompasses the entire population/stock area and no individuals occupy refuge habitats that cannot be surveyed (e.g., untrawlable rocky bottom). When a survey area does not encompass the entire population/stock area, then availability will be less than 1, and may be different depending on what component (e.g., sex, size class) of the stock is considered. In the assessment model, size-specific survey abundance is related to size-specific stock abundance by

$$N_z^{survey} = C_z^{survey} \cdot A_z^{survey} \cdot N_z^{stock} \tag{2}$$

where *z* represents size (i.e., carapace width), *N* represents size-specific abundance, *A* represents size-specific availability, and *C* represents size-specific survey catchability. It is worth pointing out that N_z^{survey} represents the survey catch abundance expanded, using area-swept methods, to the area corresponding to the availability.

Availability in the NMFS EBS bottom trawl survey is considered to be 1 for all Tanner crab in the EBS stock, because the survey area is considered to encompass the stock's distribution. Because the SBS selectivity studies were conducted on smaller areas than the full survey, availability to the NMFS and BSFRF gear in these studies may be less than 1, and may depend on size and sex. The BSFRF gear is assumed to catch all crab within the footprint of a tow (i.e., it is non-selective and provides an estimate of absolute abundance), so the following relationships are assumed in the assessment model to hold:

$$N_z^{NMFS\ EBS} = 1 \cdot C_z^{NMFS} \cdot N_z^{EBS} \tag{3}$$

$$N_z^{NMFS\ SBS} = A_z^{SBS} \cdot C_z^{NMFS} \cdot N_z^{EBS} \tag{4}$$

$$N_z^{BSFRF\ SBS} = A_z^{SBS} \cdot 1 \cdot N_z^{EBS} \tag{5}$$

where the assumptions $A_z^{EBS} \equiv 1$ and $C_z^{BSFRF} \equiv 1$ in the equations above.

Using Equations 2-4, it is also possible to estimate NMFS survey catchability (C_z^{NMFS}) directly from the SBS study data. Dividing Equation 3 by Equation 4 yields:

$$C_z^{NMFS} = \frac{N_z^{NMFS\ SBS}}{N_z^{BSFRF\ SBS}} \tag{6}$$

which provides an empirical estimate of NMFS survey catchability outside the assessment model.

Catch-comparison analysis

Equation 5 can also be applied to the individual SBS paired hauls singly or *en masse*, as in Kotwicki et al. (2017). When considered to represent a single set of paired-tow hauls, Equation 5 can be rewritten in terms of the numbers of crab sampled in a paired haul:

$$C_z^{NMFS} = \frac{N_z^{NMFS\ SBS}}{N_z^{BSFRF\ SBS}} = \frac{n_z^{NMFS\ SBS}.\left(\frac{A^{SBS}}{\alpha^{NMFS}.\Sigma^{NMFS}}\right)}{n_z^{BSFRF\ SBS}.\left(\frac{A^{SBS}}{\alpha^{BSFRF}.\Sigma^{BSFRF}}\right)} \tag{7}$$

where the n's are the actual numbers sampled by each gear, the α's are the areas swept by each gear, the Σ's are the sampling fractions for each haul type, and A^{SBS} represents the study area the catch is expanded to. Equation 6 can be rearranged (after some tedious algebra) so that the fraction of all crab caught in size class z that were caught by the NMFS gear, $\phi = \frac{n_z^{NMFS\ SBS}}{n_z^{NMFS\ SBS}+n_z^{BSFRF\ SBS}}$, can be expressed as:

$$\phi_z = \frac{n_z^{NMFS\ SBS}}{n_z^{NMFS\ SBS}+n_z^{BSFRF\ SBS}} = \frac{C_z^{NMFS}}{C_z^{NMFS}+R_\alpha \cdot R_\Sigma} \tag{8}$$

where $R_\alpha = \frac{\alpha^{BSFRF}}{\alpha^{NMFS}}$ is the ratio of areas swept by the two gears and $R_\Sigma = \frac{\Sigma^{BSFRF}}{\Sigma^{NMFS}}$ is the ratio of sampling fractions. The number of crab caught in size bin *z* by the NMFS gear, conditional on the total number of crab caught by both gears in *z* can be modeled as a binomially-distributed random variable with probability of success ϕ_z (Somerton et al., 2013). On the logit scale, Equation 7 becomes

$$logit(\phi_z) = \ln\left(\frac{\phi_z}{1-\phi_z}\right) = \ln(C_z^{NMFS}) - ln(R_\alpha \cdot R_\Sigma) \tag{9}$$

Fryer et al (2003) and Somerton et al. (2013) modeled $logit(\phi_z)$ as smooth functions of size and other haul-specific environmental characteristics (e.g., depth and sediment size). Here, I followed Brooks (2020) instead and modeled $\ln(C_z^{NMFS})$ directly as a smooth function of size. Thus, I fit different models of the form

$$logit(\phi_z) = \ln(C_z^{NMFS}) - ln(R_\alpha \cdot R_\Sigma) = s(z) - ln(R_\alpha \cdot R_\Sigma) \tag{10}$$

to the SBS data using the R package "selfisher" (R Core Team, 2020; Brooks, 2020), where $ln(R_\alpha \cdot R_\Sigma)$ was treated as a haul-specific offset and several candidate models for the smooth function *s*(*z*), including a logistic function and cubic splines with different degrees of freedom, were evaluated. Given time constraints, I was not able to test whether or not incorporating environmental characteristics such as haul depth or sediment size would be appropriate. This is an area for future research.

Data from SBS hauls taken during 2016 and 2017, in which the SBS studies were specifically focused on Tanner crab, were included in the model fits. Analyses were performed separately for males and females to develop sex-specific catchability curves. Because the assessment model assumes a single catchability curve applies (by sex) to the entire 1982-2019 time period, no year effects were included in the model fits. The model that "best" fit the data was identified from among the set of candidate models using BIC (Bayes Information Criterion).

Results

Direct estimates of survey catchability

The NMFS and BSFRF size compositions and resulting "raw" empirical catchability curves from the 2013-2017 SBS selectivity studies are shown in Figures 1 and 2. These empirical catchability curves exhibit a fair bit of interannual variability in size-specific catchability for both males and females. They

also suggest that the shapes of the selectivity curves are not really logistic (in contrast to assumptions made in the current assessment model).

Catch-comparison analysis

The models for $\ln(C_z^{NMFS})$ that best fit the SBS haul data for 2016 and 2017 were cubic splines with 5 and 8 degrees of freedom for females and males, respectively (Tables 1 and 2; Figure3). The model comparisons found that logistic curves fit the data much worse for both sexes than did the best spline curve.

Acknowledgments

The author would like to thank Scott Goodman and Madi Shipley at Natural Resources Consulting, Inc. for providing the BSFRF SBS data used in the assessment.

References

Fryer, R.J., A.F. Zuur and N. Graham. 2003. Using mixed models to combine smooth size-selection and catch-comparison curves over hauls. Can. J. Fish. Aquat. Sci. 60(4): 448-459. http://dx.doi.ord/10.1139/f03-029.

Mollie Brooks (2020). selfisher: Selectivity of Fisheries Gear, Modeled using Template Model Builder. R package version 0.3.0.200601. https://github.com/mebrooks/selfisher.

Rugolo L.J. and B.J. Turnock. 2012b. 2012 Stock Assessment and Fishery Evaluation Report for the Tanner Crab Fisheries of the Bering Sea and Aleutian Islands Regions. In: Stock Assessment and Fishery Evaluation Report for the King and Tanner Crab Fisheries of the Bering Sea and Aleutian Islands: 2012 Crab SAFE. North Pacific Fishery Management Council. Anchorage, AK. pp. 267-416.

Kotwicki, S., R.R. Lauth, K. Williams, and S.E. Goodman. 2017. Selectivity ratio: A useful tool for comparing size selectivity of multiple survey gears. Fish. Res. 191: 76-86. http://dx.doi.org/10.1016/fishres.2017.02.012.

Somerton, D.A., R.A. McConnaughey and S.S. Intelmann. 2017. Evaluating the use of acoustic bottom typing to inform models of bottom trawl efficiency. Fish. Res. 185:14-16. http://dx.doi.org/10.1016/j.fishres.2016.09.29.

Somerton, D. A. and R. S. Otto. 1999. Net efficiency of a survey trawl for snow crab, *Chionoecetes opilio*, and Tanner crab, *C. bairdi*. Fish. Bull. 97:617-625.

Somerton, D.A., K.L. Weinberg, and Scott E. Goodman. Catchability of snow crab (*Chionoecetes opilio*) by the eastern Bering Sea bottom trawl survey estimated using a catch comparison experiment. 2013. Can. J. Fish. Aquat. Sci. 70: 1699-1708. http://dx.doi.org/10.1139/cjfas-2013-0100

Stockhausen, W. 2019. 2019 Stock Assessment and Fishery Evaluation Report for the Tanner Crab Fisheries of the Bering Sea and Aleutian Islands Regions. In: Stock Assessment and Fishery Evaluation Report for the King and Tanner Crab Fisheries of the Bering Sea and Aleutian Islands: 2019 Final Crab SAFE. North Pacific Fishery Management Council. Anchorage, AK.

Tables

Table 1. Model fitting results for females. Best fitting model is in first row.

smooth type	degrees of freedom	delta BIC
cubic spline	5	0
	6	1.7
	7	4.6
	8	12
	10	18.9
	9	21.6
	4	36.8
	3	207.8
logistic	2	779.2

Table 2. Model fitting results for males. Best fitting model is in first row.

smooth type	degrees of freedom	delta BIC
cubic spline	8	0
	7	1.2
	9	7.2
	6	7.7
	10	15
	5	47.7
	4	166.6
	3	300.5
logistic	2	654

Figures

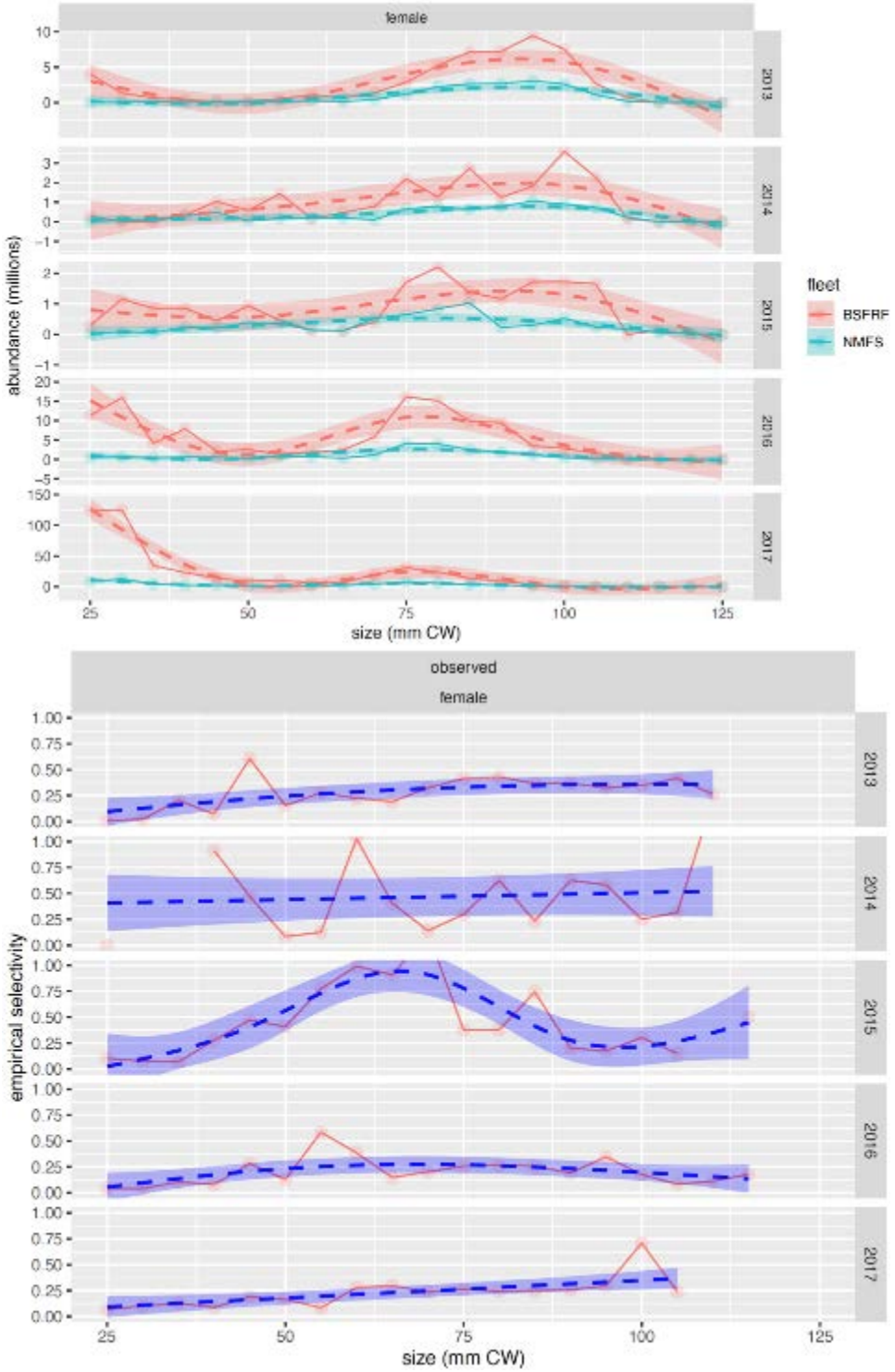

Figure 1. Upper: BSFRF (orange) and NMFS (green) size compositions for female Tanner crab from the SBS study areas for 2013-2017. Solid lines and dots are "raw" estimates, dashed lines are smoothed fits using cubic splines. Lower: empirical catchability curves calculated using Equation 5. Red lines and dots: "raw" curves, dashed lines and fills: smoothed fits.

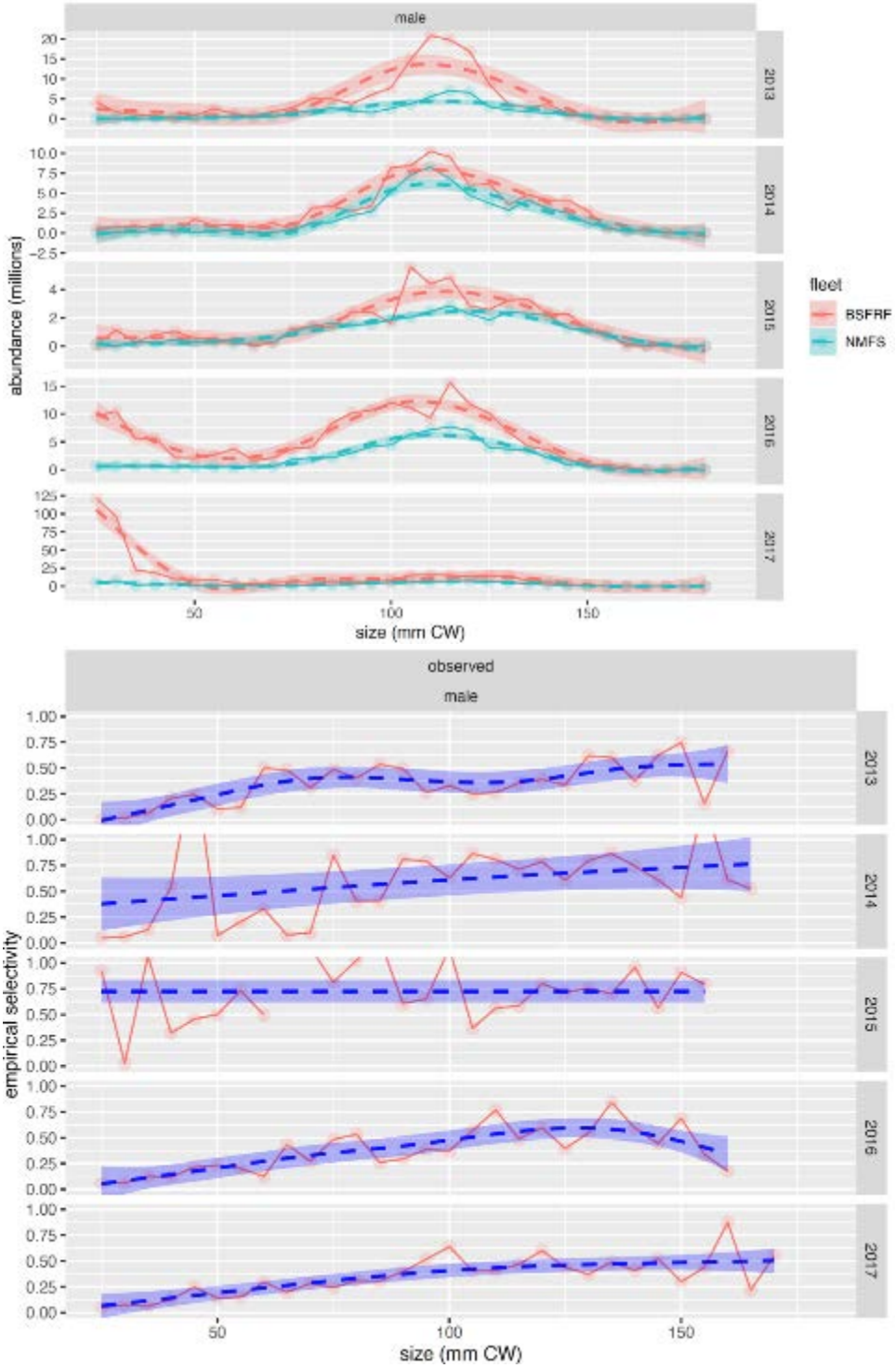

Figure 2. Upper: BSFRF (orange) and NMFS (green) size compositions for male Tanner crab from the SBS study areas for 2013-2017. Solid lines and dots are "raw" estimates, dashed lines are smoothed fits using cubic splines. Lower: empirical catchability curves calculated using Equation 5. Red lines and dots: "raw" curves, dashed lines and fills: smoothed fits.

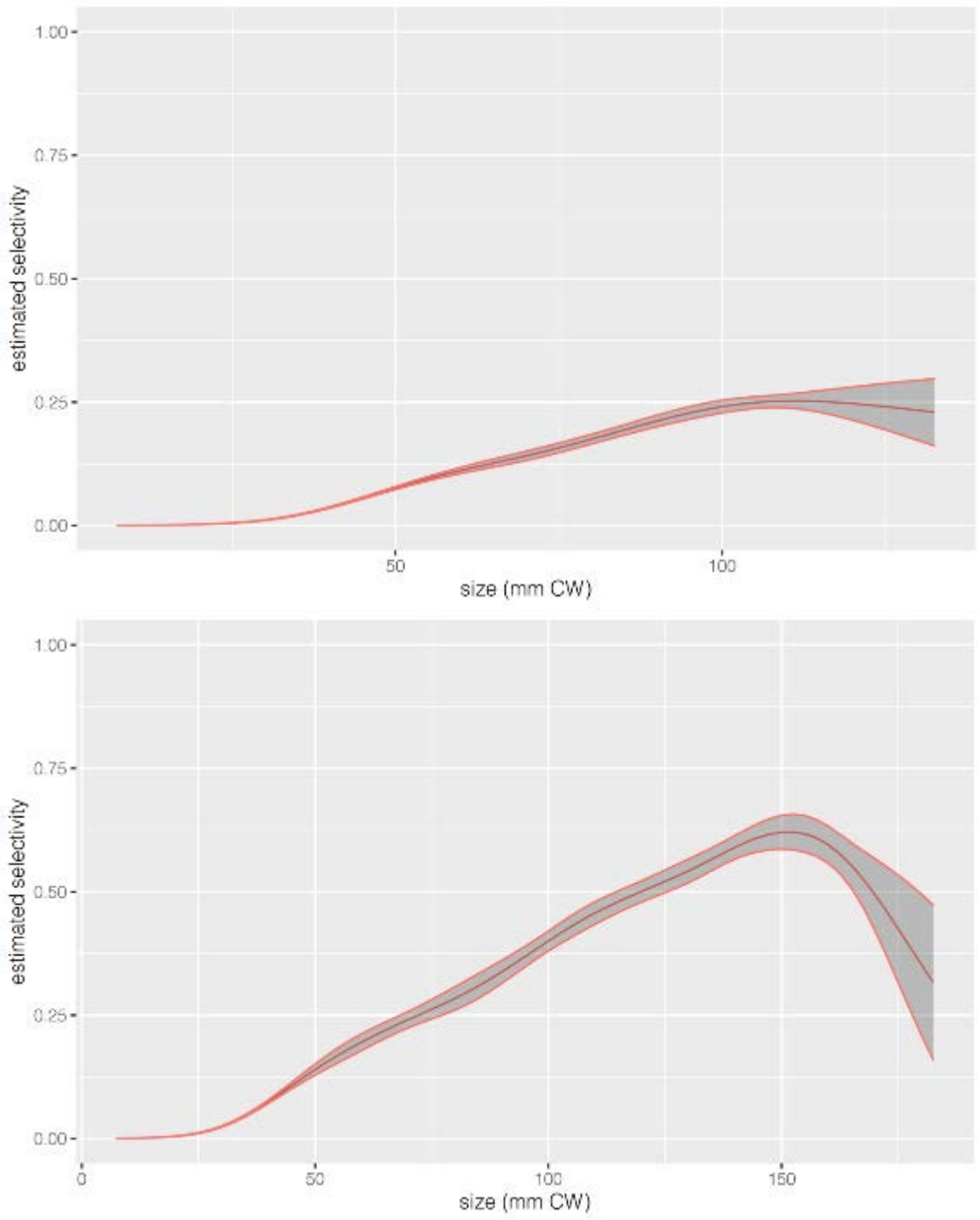

Figure 3. Estimated empirical catchability curves based on the best fitting models to the 2016-2017 SBS data using catch-comparison analysis assuming catchability is a smooth function of crab. The center line in each plot represents the mean, the fills represent 80% confidence intervals. Note the difference in x-axis scales.

Appendix 5: Fits to Aggregated Fishery Catch Data – 19.03(2020) vs 19.03 vs 20.07 vs 20.10

William Stockhausen

01 September, 2020

Contents

Model fits to aggregated fisheries catch data

Fits to the aggregated fisheries catch data available to the model(s) are presented in this section. Not all of the fits presented are necessarily included in the parameter optimization for each model; some fits to datasets for a particular model may be included for comparison purposes with other models which include those data in their optimization. The reader should consult the main assessment document to determine which fits are included in the optimization for any particular model.

Fishery retained catch biomass

Fits

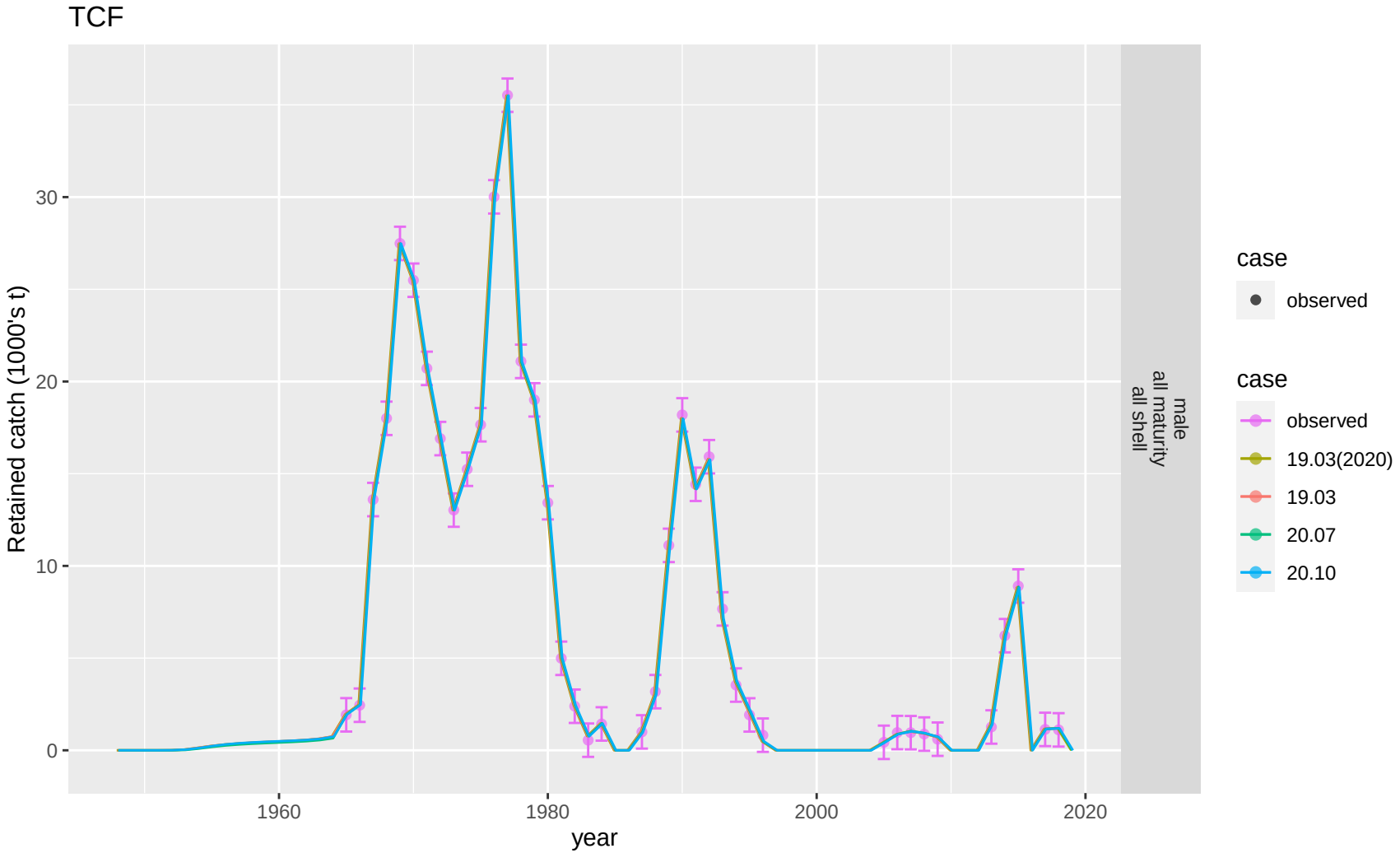

Figure 1: Comparison of observed and predicted male retained catch biomass for TCF.

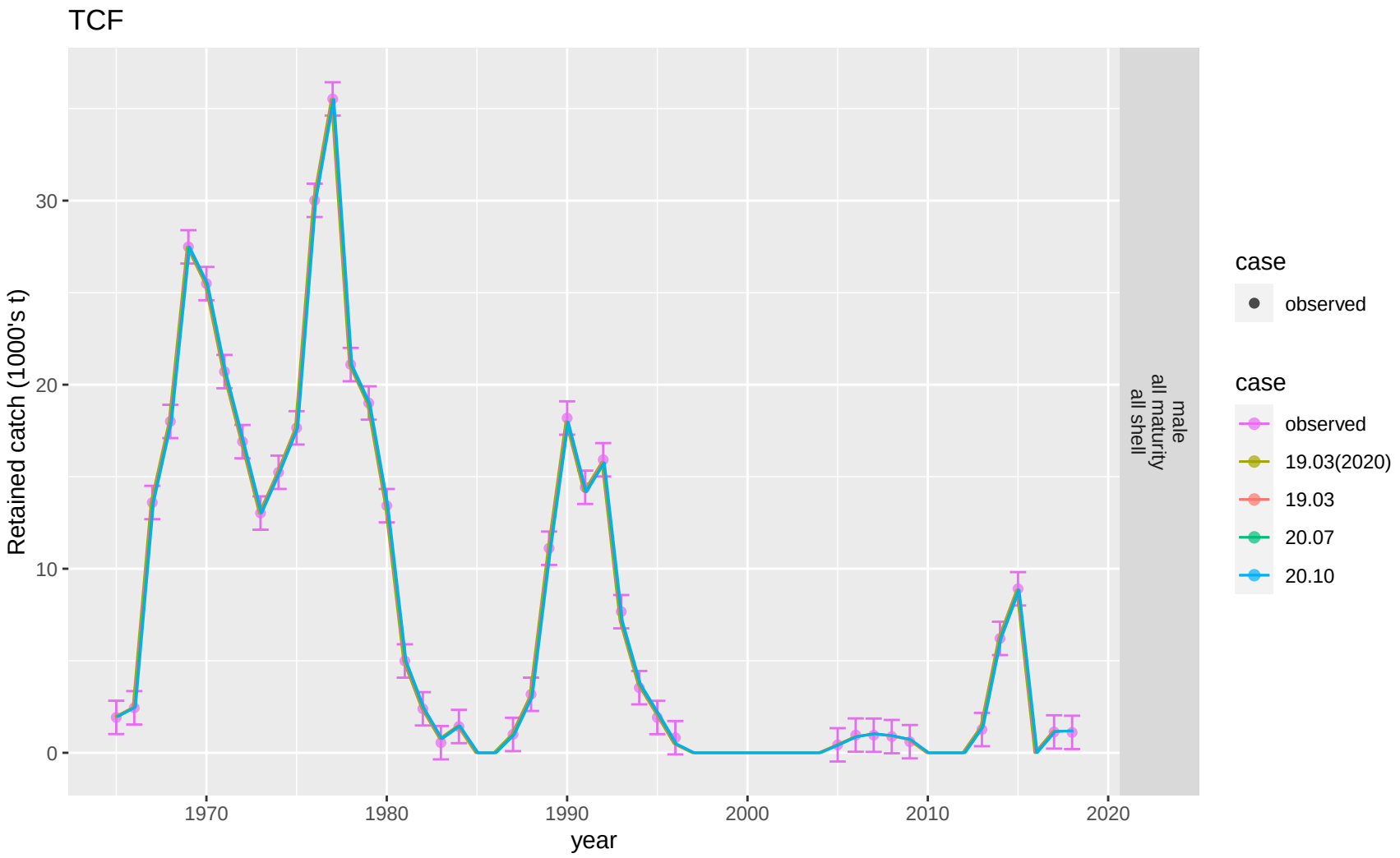

Figure 2: Comparison of observed and predicted male retained catch biomass for TCF. Observed time period.

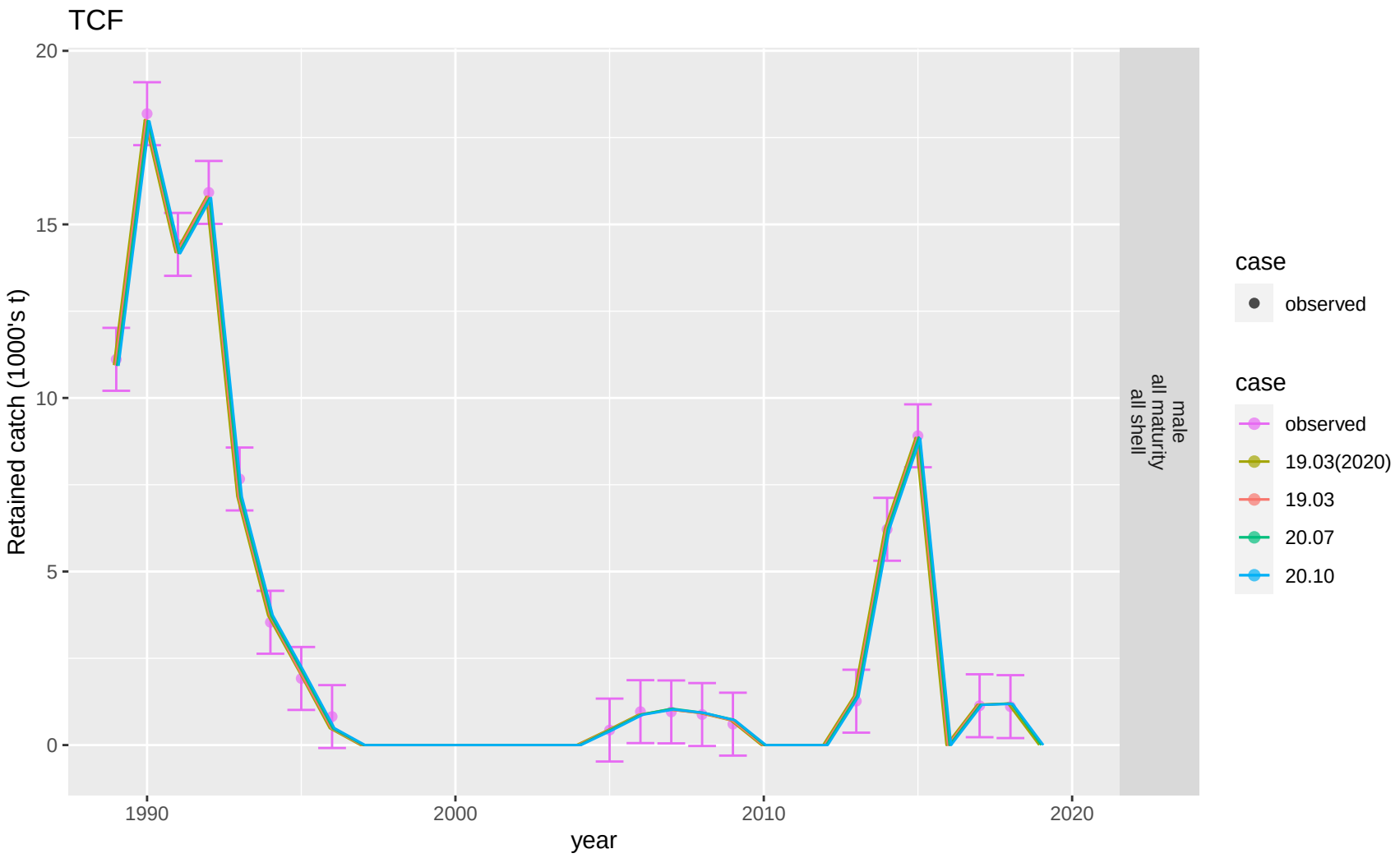

Figure 3: Comparison of observed and predicted male retained catch biomass for TCF. Recent time period.

Z-scores

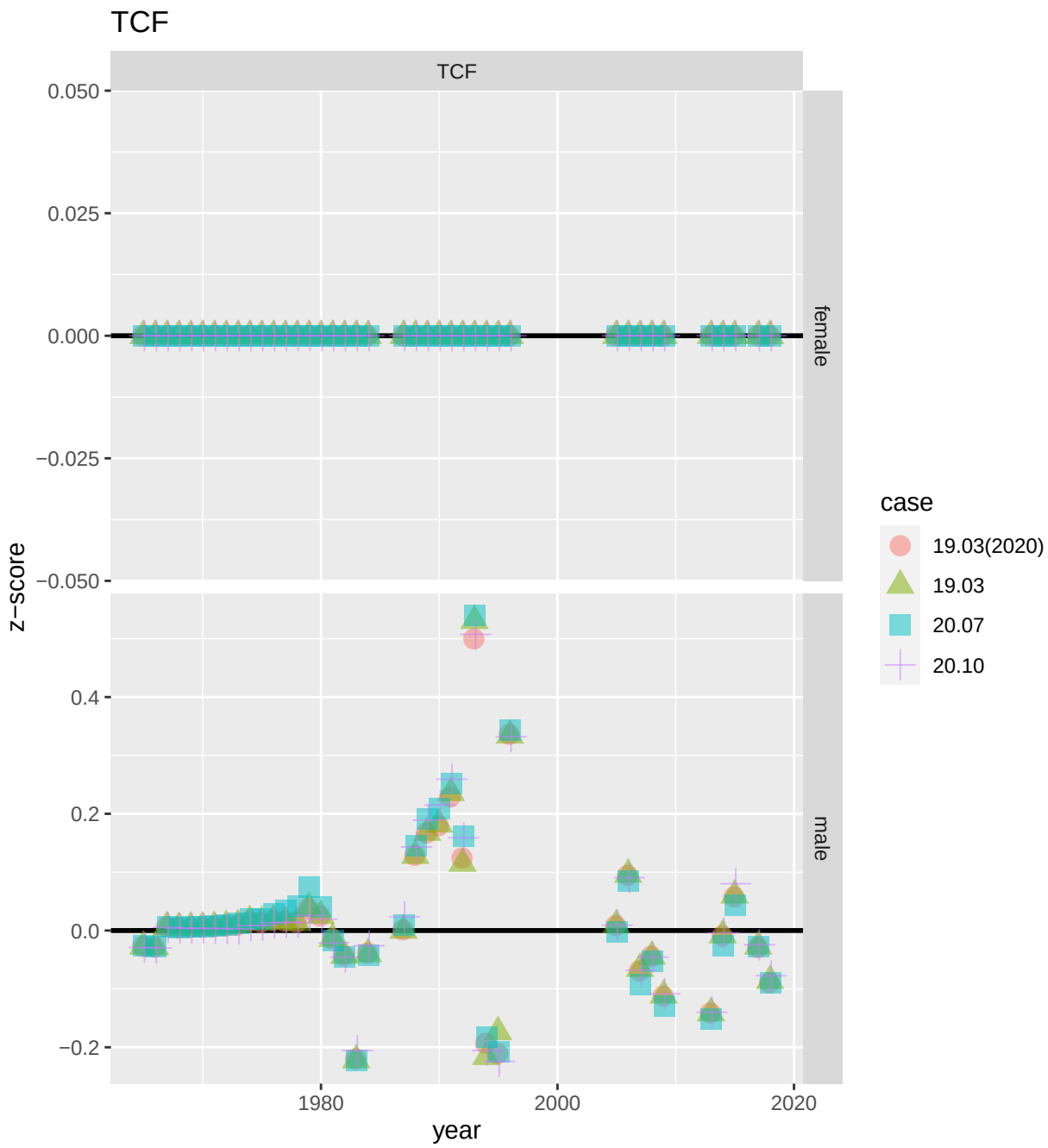

Figure 4: Z-scores for retained catch biomass in TCF.

Fishery retained catch abundance

Fits

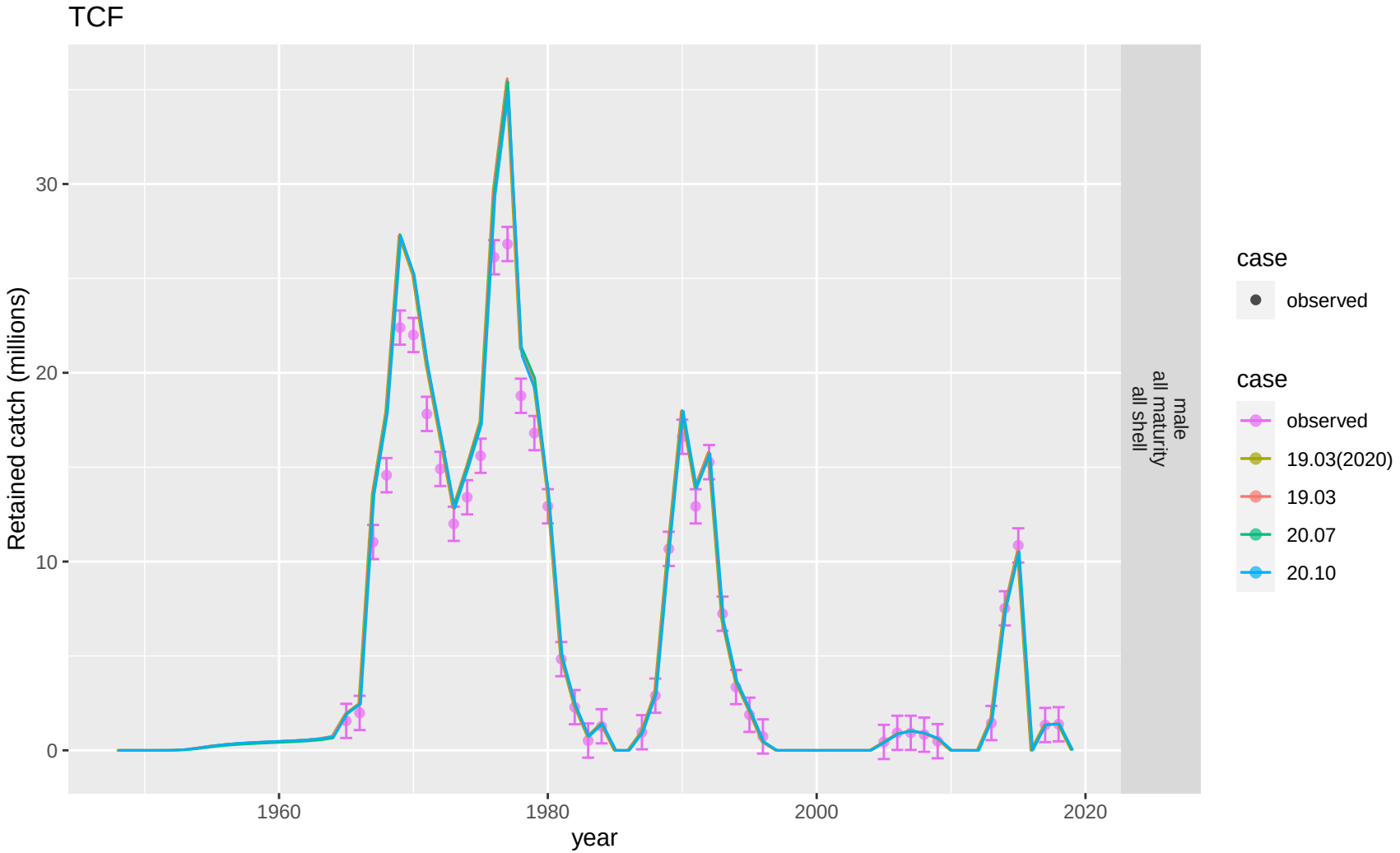

Figure 5: Comparison of observed and predicted male retained catch abundance for TCF.

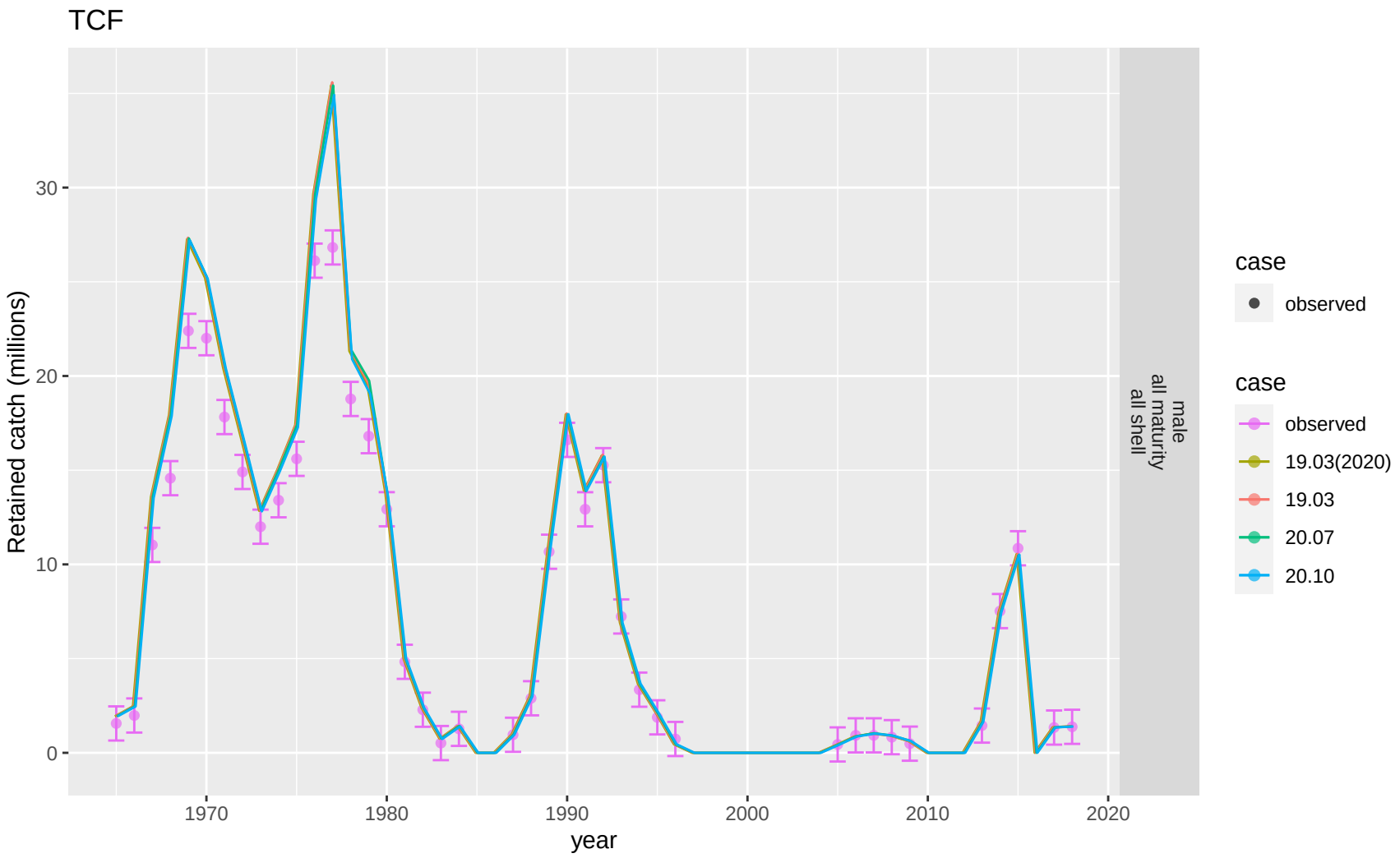

Figure 6: Comparison of observed and predicted male retained catch abundance for TCF. Recent time period.

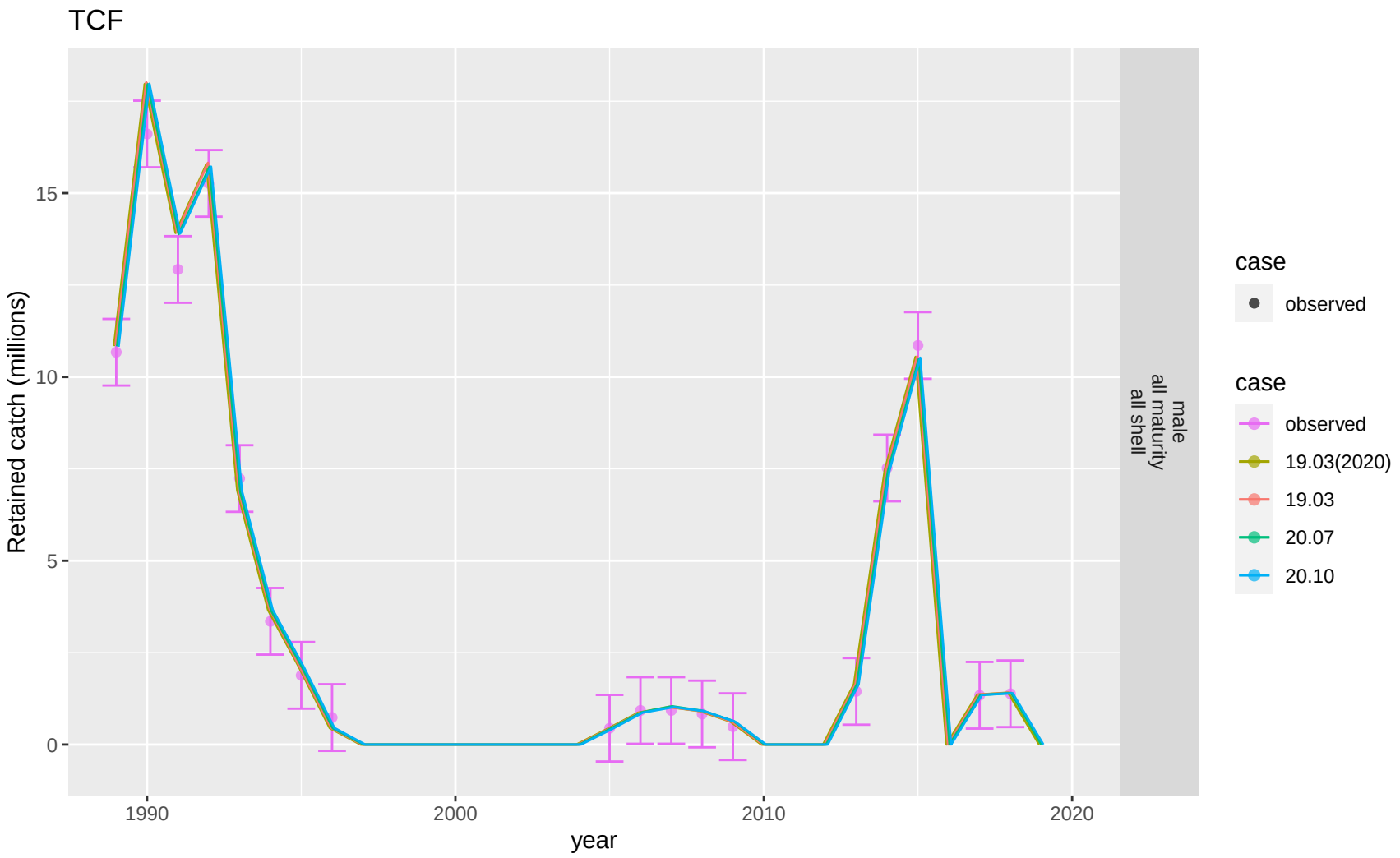

Figure 7: Comparison of observed and predicted male retained catch abundance for TCF. Observed time period.

Z-scores

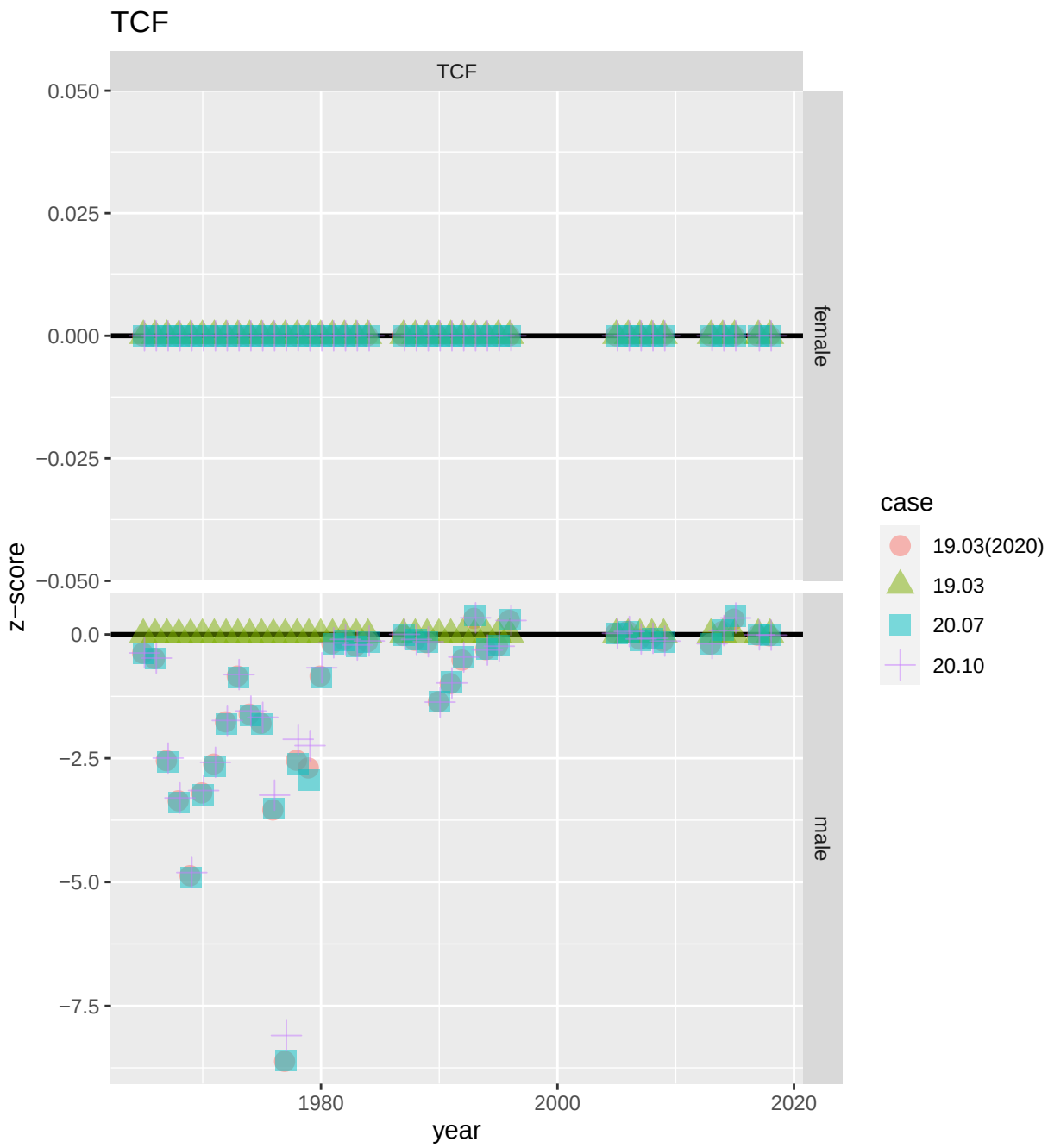

Figure 8: Z-scores for retained catch abundance in TCF.

Fishery total catch biomass

Fits

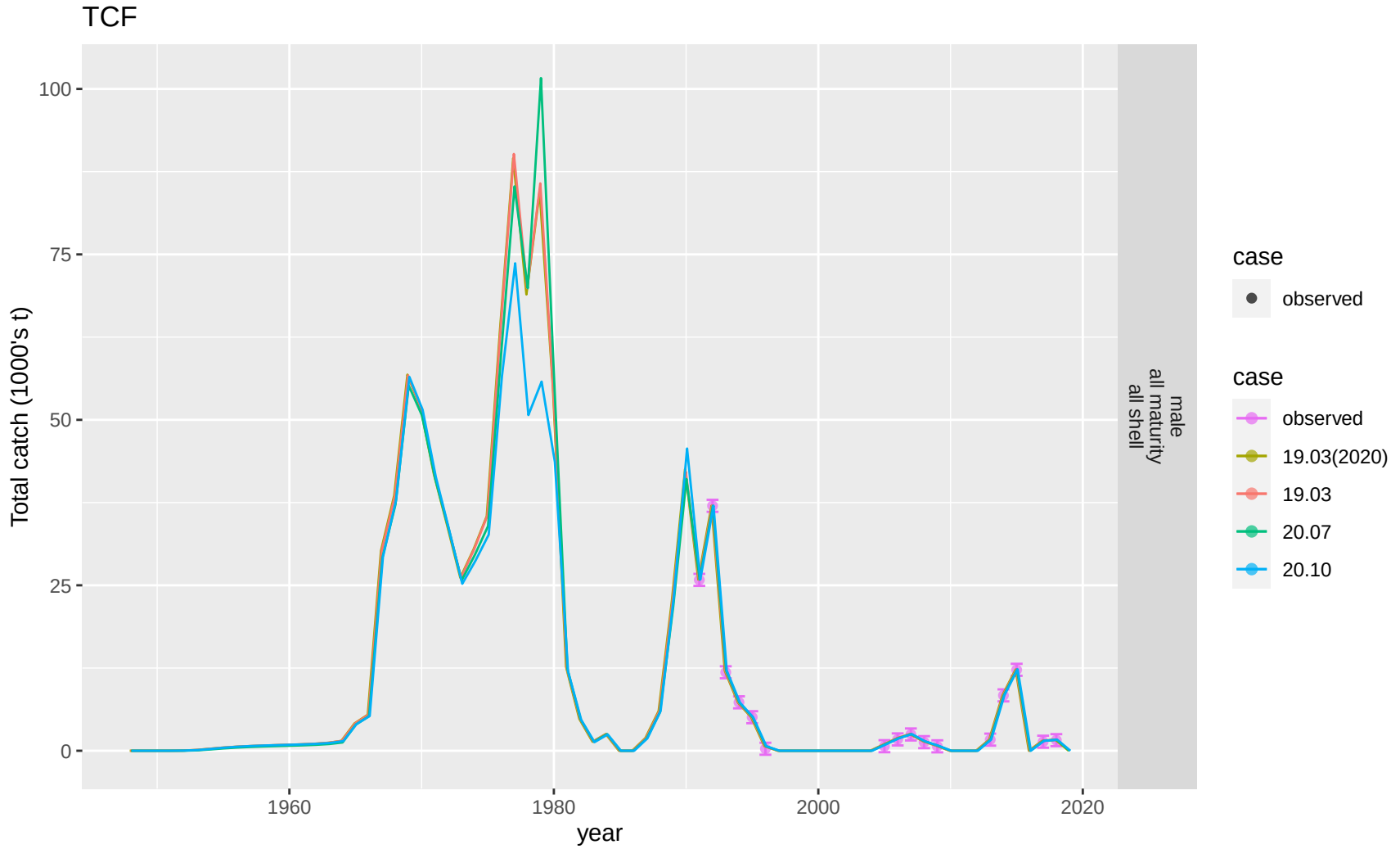

Figure 9: Comparison of observed and predicted total male catch biomass for TCF.

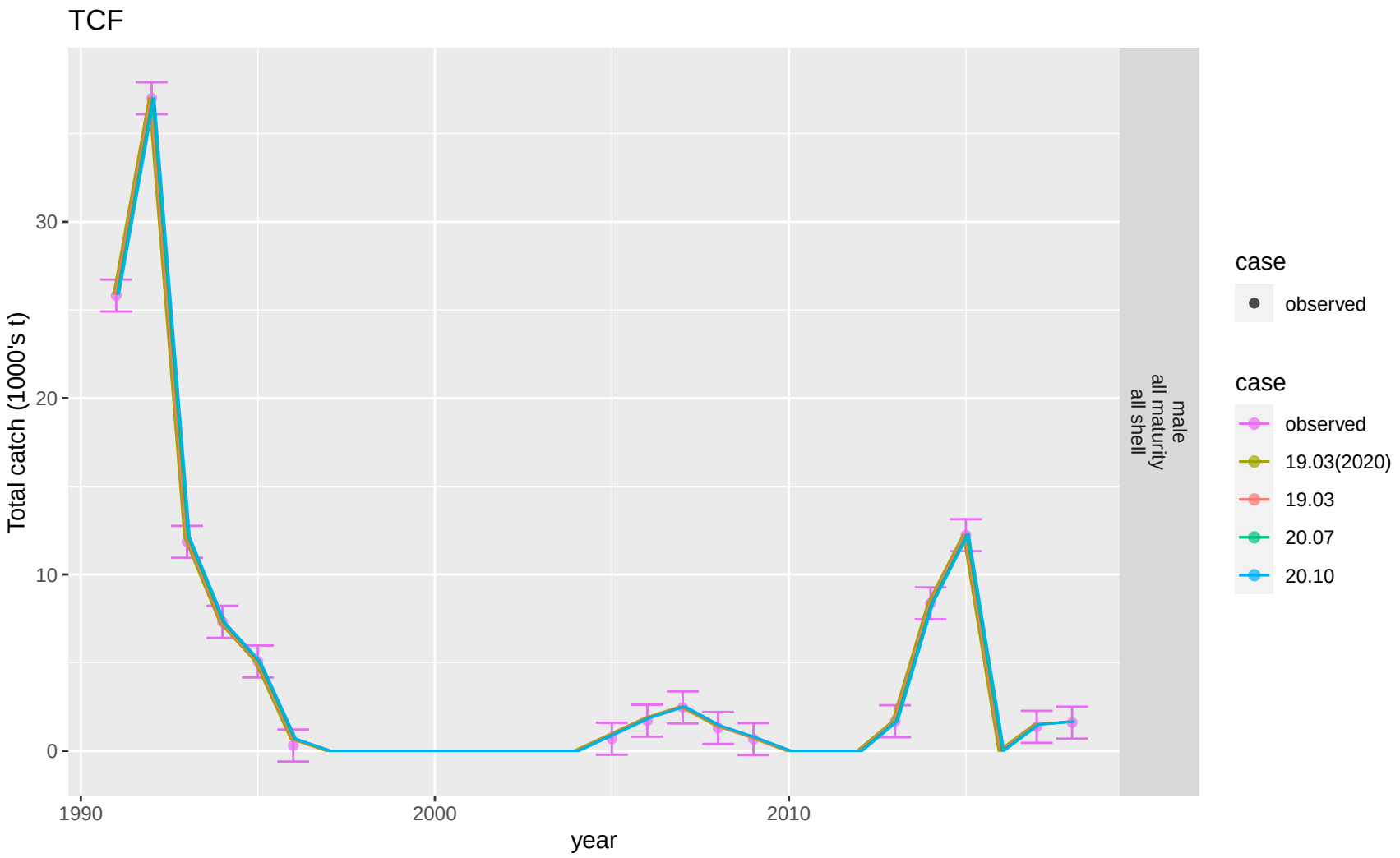

Figure 10: Comparison of observed and predicted total male catch biomass for TCF. Observed time period.

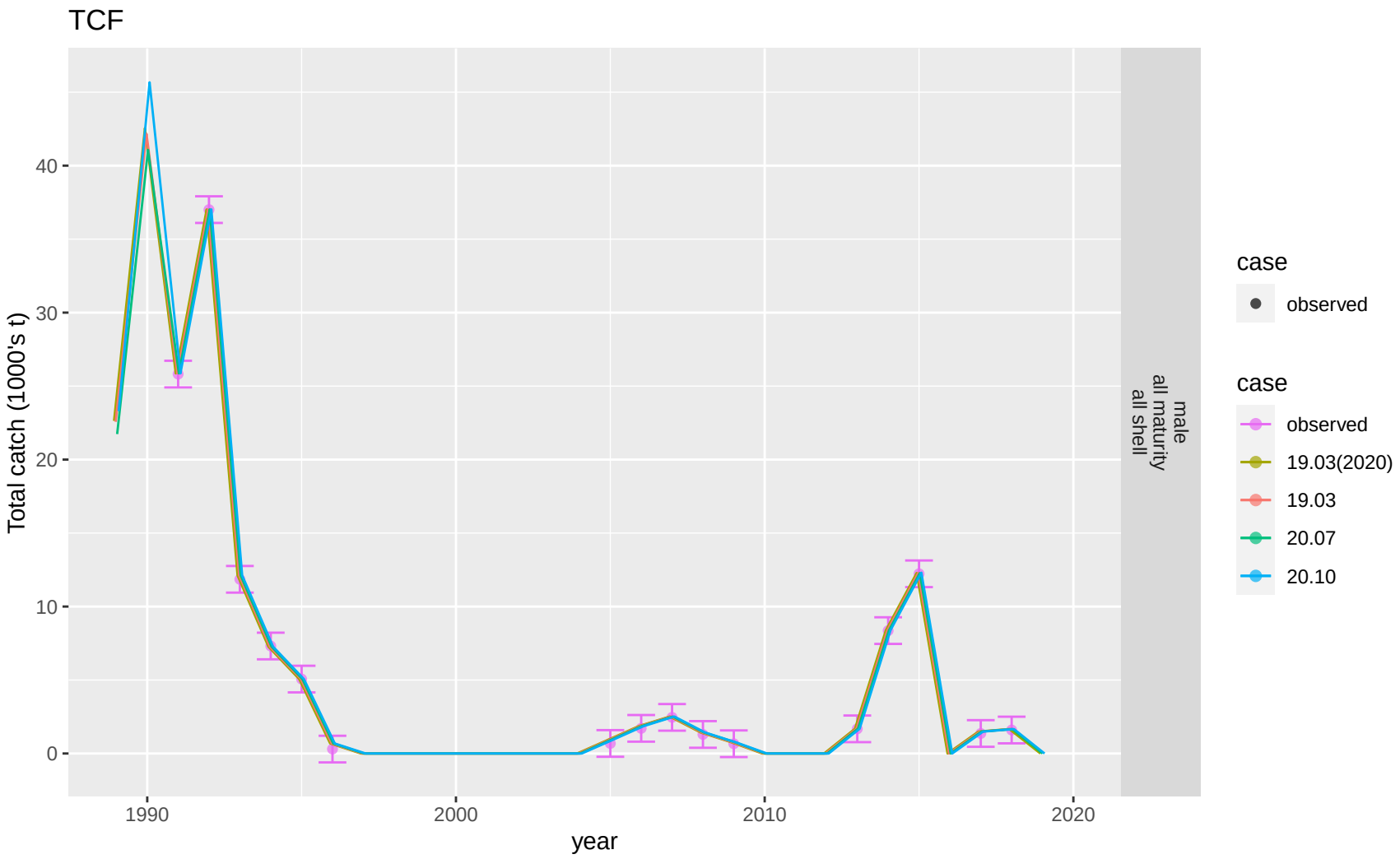

Figure 11: Comparison of observed and predicted total male catch biomass for TCF. Recent time period.

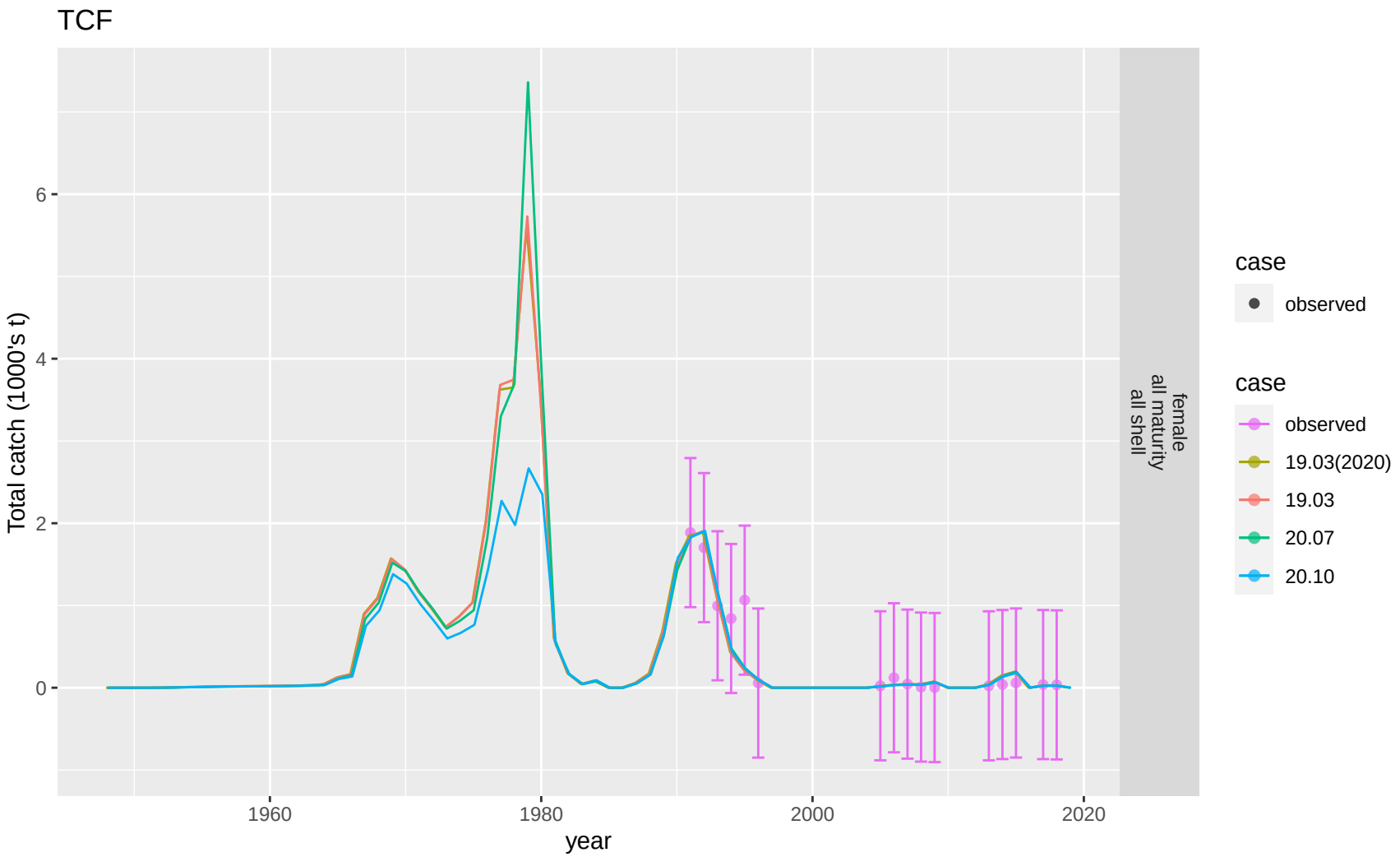

Figure 12: Comparison of observed and predicted total female catch biomass for TCF.

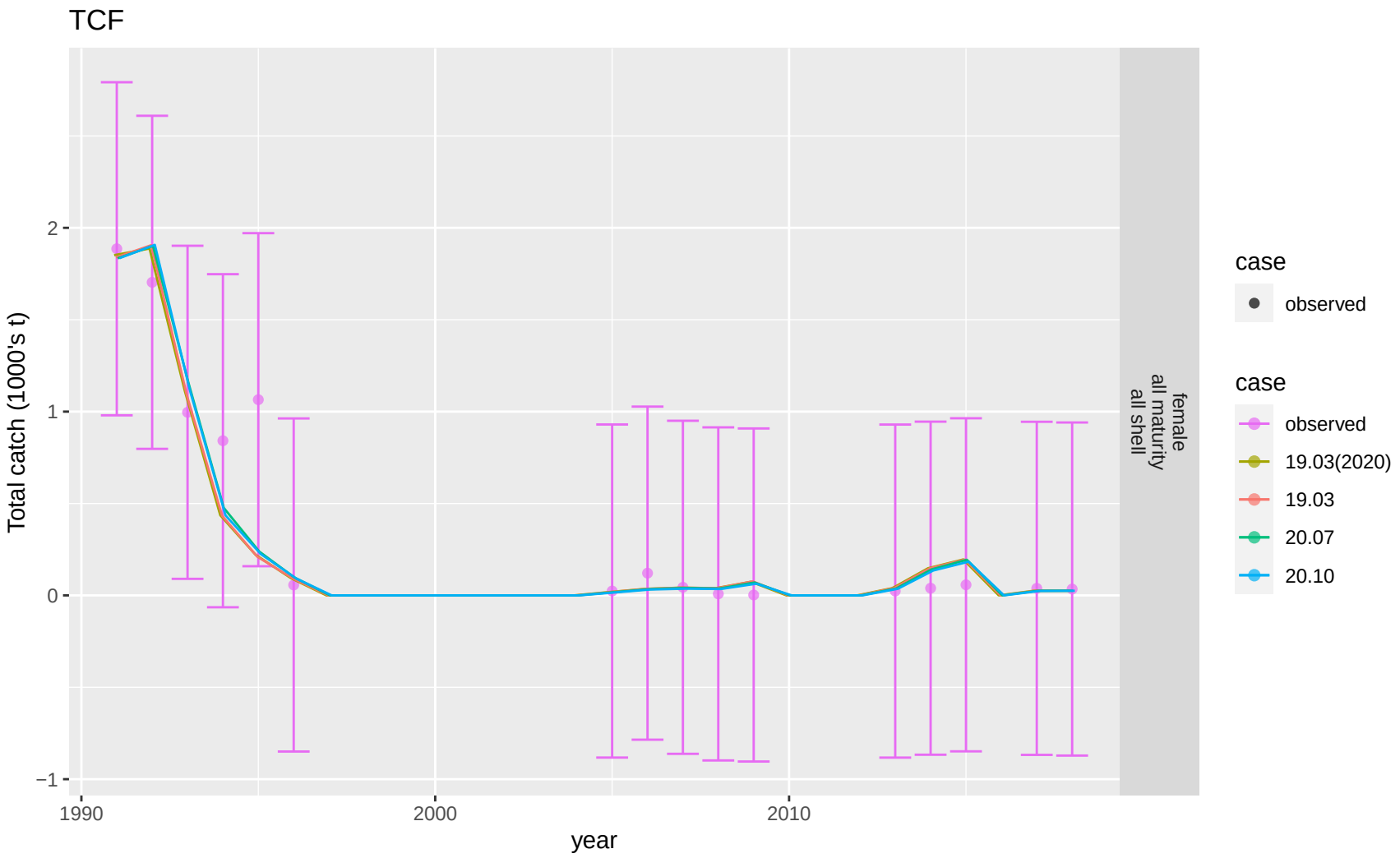

Figure 13: Comparison of observed and predicted total female catch biomass for TCF. Observed time period.

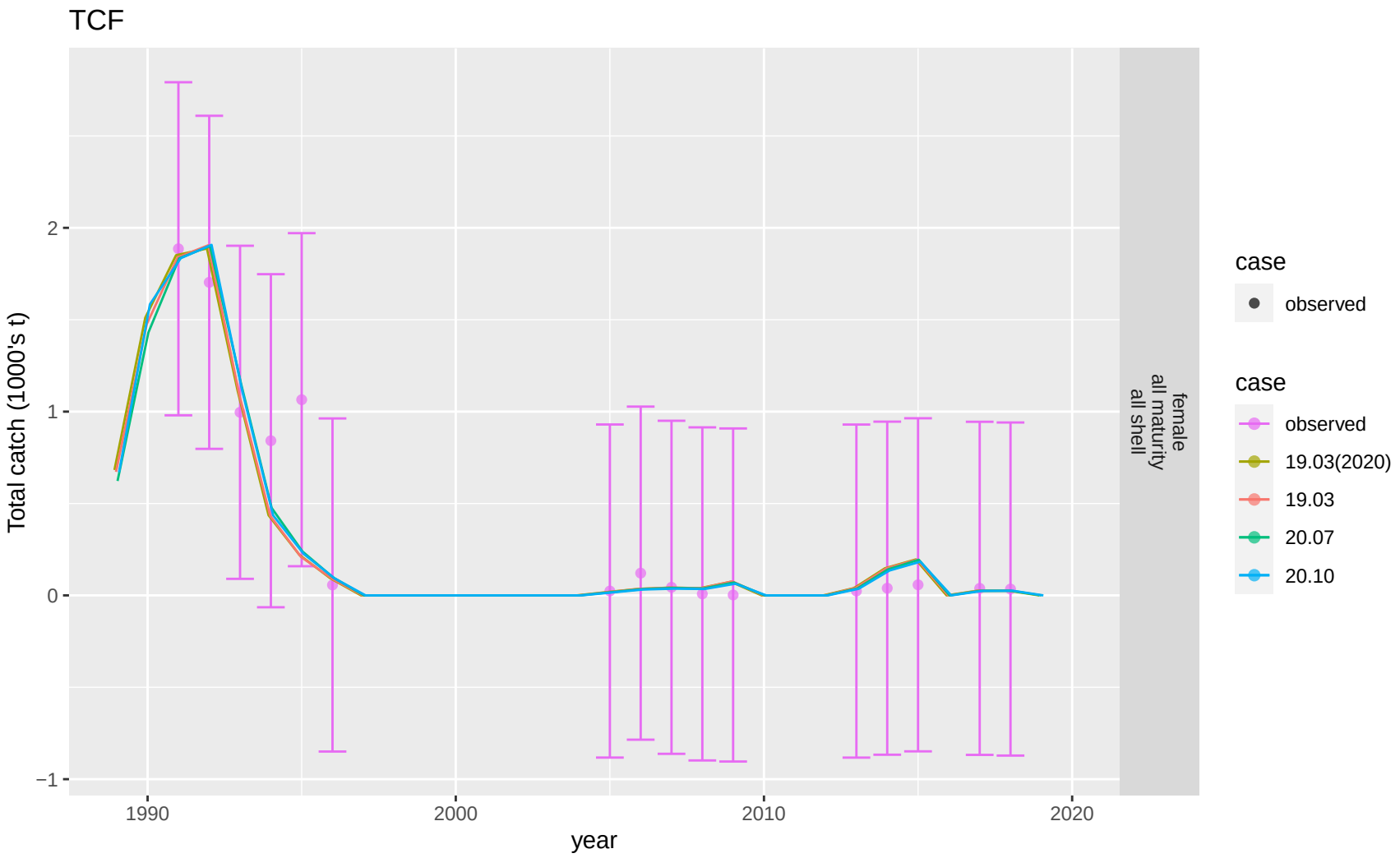

Figure 14: Comparison of observed and predicted total female catch biomass for TCF. Recent time period.

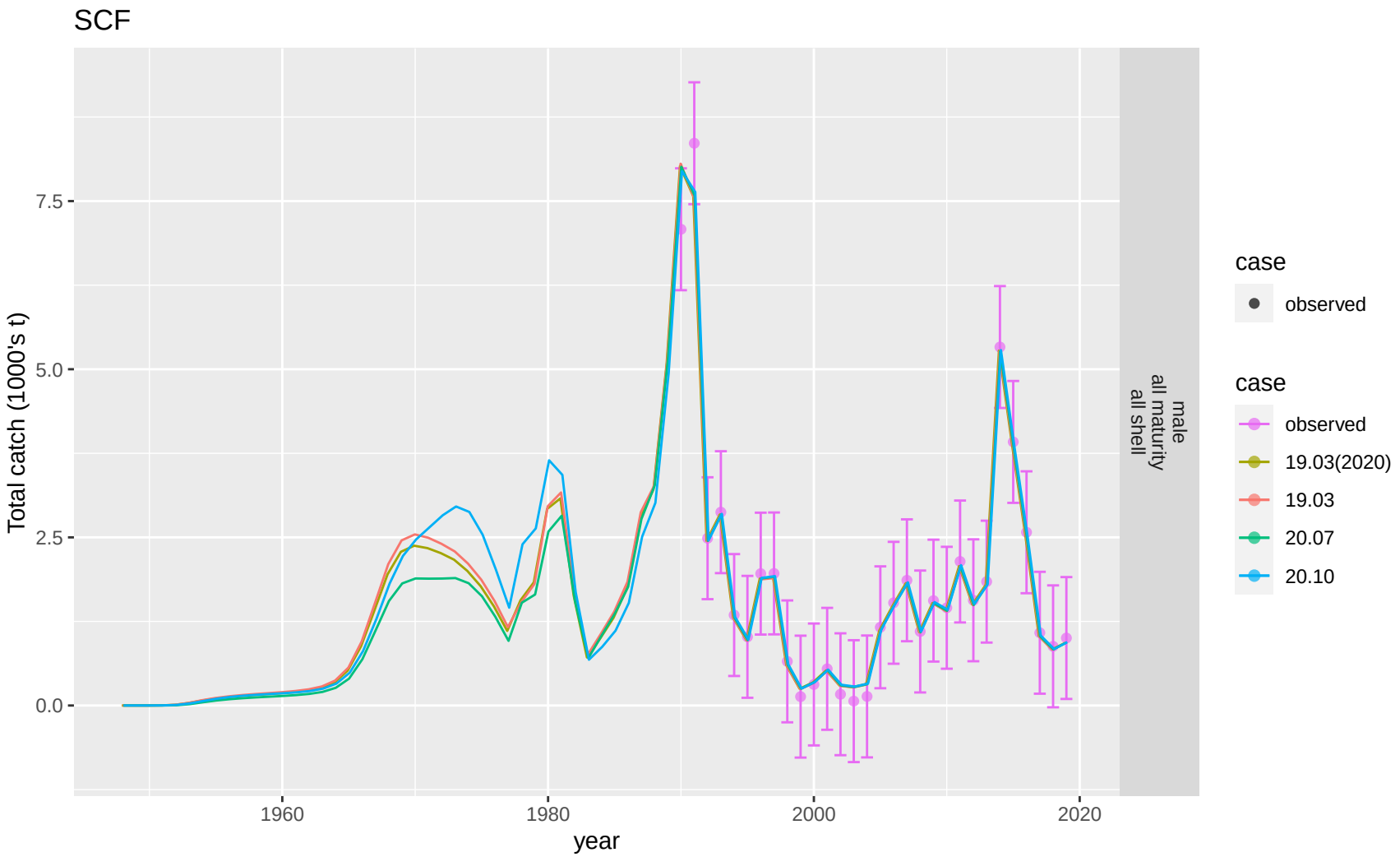

Figure 15: Comparison of observed and predicted total male catch biomass for SCF.

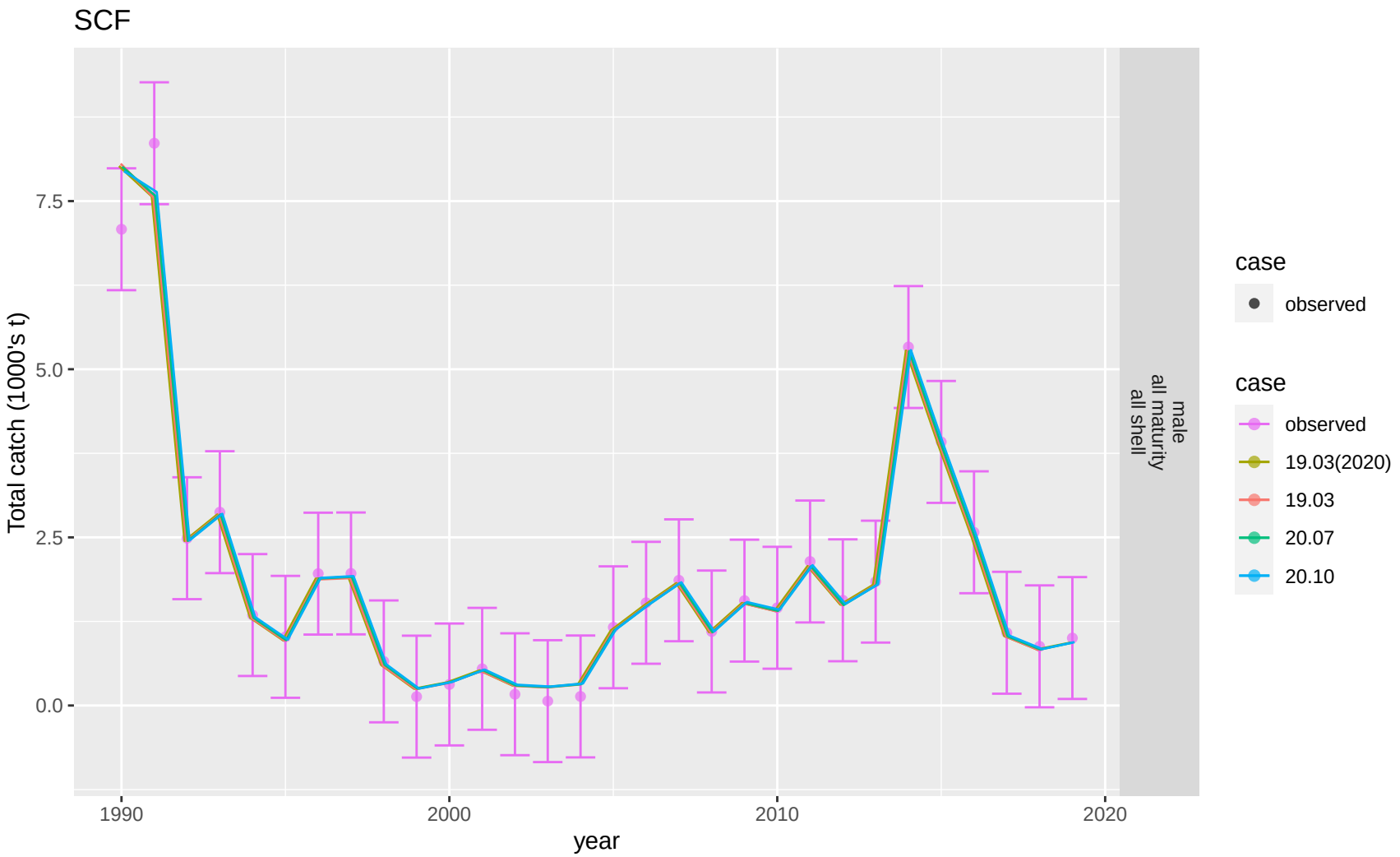

Figure 16: Comparison of observed and predicted total male catch biomass for SCF. Observed time period.

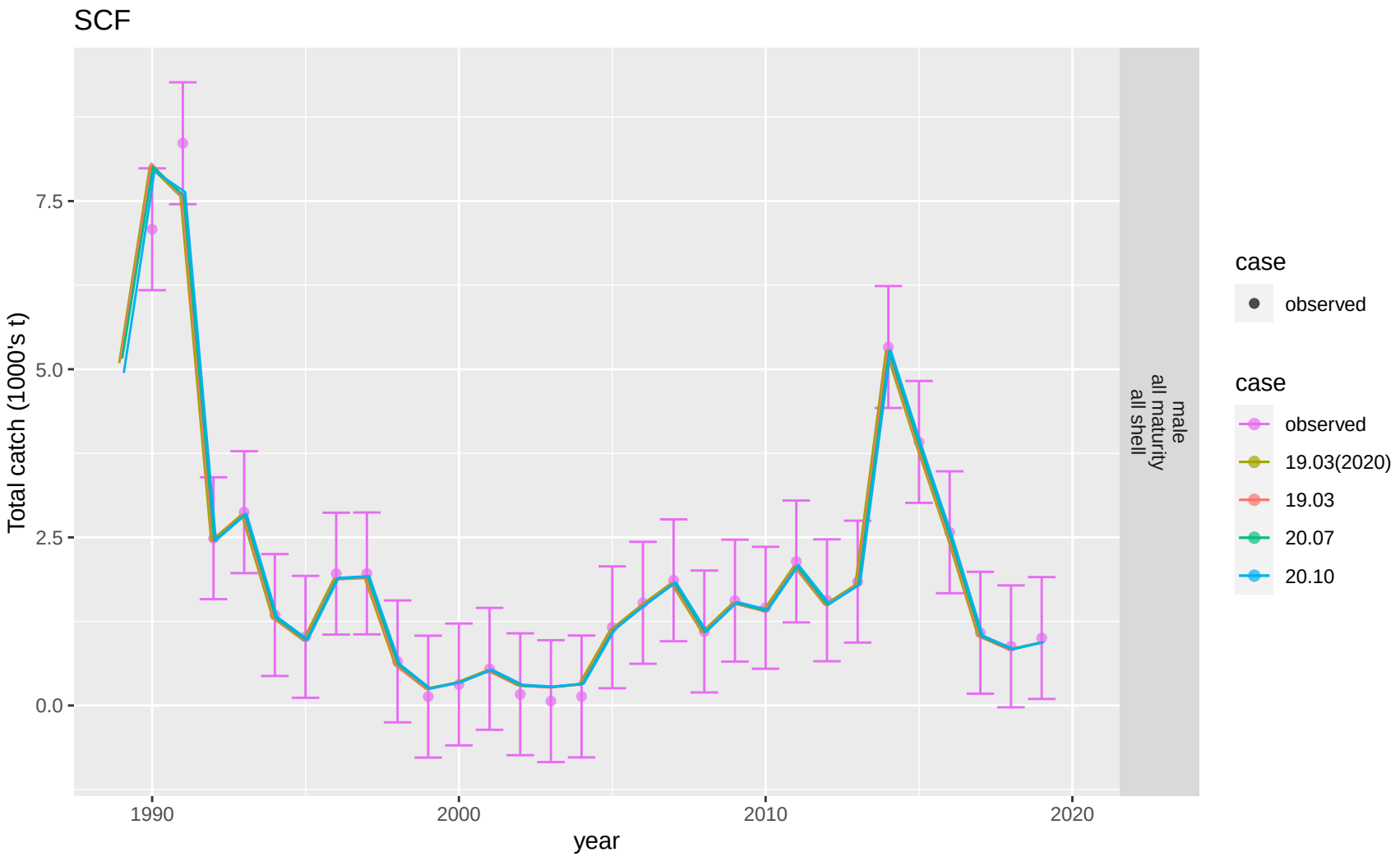

Figure 17: Comparison of observed and predicted total male catch biomass for SCF. Recent time period.

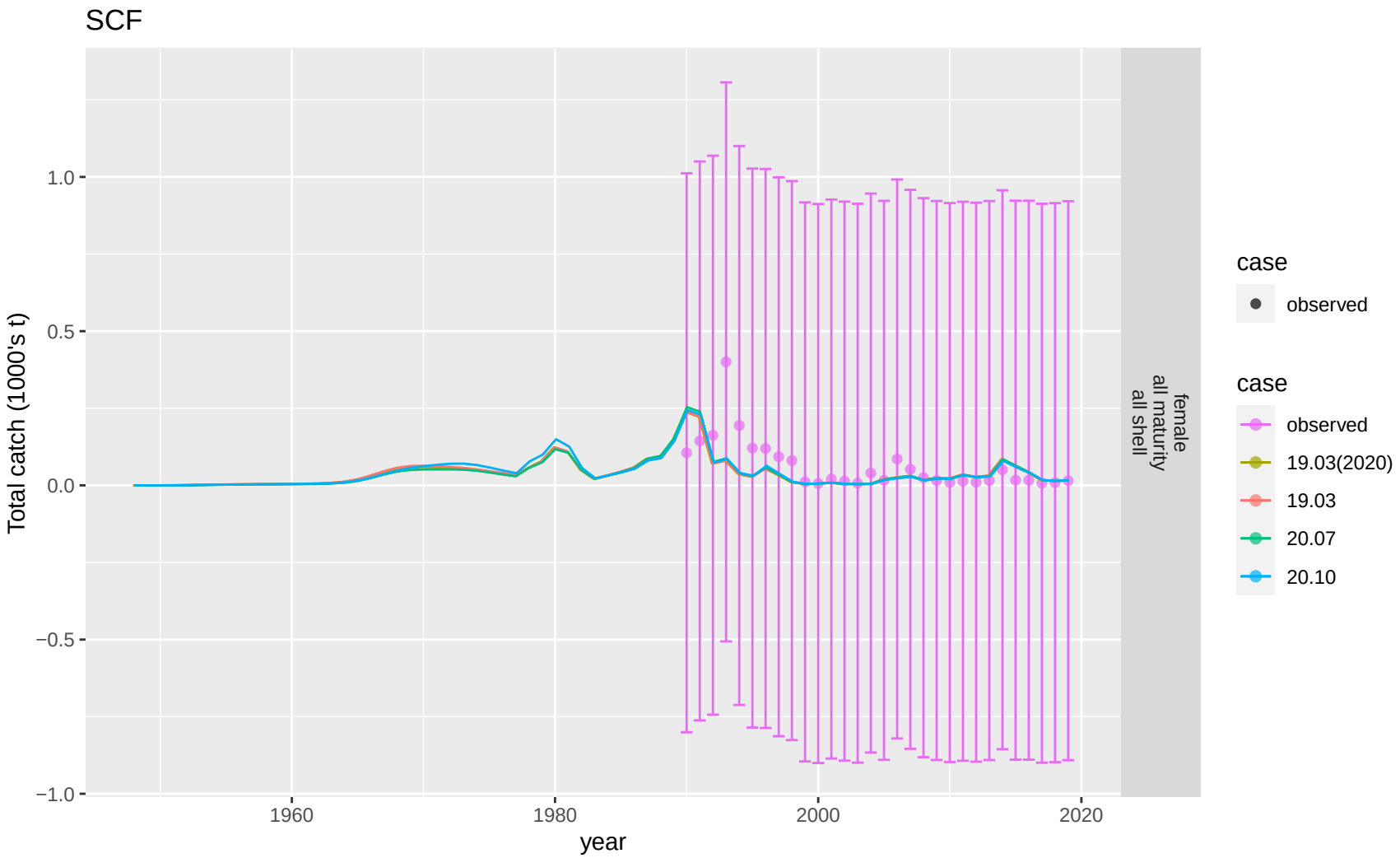

Figure 18: Comparison of observed and predicted total female catch biomass for SCF.

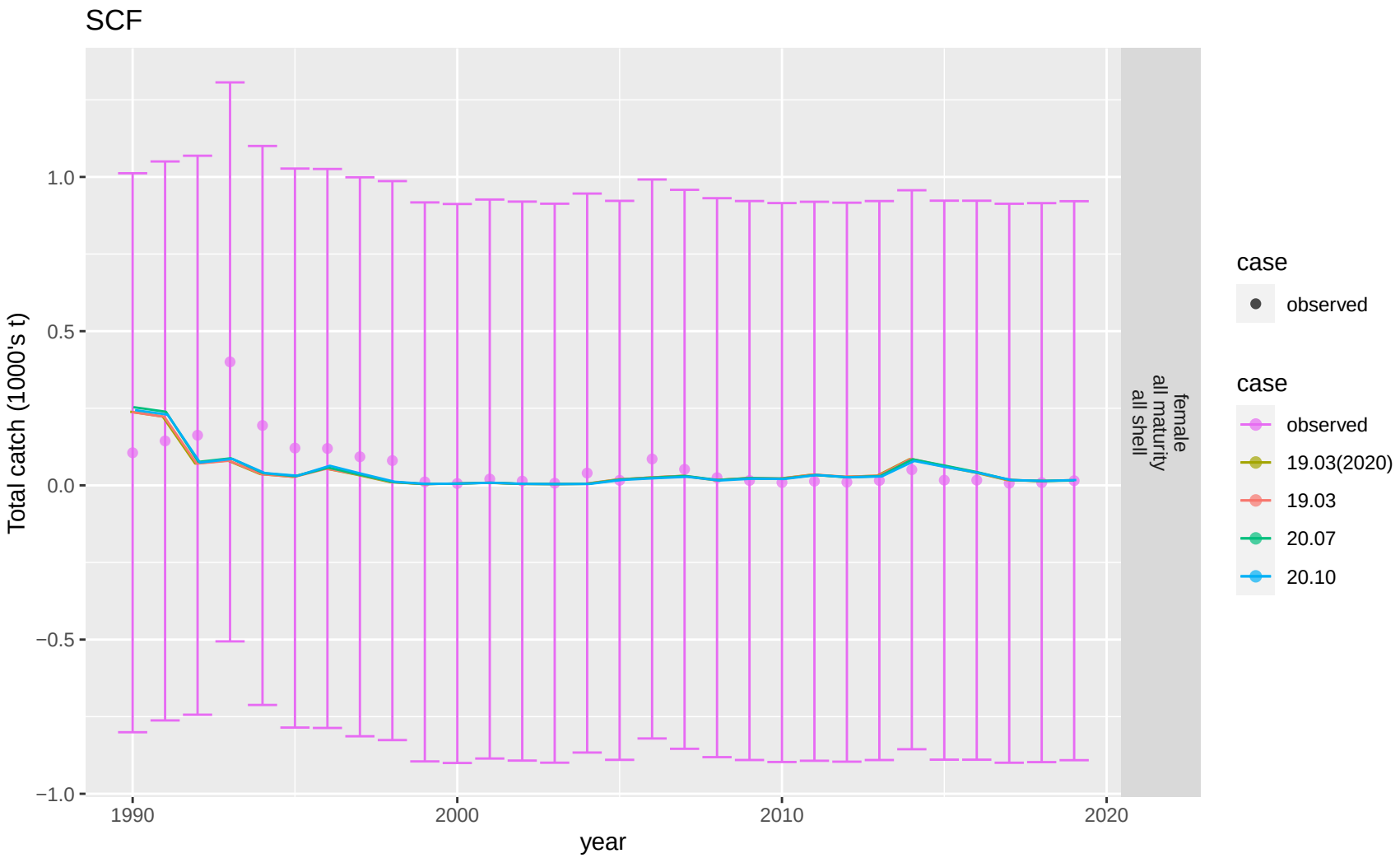

Figure 19: Comparison of observed and predicted total female catch biomass for SCF. Observed time period.

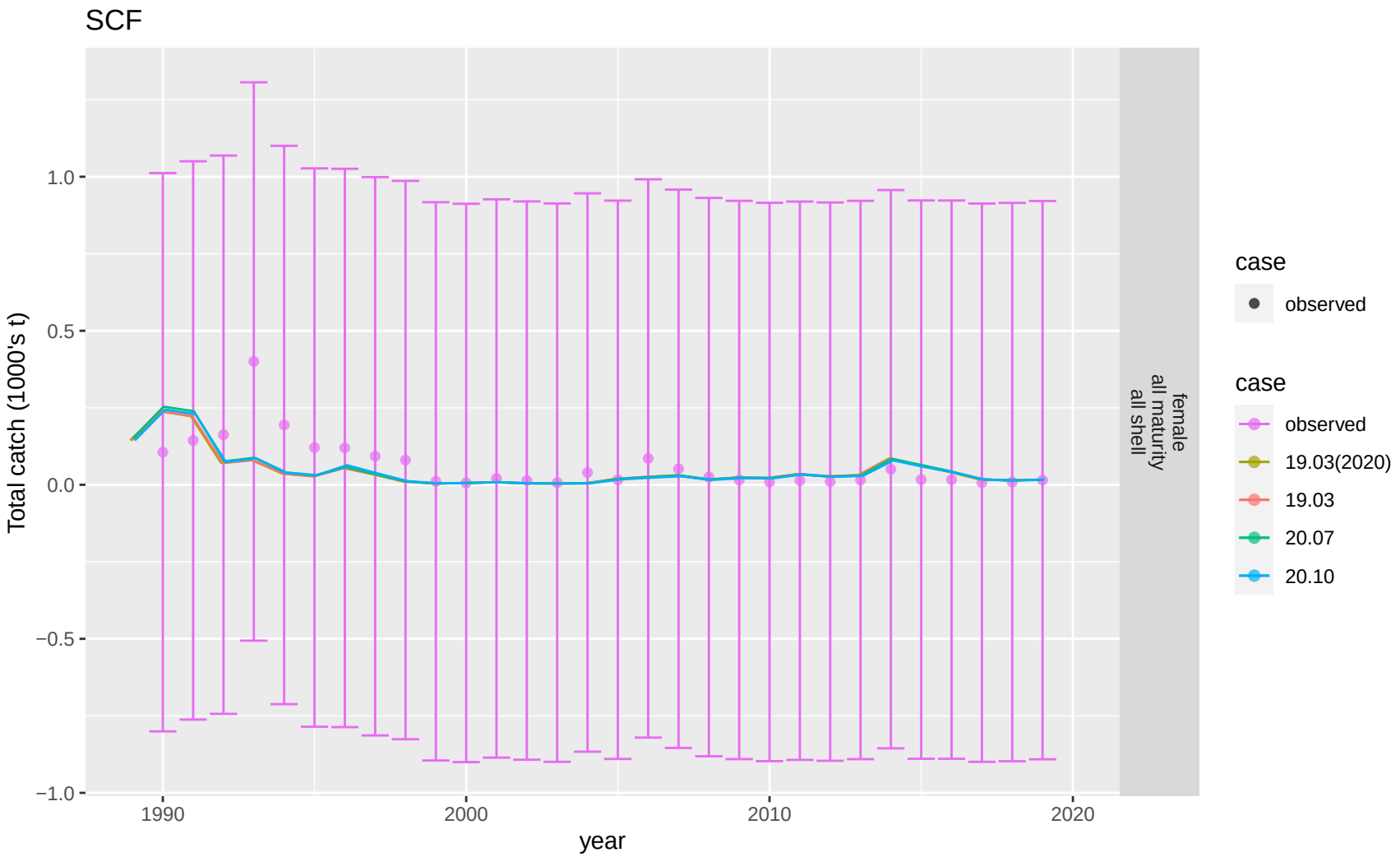

Figure 20: Comparison of observed and predicted total female catch biomass for SCF. Recent time period.

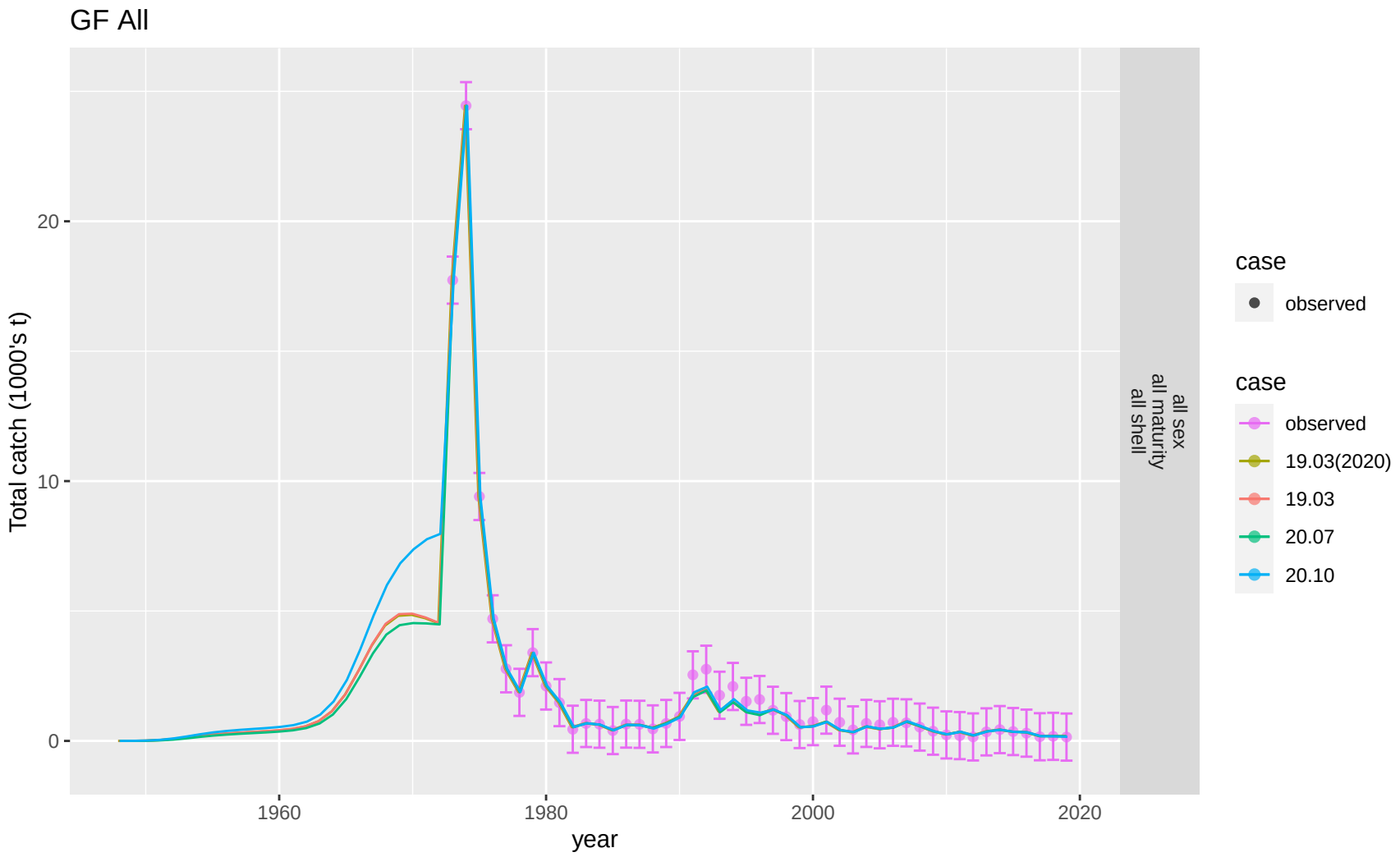

Figure 21: Comparison of observed and predicted total all sex catch biomass for GF All.

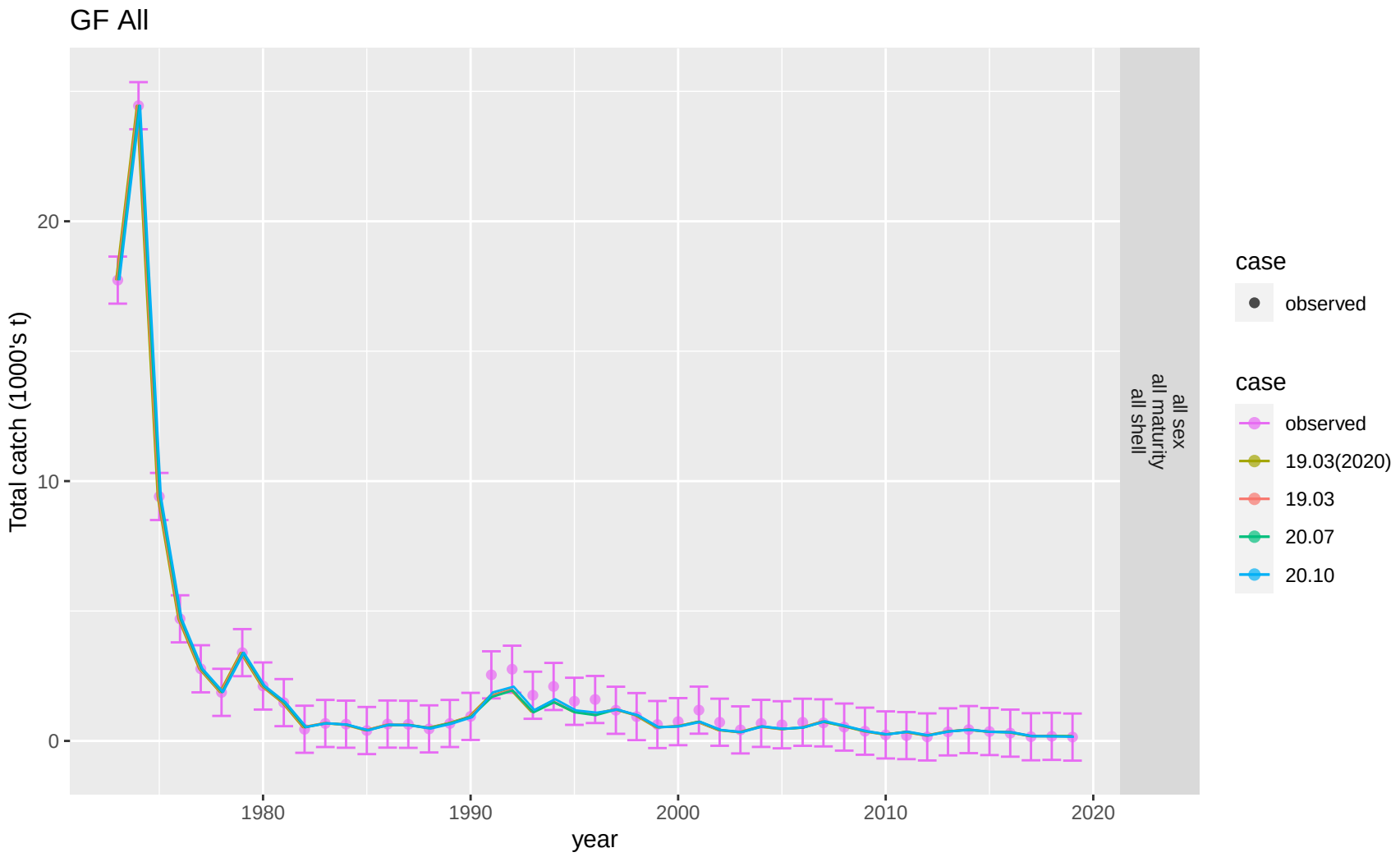

Figure 22: Comparison of observed and predicted total all sex catch biomass for GF All. Observed time period.

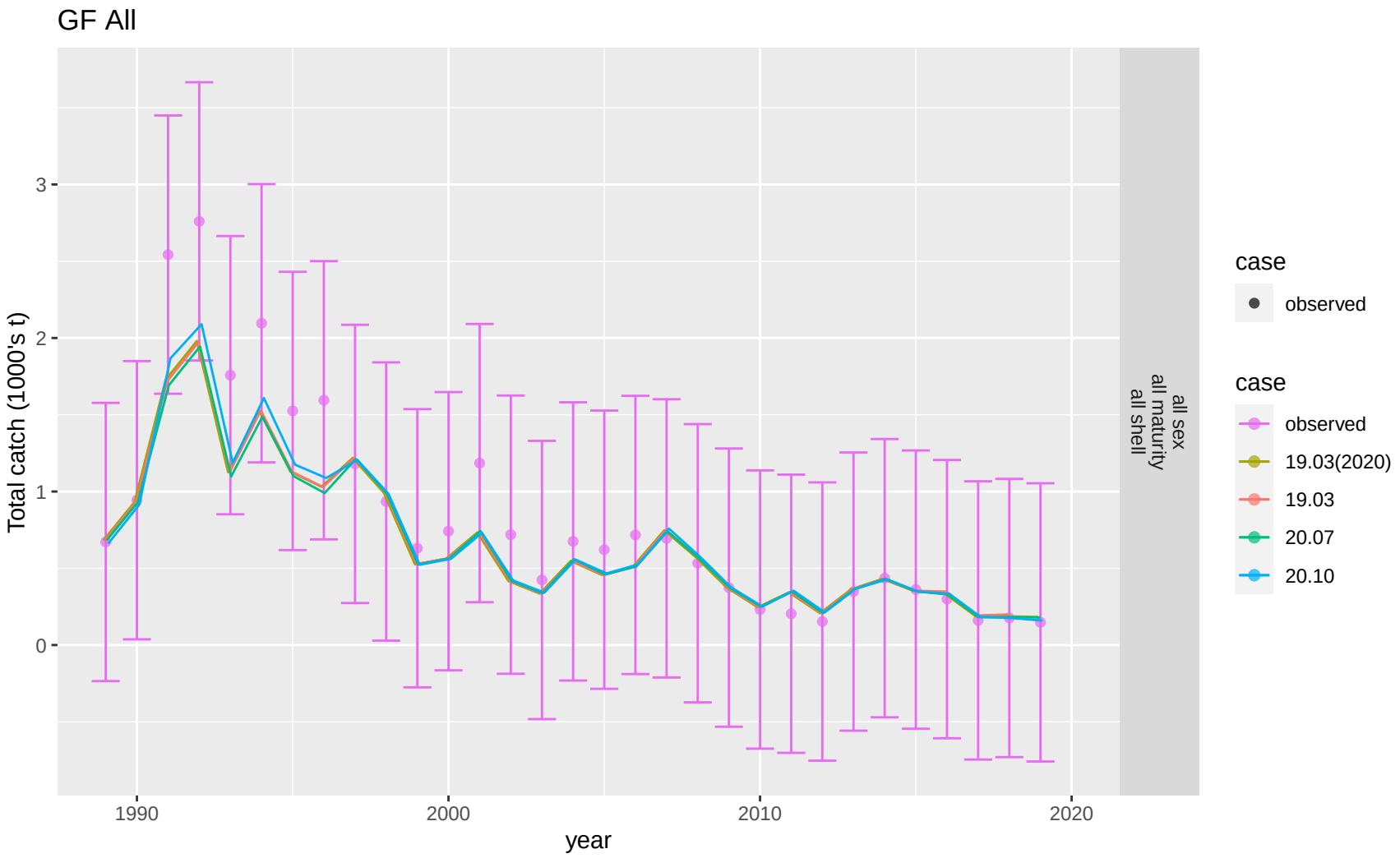

Figure 23: Comparison of observed and predicted total all sex catch biomass for GF All. Recent time period.

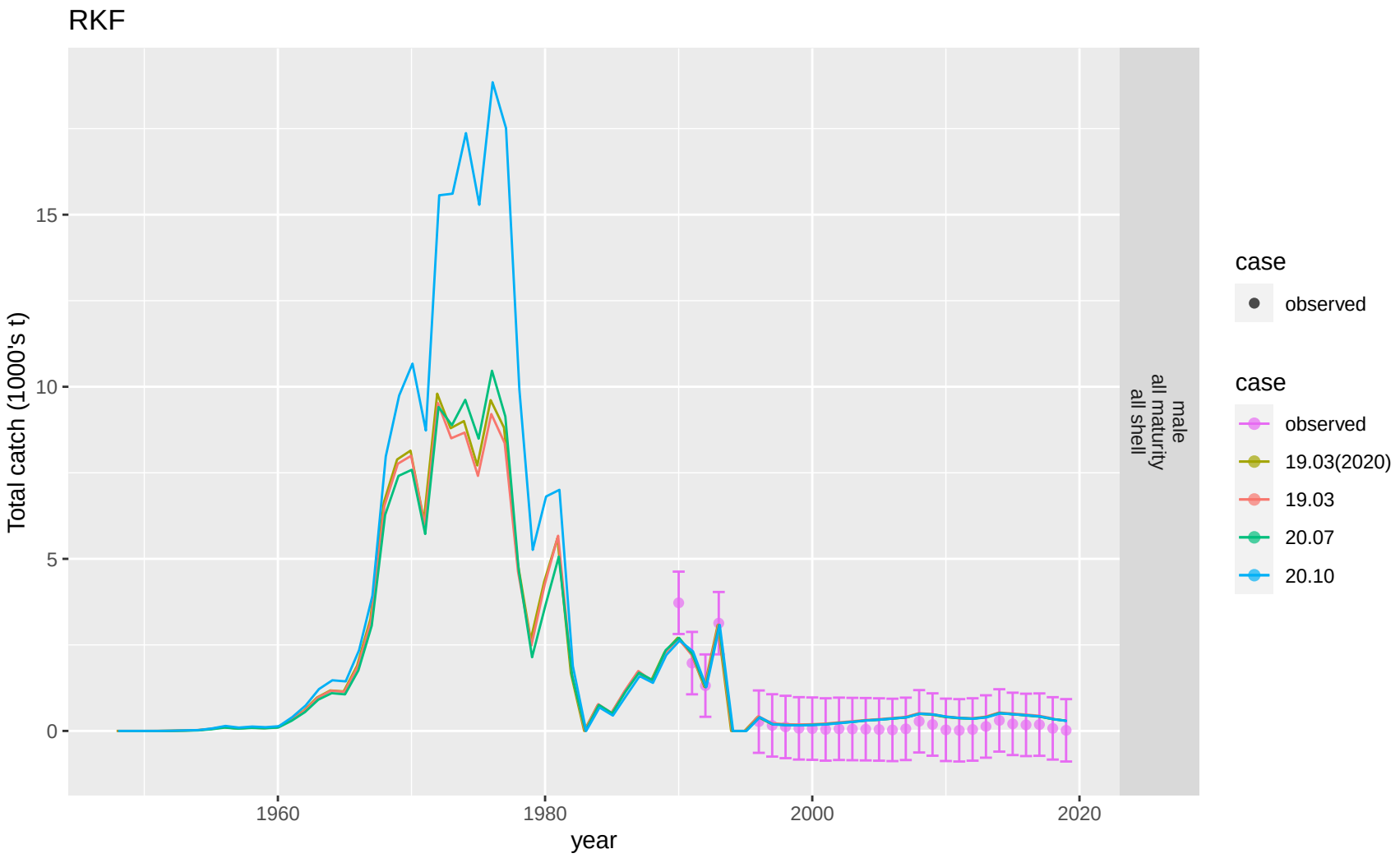

Figure 24: Comparison of observed and predicted total male catch biomass for RKF.

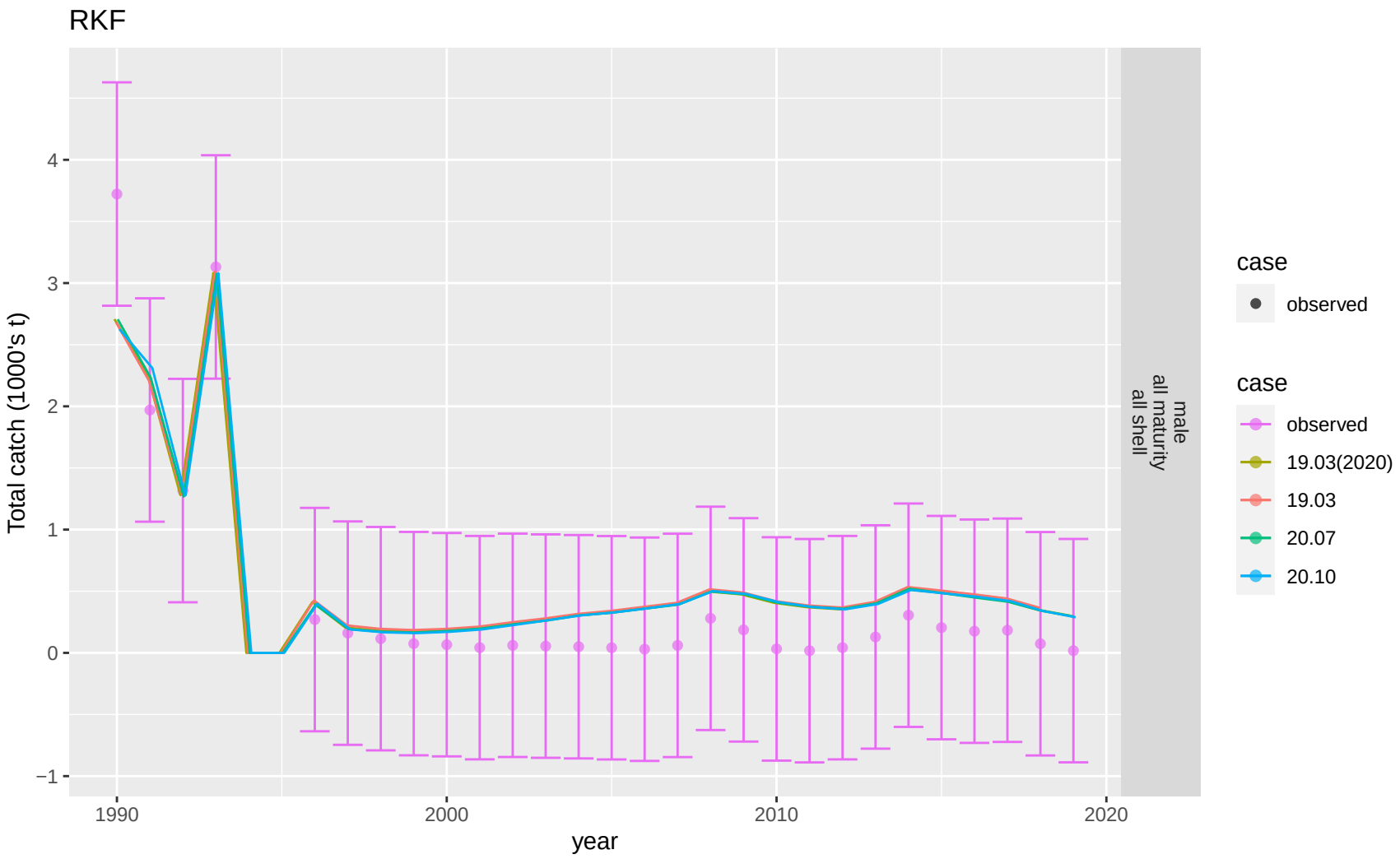

Figure 25: Comparison of observed and predicted total male catch biomass for RKF. Observed time period.

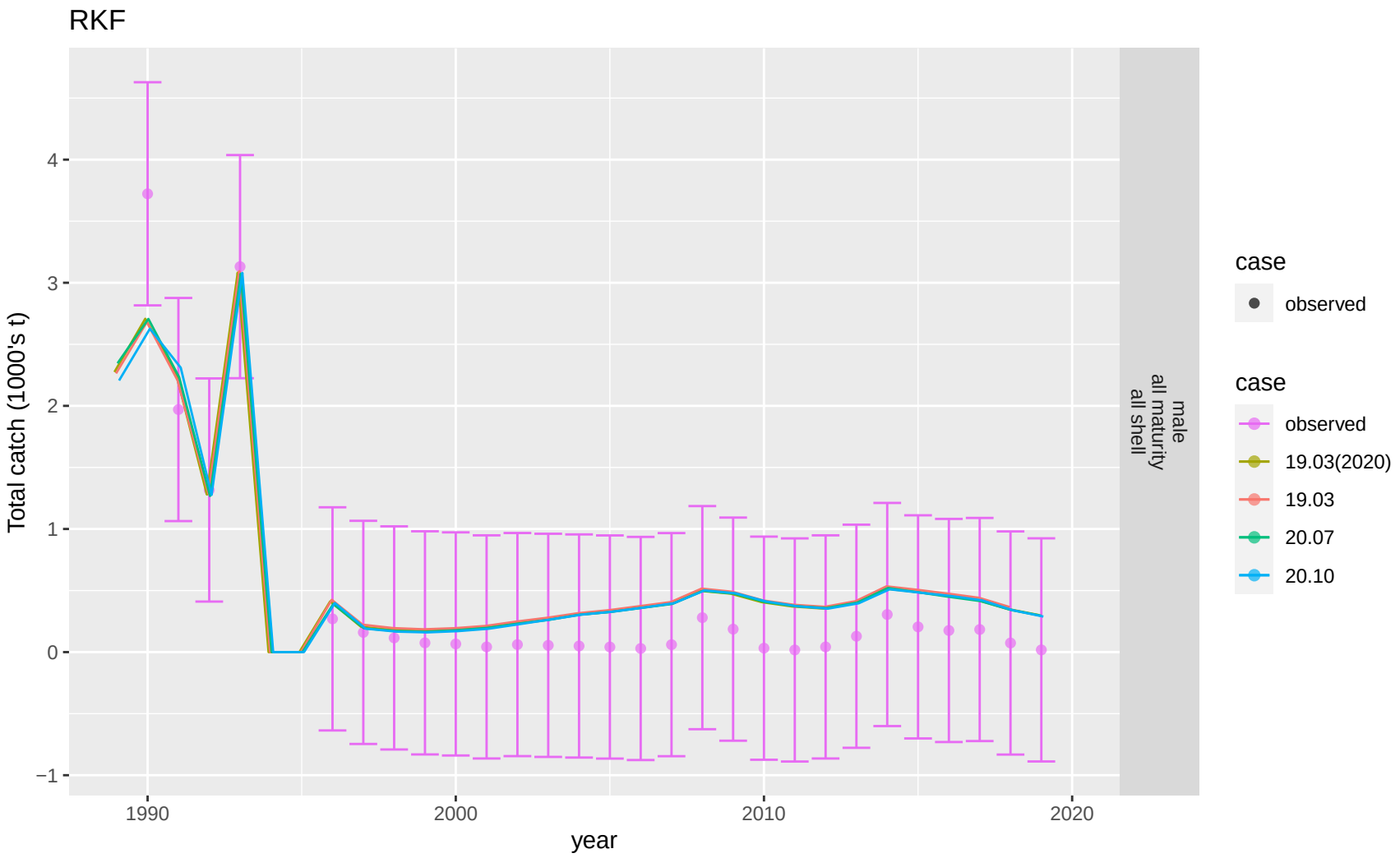

Figure 26: Comparison of observed and predicted total male catch biomass for RKF. Recent time period.

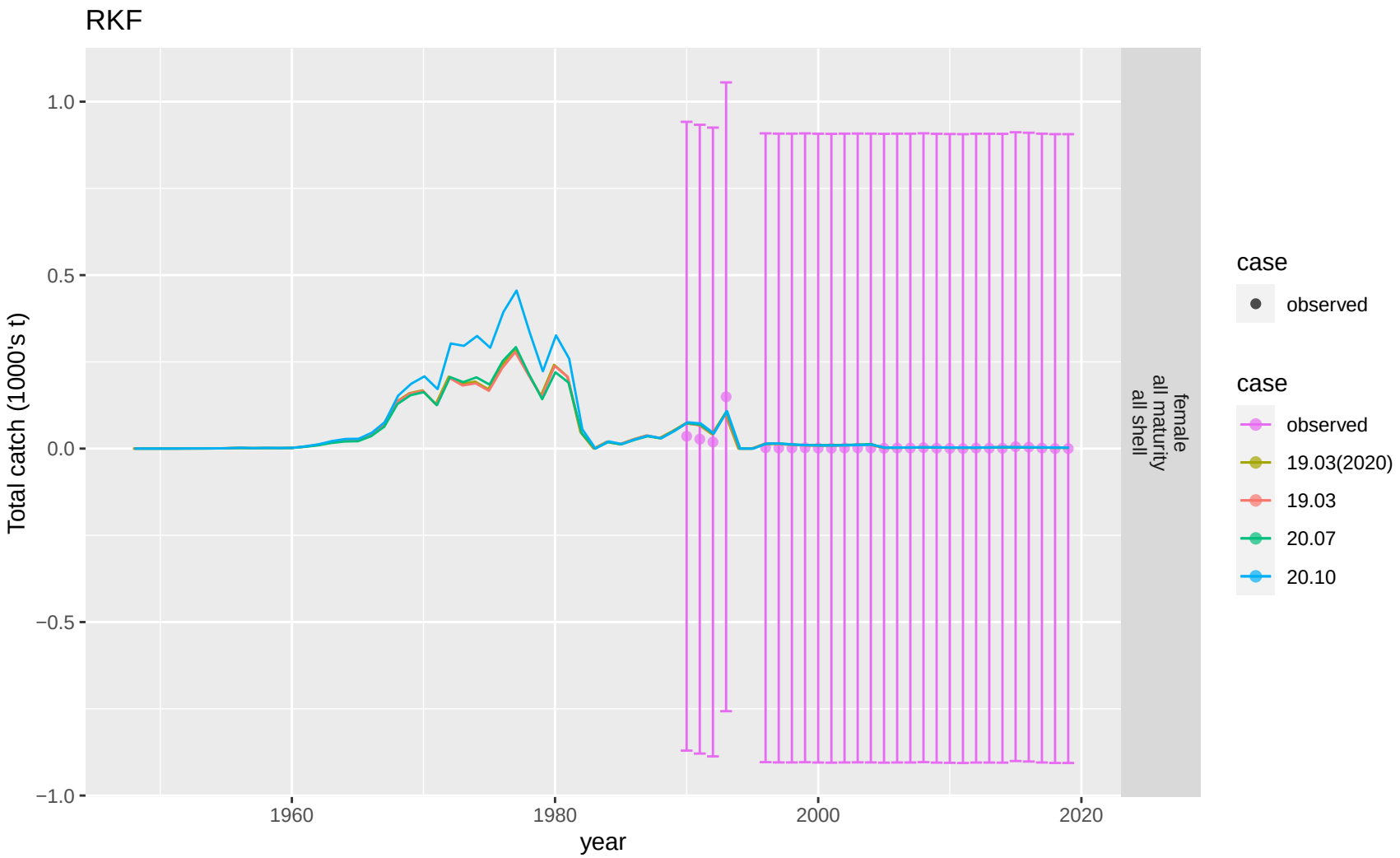

Figure 27: Comparison of observed and predicted total female catch biomass for RKF.

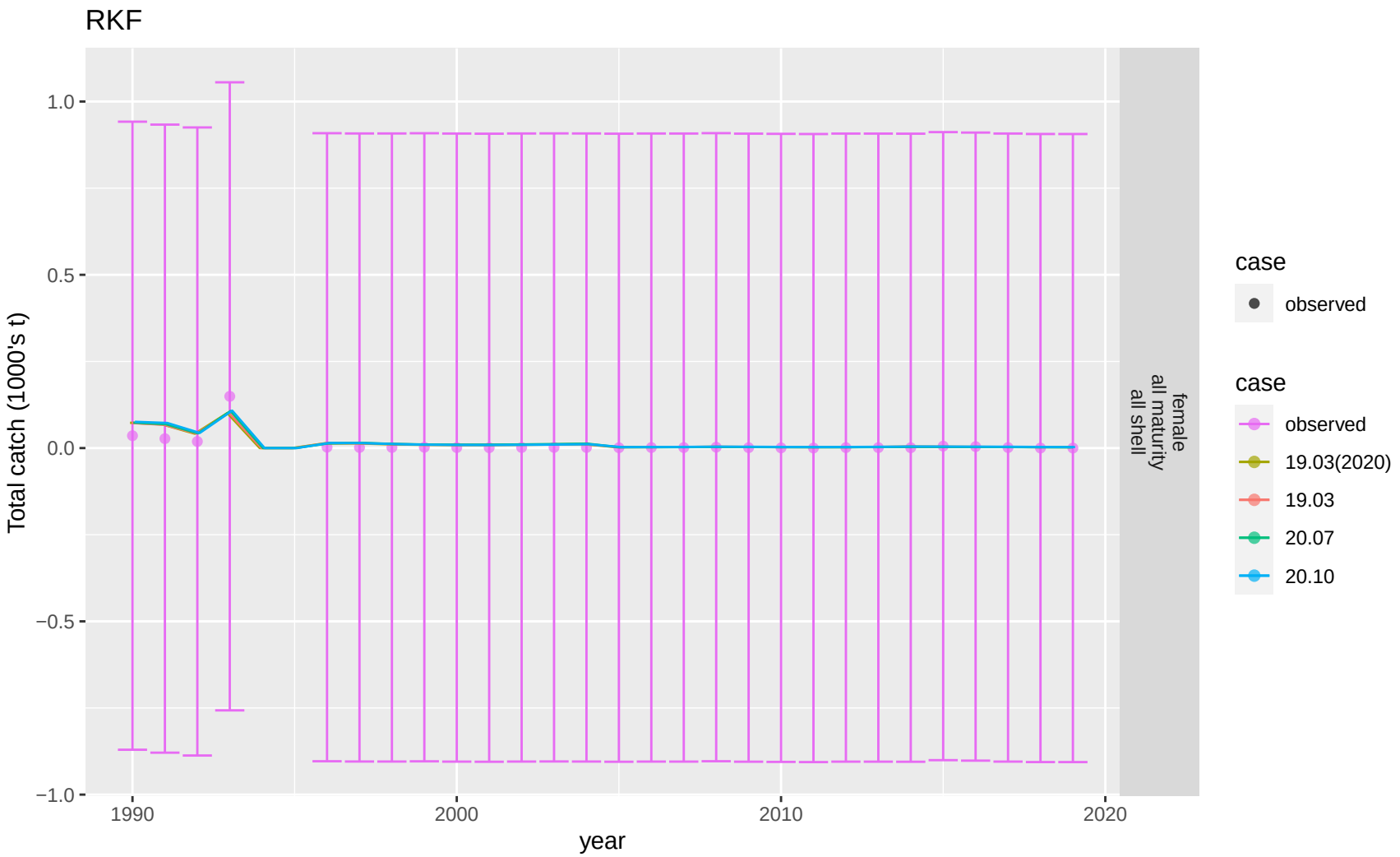

Figure 28: Comparison of observed and predicted total female catch biomass for RKF. Observed time period.

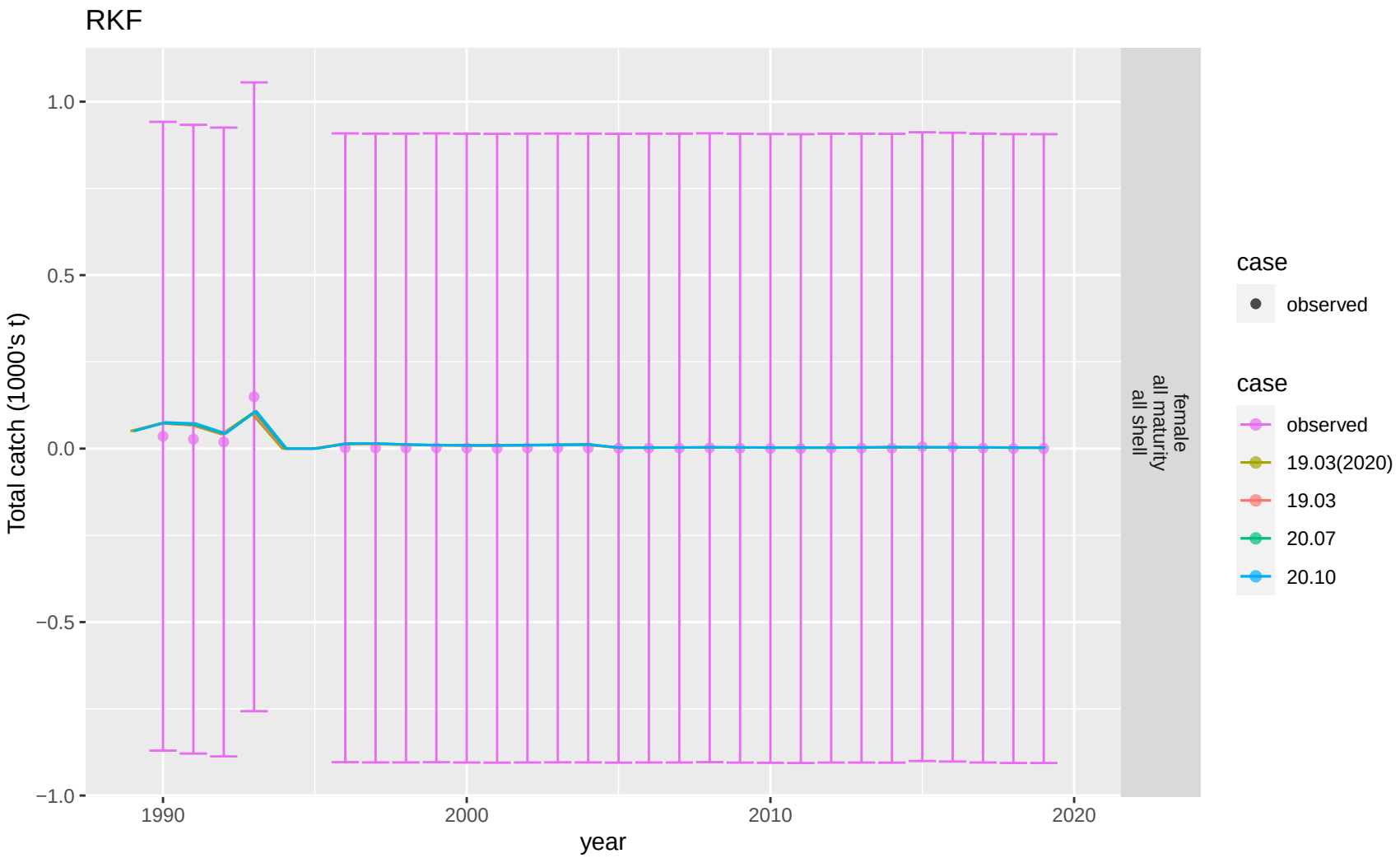

Figure 29: Comparison of observed and predicted total female catch biomass for RKF. Recent time period.

Z-scores

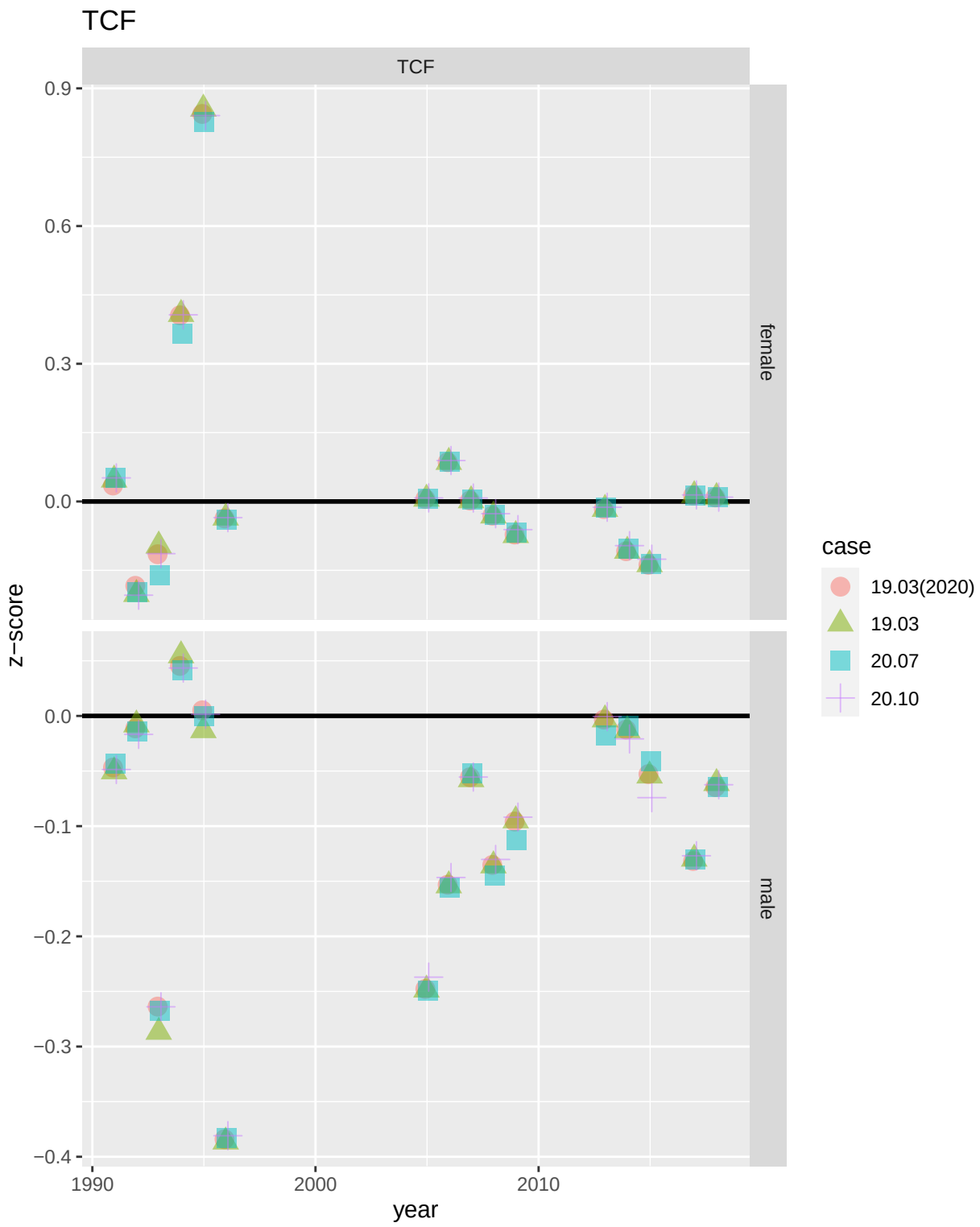

Figure 30: Z-scores for total catch biomass in TCF.

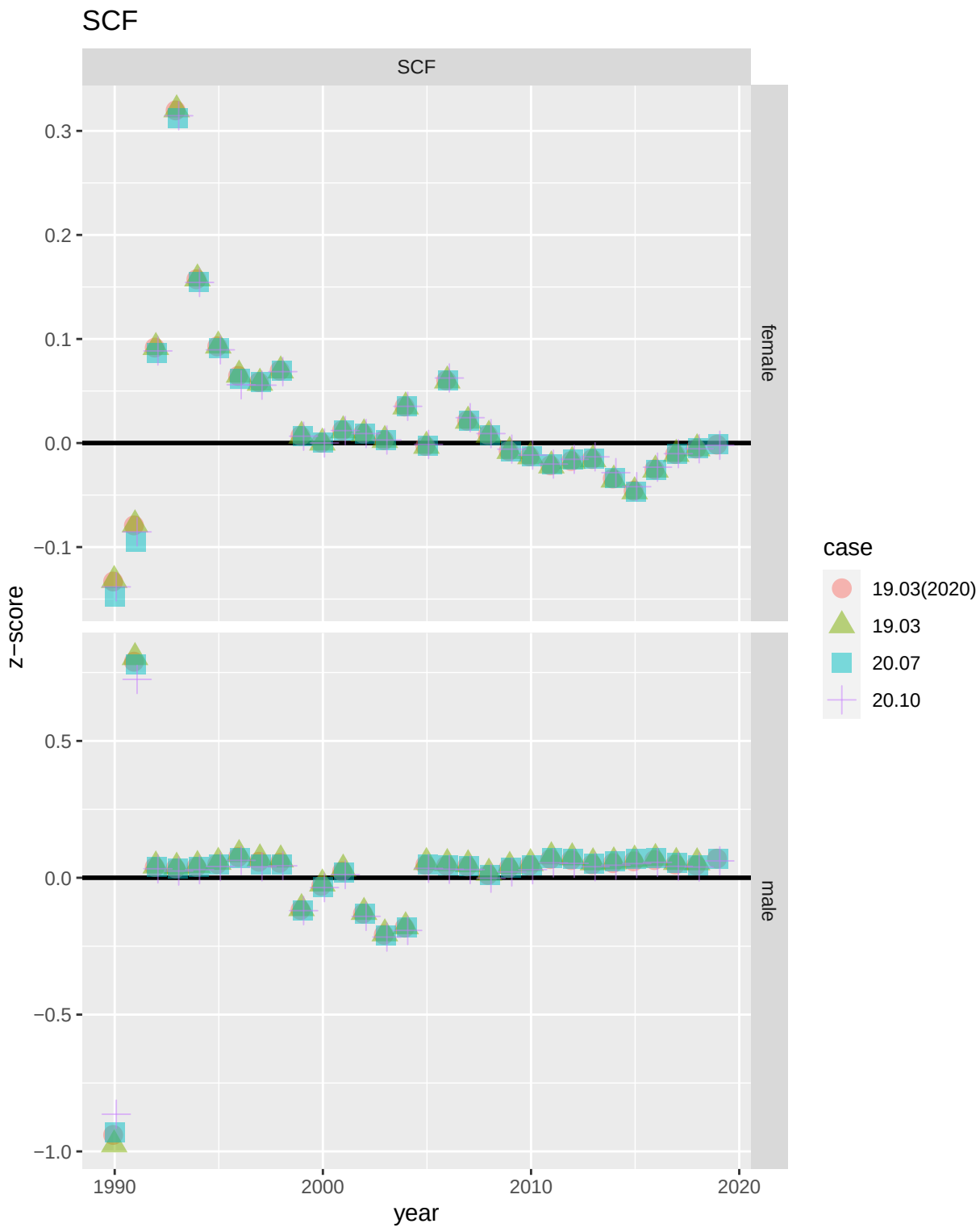

Figure 31: Z-scores for total catch biomass in SCF.

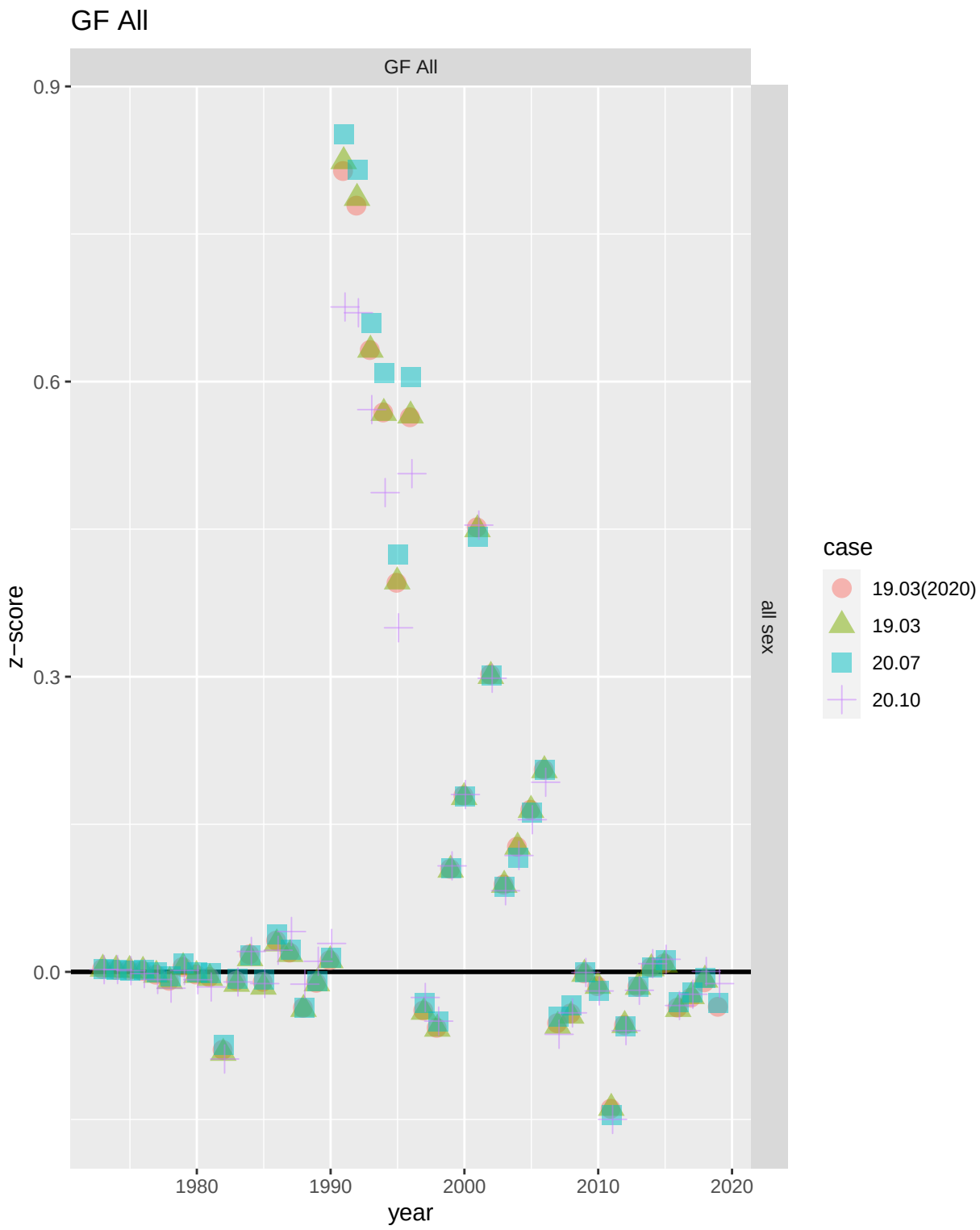

Figure 32: Z-scores for total catch biomass in GF All.

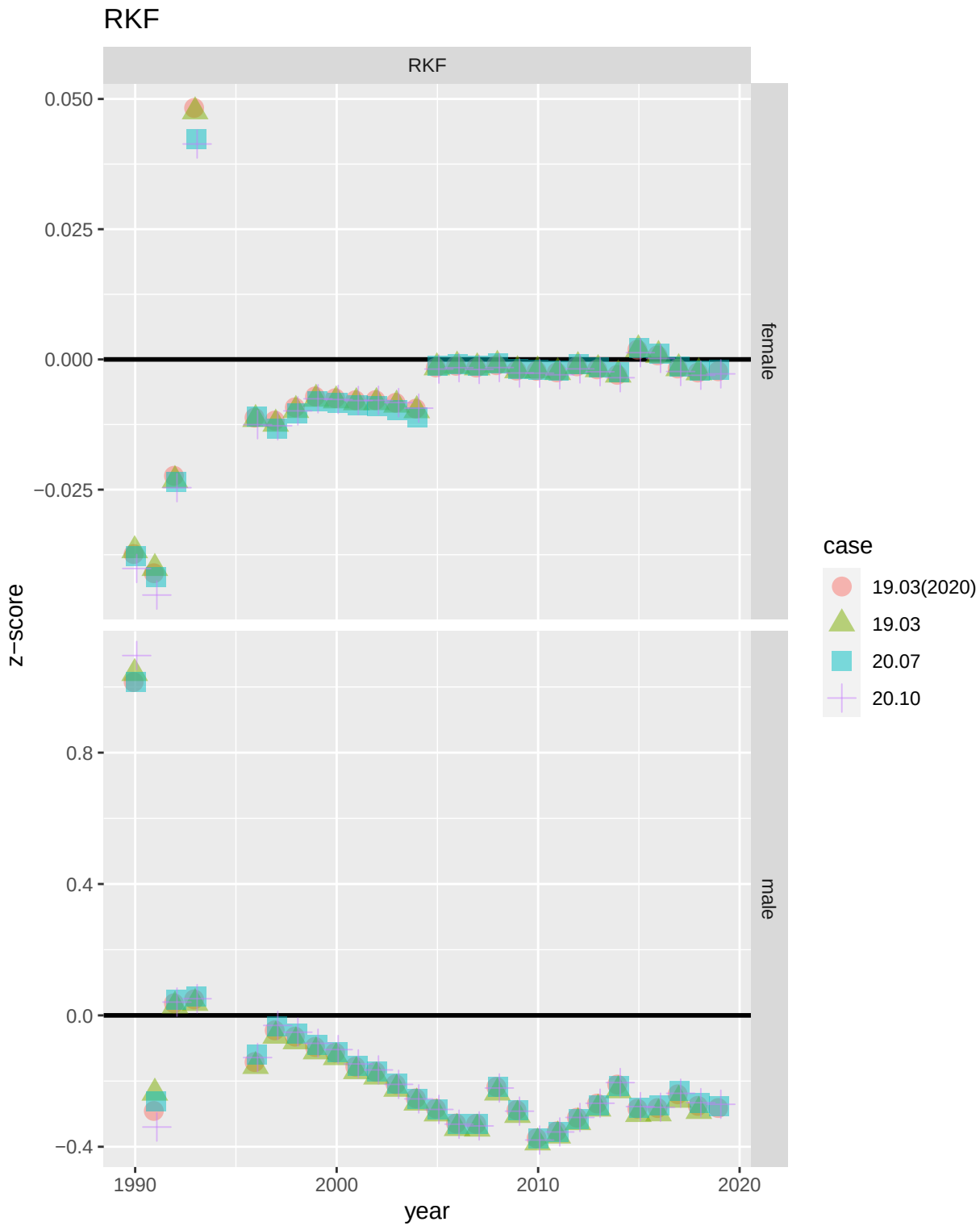

Figure 33: Z-scores for total catch biomass in RKF.

Fishery total catch abundance

Fits

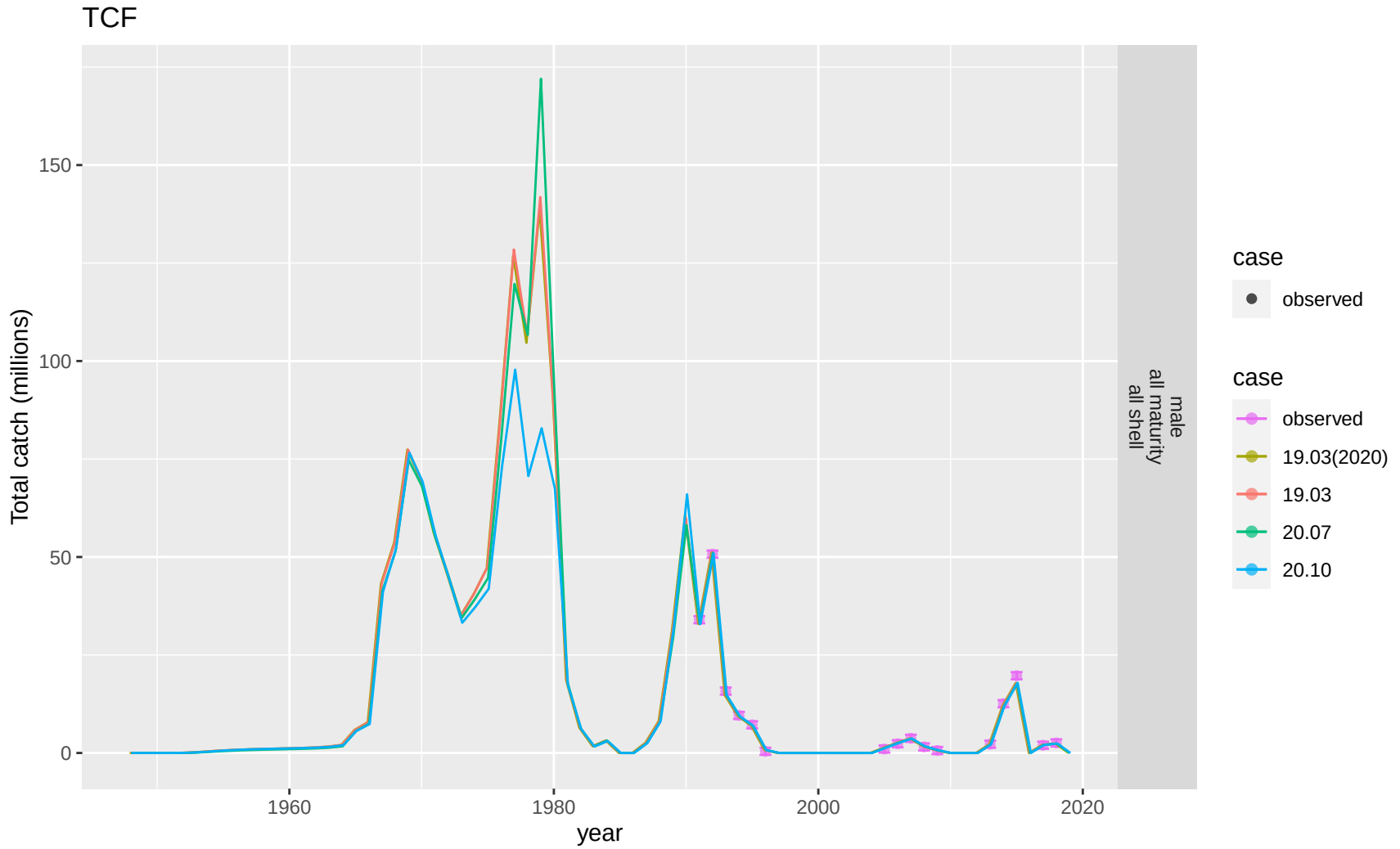

Figure 34: Comparison of observed and predicted male total catch abundance for TCF.

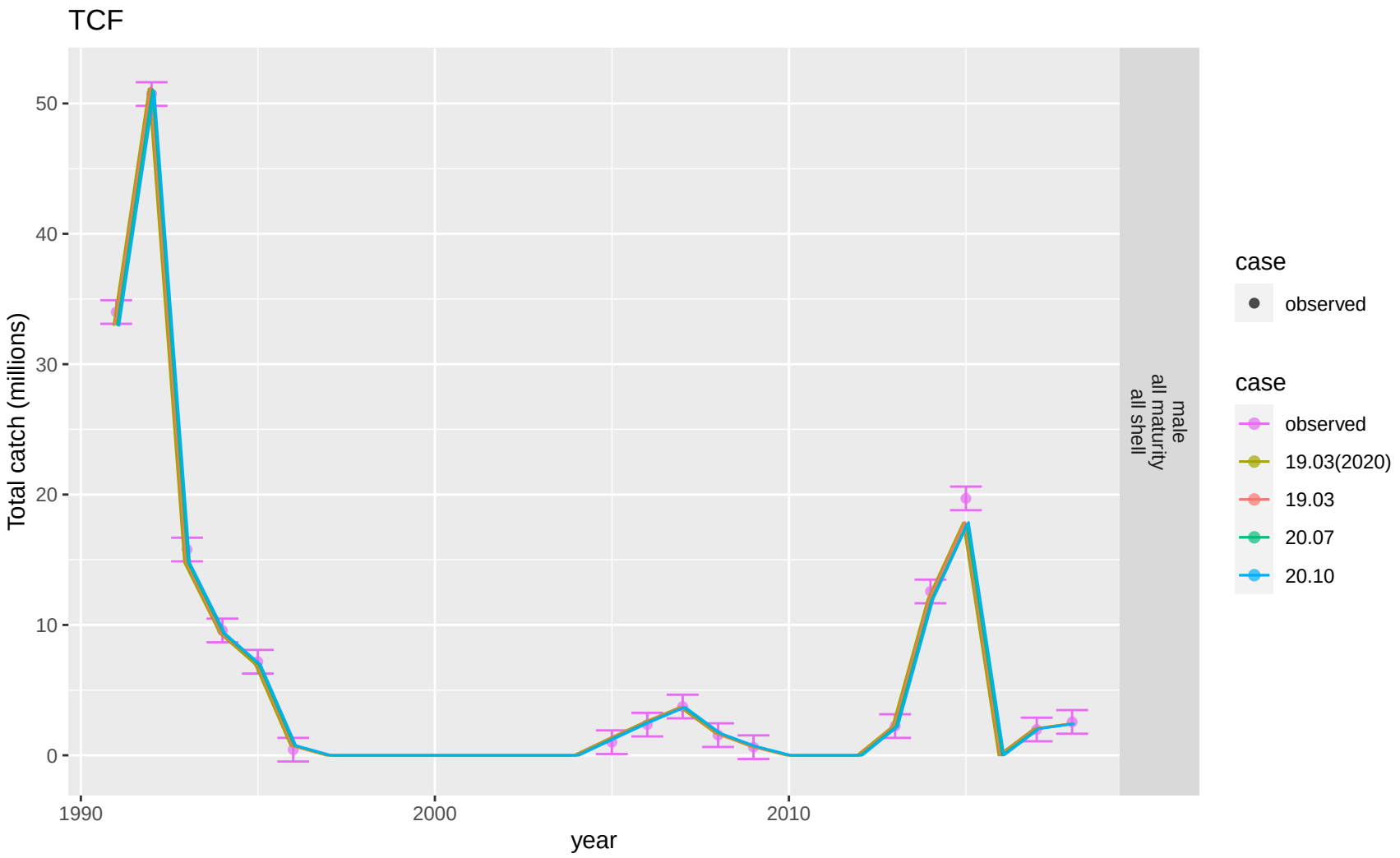

Figure 35: Comparison of observed and predicted male total catch abundance for TCF. Observed time period.

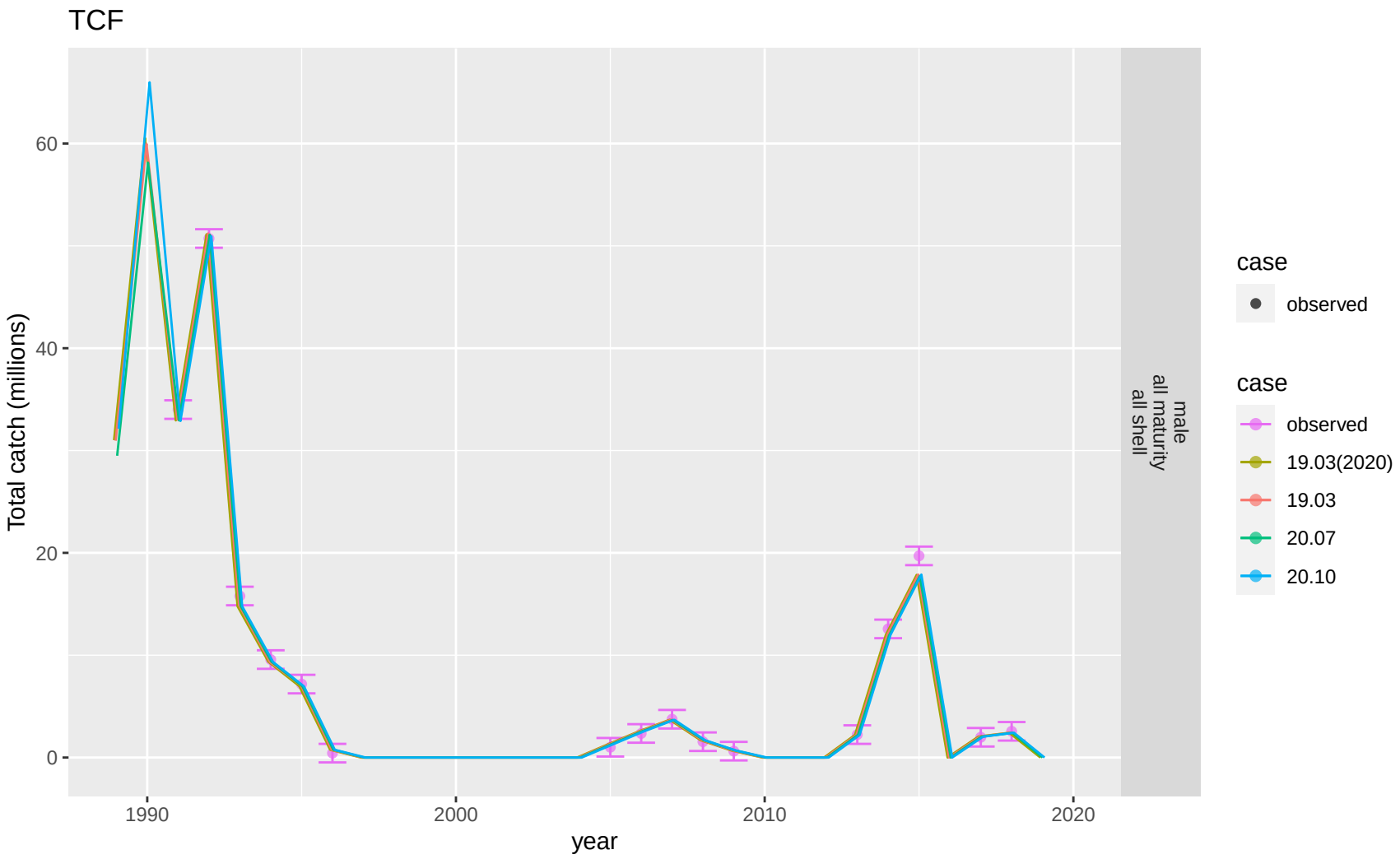

Figure 36: Comparison of observed and predicted male total catch abundance for TCF. Recent time period.

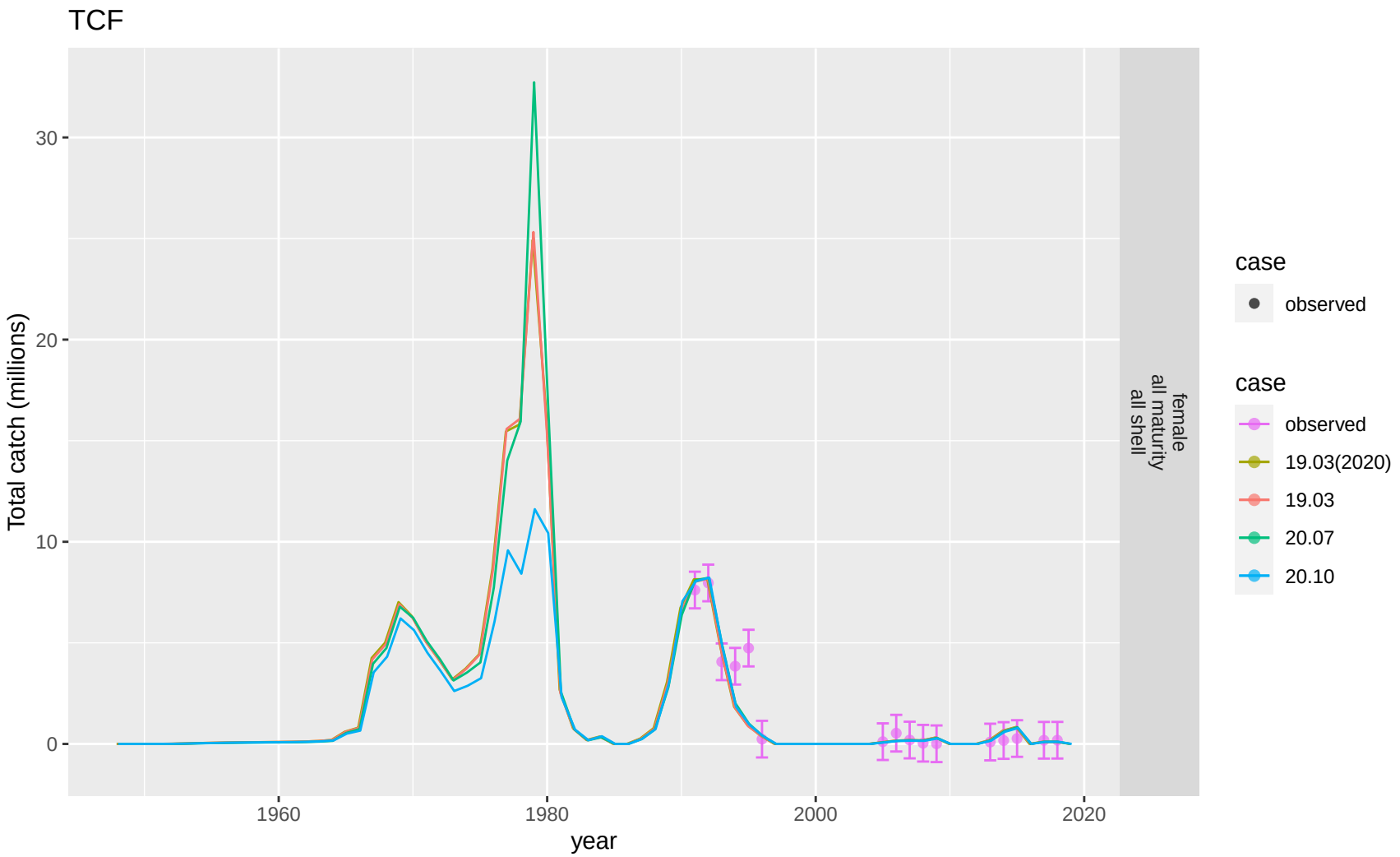

Figure 37: Comparison of observed and predicted female total catch abundance for TCF.

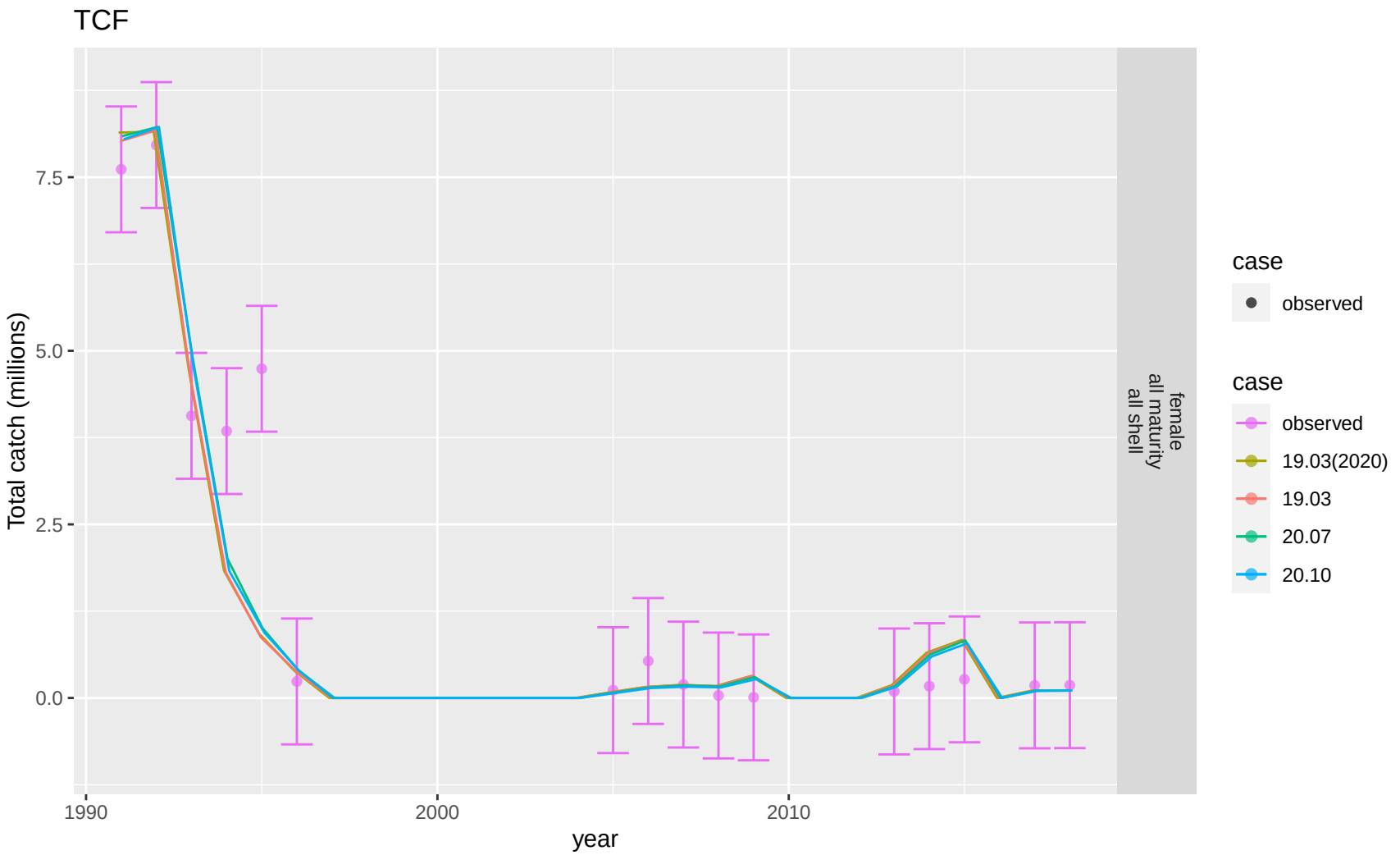

Figure 38: Comparison of observed and predicted female total catch abundance for TCF. Observed time period.

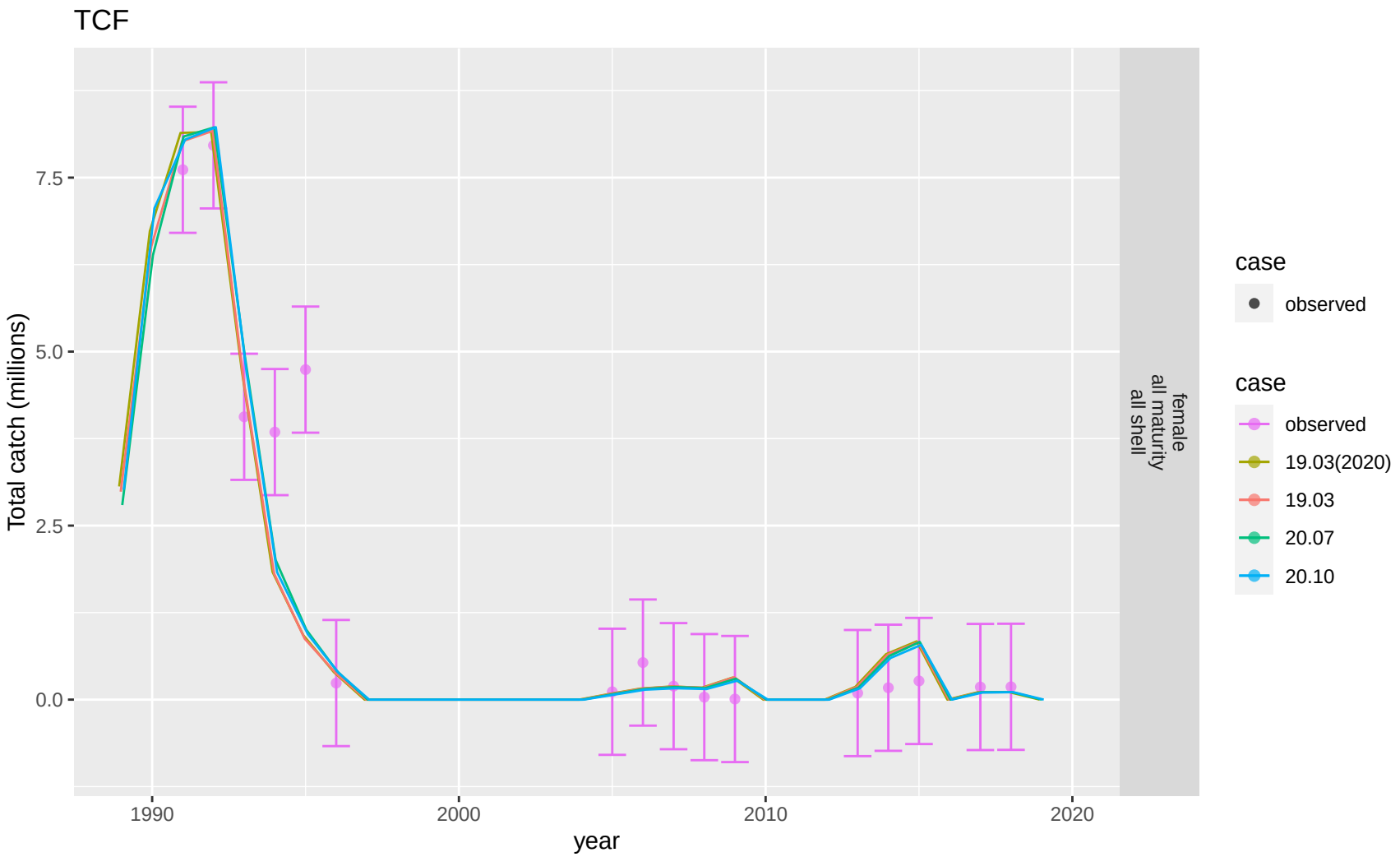

Figure 39: Comparison of observed and predicted female total catch abundance for TCF. Recent time period.

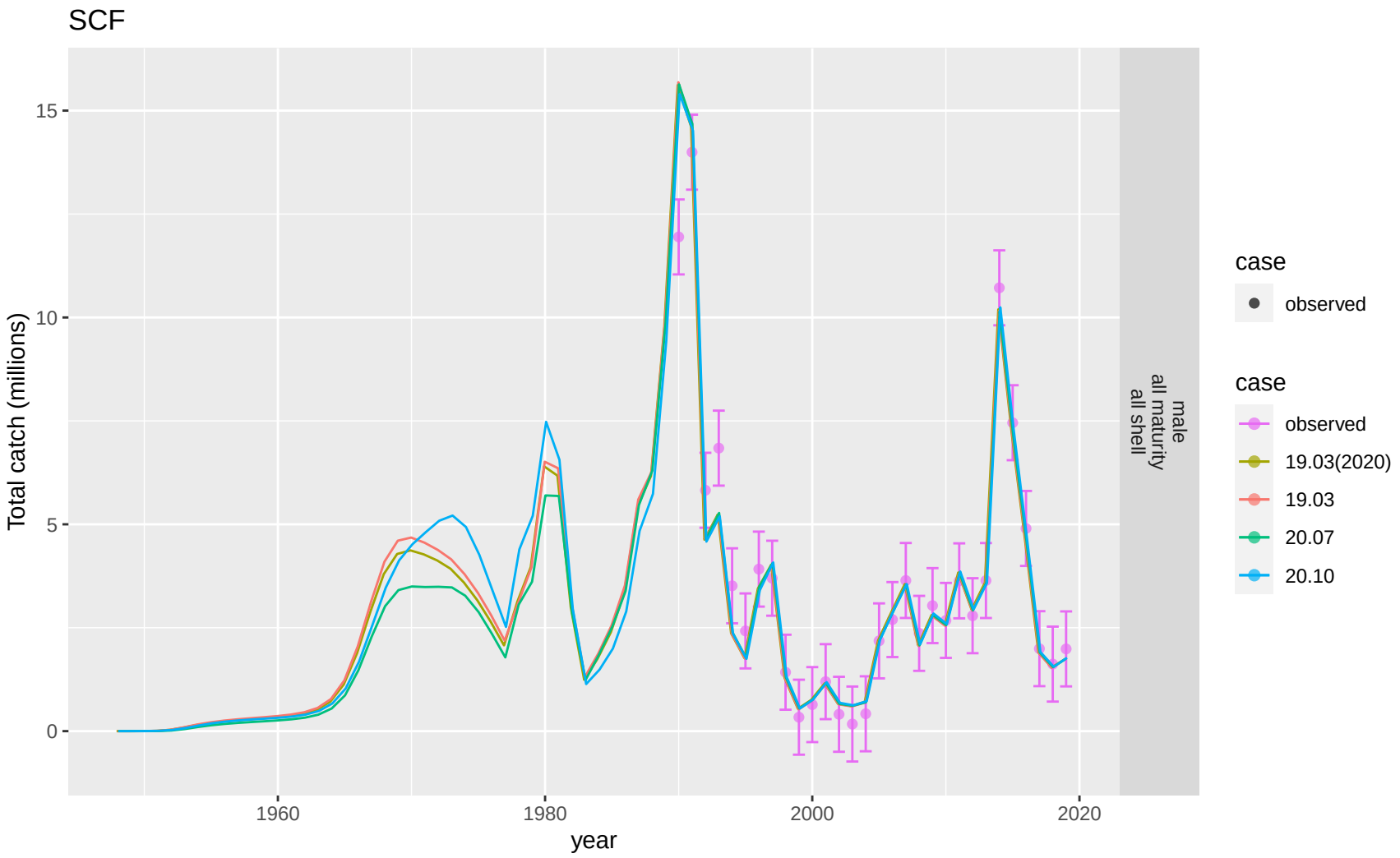

Figure 40: Comparison of observed and predicted male total catch abundance for SCF.

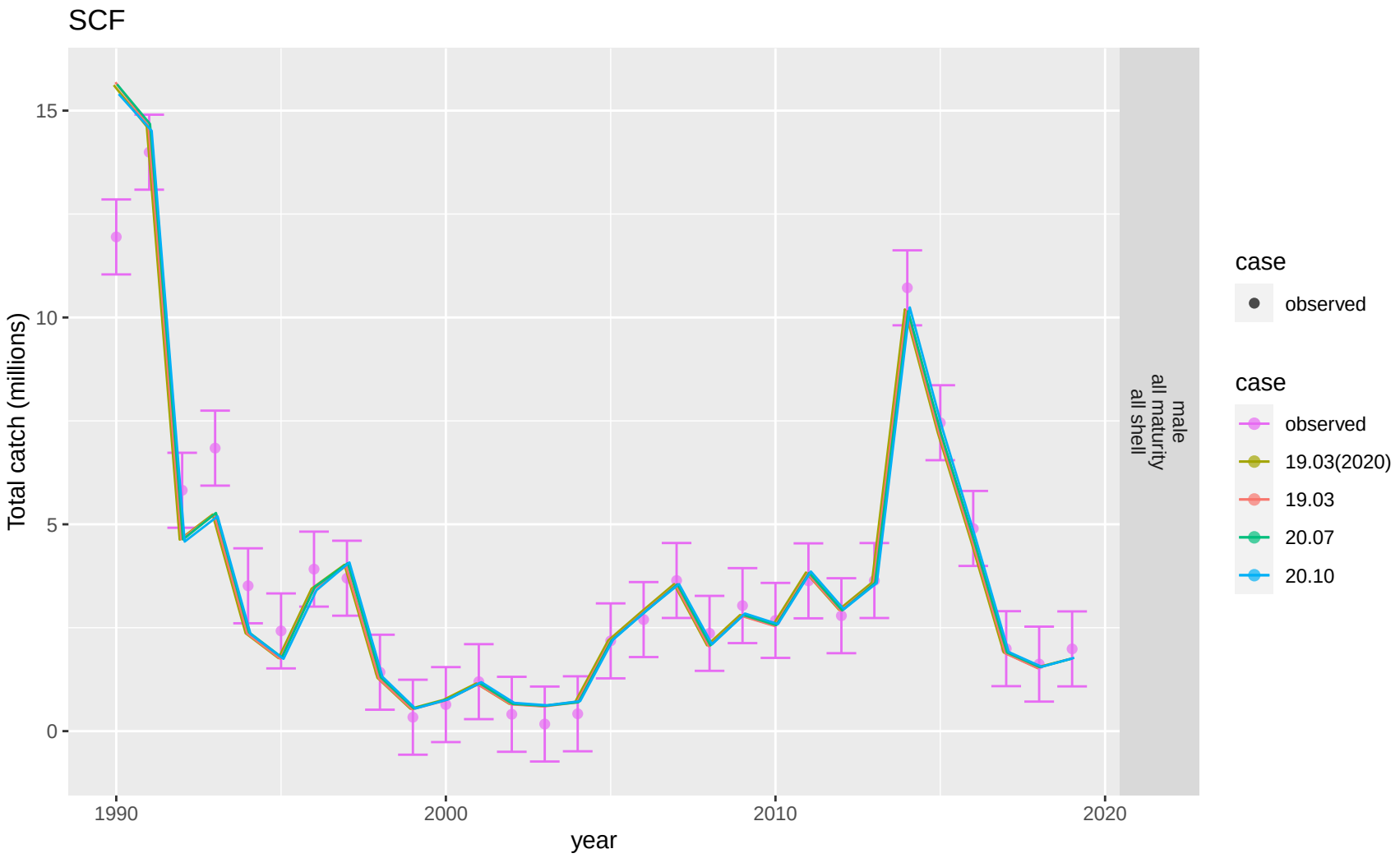

Figure 41: Comparison of observed and predicted male total catch abundance for SCF. Observed time period.

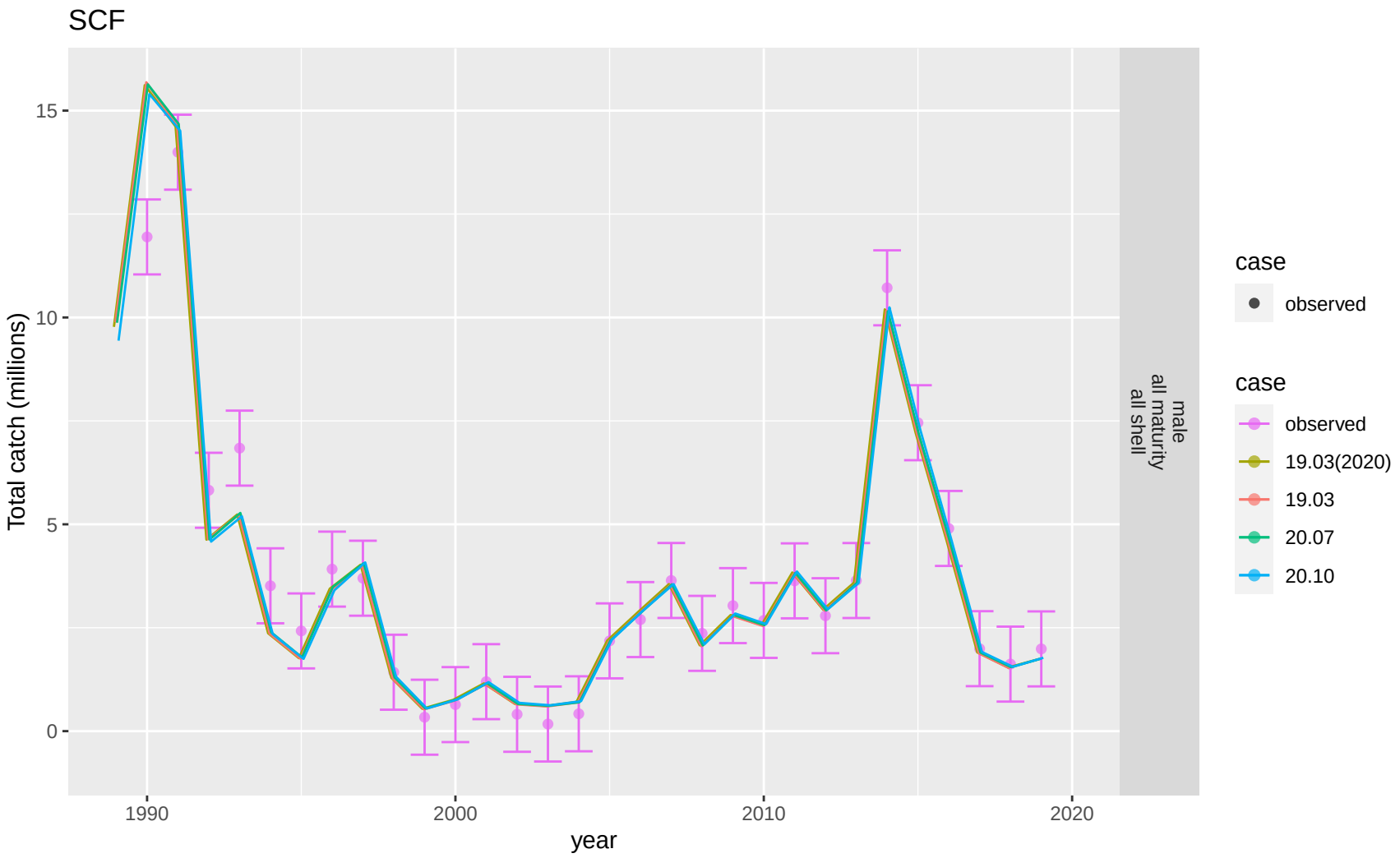

Figure 42: Comparison of observed and predicted male total catch abundance for SCF. Recent time period.

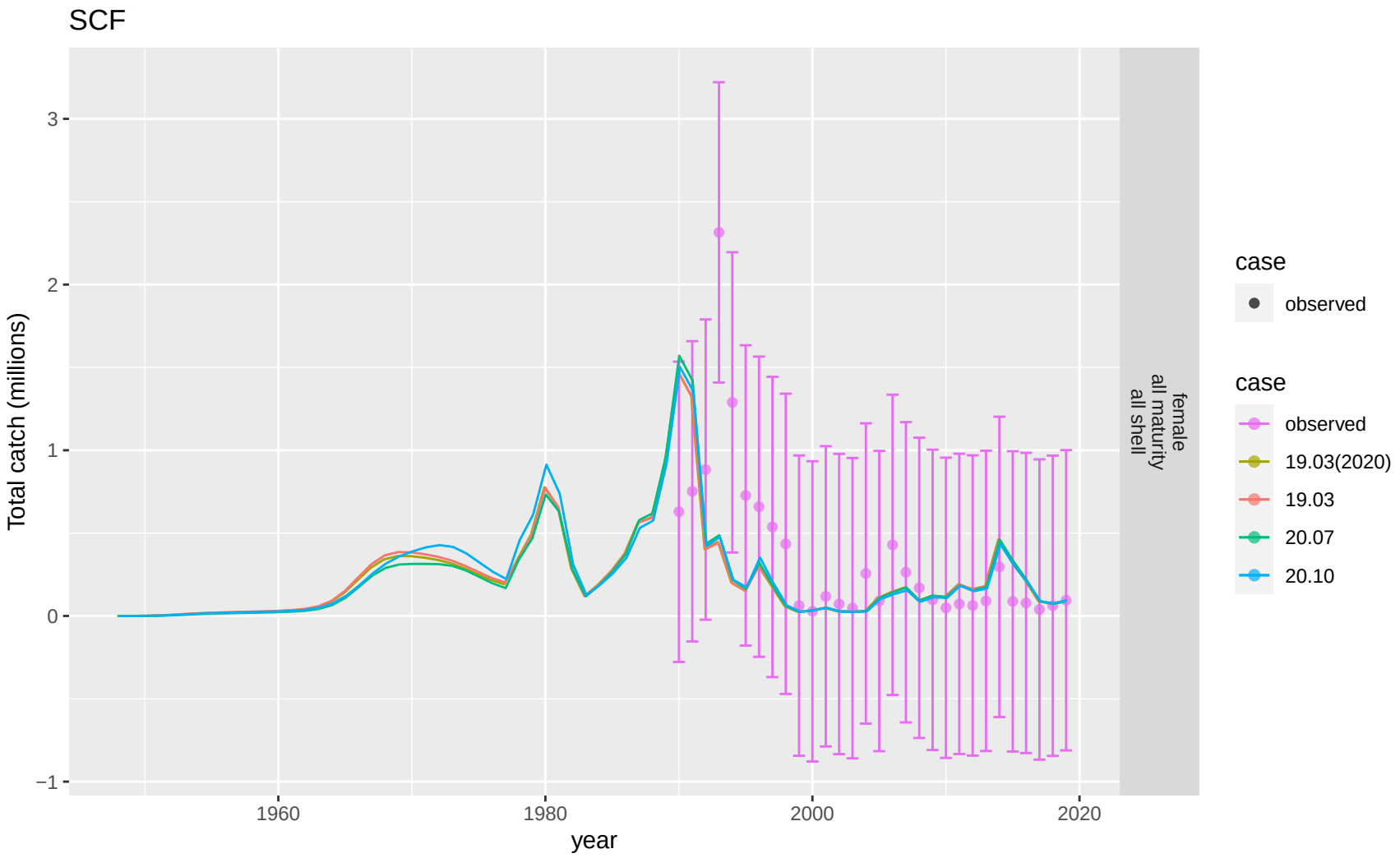

Figure 43: Comparison of observed and predicted female total catch abundance for SCF.

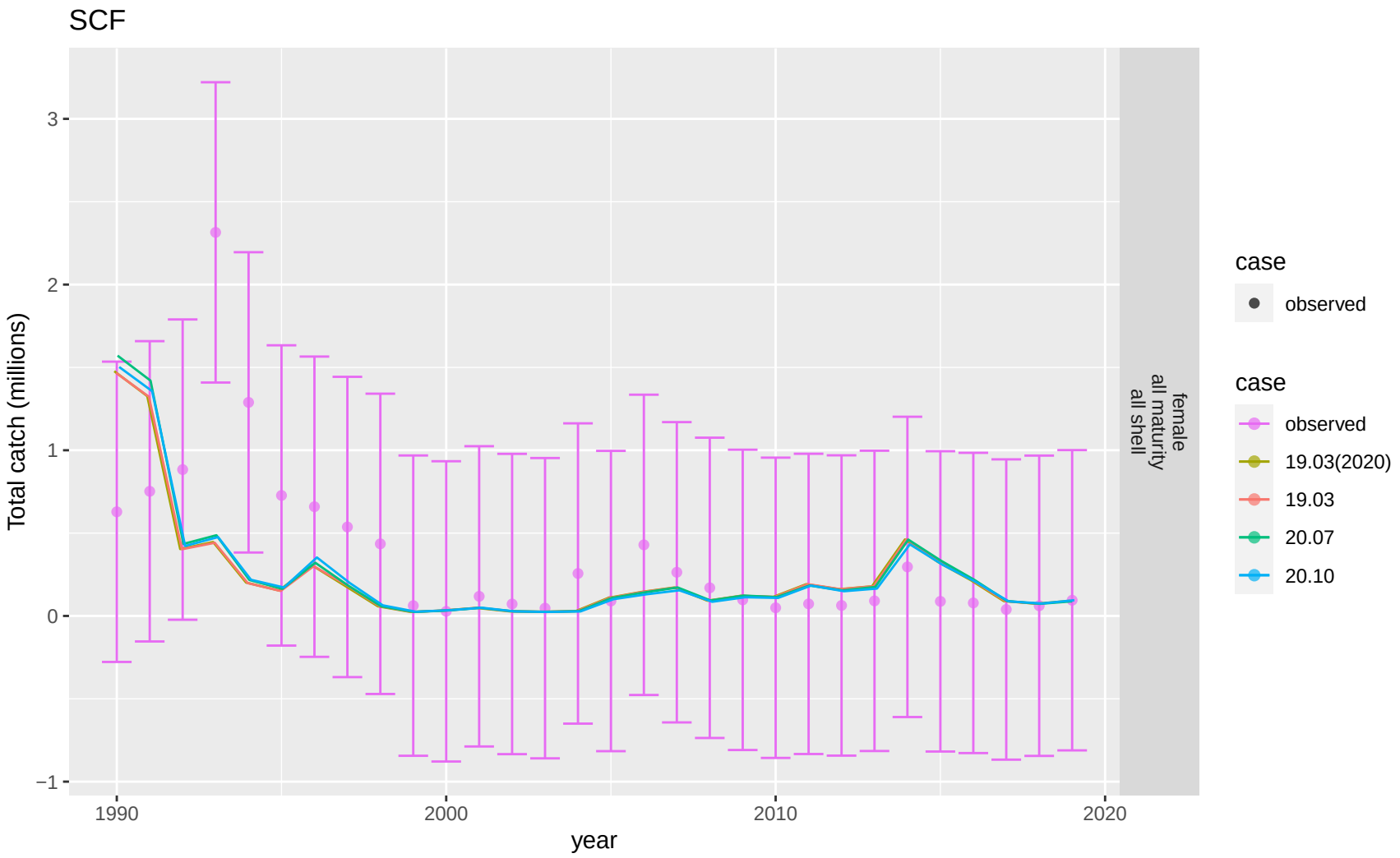

Figure 44: Comparison of observed and predicted female total catch abundance for SCF. Observed time period.

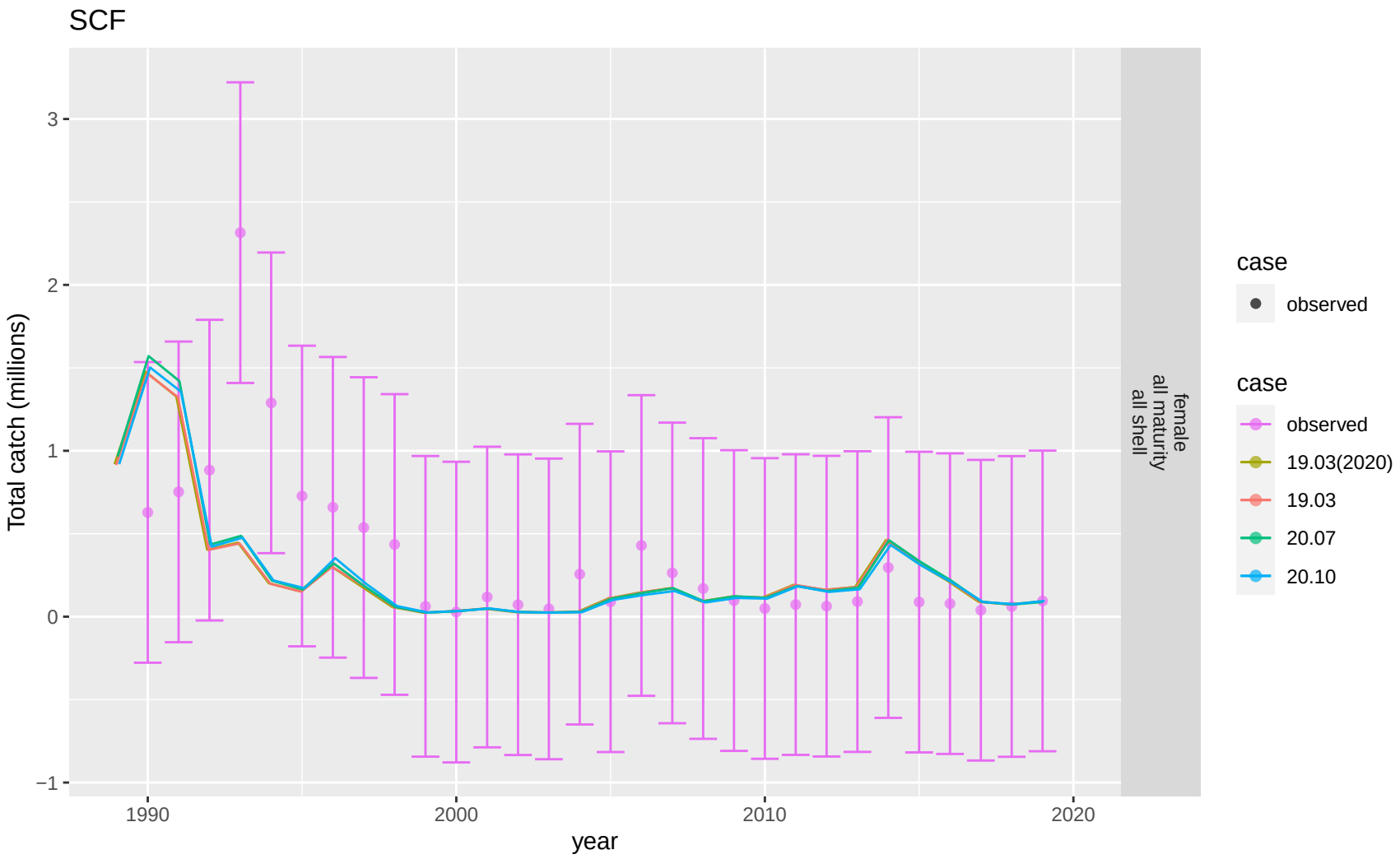

Figure 45: Comparison of observed and predicted female total catch abundance for SCF. Recent time period.

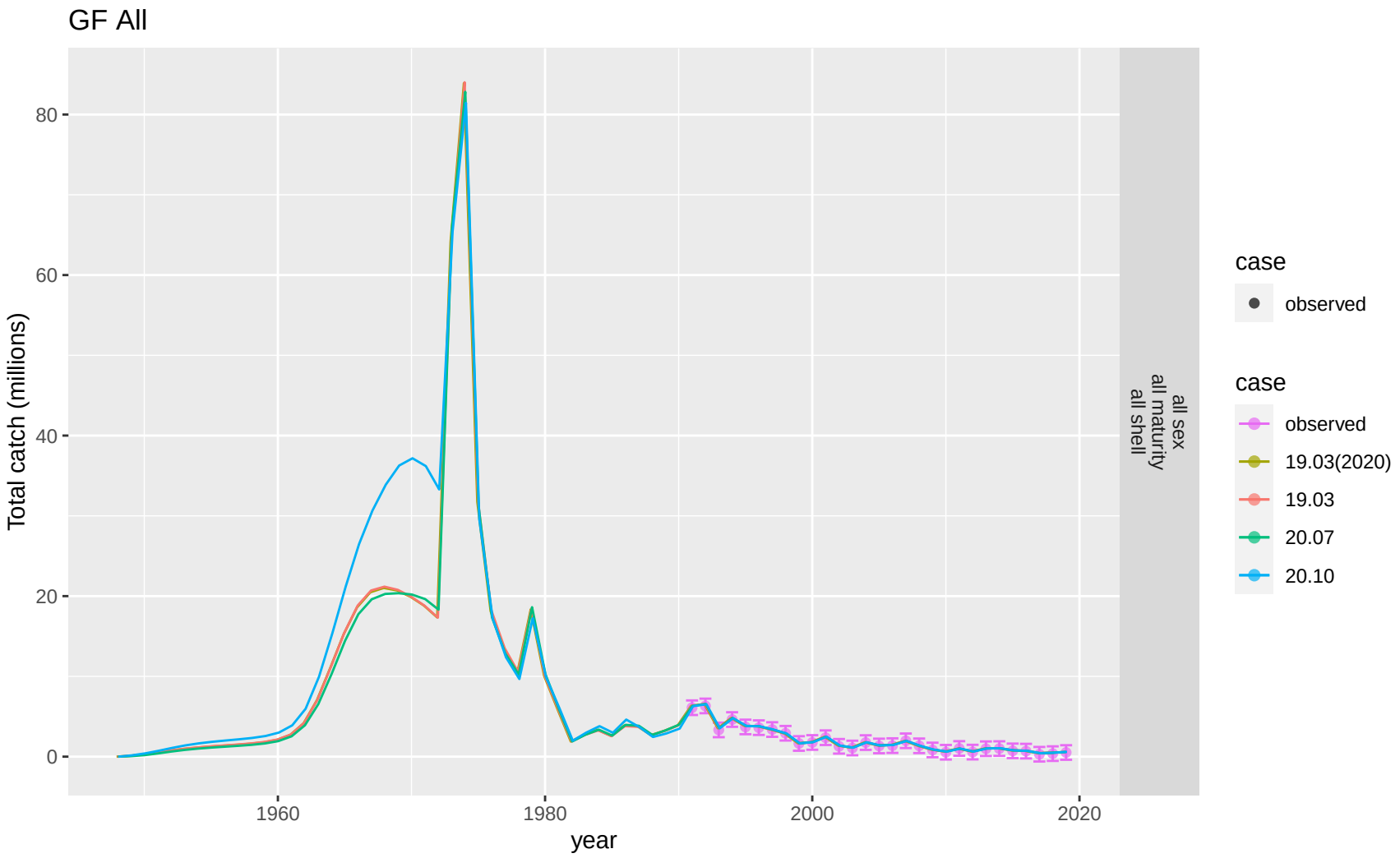

Figure 46: Comparison of observed and predicted all sex total catch abundance for GF All.

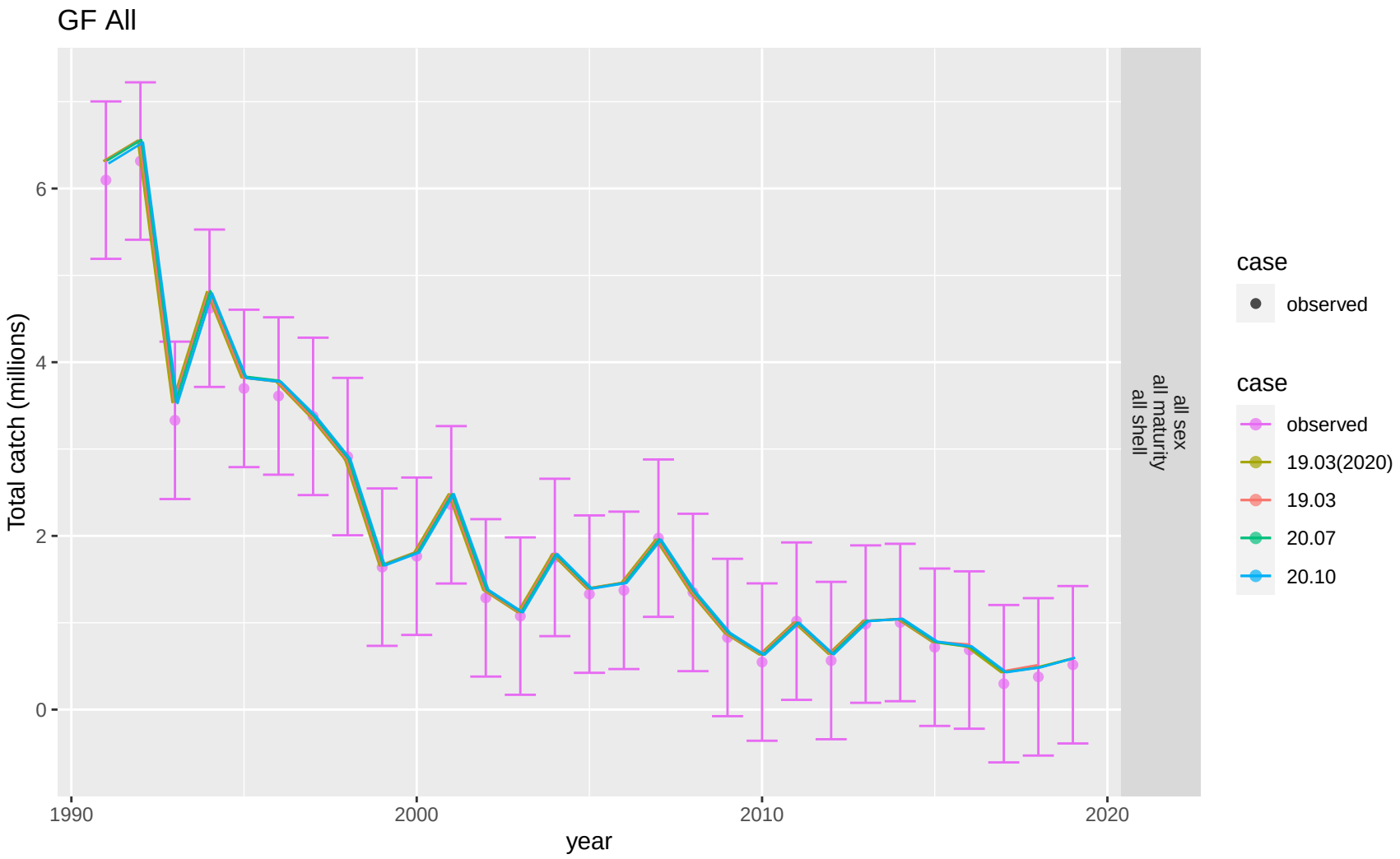

Figure 47: Comparison of observed and predicted all sex total catch abundance for GF All. Observed time period.

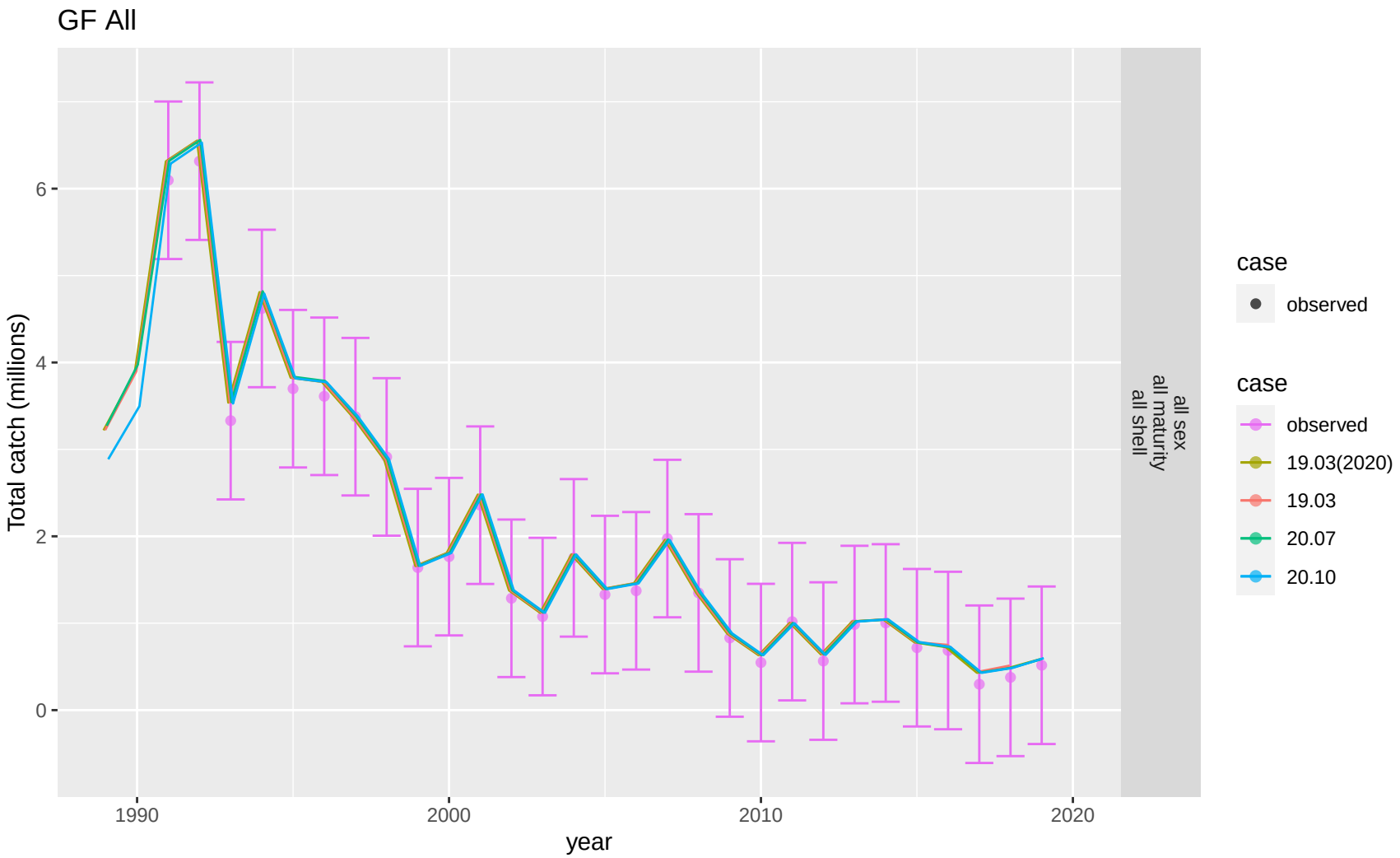

Figure 48: Comparison of observed and predicted all sex total catch abundance for GF All. Recent time period.

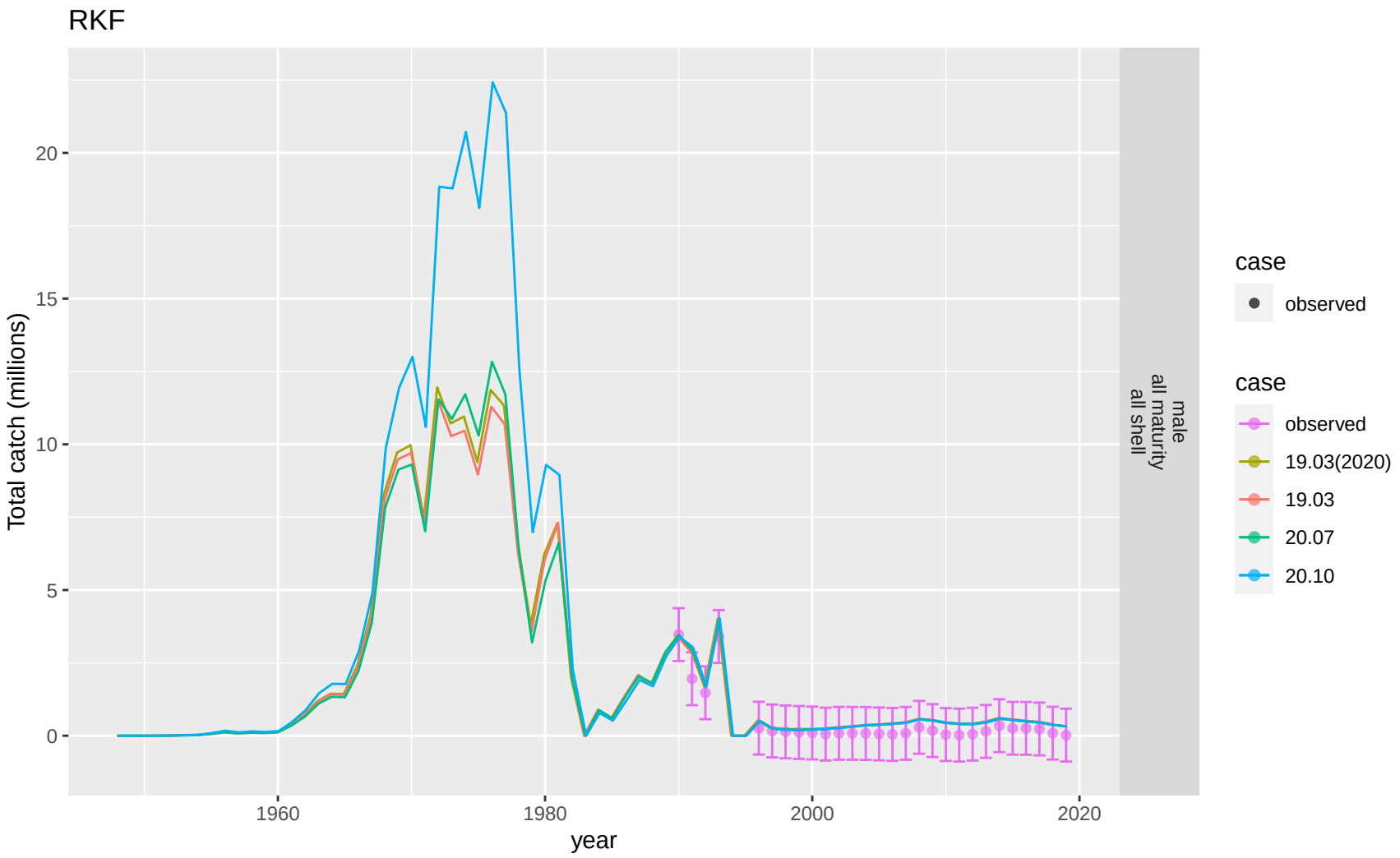

Figure 49: Comparison of observed and predicted male total catch abundance for RKF.

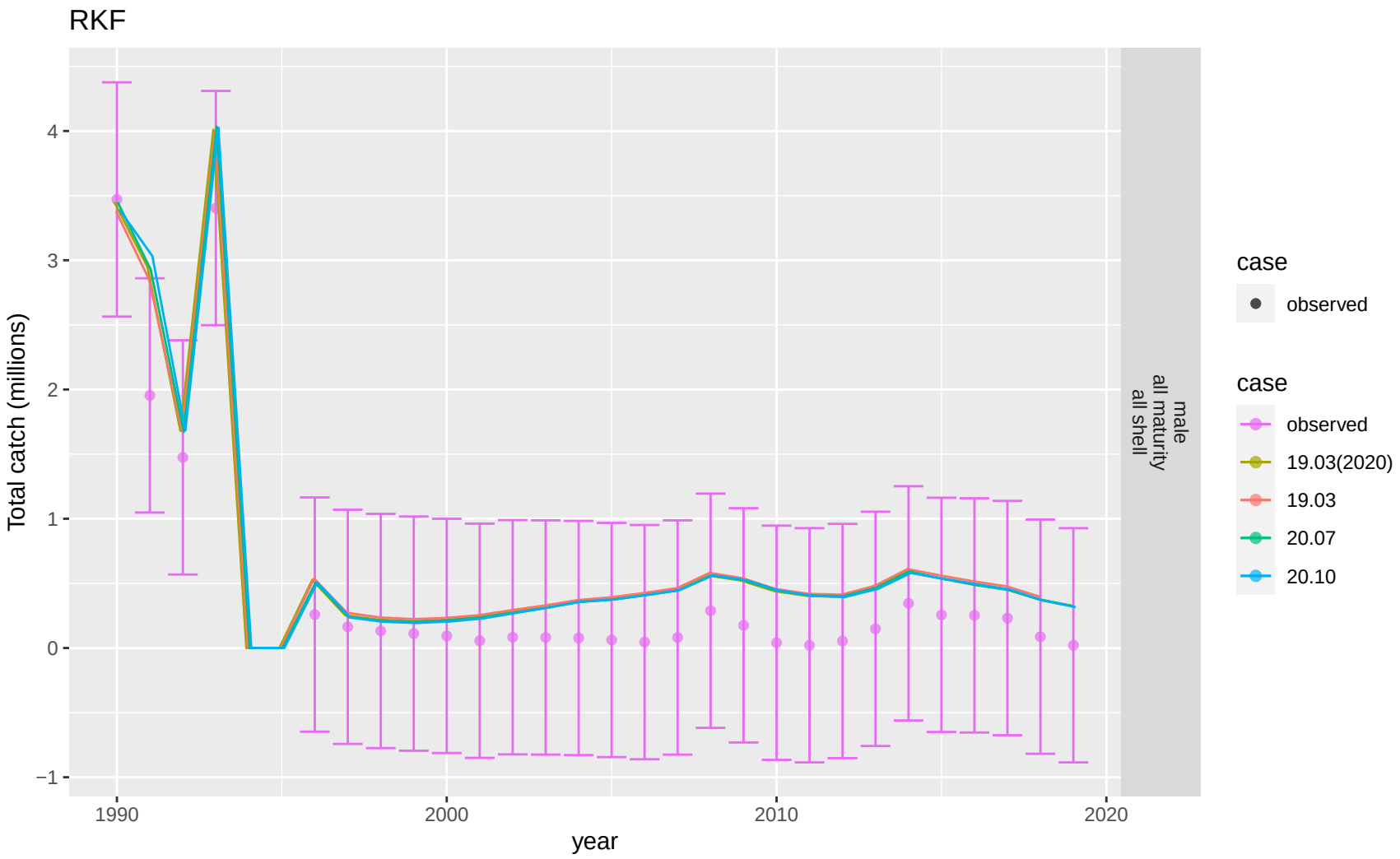

Figure 50: Comparison of observed and predicted male total catch abundance for RKF. Observed time period.

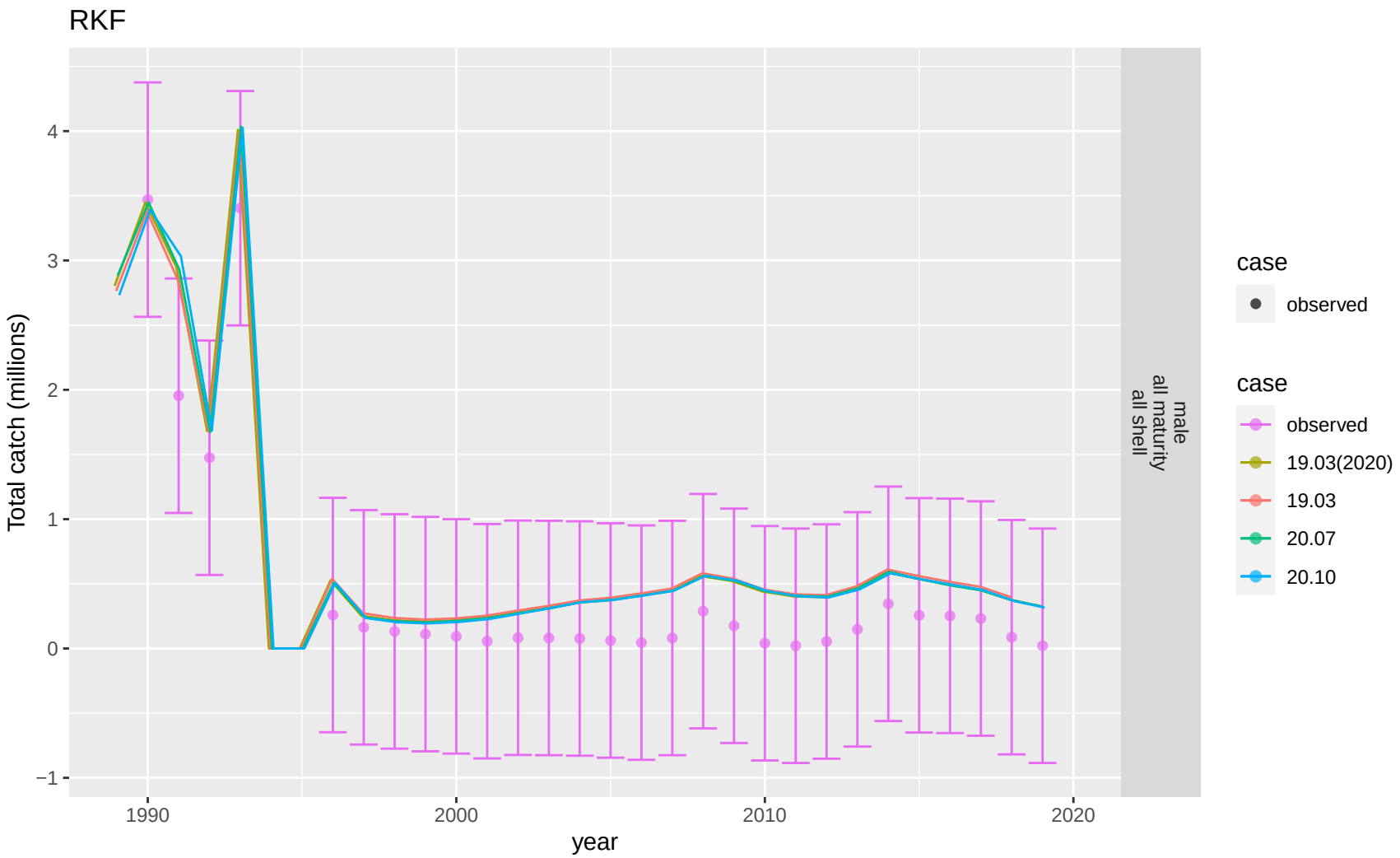

Figure 51: Comparison of observed and predicted male total catch abundance for RKF. Recent time period.

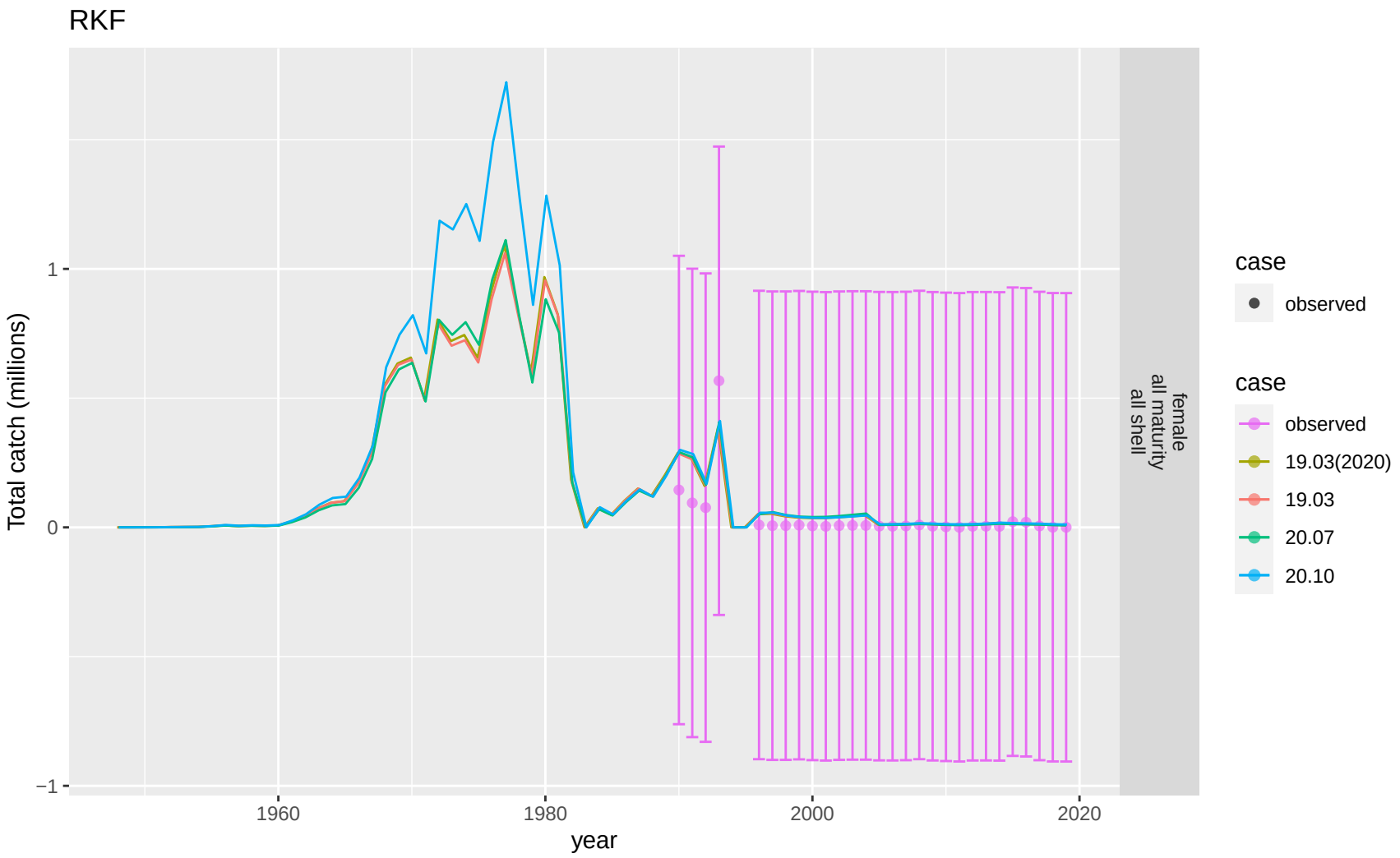

Figure 52: Comparison of observed and predicted female total catch abundance for RKF.

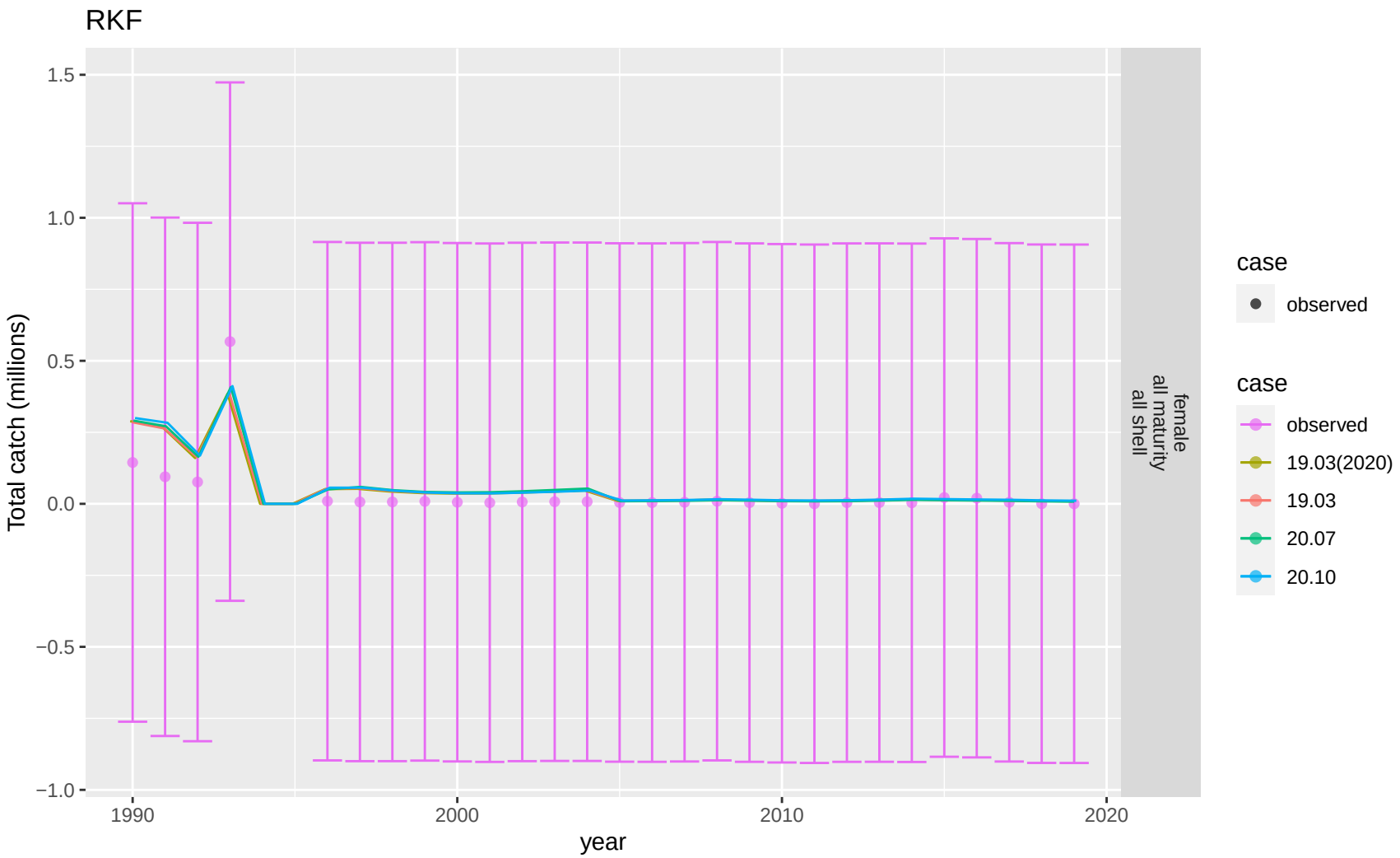

Figure 53: Comparison of observed and predicted female total catch abundance for RKF. Observed time period.

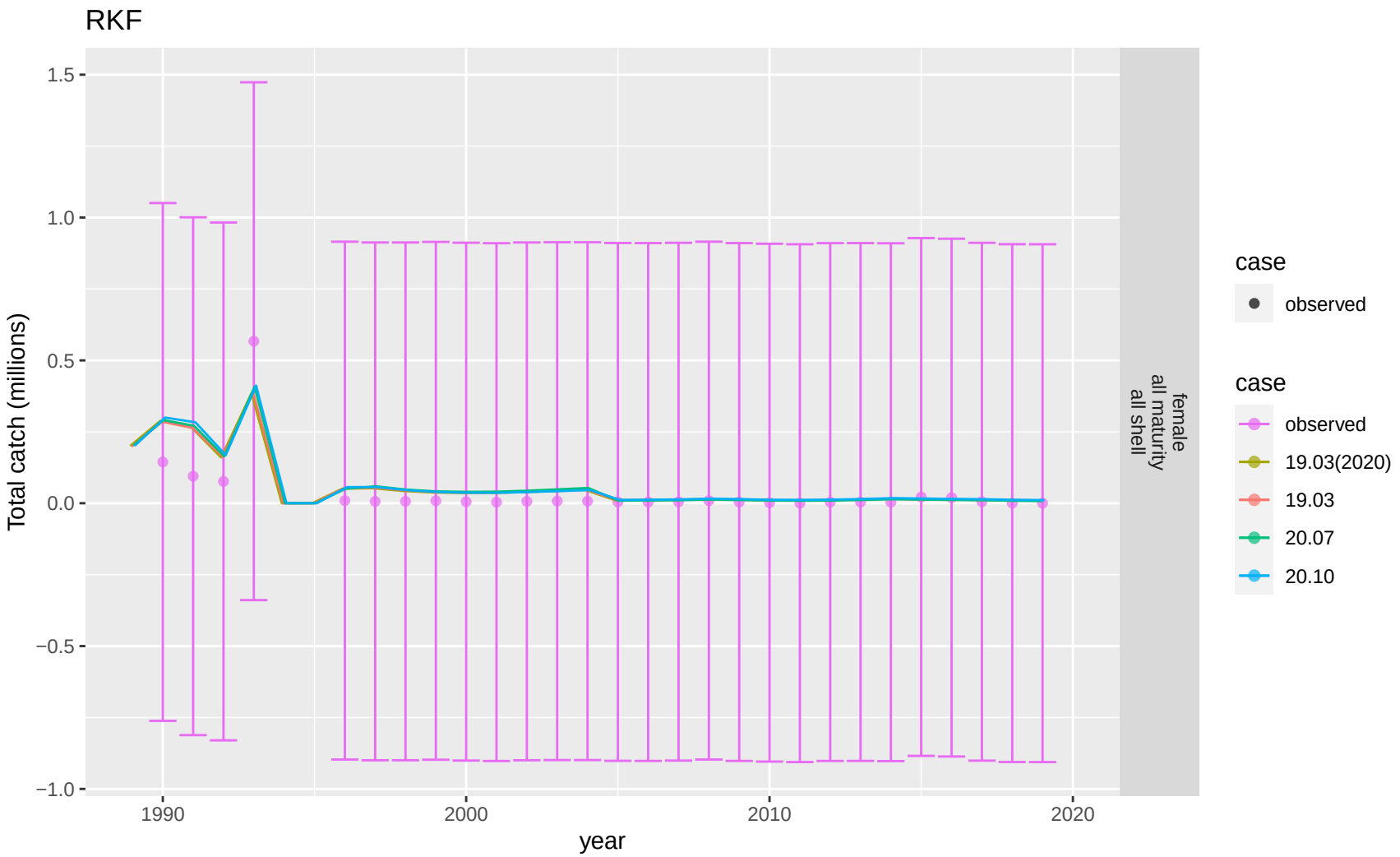

Figure 54: Comparison of observed and predicted female total catch abundance for RKF. Recent time period.

Z-scores

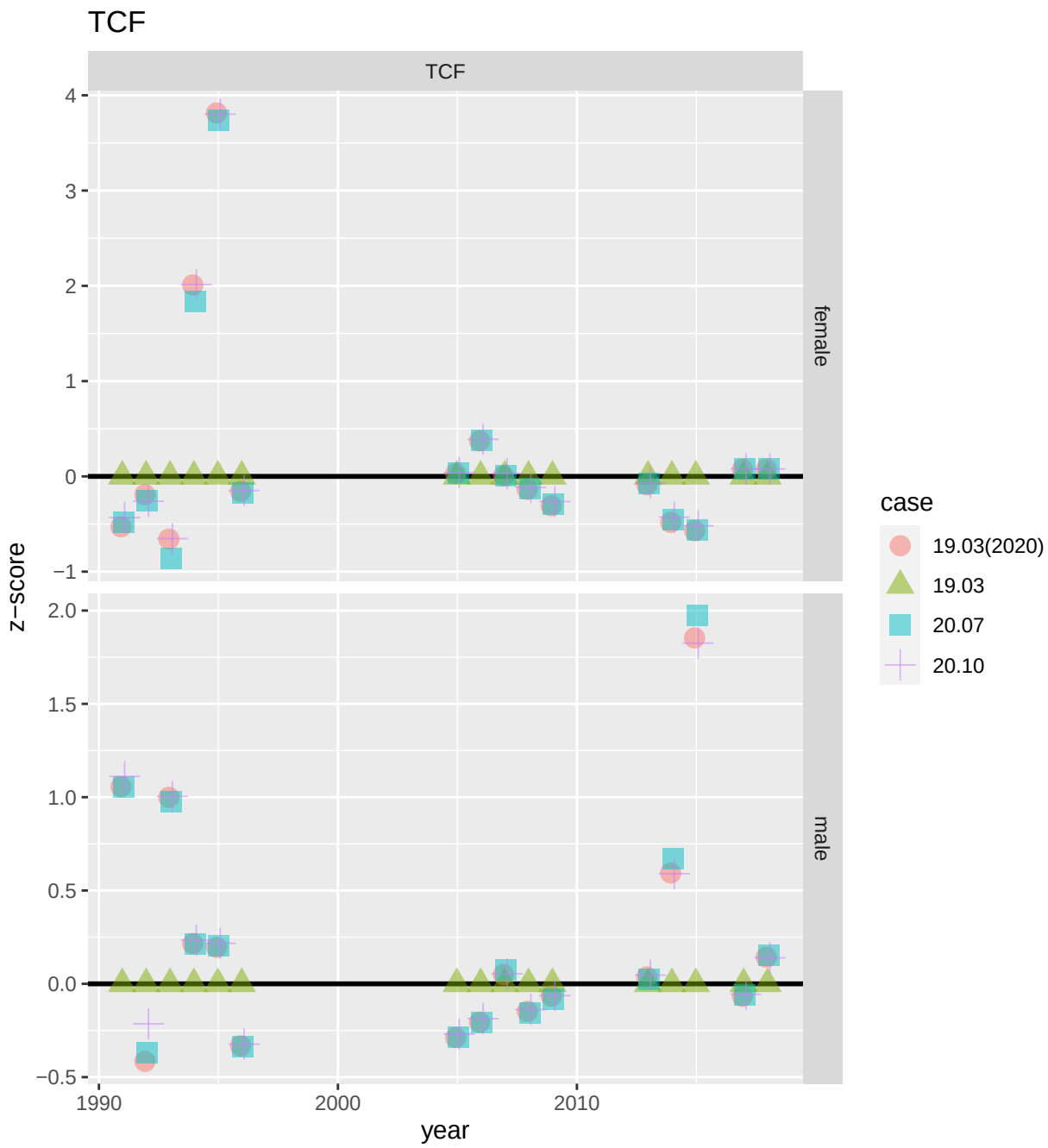

Figure 55: Z-scores for total catch abundance in TCF.

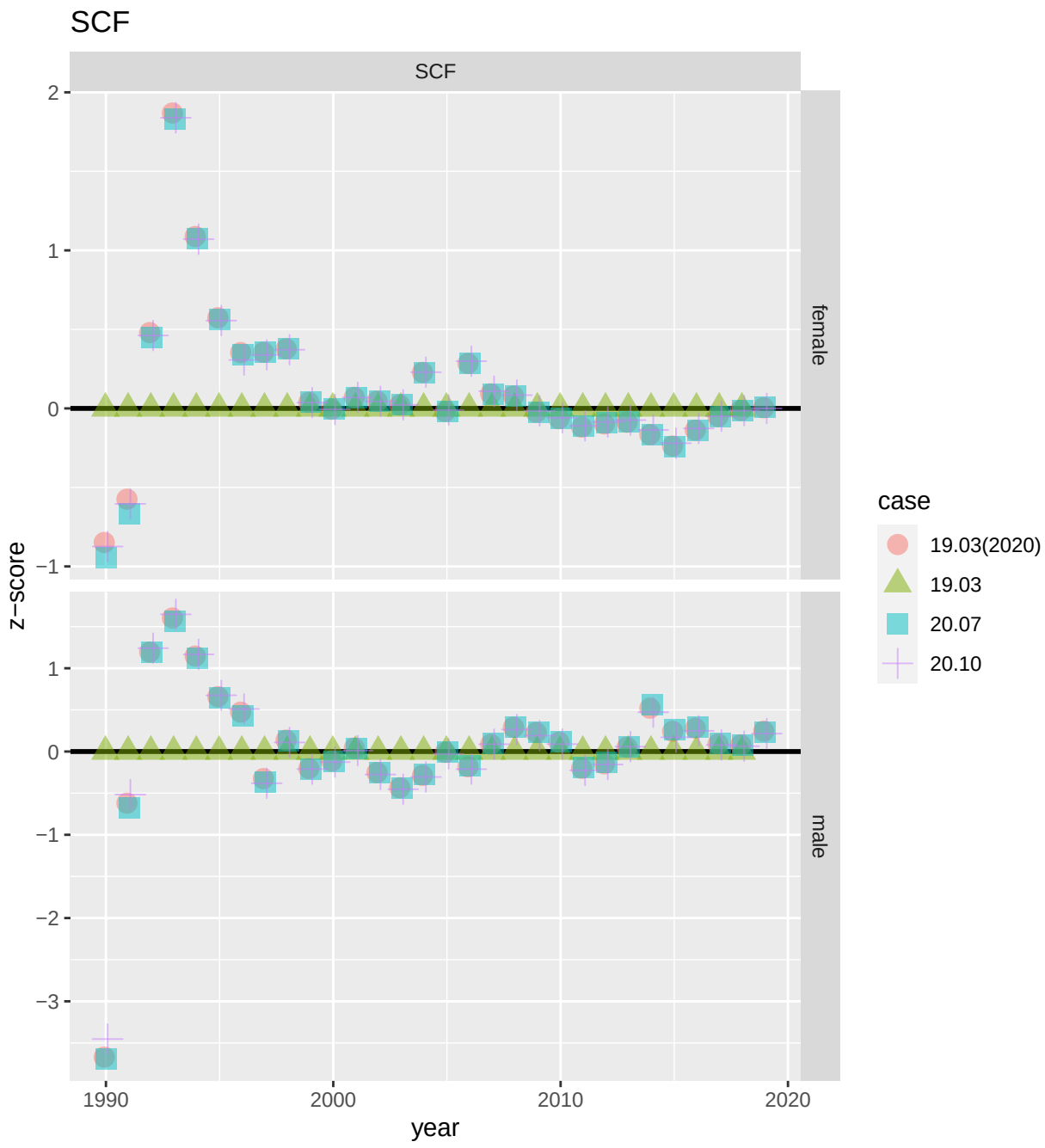

Figure 56: Z-scores for total catch abundance in SCF.

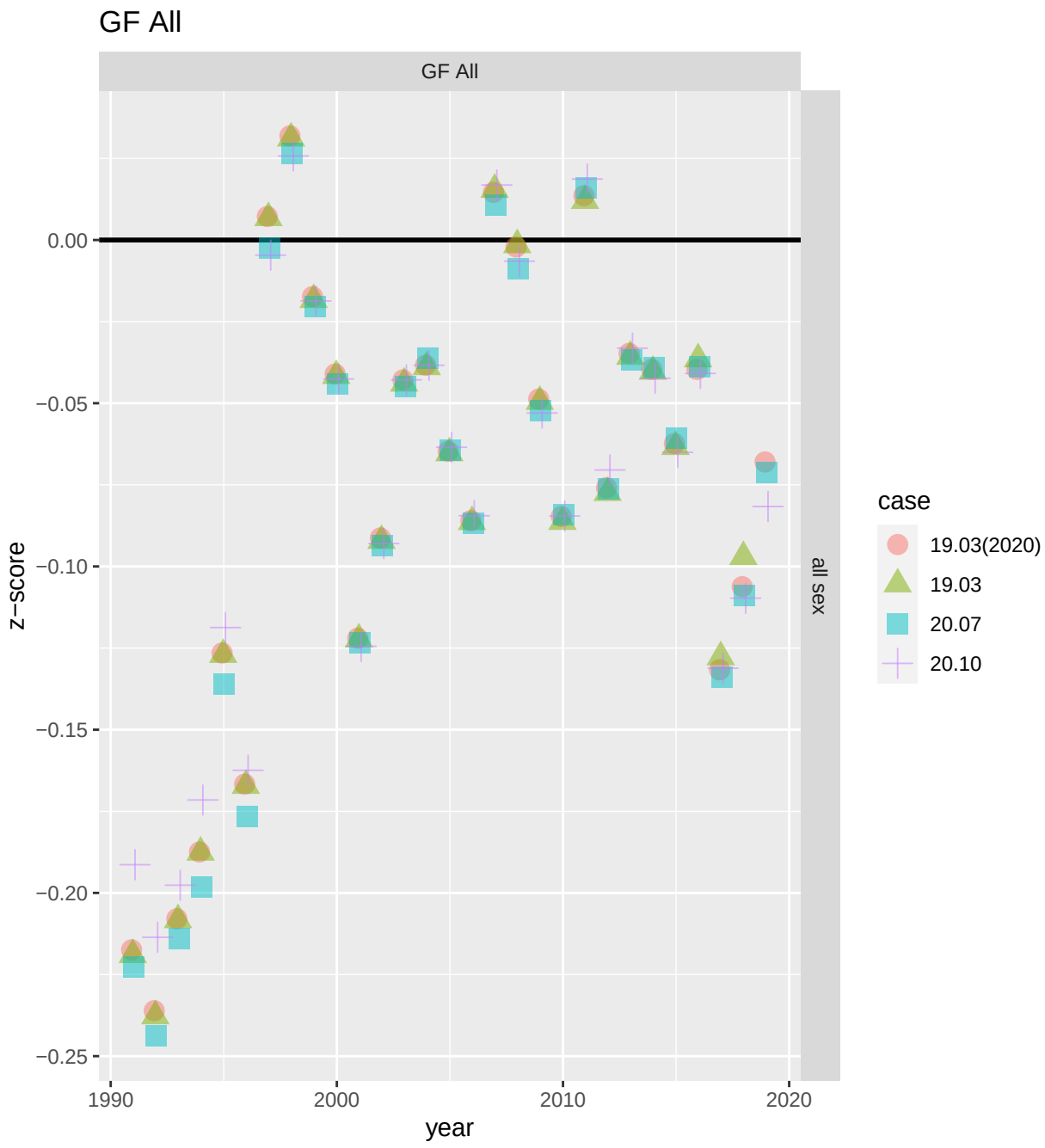

Figure 57: Z-scores for total catch abundance in GF All.

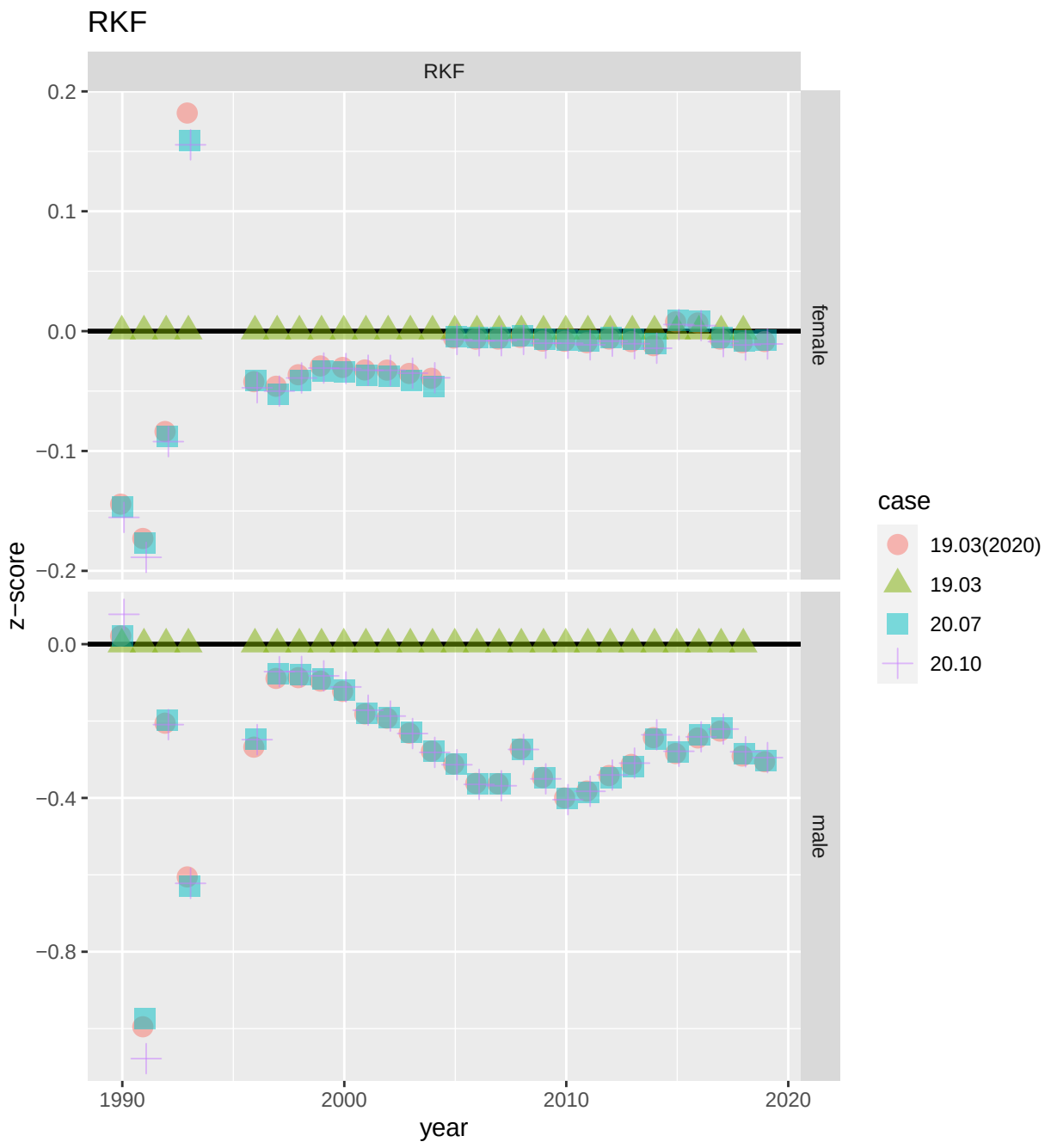

Figure 58: Z-scores for total catch abundance in RKF.

Appendix 6: Fits to Aggregated Survey Catch Data – 19.03(2020) vs 19.03 vs 20.07 vs 20.10

William Stockhausen

01 September, 2020

Contents

Model fits to aggregated survey catch data

Fits to the aggregated survey catch data available to the model(s) are presented in this section. Not all of the fits presented are necessarily included in the parameter optimization for each model; some fits to datasets for a particular model may be included for comparison purposes with other models which include those data in their optimization. The reader should consult the main assessment document to determine which fits are included in the optimization for any particular model.

Survey biomass

Fits

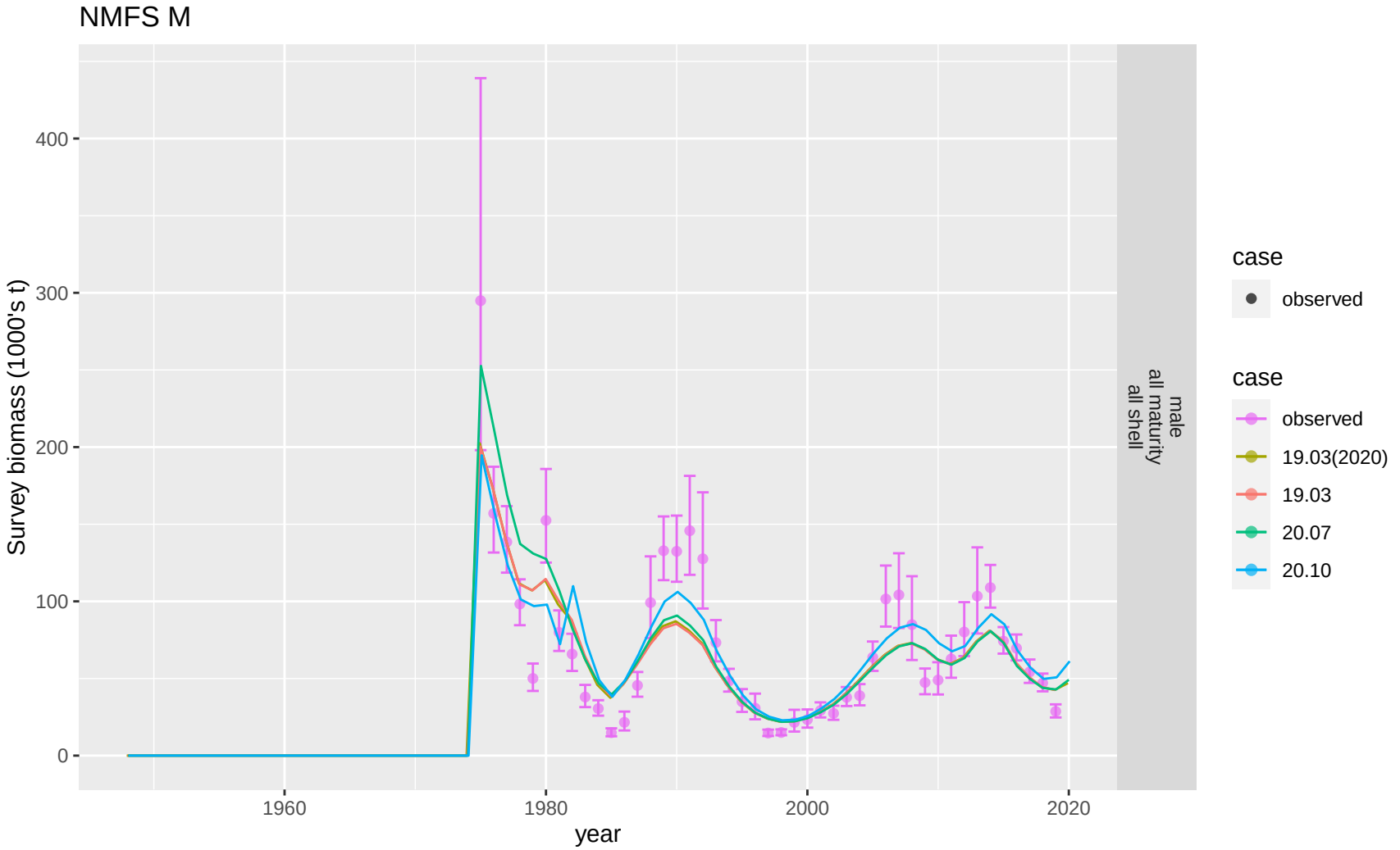

Figure 1: Comparison of observed and predicted male survey biomass for NMFS M.

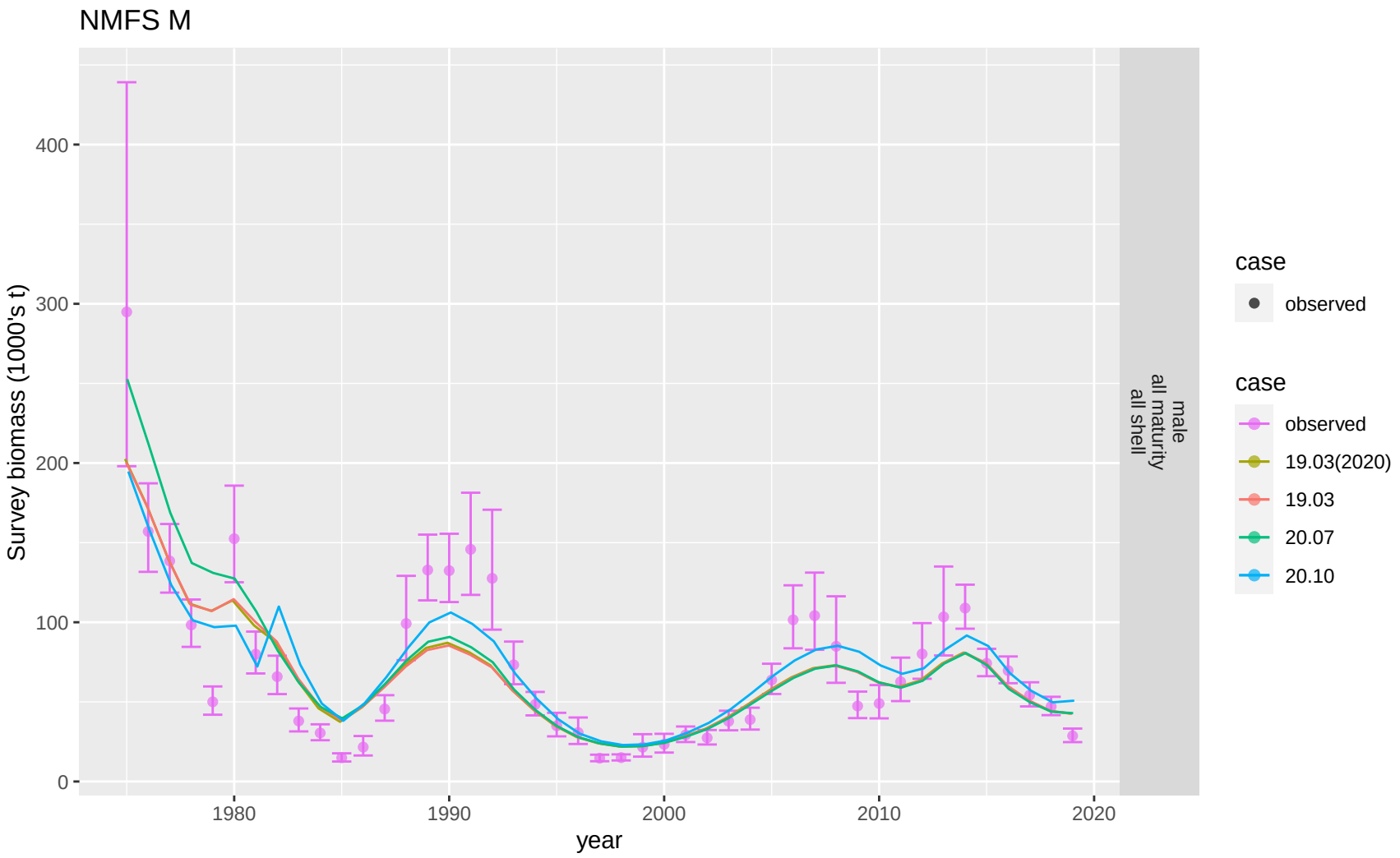

Figure 2: Comparison of observed and predicted male survey biomass for NMFS M. Observed time period.

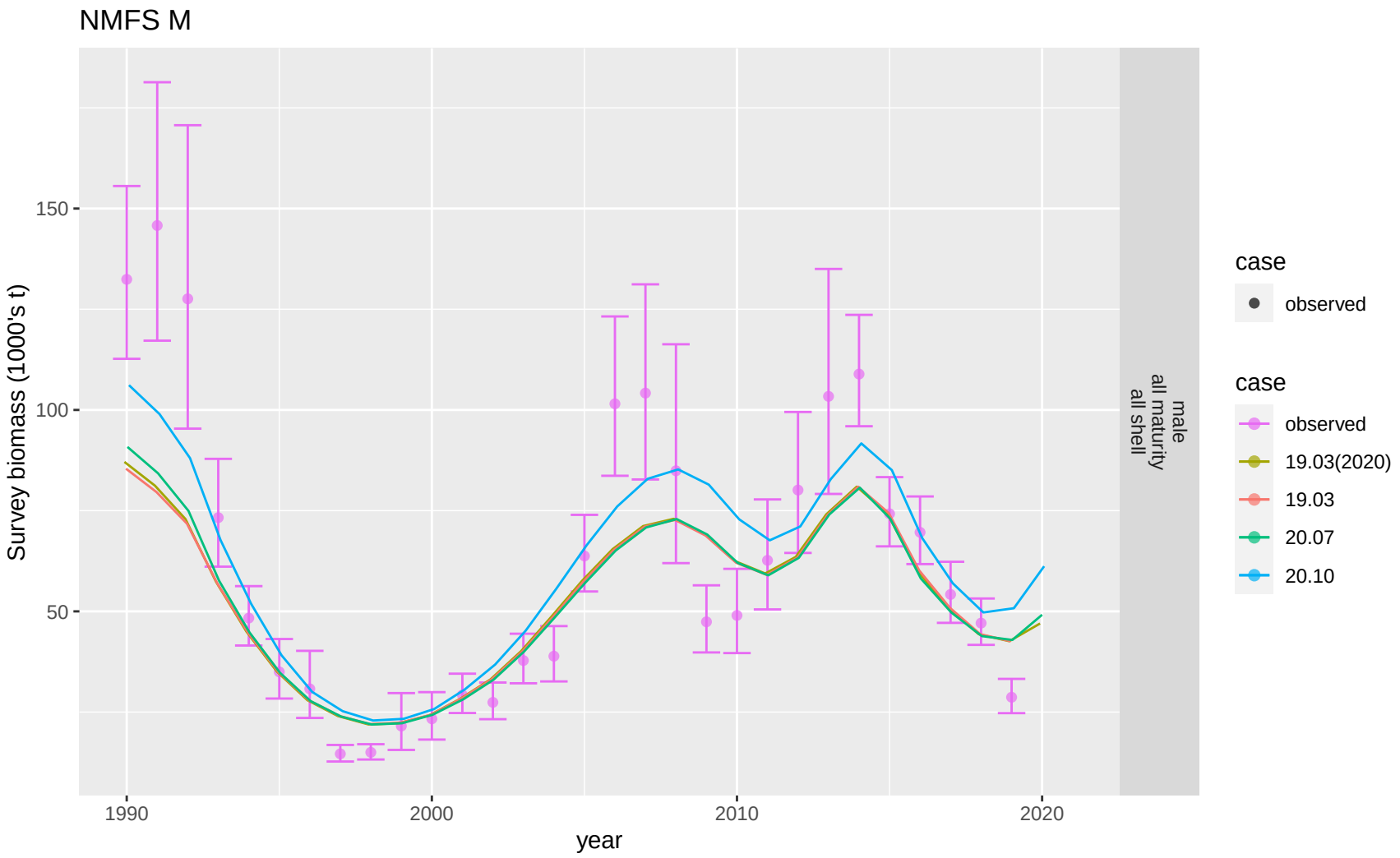

Figure 3: Comparison of observed and predicted male survey biomass for NMFS M. Recent time period.

Figure 4: Comparison of observed and predicted female survey biomass for NMFS F.

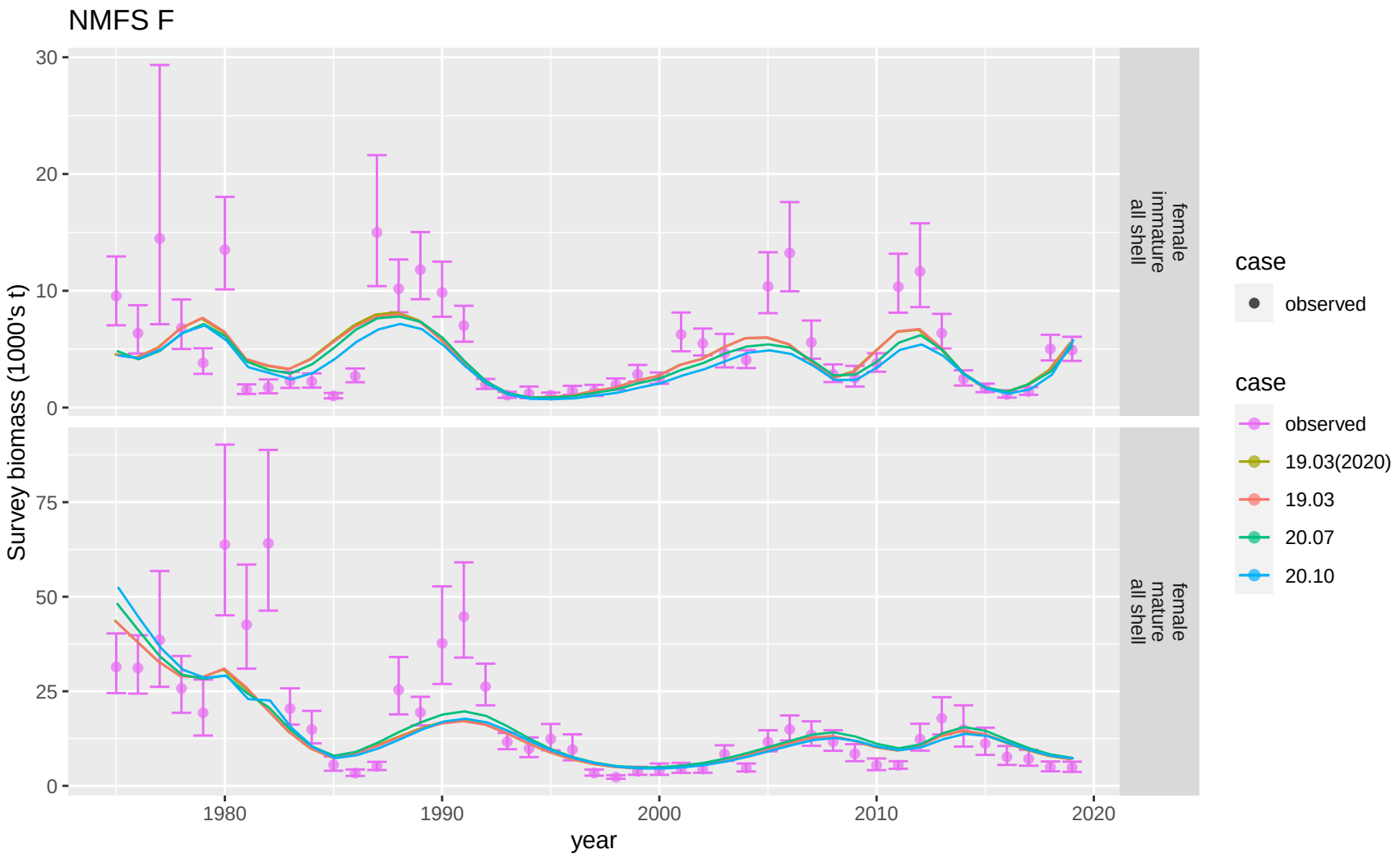

Figure 5: Comparison of observed and predicted female survey biomass for NMFS F. Observed time period.

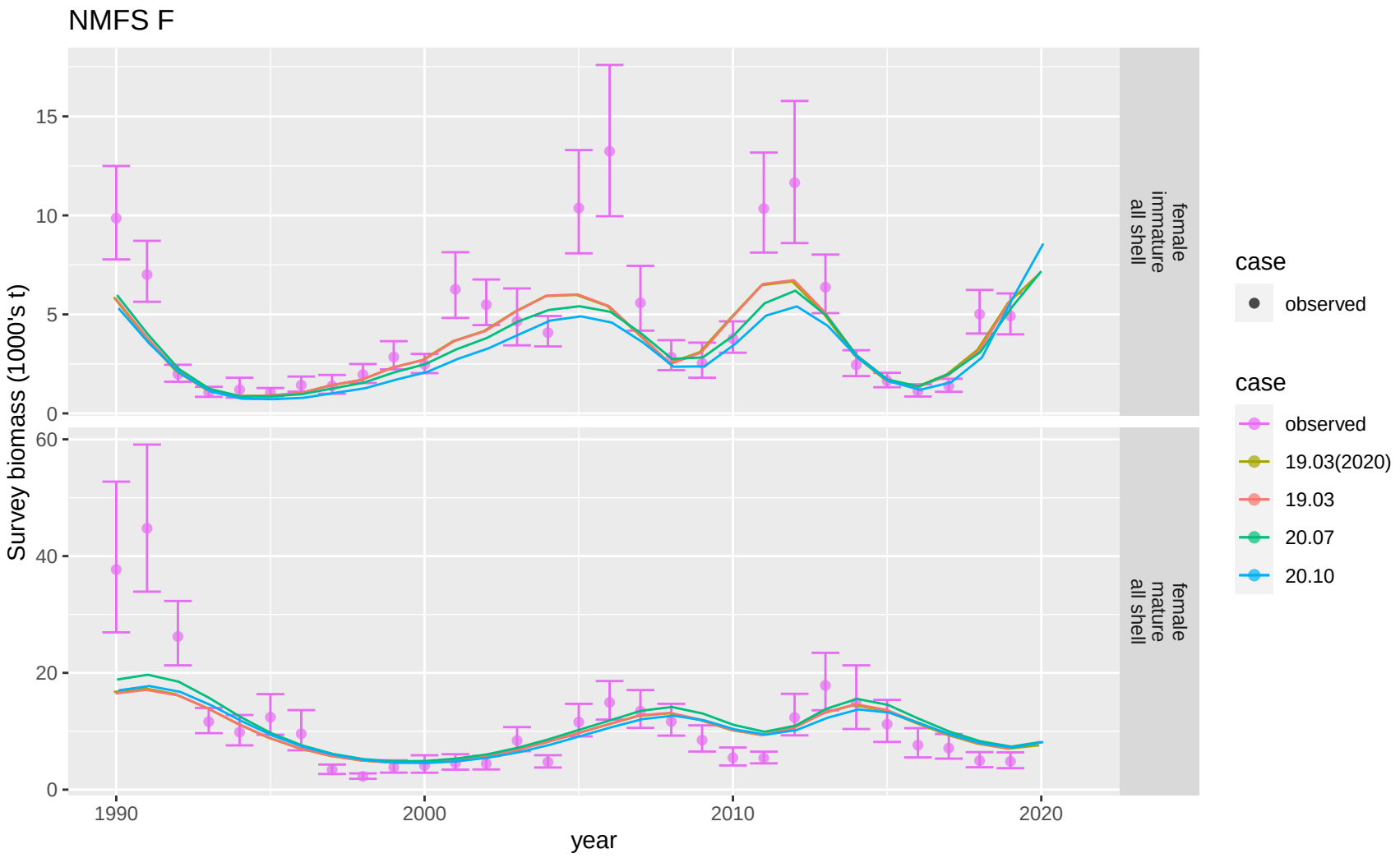

Figure 6: Comparison of observed and predicted female survey biomass for NMFS F. Recent time period.

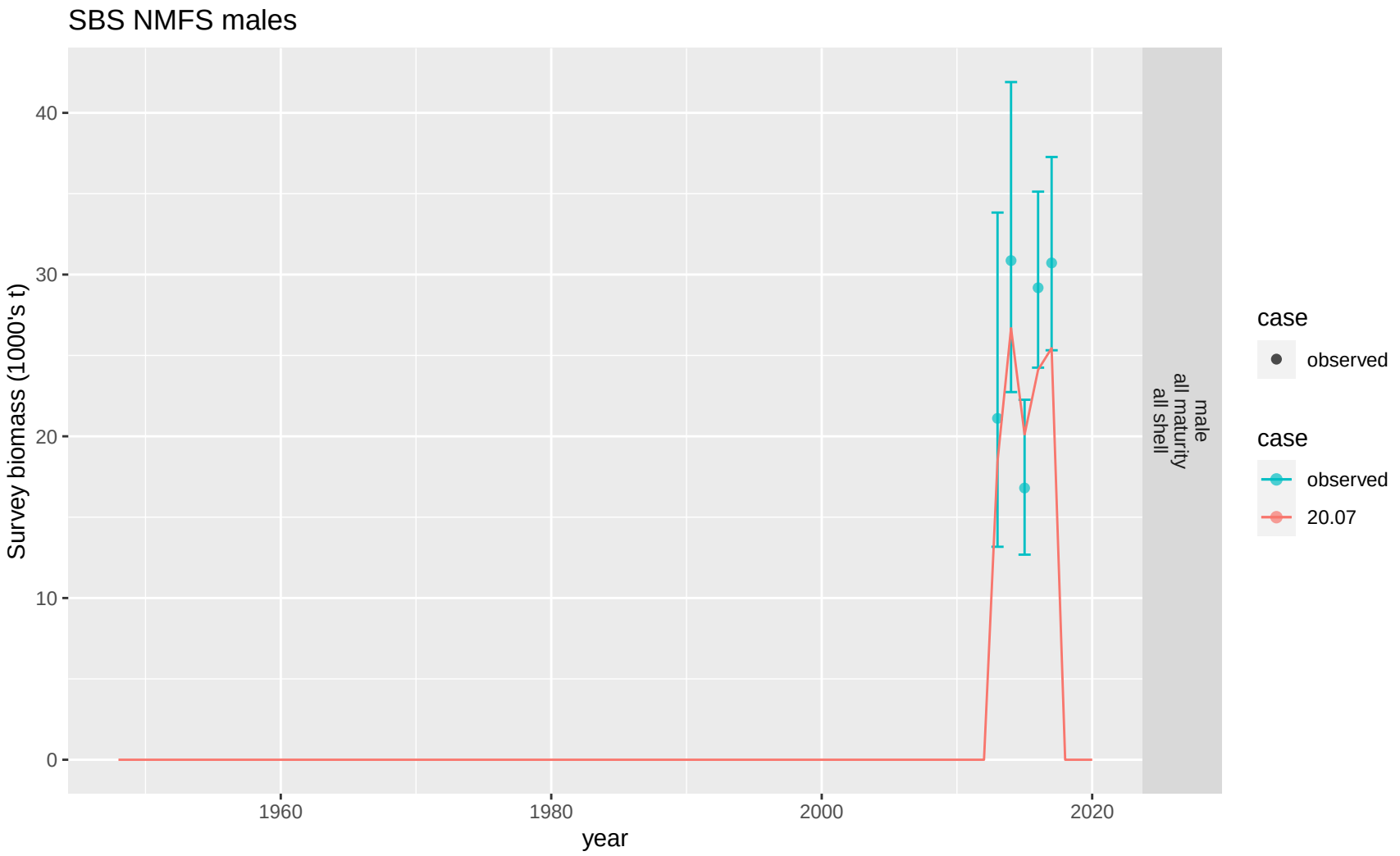

Figure 7: Comparison of observed and predicted male survey biomass for SBS NMFS males.

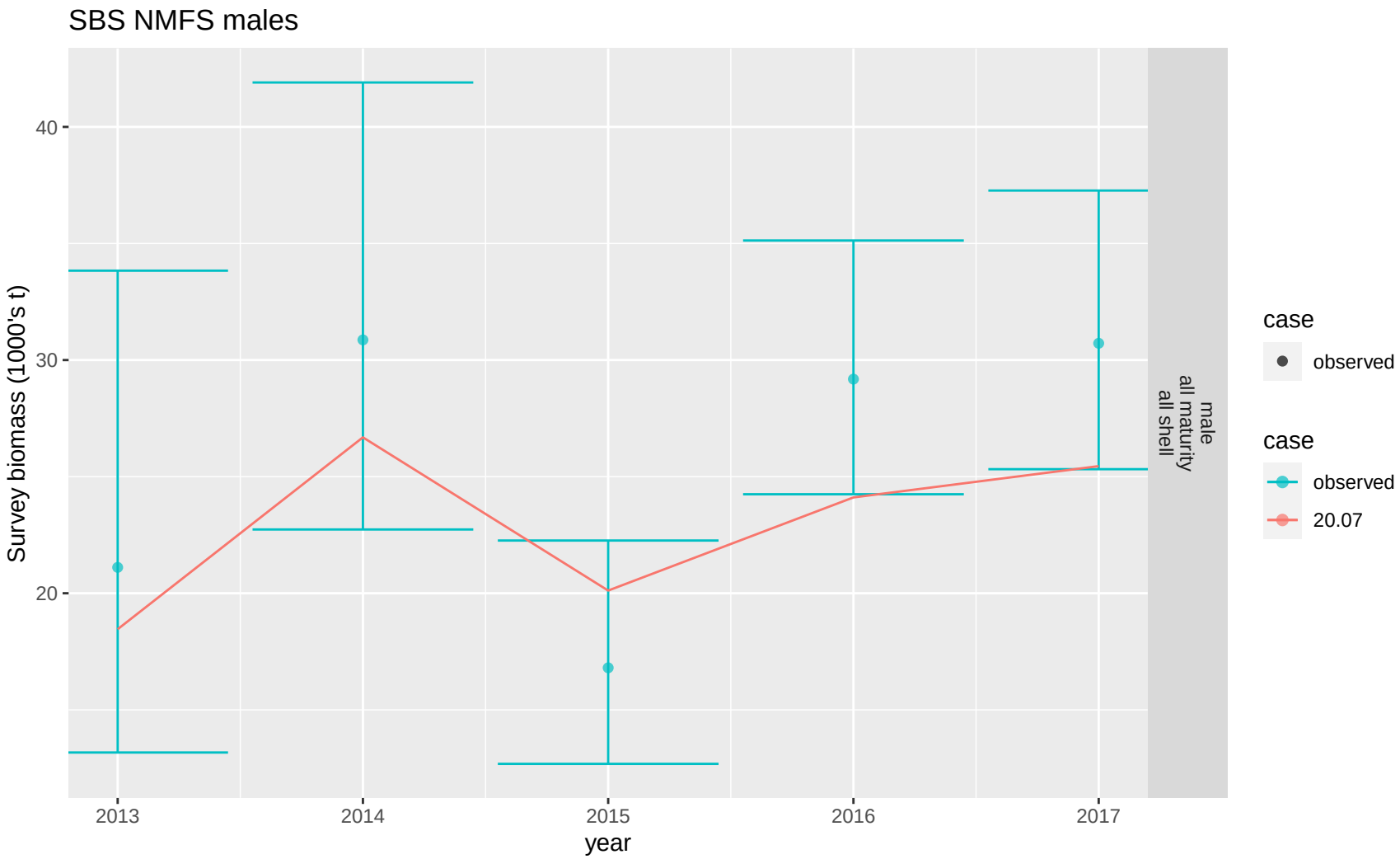

Figure 8: Comparison of observed and predicted male survey biomass for SBS NMFS males. Observed time period.

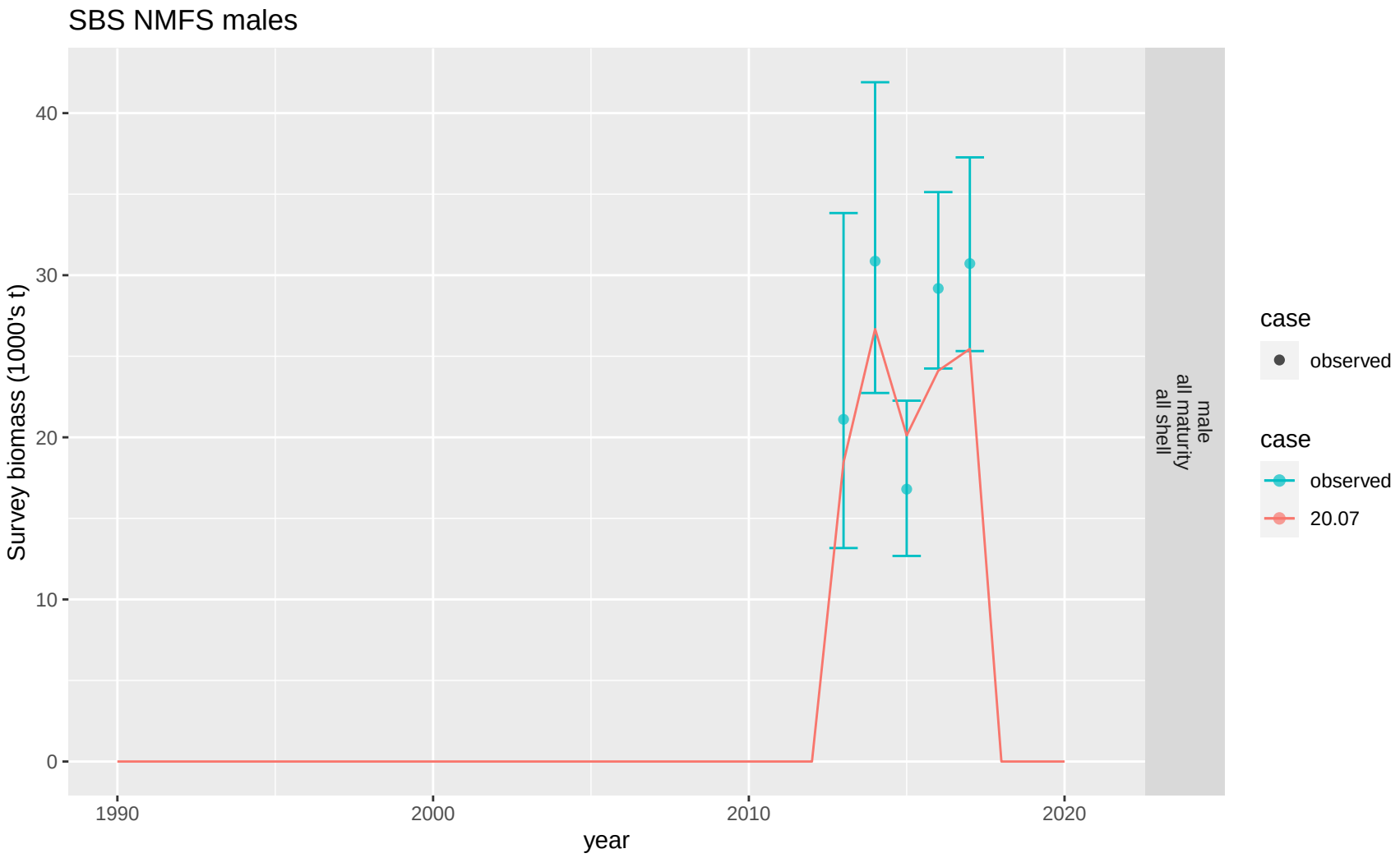

Figure 9: Comparison of observed and predicted male survey biomass for SBS NMFS males. Recent time period.

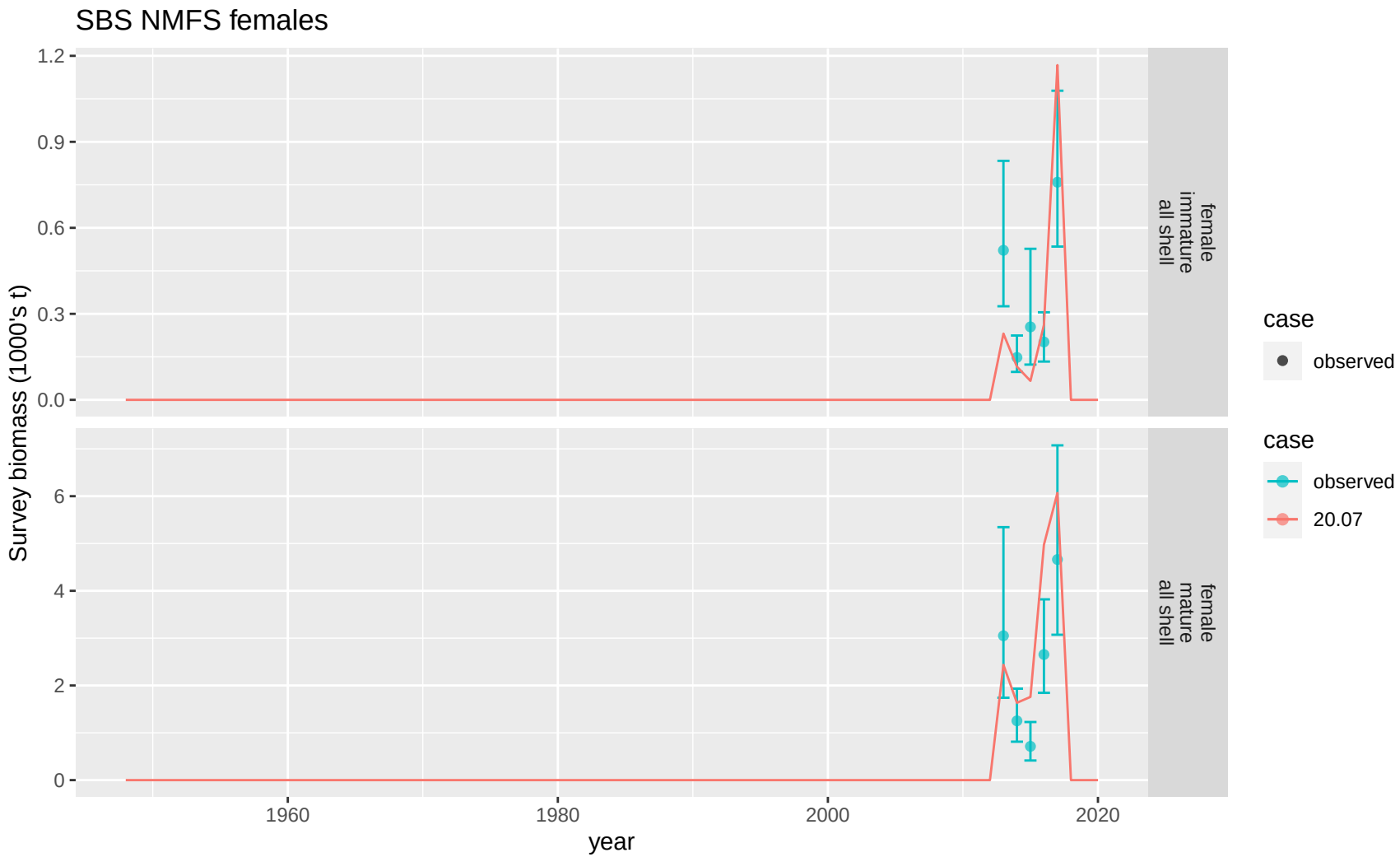

Figure 10: Comparison of observed and predicted female survey biomass for SBS NMFS females.

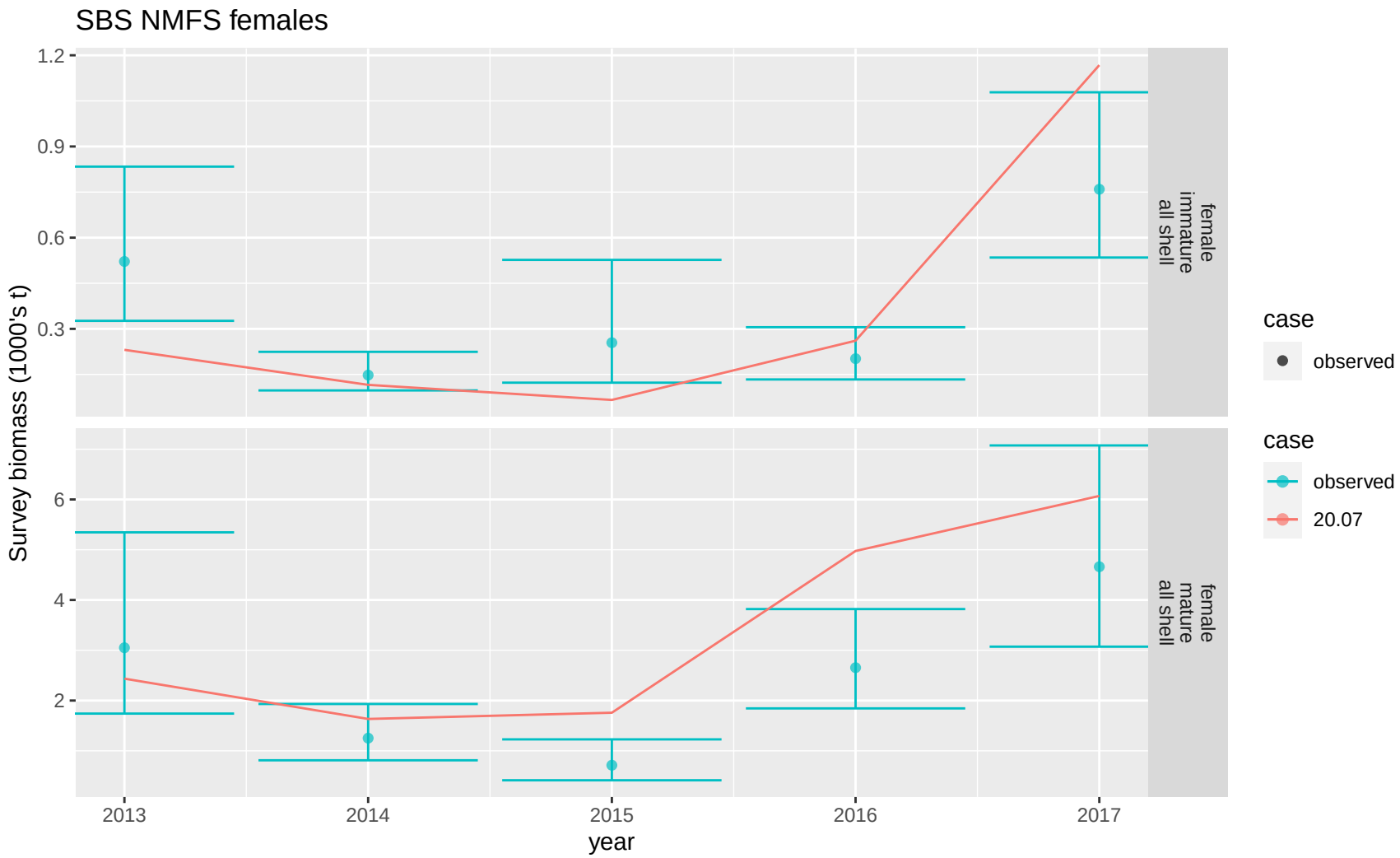

Figure 11: Comparison of observed and predicted female survey biomass for SBS NMFS females. Observed time period.

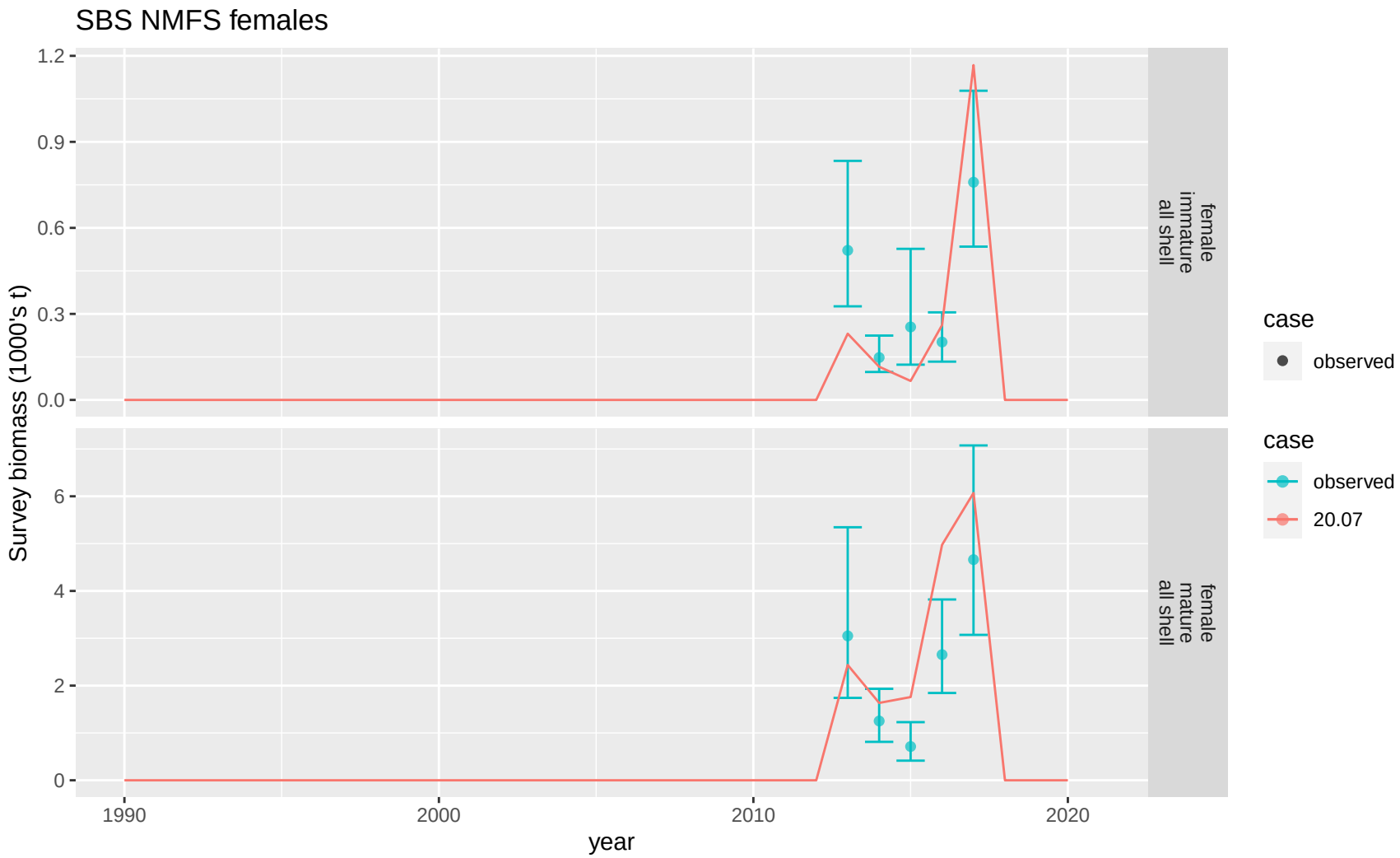

Figure 12: Comparison of observed and predicted female survey biomass for SBS NMFS females. Recent time period.

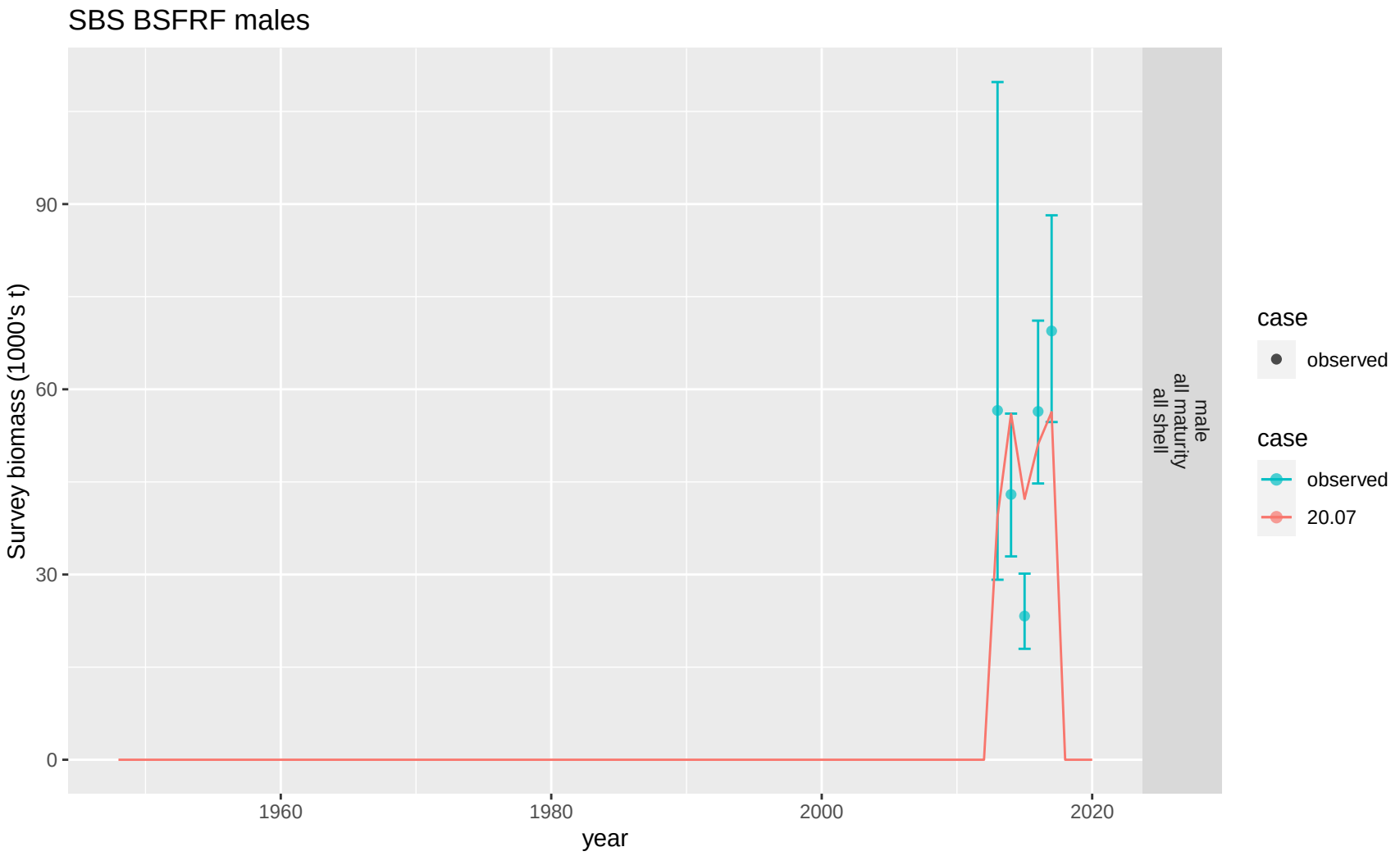

Figure 13: Comparison of observed and predicted male survey biomass for SBS BSFRF males.

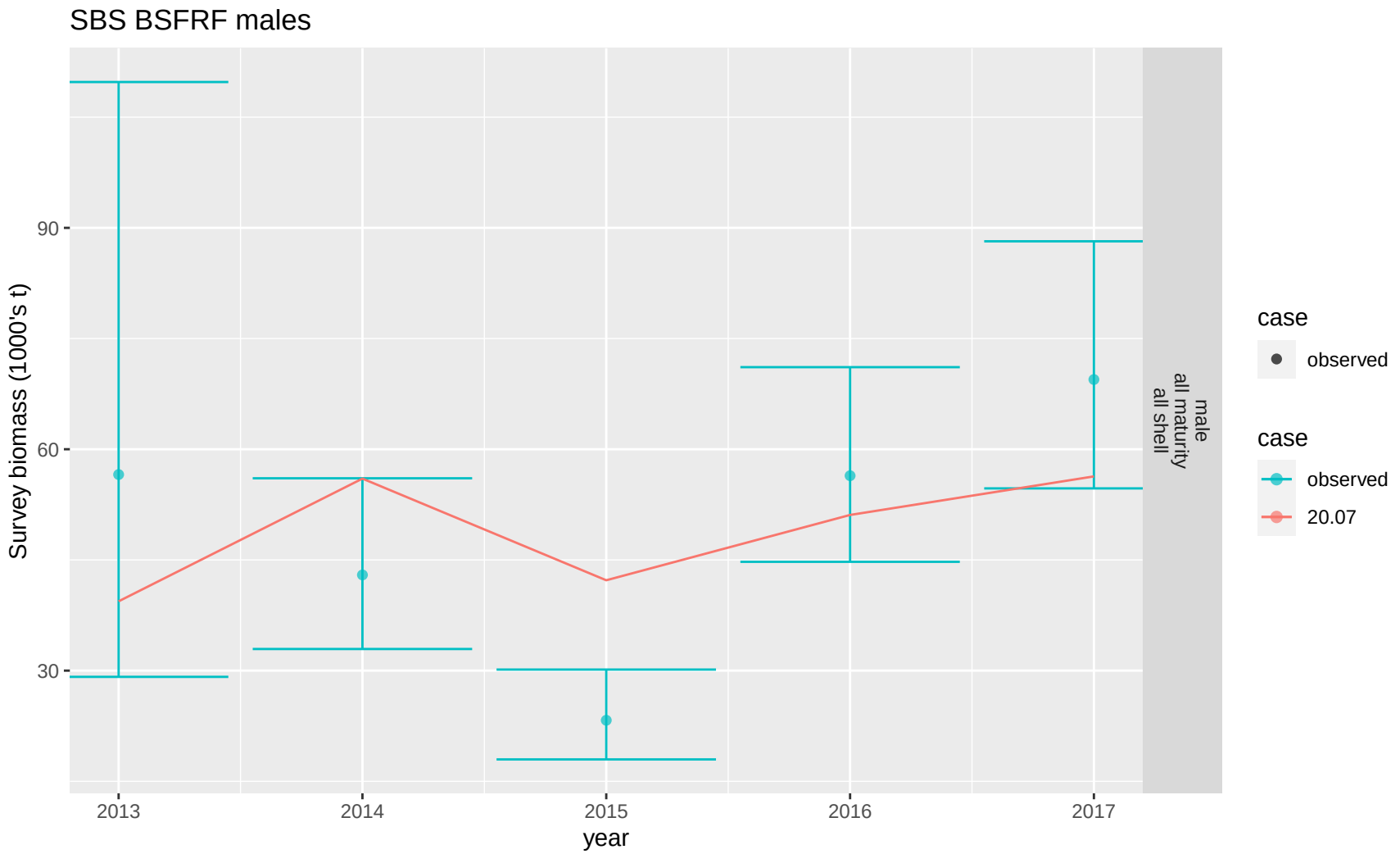

Figure 14: Comparison of observed and predicted male survey biomass for SBS BSFRF males. Observed time period.

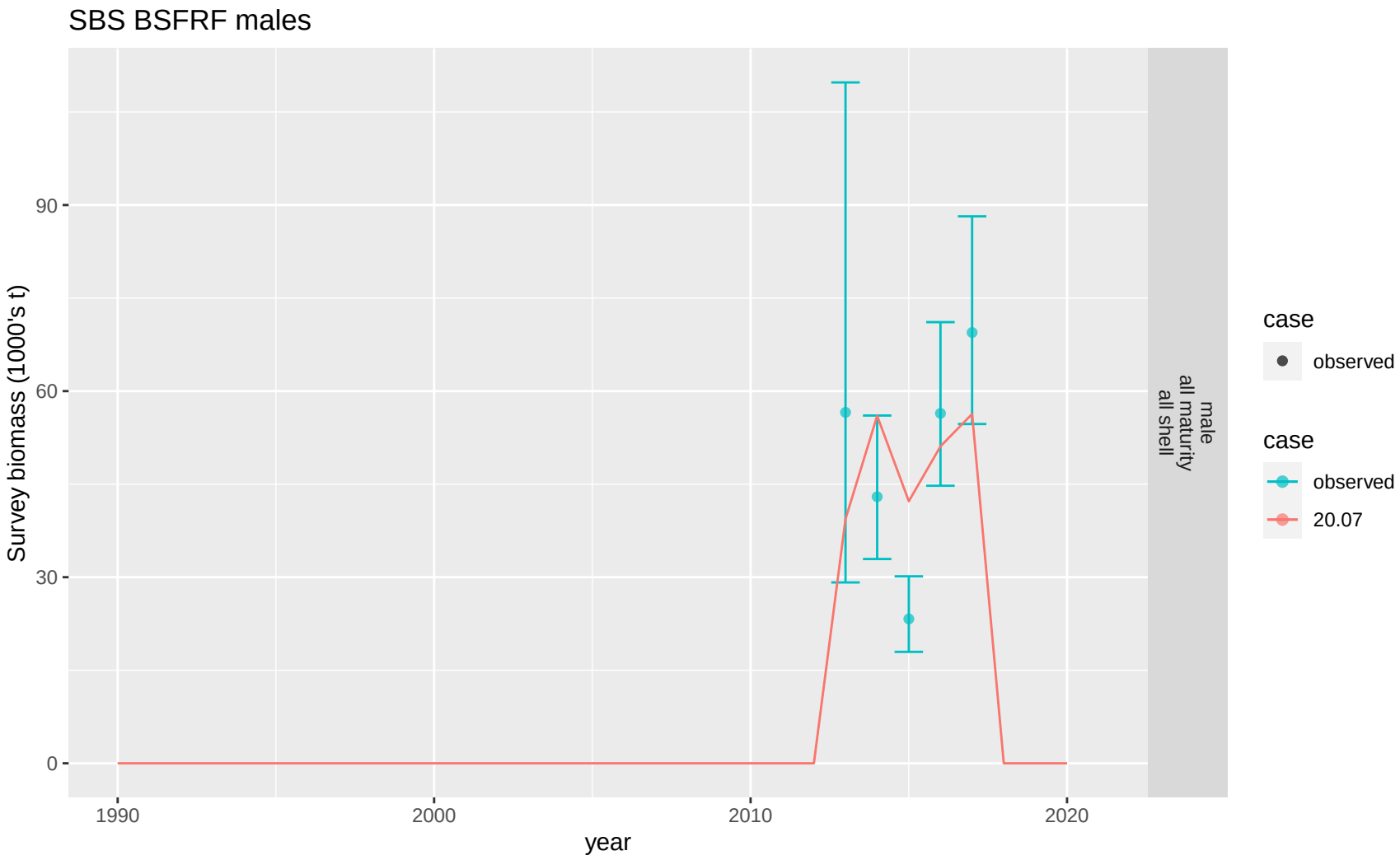

Figure 15: Comparison of observed and predicted male survey biomass for SBS BSFRF males. Recent time period.

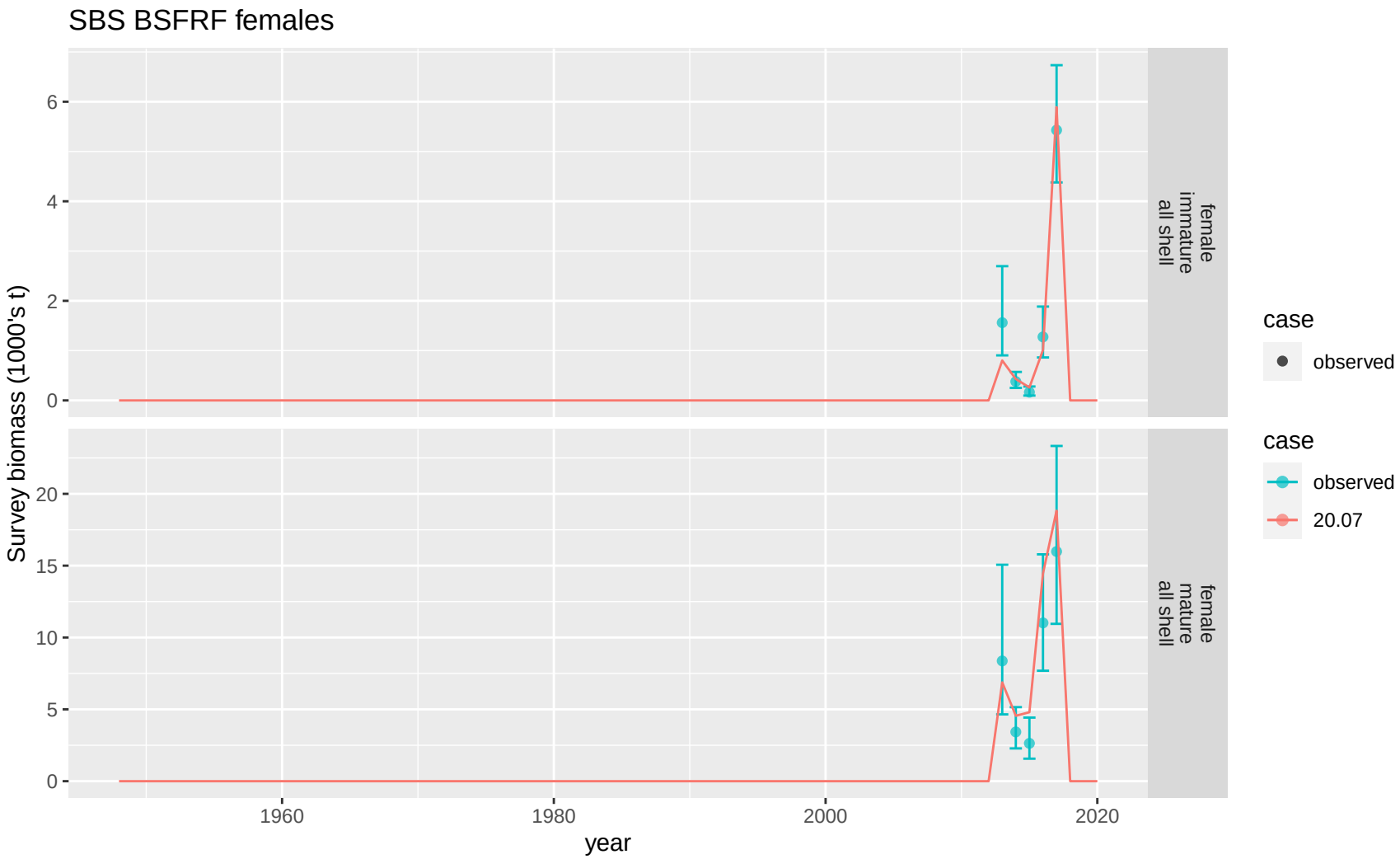

Figure 16: Comparison of observed and predicted female survey biomass for SBS BSFRF females.

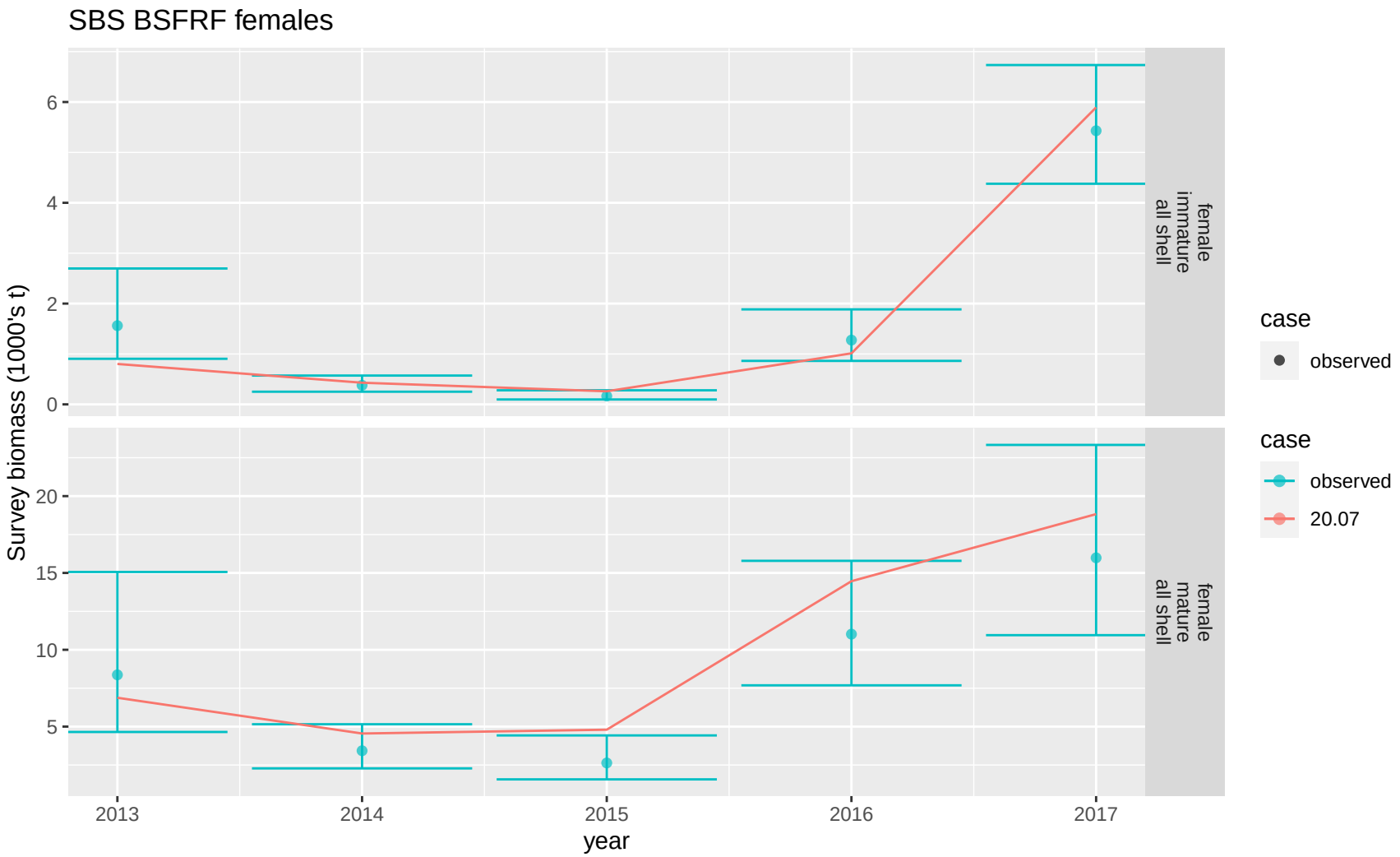

Figure 17: Comparison of observed and predicted female survey biomass for SBS BSFRF females. Observed time period.

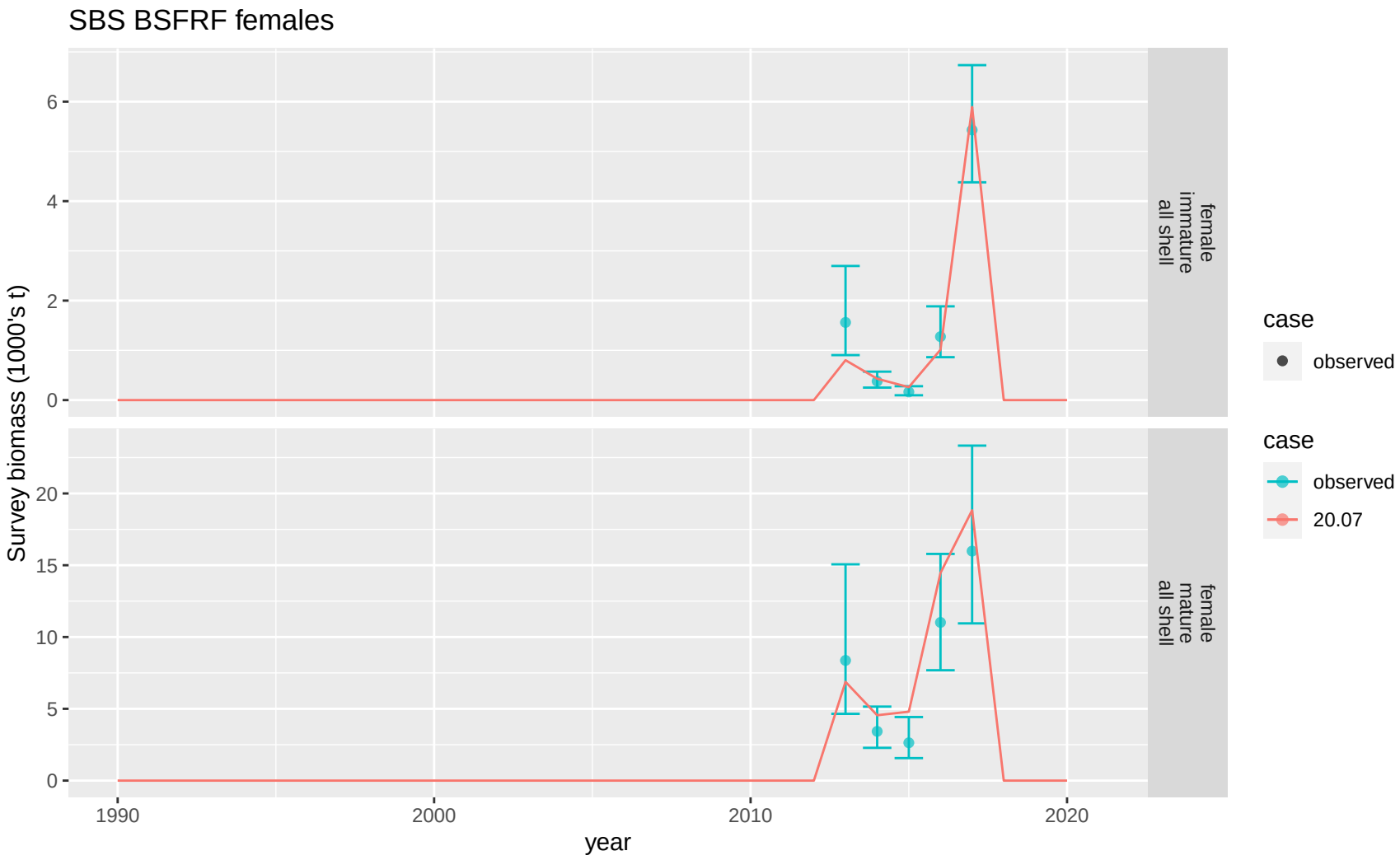

Figure 18: Comparison of observed and predicted female survey biomass for SBS BSFRF females. Recent time period.

Z-scores

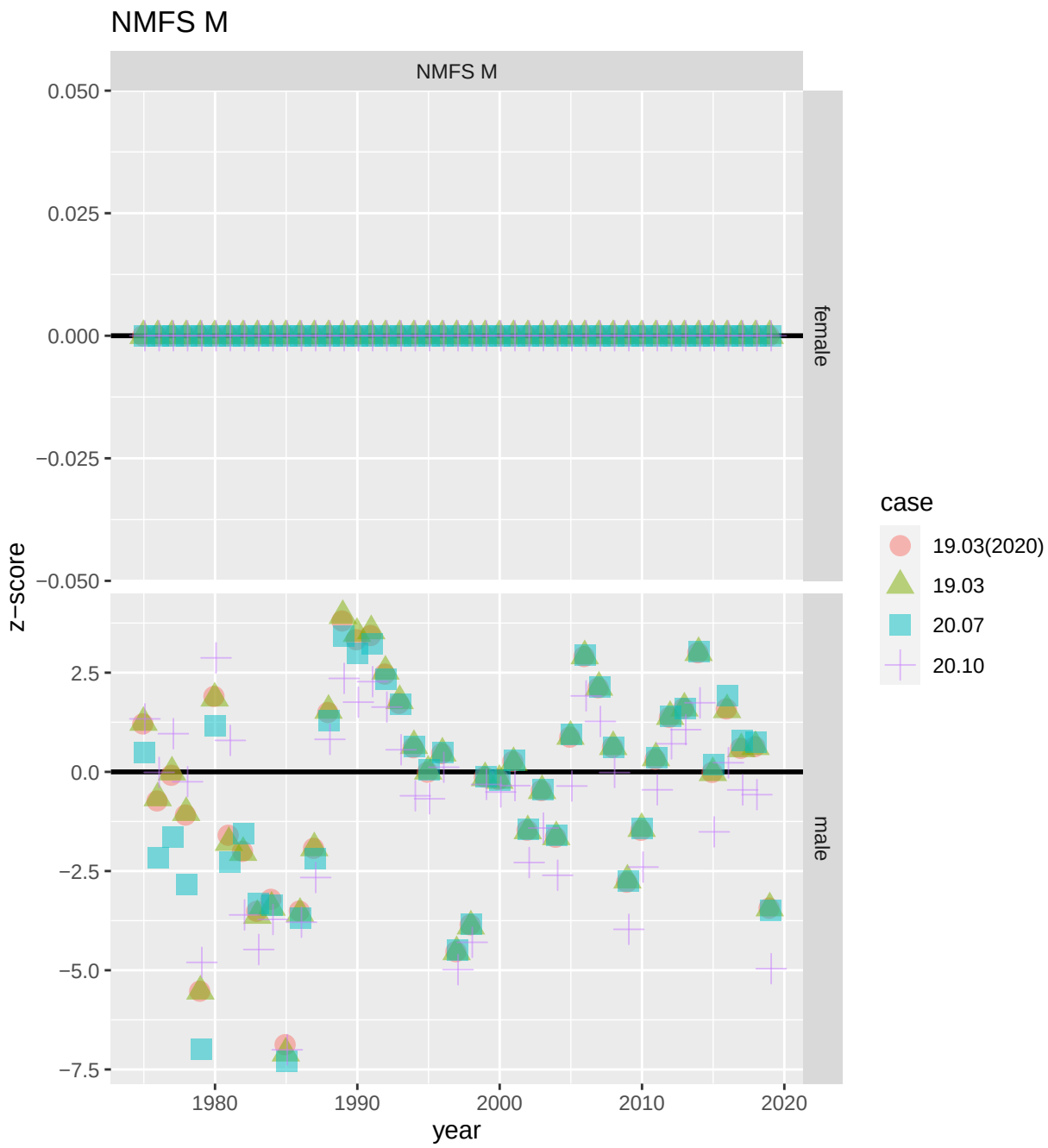

Figure 19: Z-scores for index catch biomass in NMFS M.

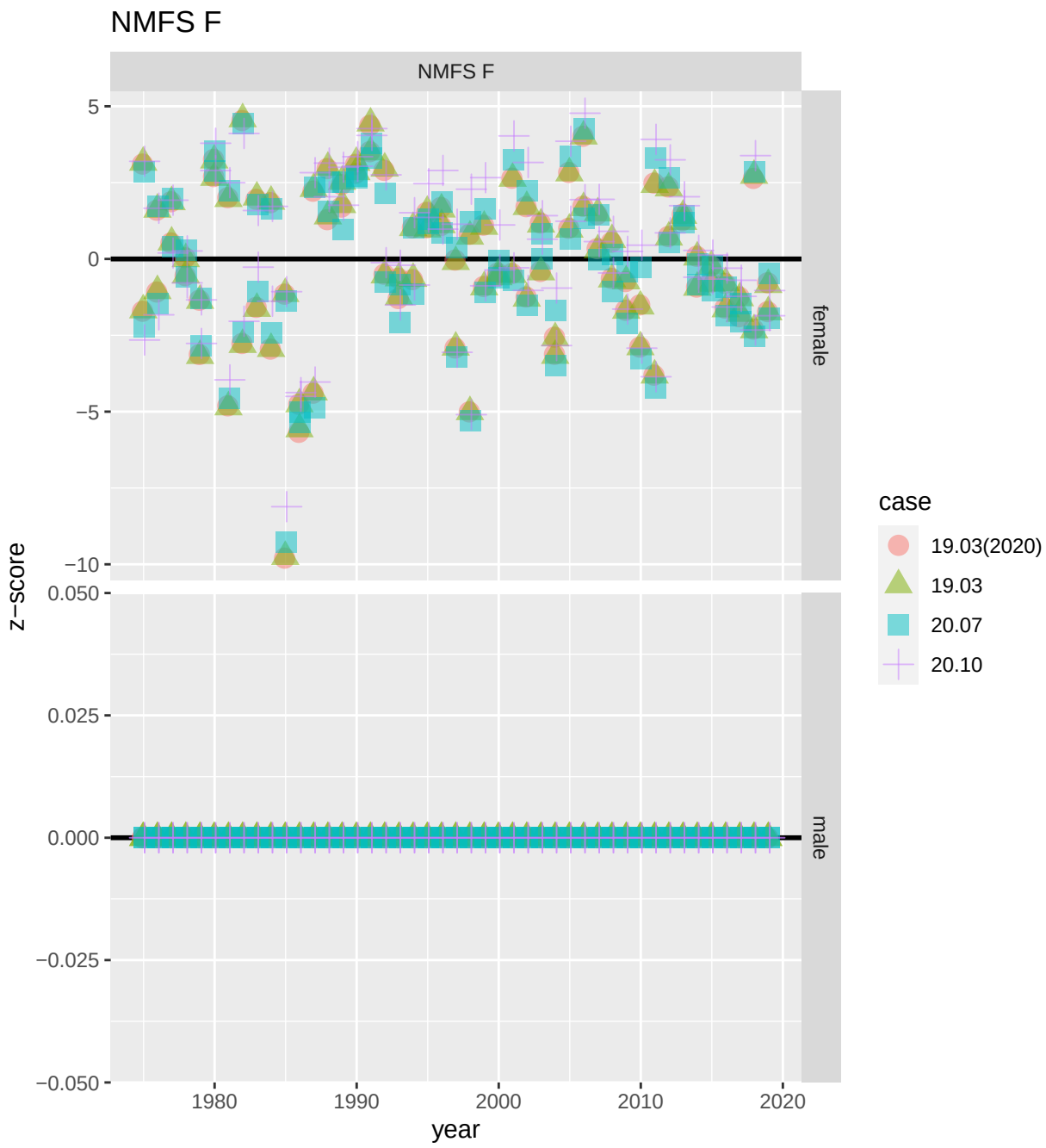

Figure 20: Z-scores for index catch biomass in NMFS F.

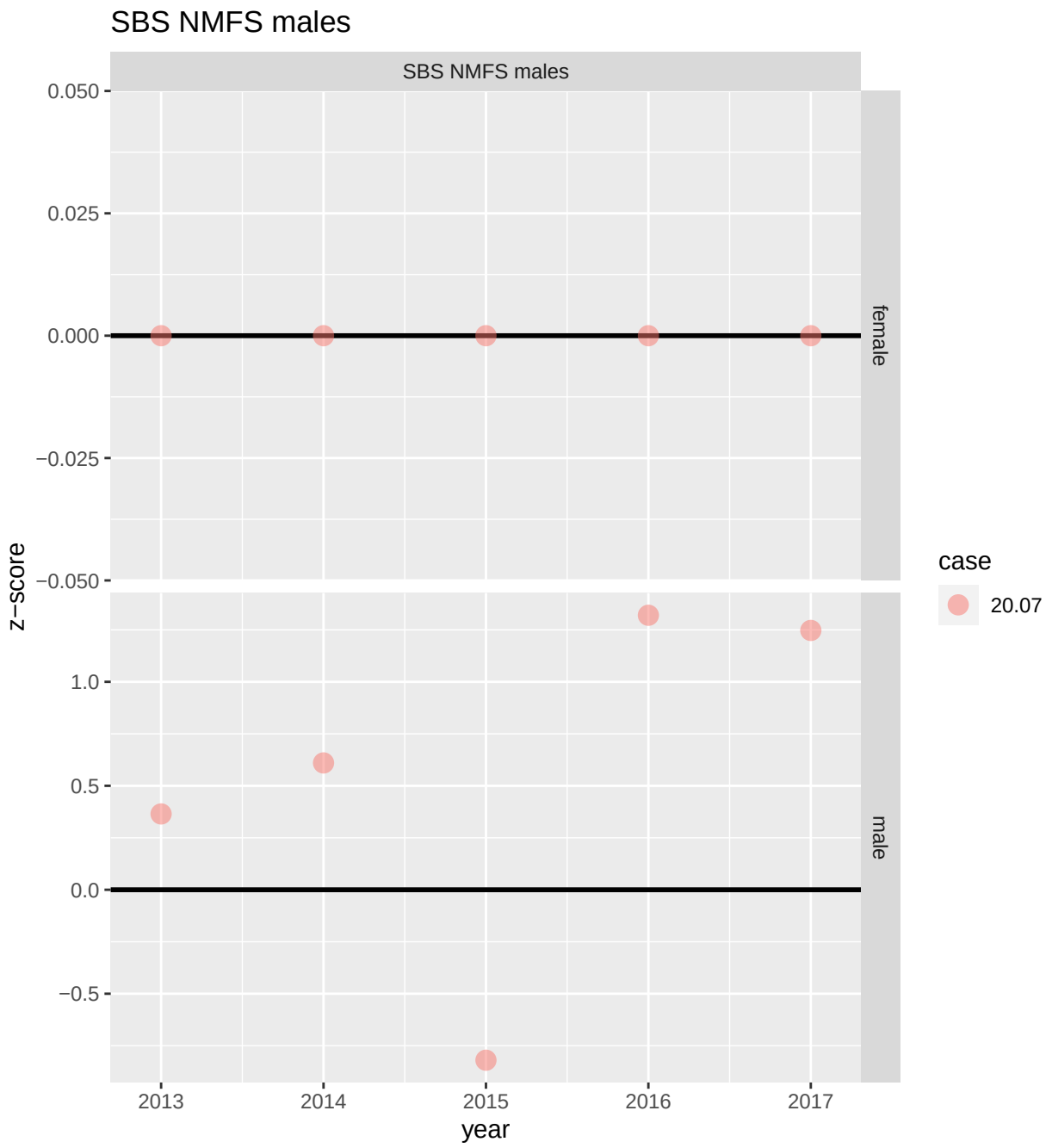

Figure 21: Z-scores for index catch biomass in SBS NMFS males.

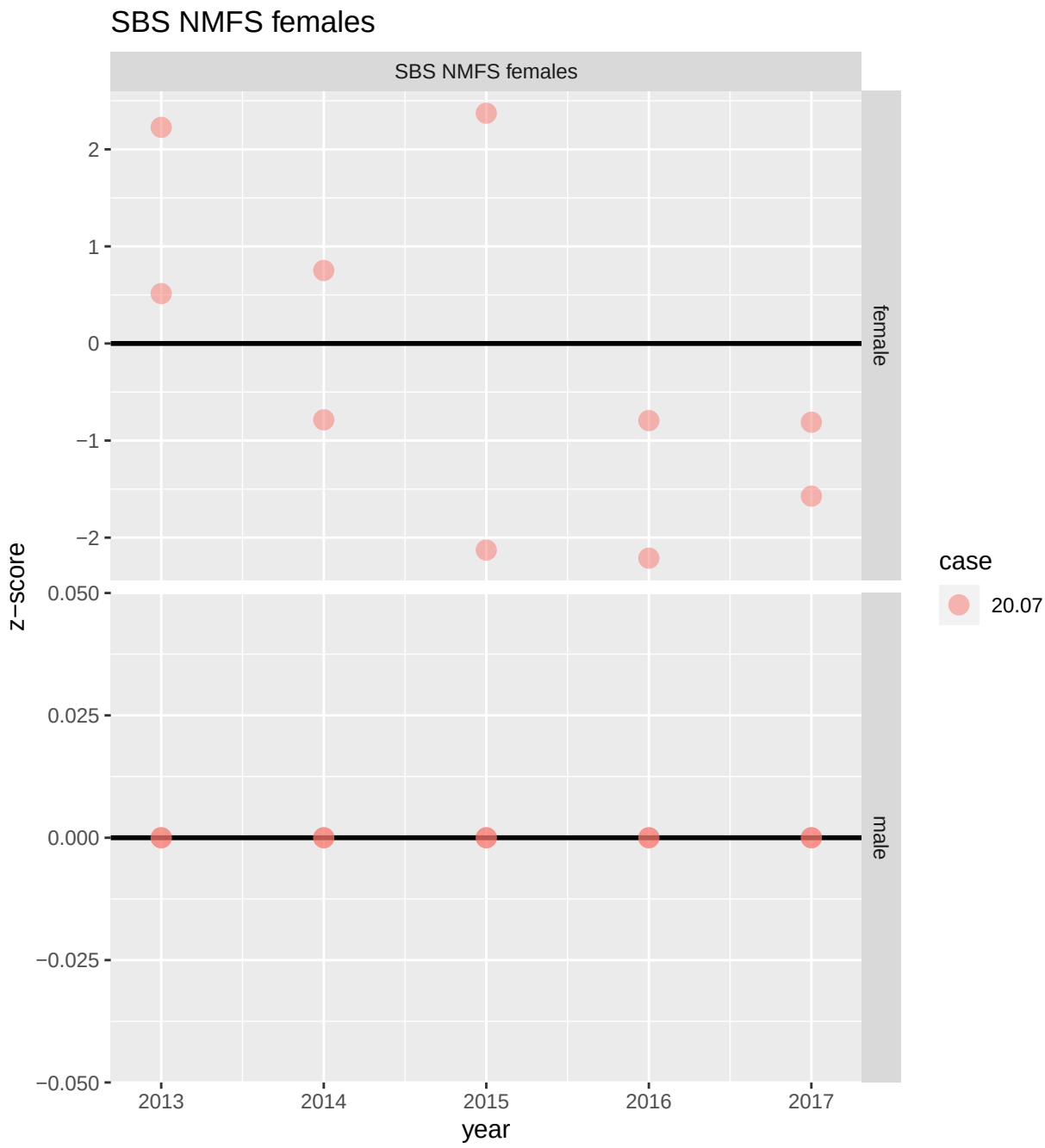

Figure 22: Z-scores for index catch biomass in SBS NMFS females.

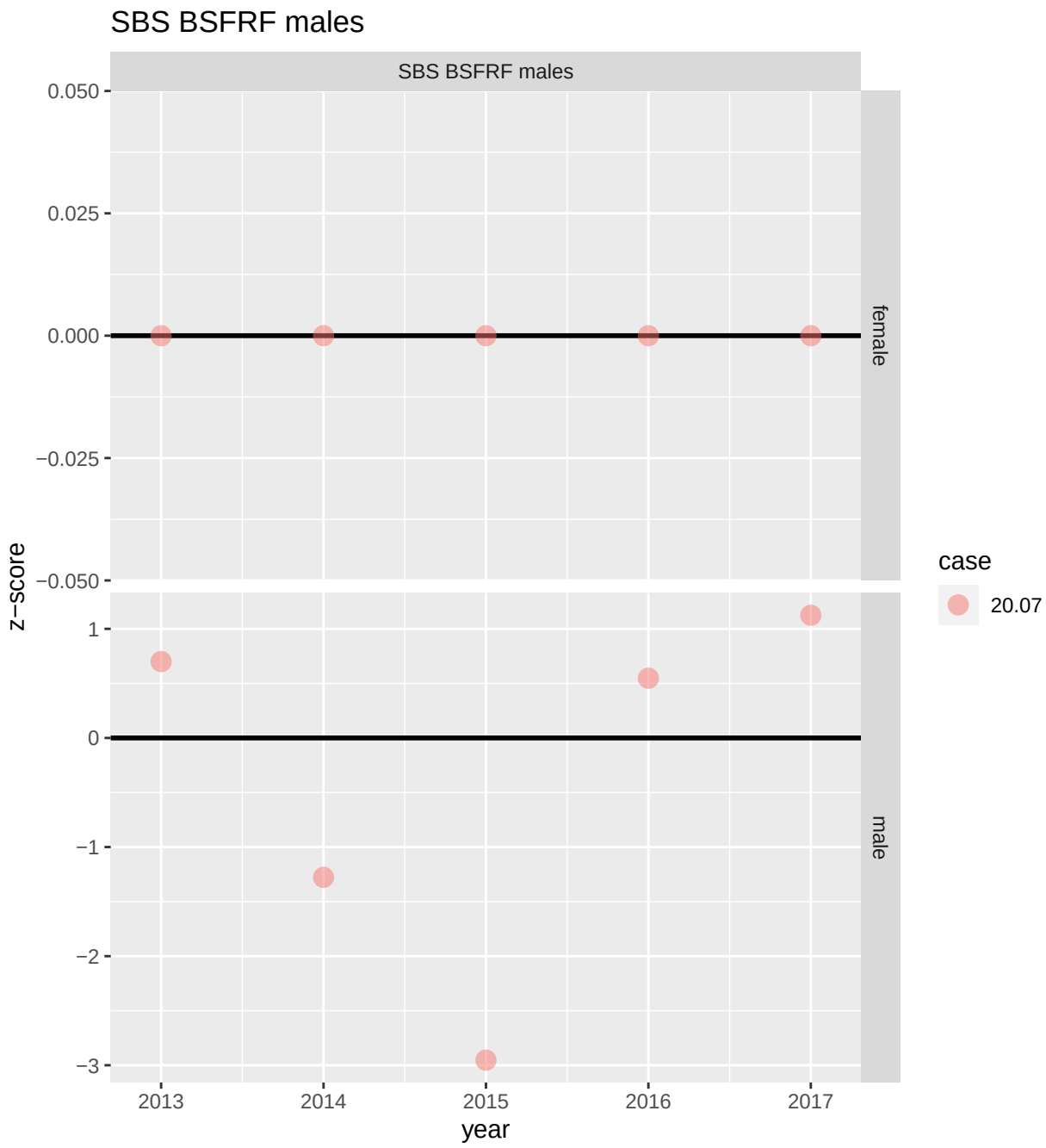

Figure 23: Z-scores for index catch biomass in SBS BSFRF males.

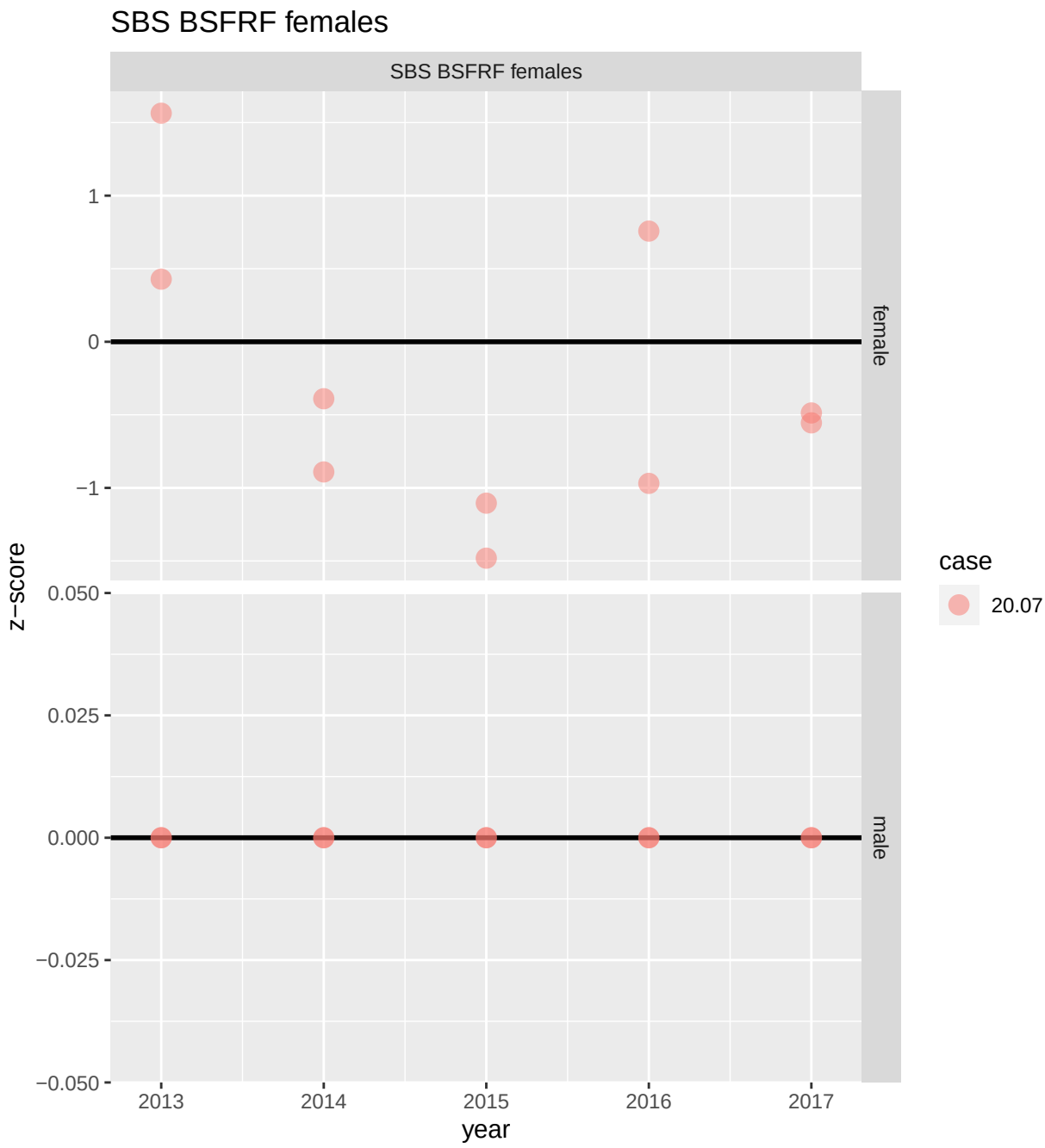

Figure 24: Z-scores for index catch biomass in SBS BSFRF females.

Survey abundance

Fits

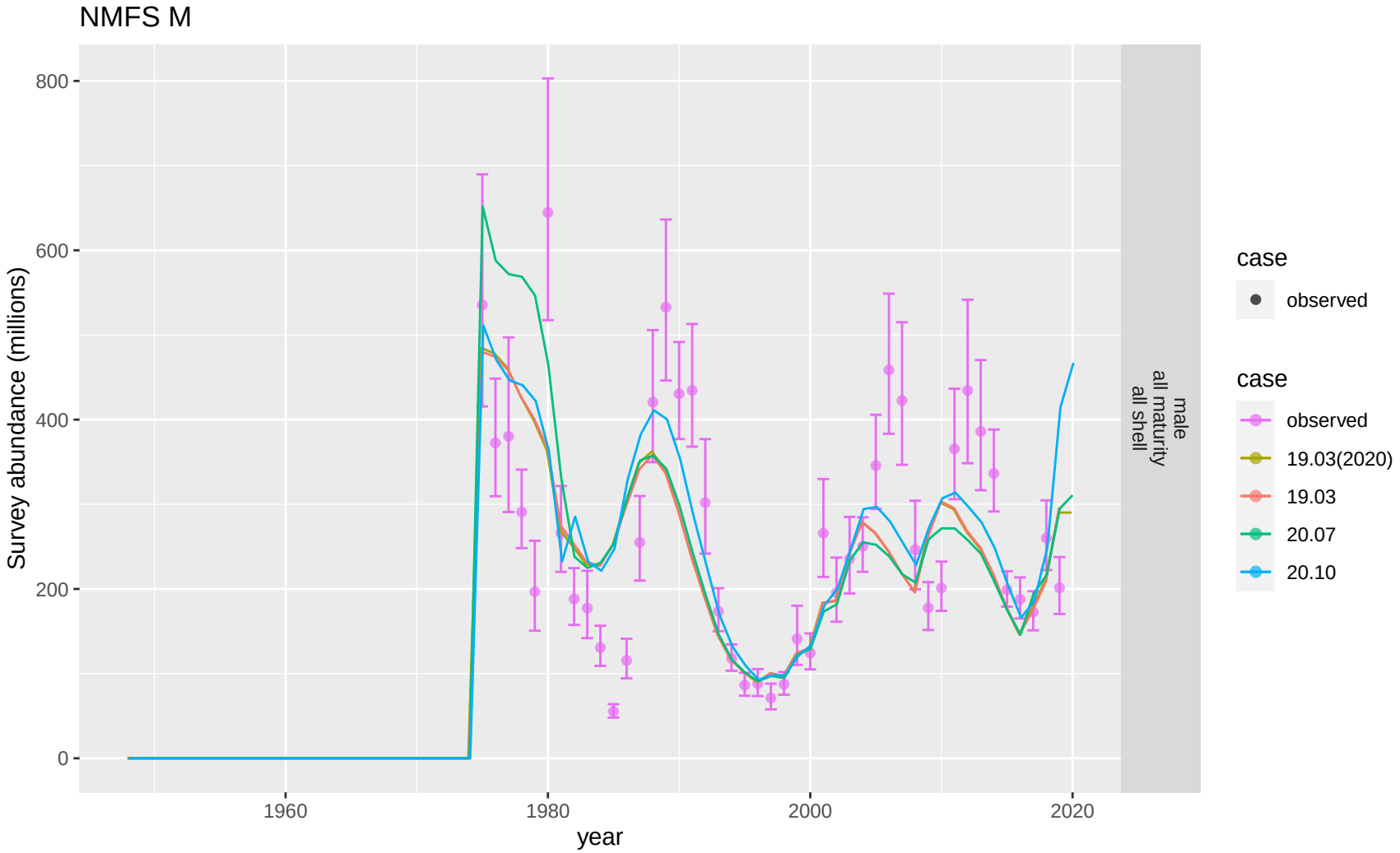

Figure 25: Comparison of observed and predicted male survey abundance for NMFS M.

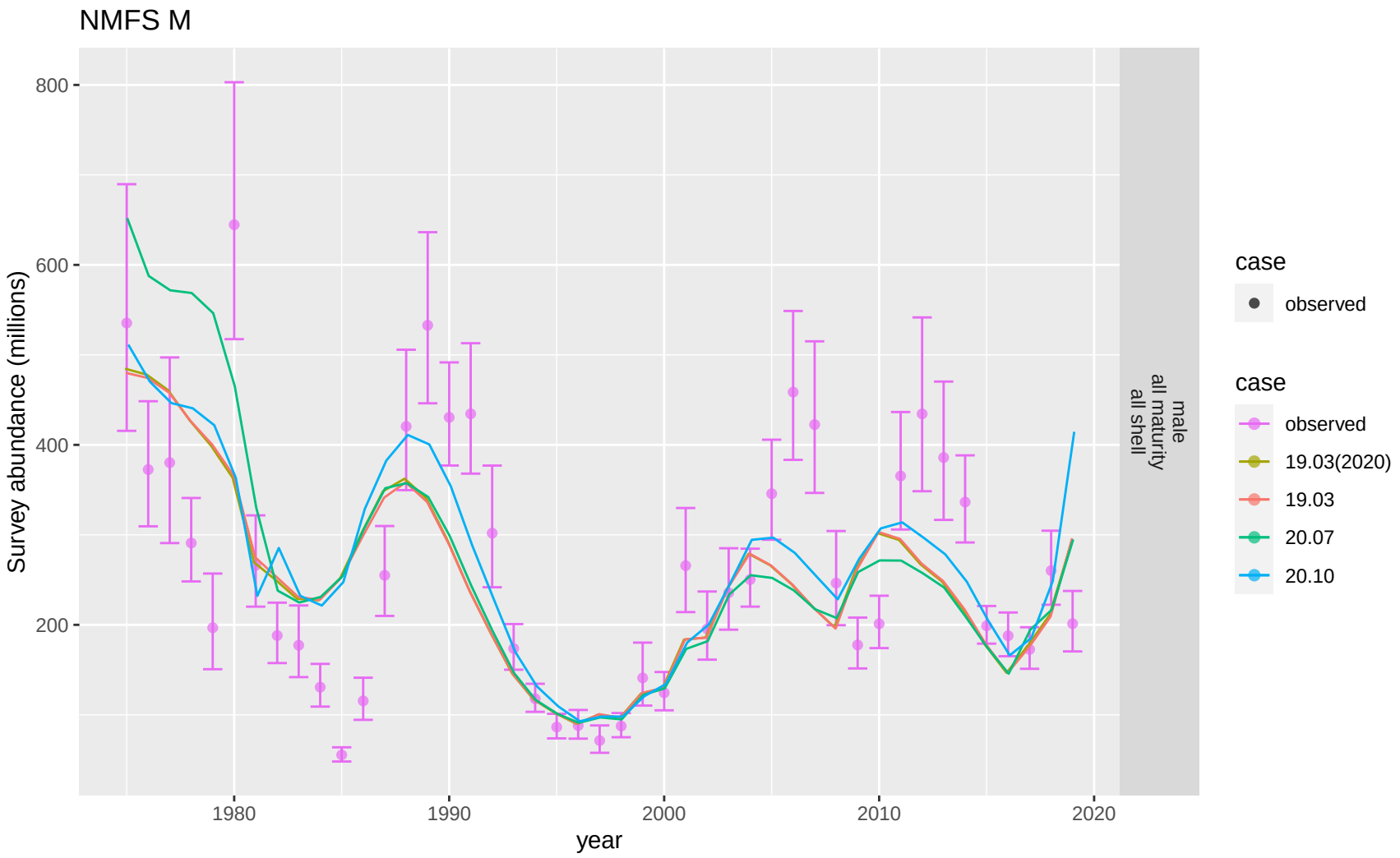

Figure 26: Comparison of observed and predicted male survey abundance for NMFS M. Observed time period.

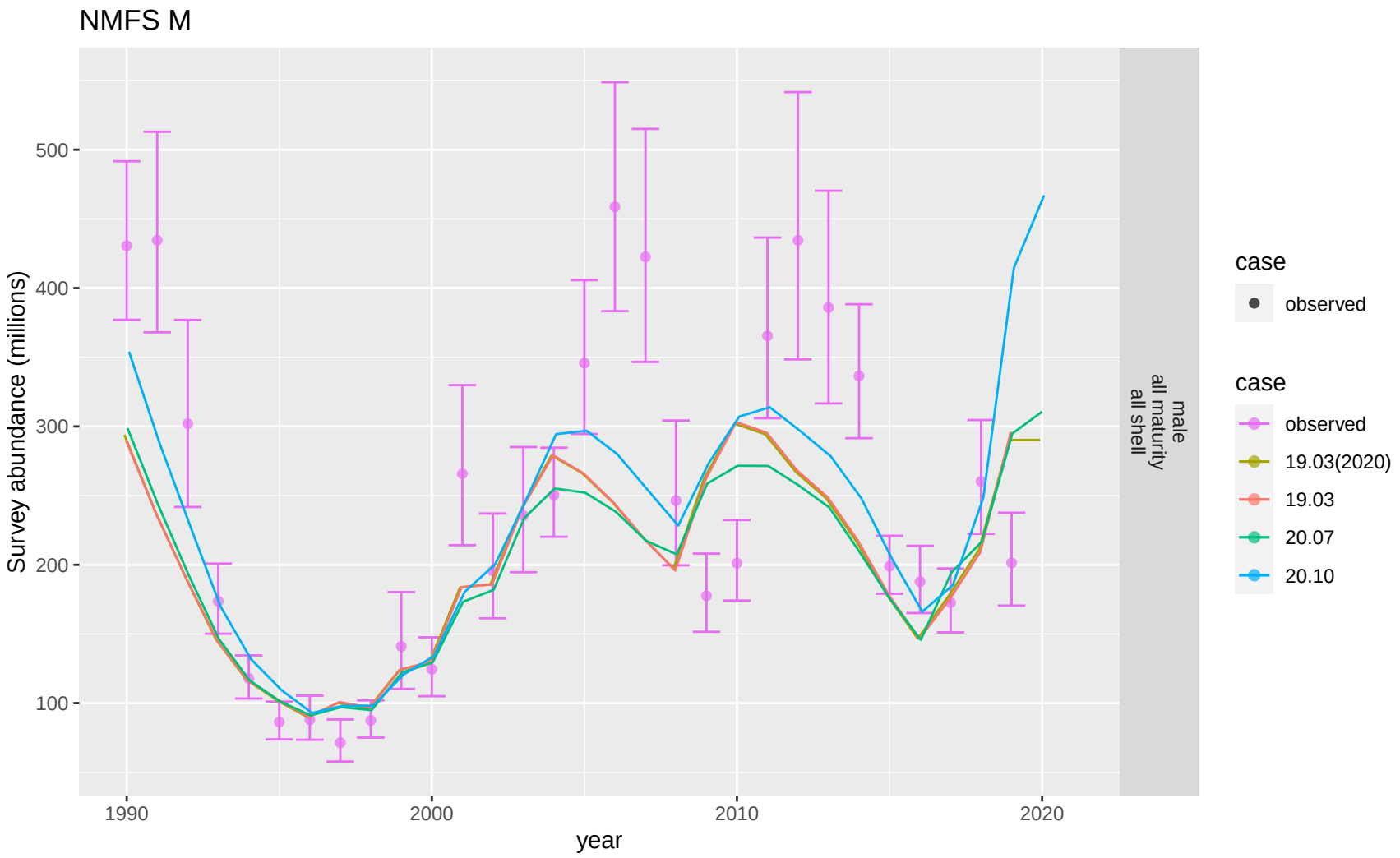

Figure 27: Comparison of observed and predicted male survey abundance for NMFS M. Recent time period.

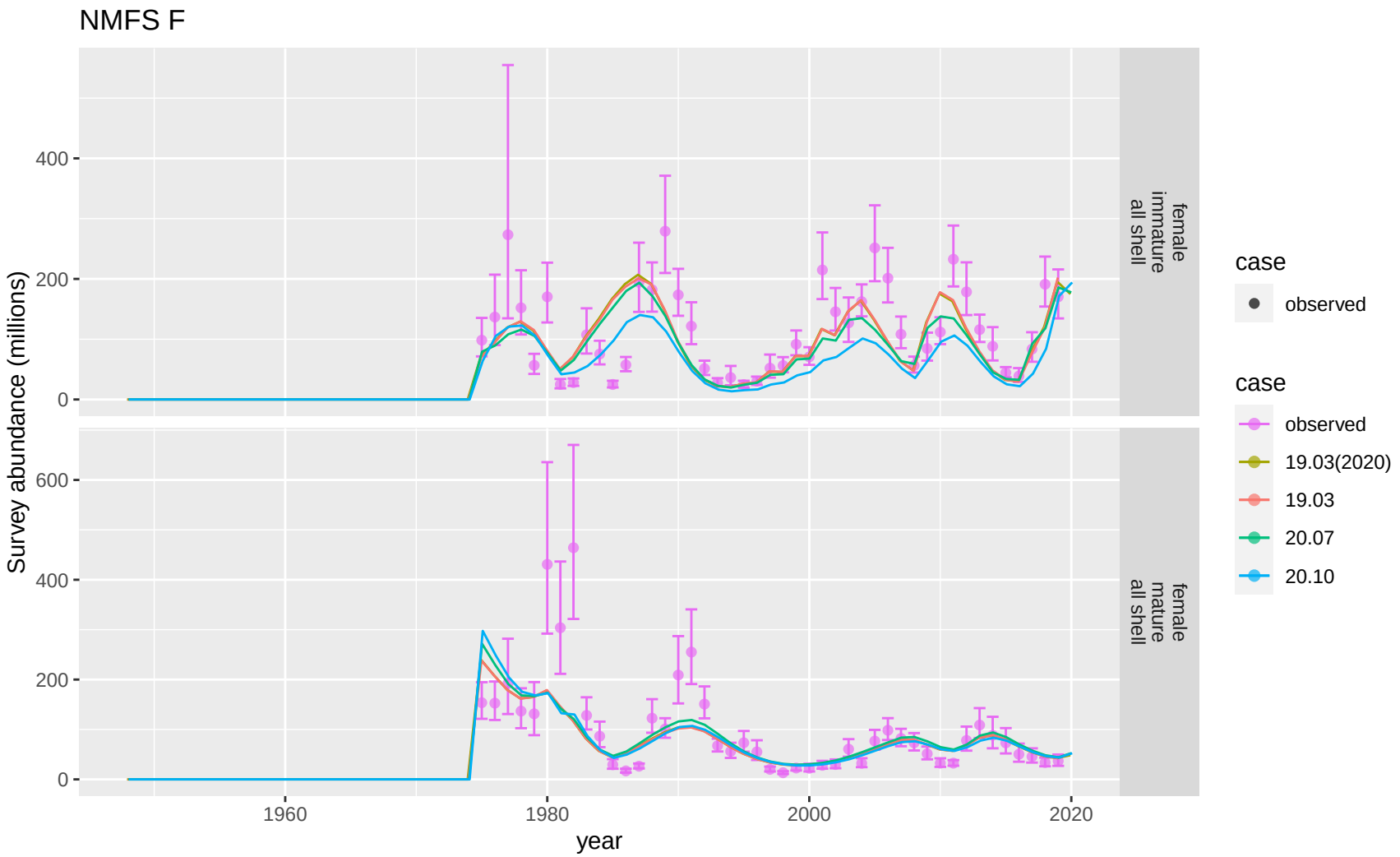

Figure 28: Comparison of observed and predicted female survey abundance for NMFS F.

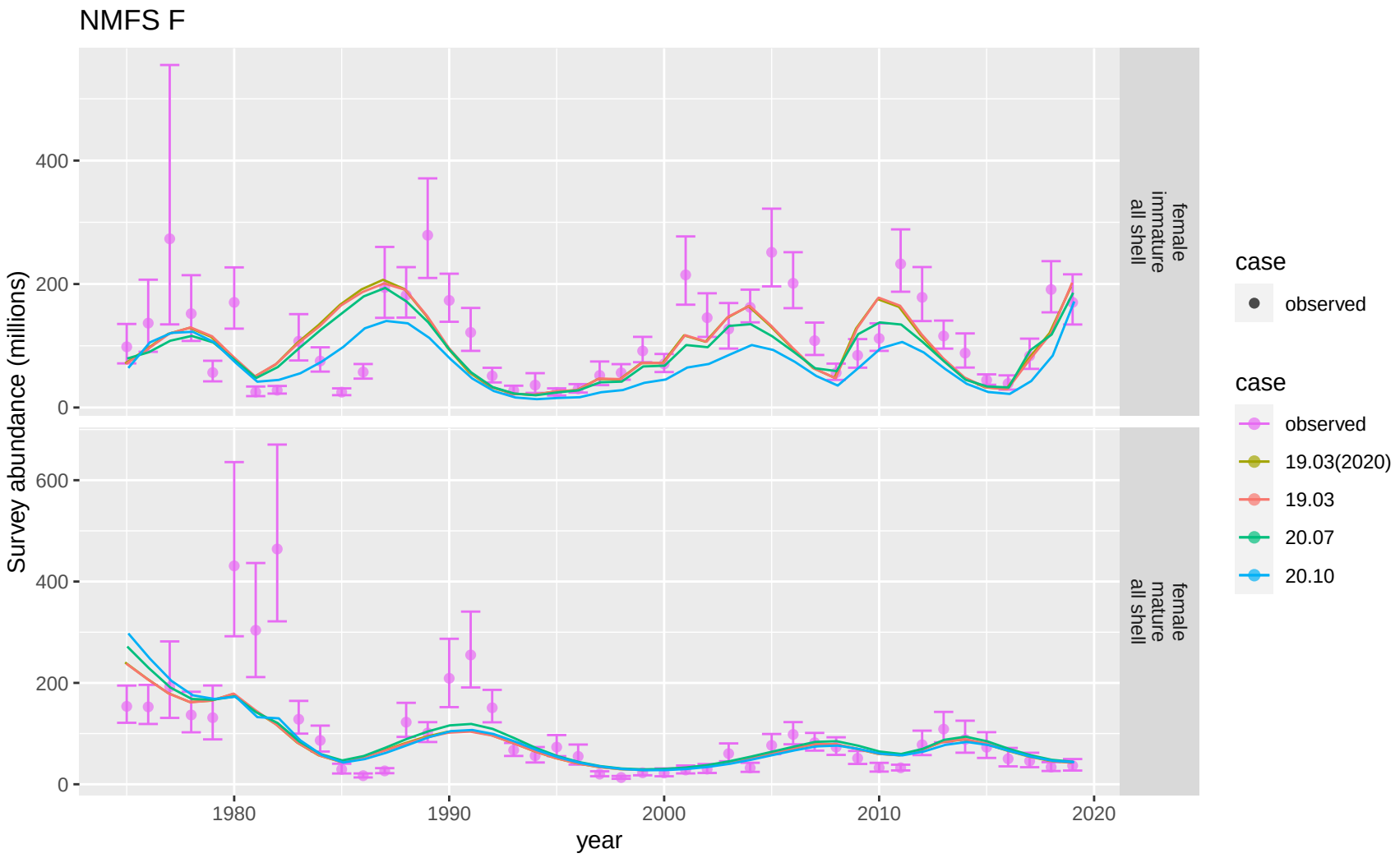

Figure 29: Comparison of observed and predicted female survey abundance for NMFS F. Observed time period.

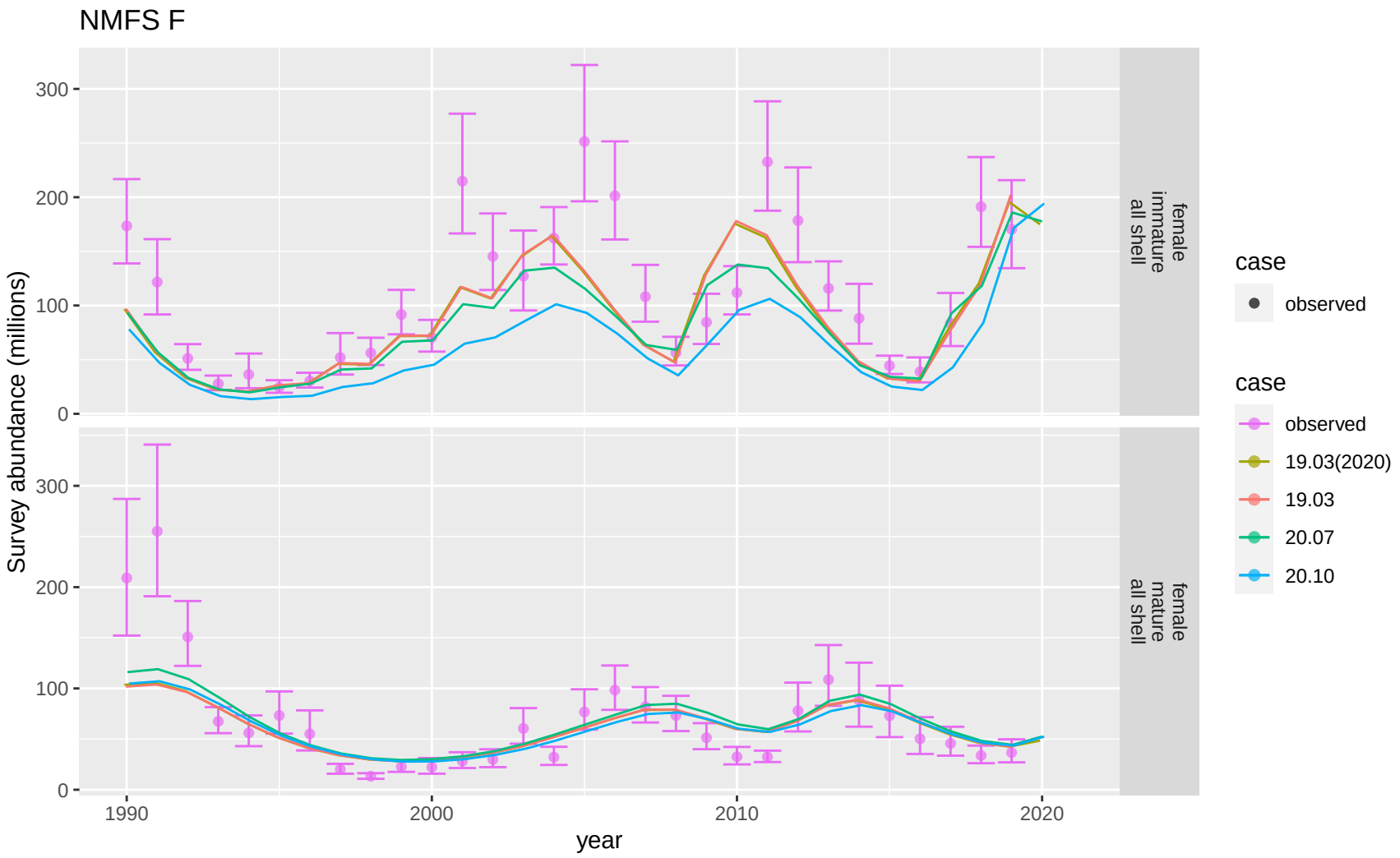

Figure 30: Comparison of observed and predicted female survey abundance for NMFS F. Recent time period.

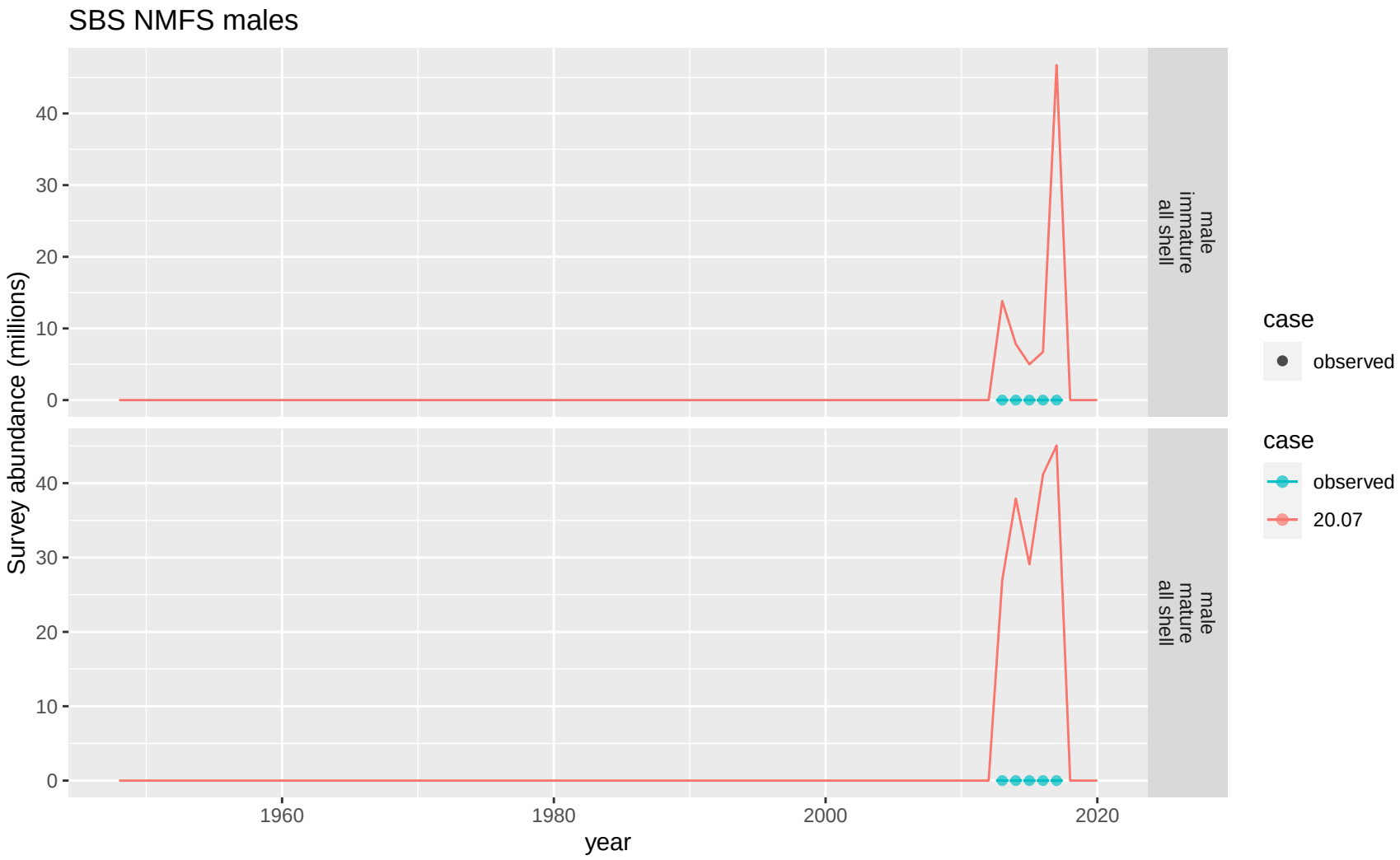

Figure 31: Comparison of observed and predicted male survey abundance for SBS NMFS males.

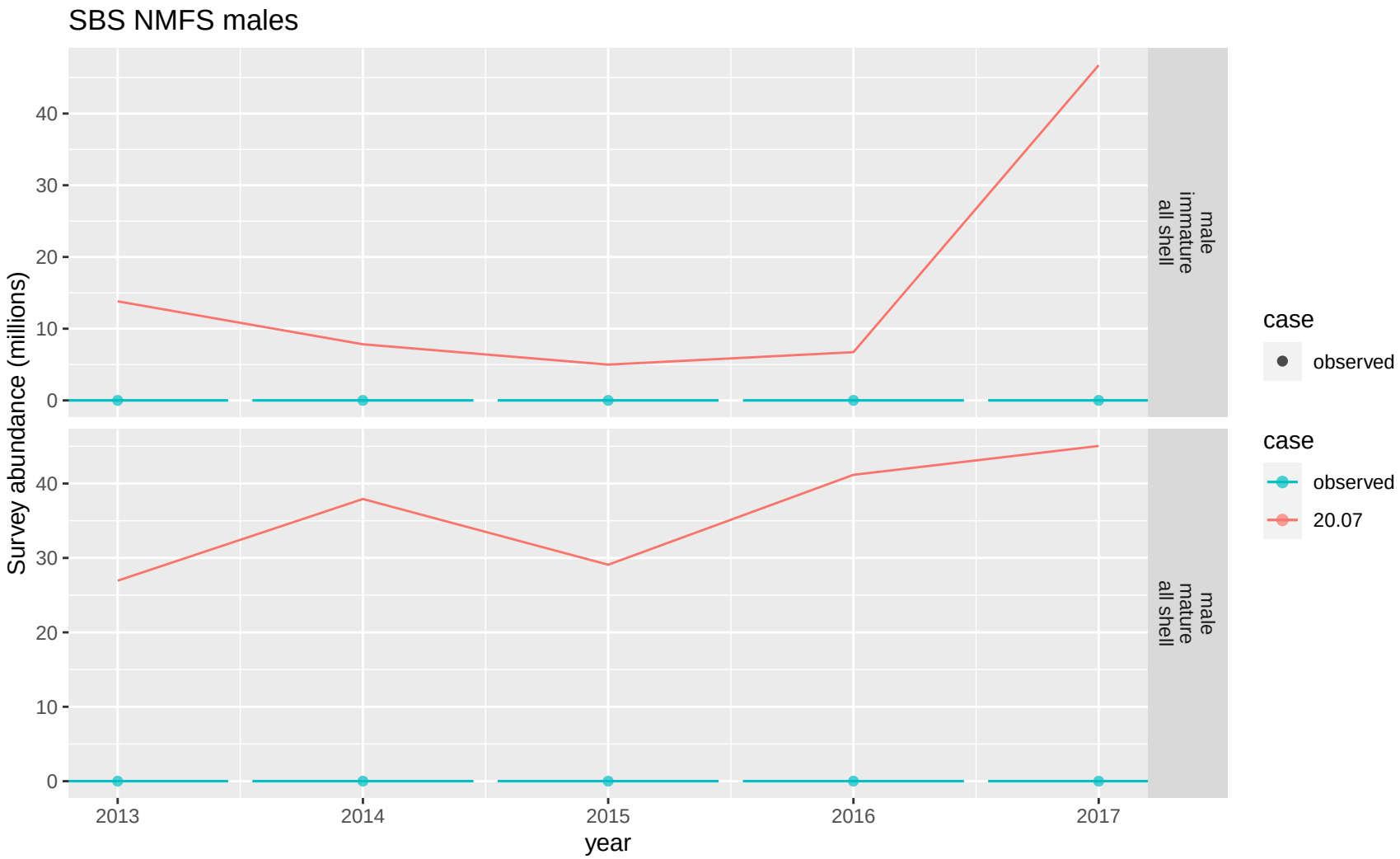

Figure 32: Comparison of observed and predicted male survey abundance for SBS NMFS males. Observed time period.

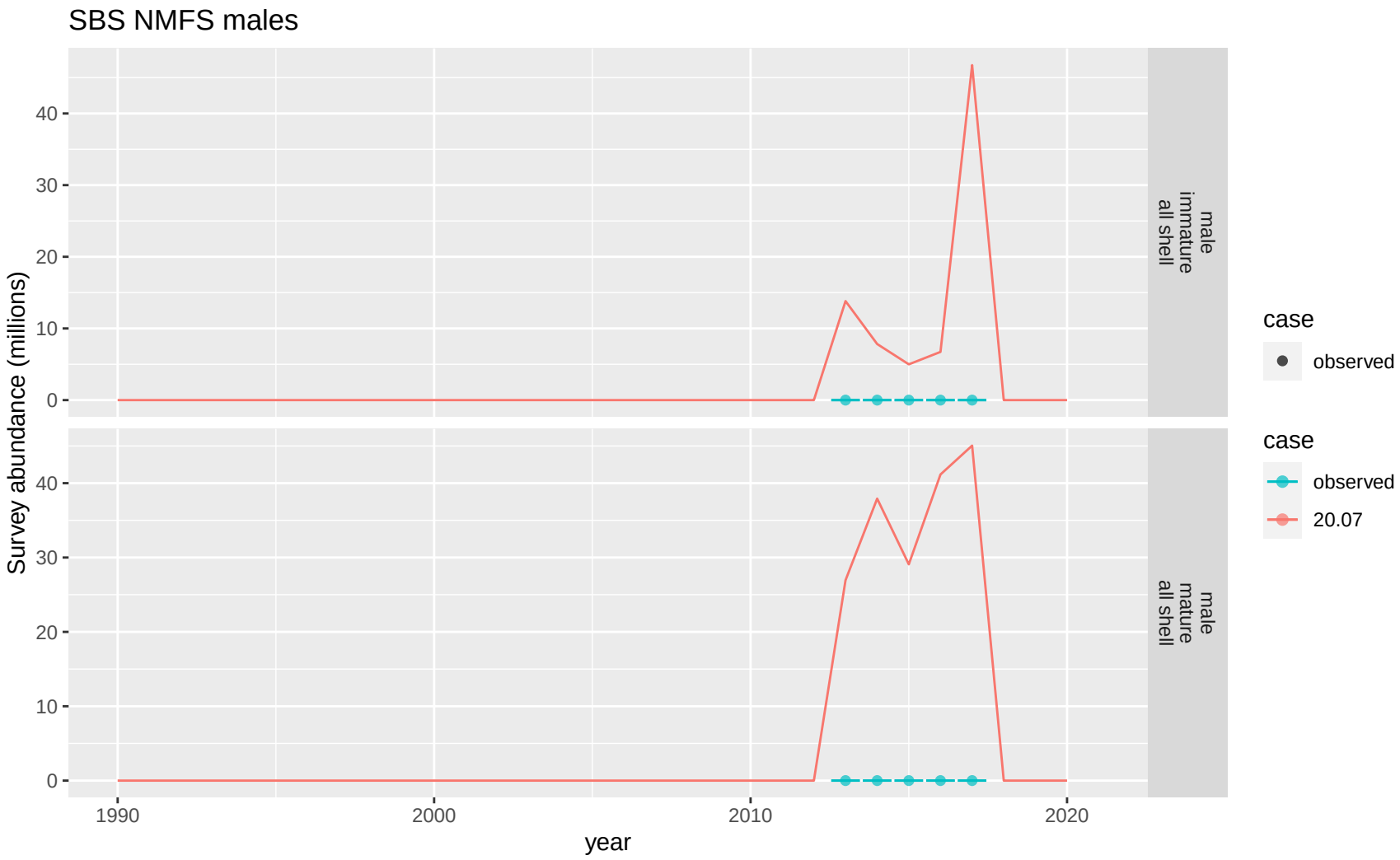

Figure 33: Comparison of observed and predicted male survey abundance for SBS NMFS males. Recent time period.

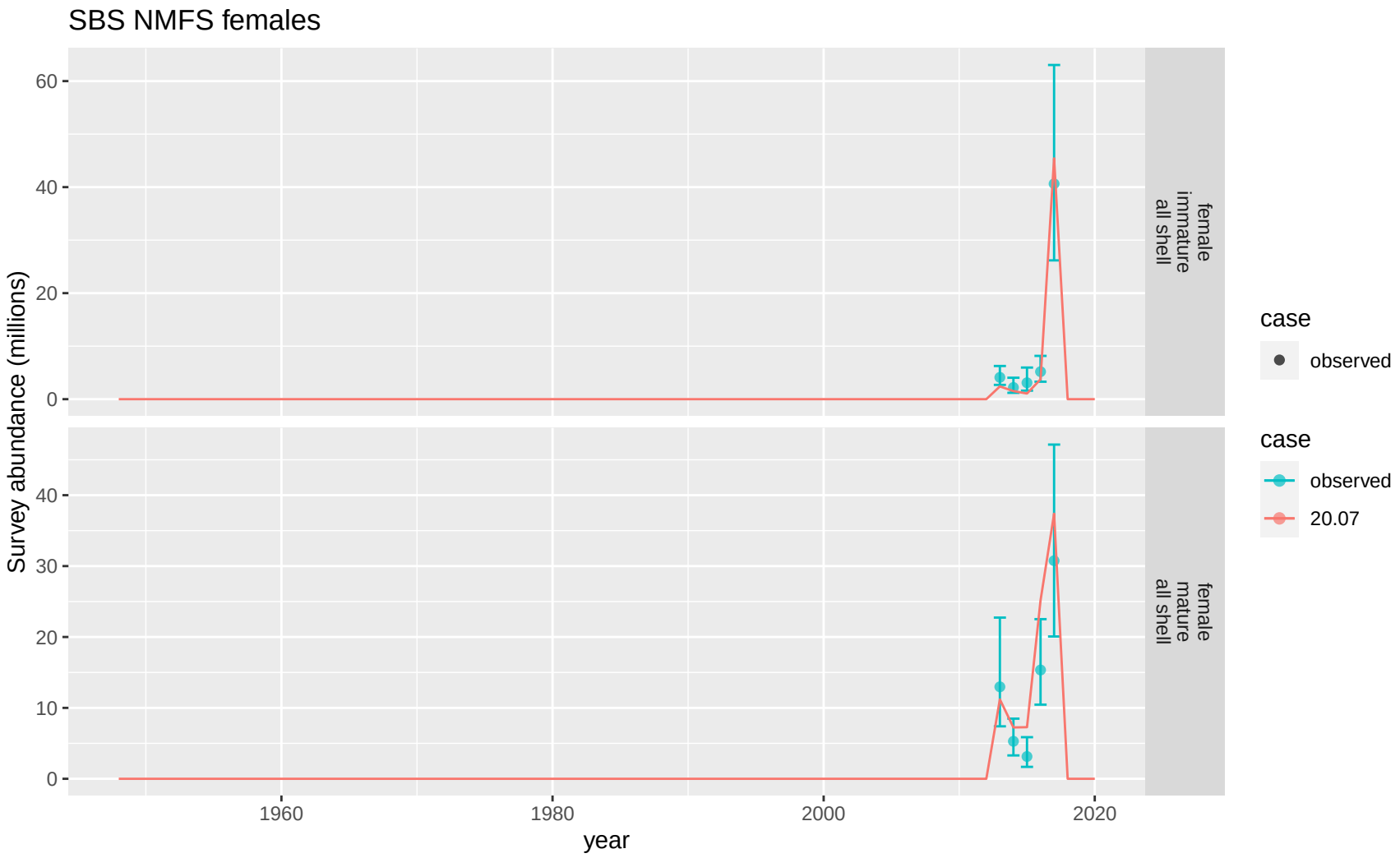

Figure 34: Comparison of observed and predicted female survey abundance for SBS NMFS females.

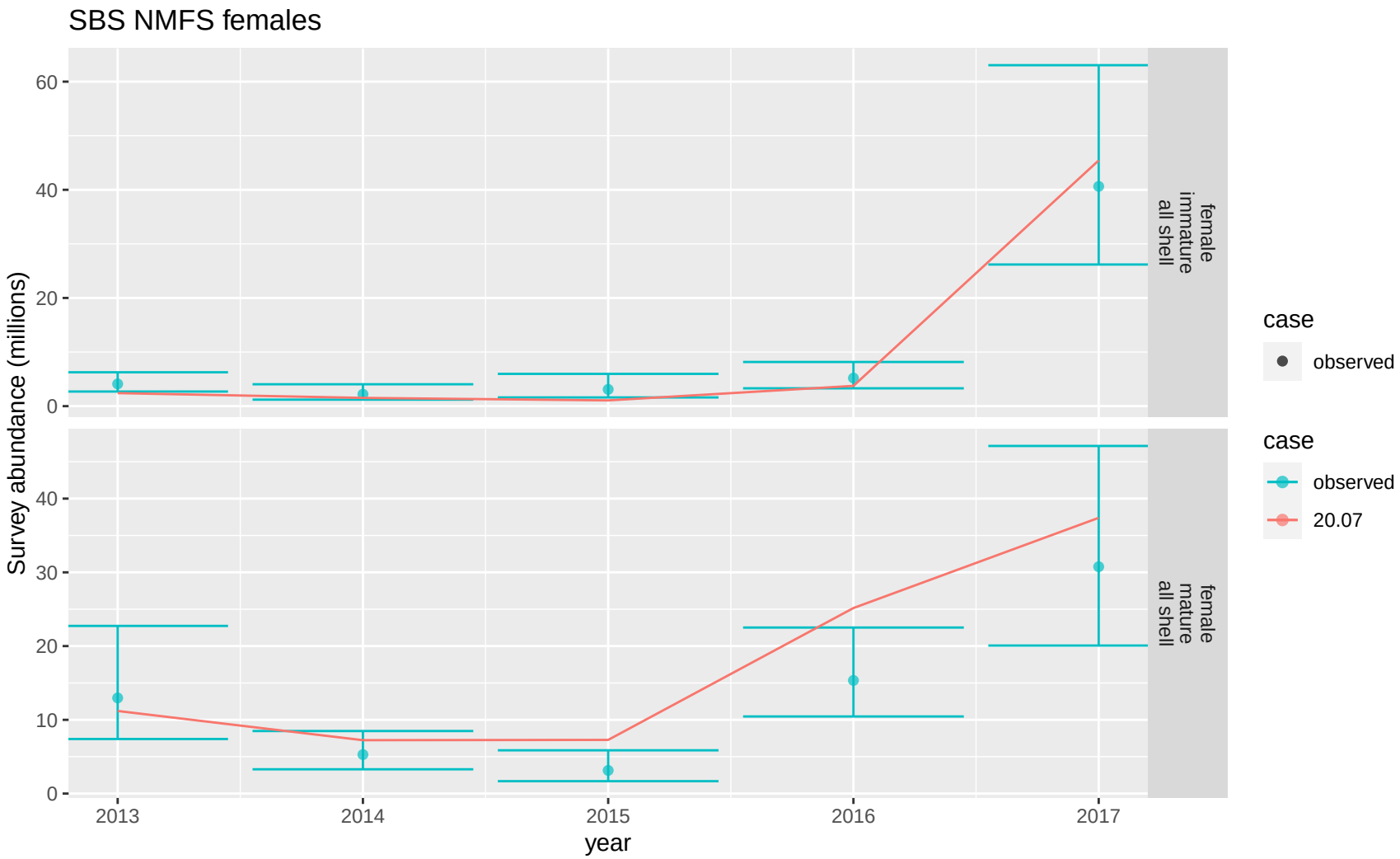

Figure 35: Comparison of observed and predicted female survey abundance for SBS NMFS females. Observed time period.

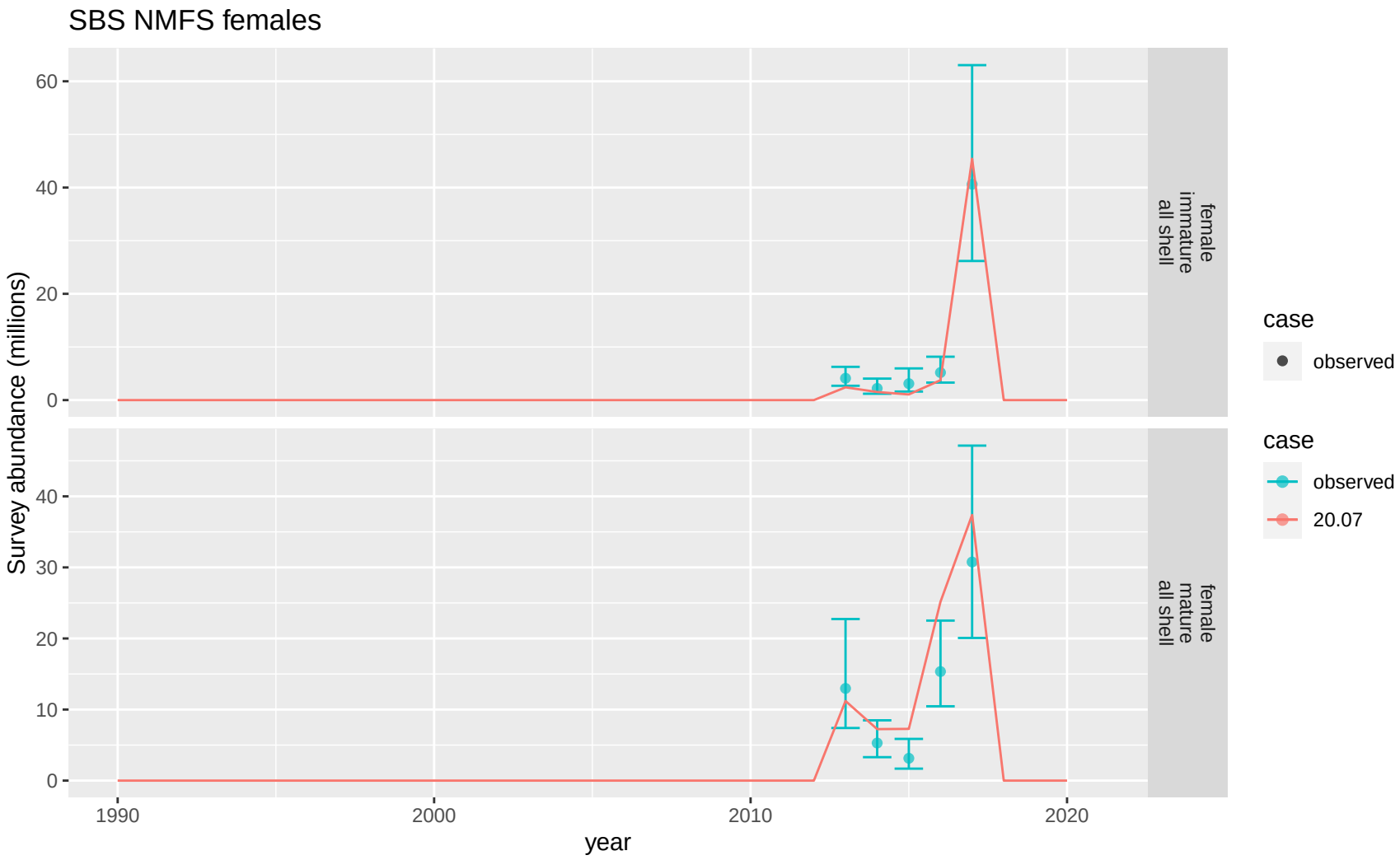

Figure 36: Comparison of observed and predicted female survey abundance for SBS NMFS females. Recent time period.

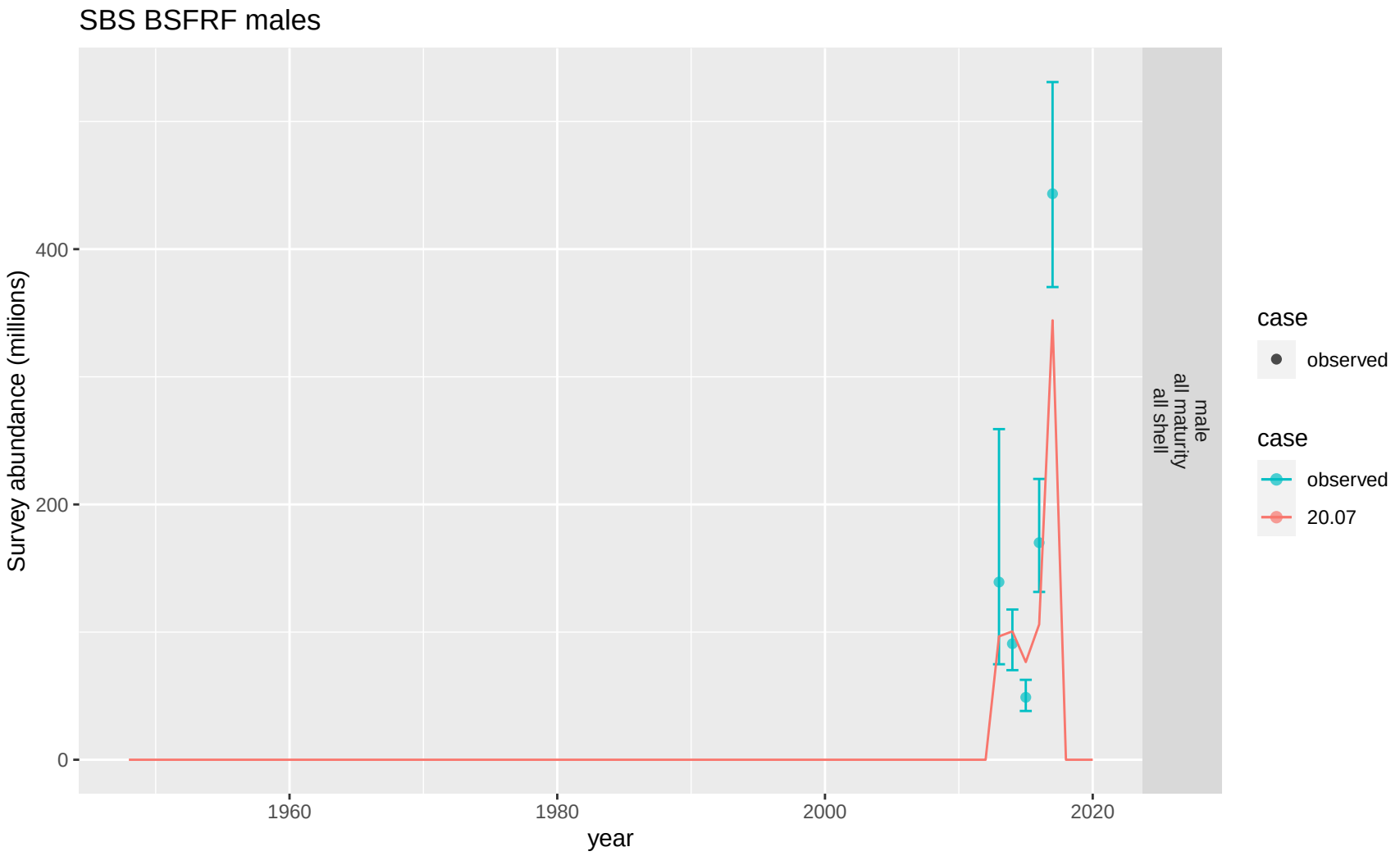

Figure 37: Comparison of observed and predicted male survey abundance for SBS BSFRF males.

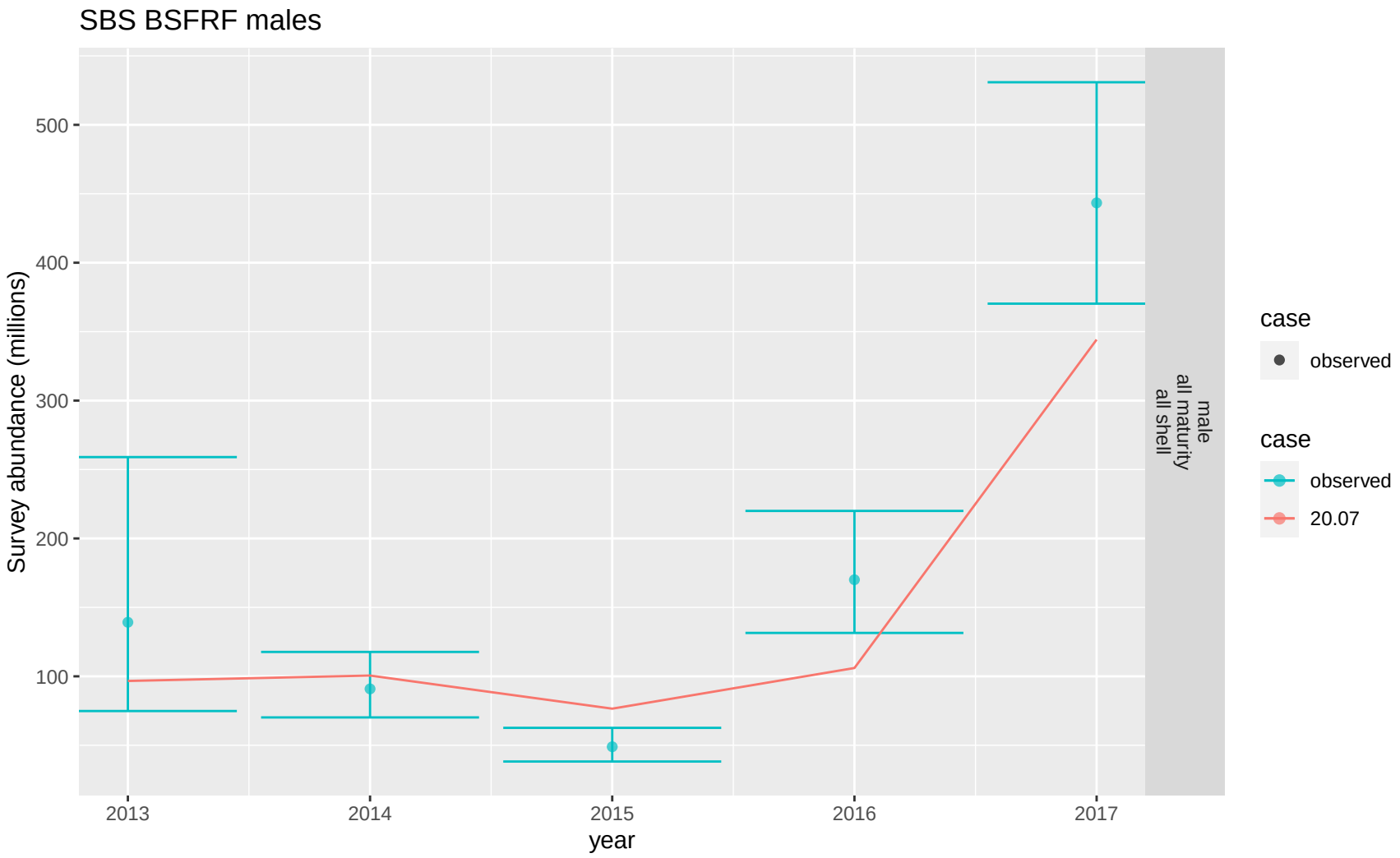

Figure 38: Comparison of observed and predicted male survey abundance for SBS BSFRF males. Observed time period.

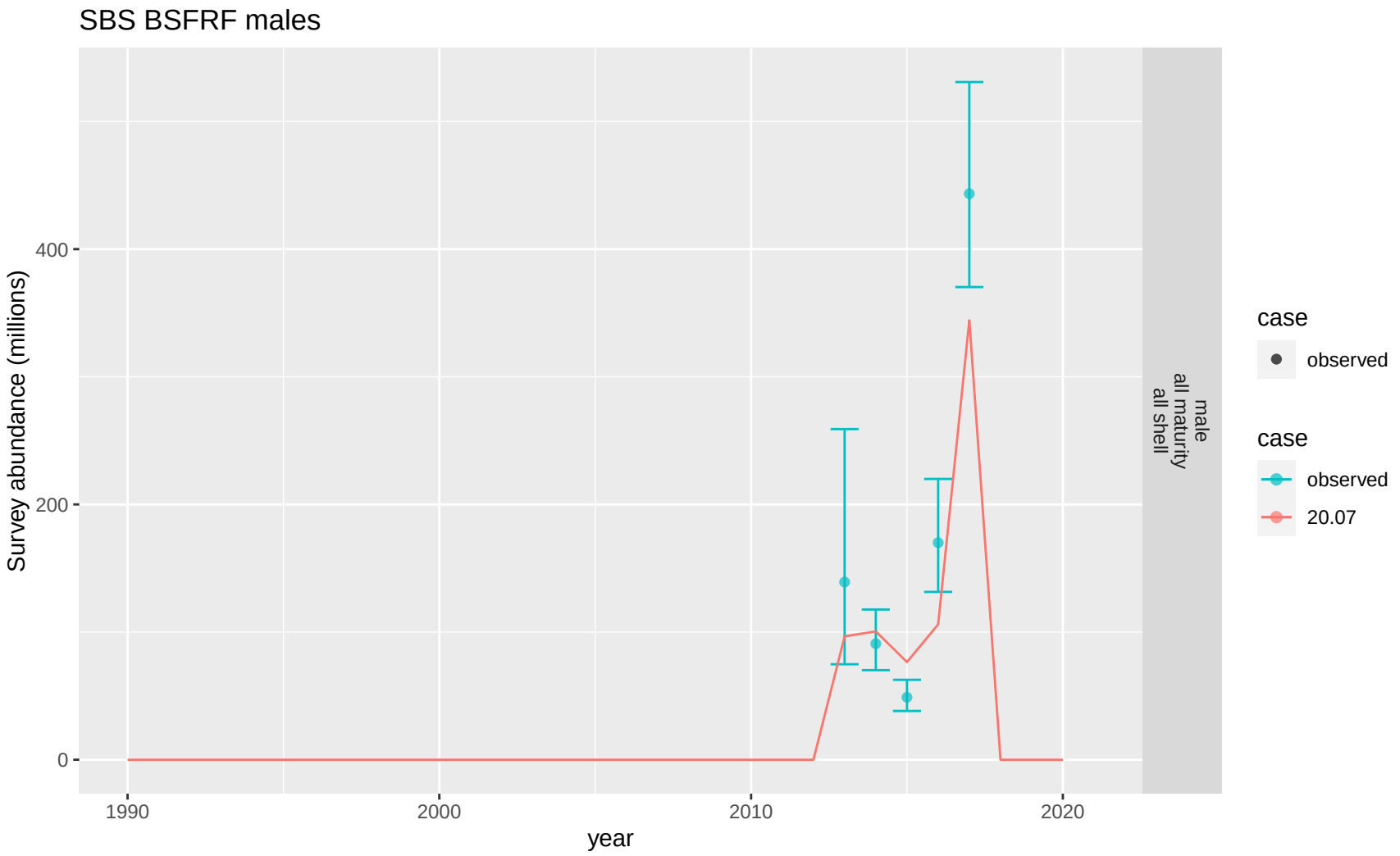

Figure 39: Comparison of observed and predicted male survey abundance for SBS BSFRF males. Recent time period.

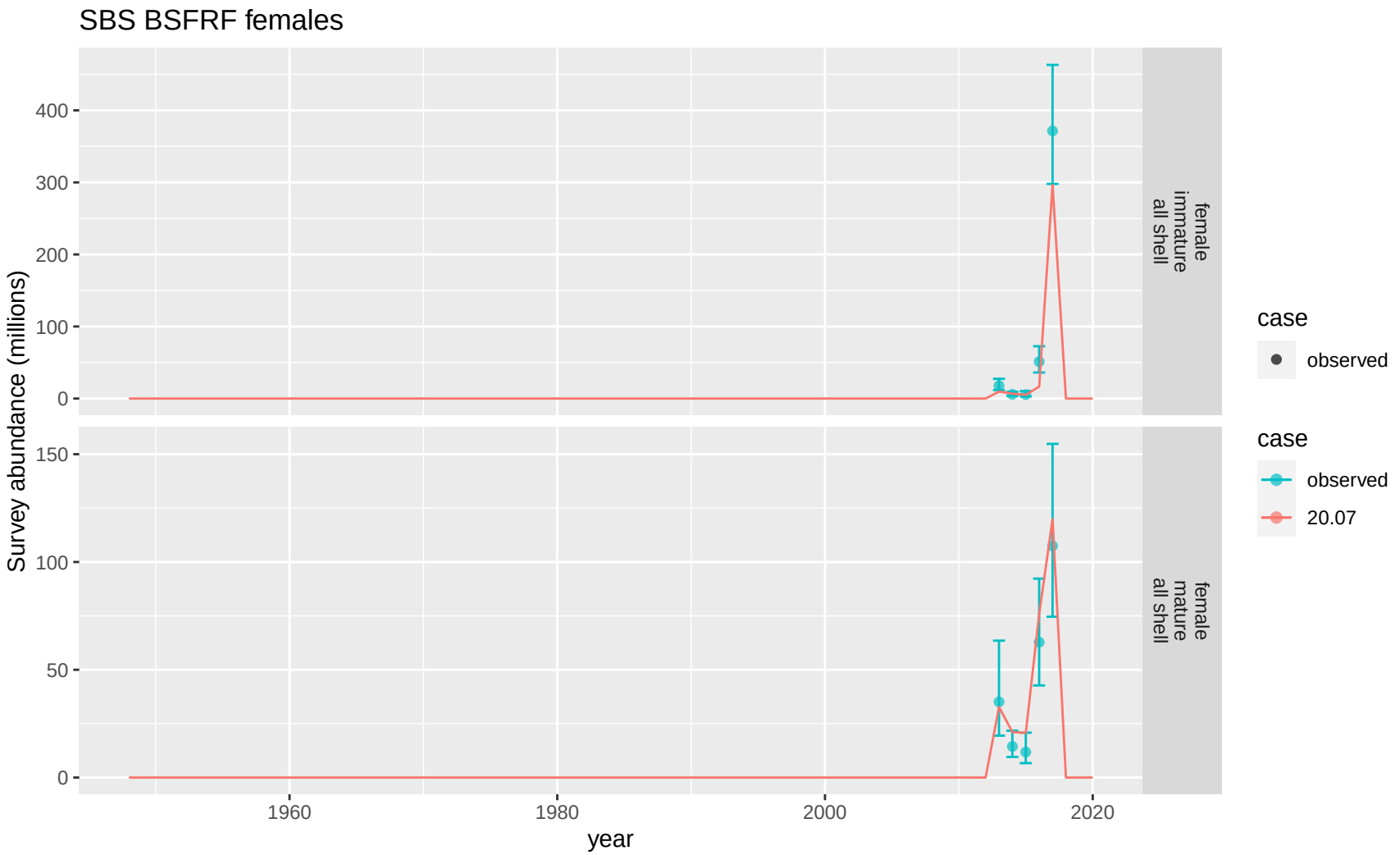

Figure 40: Comparison of observed and predicted female survey abundance for SBS BSFRF females.

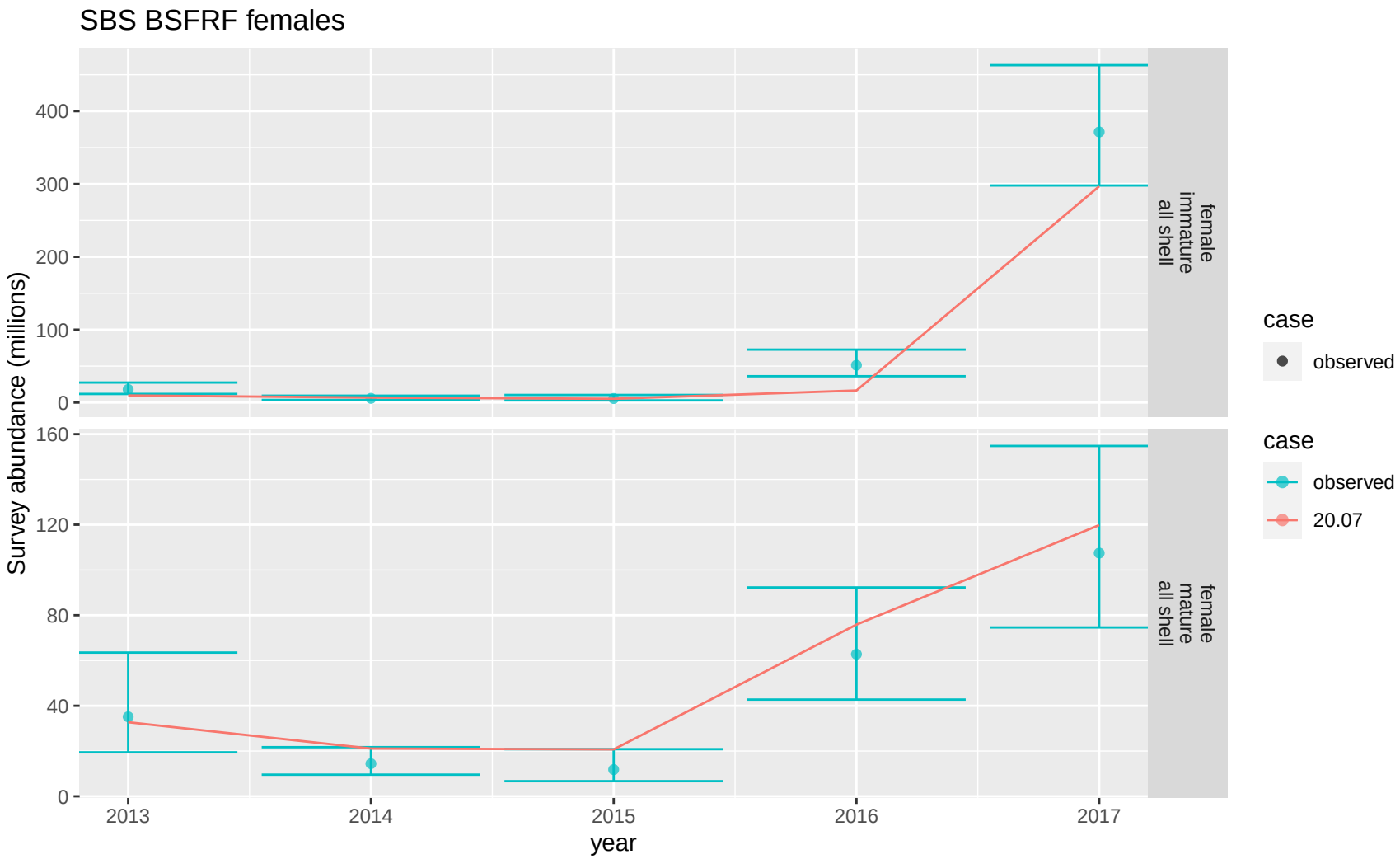

Figure 41: Comparison of observed and predicted female survey abundance for SBS BSFRF females. Observed time period.

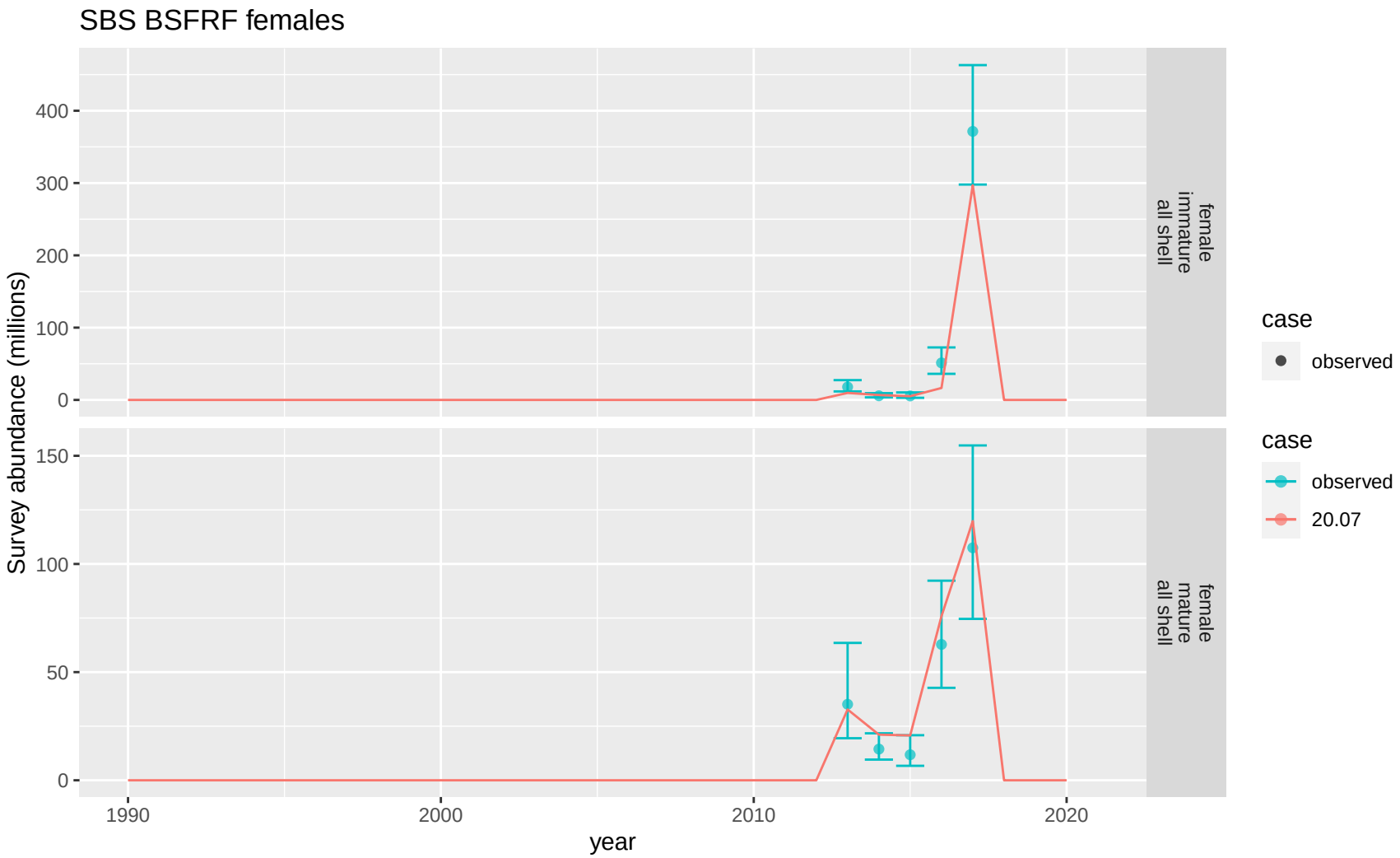

Figure 42: Comparison of observed and predicted female survey abundance for SBS BSFRF females. Recent time period.

Z-scores

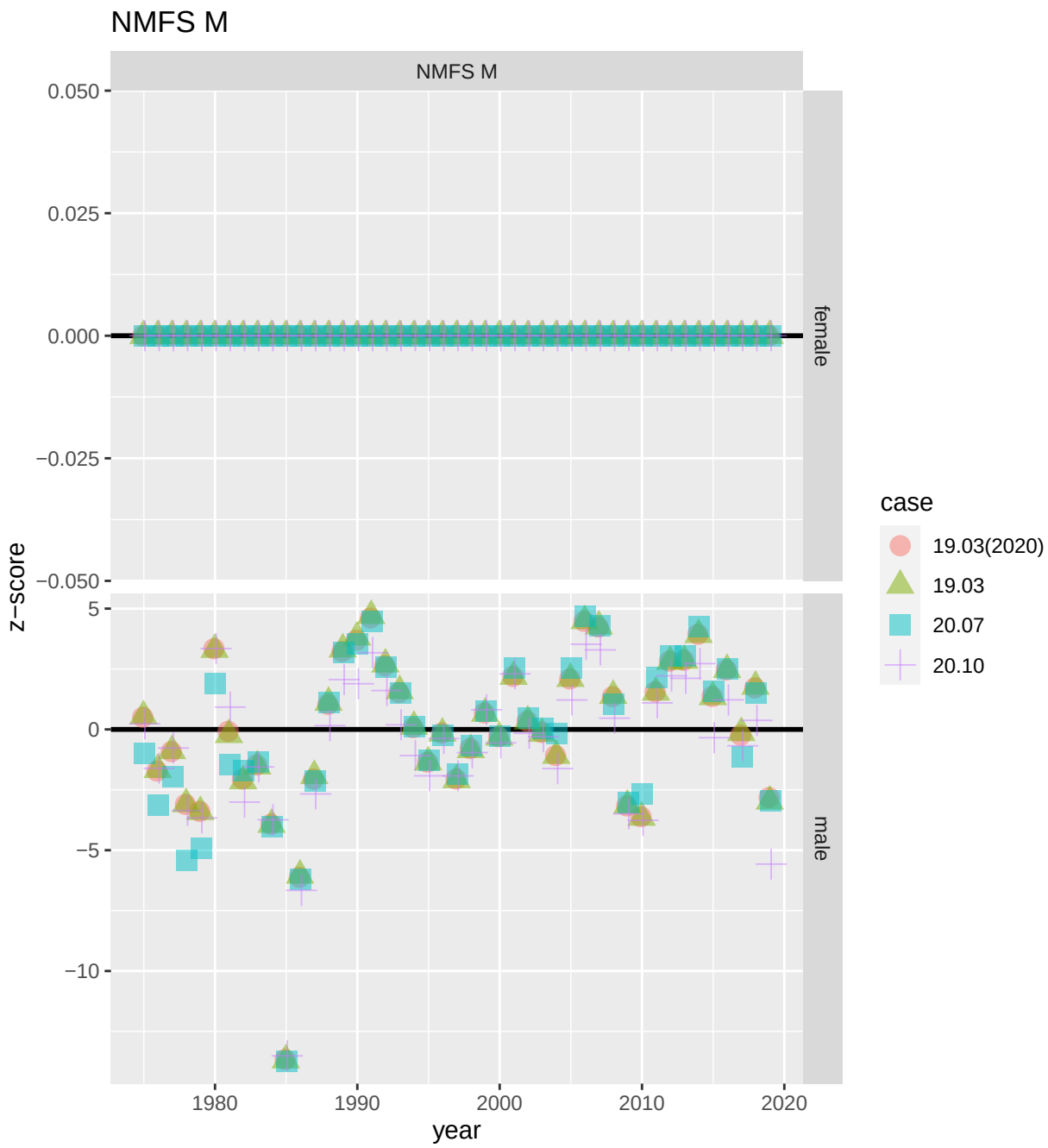

Figure 43: Z-scores for index catch abundance in NMFS M.

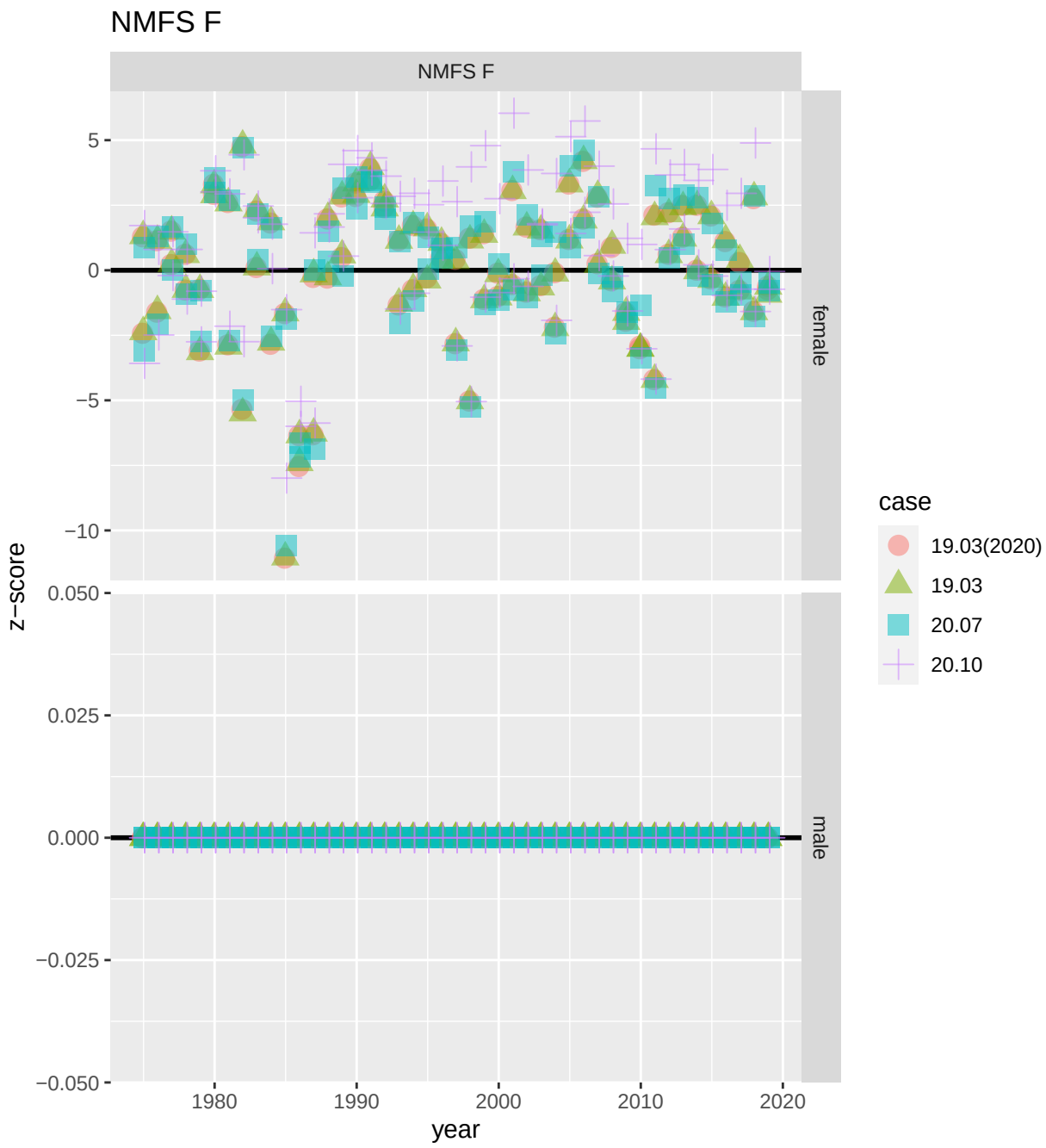

Figure 44: Z-scores for index catch abundance in NMFS F.

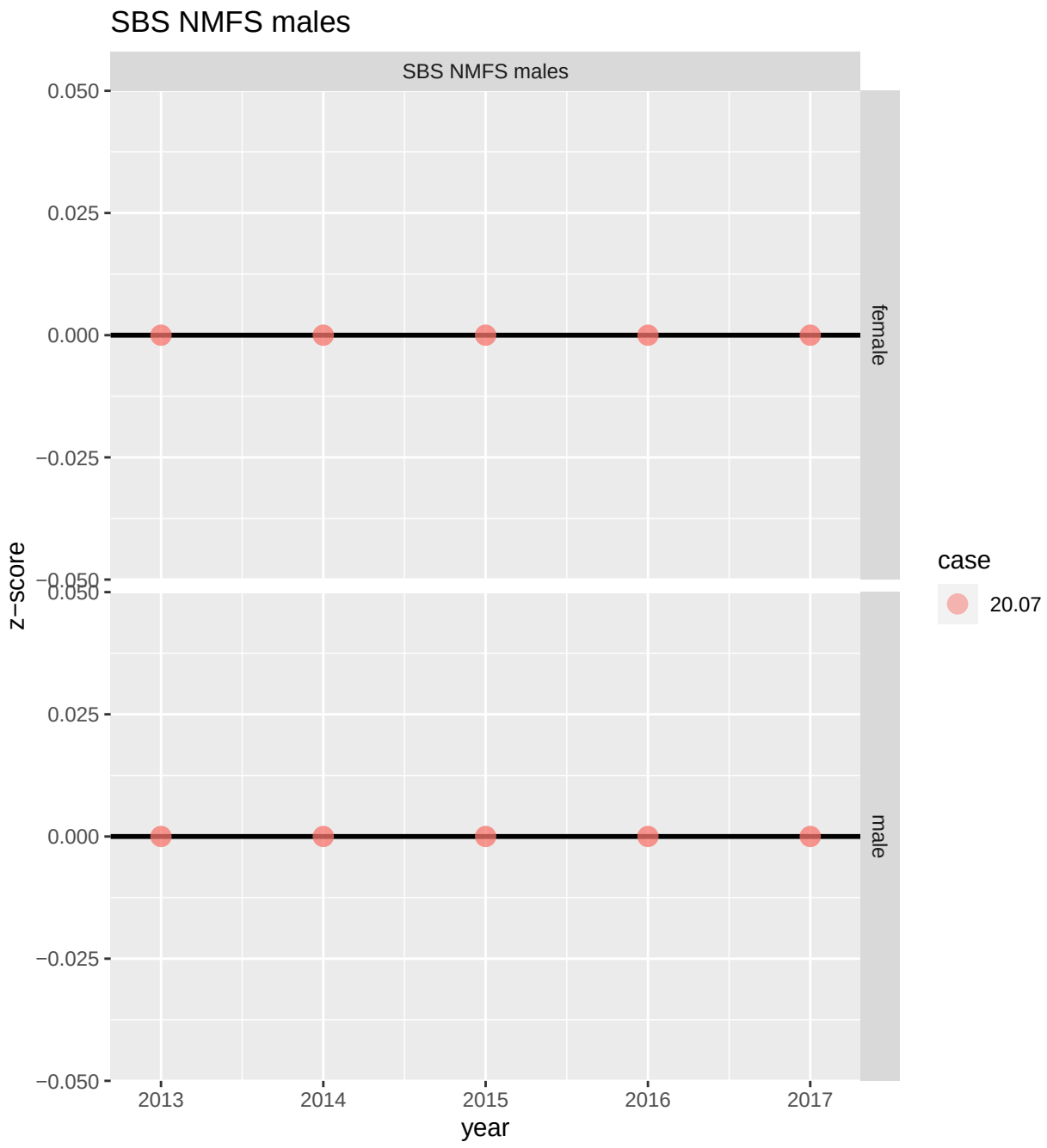

Figure 45: Z-scores for index catch abundance in SBS NMFS males.

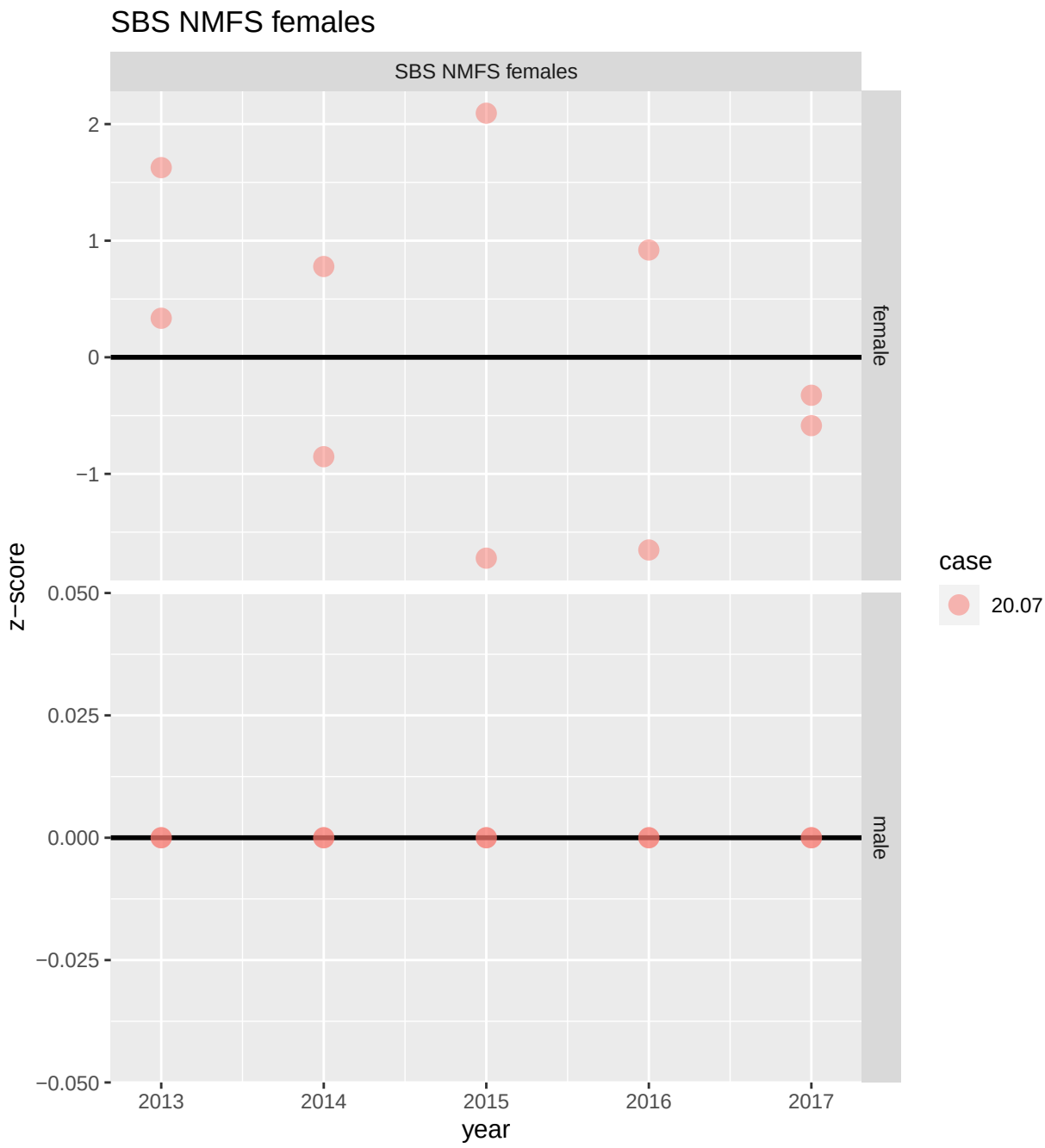

Figure 46: Z-scores for index catch abundance in SBS NMFS females.

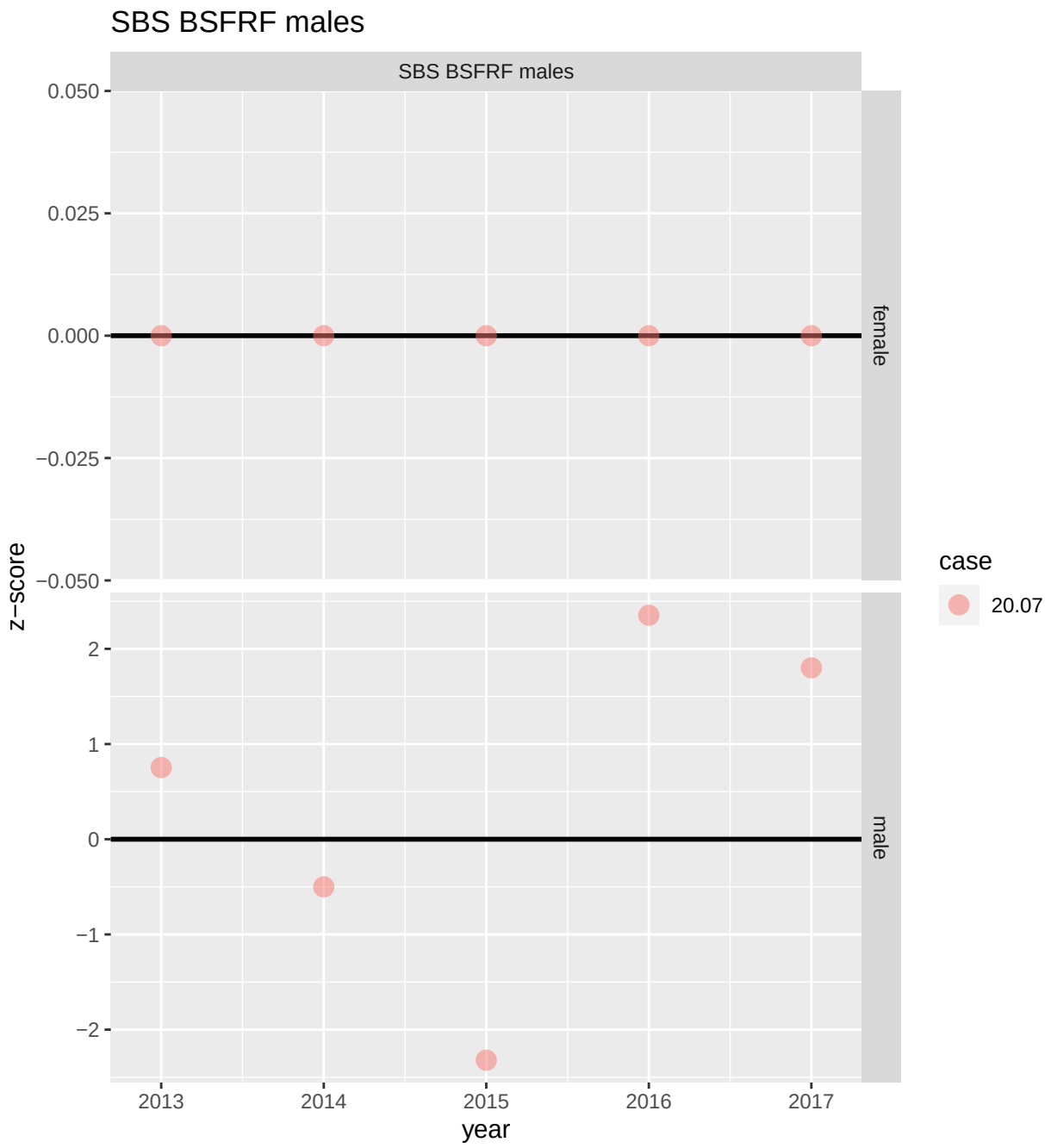

Figure 47: Z-scores for index catch abundance in SBS BSFRF males.

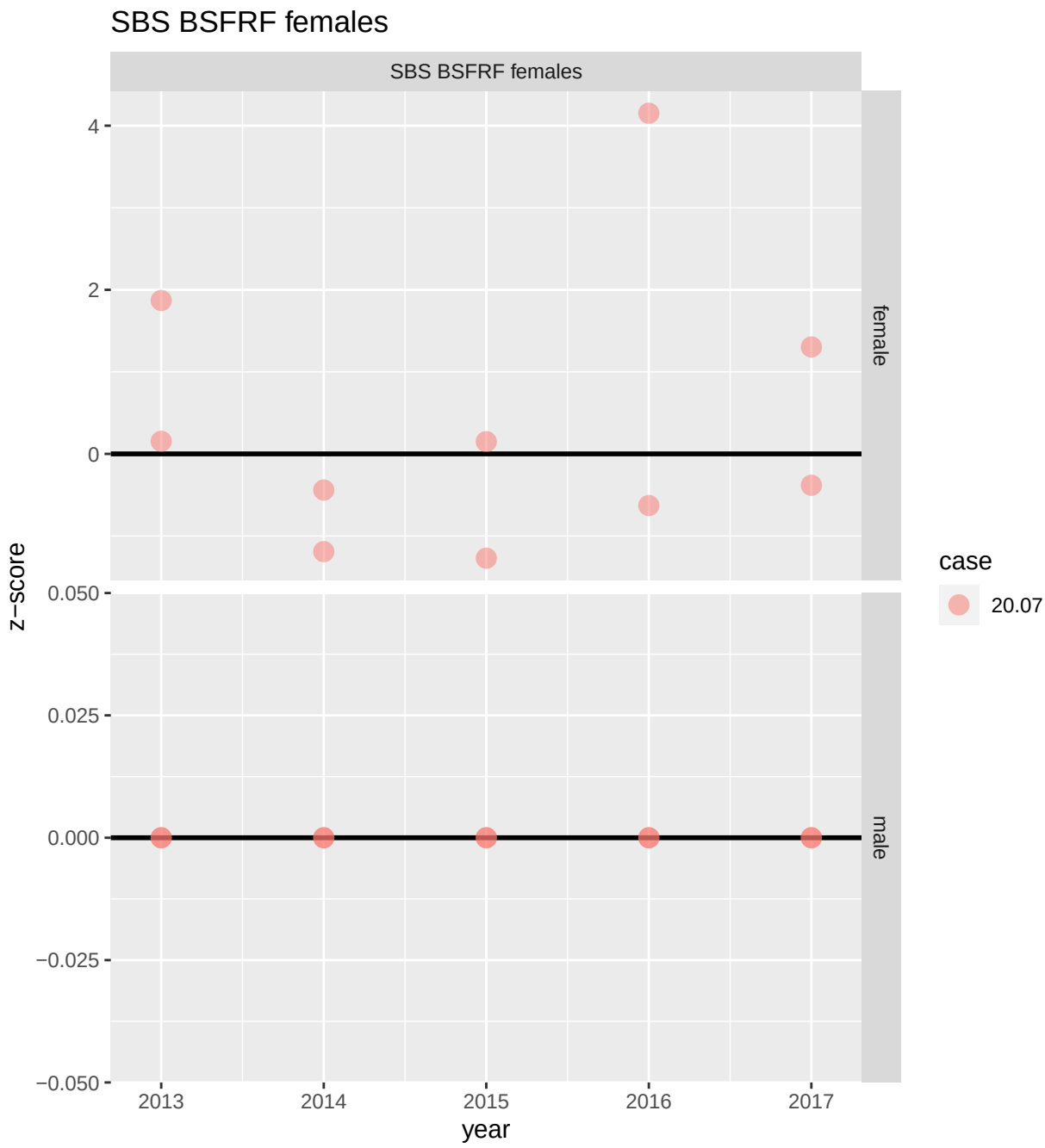

Figure 48: Z-scores for index catch abundance in SBS BSFRF females.

Appendix 7: Fits to "Other" Data – 19.03(2020) vs 19.03 vs 20.07 vs 20.10

William Stockhausen

01 September, 2020

Contents

Model fits to "other" data

Fits to growth data and male maturity datasets by the model(s) are presented in this section. Not all of the fits presented are necessarily included in the parameter optimization for each model; some fits for a particular model may be included for comparison purposes with other models which include those data in their optimization. The reader should consult the main assessment document to determine which fits are included in the optimization for any particular model.

Growth data

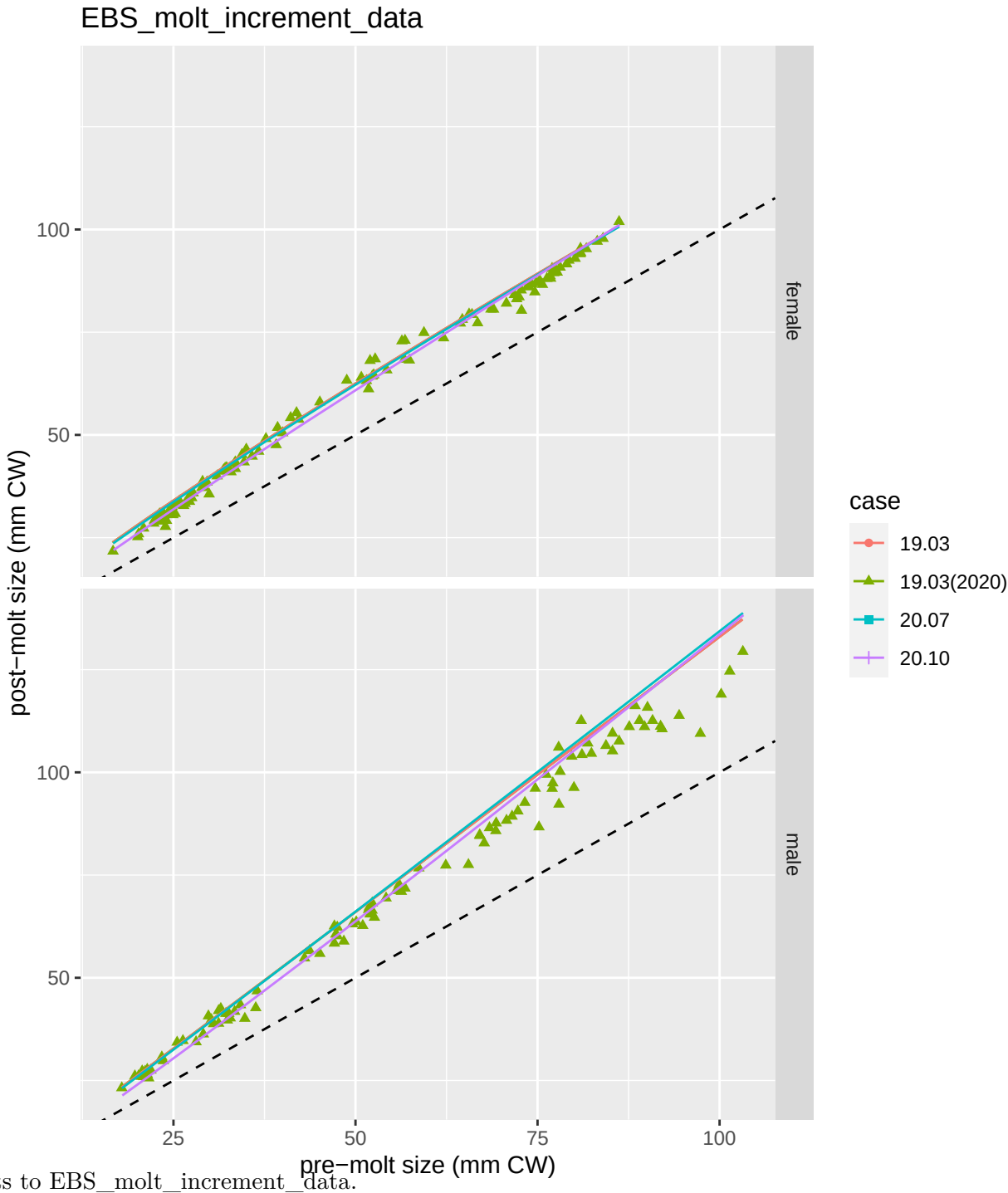

Figure 1. Model fits to EBS_molt_increment_data.

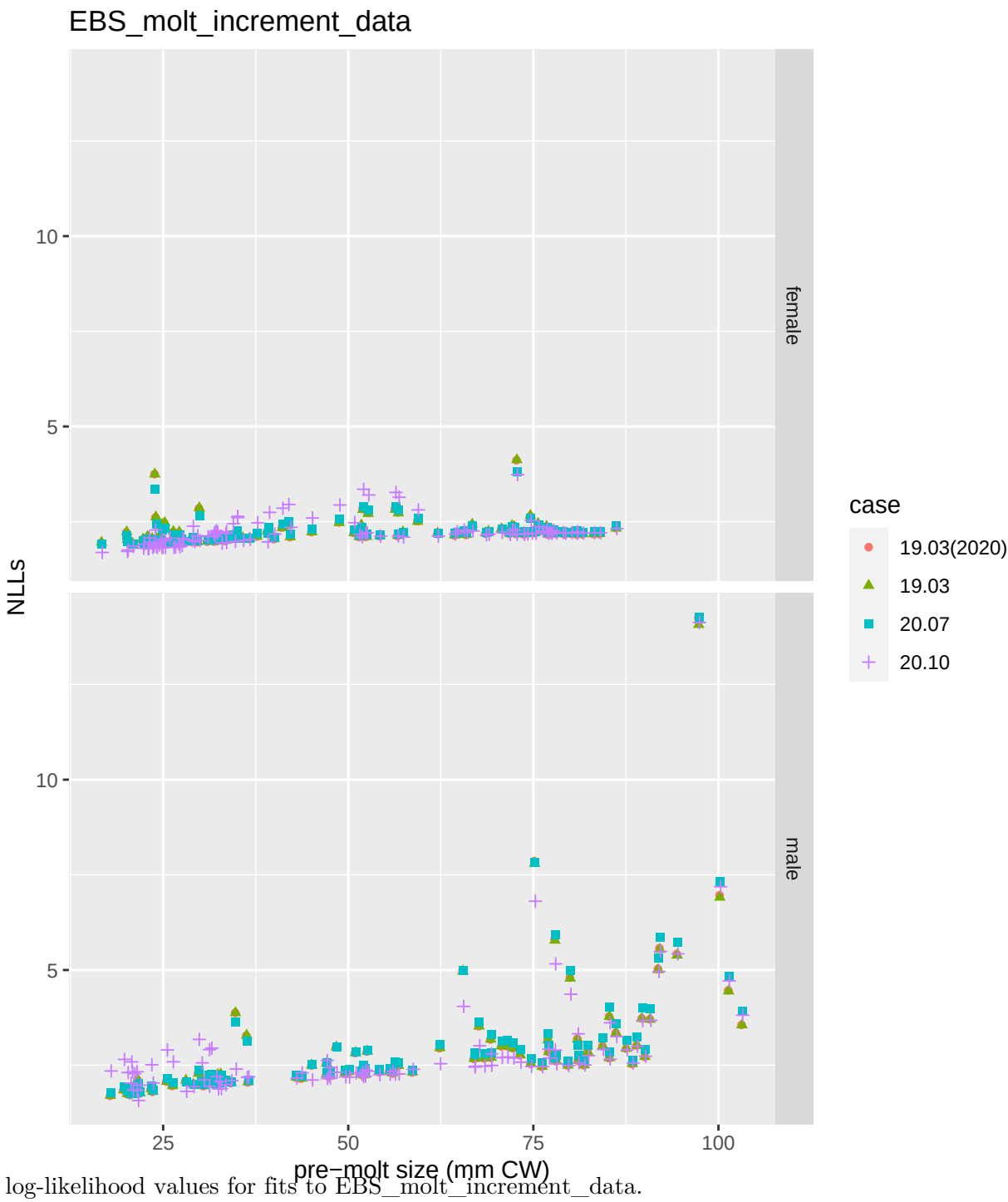

Figure 2. Negative log-likelihood values for fits to EBS_molt_increment_data.

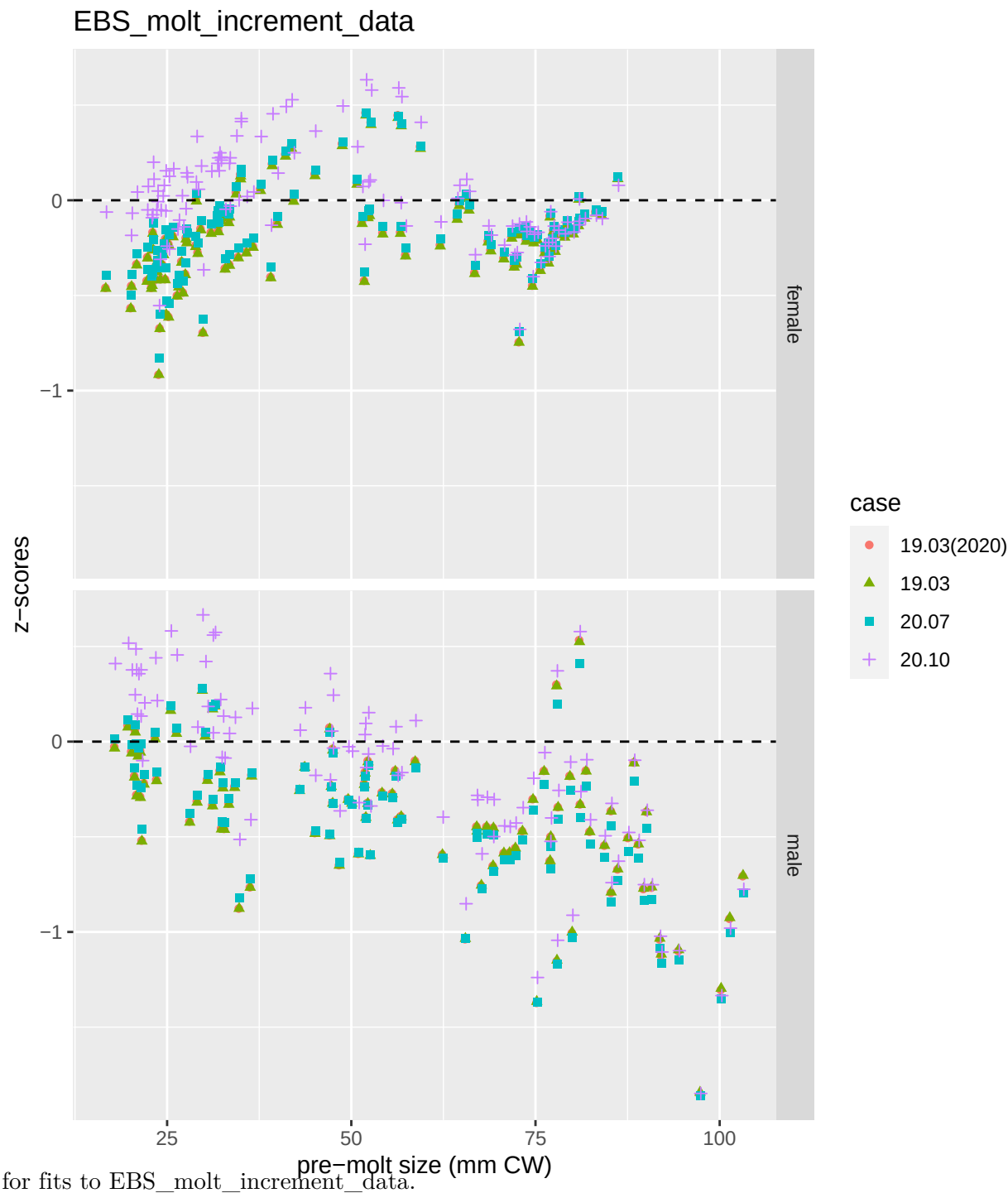

Figure 3. Z-scores for fits to EBS_molt_increment_data.

Maturity ogive data

In the male maturity dataset used in this assessment, a number of male crab less than 60 mm CW were classified as mature based on their chela height-to-carapace width ratios. For the purposes of fitting the data, these crab were assumed to be misclassified and to actually be immature. Consequently, data from size bins less than 60 mm CW, although shown in the following plots comparing model predictions to observations, were not included in the likelihood used for model optimization and are not shown in the NLL and z-score plots.

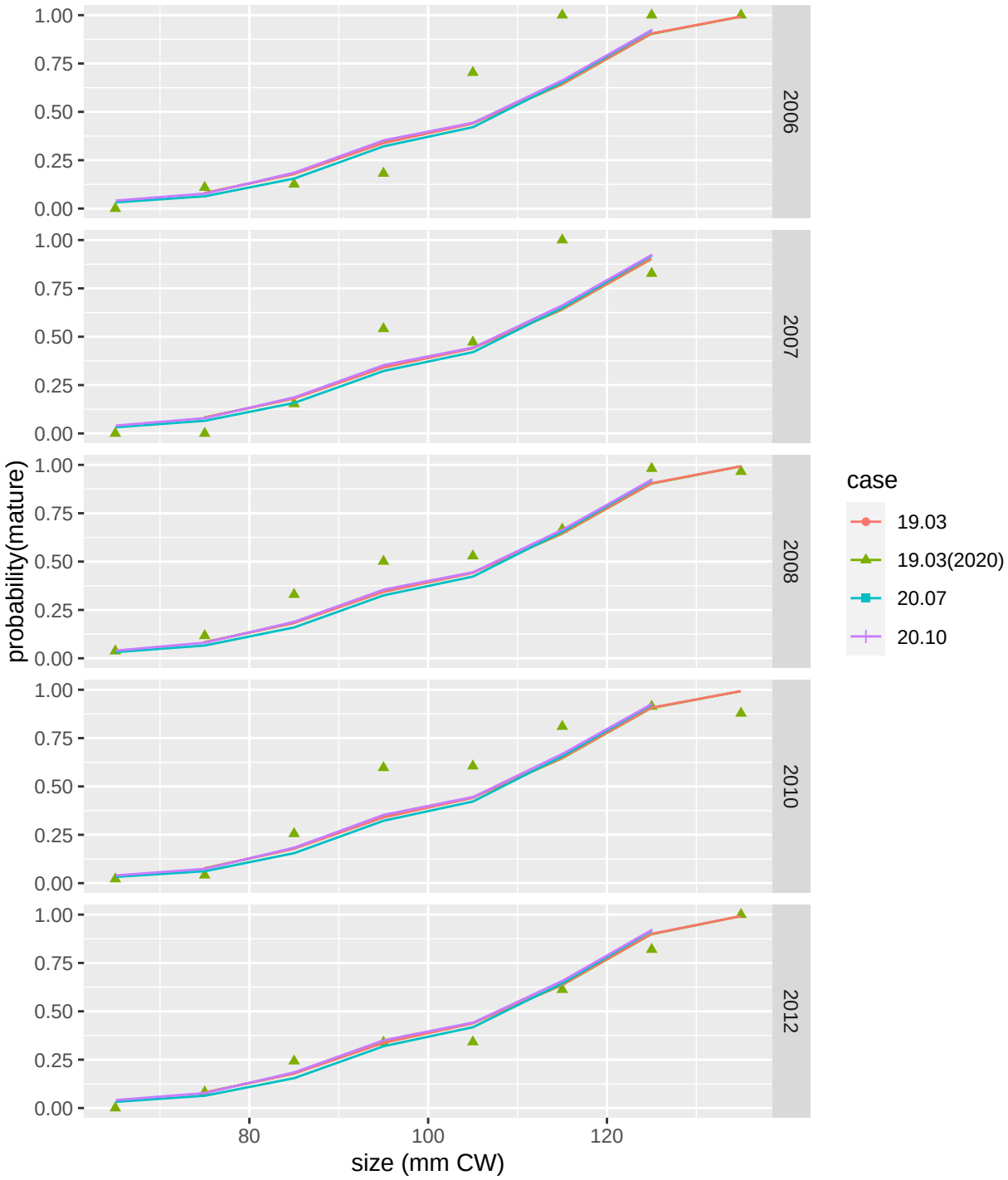

Figure 4: Model fits to EBS male maturity ogives for 2006 to 2012.

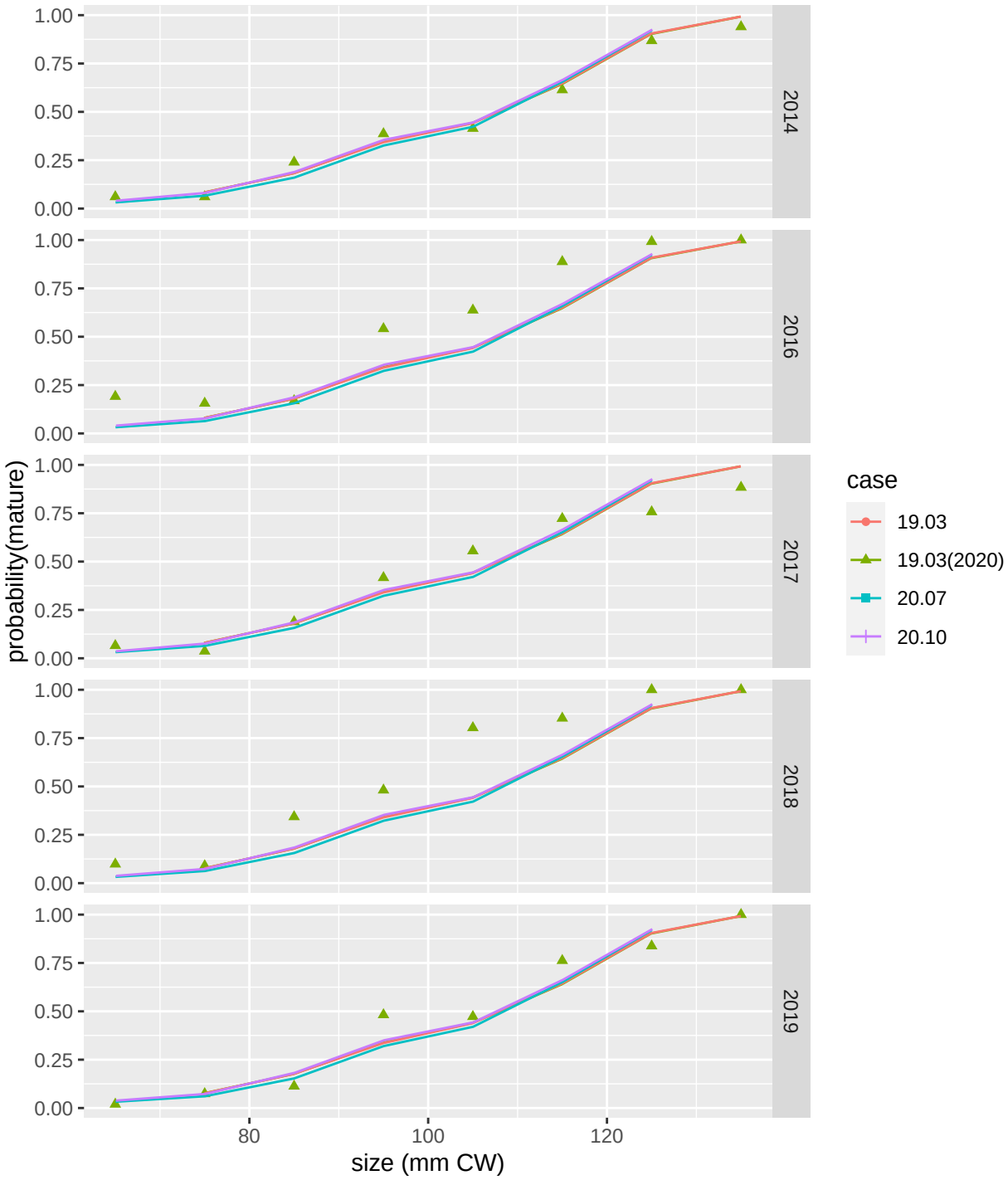

Figure 5: Model fits to EBS male maturity ogives for 2014 to 2019.

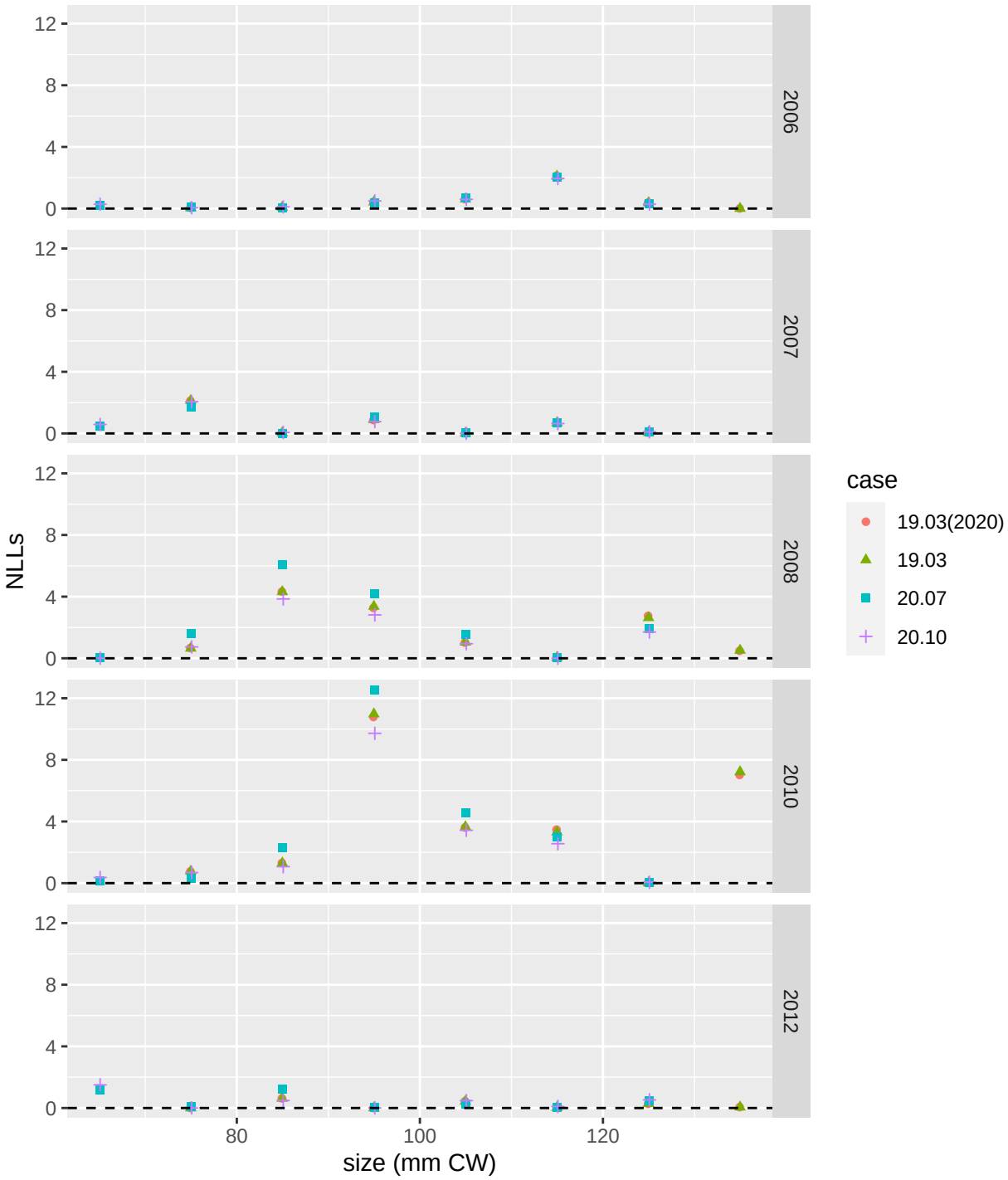

Figure 6: Negative log-likelihood values for fits to EBS male maturity ogives for 2006 to 2012.

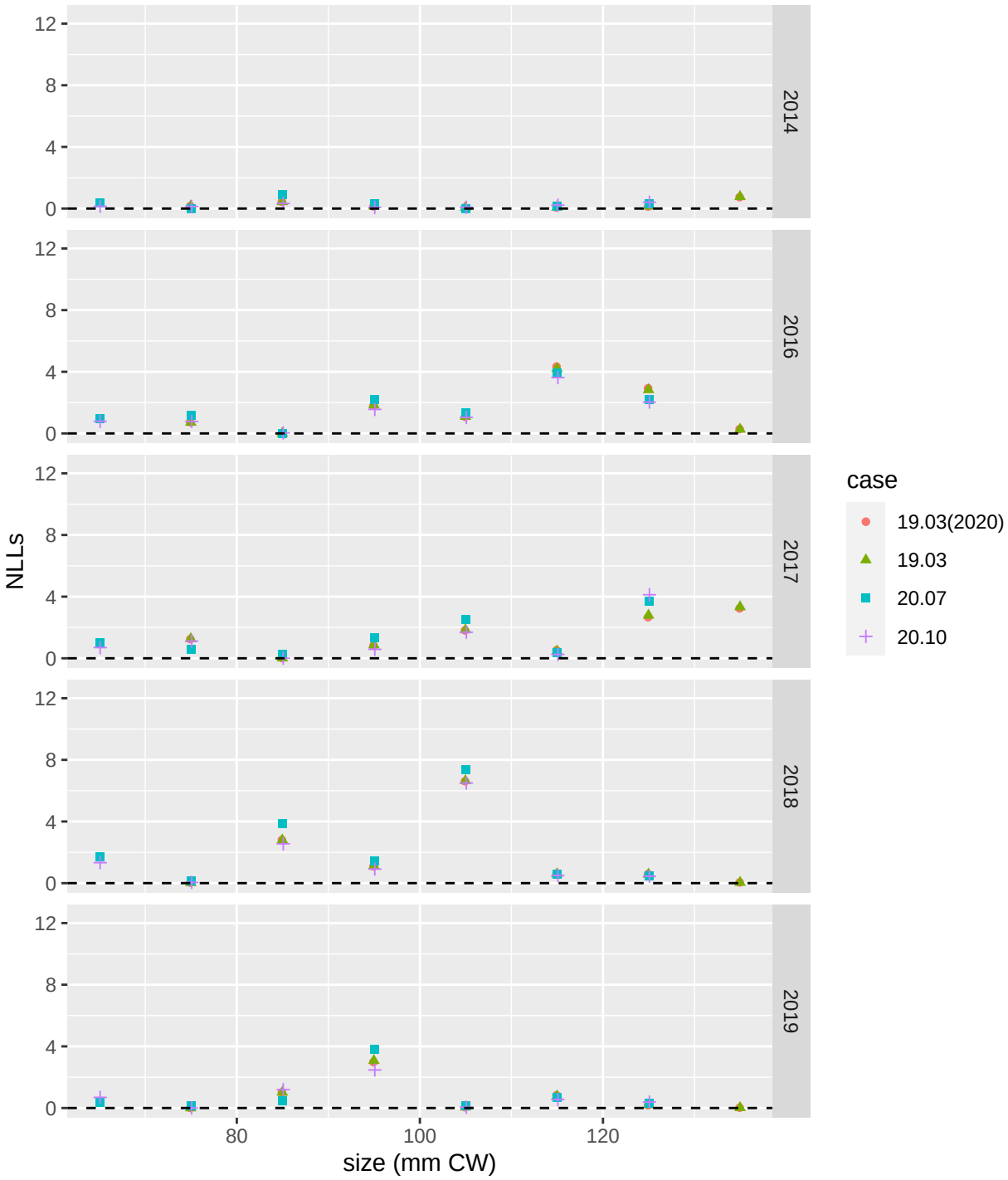

Figure 7: Negative log-likelihood values for fits to EBS male maturity ogives for 2014 to 2019.

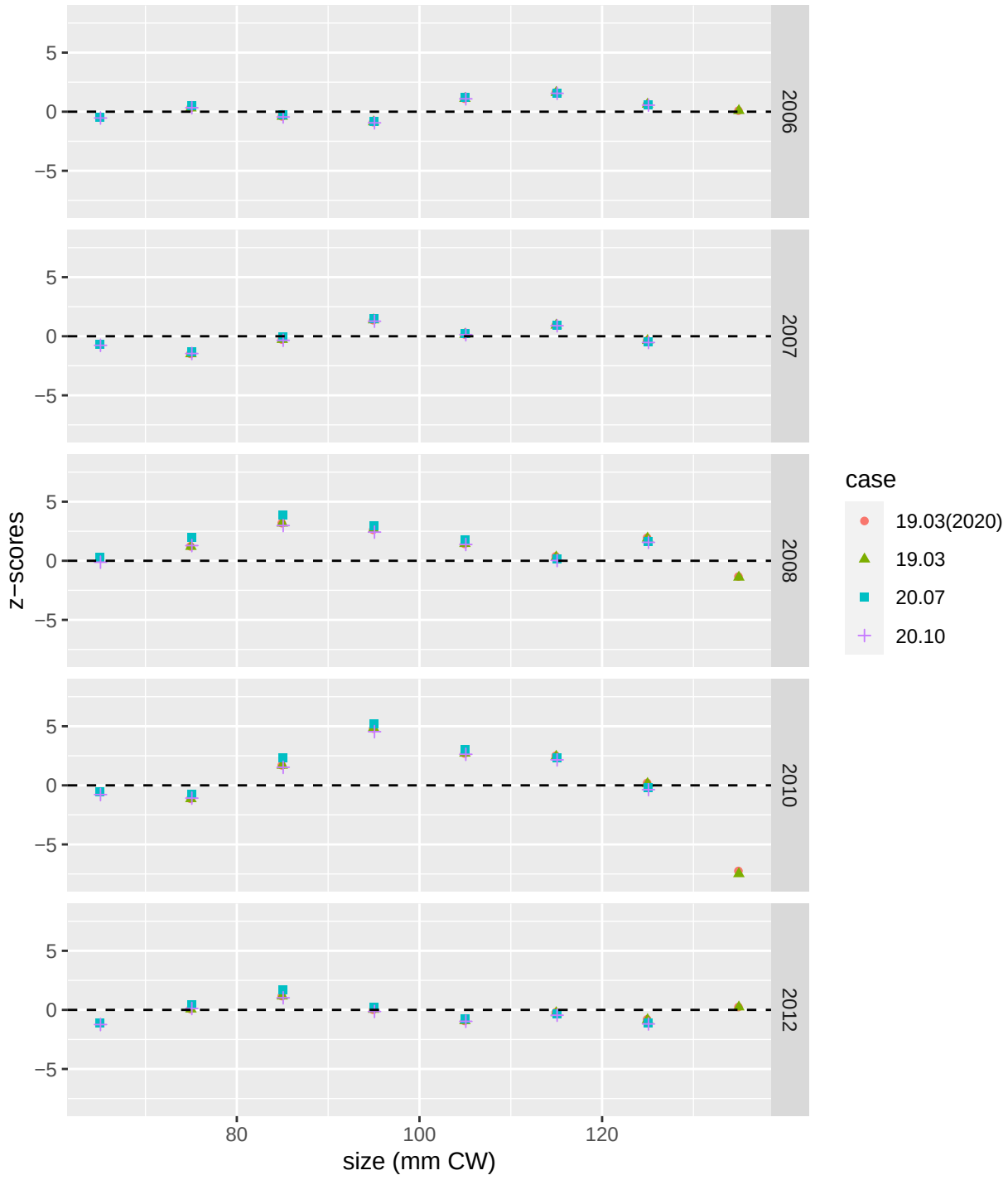

Figure 8: Z-scores for fits to EBS male maturity ogives for 2006 to 2012.

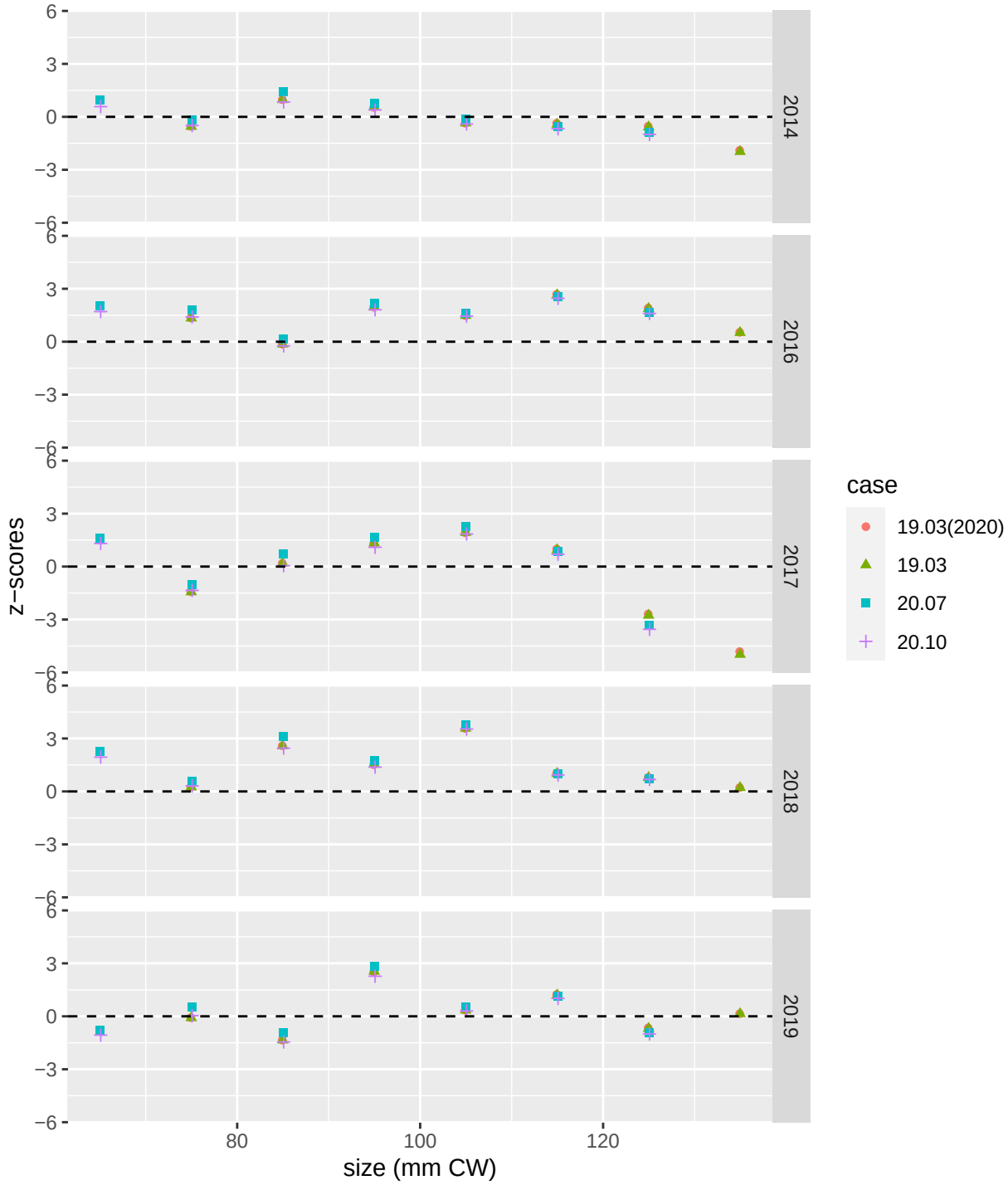

Figure 9: Z-scores for fits to EBS male maturity ogives for 2014 to 2019.

Appendix 8: Fits to All Size Composition Data – 19.03(2020) vs 19.03 vs 20.07 vs 20.10

William Stockhausen

01 September, 2020

Contents

Model fits to size compositions, by year

Fits to the size composition data available to the model(s) are presented in this section as line plots by year. Not all of the fits presented are necessarily included in the parameter optimization for each model; some fits to datasets for a particular model may be included for comparison purposes with other models which include those data in their optimization. The reader should consult the main assessment document to determine which fits are included in the optimization for any particular model.

Survey size compositions

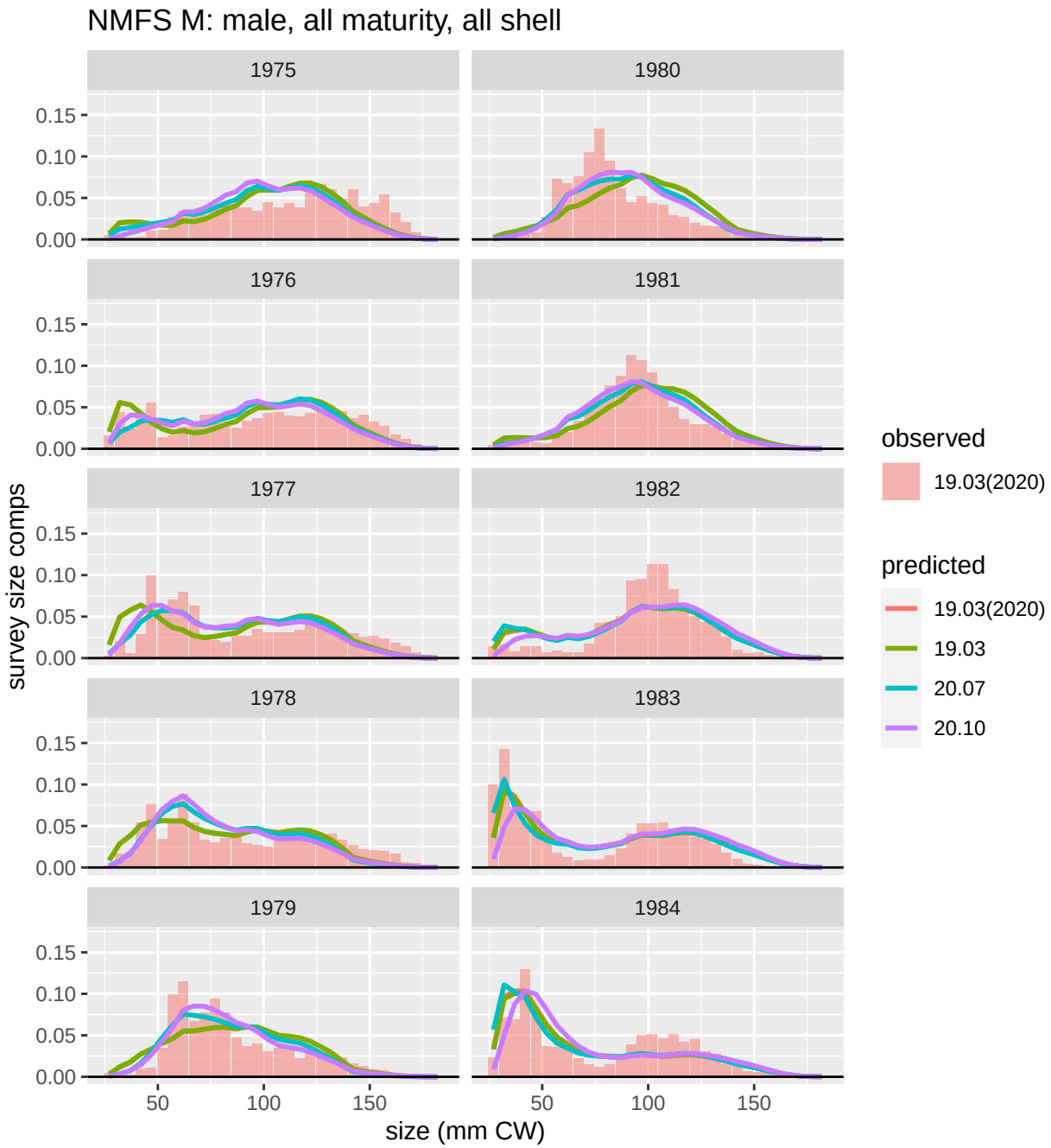

Figure 1: Comparison of observed and predicted male, all maturity, all shell survey size comps for NMFS M. Page 1 of 5.

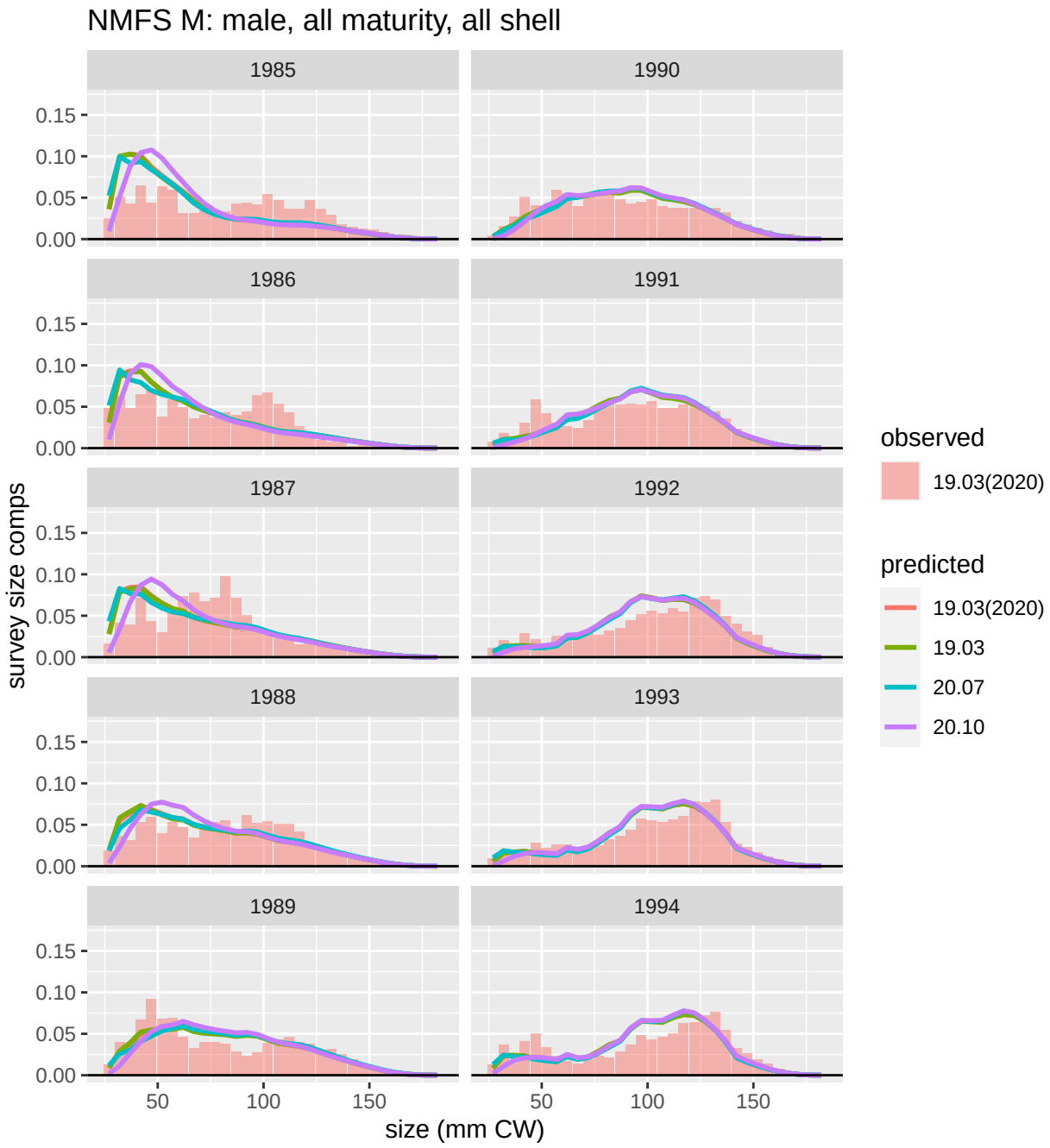

Figure 2: Comparison of observed and predicted male, all maturity, all shell survey size comps for NMFS M. Page 2 of 5.

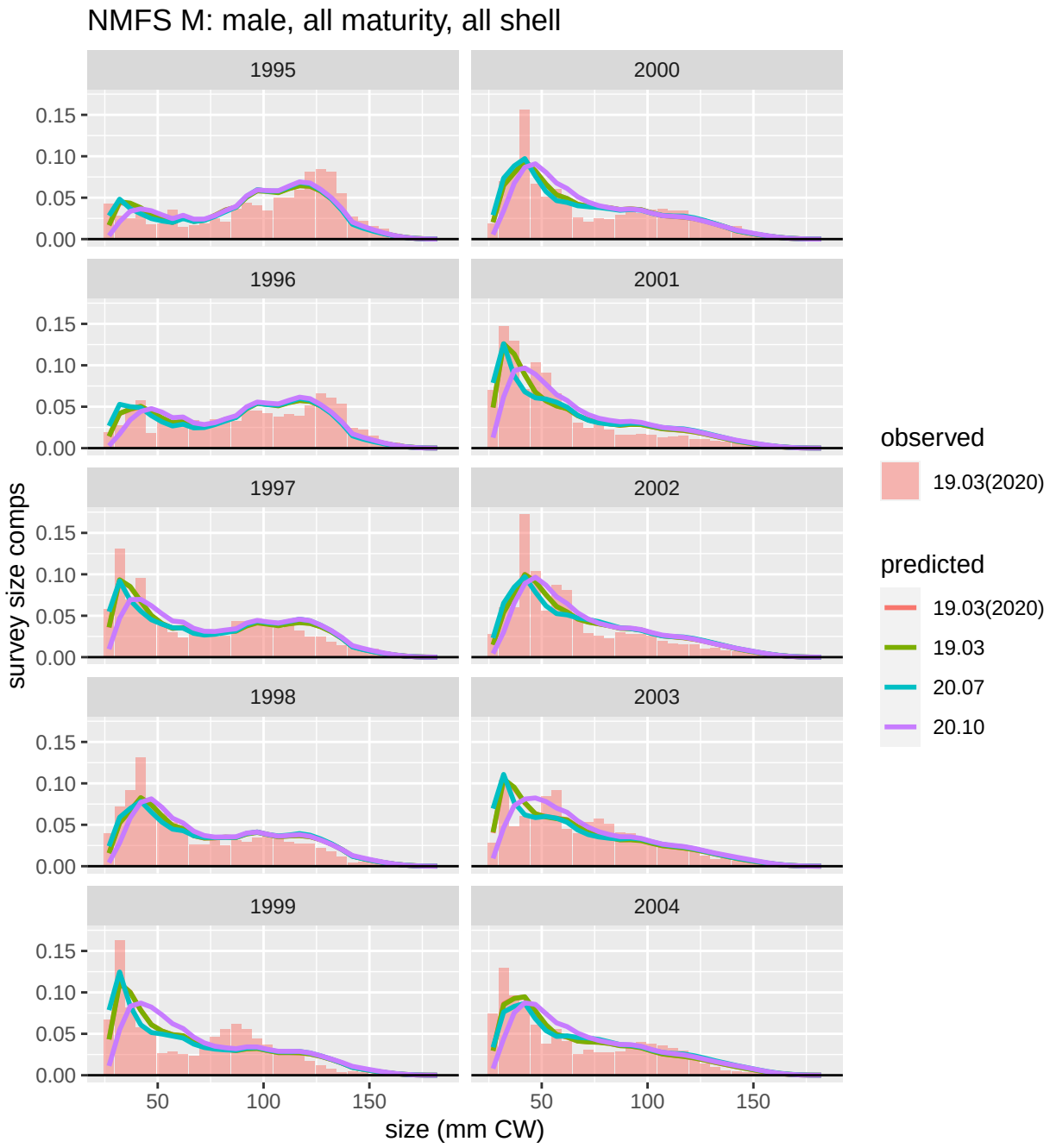

Figure 3: Comparison of observed and predicted male, all maturity, all shell survey size comps for NMFS M. Page 3 of 5.

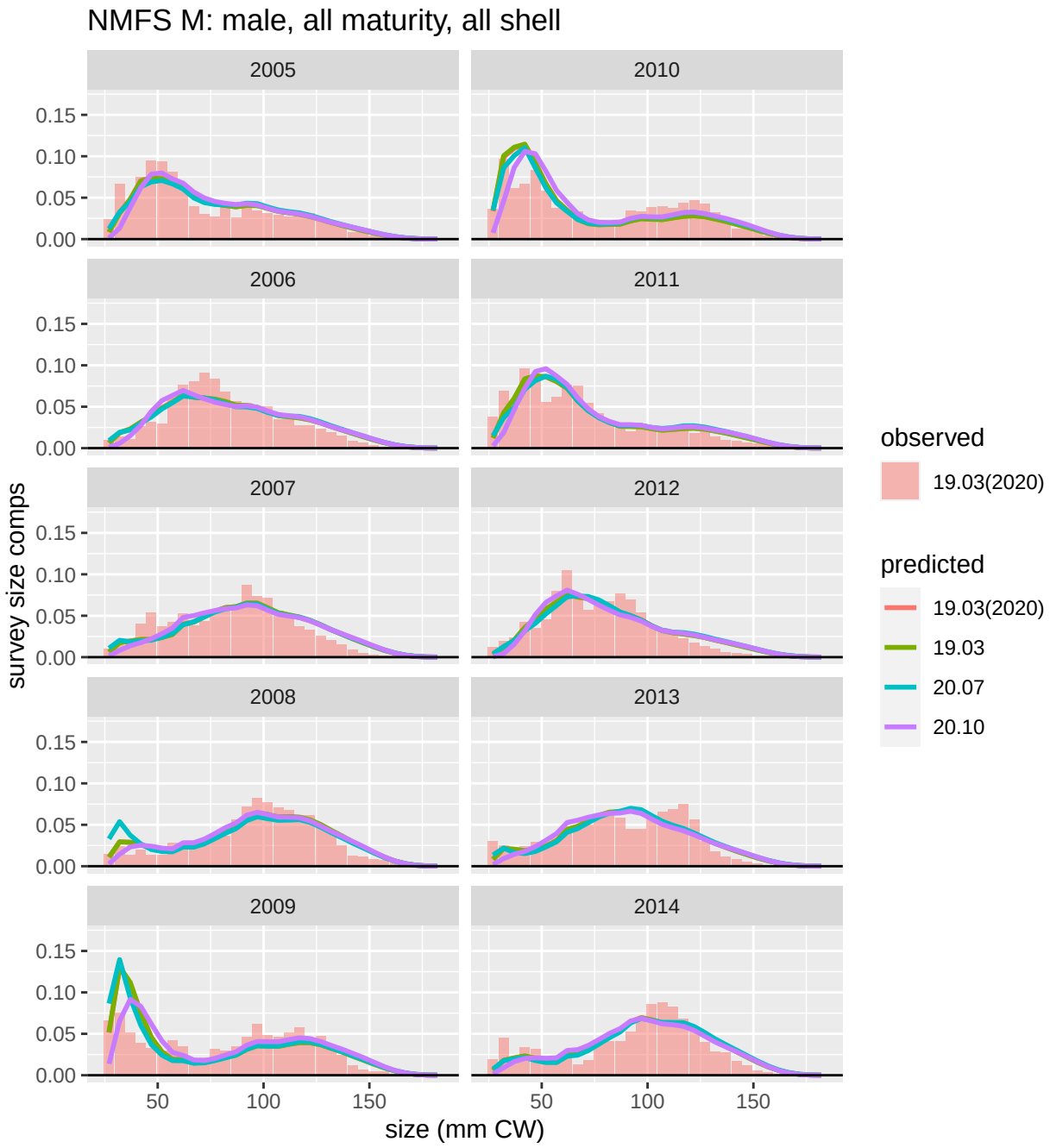

Figure 4: Comparison of observed and predicted male, all maturity, all shell survey size comps for NMFS M. Page 4 of 5.

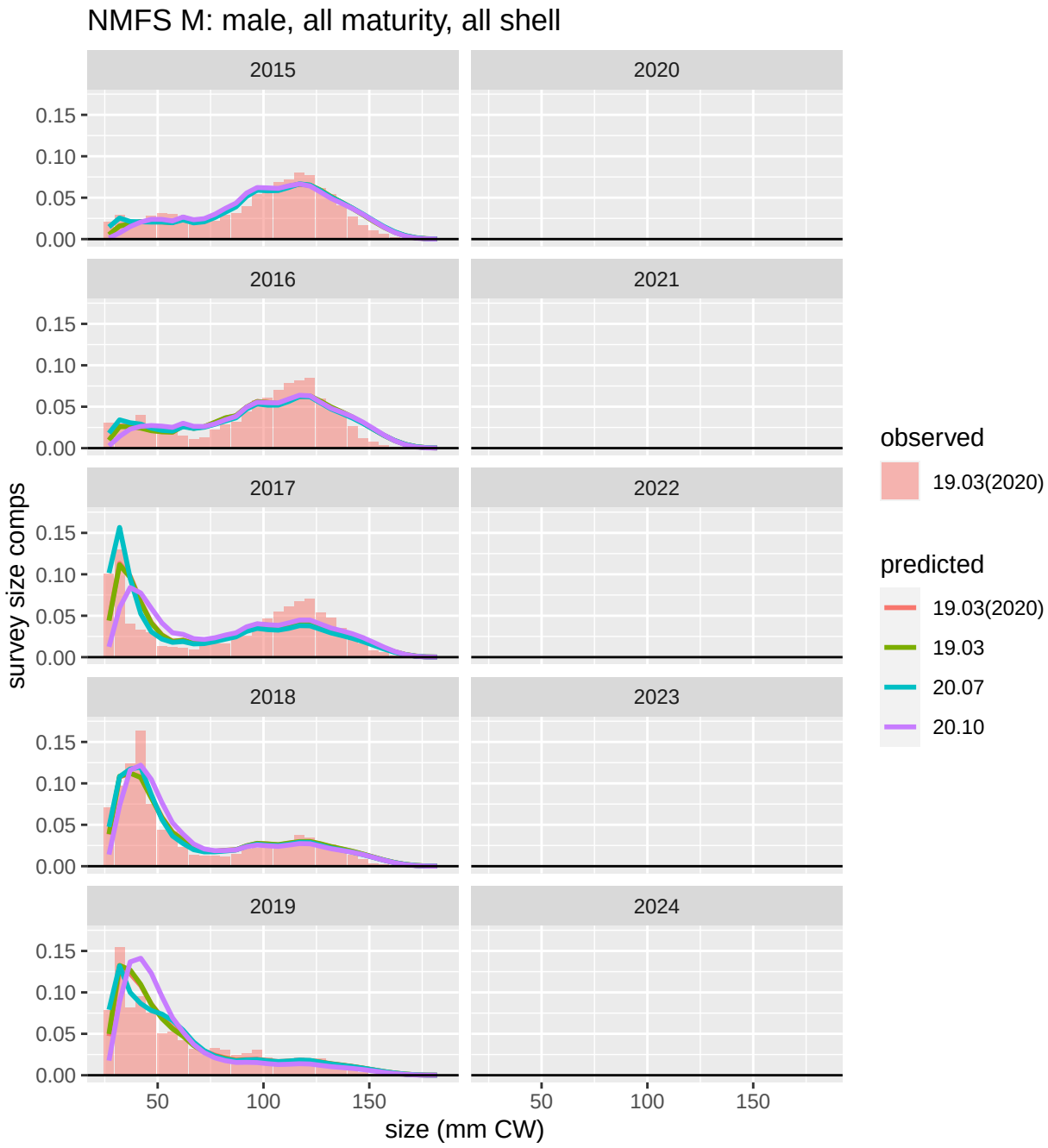

Figure 5: Comparison of observed and predicted male, all maturity, all shell survey size comps for NMFS M. Page 5 of 5.

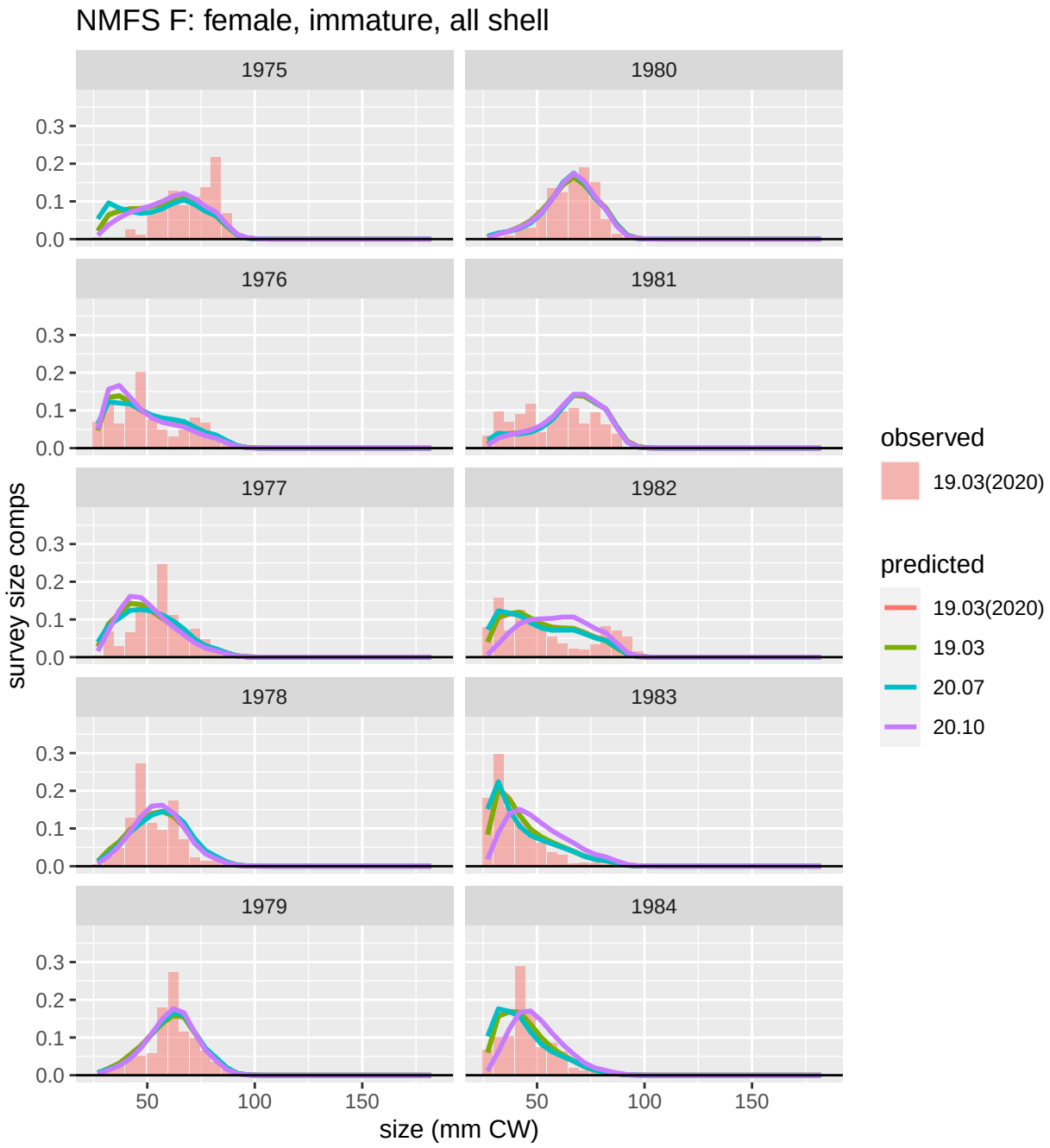

Figure 6: Comparison of observed and predicted female, immature, all shell survey size comps for NMFS F. Page 1 of 5.

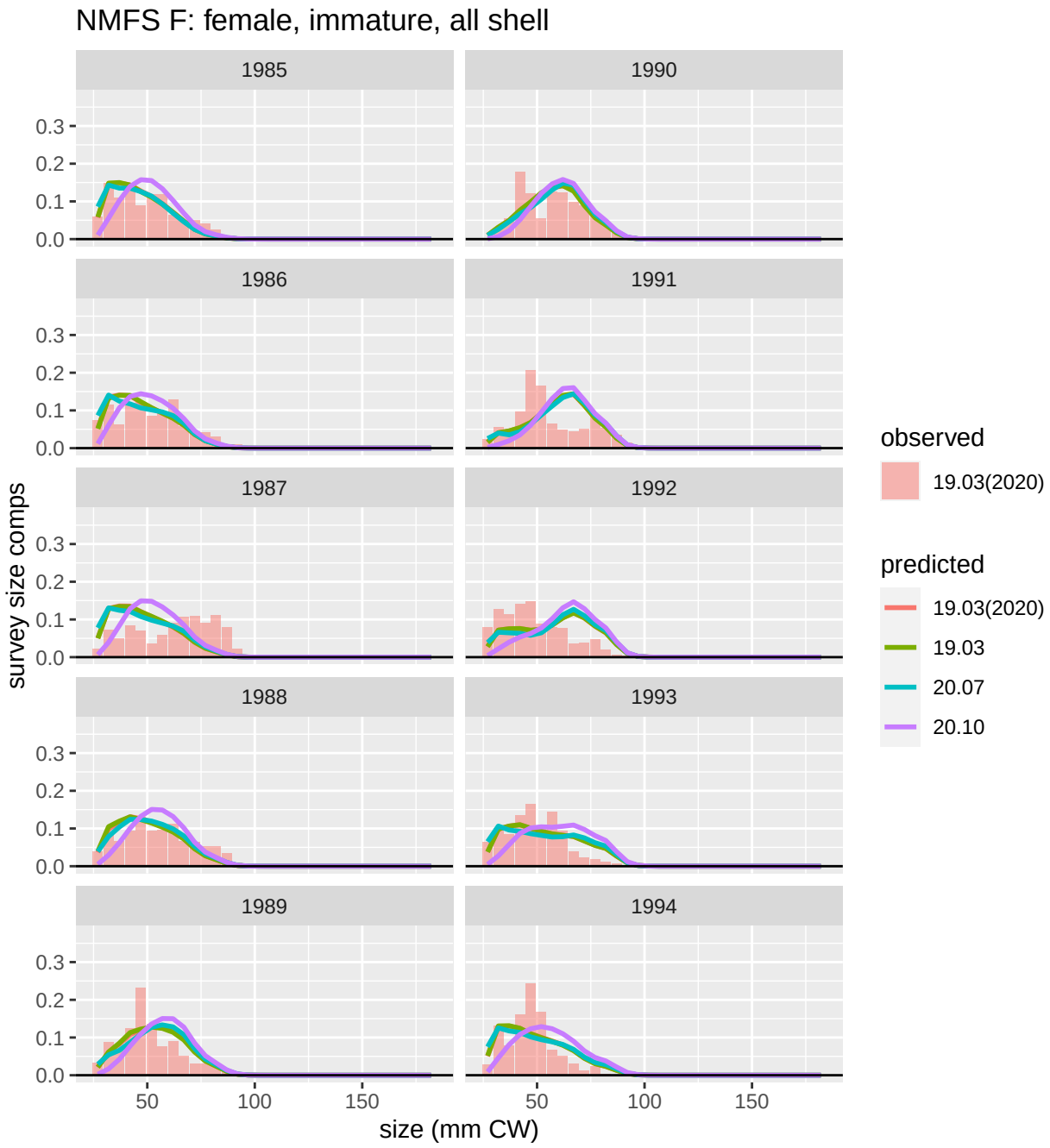

Figure 7: Comparison of observed and predicted female, immature, all shell survey size comps for NMFS F. Page 2 of 5.

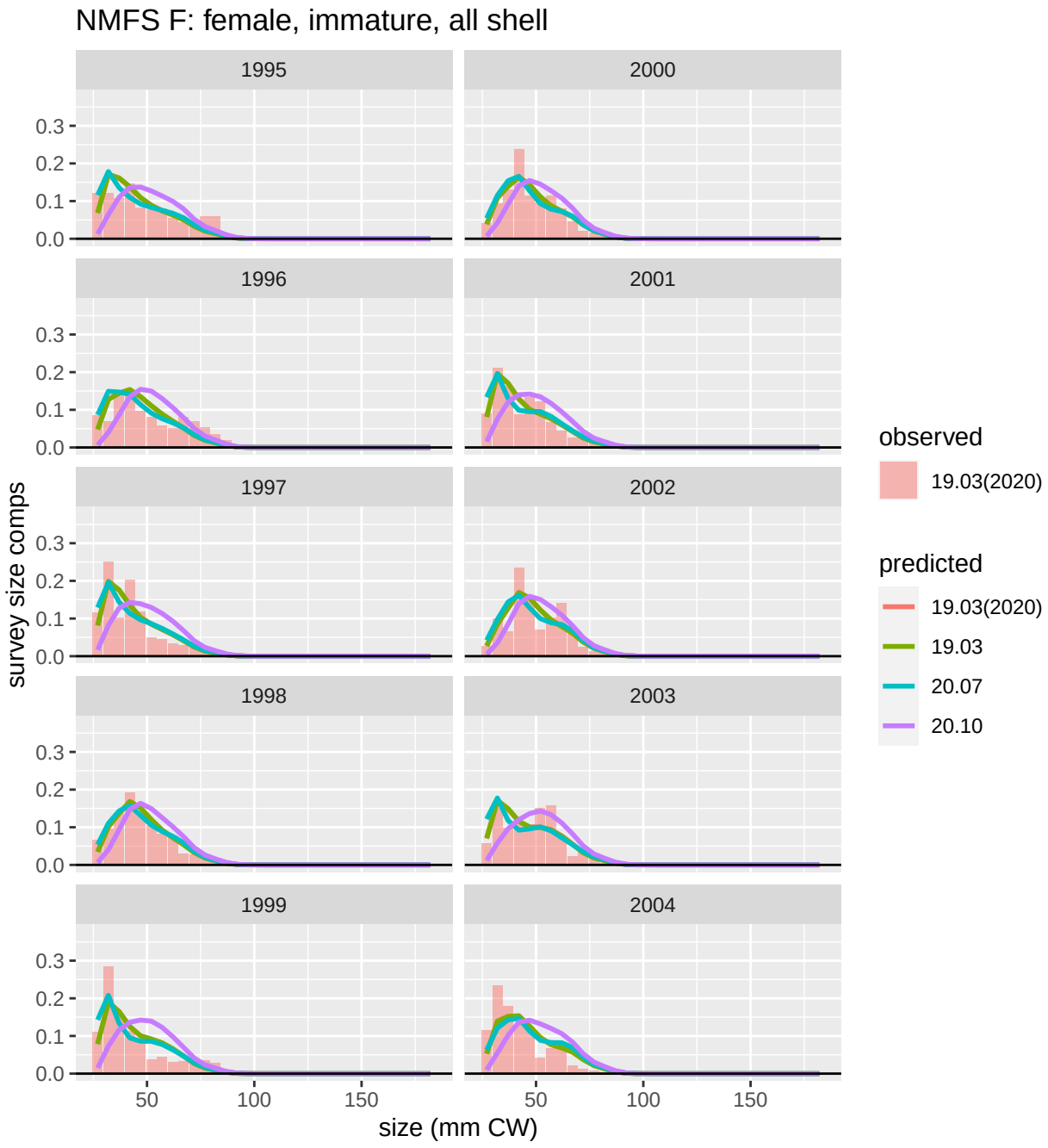

Figure 8: Comparison of observed and predicted female, immature, all shell survey size comps for NMFS F. Page 3 of 5.

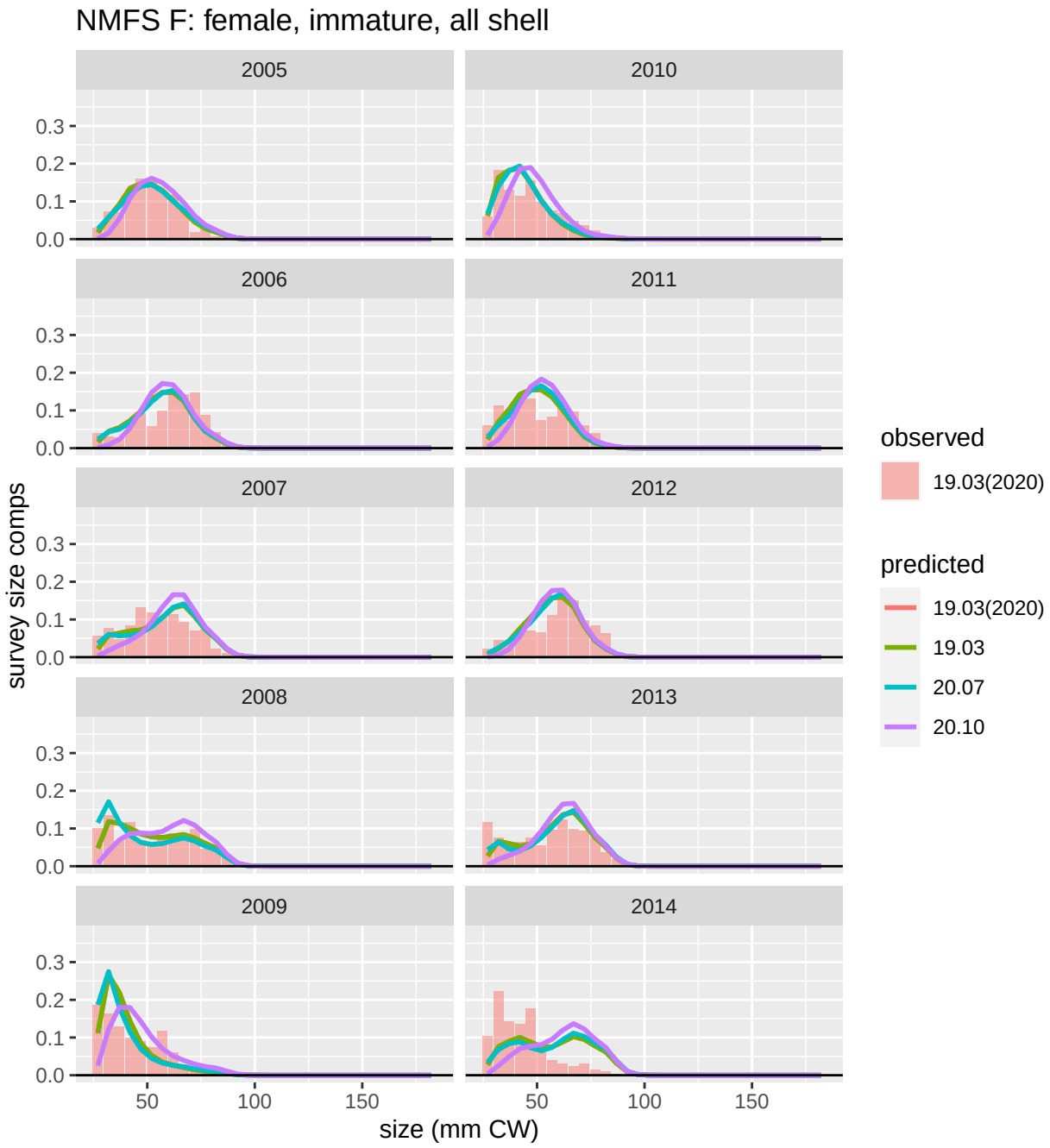

Figure 9: Comparison of observed and predicted female, immature, all shell survey size comps for NMFS F. Page 4 of 5.

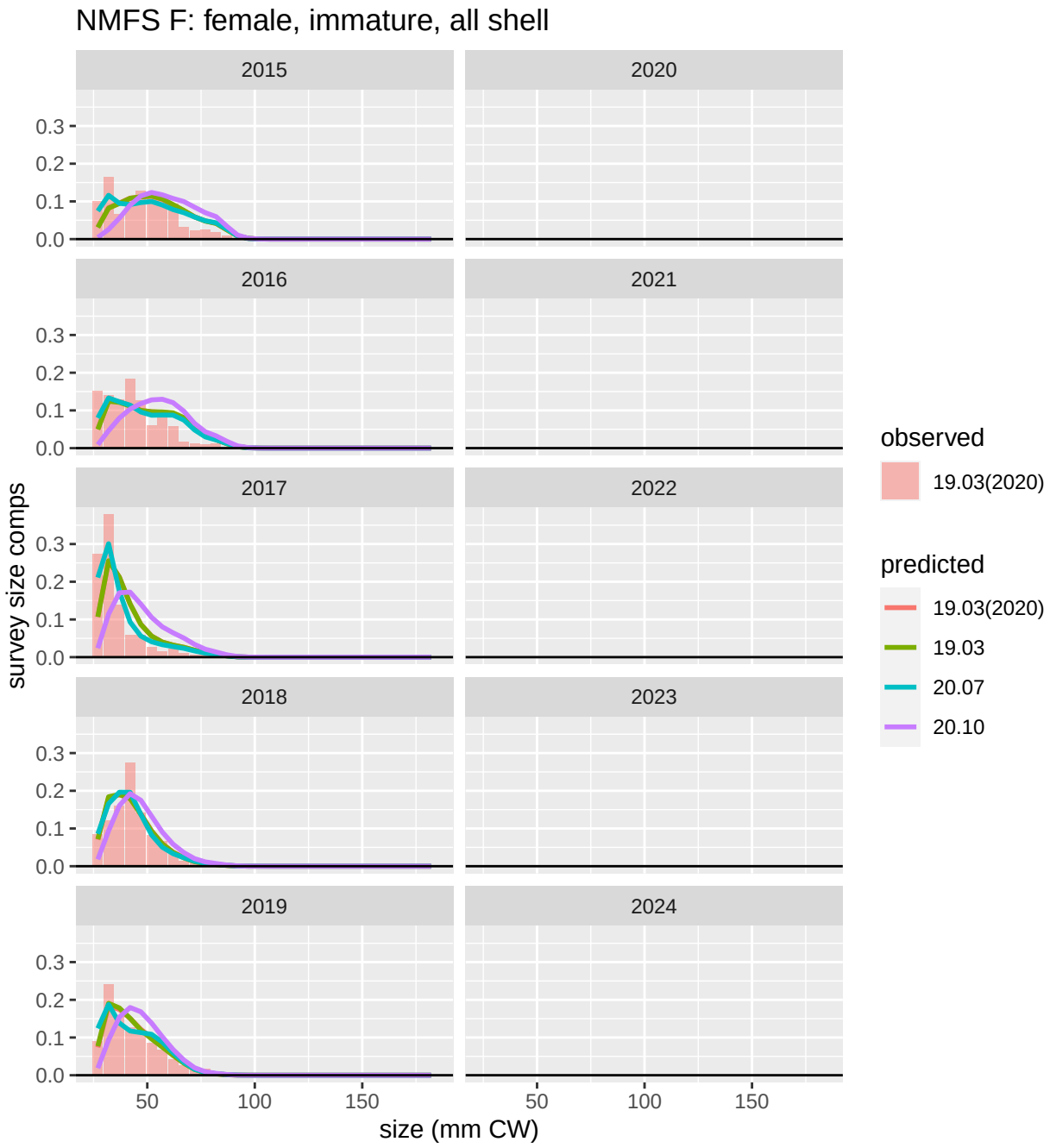

Figure 10: Comparison of observed and predicted female, immature, all shell survey size comps for NMFS F. Page 5 of 5.

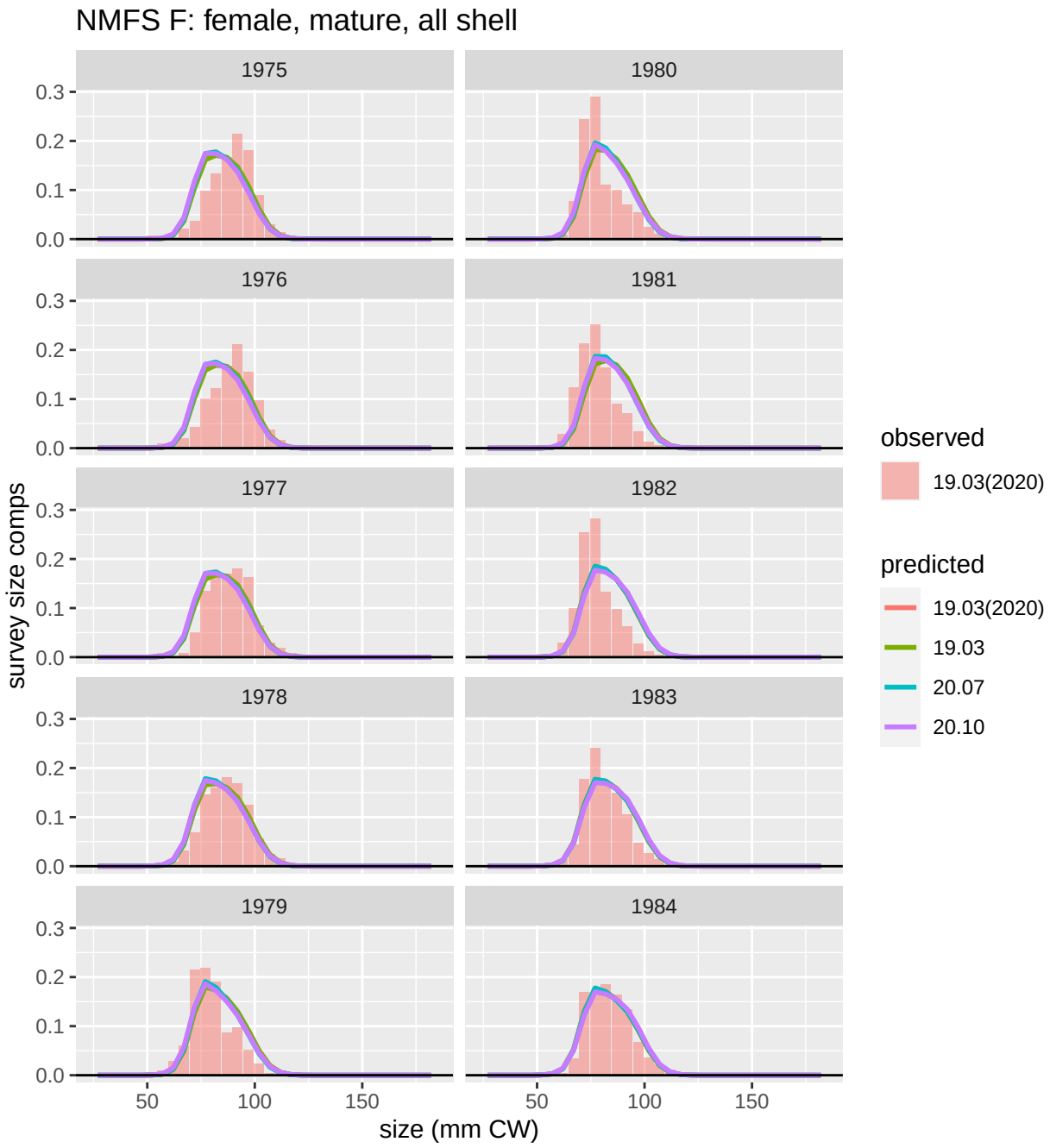

Figure 11: Comparison of observed and predicted female, mature, all shell survey size comps for NMFS F. Page 1 of 5.

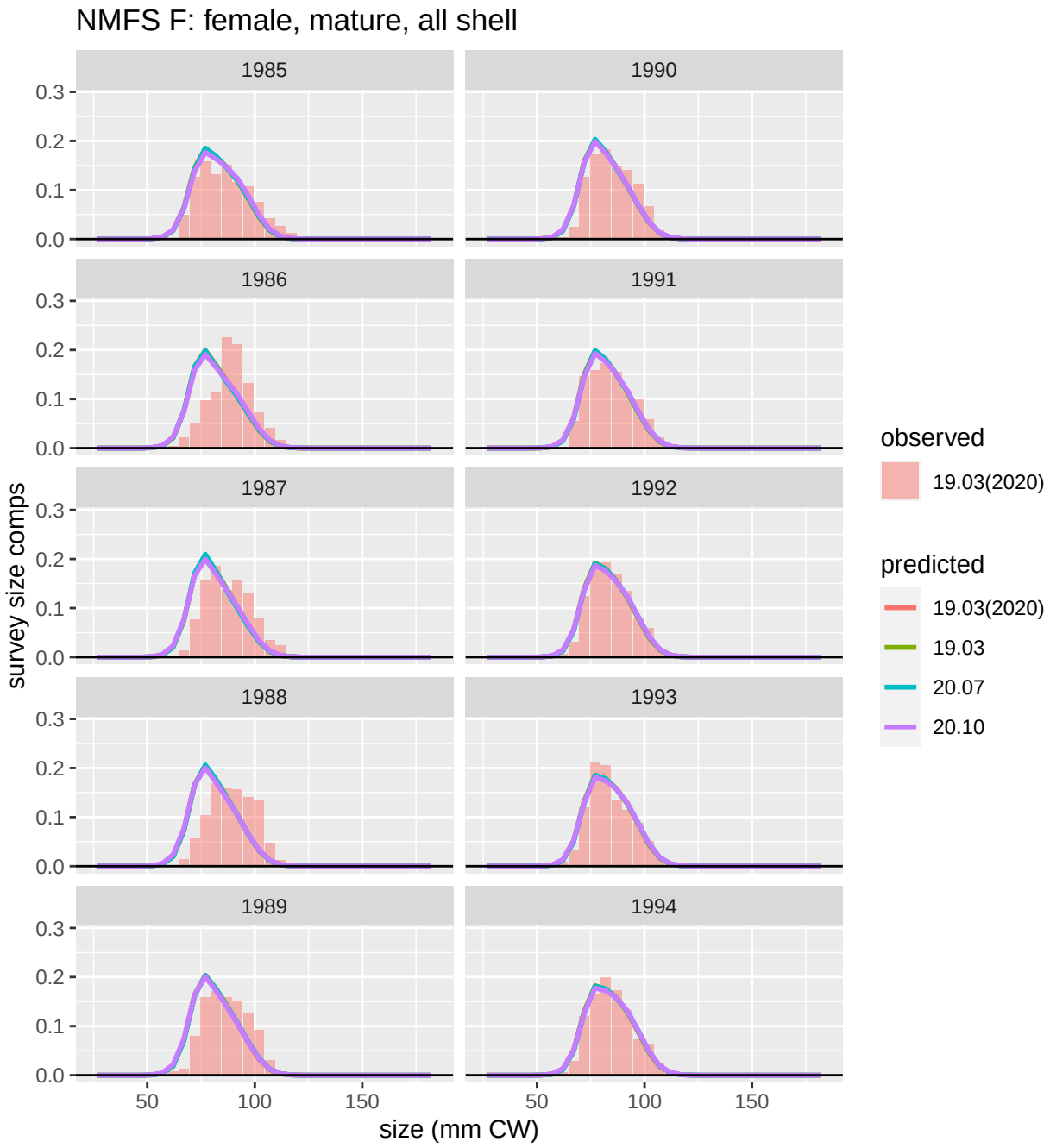

Figure 12: Comparison of observed and predicted female, mature, all shell survey size comps for NMFS F. Page 2 of 5.

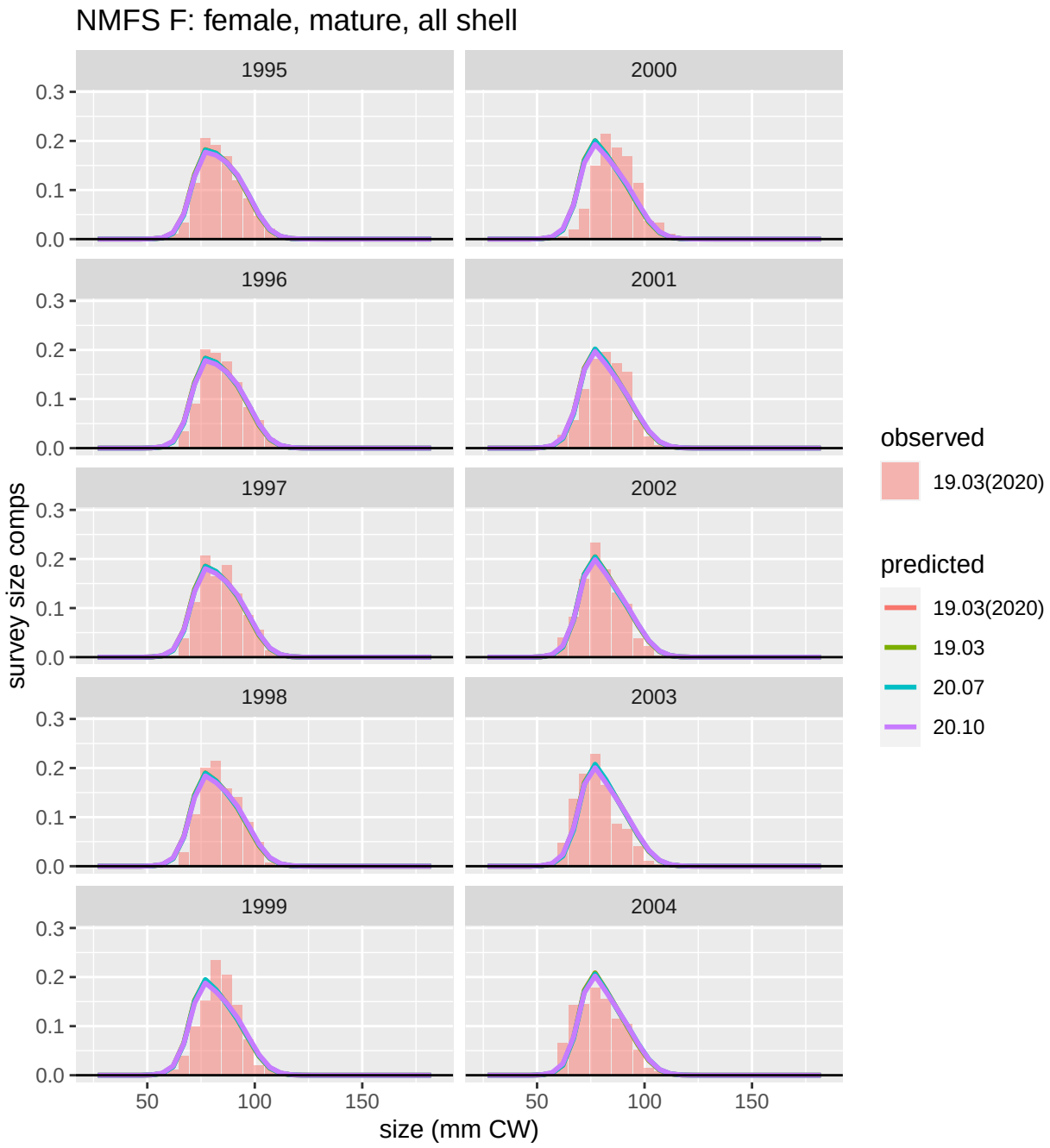

Figure 13: Comparison of observed and predicted female, mature, all shell survey size comps for NMFS F. Page 3 of 5.

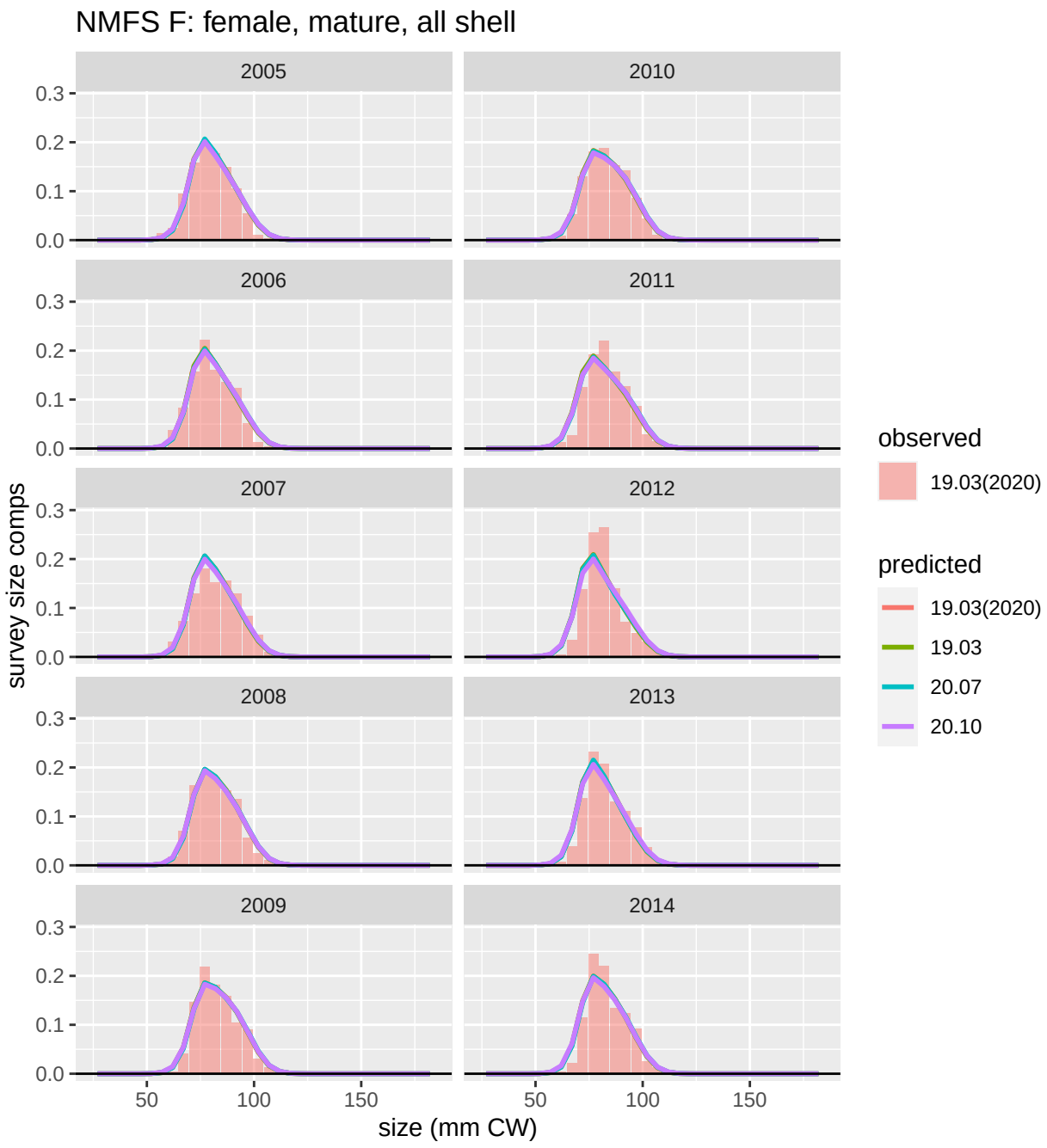

Figure 14: Comparison of observed and predicted female, mature, all shell survey size comps for NMFS F. Page 4 of 5.

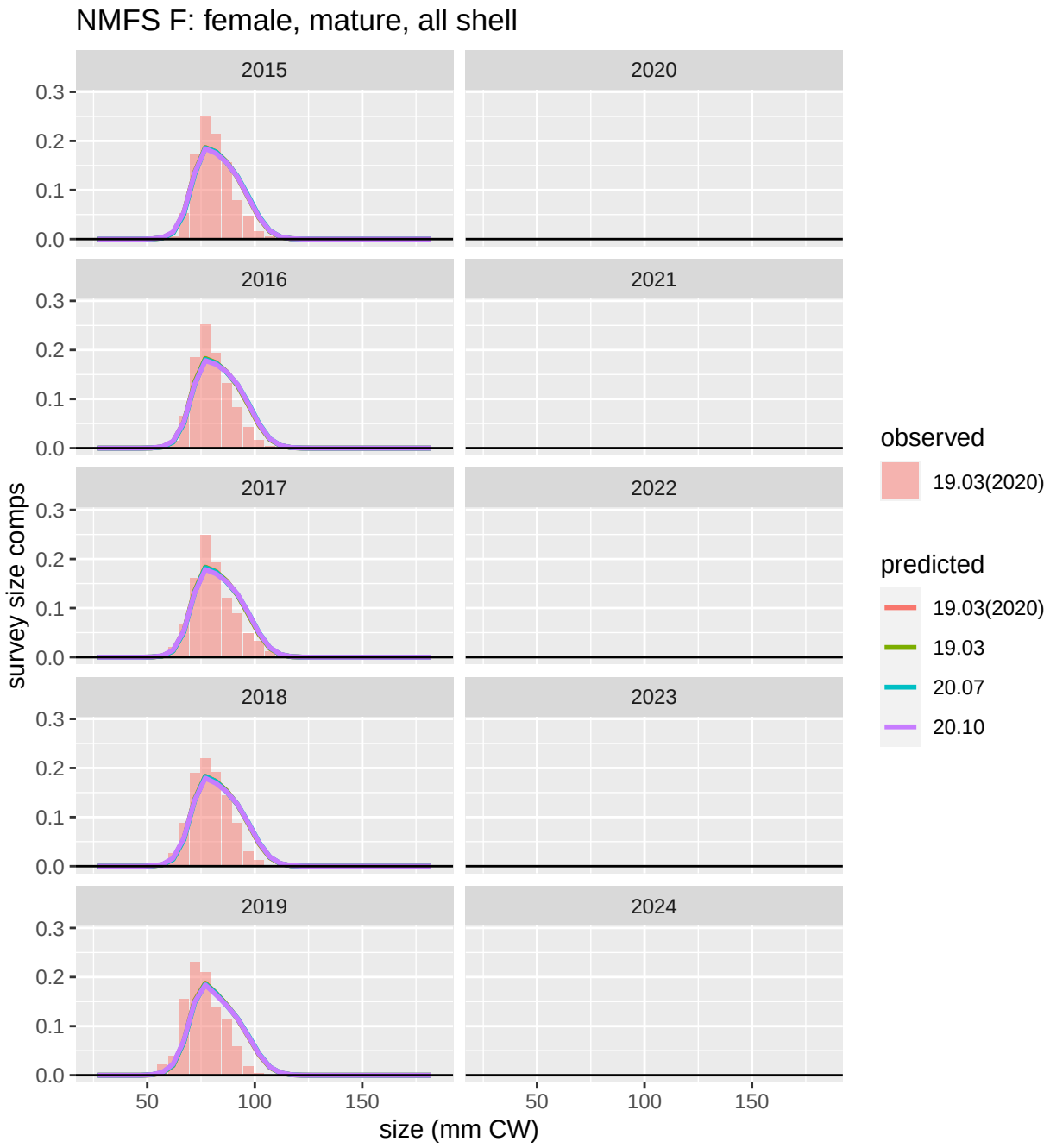

Figure 15: Comparison of observed and predicted female, mature, all shell survey size comps for NMFS F. Page 5 of 5.

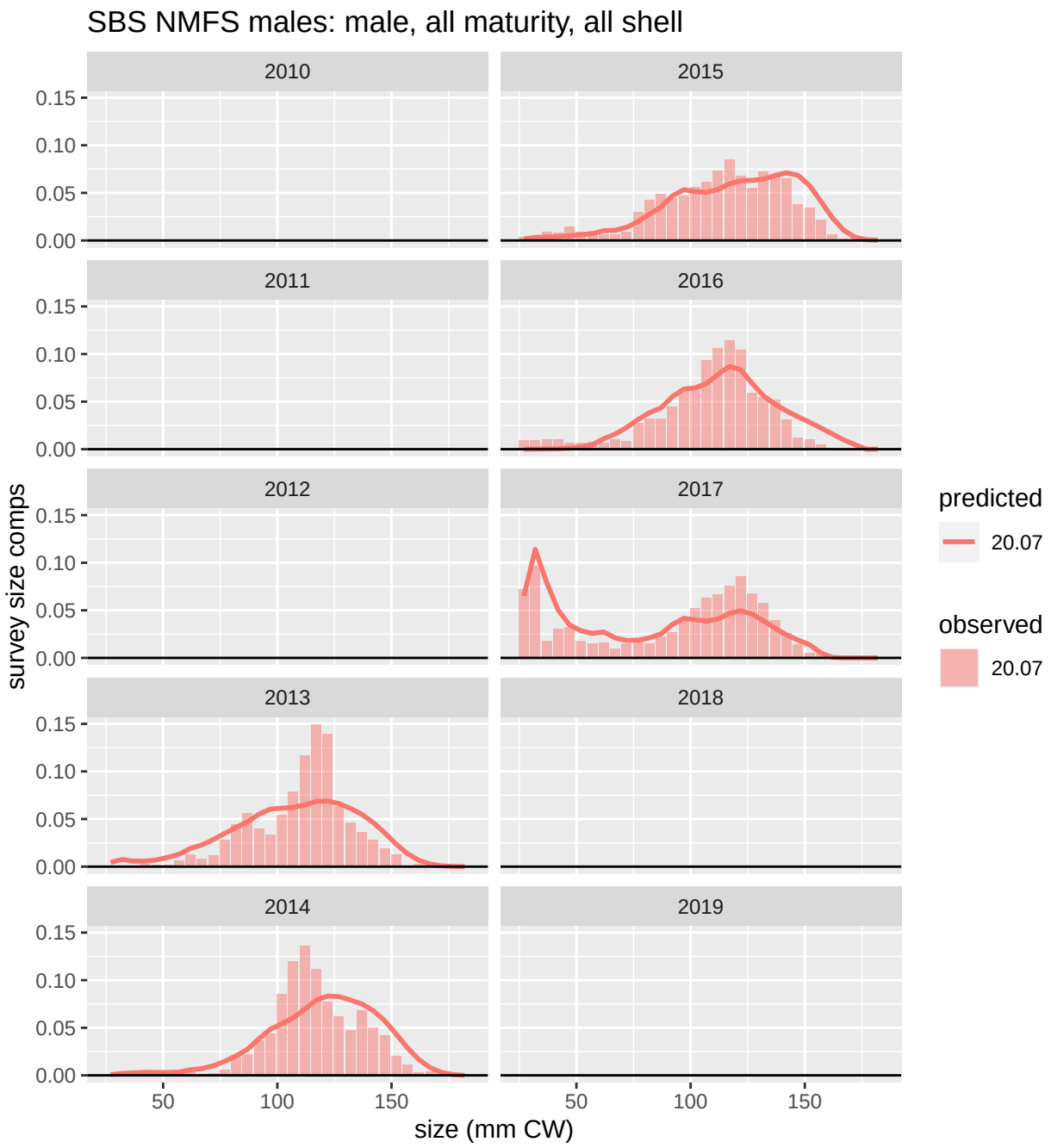

Figure 16: Comparison of observed and predicted male, all maturity, all shell survey size comps for SBS NMFS males. Page 1 of 1.

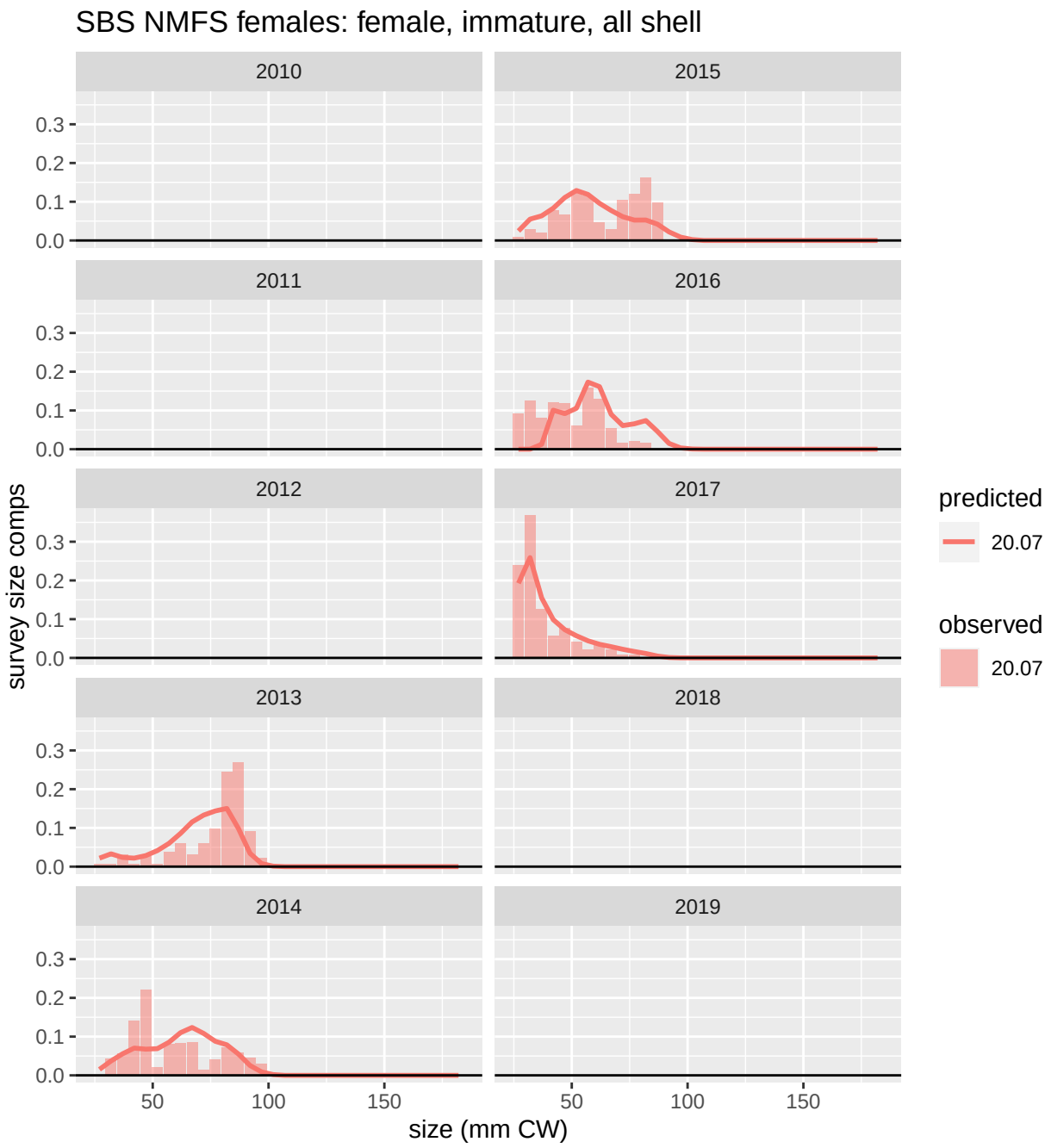

Figure 17: Comparison of observed and predicted female, immature, all shell survey size comps for SBS NMFS females. Page 1 of 1.

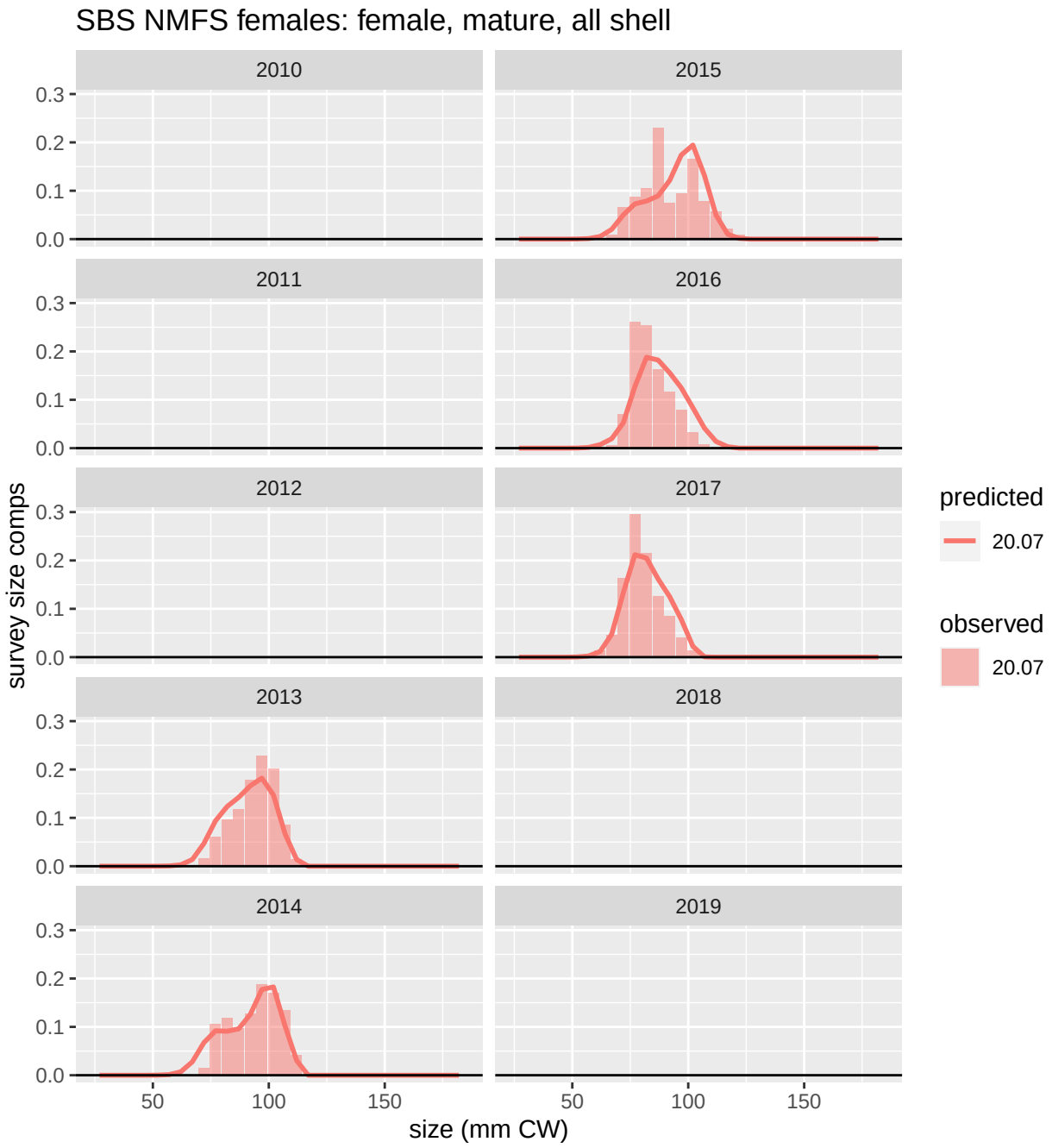

Figure 18: Comparison of observed and predicted female, mature, all shell survey size comps for SBS NMFS females. Page 1 of 1.

Figure 19: Comparison of observed and predicted male, all maturity, all shell survey size comps for SBS BSFRF males. Page 1 of 1.

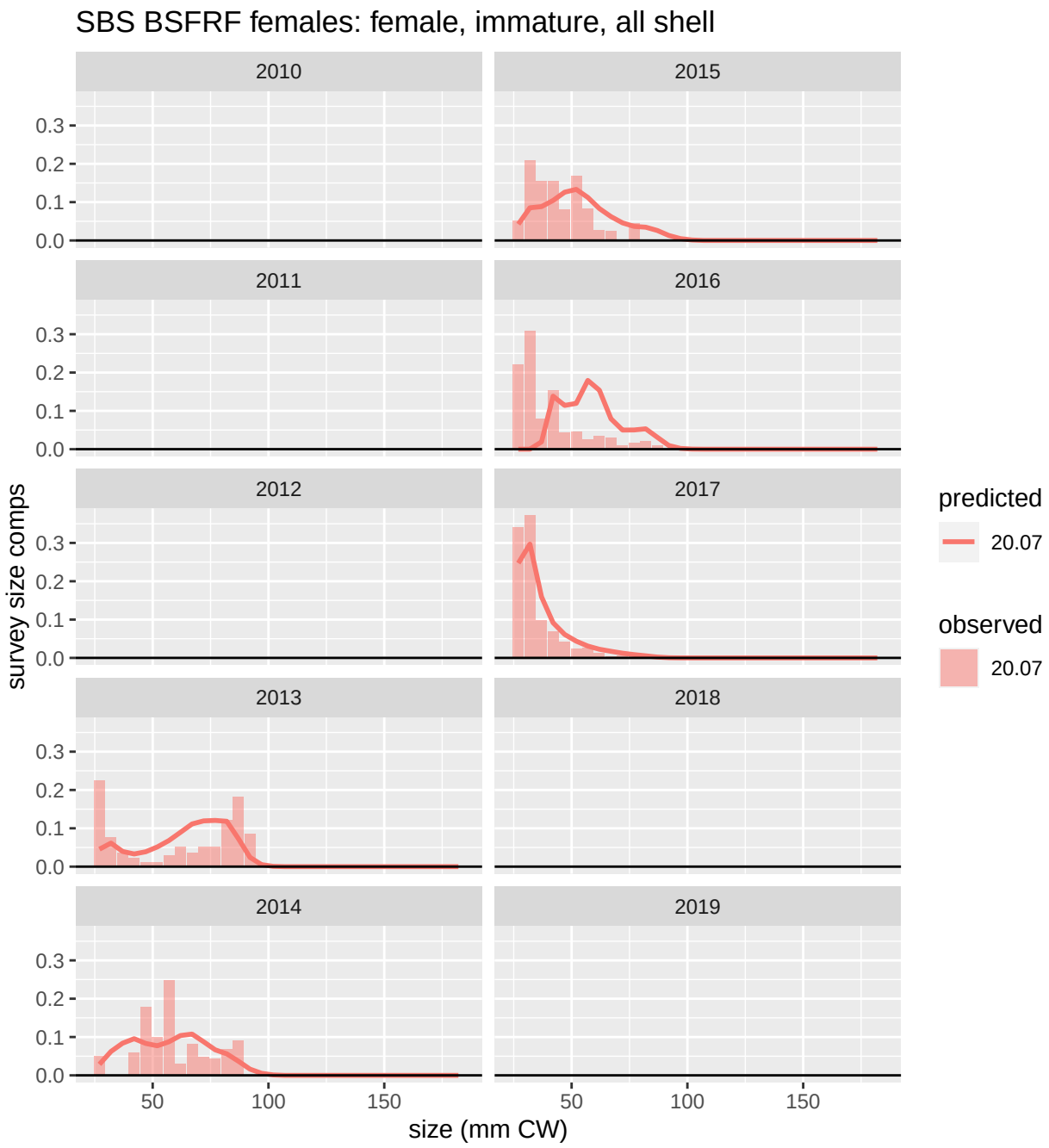

Figure 20: Comparison of observed and predicted female, immature, all shell survey size comps for SBS BSFRF females. Page 1 of 1.

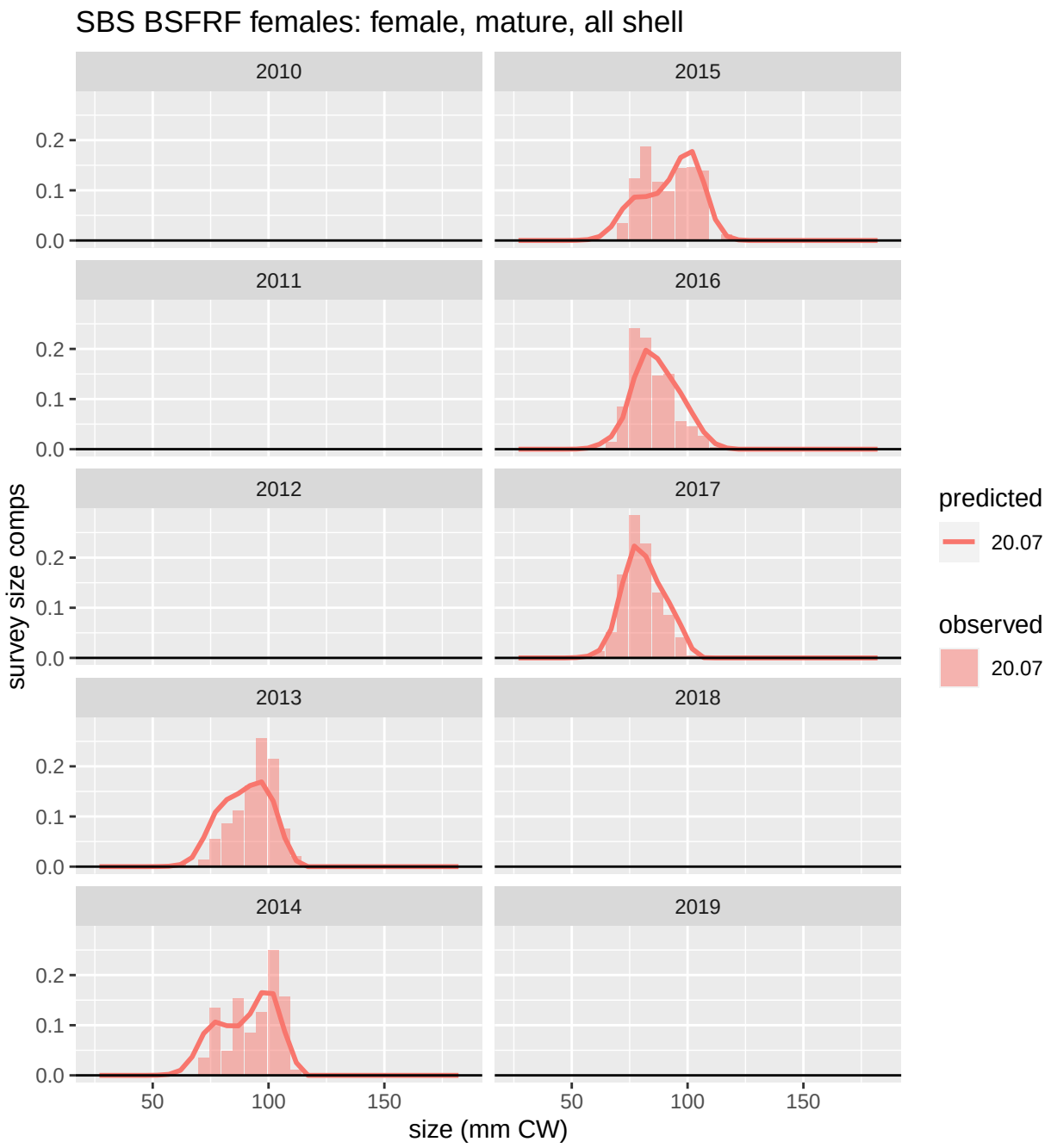

Figure 21: Comparison of observed and predicted female, mature, all shell survey size comps for SBS BSFRF females. Page 1 of 1.

Fishery retained catch size compositions

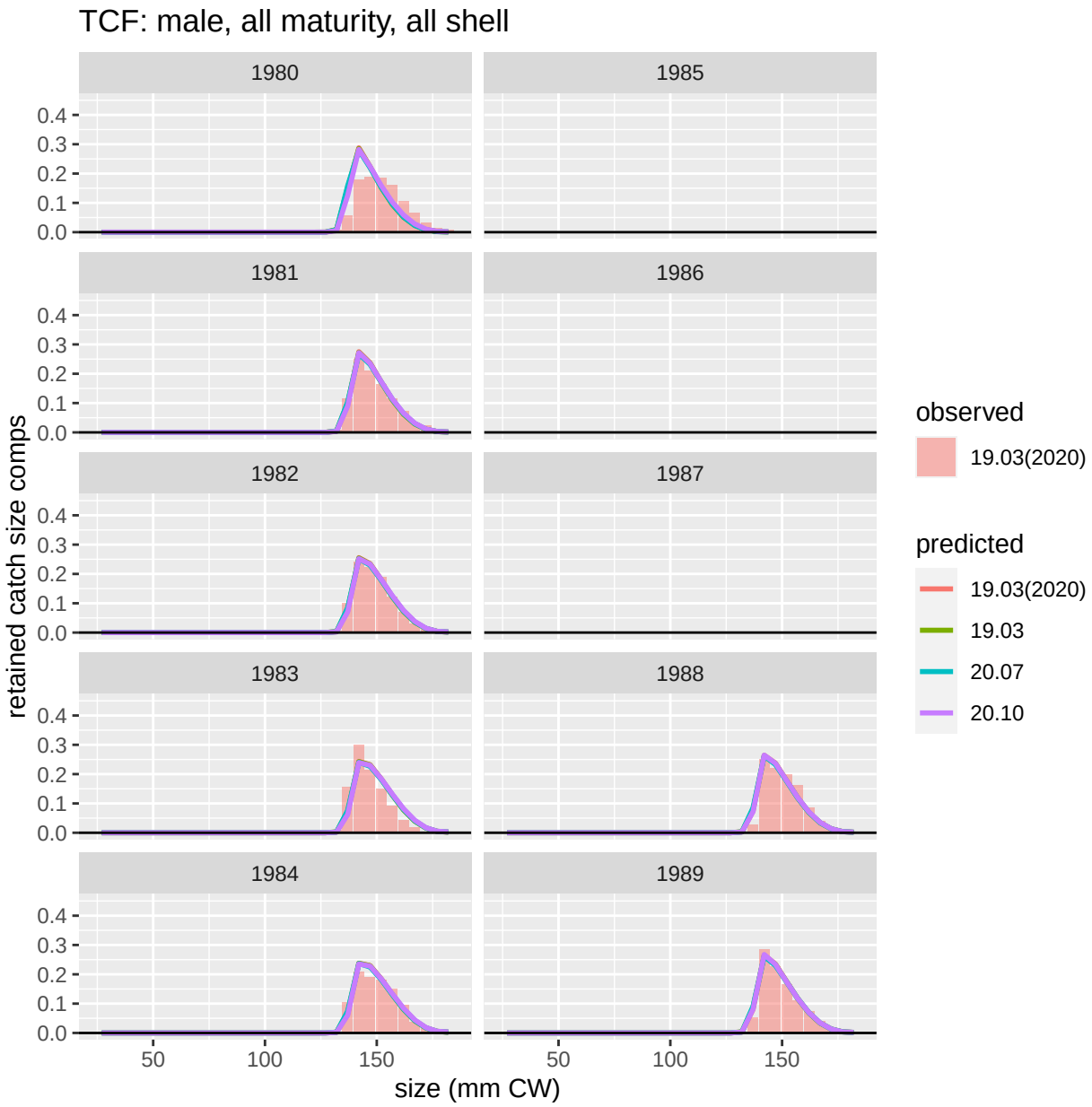

Figure 22: Comparison of observed and predicted male, all maturity, all shell retained catch size comps for TCF. Page 1 of 4.

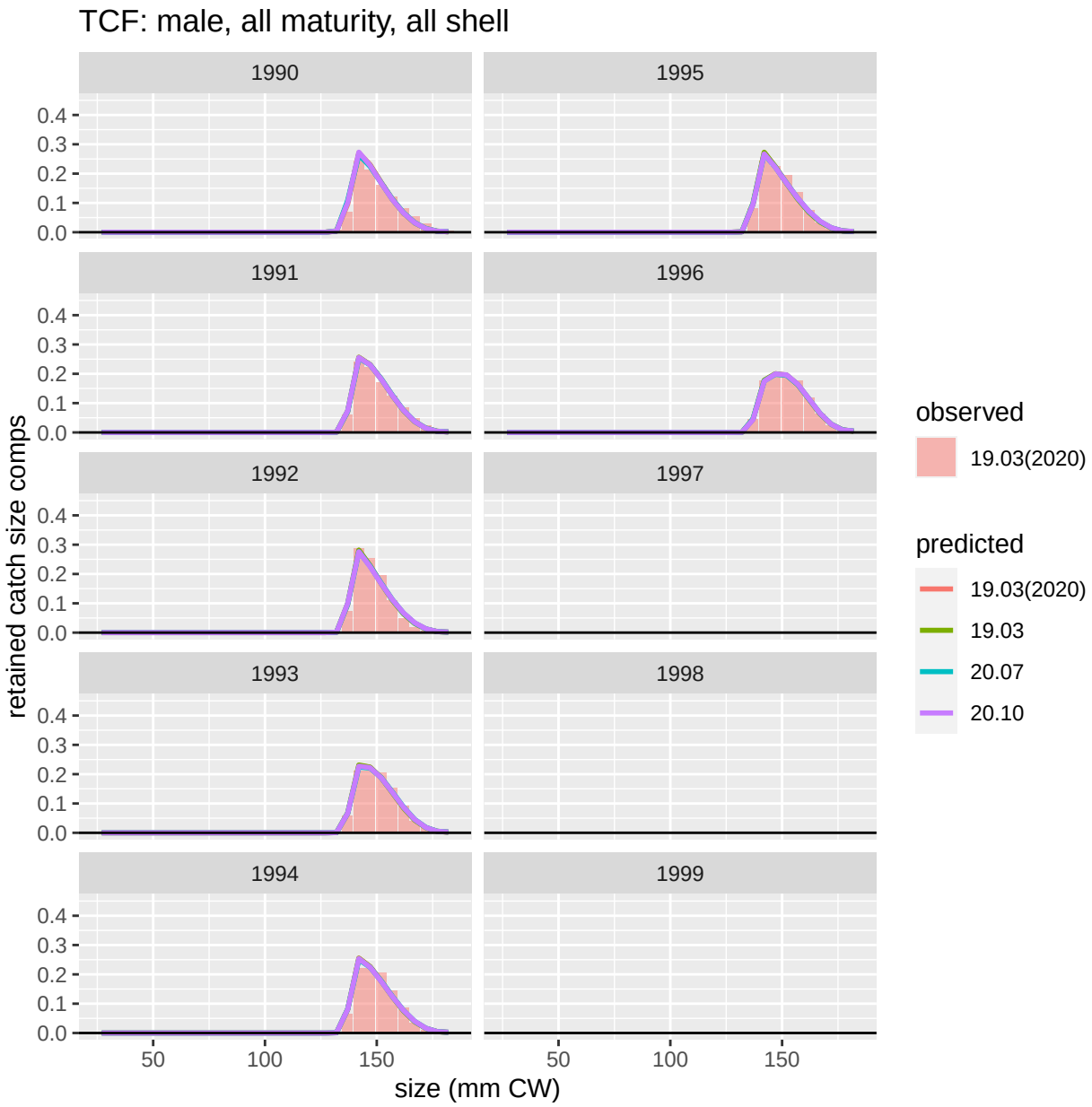

Figure 23: Comparison of observed and predicted male, all maturity, all shell retained catch size comps for TCF. Page 2 of 4.

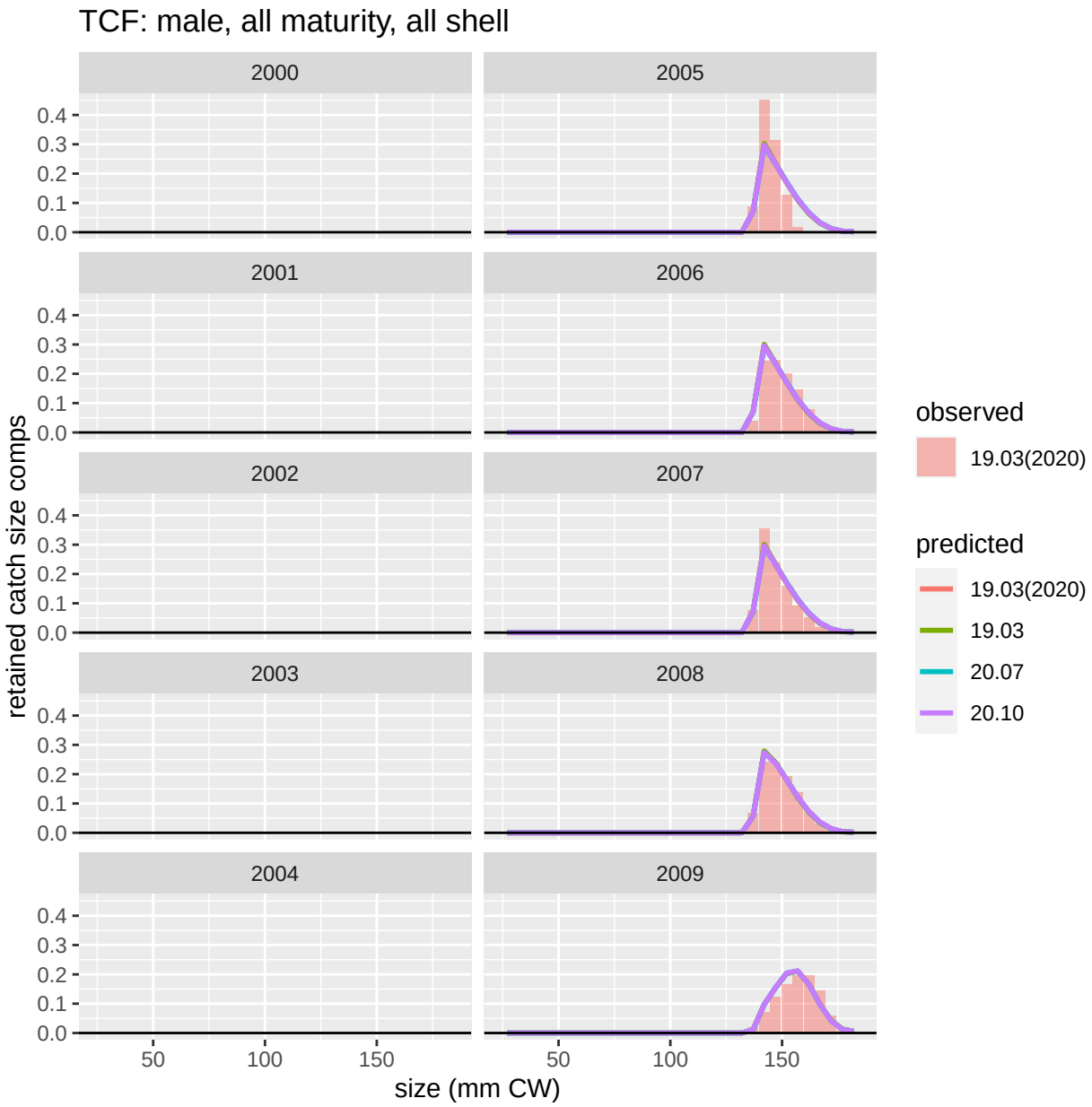

Figure 24: Comparison of observed and predicted male, all maturity, all shell retained catch size comps for TCF. Page 3 of 4.

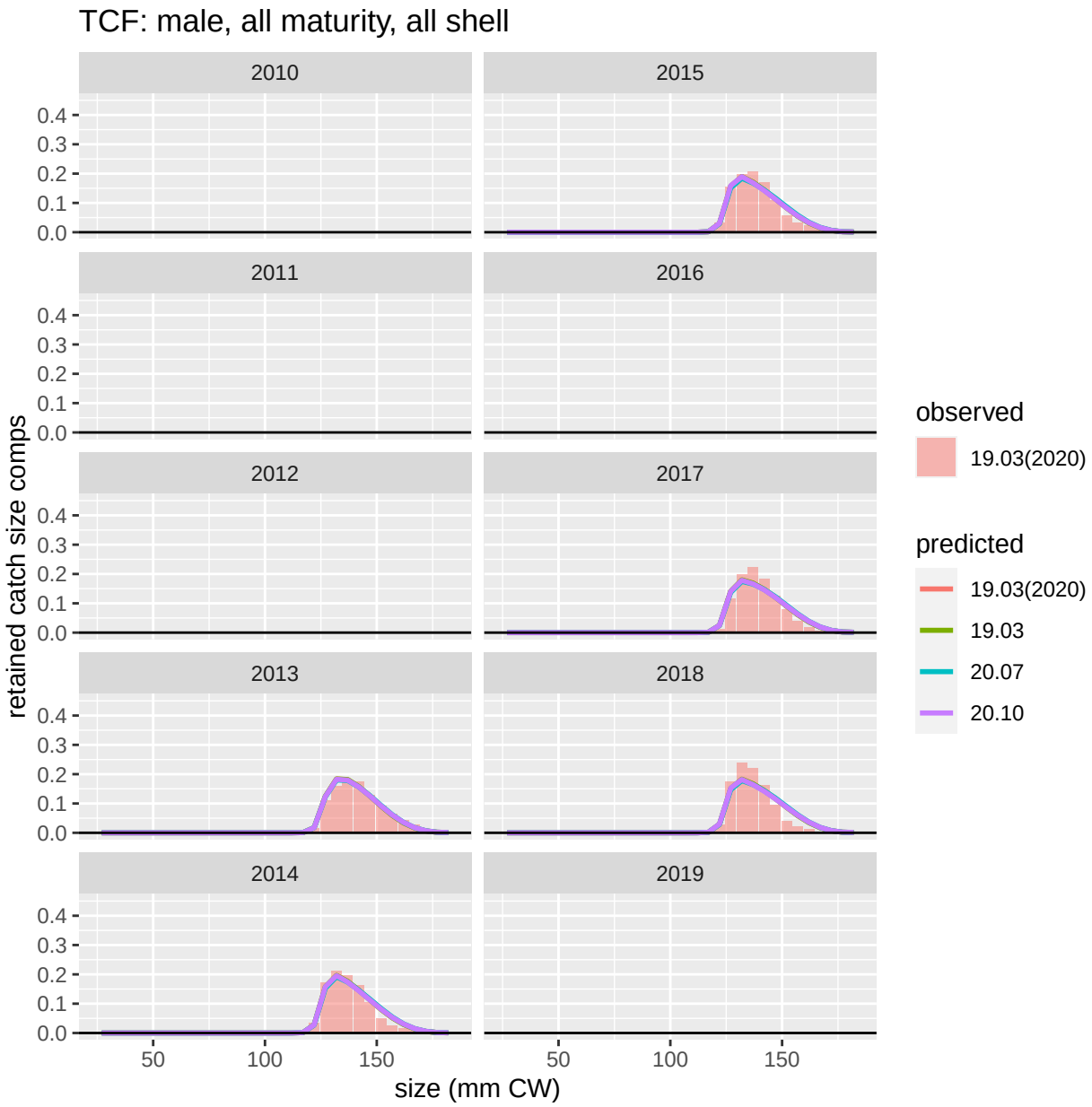

Figure 25: Comparison of observed and predicted male, all maturity, all shell retained catch size comps for TCF. Page 4 of 4.

Fishery total catch size compositions

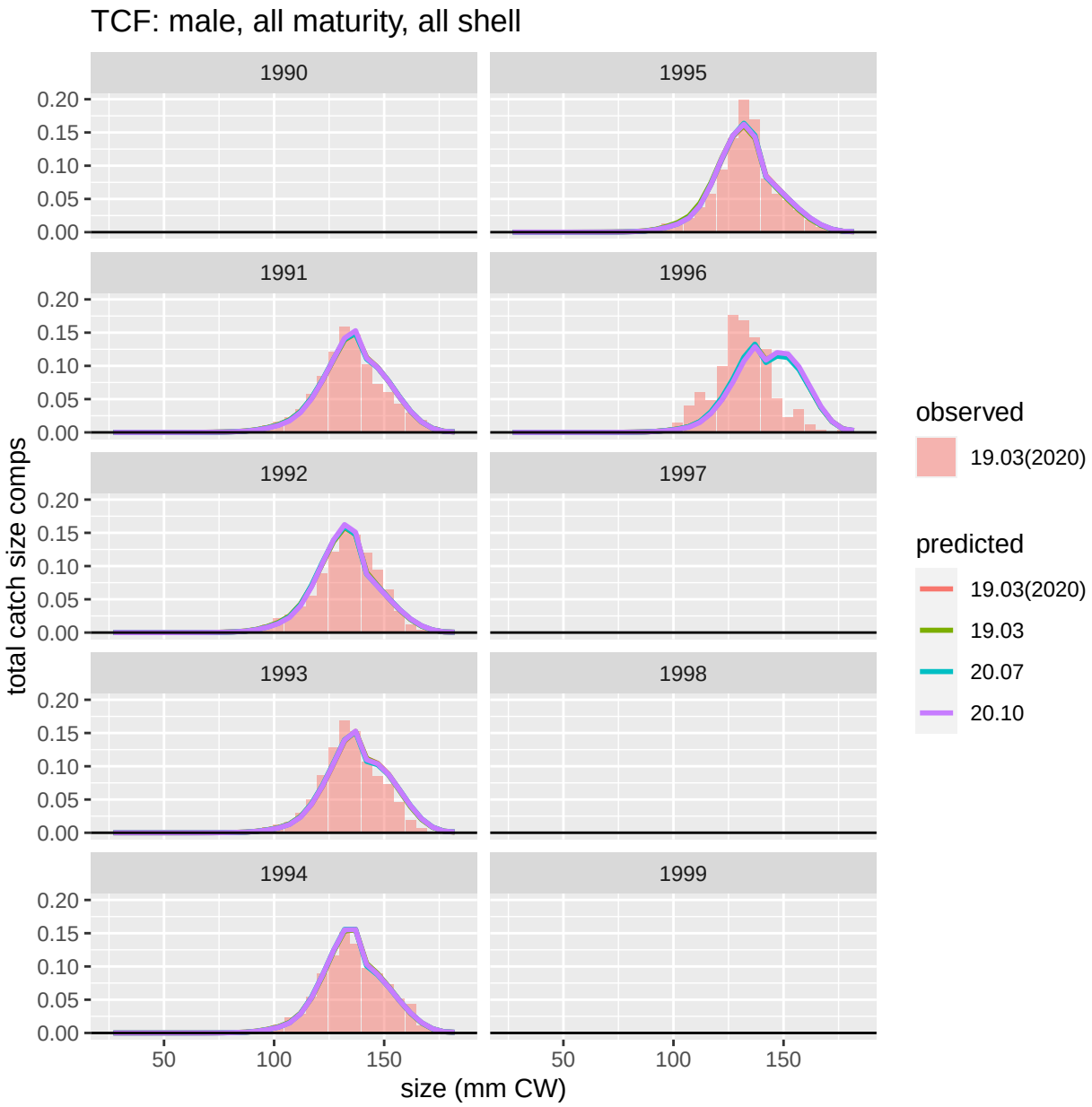

Figure 26: Comparison of observed and predicted male, all maturity, all shell total catch size comps for TCF. Page 1 of 3.

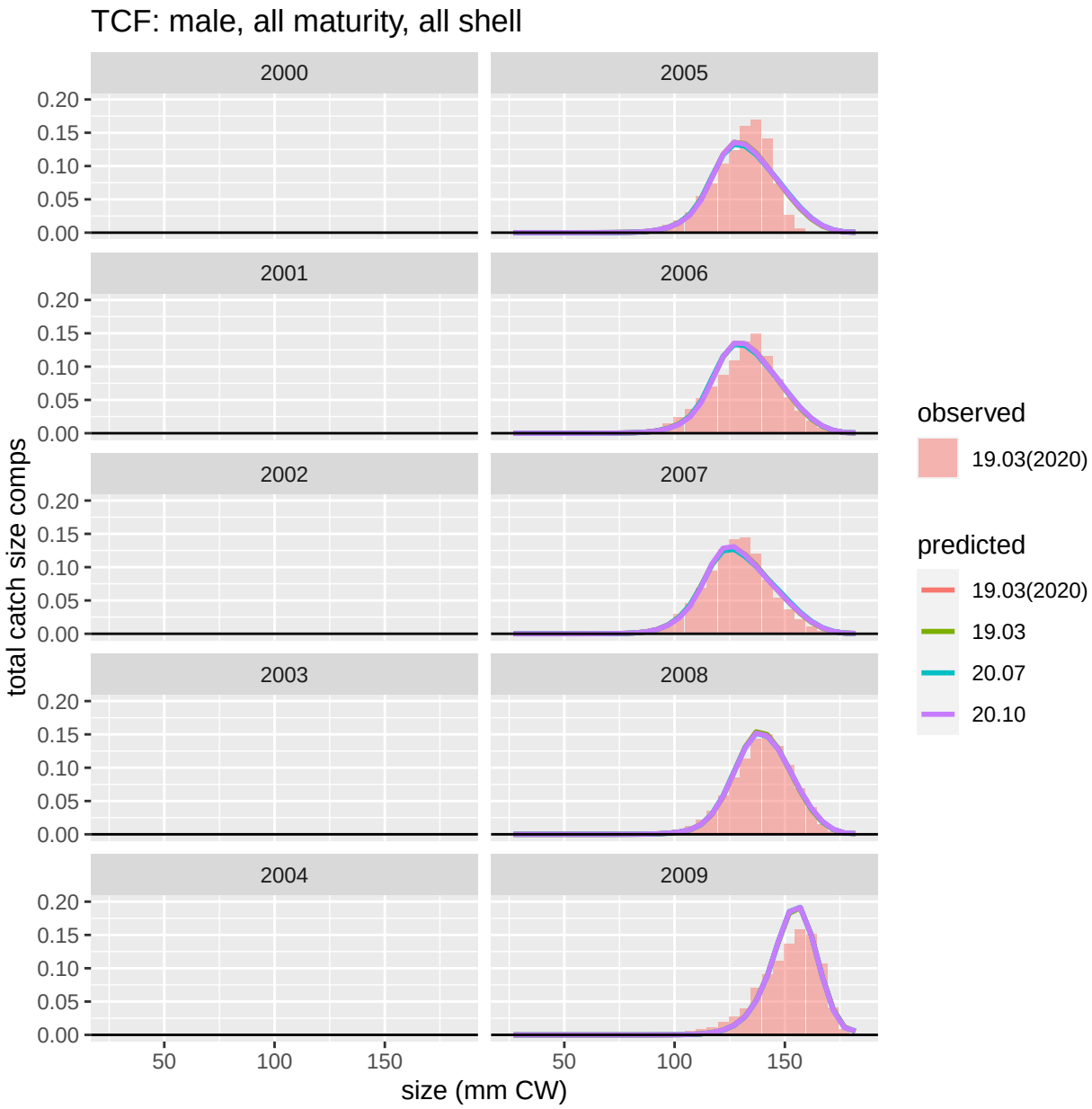

Figure 27: Comparison of observed and predicted male, all maturity, all shell total catch size comps for TCF. Page 2 of 3.

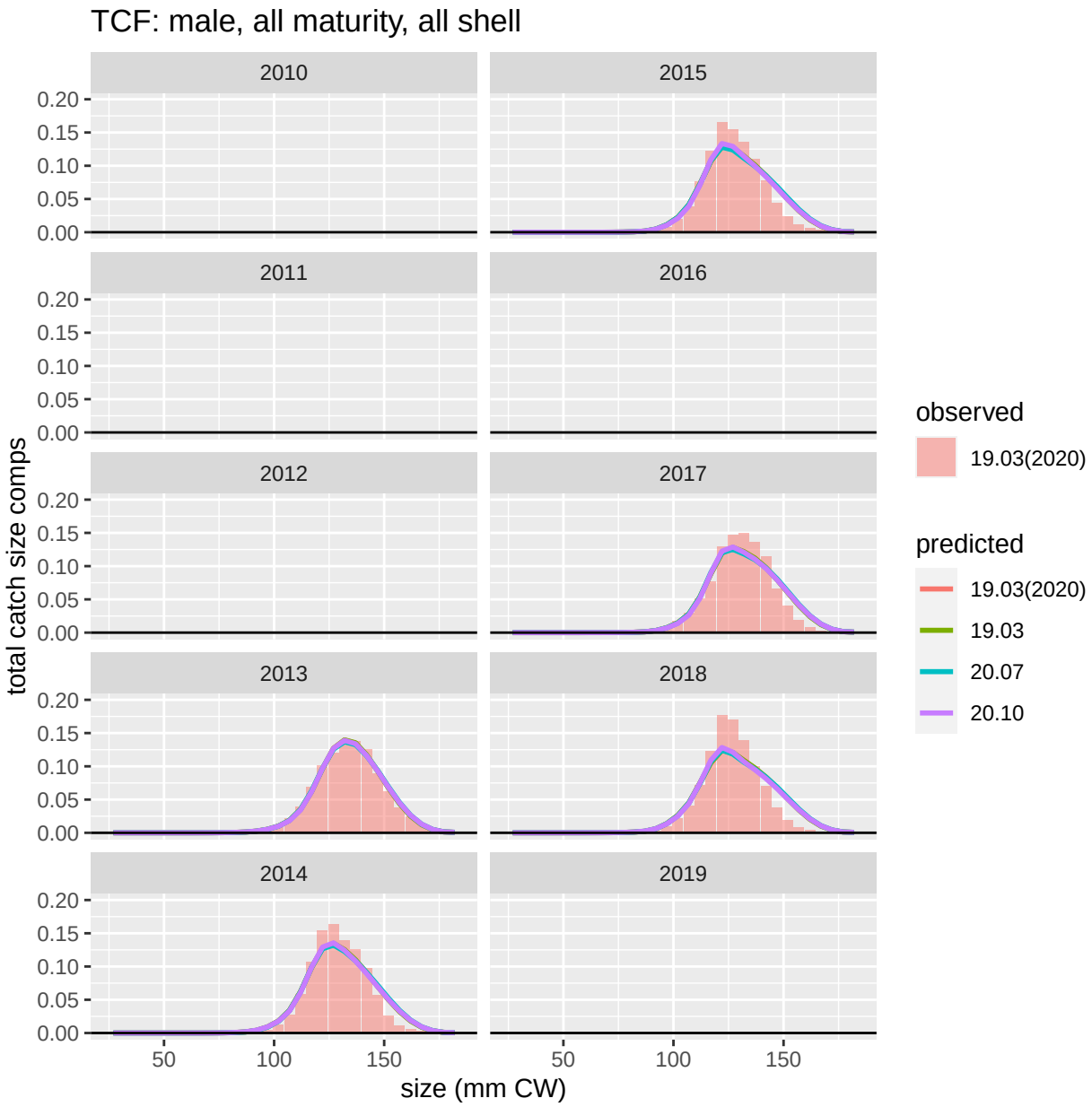

Figure 28: Comparison of observed and predicted male, all maturity, all shell total catch size comps for TCF. Page 3 of 3.

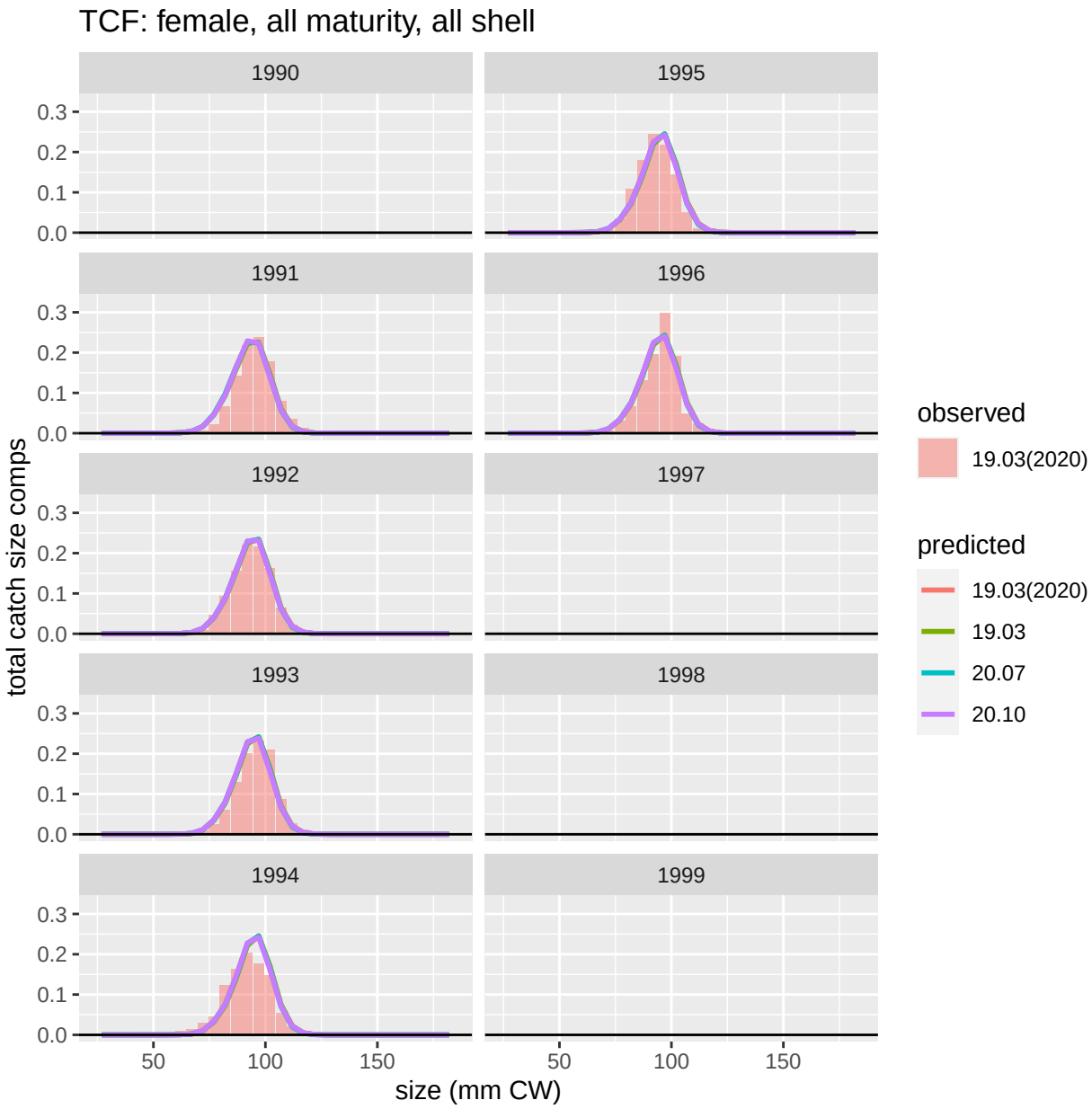

Figure 29: Comparison of observed and predicted female, all maturity, all shell total catch size comps for TCF. Page 1 of 3.

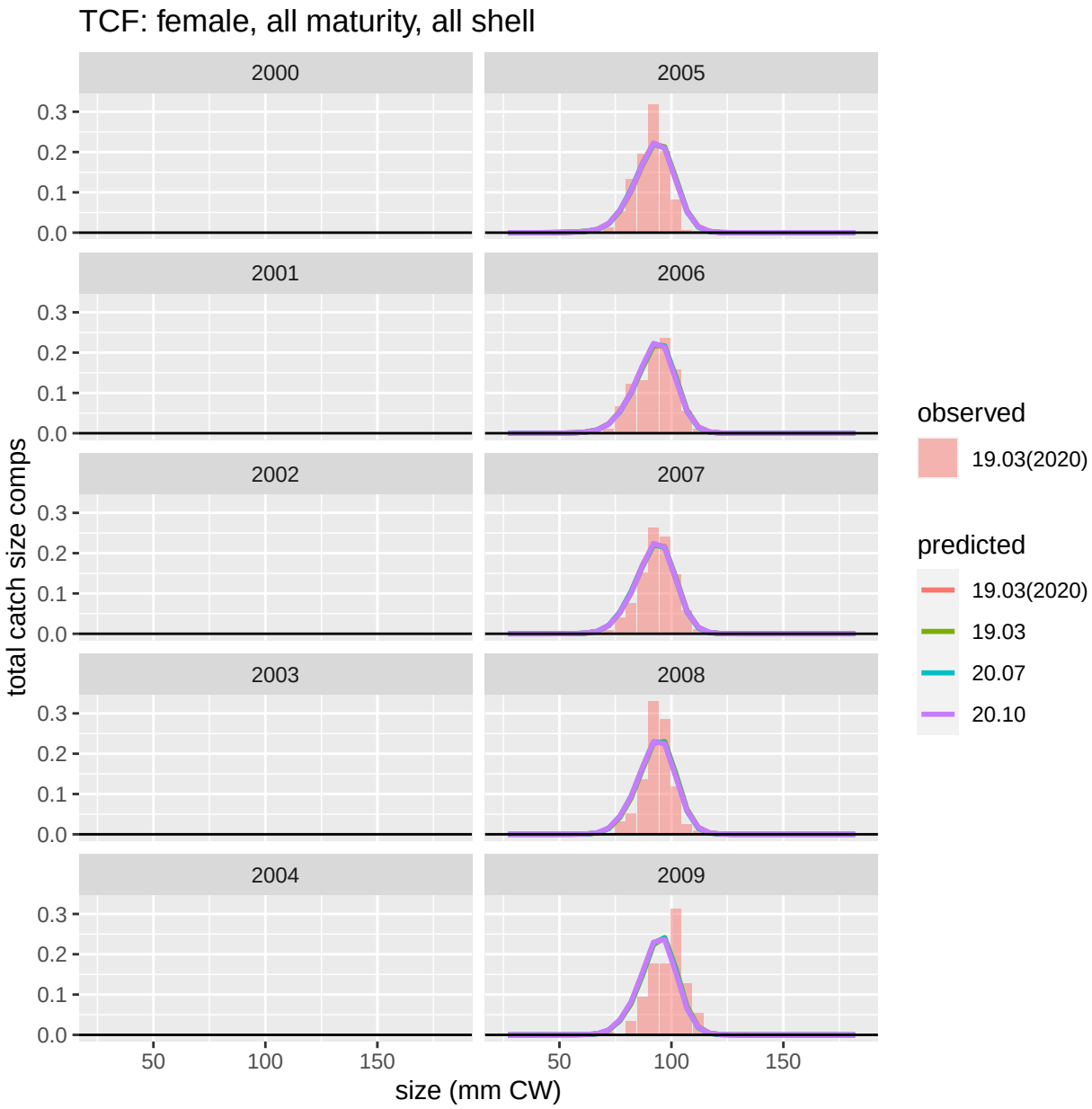

Figure 30: Comparison of observed and predicted female, all maturity, all shell total catch size comps for TCF. Page 2 of 3.

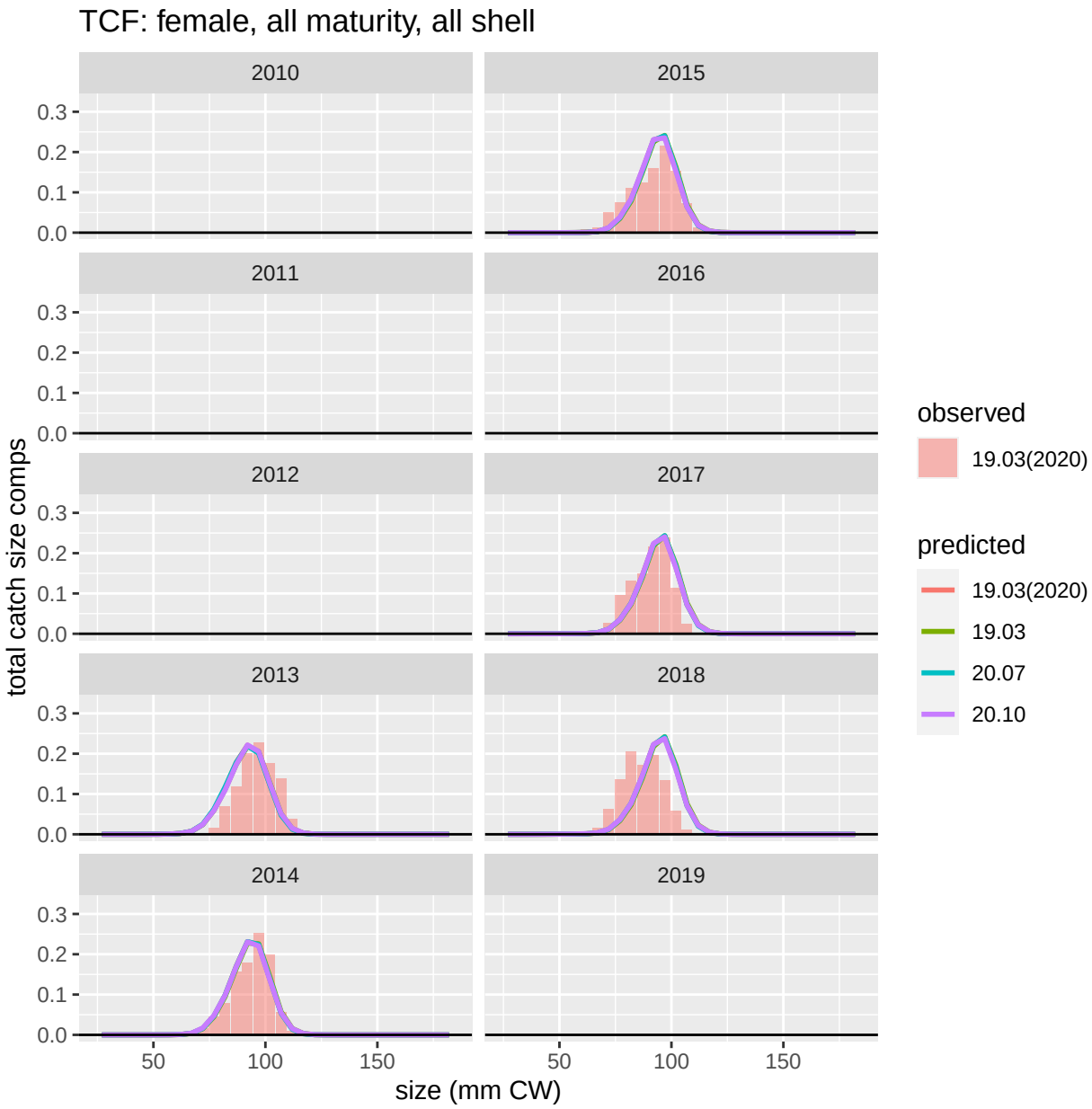

Figure 31: Comparison of observed and predicted female, all maturity, all shell total catch size comps for TCF. Page 3 of 3.

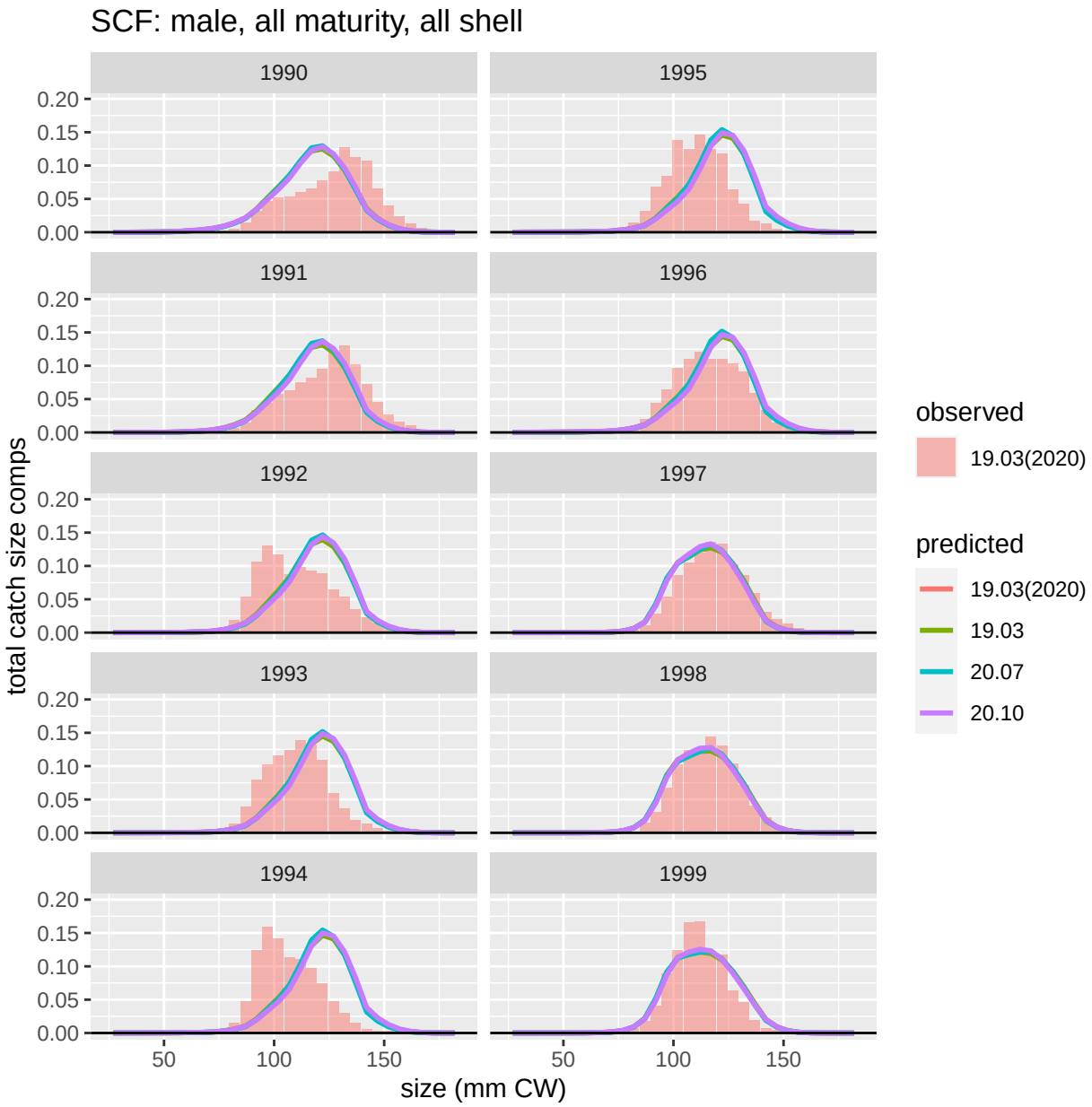

Figure 32: Comparison of observed and predicted male, all maturity, all shell total catch size comps for SCF. Page 1 of 3.

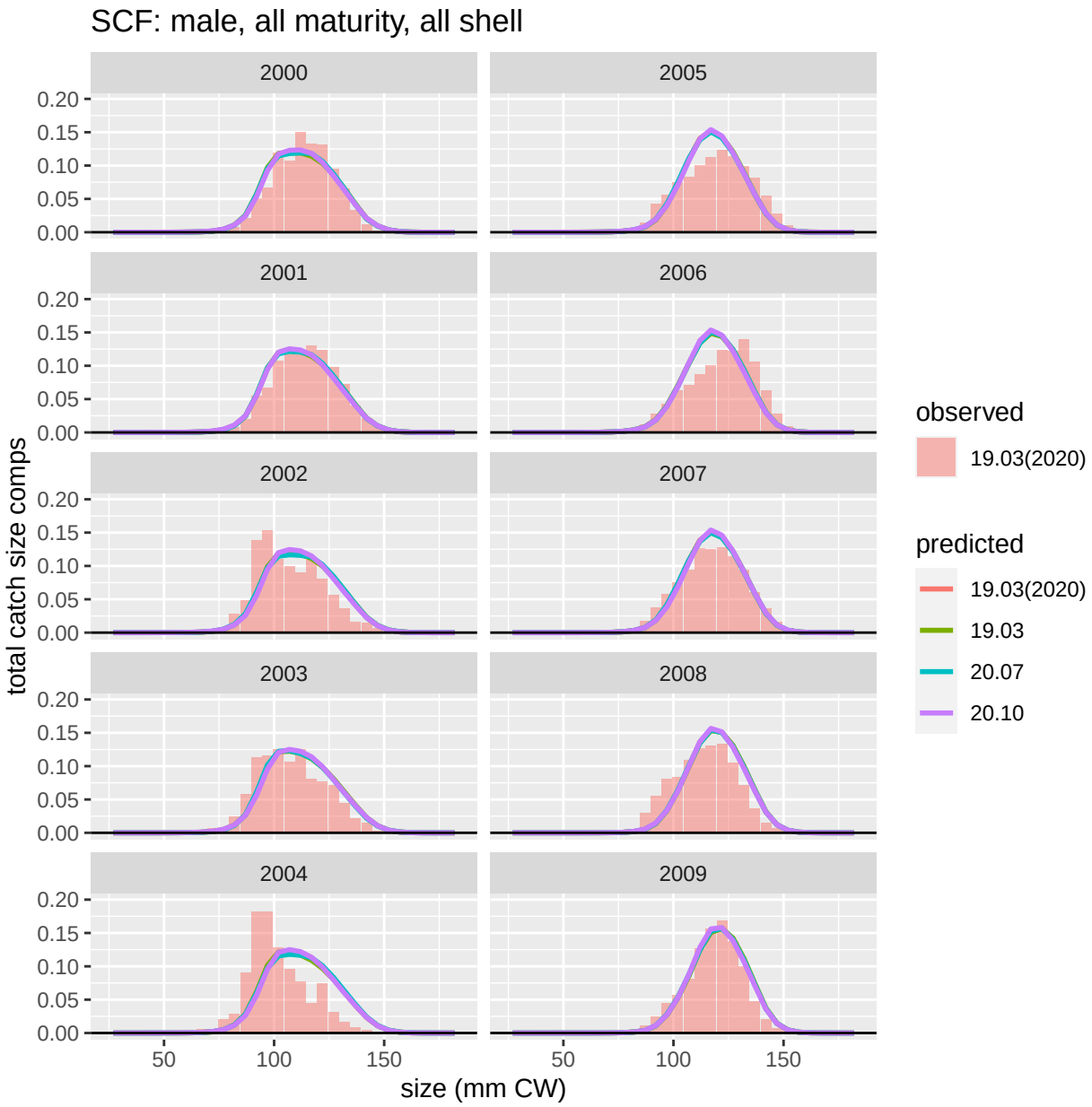

Figure 33: Comparison of observed and predicted male, all maturity, all shell total catch size comps for SCF. Page 2 of 3.

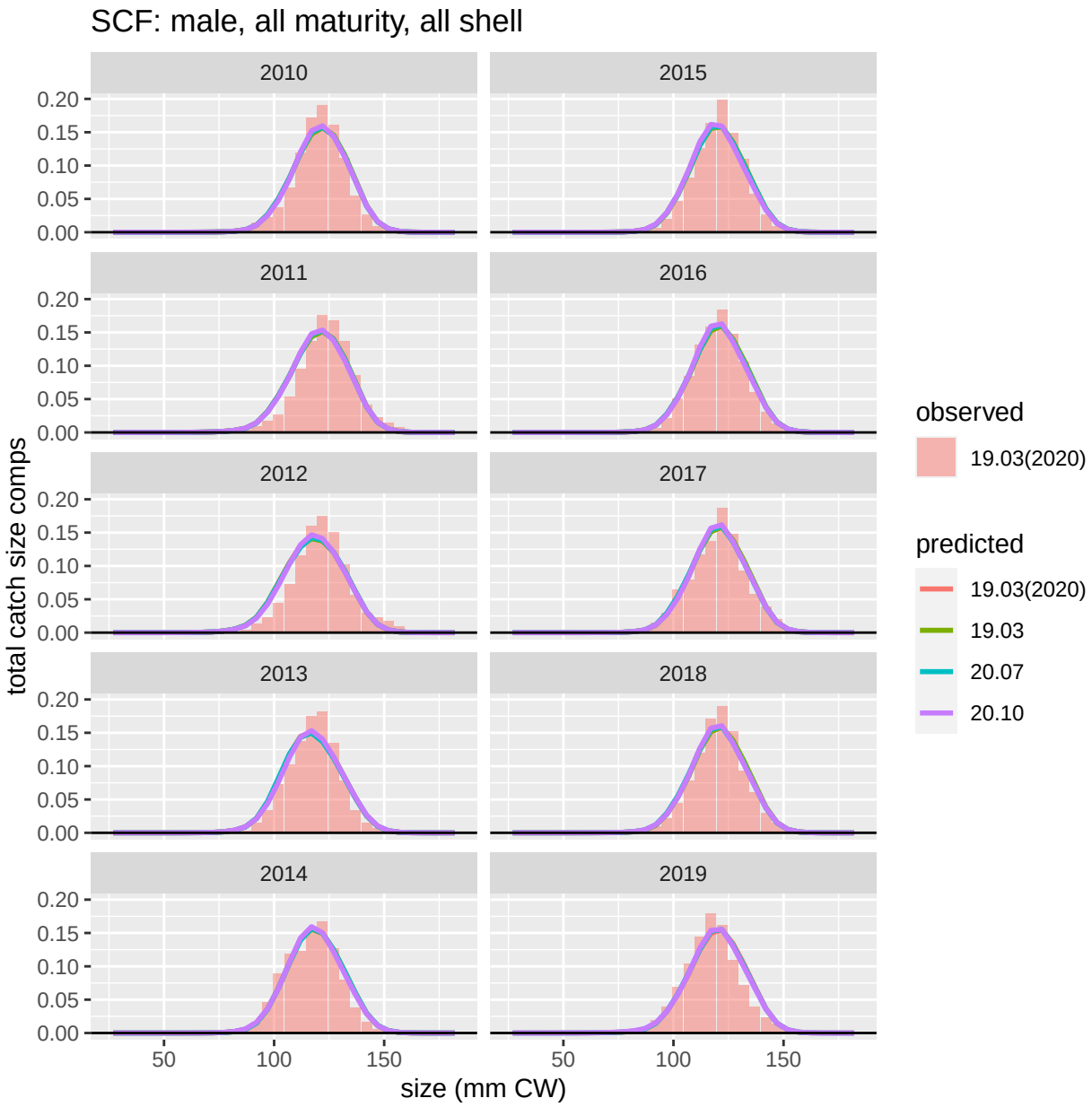

Figure 34: Comparison of observed and predicted male, all maturity, all shell total catch size comps for SCF. Page 3 of 3.

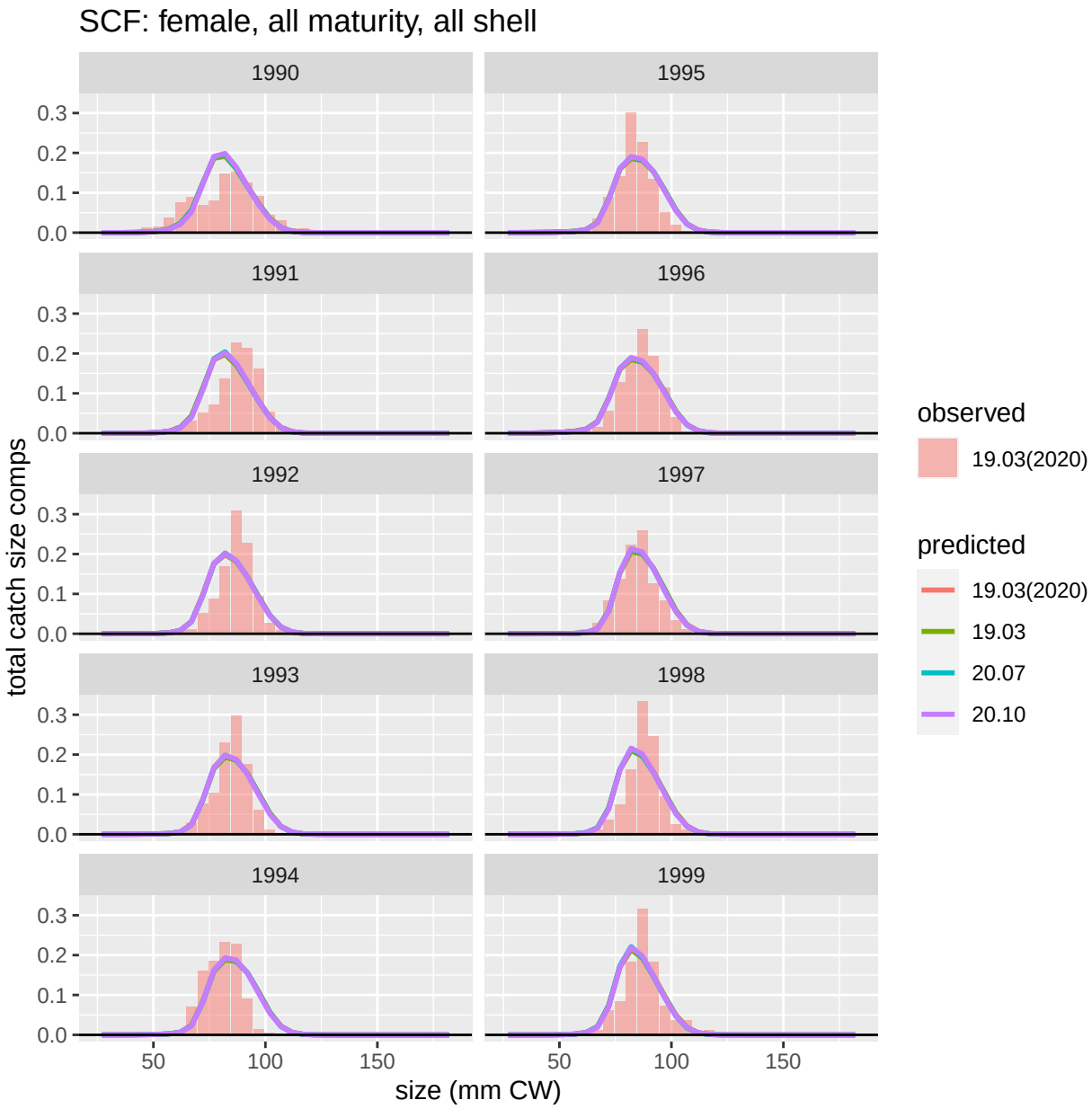

Figure 35: Comparison of observed and predicted female, all maturity, all shell total catch size comps for SCF. Page 1 of 3.

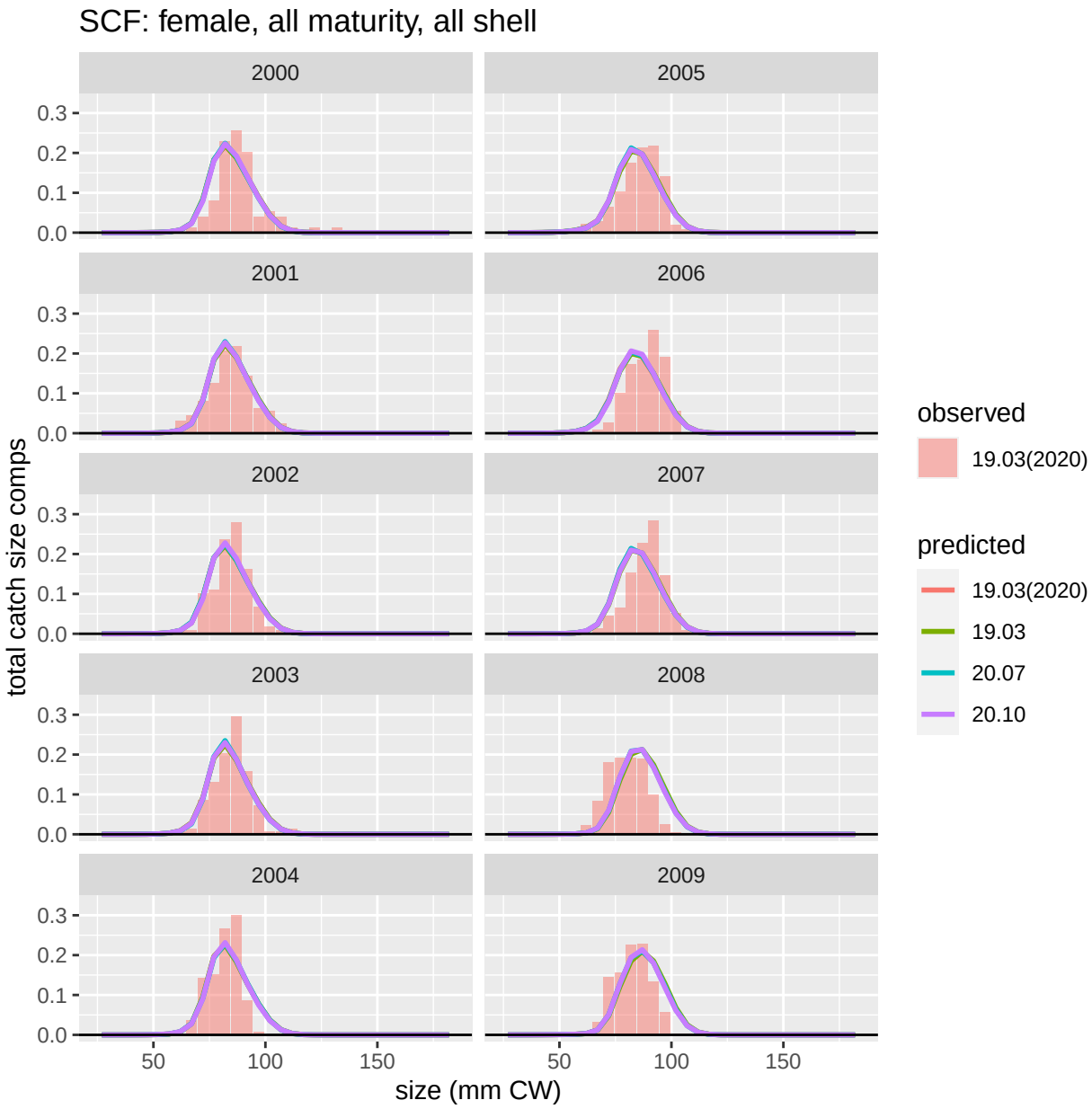

Figure 36: Comparison of observed and predicted female, all maturity, all shell total catch size comps for SCF. Page 2 of 3.

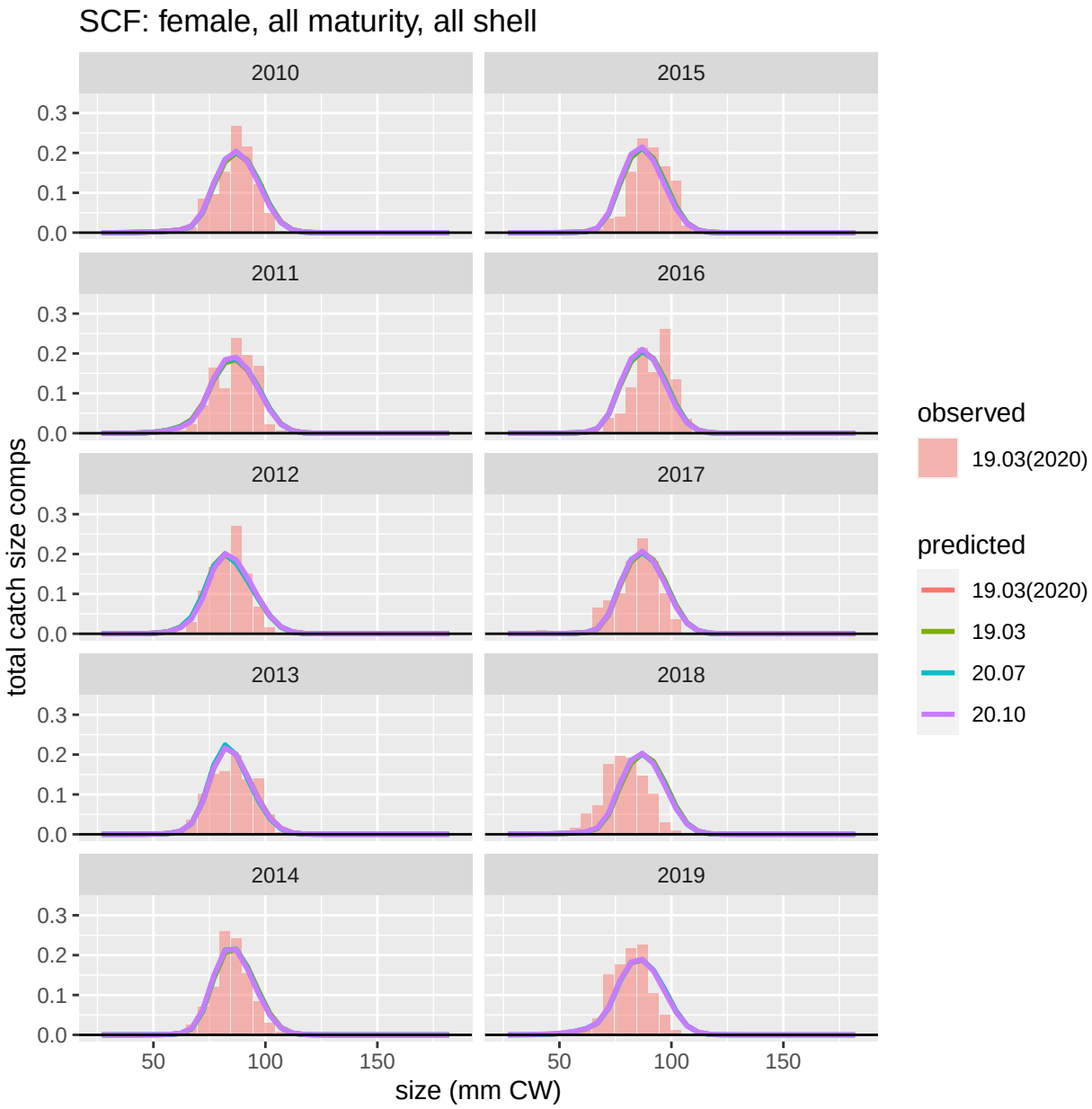

Figure 37: Comparison of observed and predicted female, all maturity, all shell total catch size comps for SCF. Page 3 of 3.

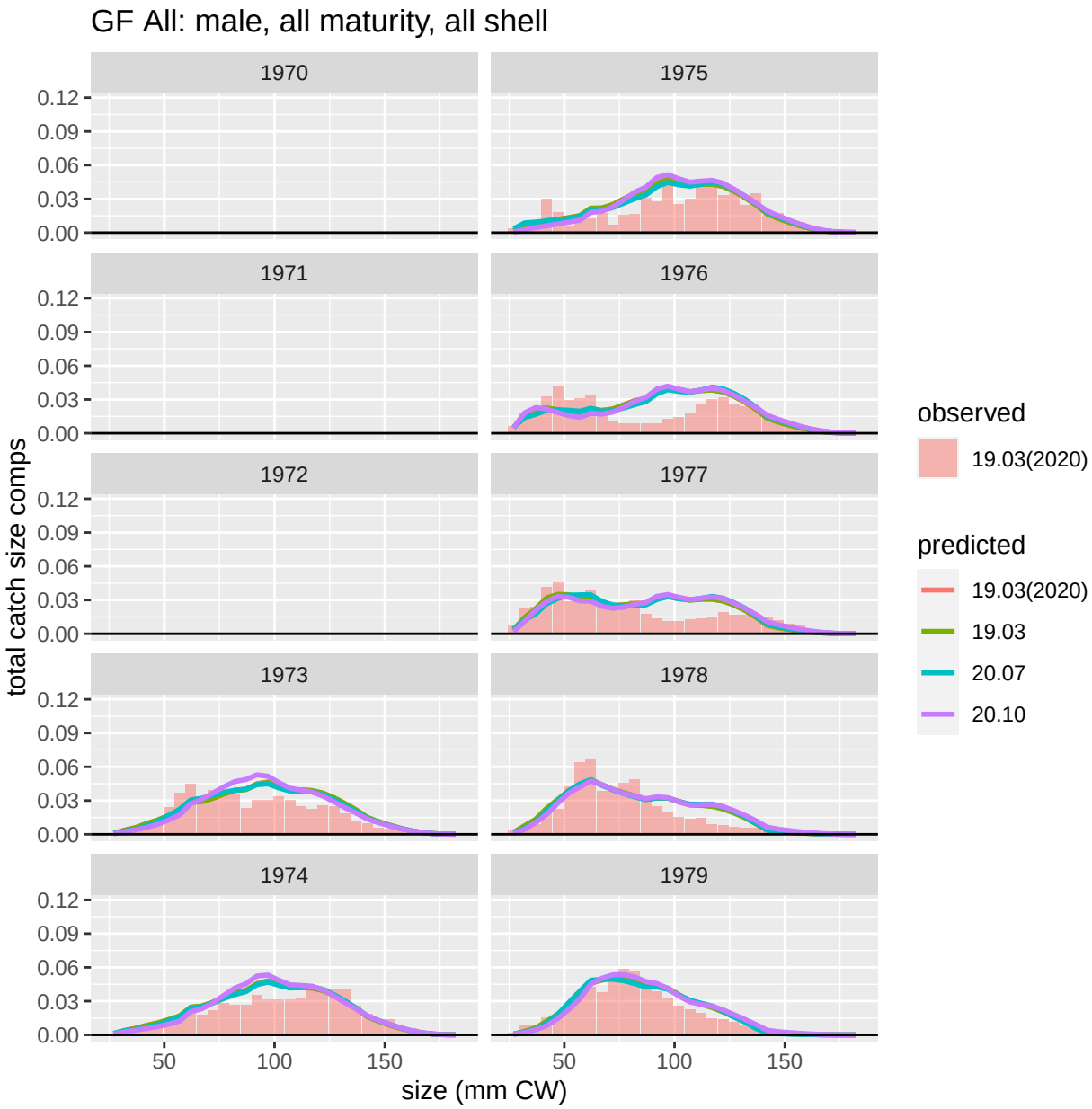

Figure 38: Comparison of observed and predicted male, all maturity, all shell total catch size comps for GF All. Page 1 of 5.

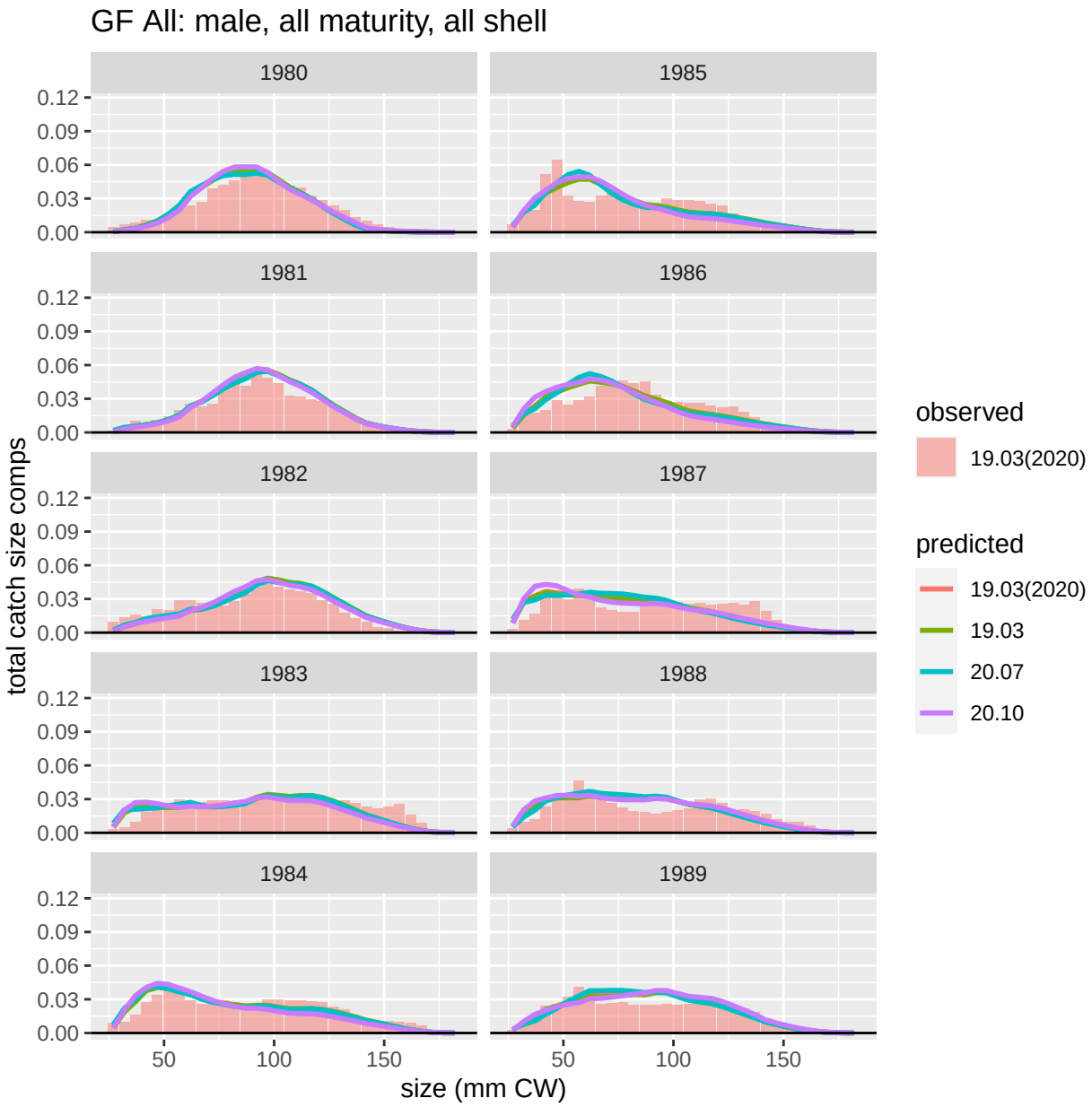

Figure 39: Comparison of observed and predicted male, all maturity, all shell total catch size comps for GF All. Page 2 of 5.

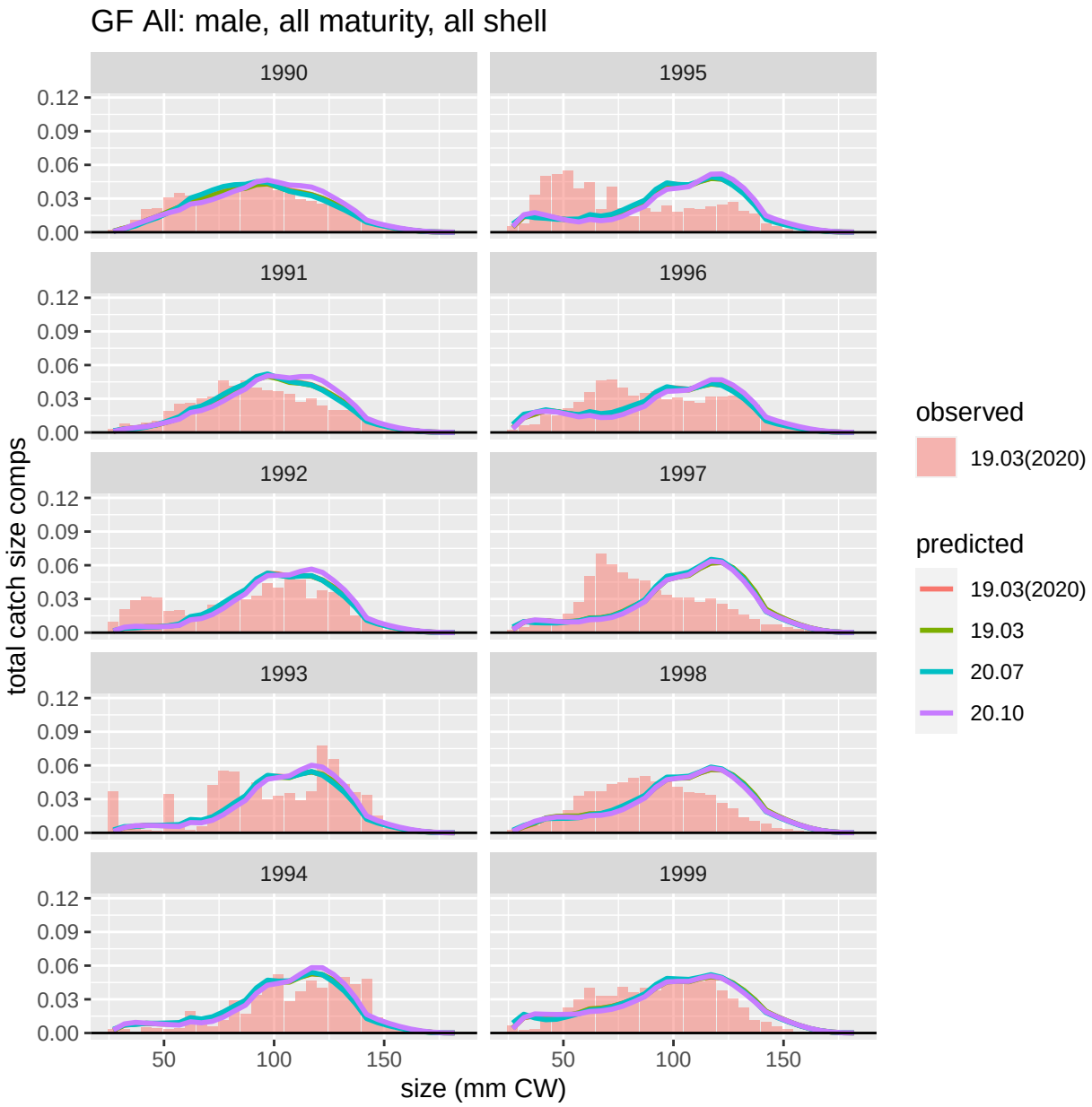

Figure 40: Comparison of observed and predicted male, all maturity, all shell total catch size comps for GF All. Page 3 of 5.

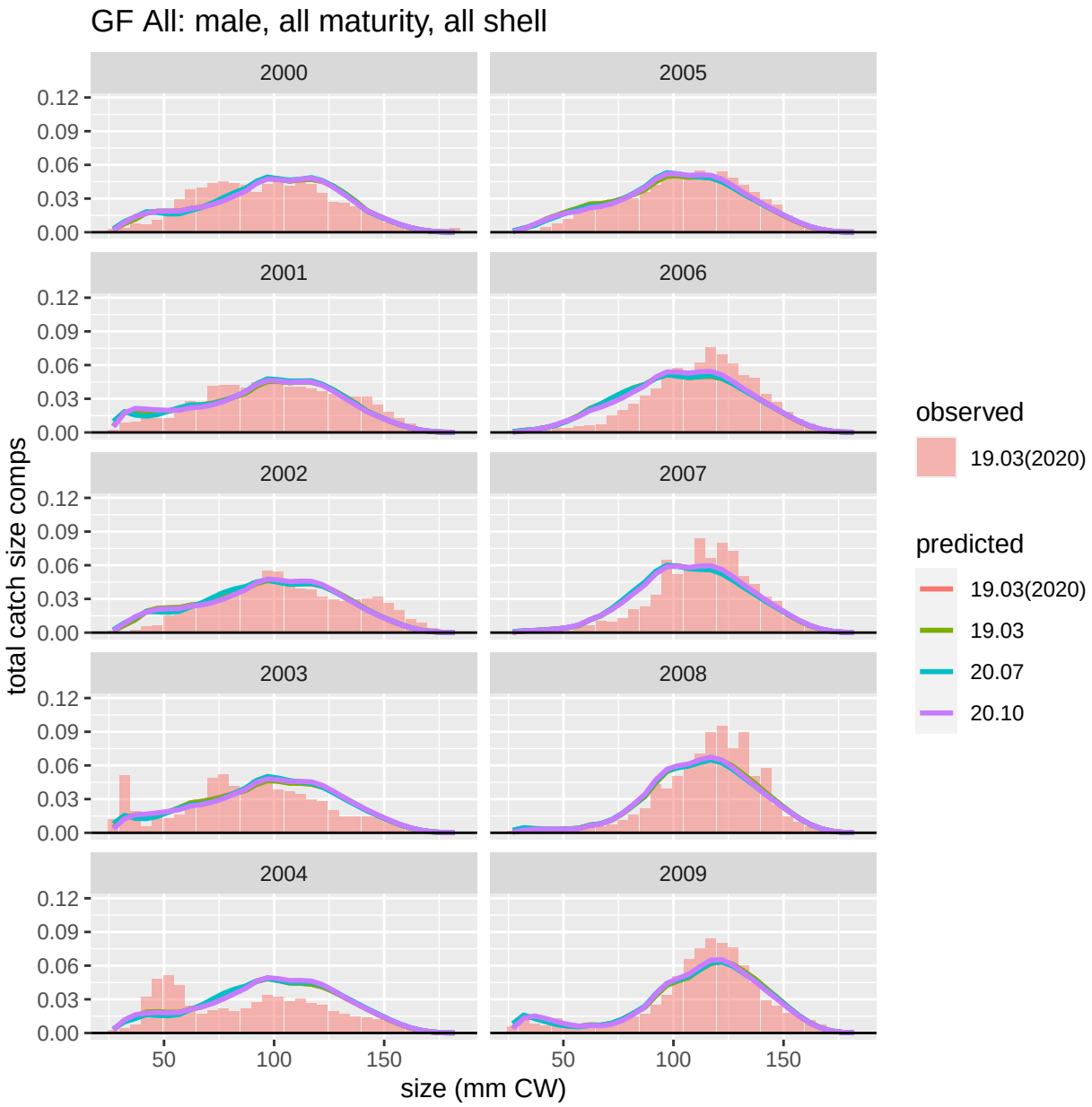

Figure 41: Comparison of observed and predicted male, all maturity, all shell total catch size comps for GF All. Page 4 of 5.

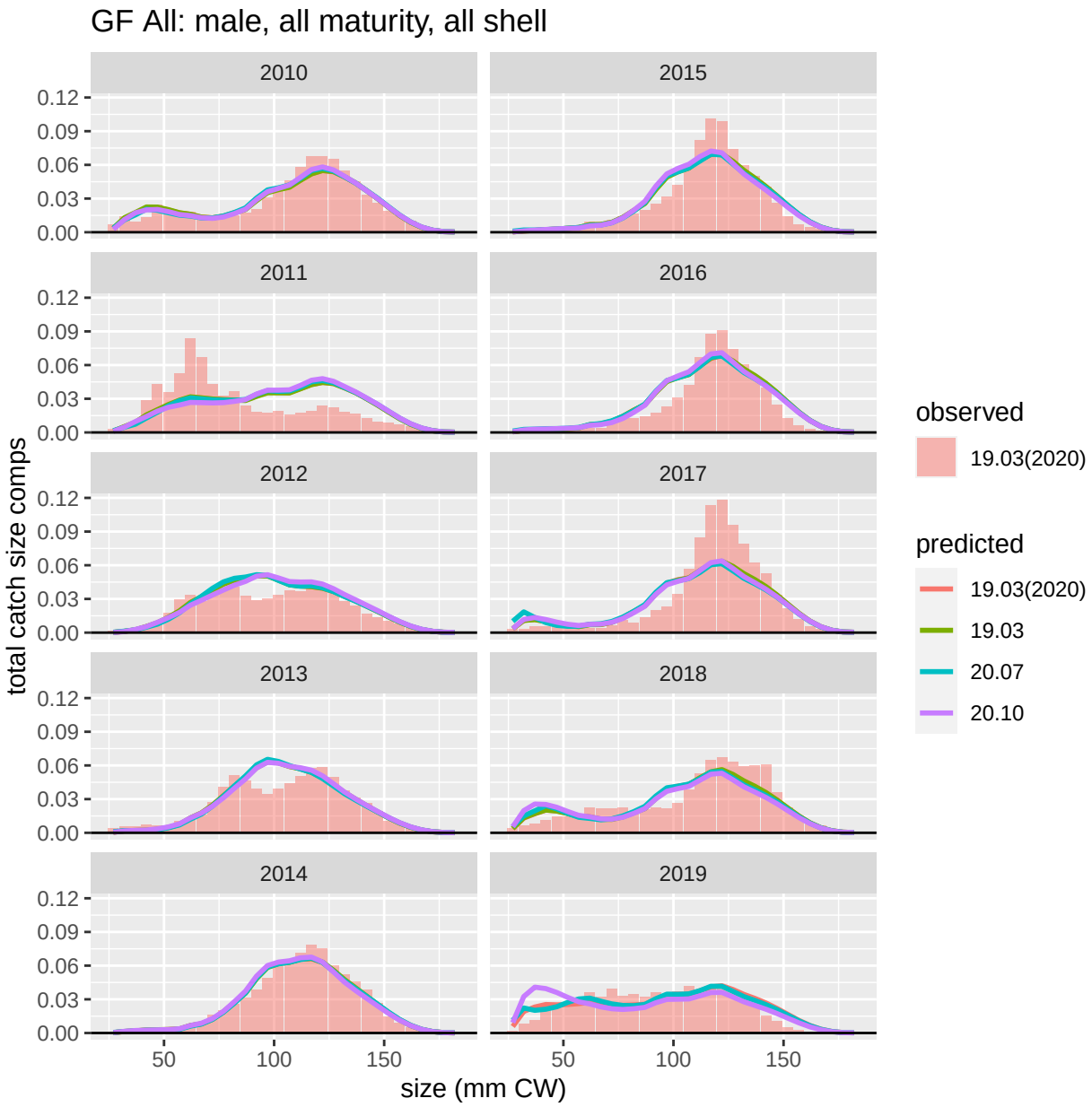

Figure 42: Comparison of observed and predicted male, all maturity, all shell total catch size comps for GF All. Page 5 of 5.

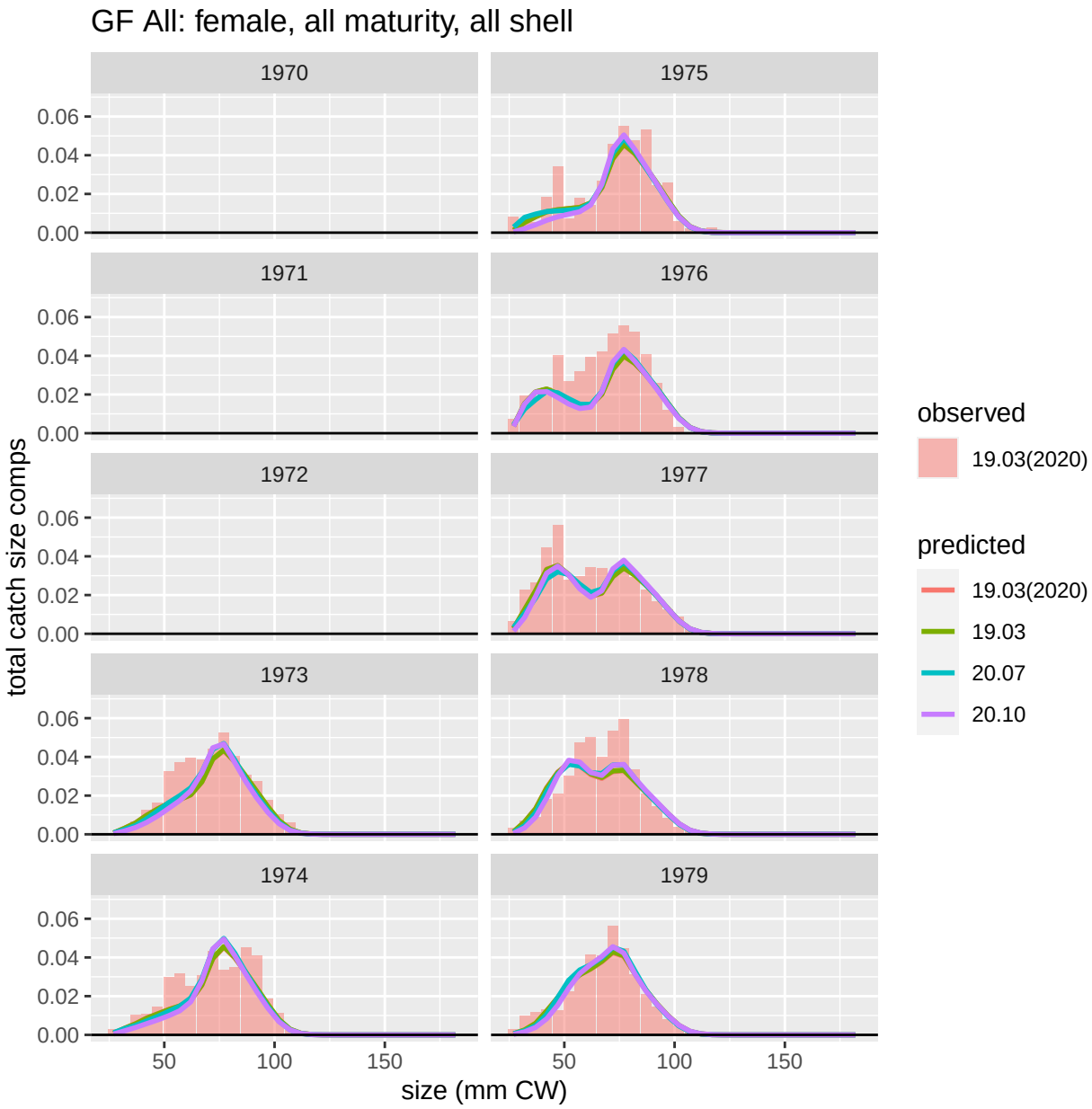

Figure 43: Comparison of observed and predicted female, all maturity, all shell total catch size comps for GF All. Page 1 of 5.

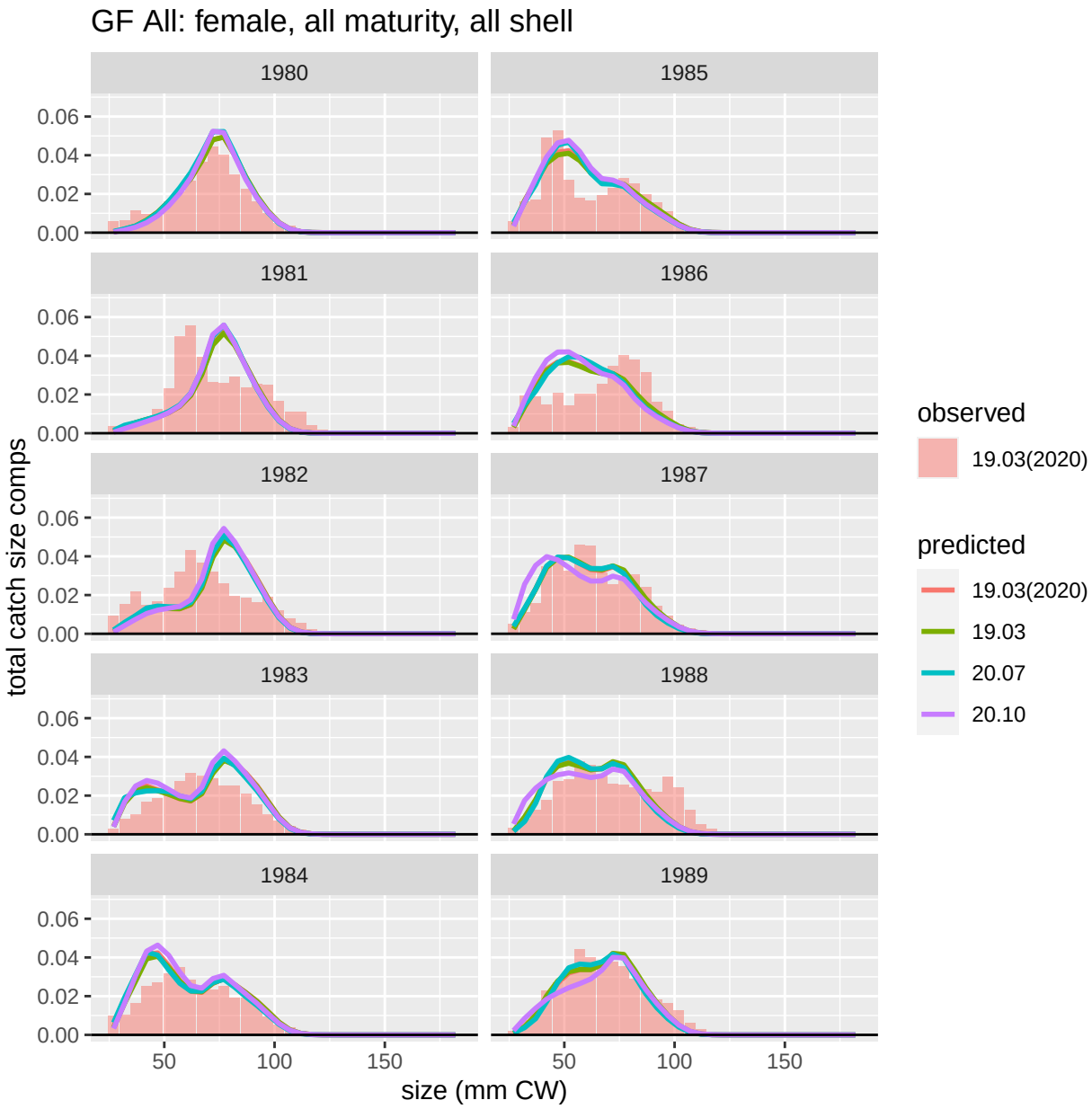

Figure 44: Comparison of observed and predicted female, all maturity, all shell total catch size comps for GF All. Page 2 of 5.

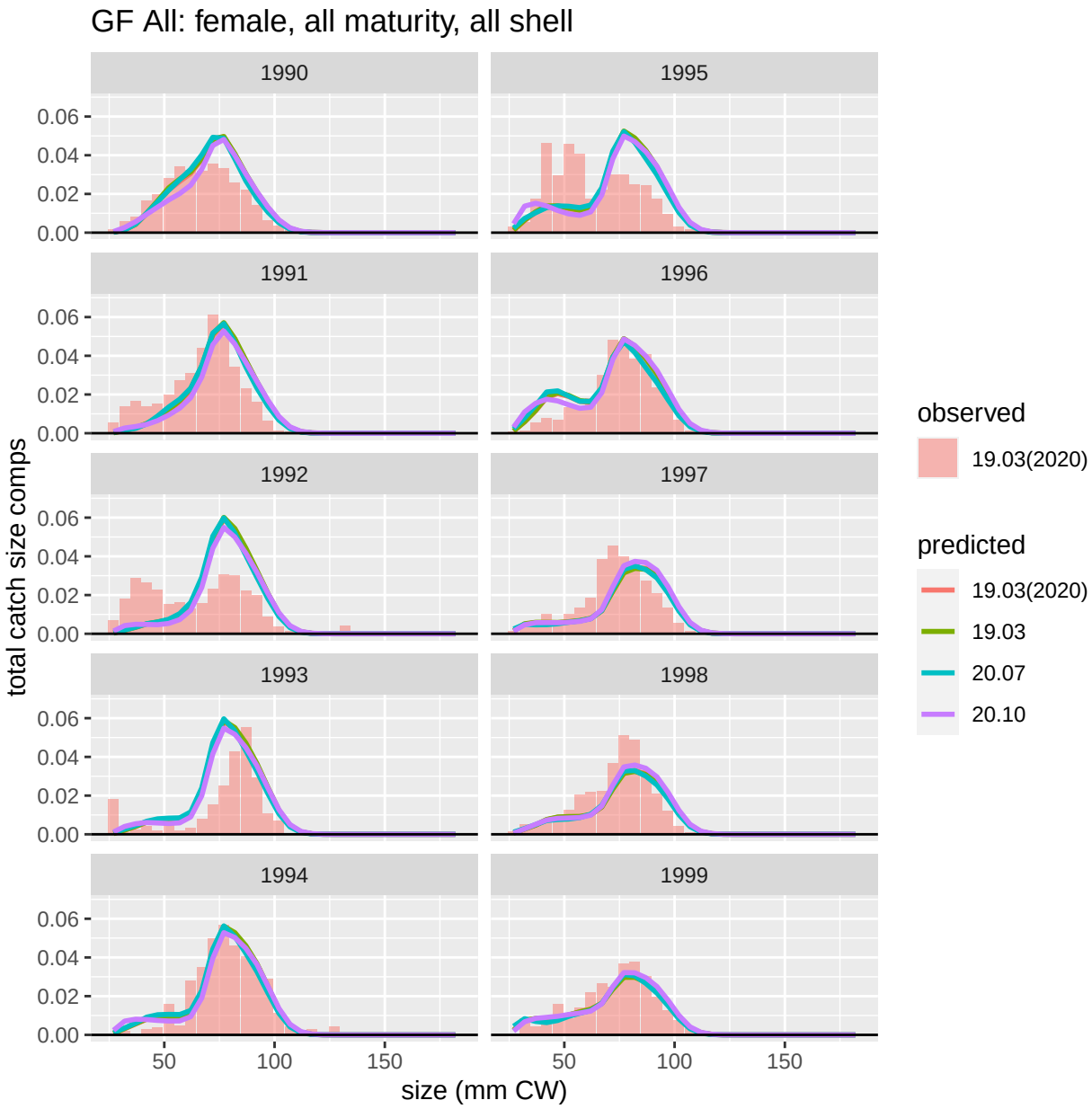

Figure 45: Comparison of observed and predicted female, all maturity, all shell total catch size comps for GF All. Page 3 of 5.

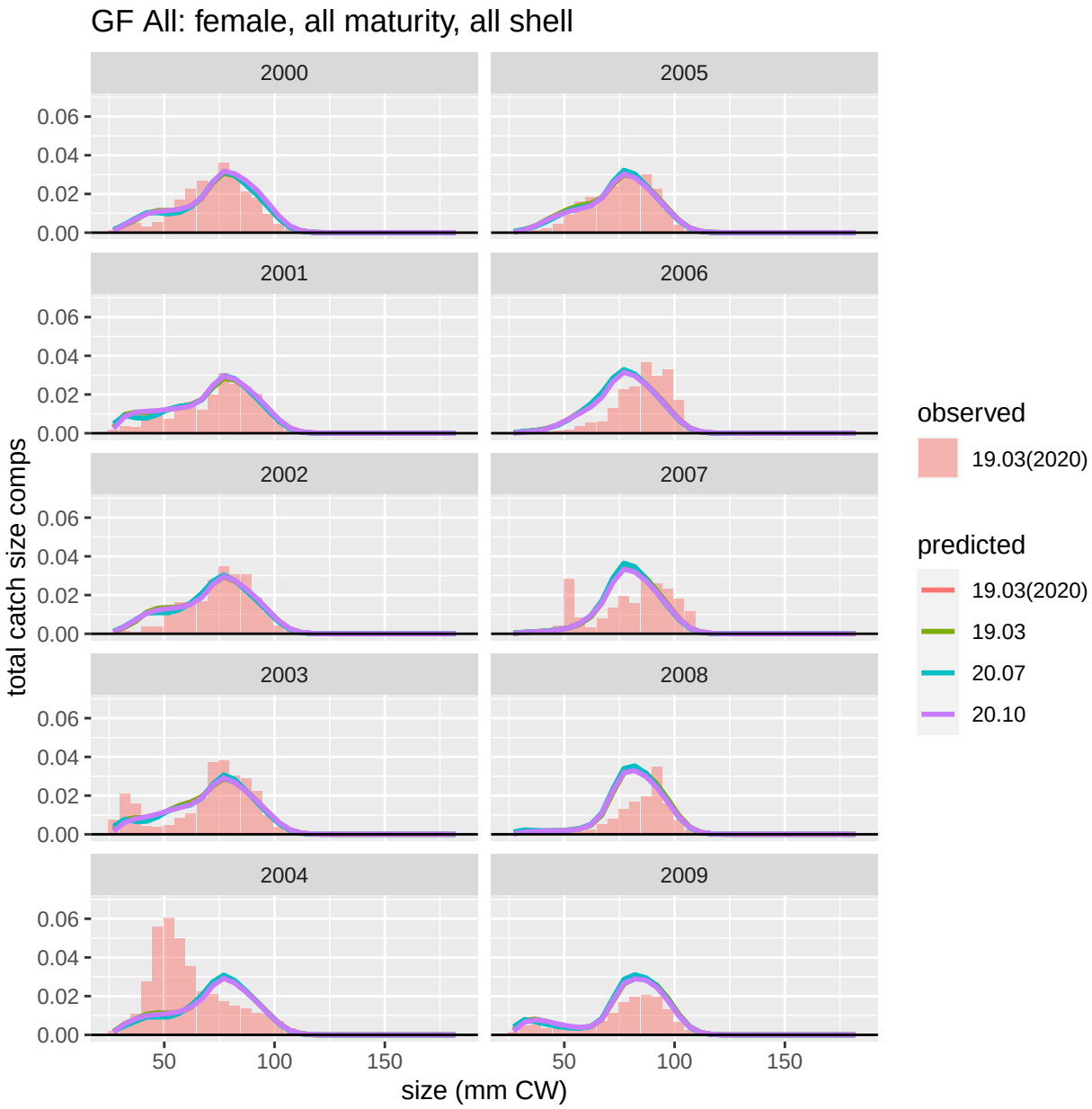

Figure 46: Comparison of observed and predicted female, all maturity, all shell total catch size comps for GF All. Page 4 of 5.

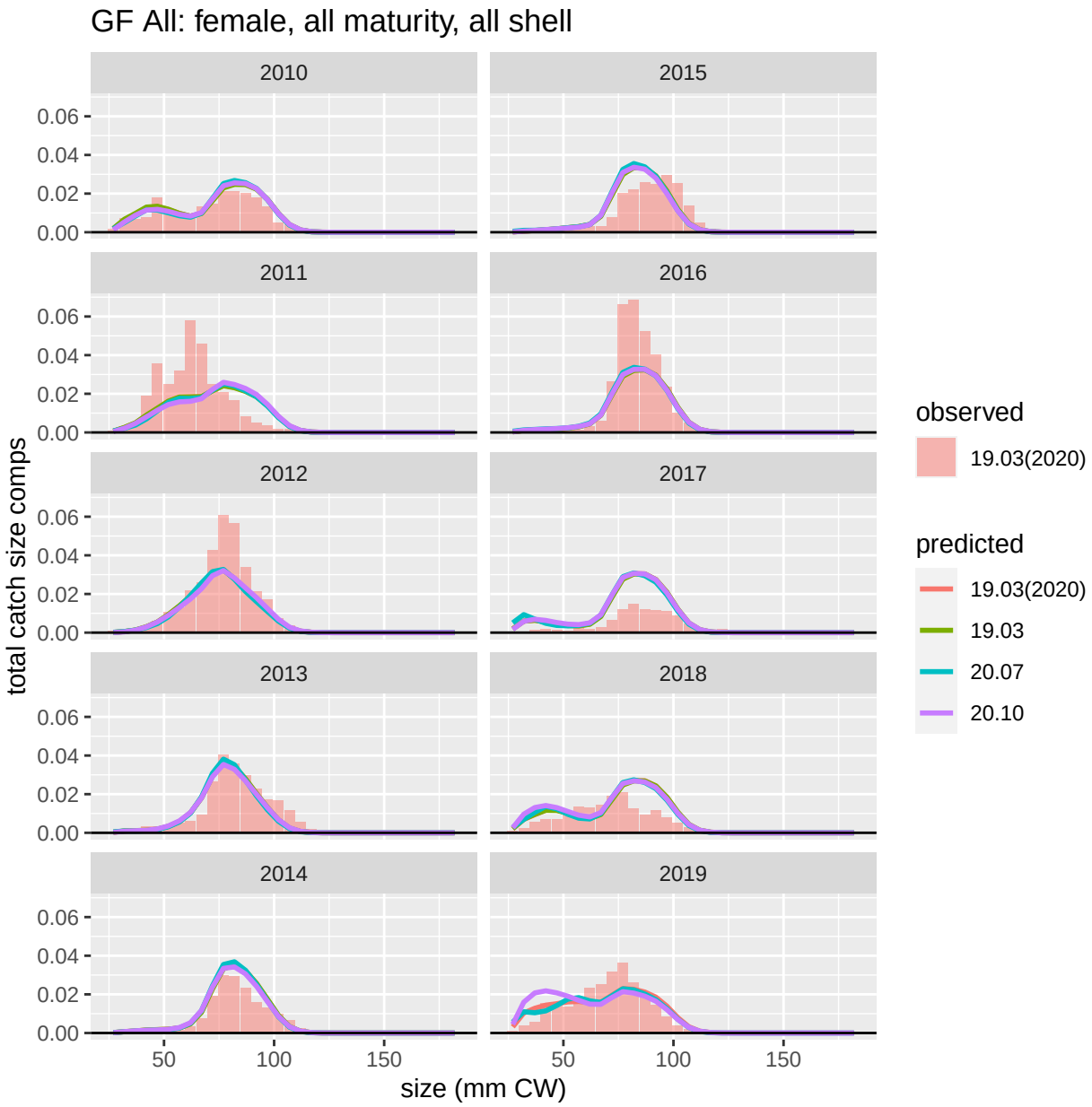

Figure 47: Comparison of observed and predicted female, all maturity, all shell total catch size comps for GF All. Page 5 of 5.

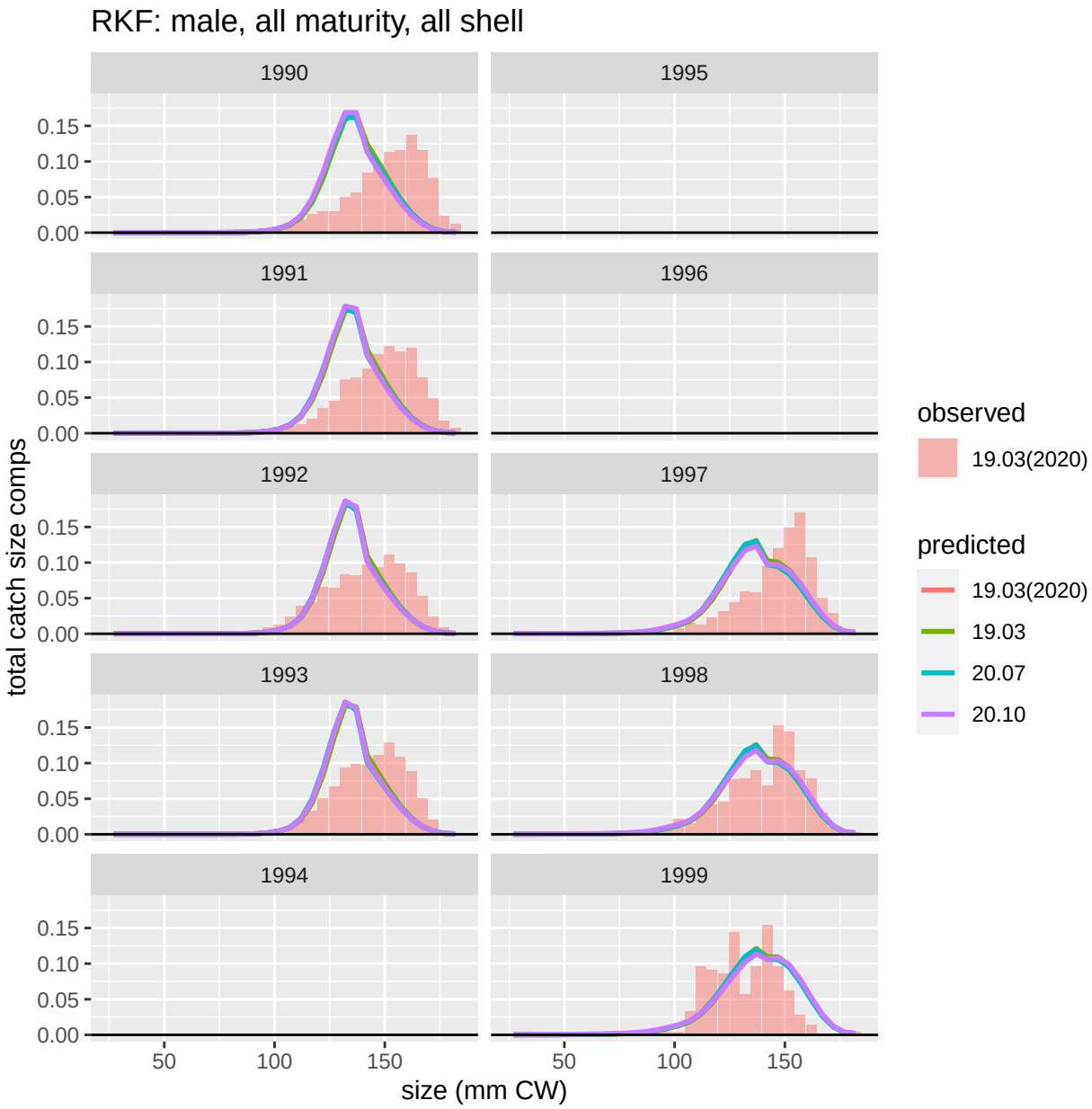

Figure 48: Comparison of observed and predicted male, all maturity, all shell total catch size comps for RKF. Page 1 of 3.

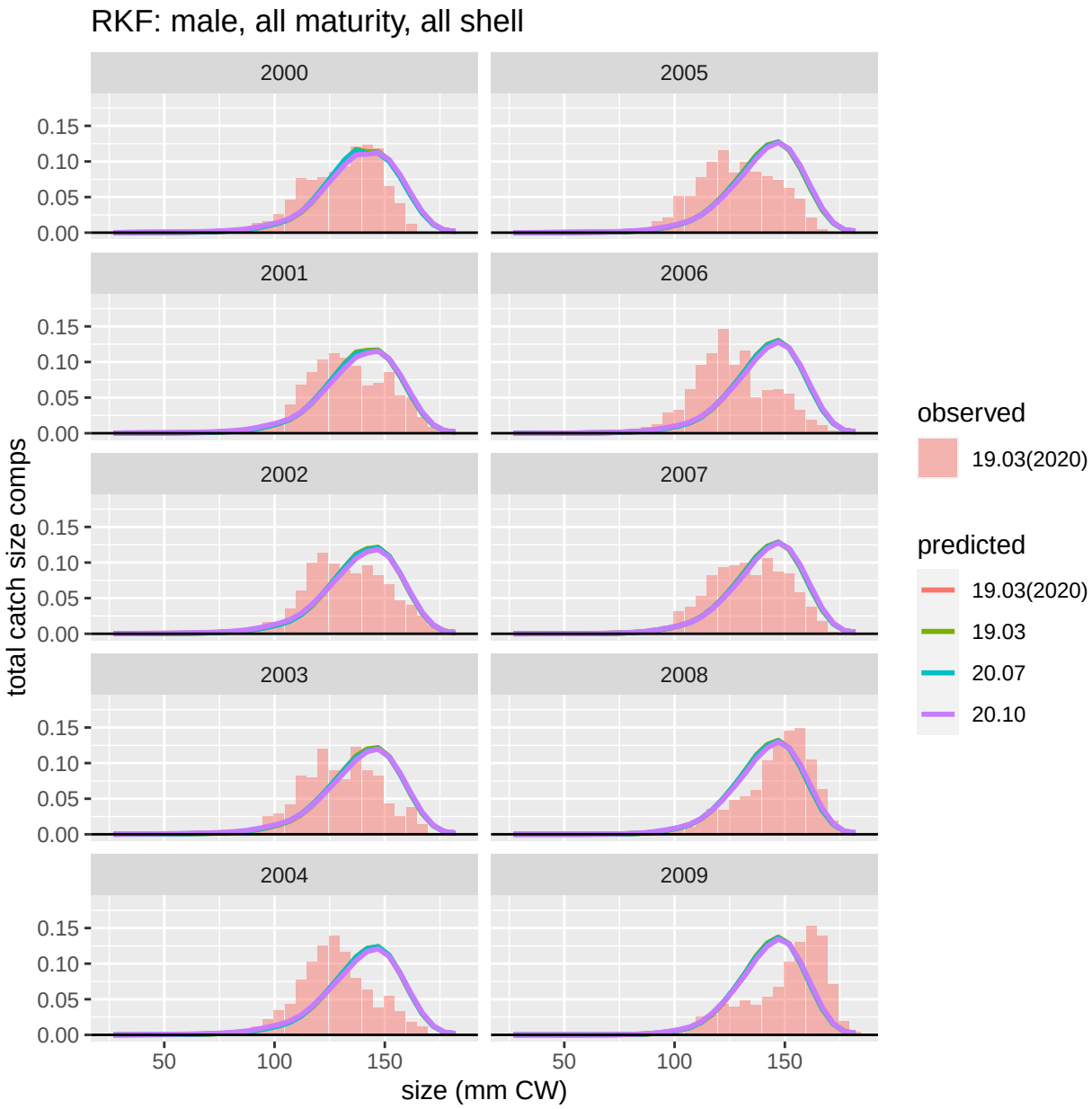

Figure 49: Comparison of observed and predicted male, all maturity, all shell total catch size comps for RKF. Page 2 of 3.

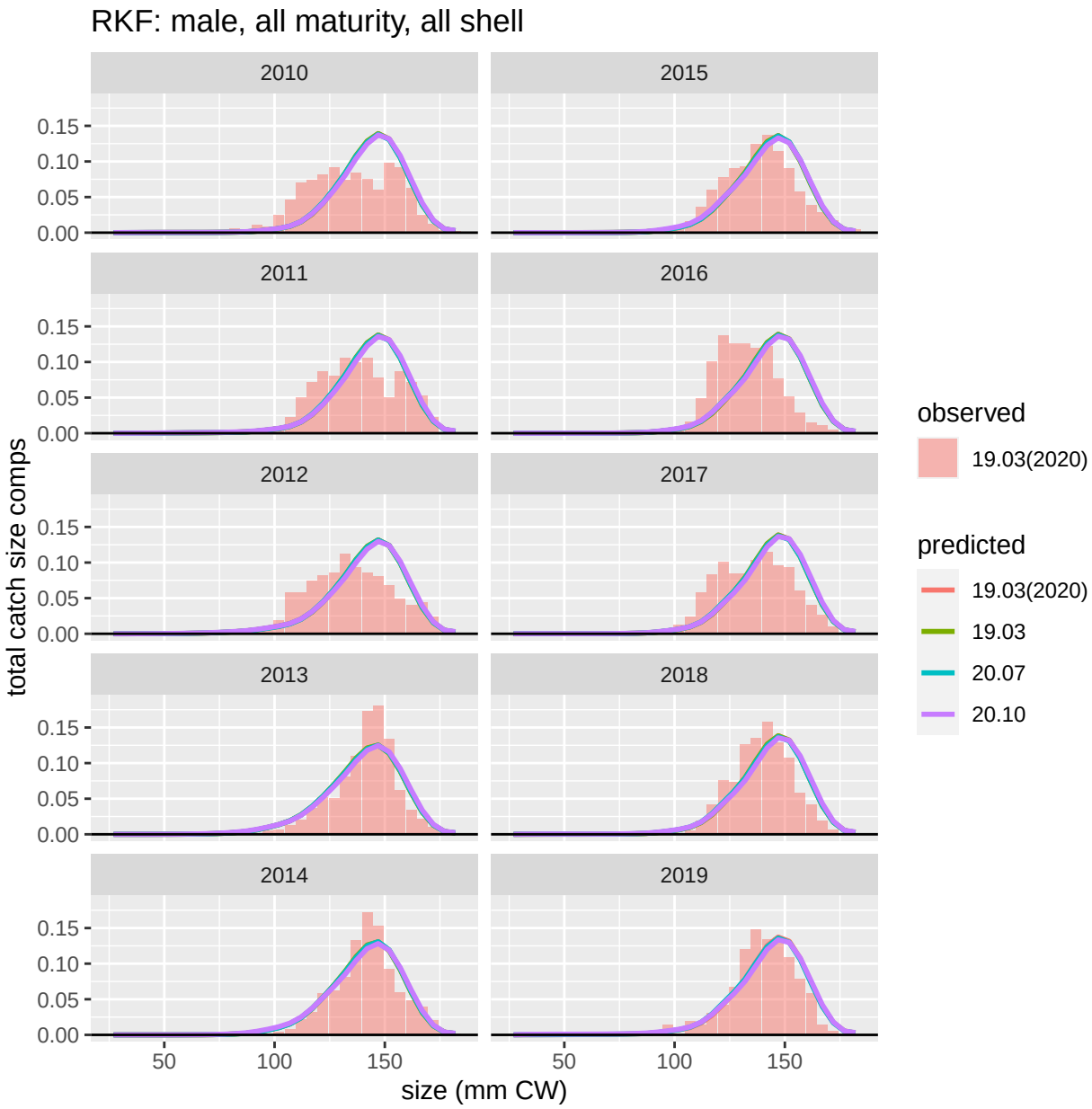

Figure 50: Comparison of observed and predicted male, all maturity, all shell total catch size comps for RKF. Page 3 of 3.

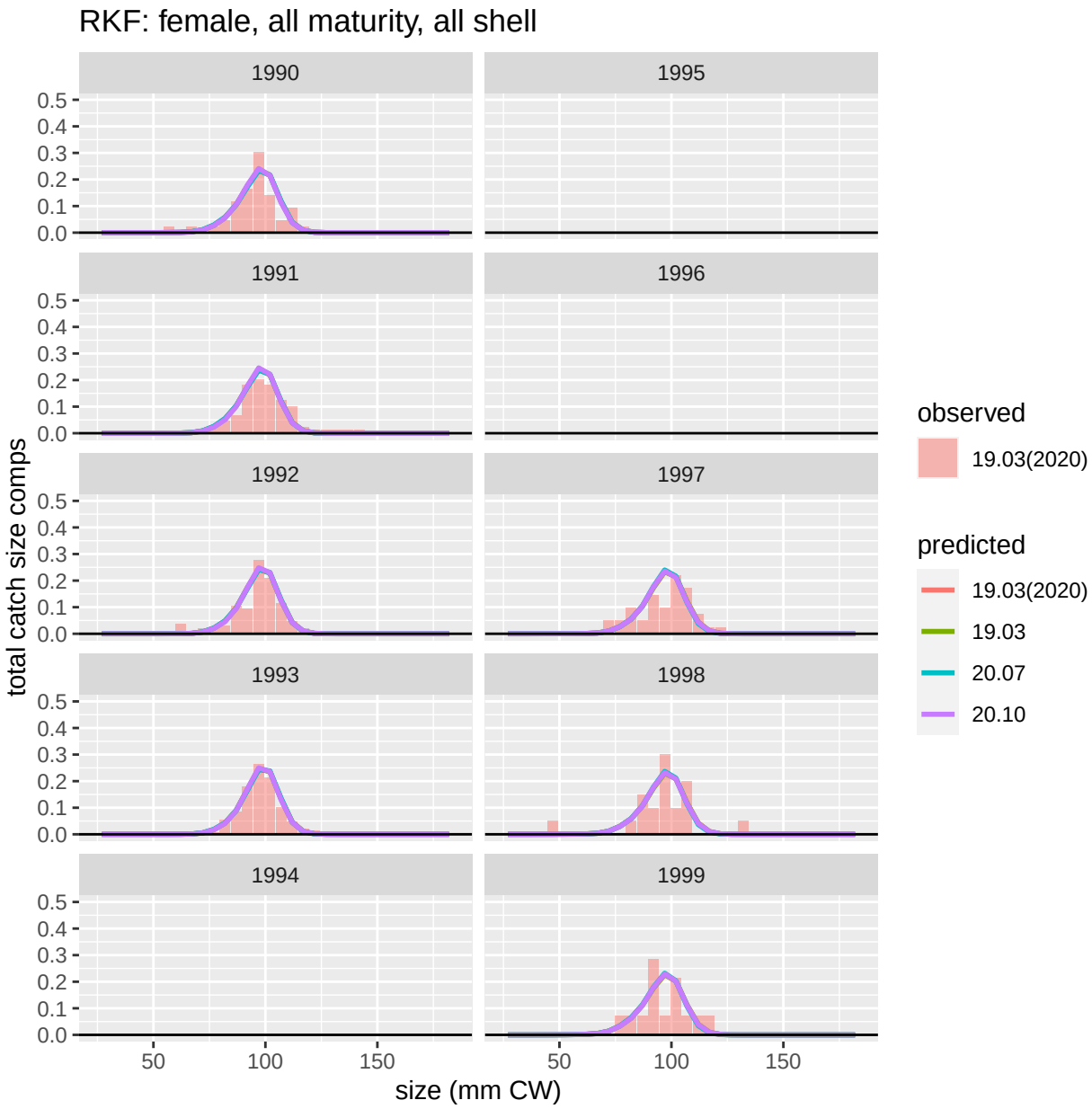

Figure 51: Comparison of observed and predicted female, all maturity, all shell total catch size comps for RKF. Page 1 of 3.

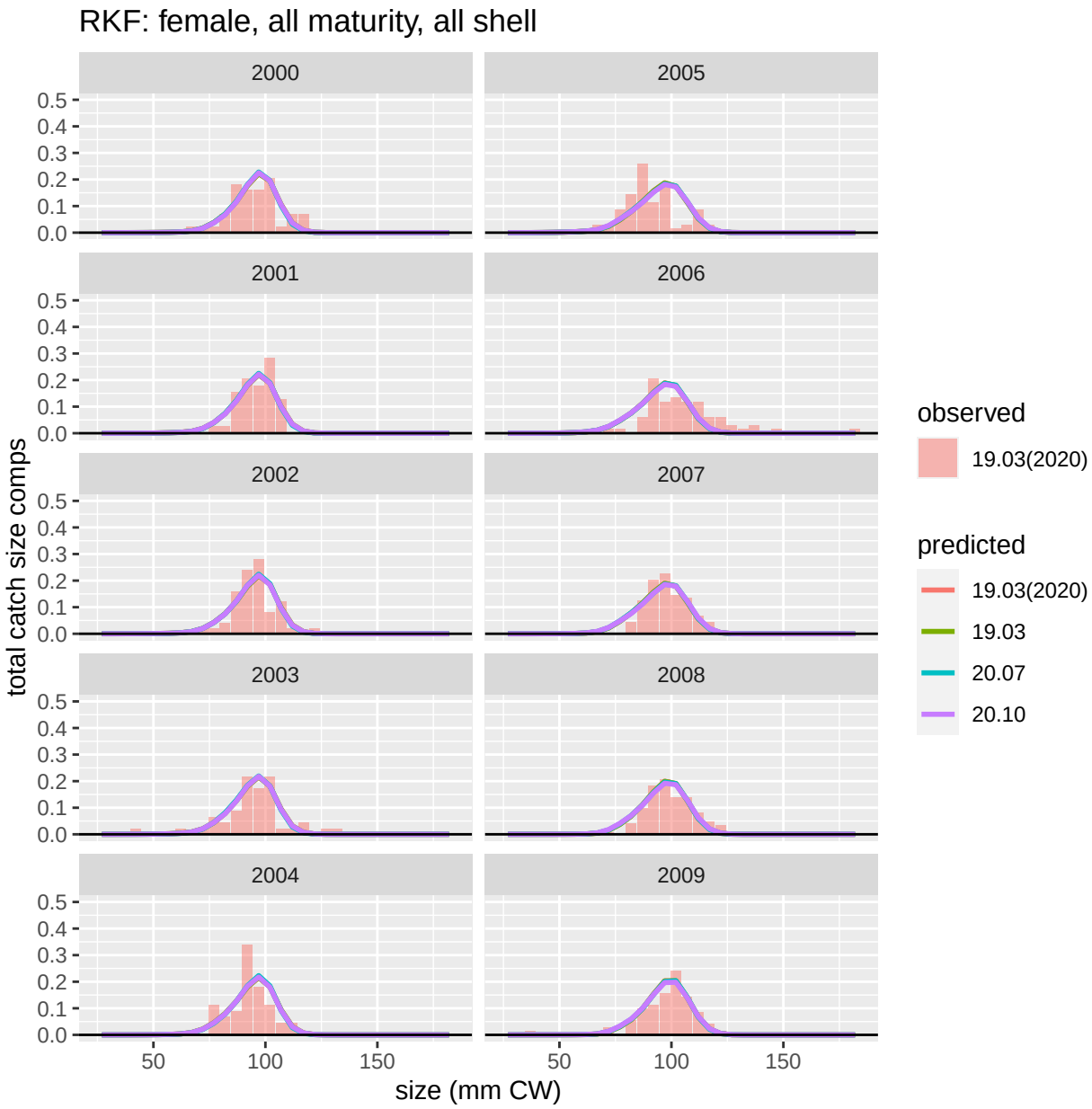

Figure 52: Comparison of observed and predicted female, all maturity, all shell total catch size comps for RKF. Page 2 of 3.

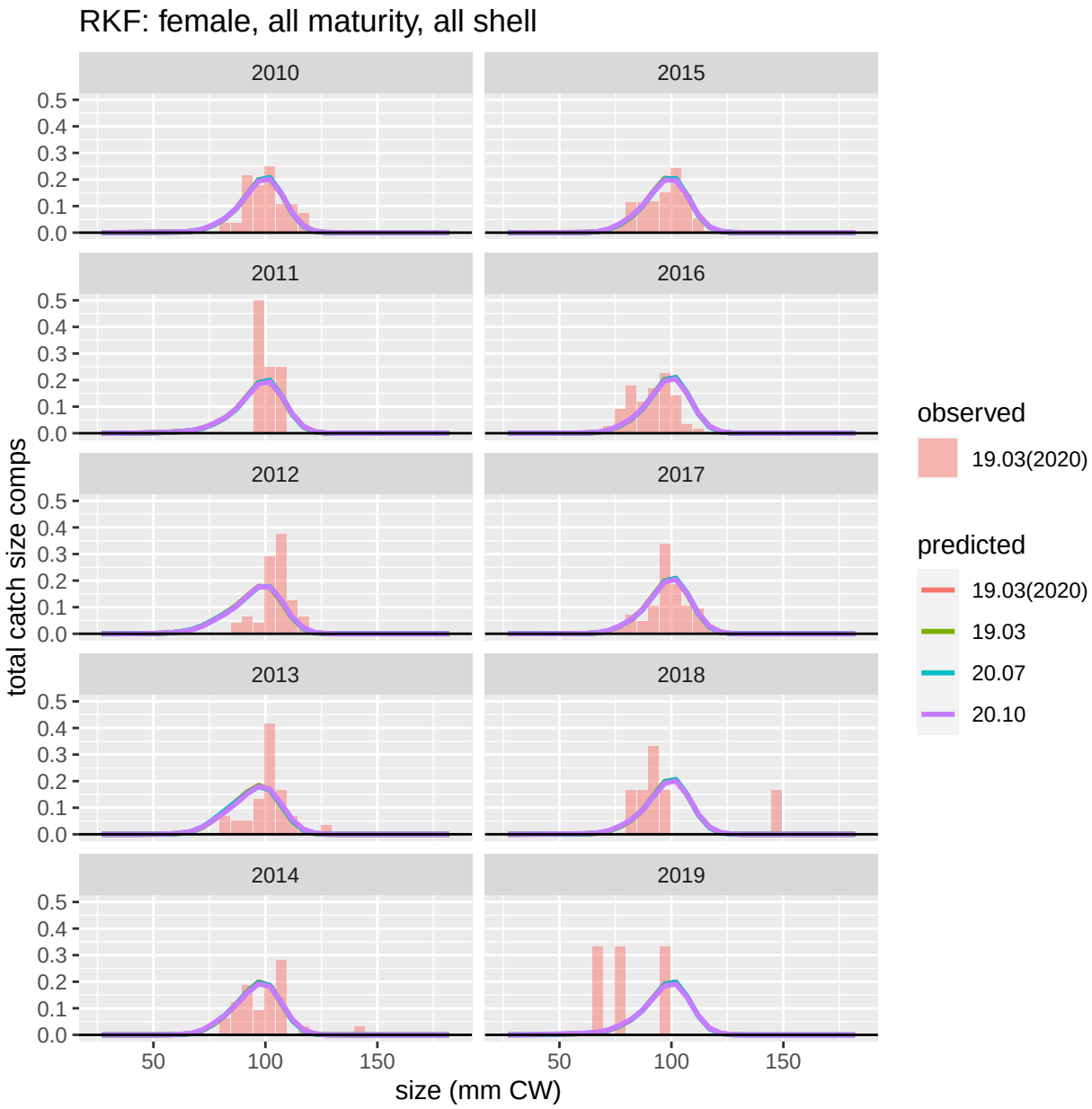

Figure 53: Comparison of observed and predicted female, all maturity, all shell total catch size comps for RKF. Page 3 of 3.

Appendix 9: Diagnostics for Fits to Fisheries Size Composition Data –19.03(2020) vs 19.03 vs 20.07 vs 20.10

William Stockhausen

01 September, 2020

Contents

Introduction

Fits to fishery retained catch and total catch size composition data available to the model(s) are presented in this section. Included are plots of mean fits to size compositions, Pearson's residuals as bubble plots, and effective sample sizes. Not all of the fits presented are necessarily included in the parameter optimization for each model; some fits to datasets for a particular model may be included for comparison purposes with other models which include those data in their optimization. The reader should consult the main assessment document to determine which fits are included in the optimization for any particular model.

Retained catch mean size compositions

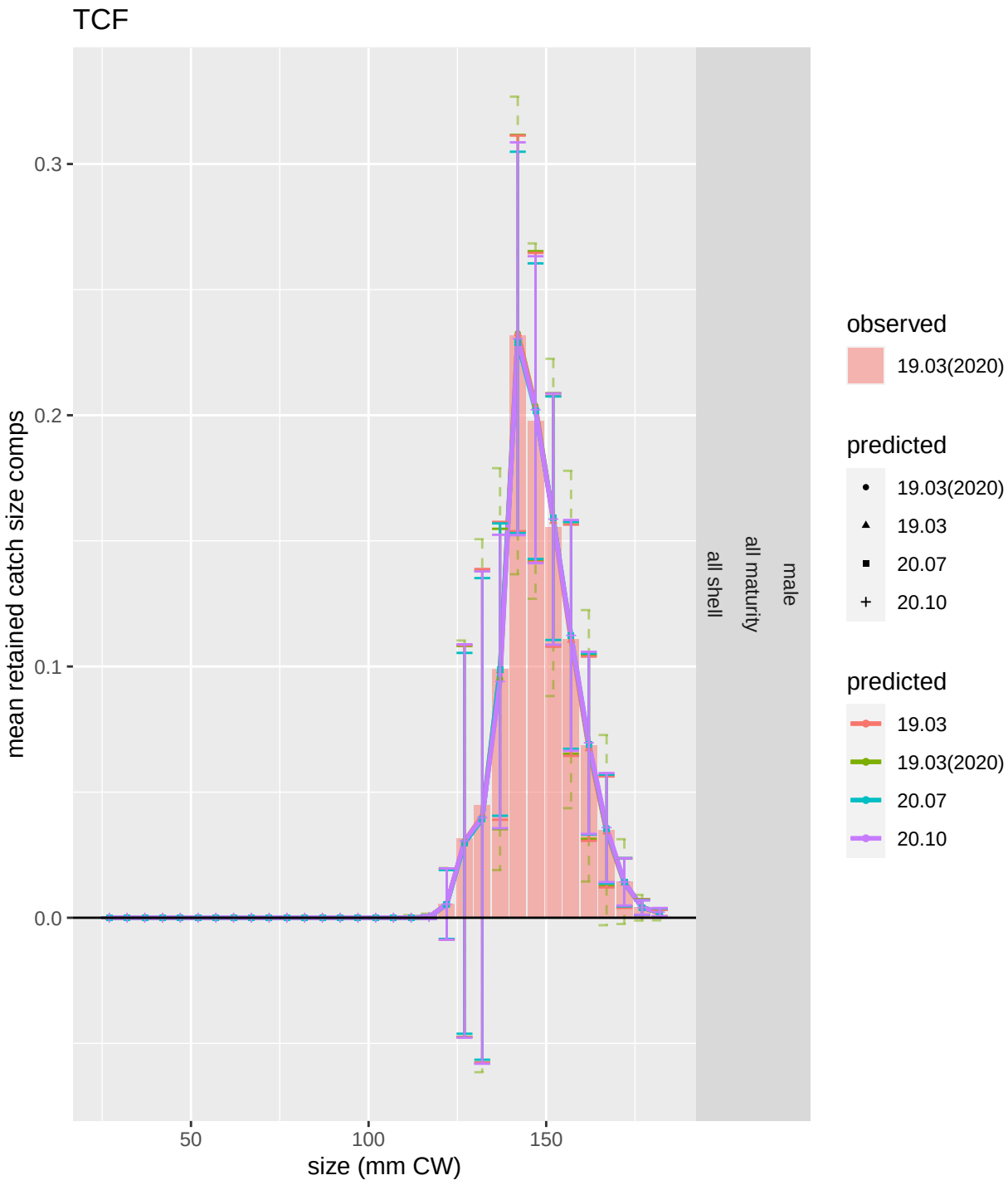

Figure 1: Comparison of observed and predicted mean retained catch size comps for TCF.

Total catch mean size compositions

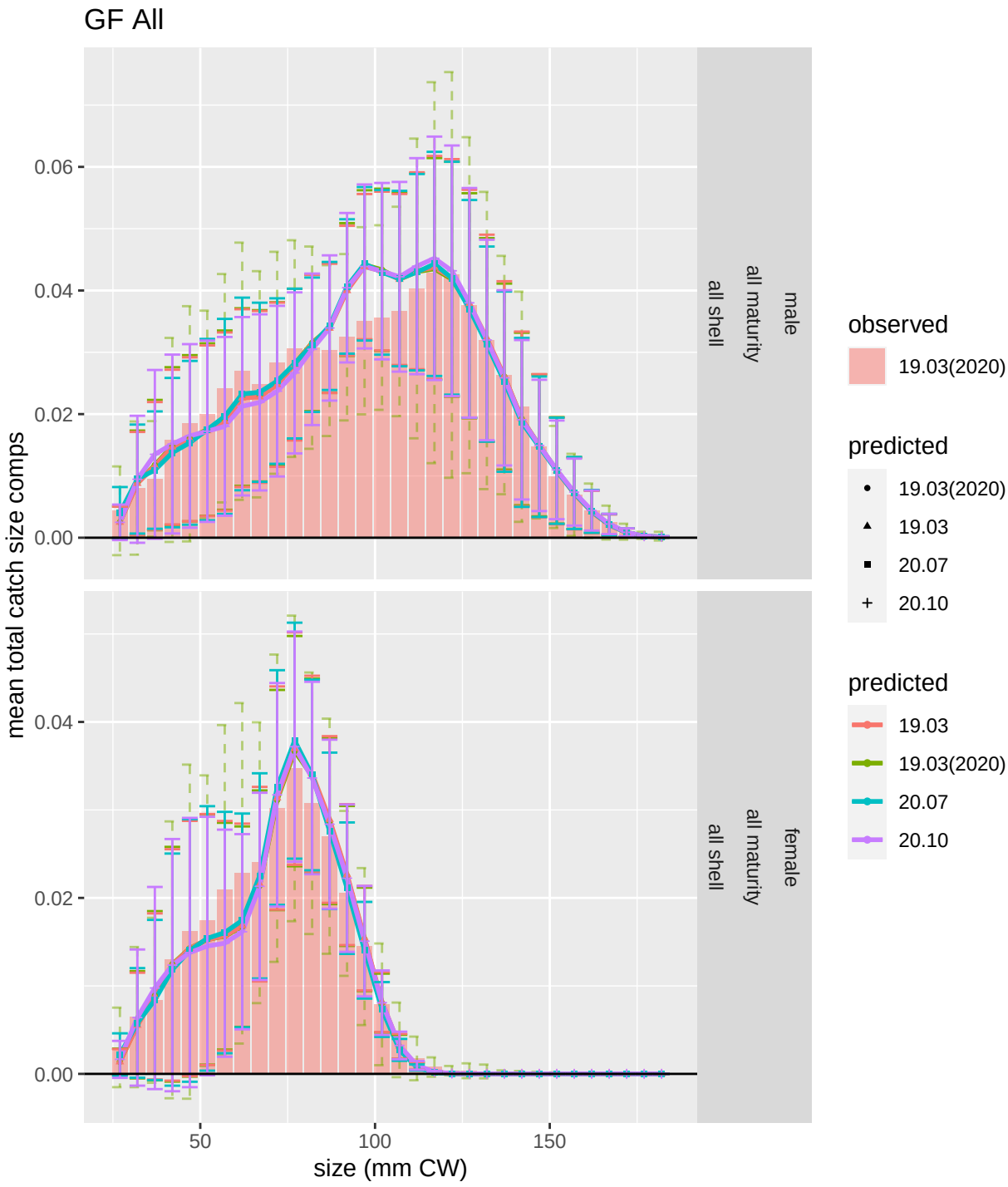

Figure 2: Comparison of observed and predicted mean total catch size comps for GF All.

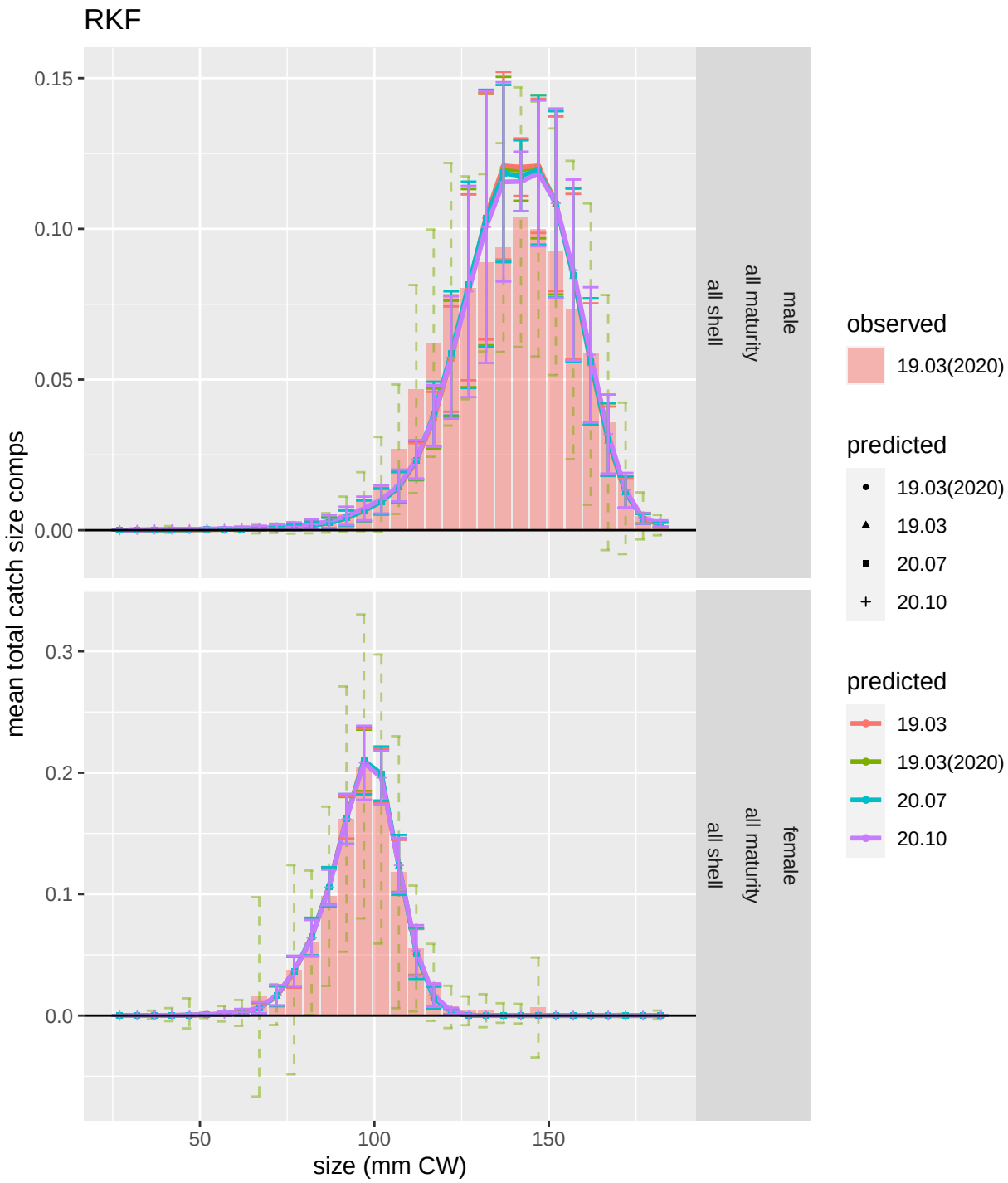

Figure 3: Comparison of observed and predicted mean total catch size comps for RKF.

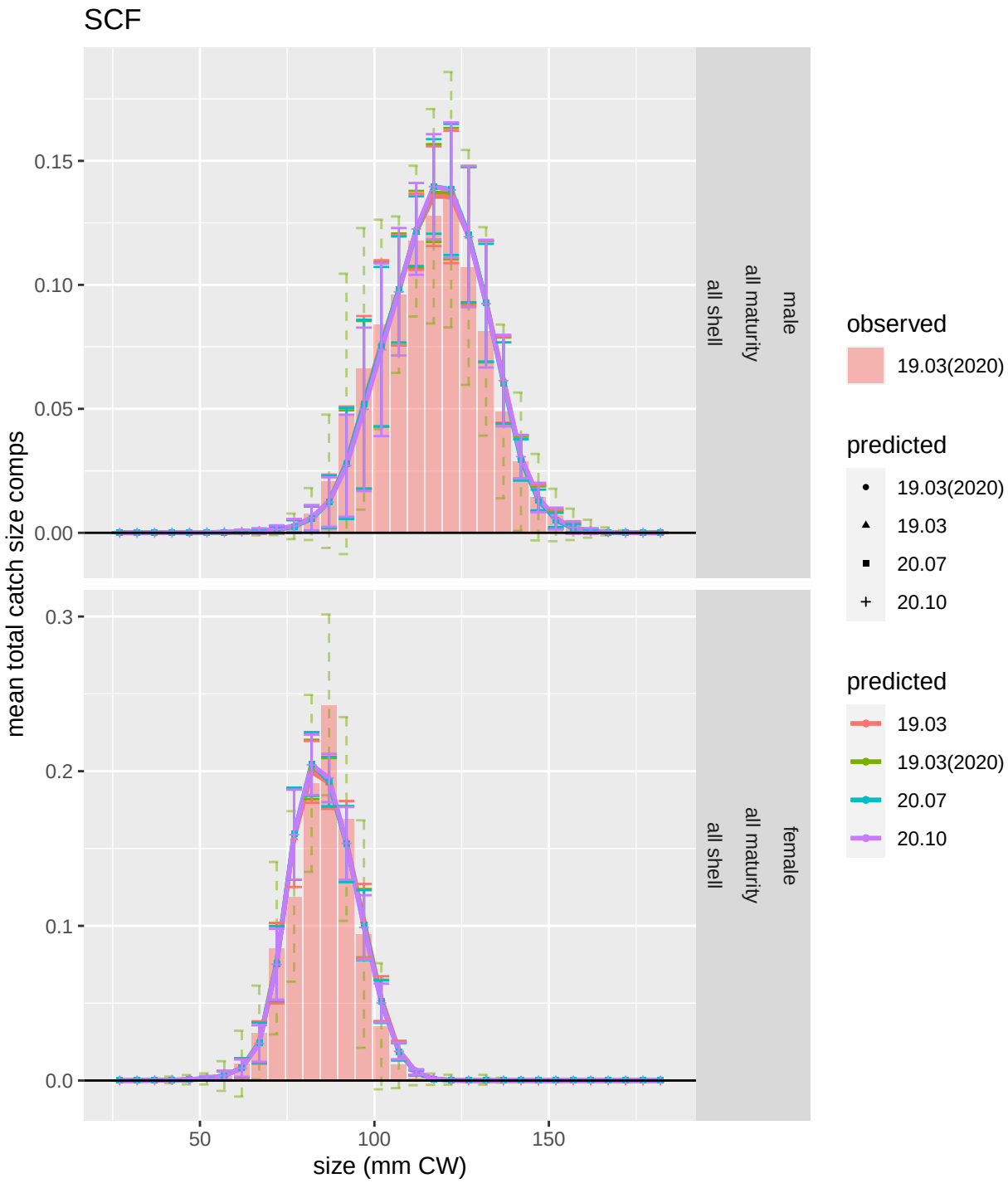

Figure 4: Comparison of observed and predicted mean total catch size comps for SCF.

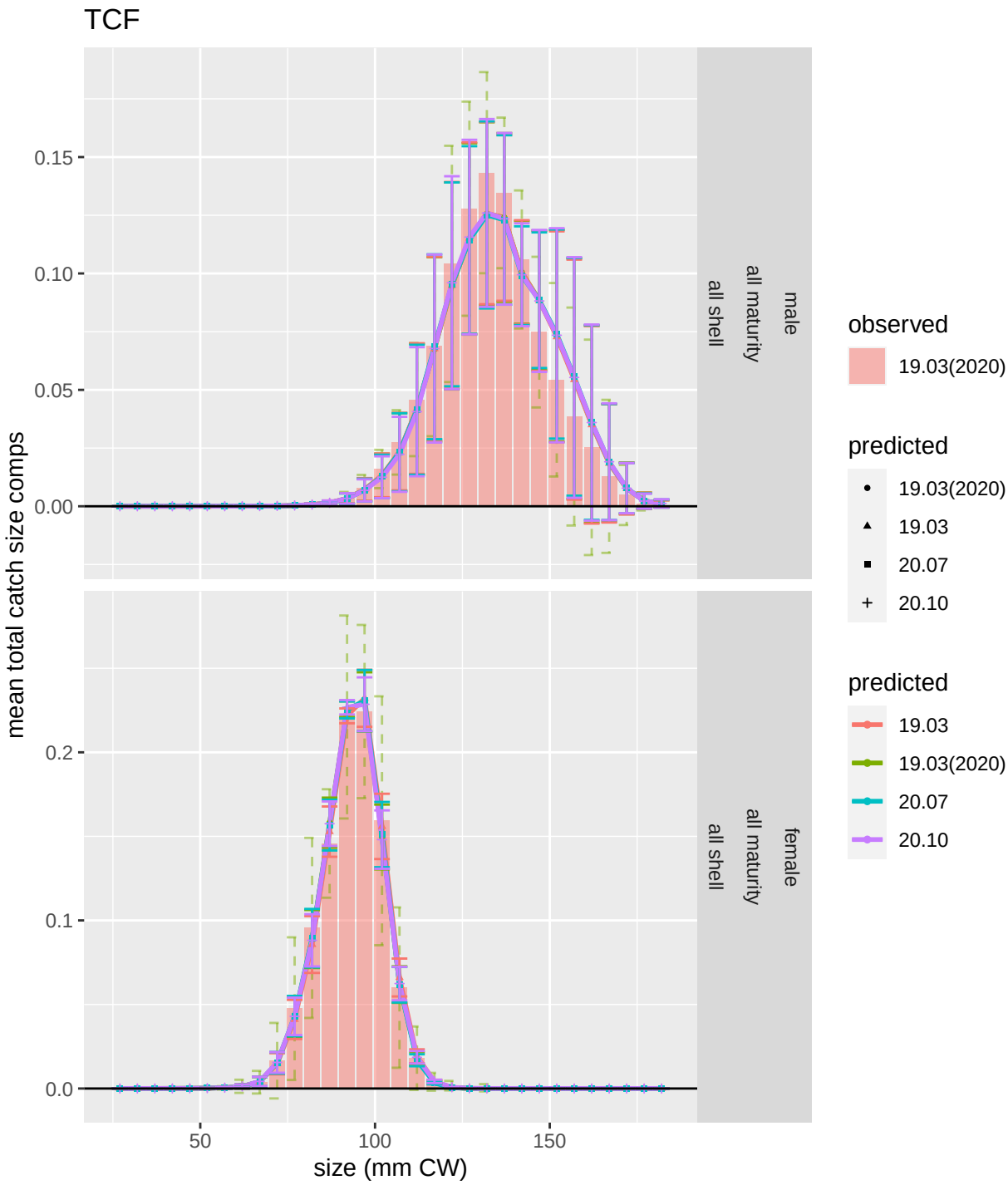

Figure 5: Comparison of observed and predicted mean total catch size comps for TCF.

Fishery retained catch size composition residuals

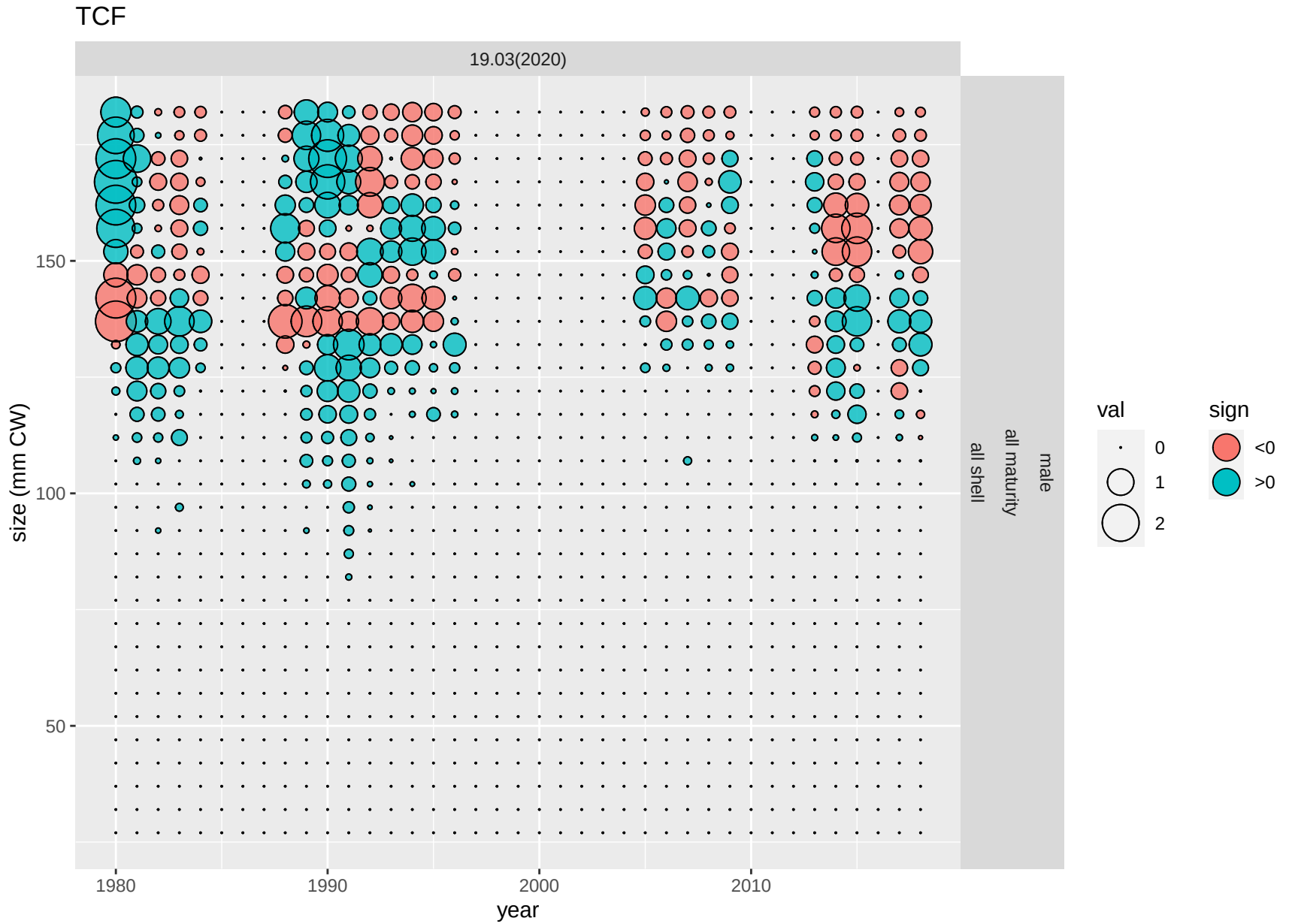

Figure 6: Pearson's residuals for male proportions-at-size from the TCF for scenario 19.03(2020).

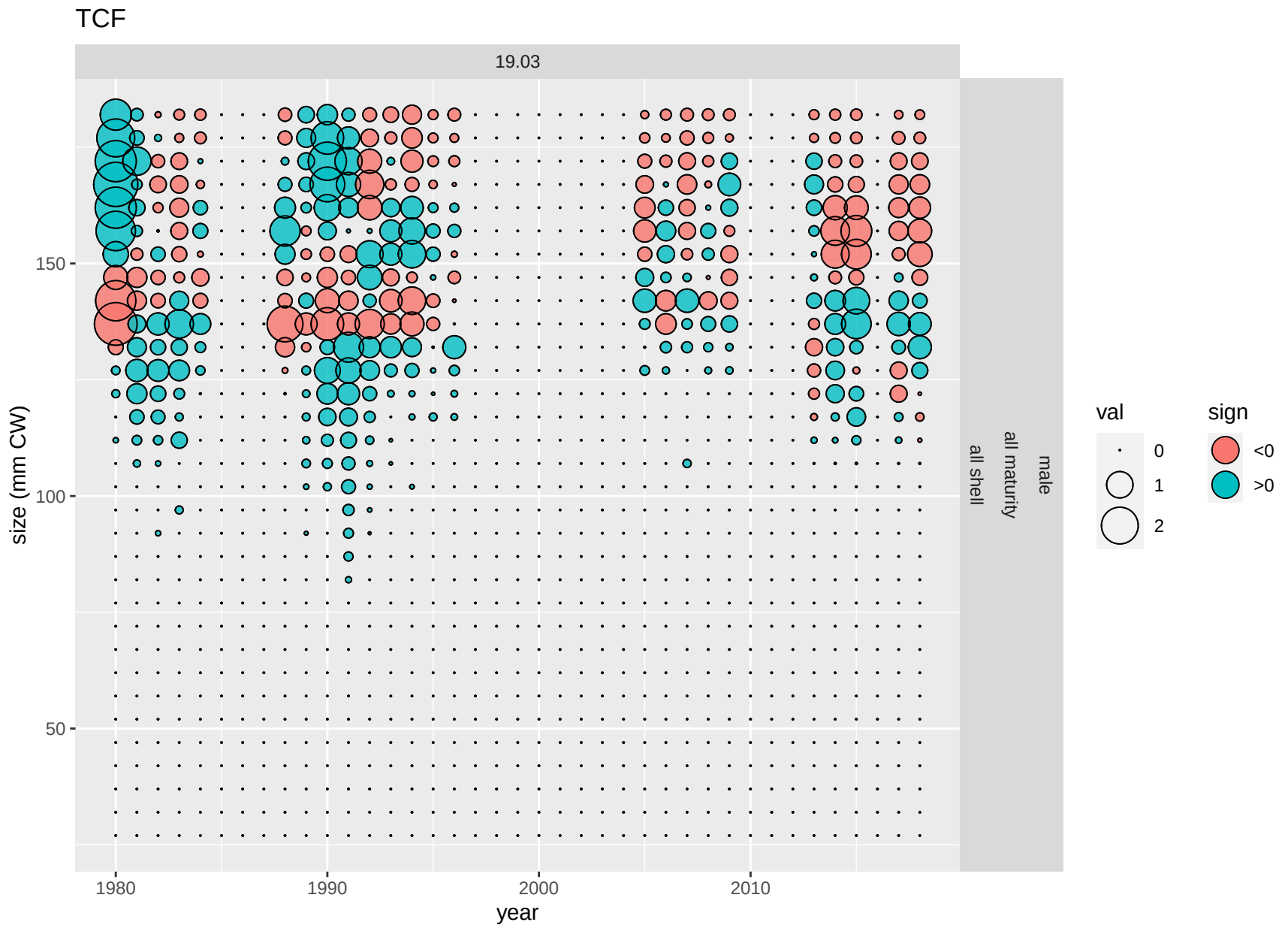

Figure 7: Pearson's residuals for male proportions-at-size from the TCF for scenario 19.03.

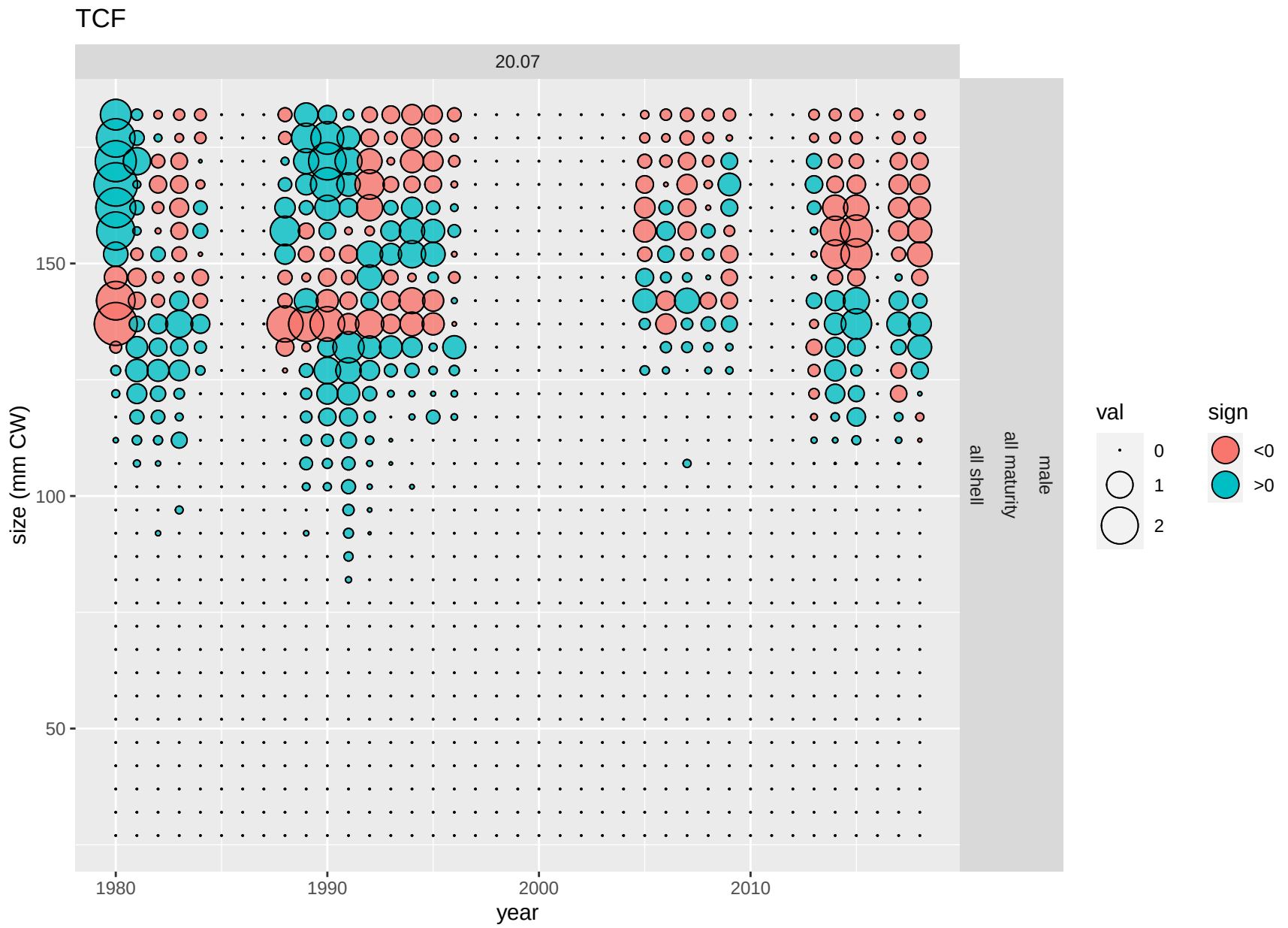

Figure 8: Pearson's residuals for male proportions-at-size from the TCF for scenario 20.07.

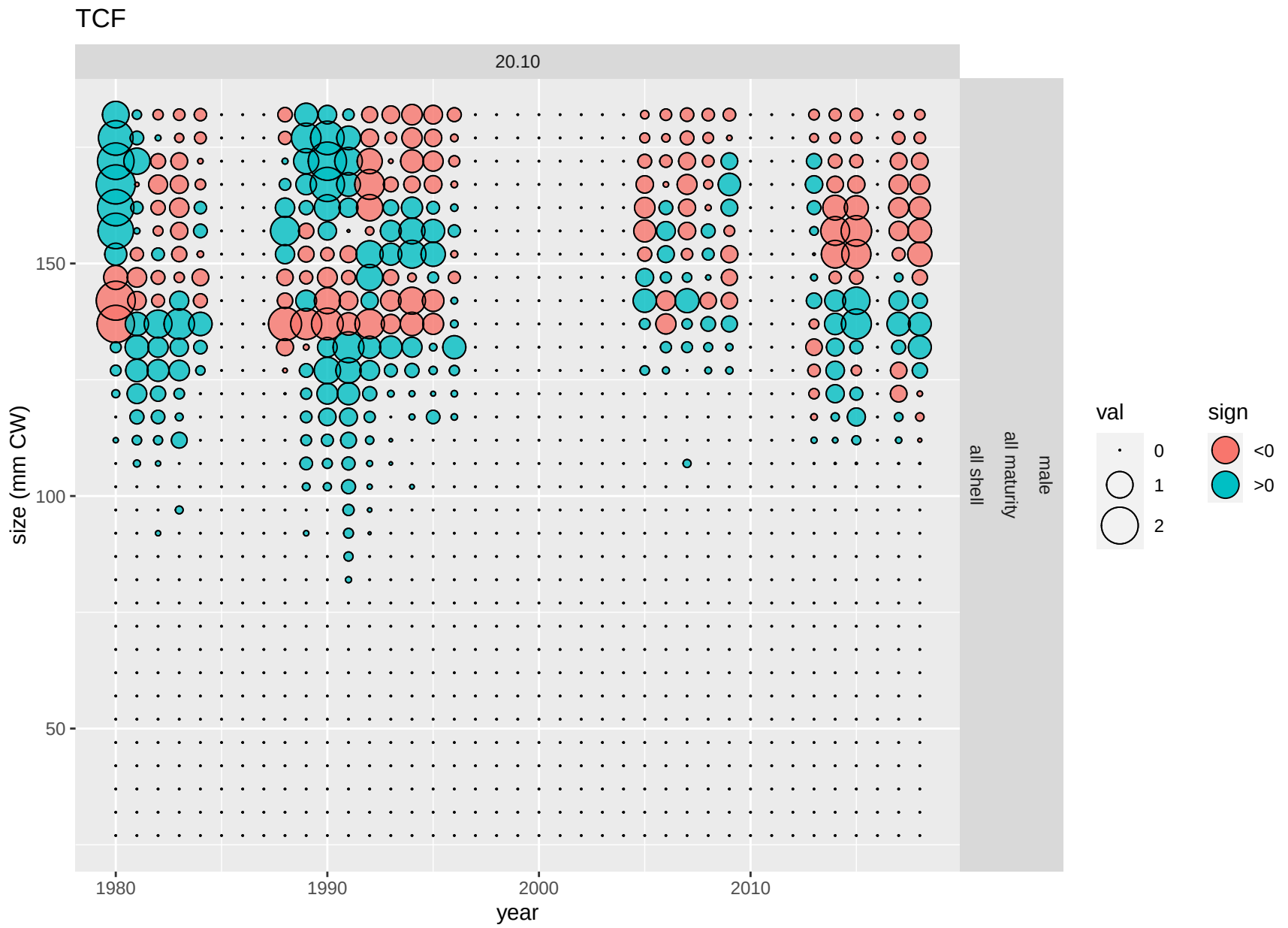

Figure 9: Pearson's residuals for male proportions-at-size from the TCF for scenario 20.10.

Effective Ns for retained catch size compositions

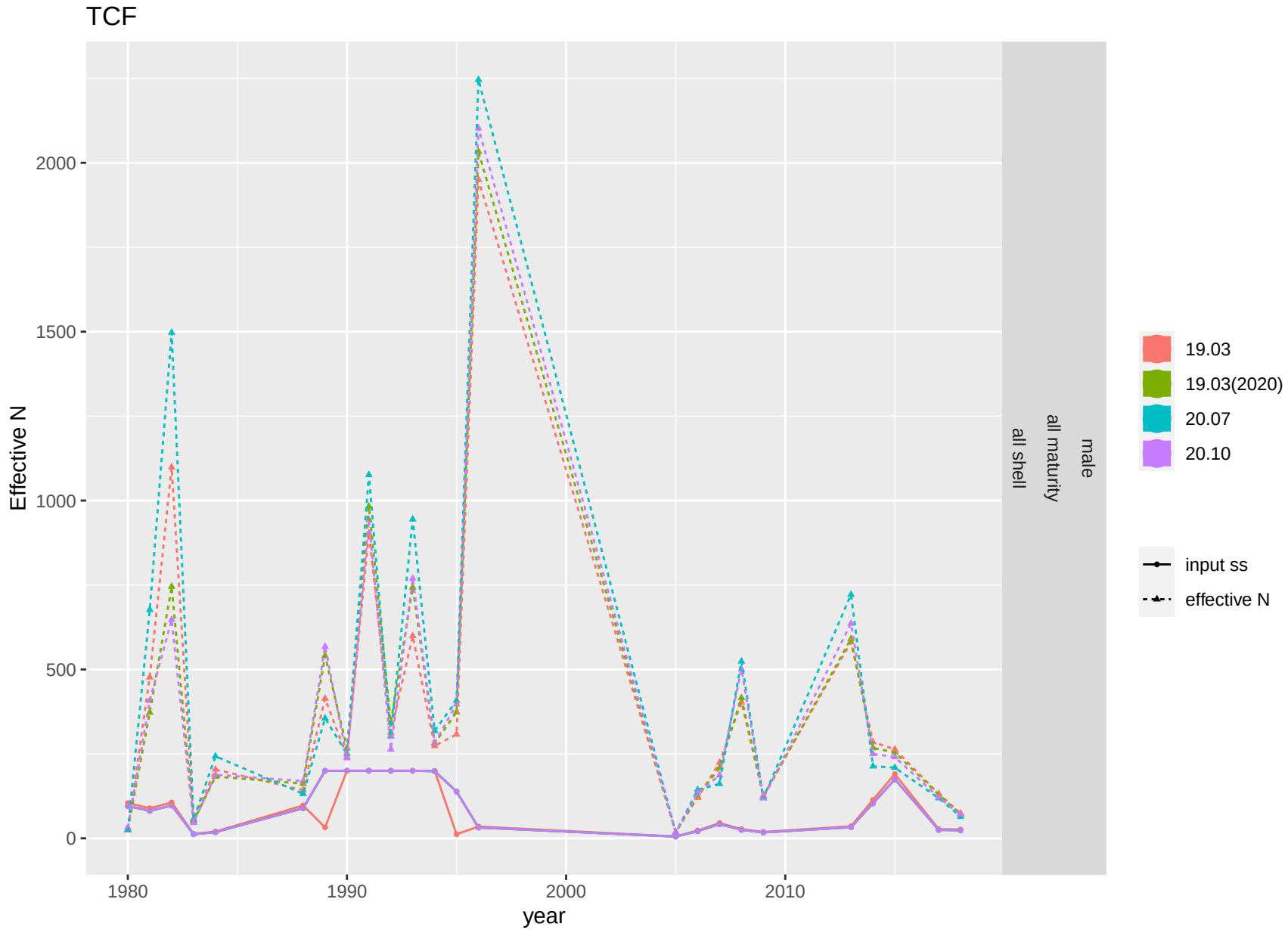

Figure 10: Input and effective sample sizes from retained catch size compositions from the TCF fishery.

Total catch size composition residuals

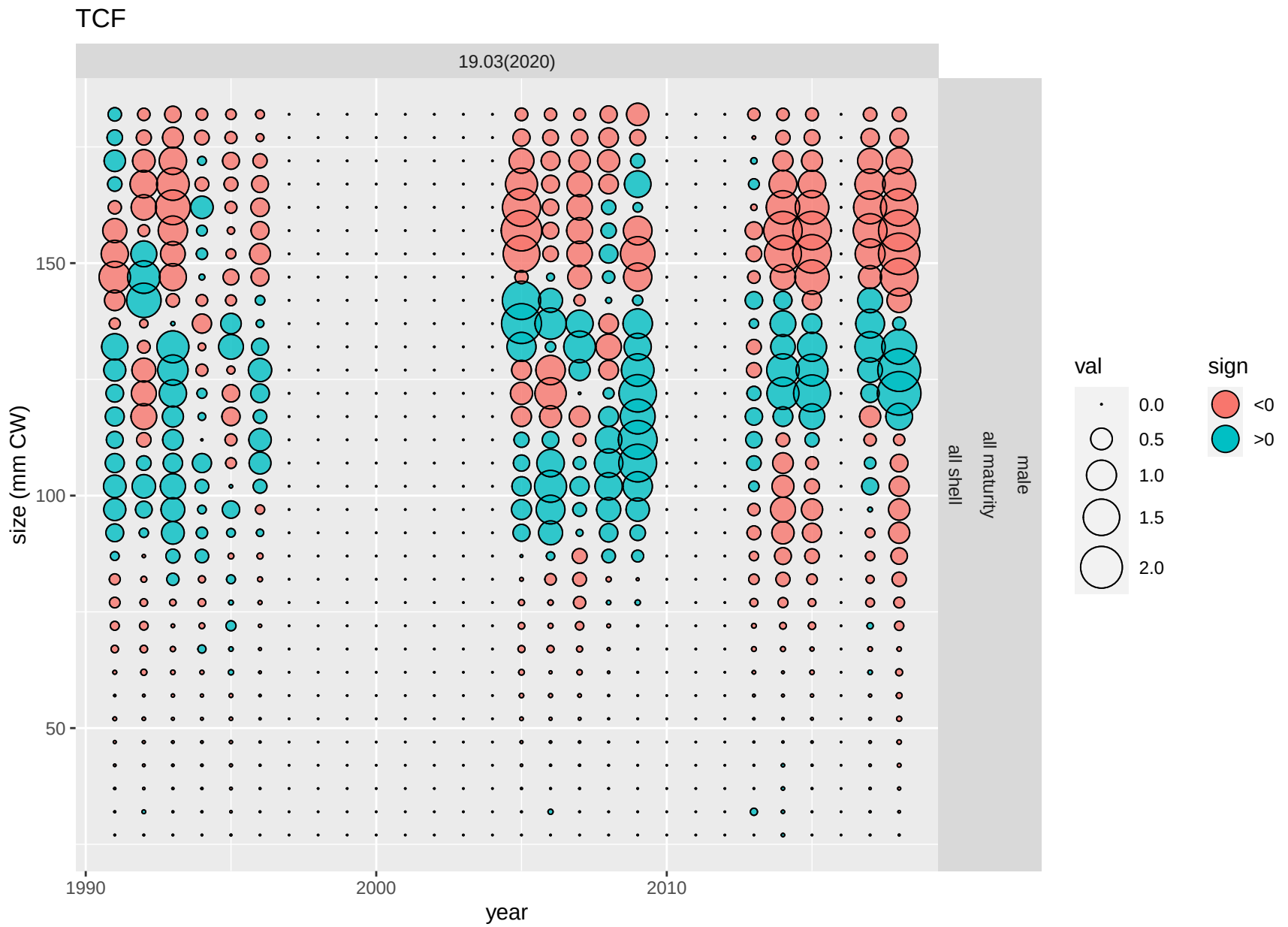

Figure 11: Pearson's residuals for male proportions-at-size from the TCF for scenario 19.03(2020).

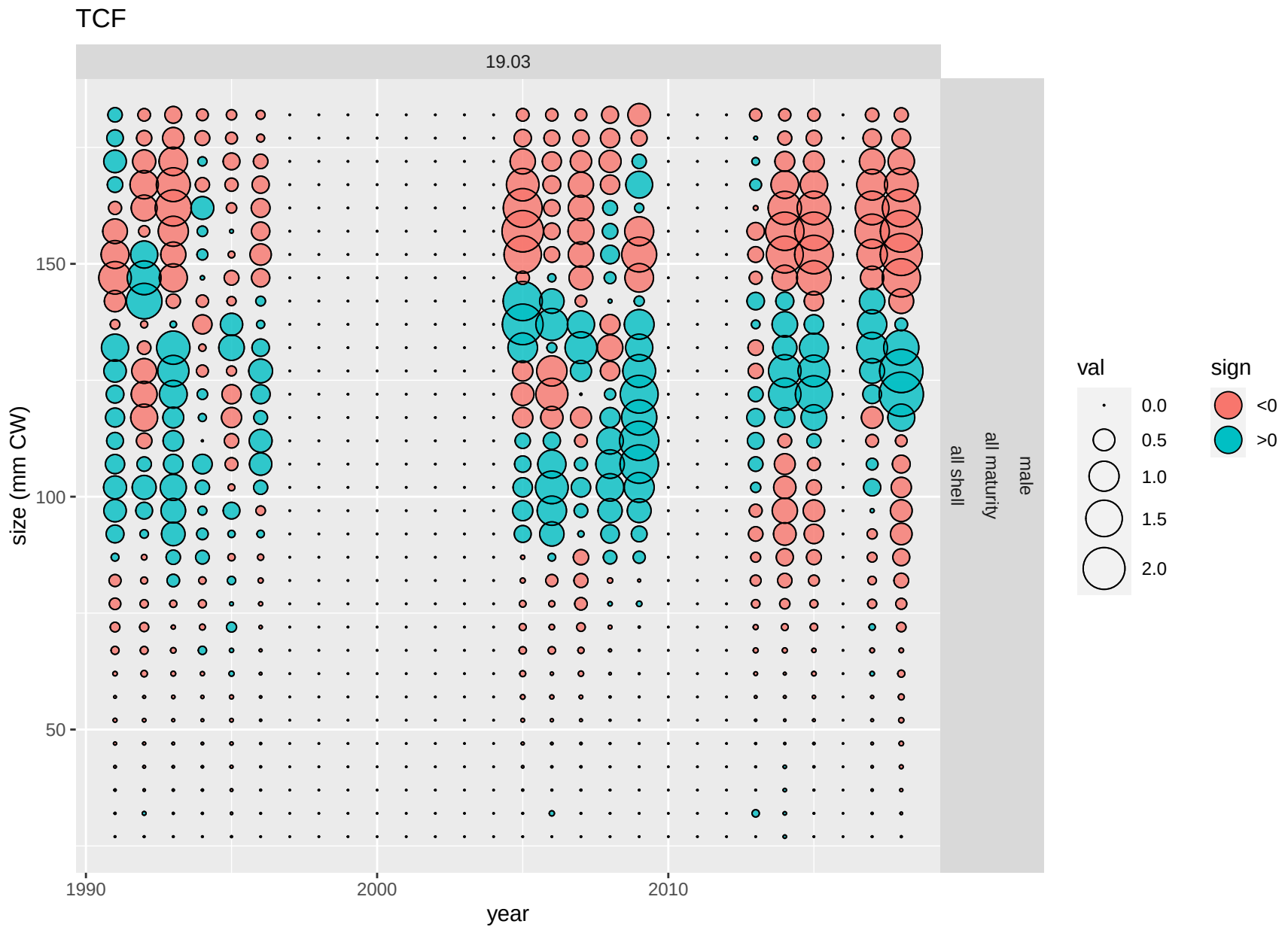

Figure 12: Pearson's residuals for male proportions-at-size from the TCF for scenario 19.03.

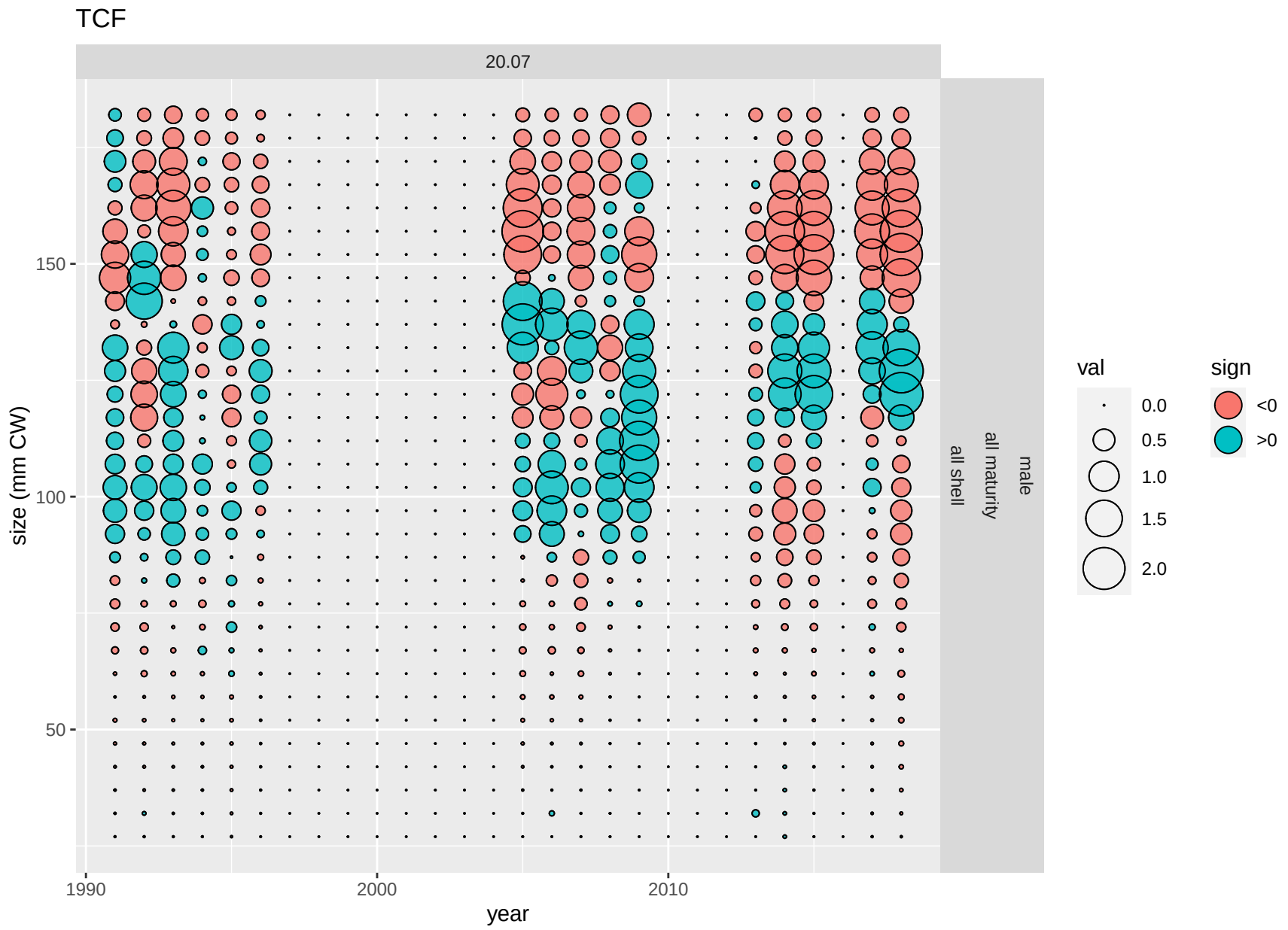

Figure 13: Pearson's residuals for male proportions-at-size from the TCF for scenario 20.07.

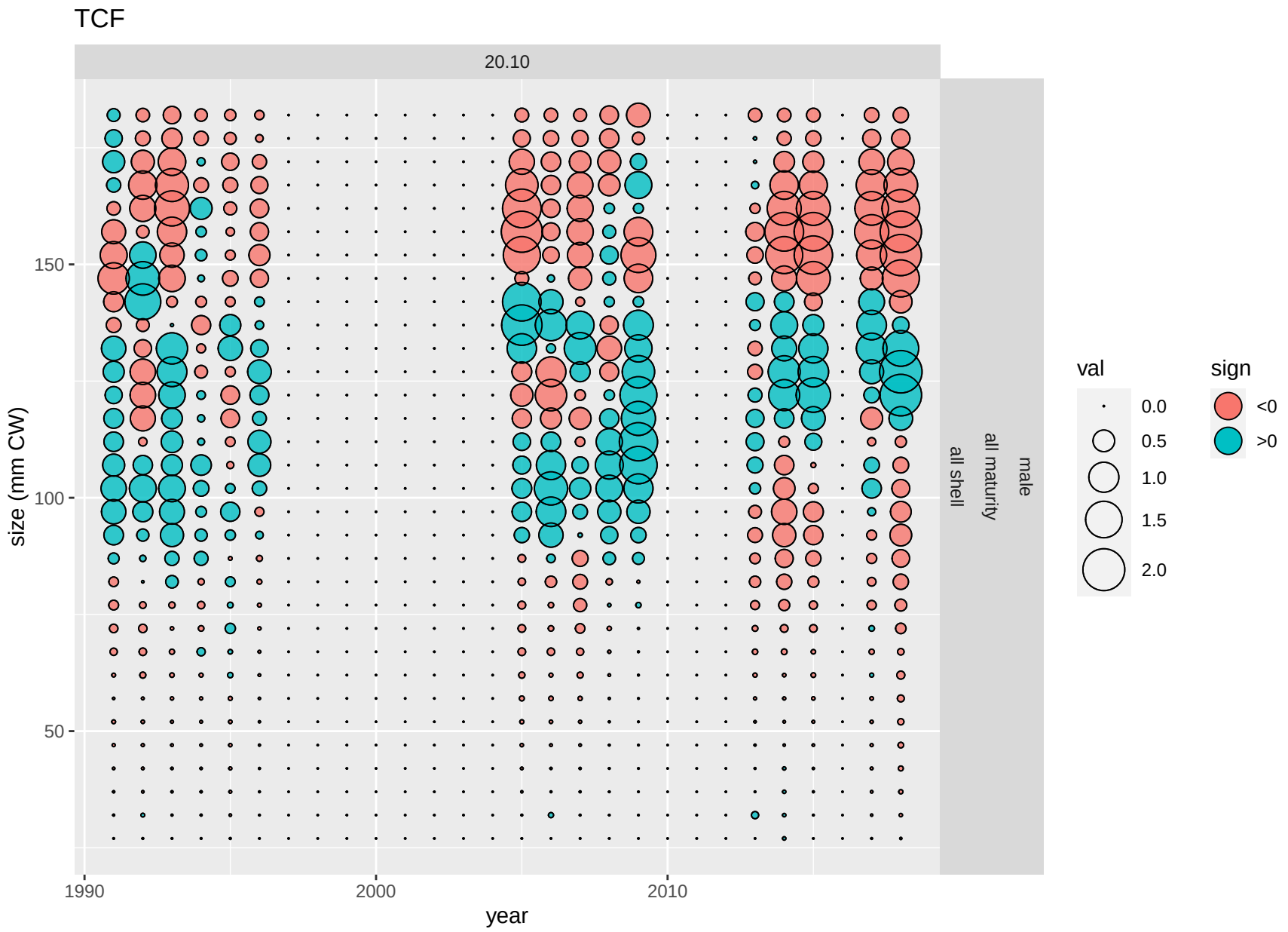

Figure 14: Pearson's residuals for male proportions-at-size from the TCF for scenario 20.10.

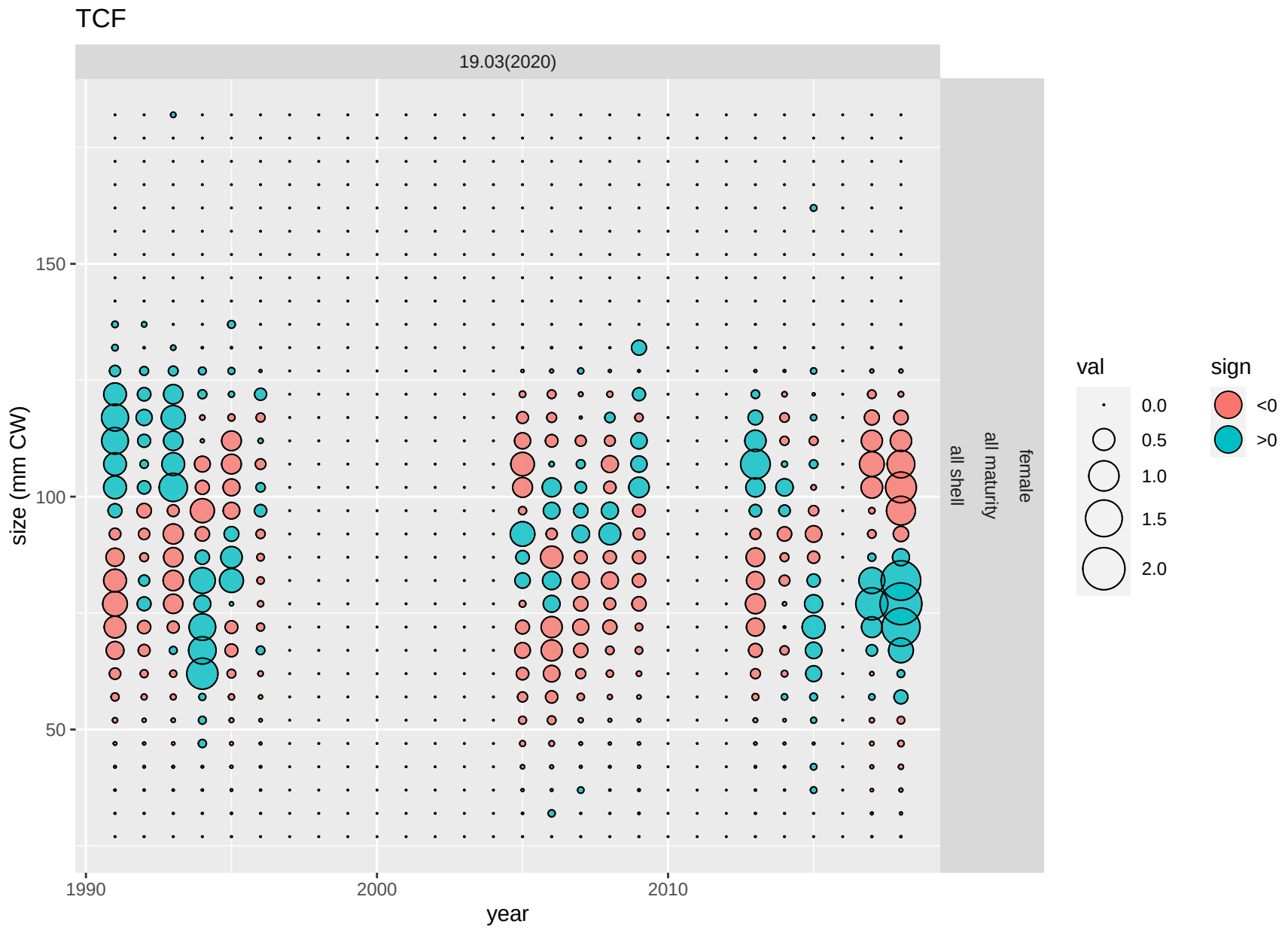

Figure 15: Pearson's residuals for female proportions-at-size from the TCF for scenario 19.03(2020).

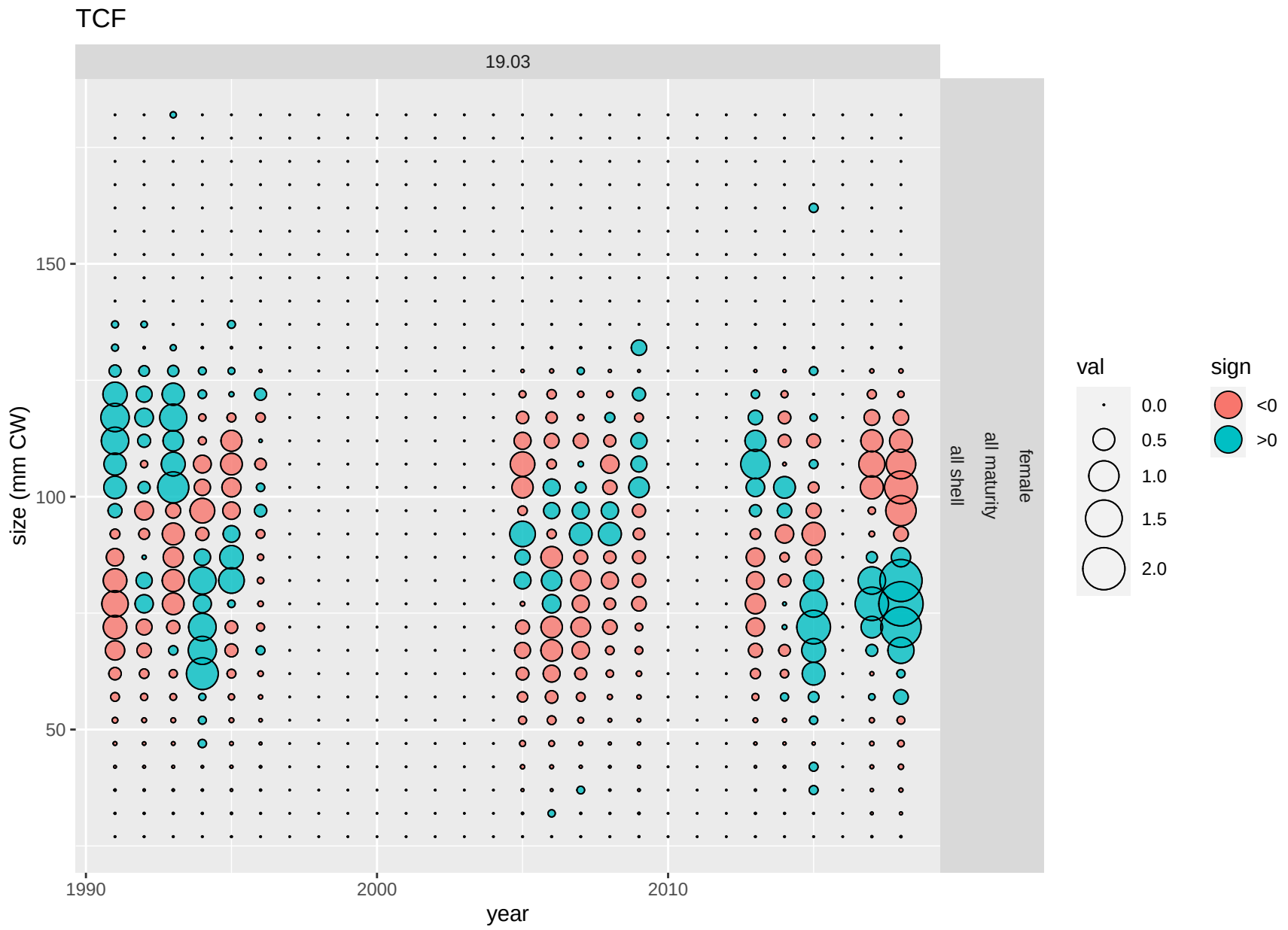

Figure 16: Pearson's residuals for female proportions-at-size from the TCF for scenario 19.03.

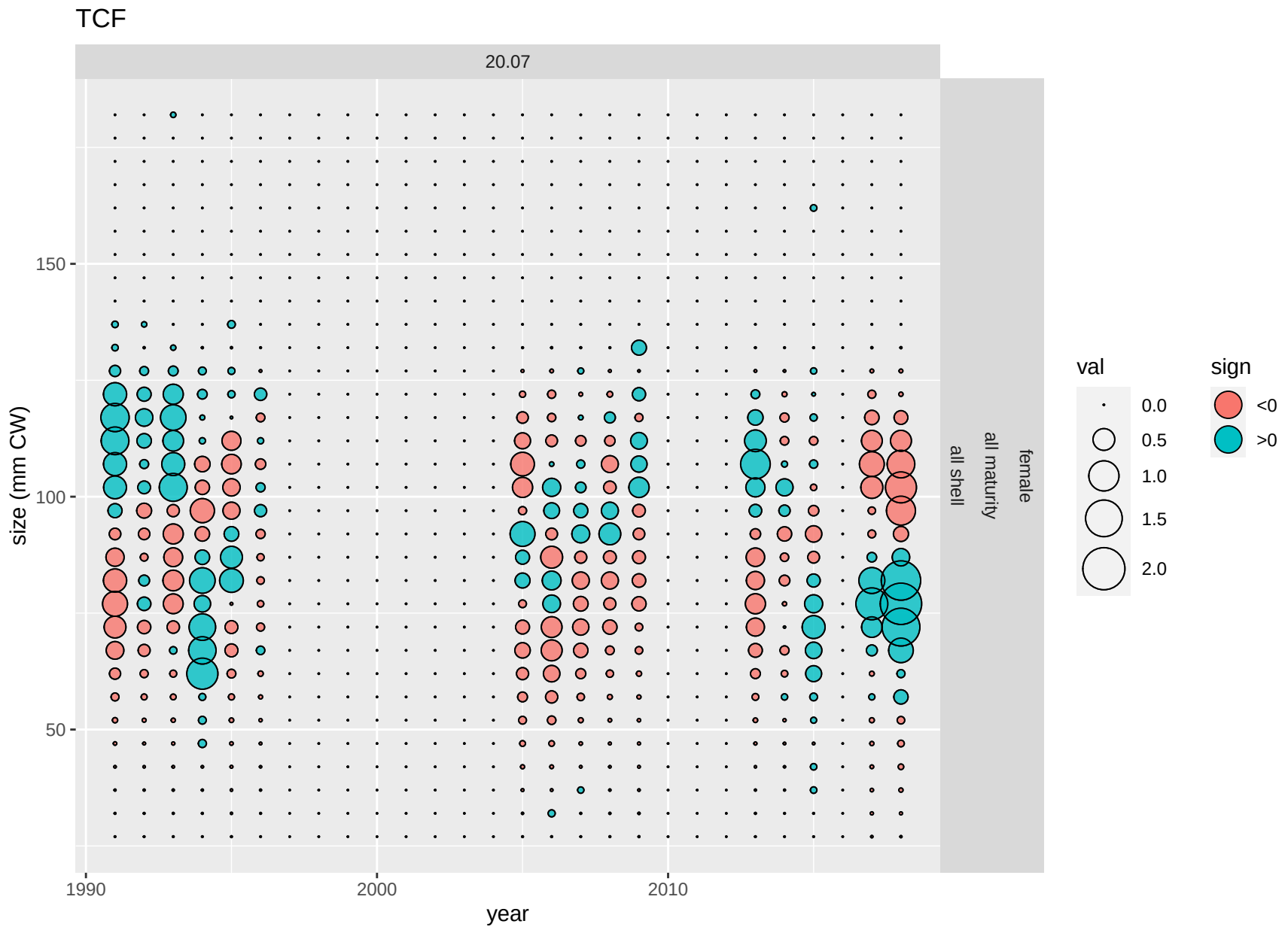

Figure 17: Pearson's residuals for female proportions-at-size from the TCF for scenario 20.07.

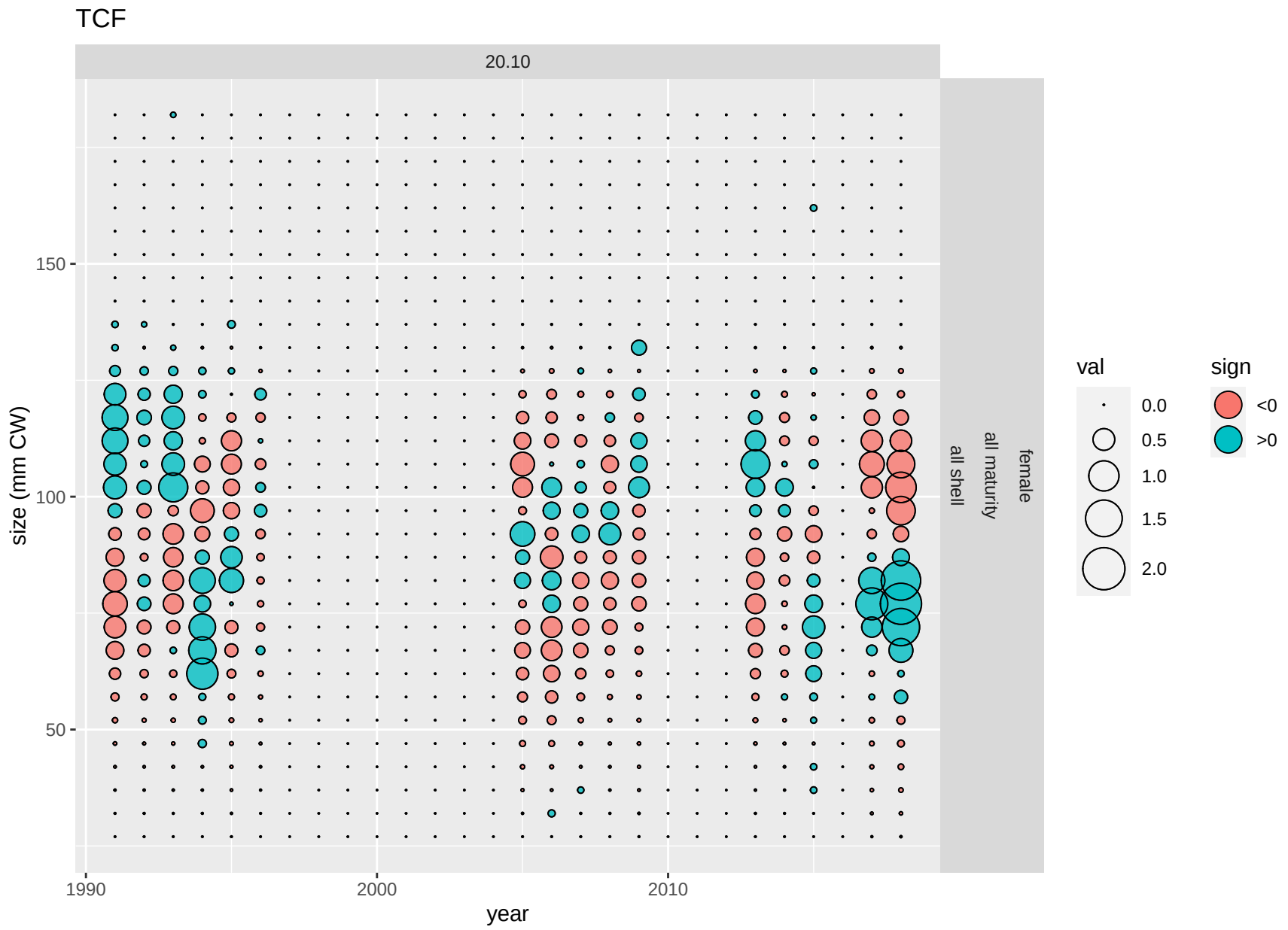

Figure 18: Pearson's residuals for female proportions-at-size from the TCF for scenario 20.10.

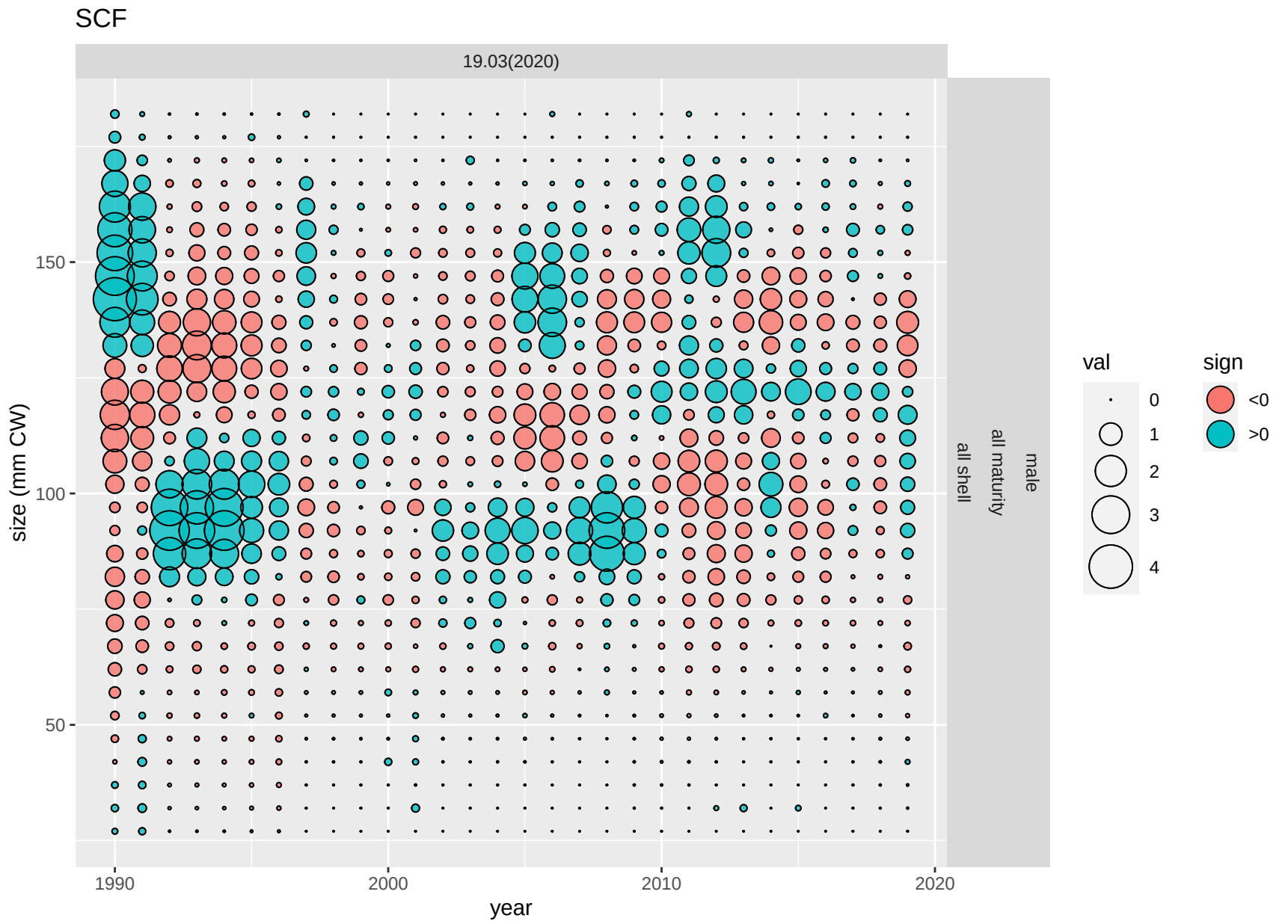

Figure 19: Pearson's residuals for male proportions-at-size from the SCF for scenario 19.03(2020).

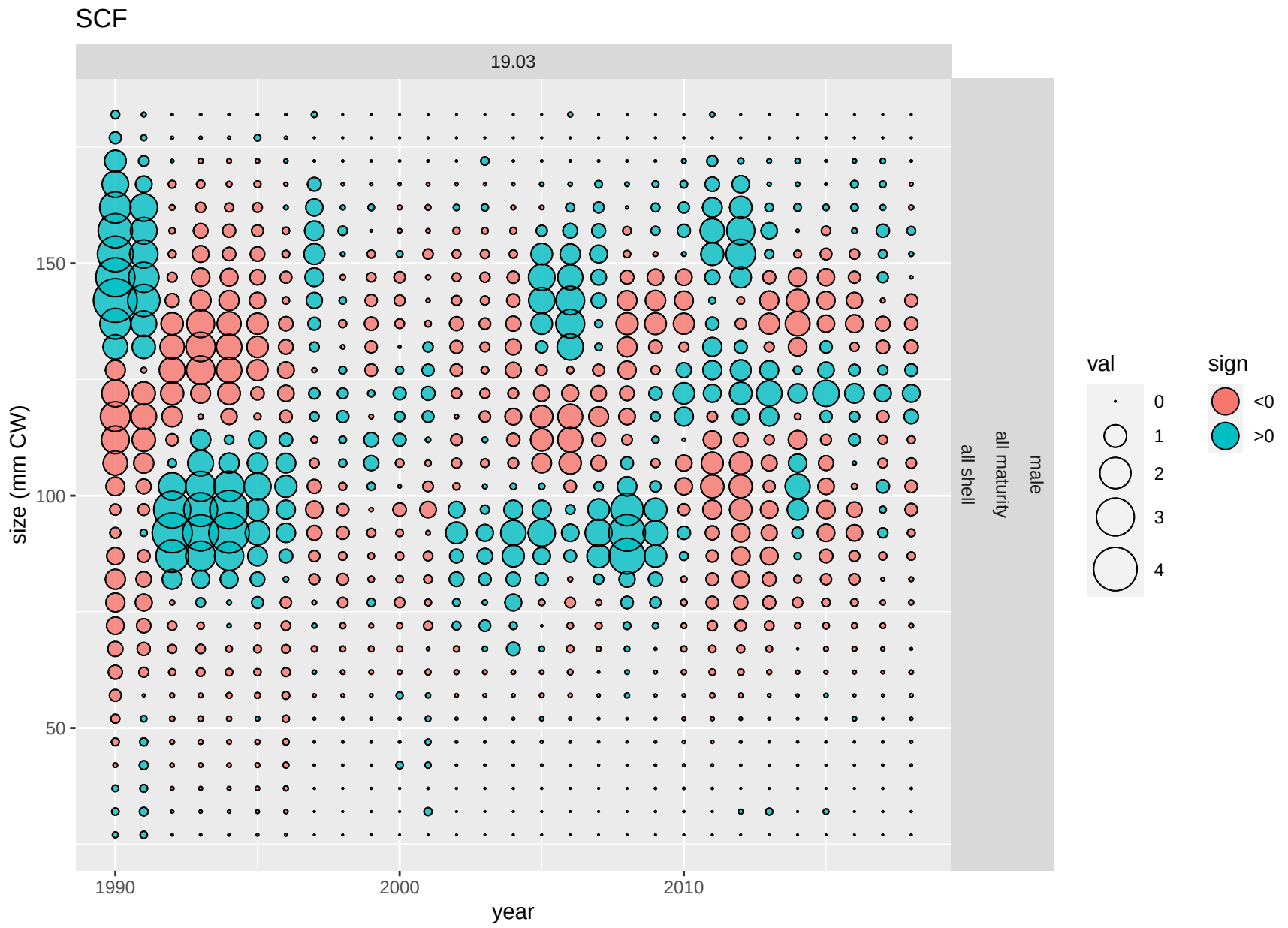

Figure 20: Pearson's residuals for male proportions-at-size from the SCF for scenario 19.03.

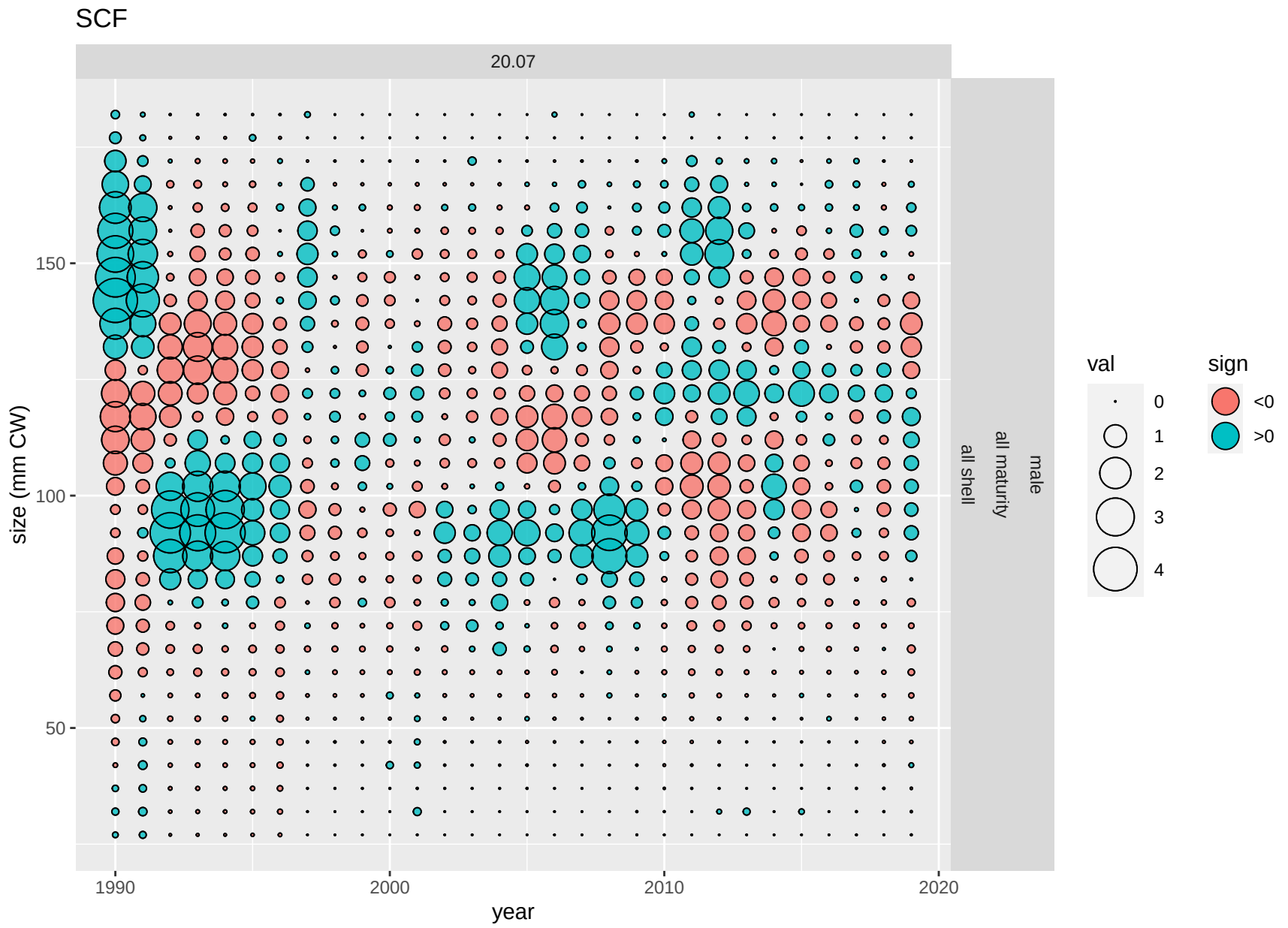

Figure 21: Pearson's residuals for male proportions-at-size from the SCF for scenario 20.07.

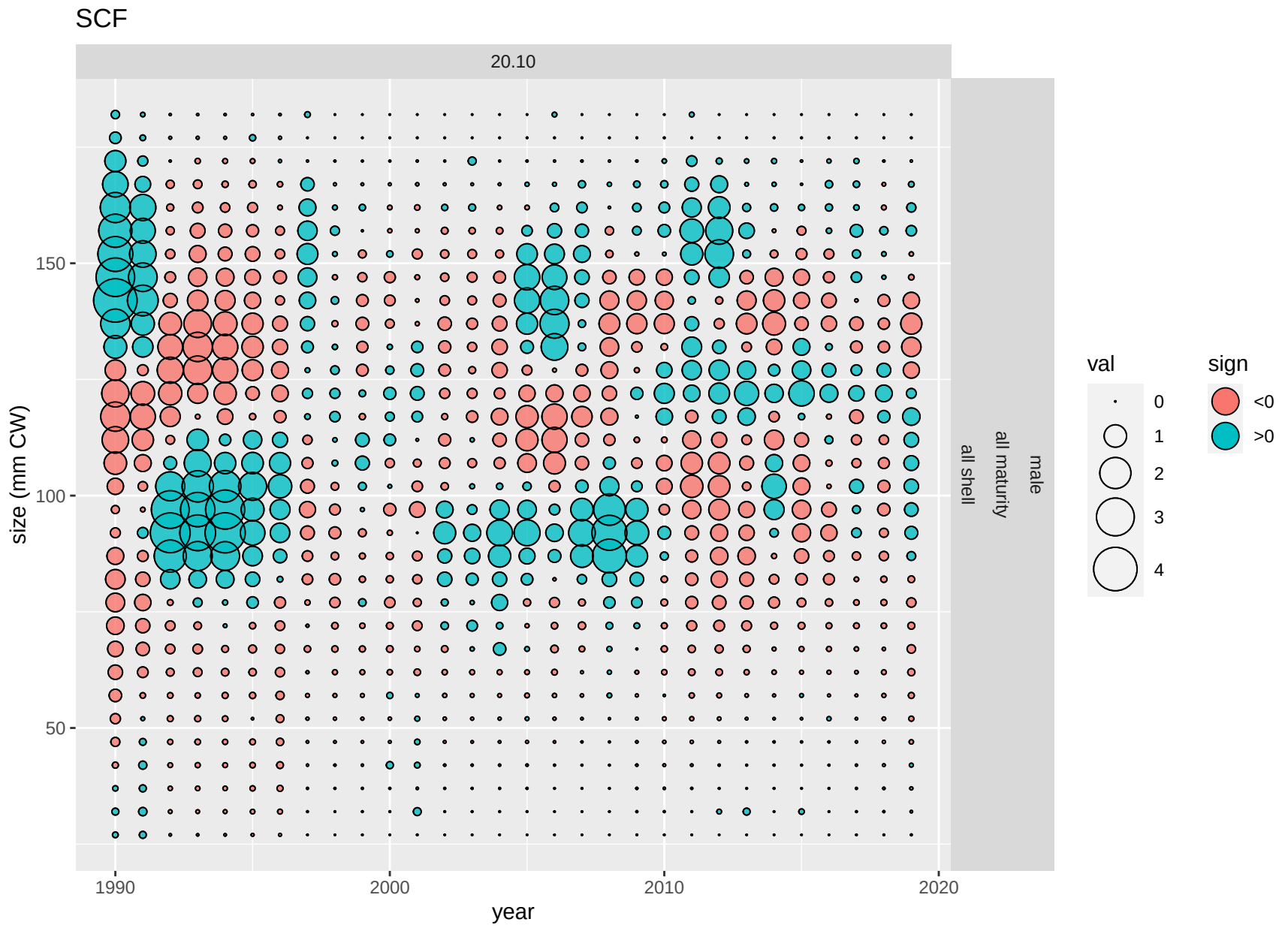

Figure 22: Pearson's residuals for male proportions-at-size from the SCF for scenario 20.10.

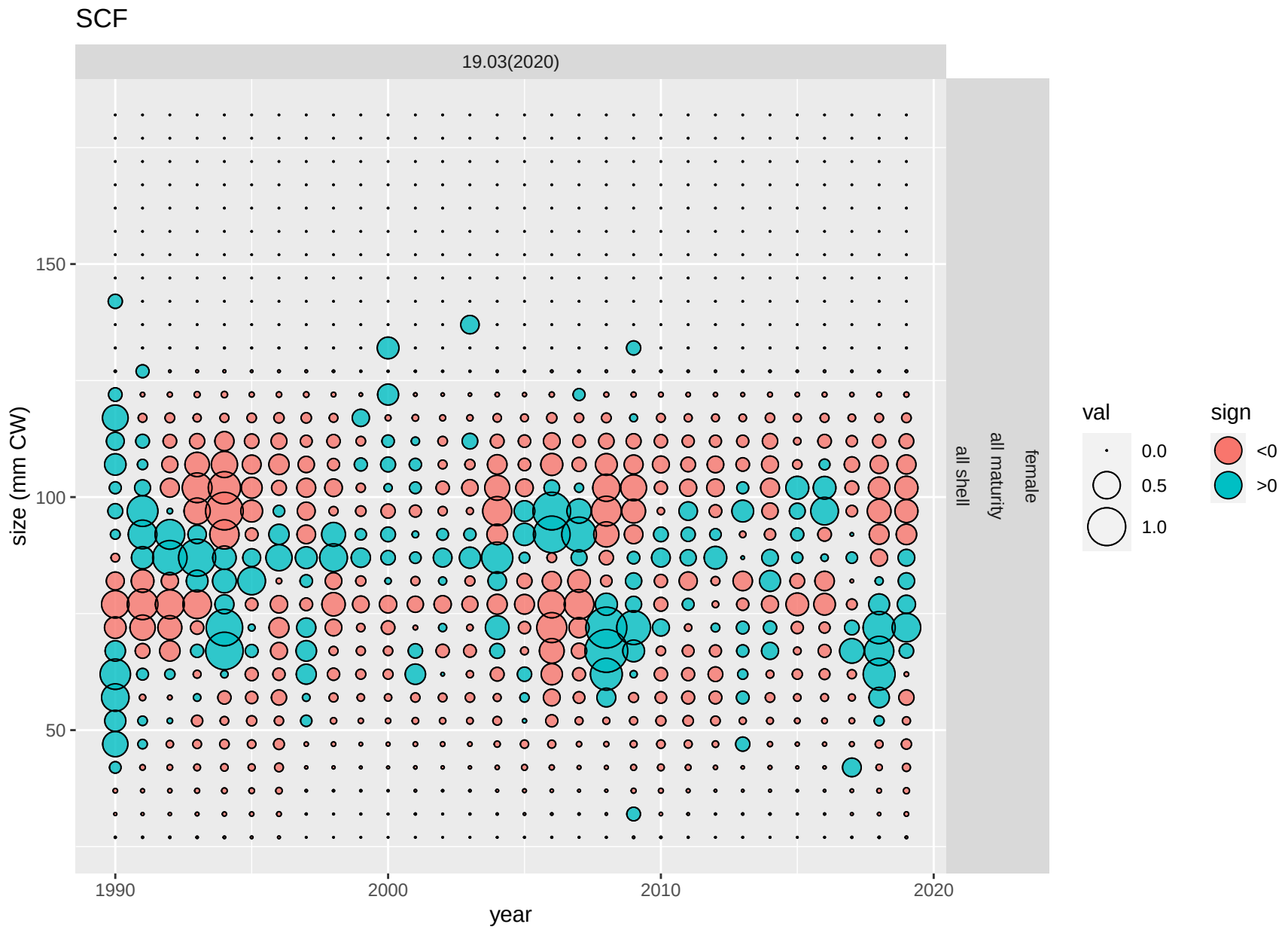

Figure 23: Pearson's residuals for female proportions-at-size from the SCF for scenario 19.03(2020).

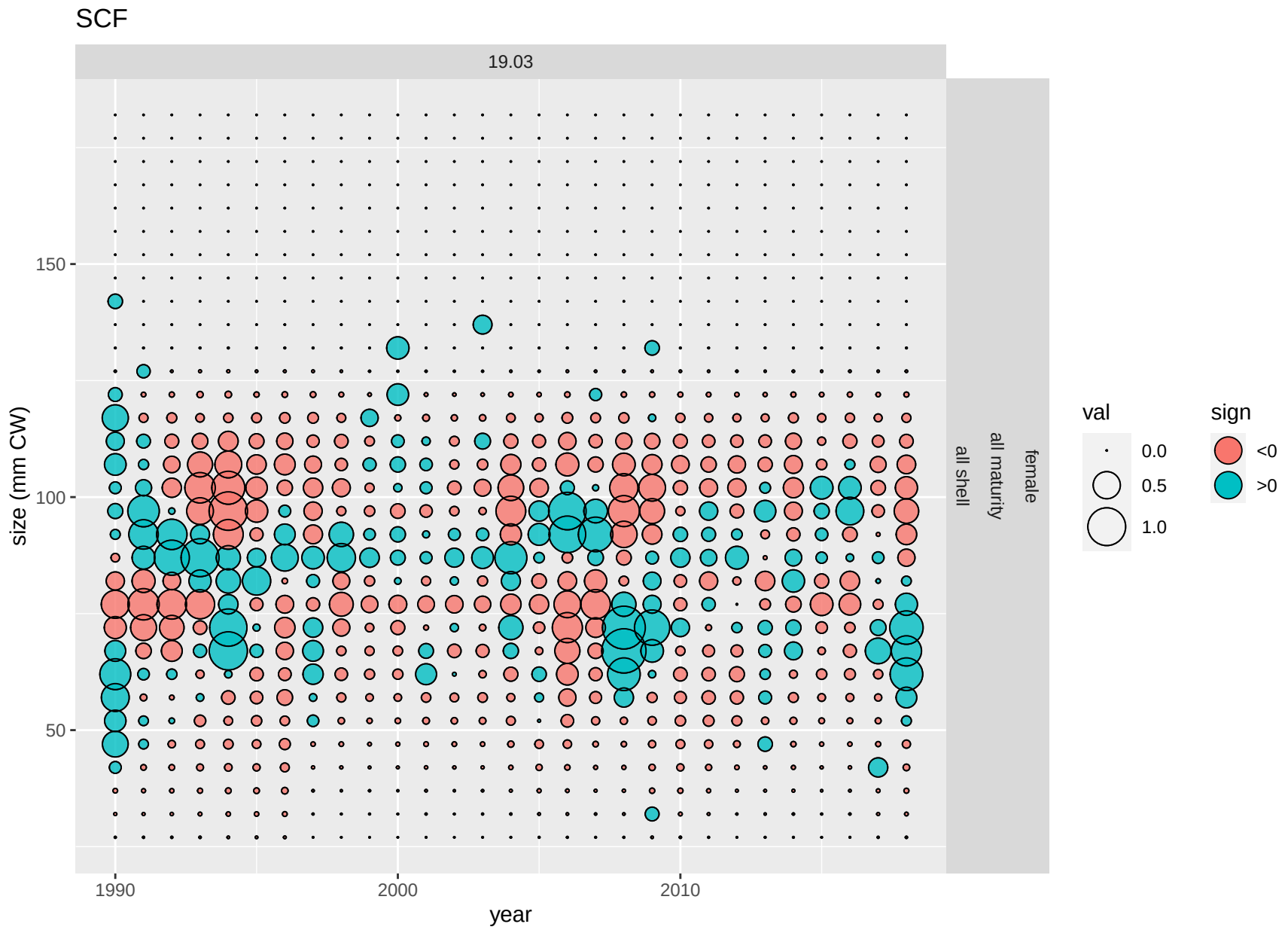

Figure 24: Pearson's residuals for female proportions-at-size from the SCF for scenario 19.03.

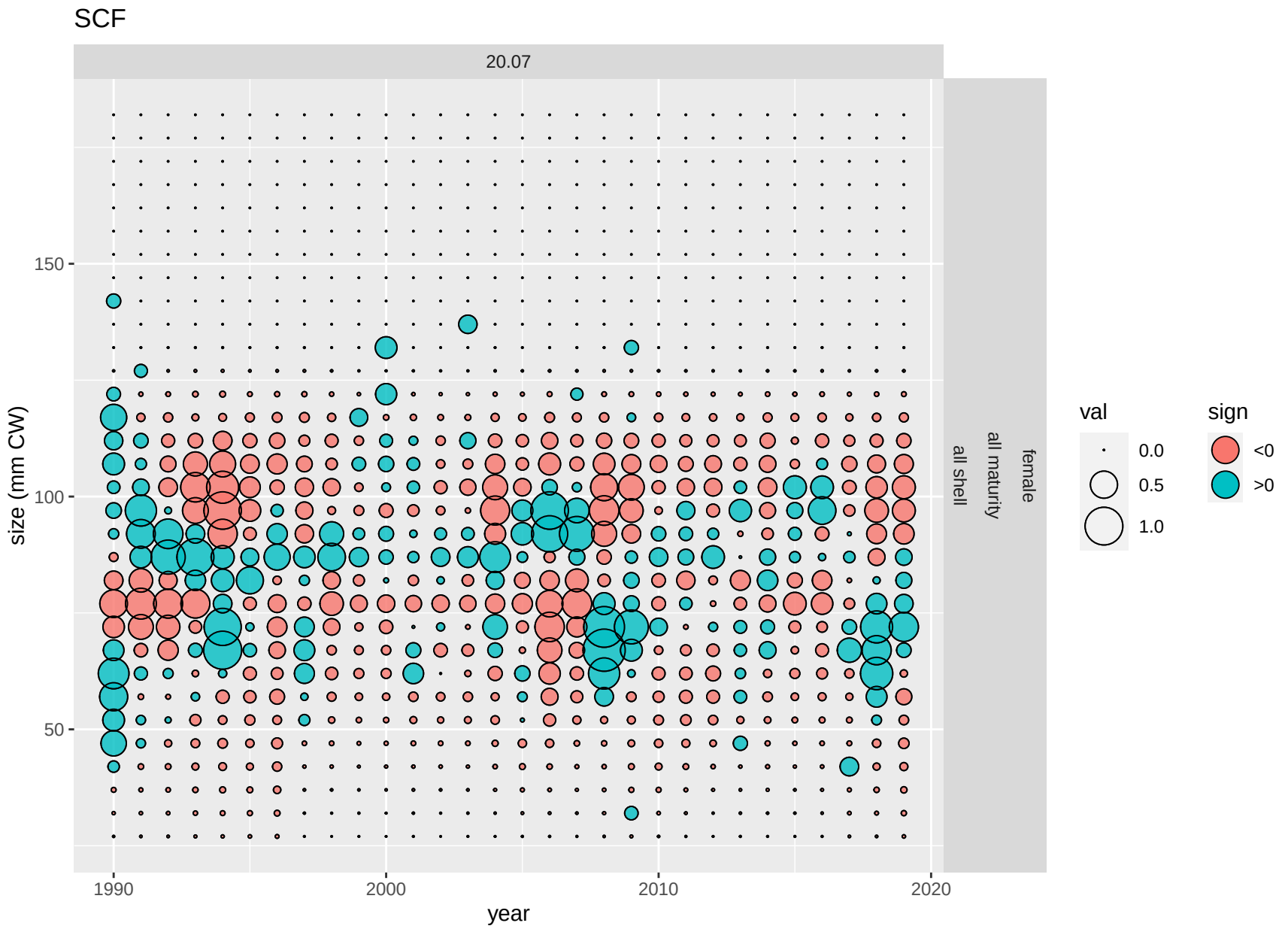

Figure 25: Pearson's residuals for female proportions-at-size from the SCF for scenario 20.07.

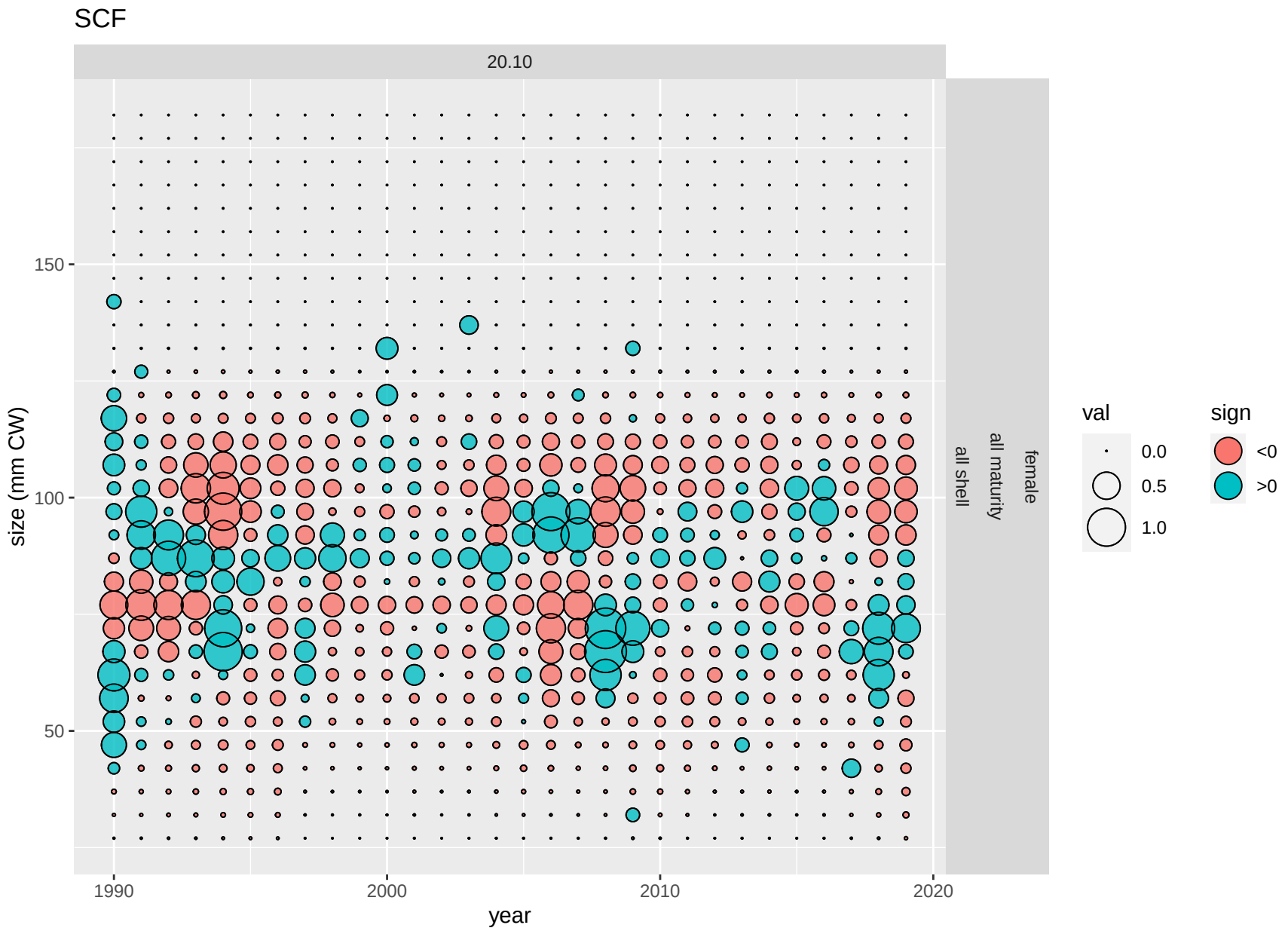

Figure 26: Pearson's residuals for female proportions-at-size from the SCF for scenario 20.10.

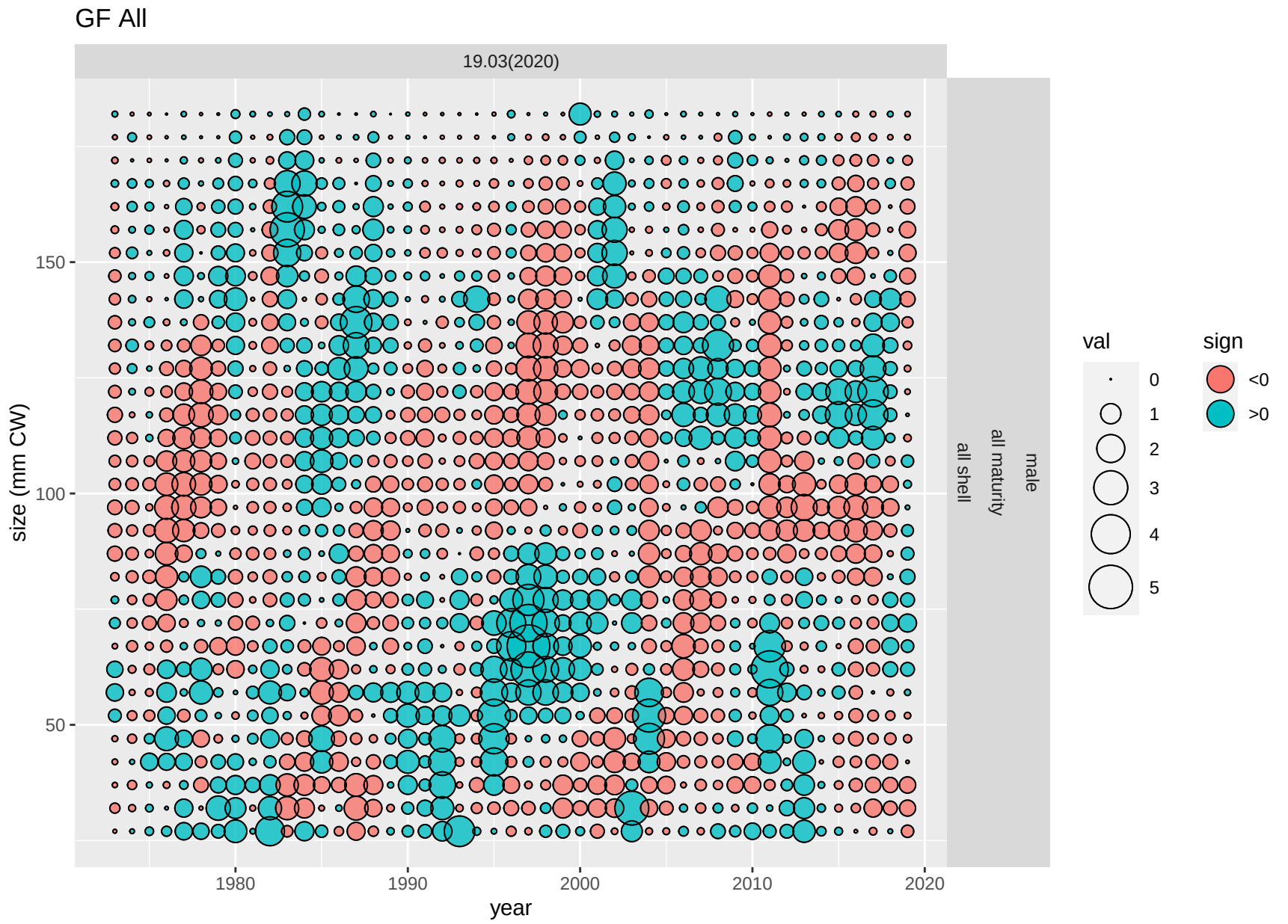

Figure 27: Pearson's residuals for male proportions-at-size from the GF All for scenario 19.03(2020).

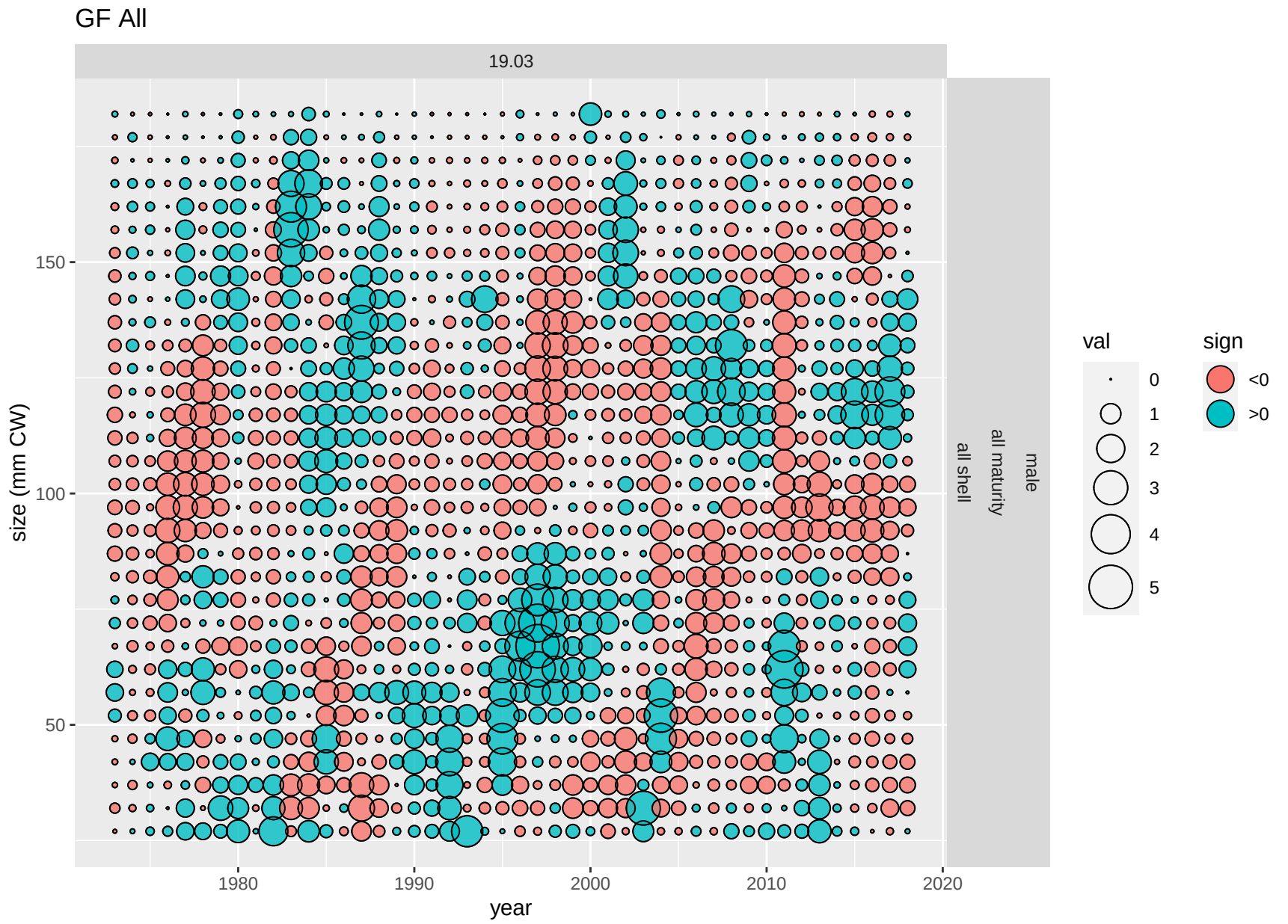

Figure 28: Pearson's residuals for male proportions-at-size from the GF All for scenario 19.03.

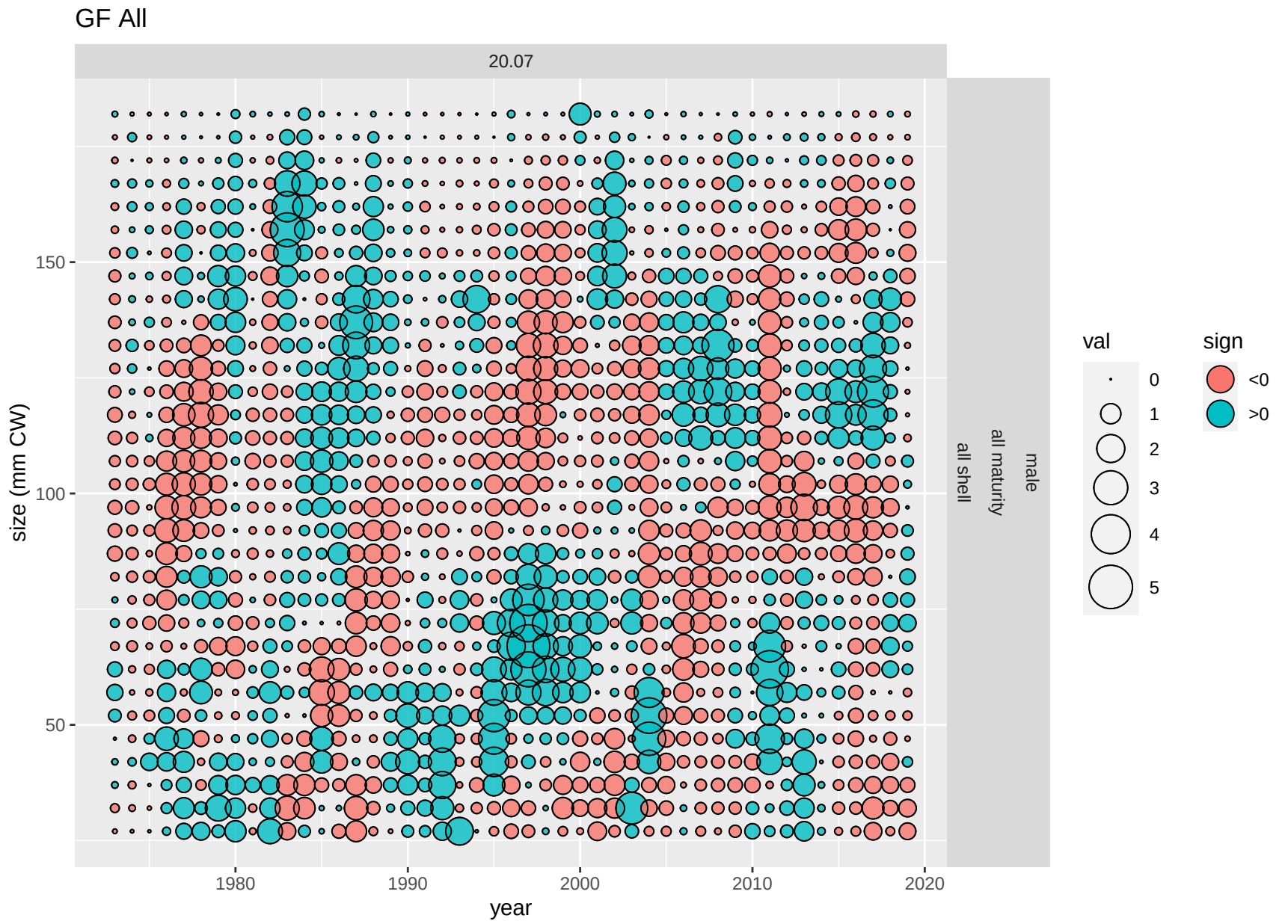

Figure 29: Pearson's residuals for male proportions-at-size from the GF All for scenario 20.07.

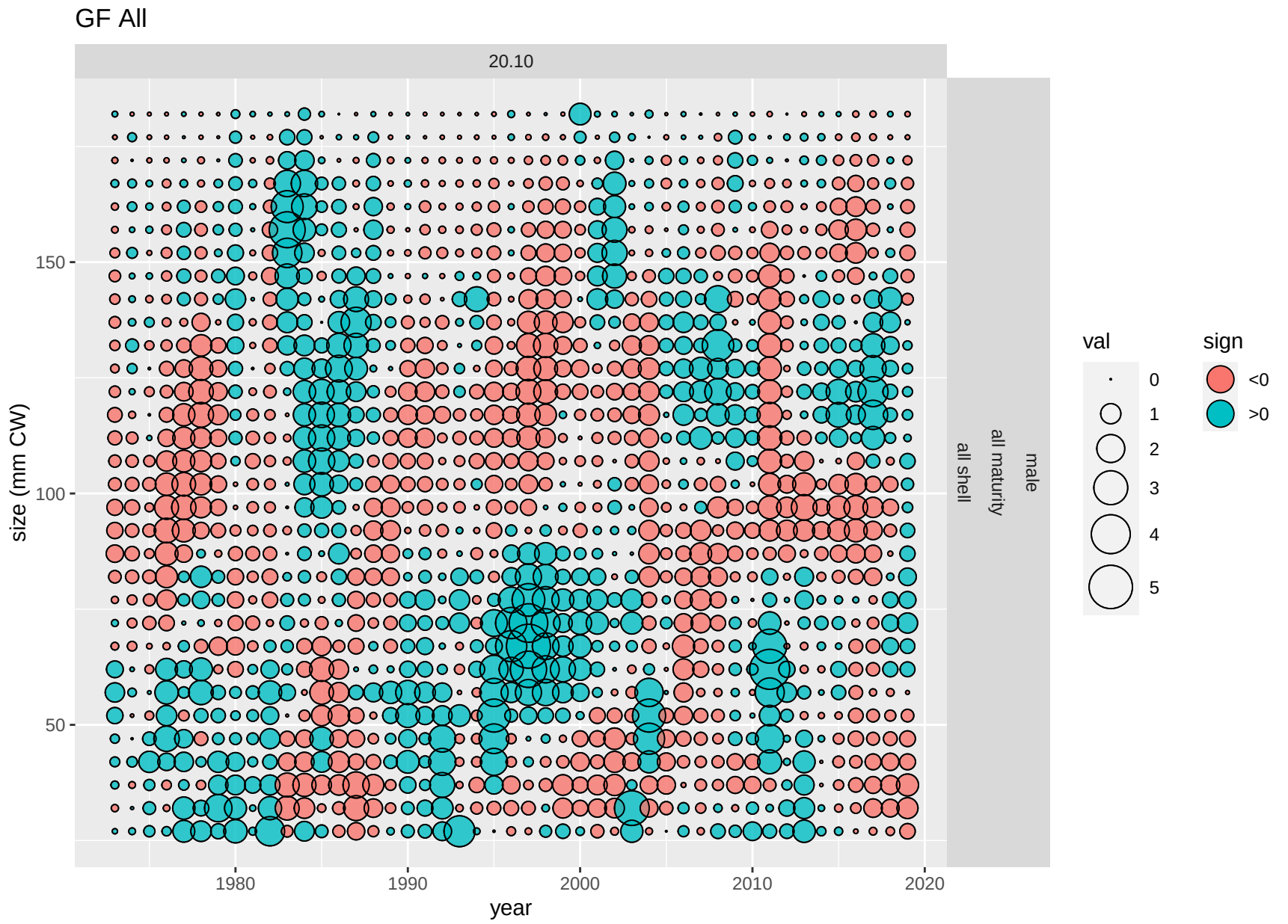

Figure 30: Pearson's residuals for male proportions-at-size from the GF All for scenario 20.10.

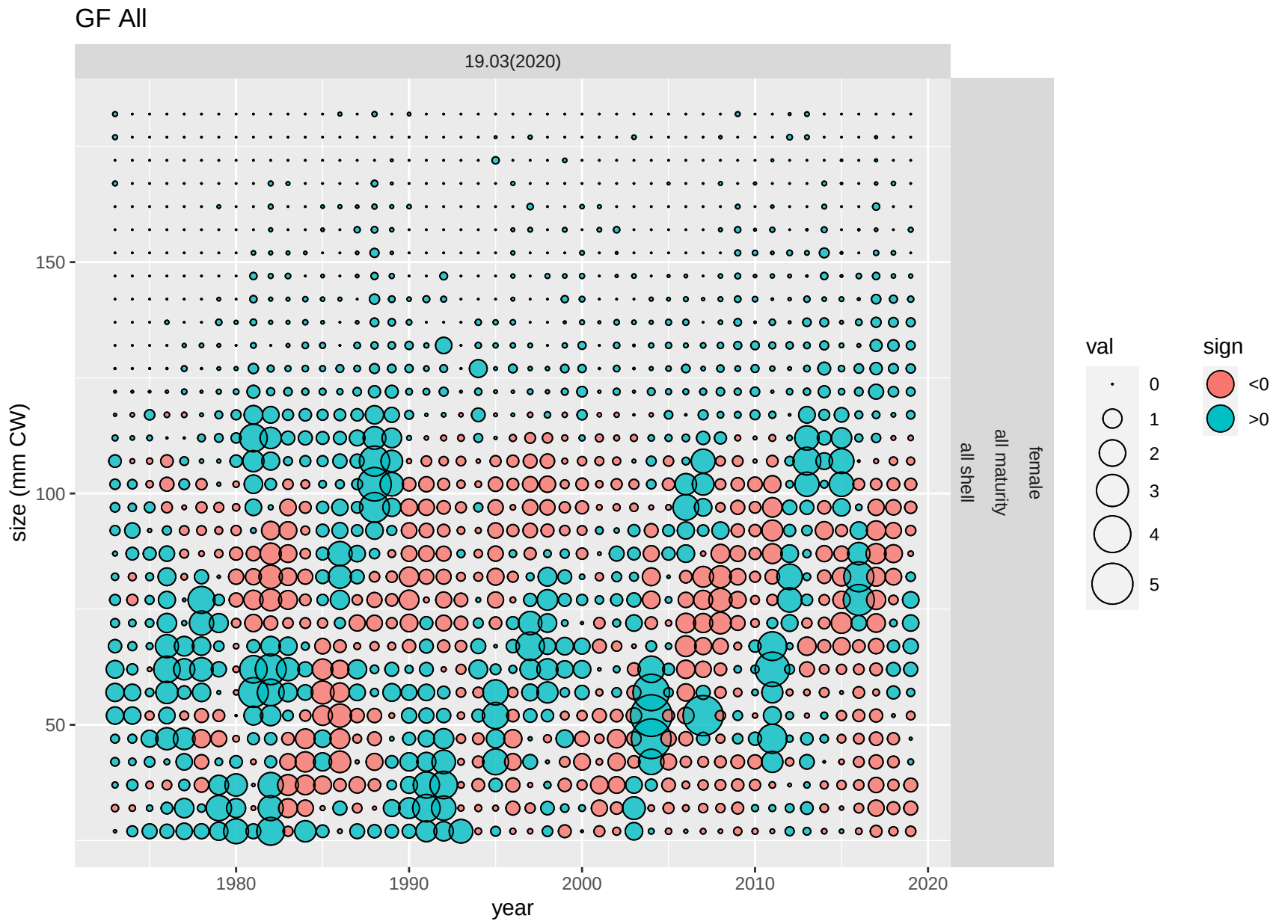

Figure 31: Pearson's residuals for female proportions-at-size from the GF All for scenario 19.03(2020).

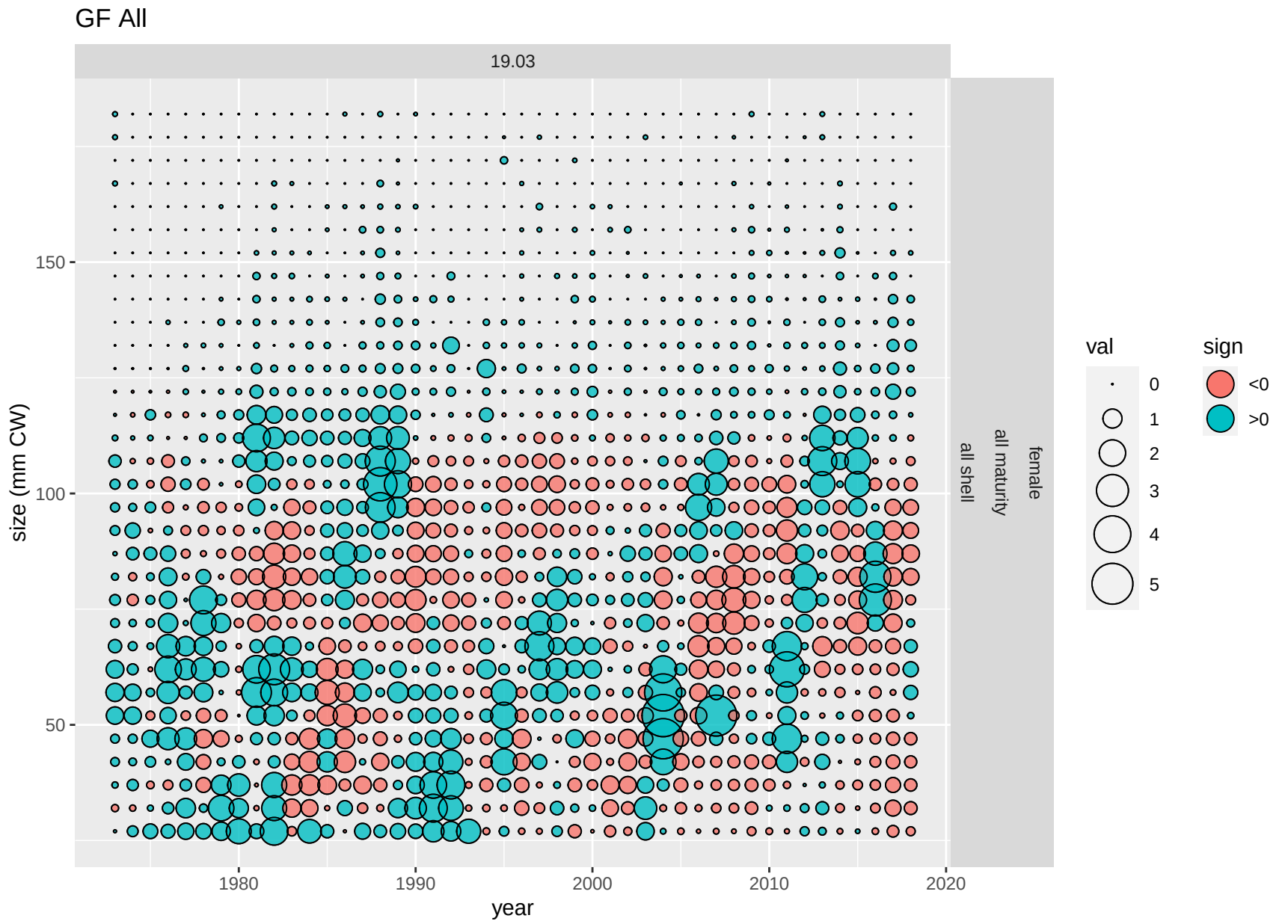

Figure 32: Pearson's residuals for female proportions-at-size from the GF All for scenario 19.03.

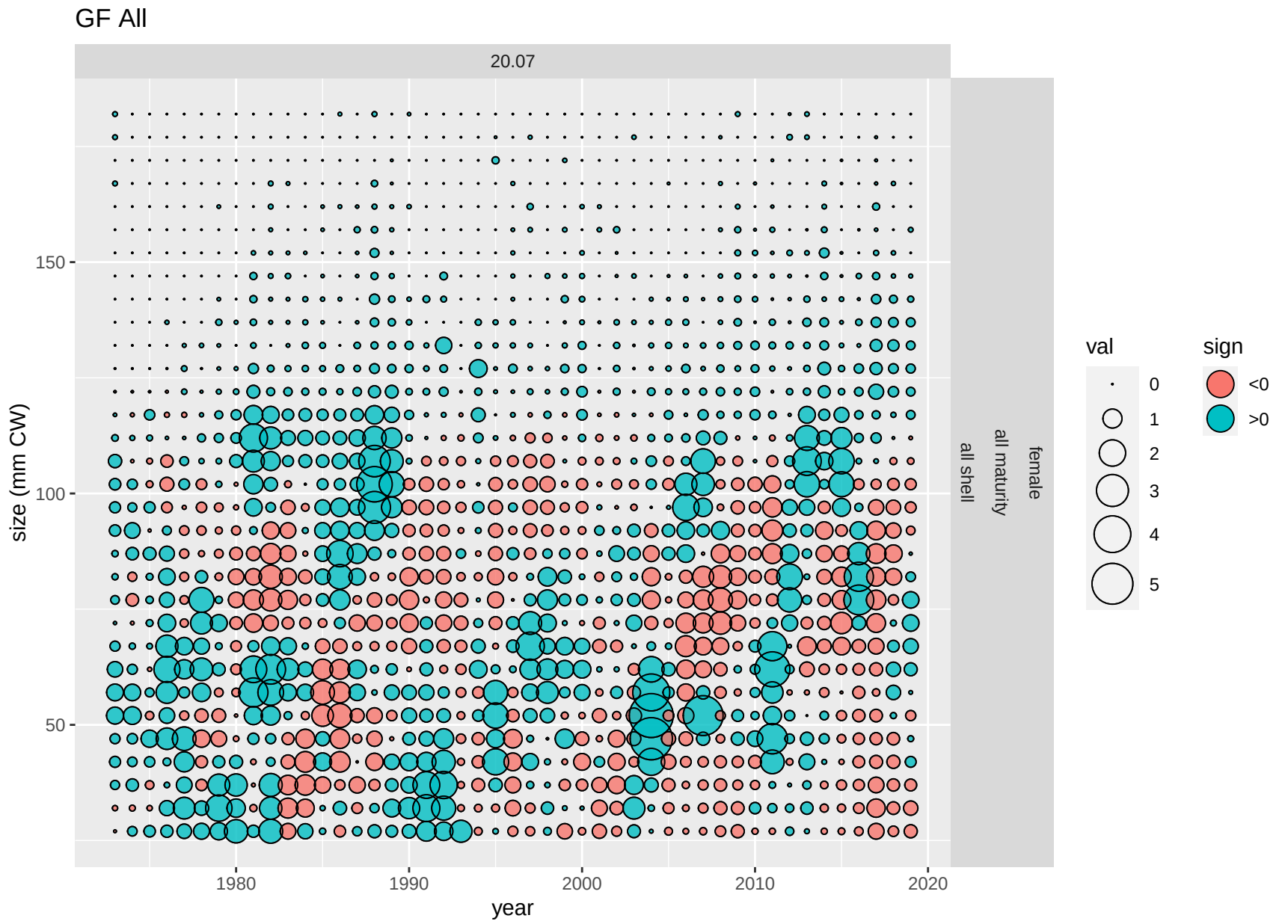

Figure 33: Pearson's residuals for female proportions-at-size from the GF All for scenario 20.07.

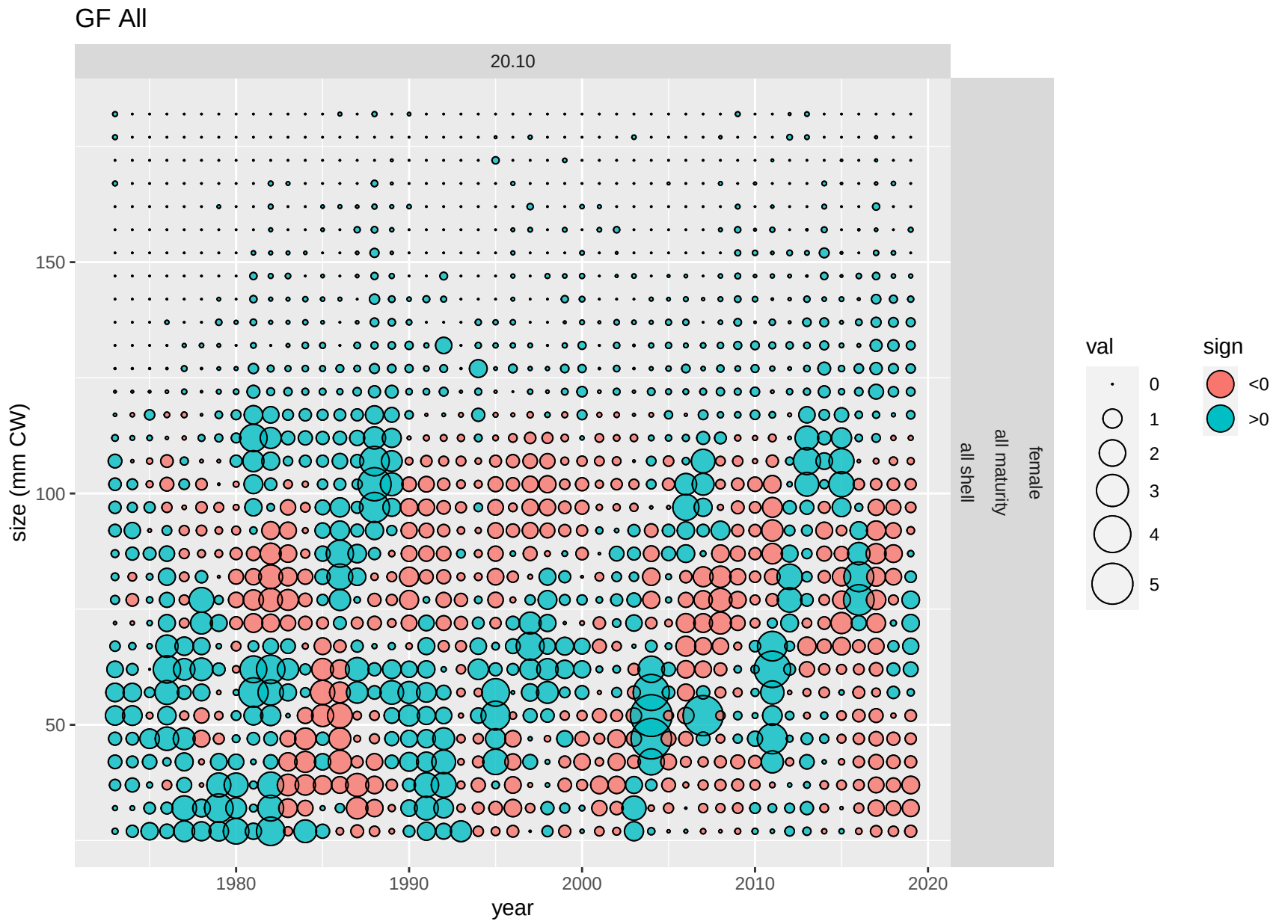

Figure 34: Pearson's residuals for female proportions-at-size from the GF All for scenario 20.10.

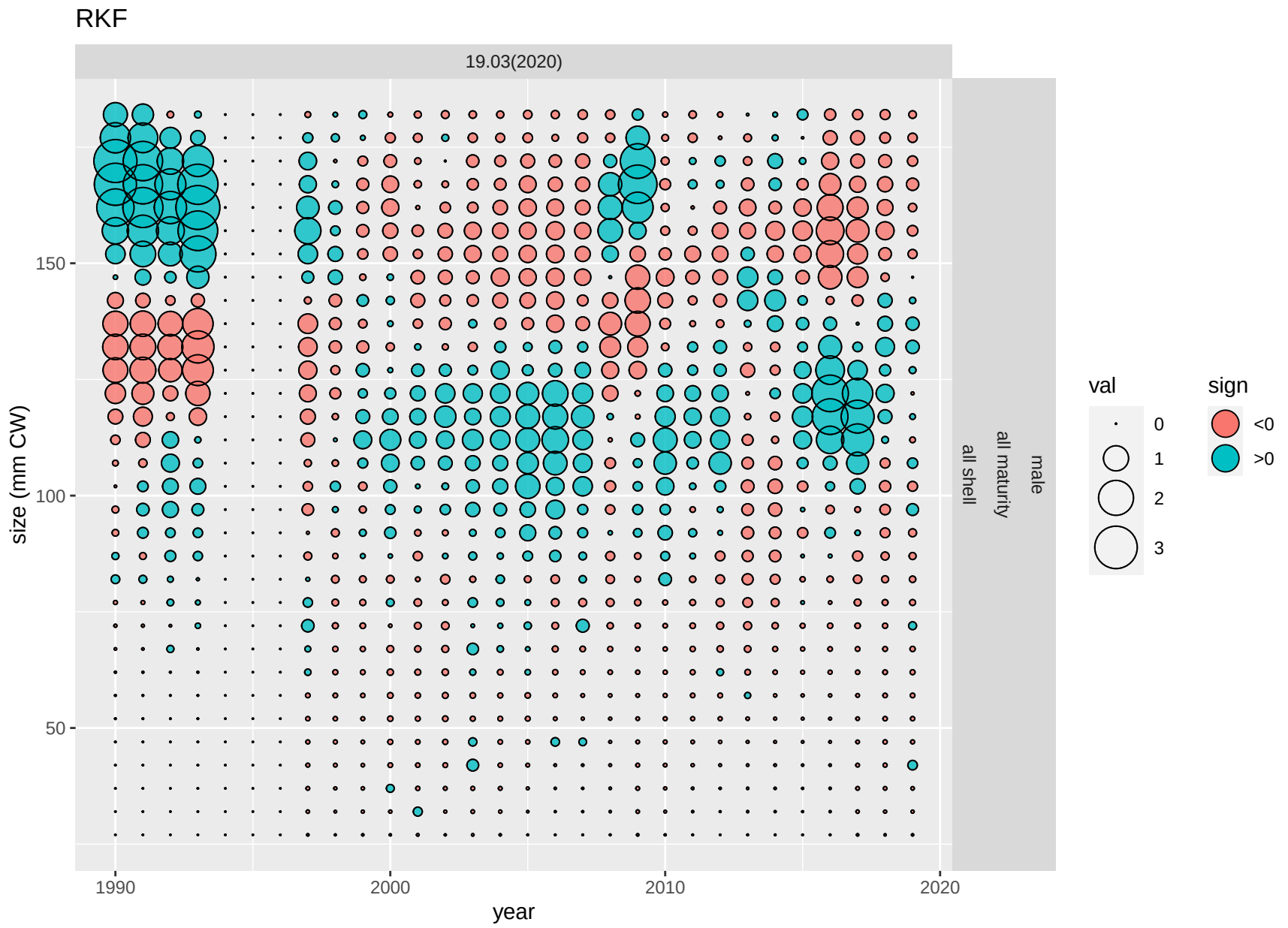

Figure 35: Pearson's residuals for male proportions-at-size from the RKF for scenario 19.03(2020).

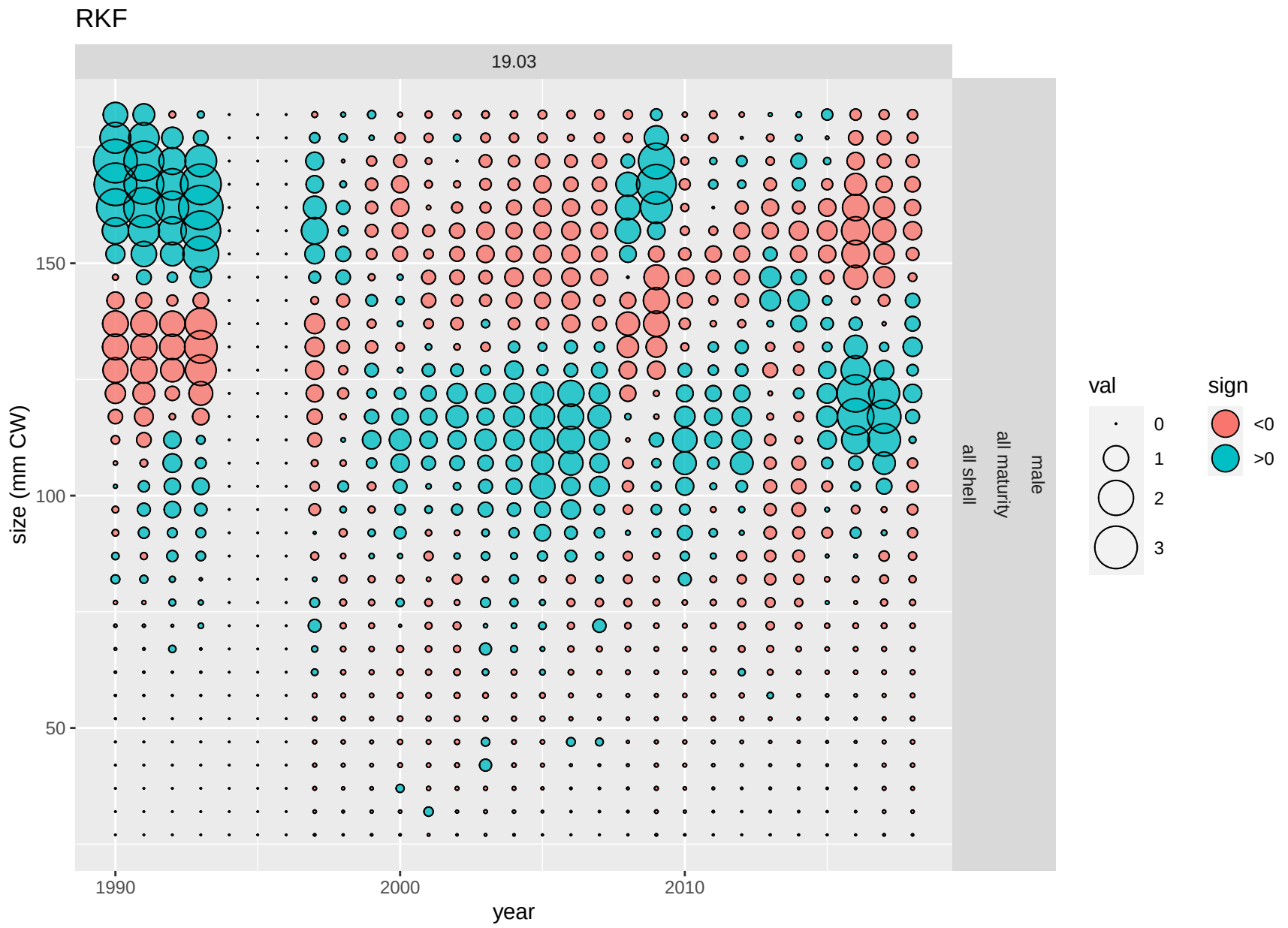

Figure 36: Pearson's residuals for male proportions-at-size from the RKF for scenario 19.03.

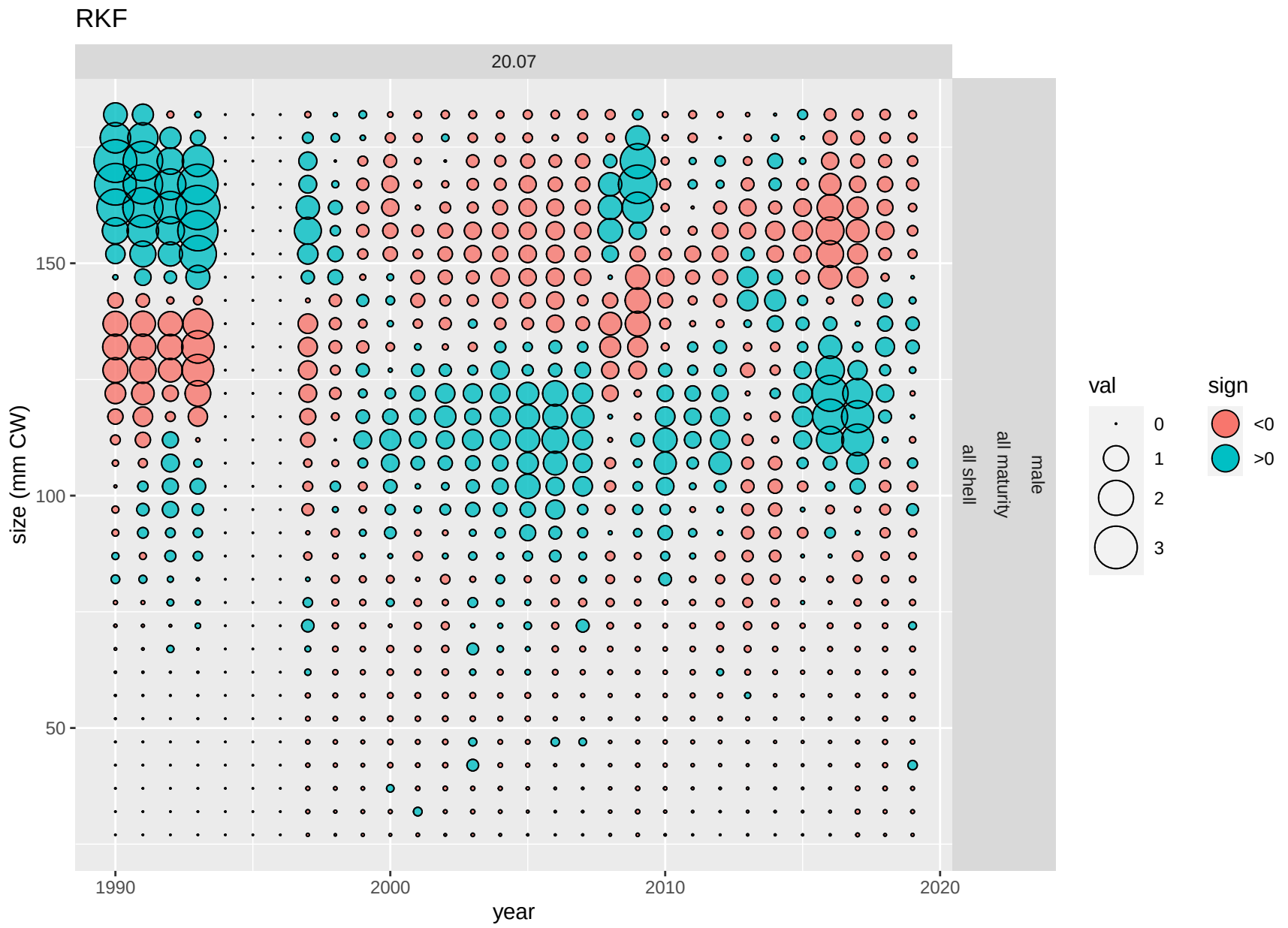

Figure 37: Pearson's residuals for male proportions-at-size from the RKF for scenario 20.07.

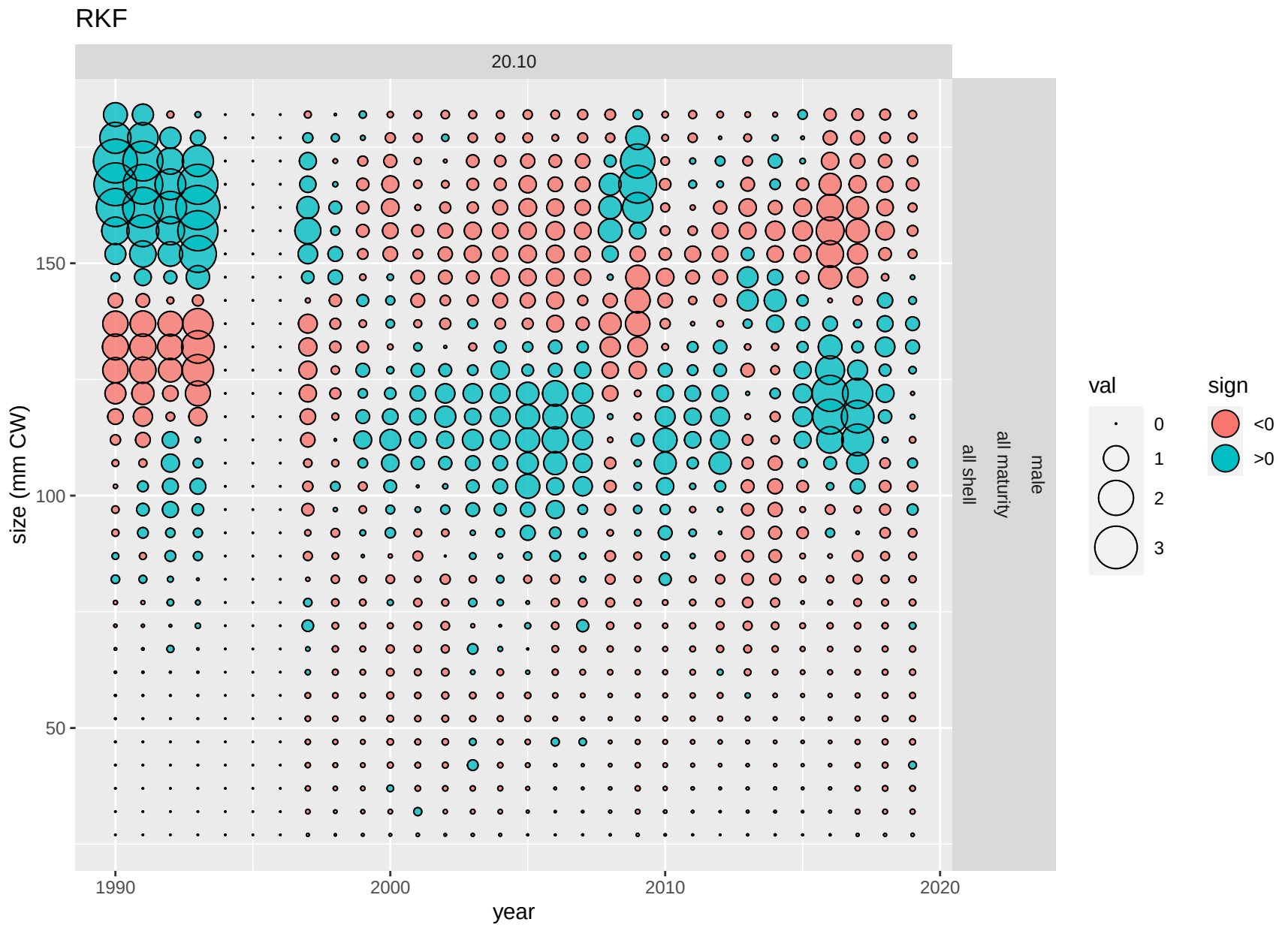

Figure 38: Pearson's residuals for male proportions-at-size from the RKF for scenario 20.10.

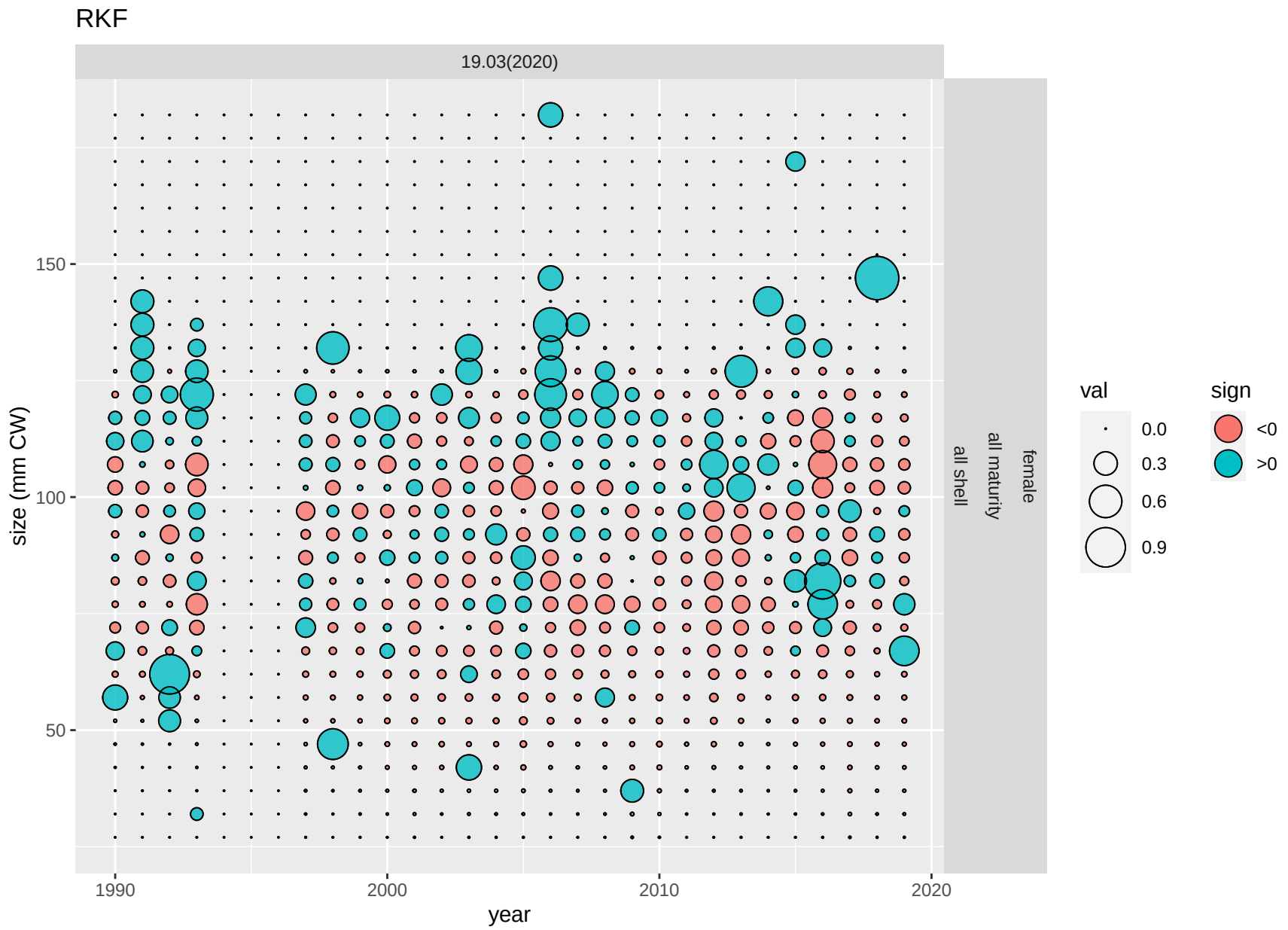

Figure 39: Pearson's residuals for female proportions-at-size from the RKF for scenario 19.03(2020).

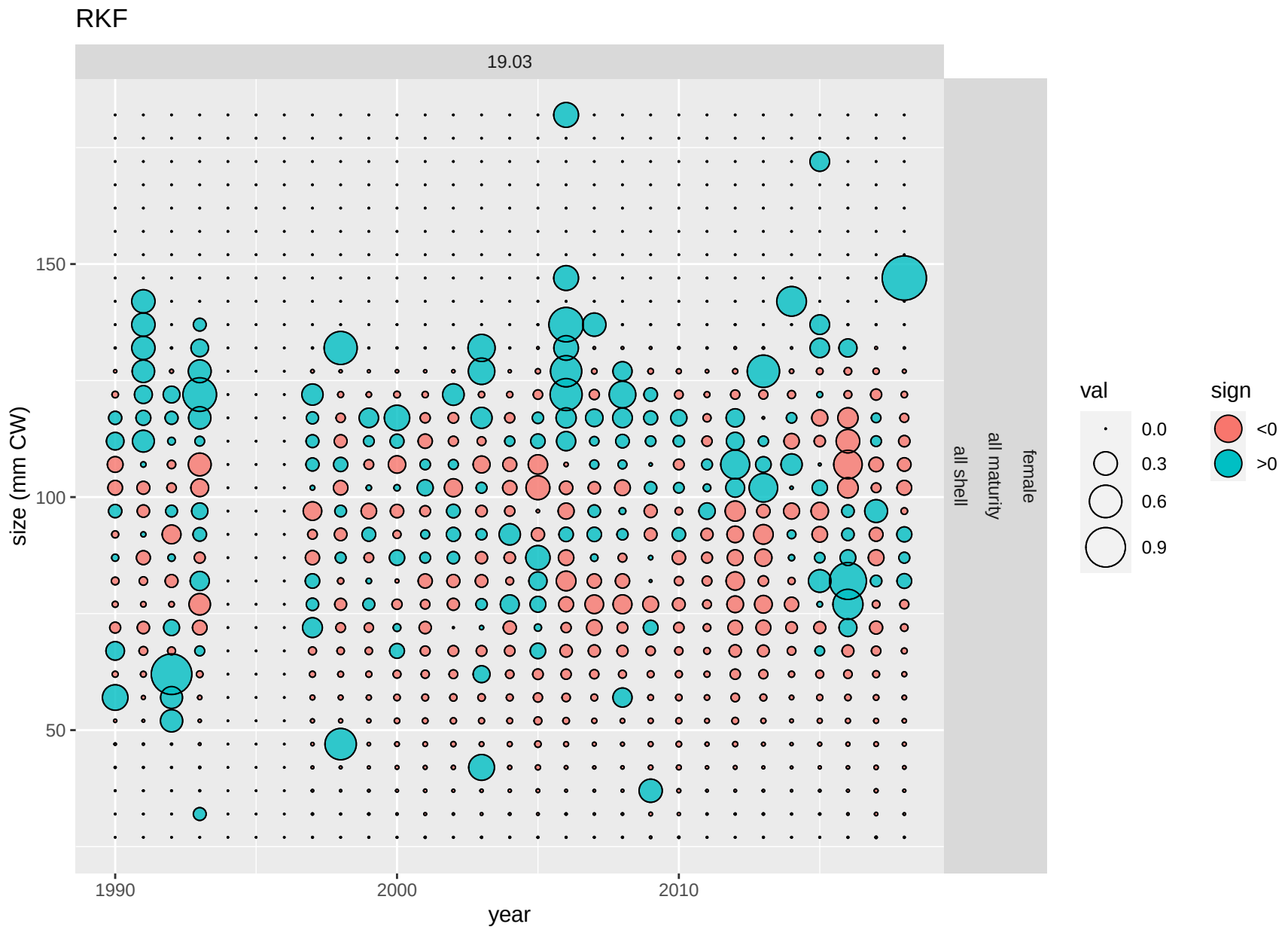

Figure 40: Pearson's residuals for female proportions-at-size from the RKF for scenario 19.03.

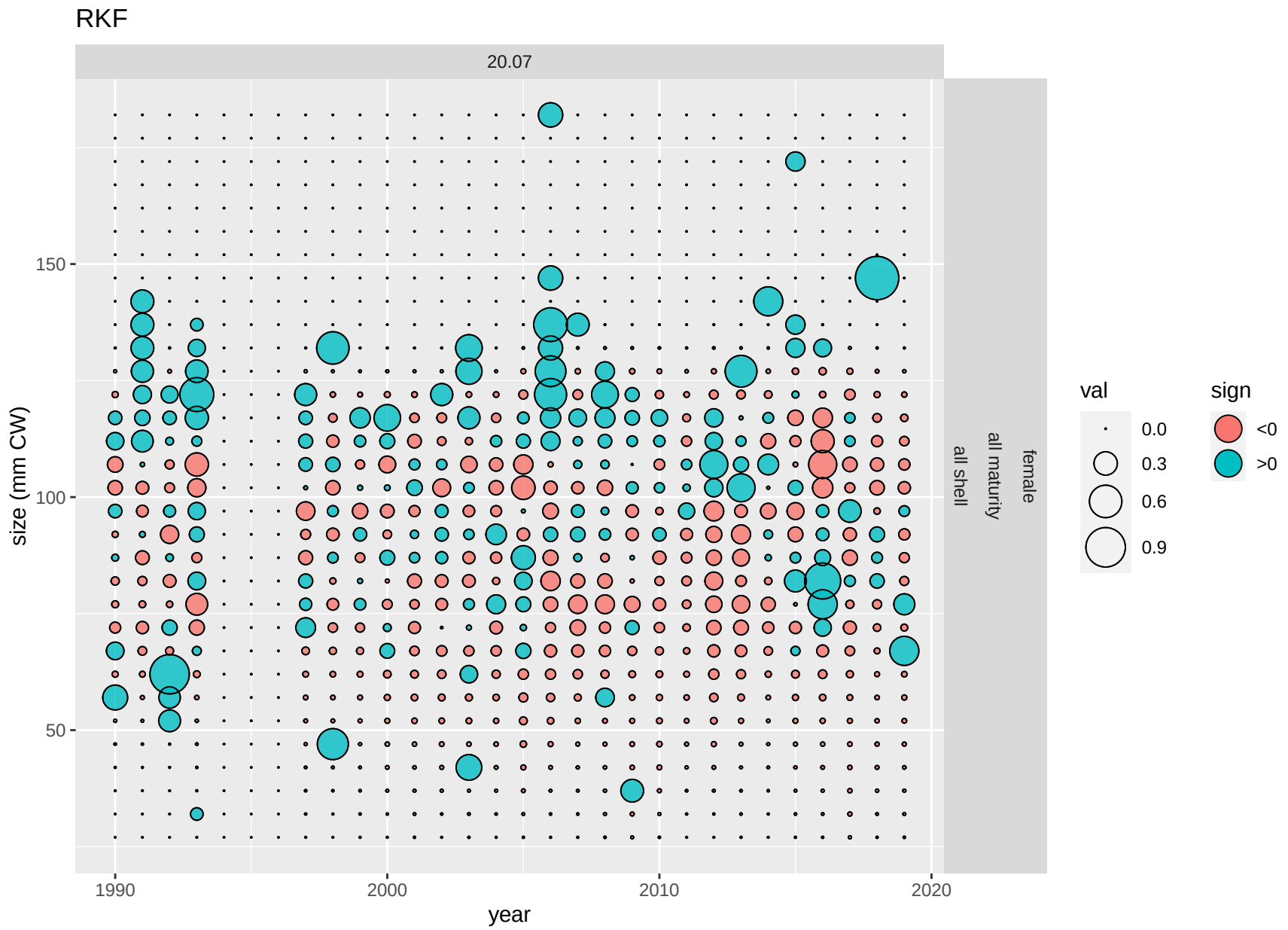

Figure 41: Pearson's residuals for female proportions-at-size from the RKF for scenario 20.07.

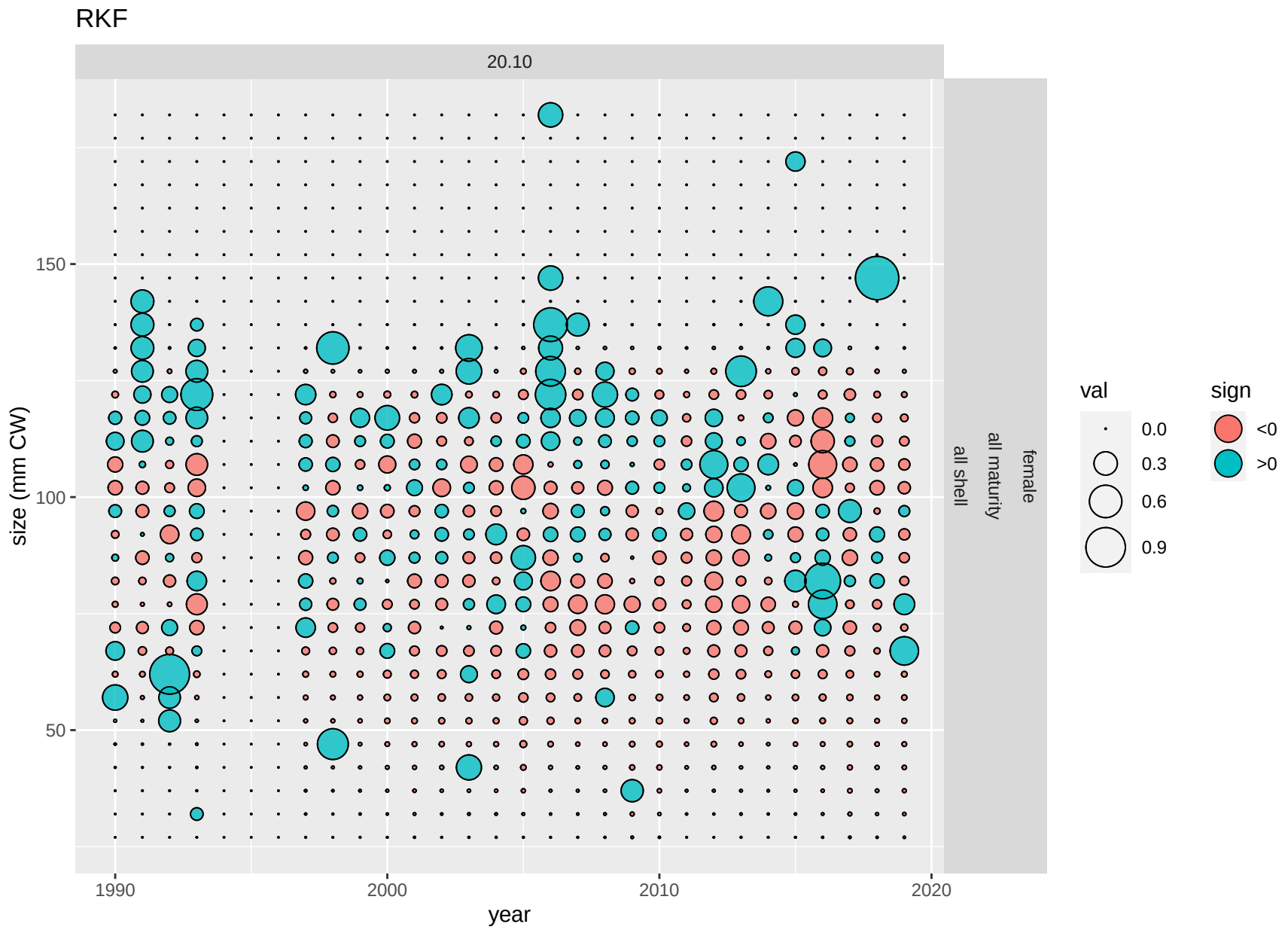

Figure 42: Pearson's residuals for female proportions-at-size from the RKF for scenario 20.10.

Effective Ns for total catch size compositions

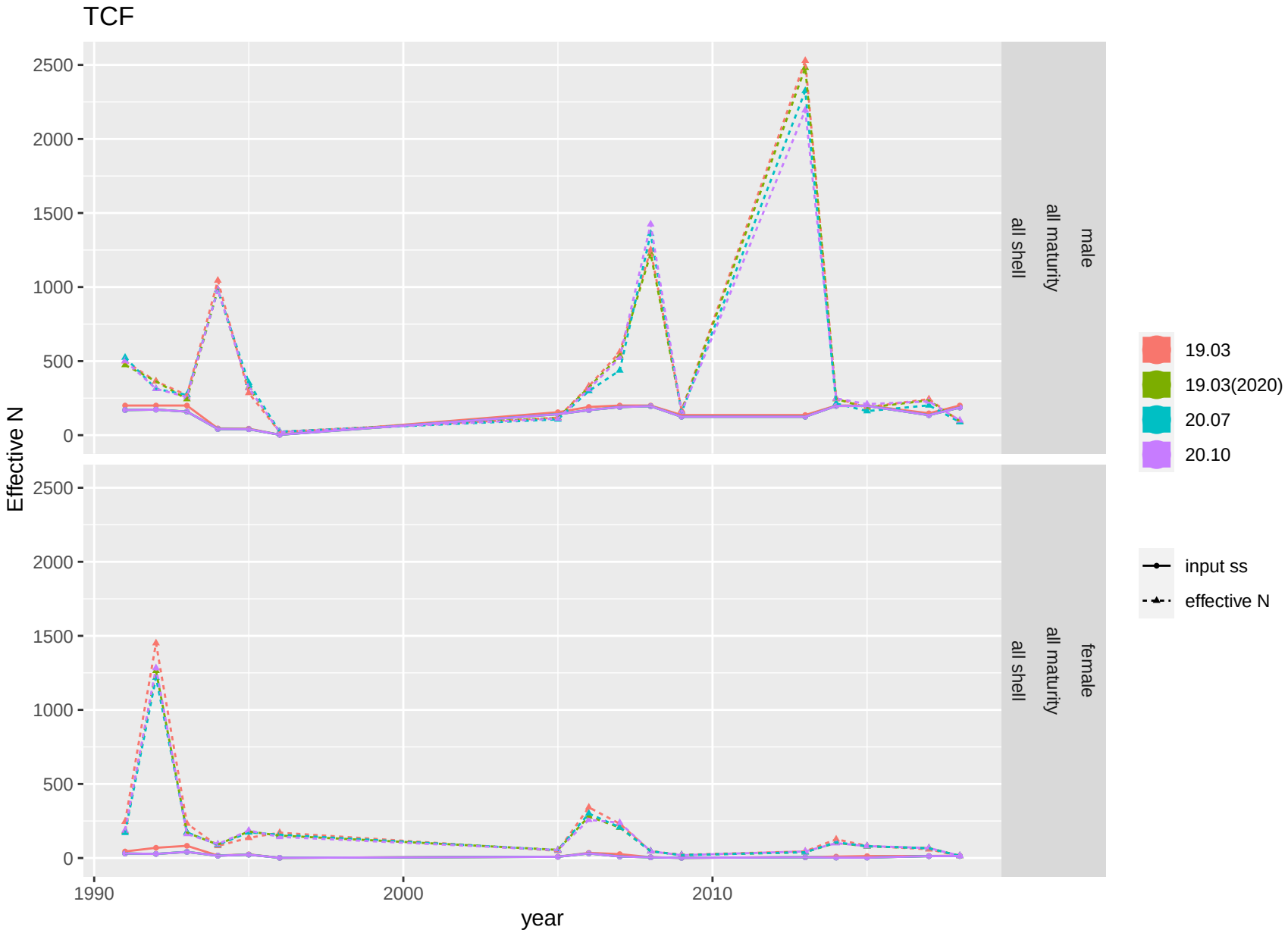

Figure 43: Input and effective sample sizes from total catch size compositions from the TCF fishery.

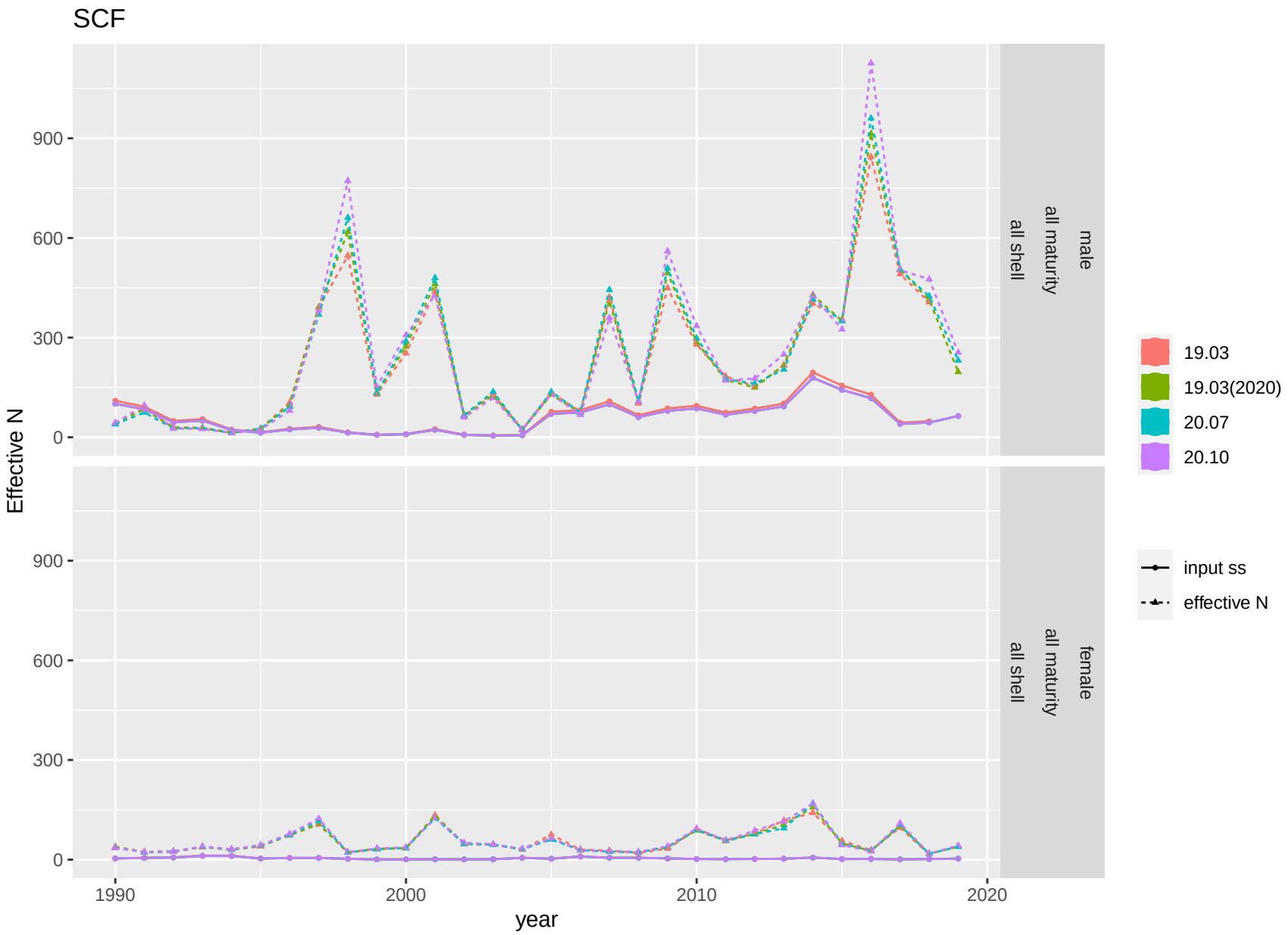

Figure 44: Input and effective sample sizes from total catch size compositions from the SCF fishery.

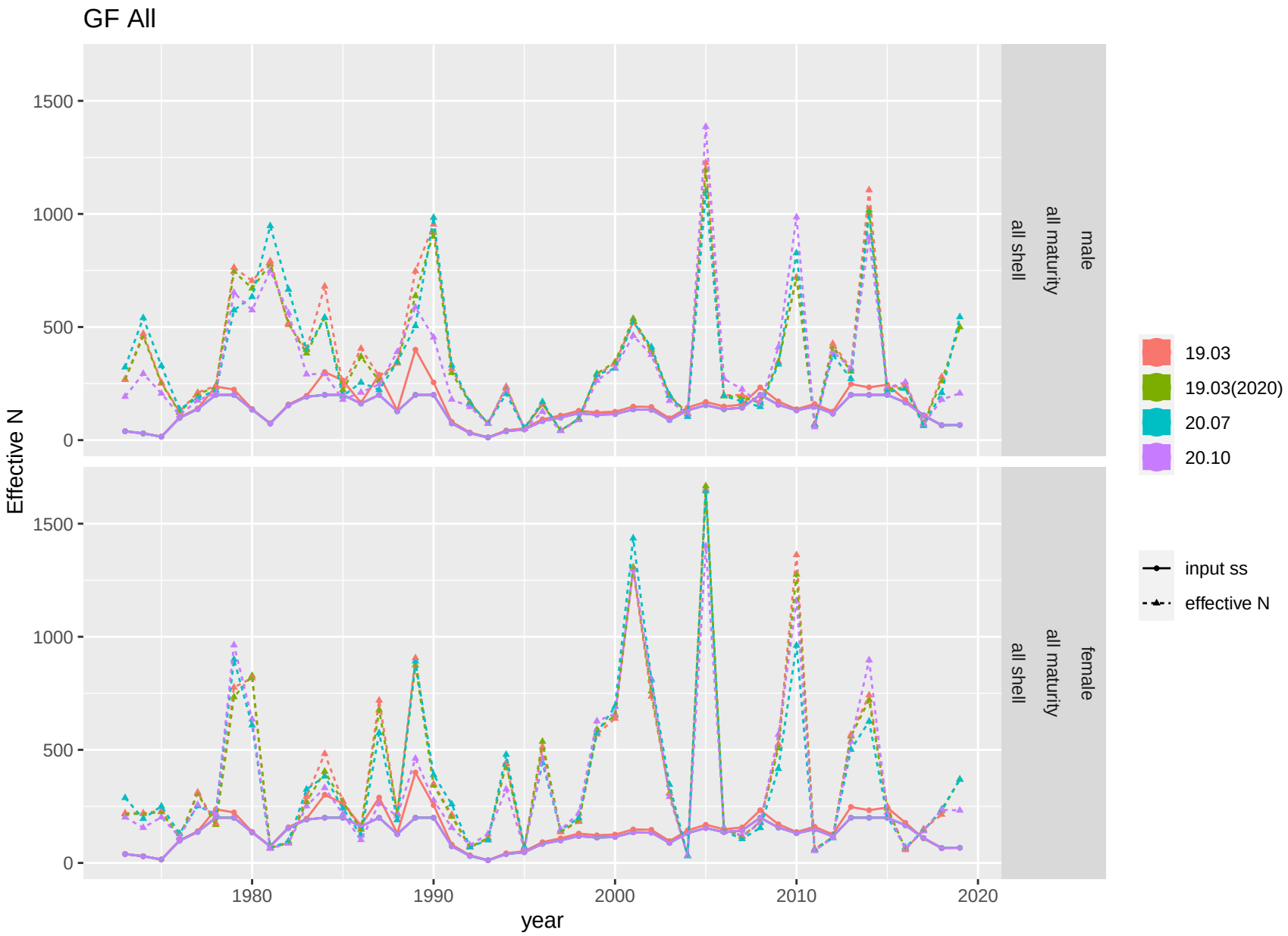

Figure 45: Input and effective sample sizes from total catch size compositions from the GF All fishery.

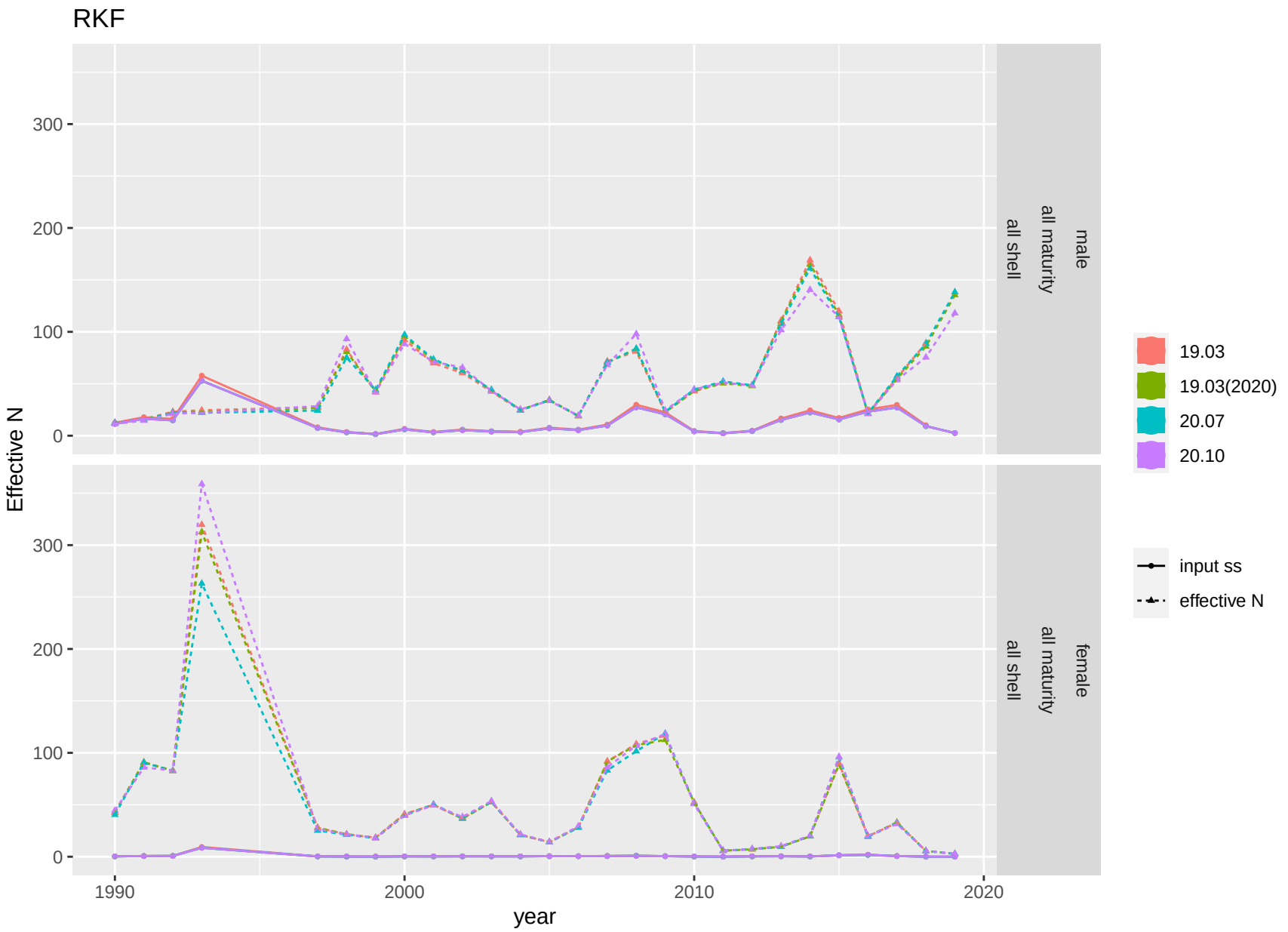

Figure 46: Input and effective sample sizes from total catch size compositions from the RKF fishery.

Appendix 10: Diagnostics for Fits to Surveys Size Composition Data –19.03(2020) vs 19.03 vs 20.07 vs 20.10

William Stockhausen

01 September, 2020

Contents

Introduction

Fits to survey size composition data available to the model(s) are presented in this section. Included are plots of mean fits to size compositions, Pearson's residuals as bubble plots, and effective sample sizes. Not all of the fits presented are necessarily included in the parameter optimization for each model; some fits to datasets for a particular model may be included for comparison purposes with other models which include those data in their optimization. The reader should consult the main assessment document to determine which fits are included in the optimization for any particular model.

Mean survey size compositions

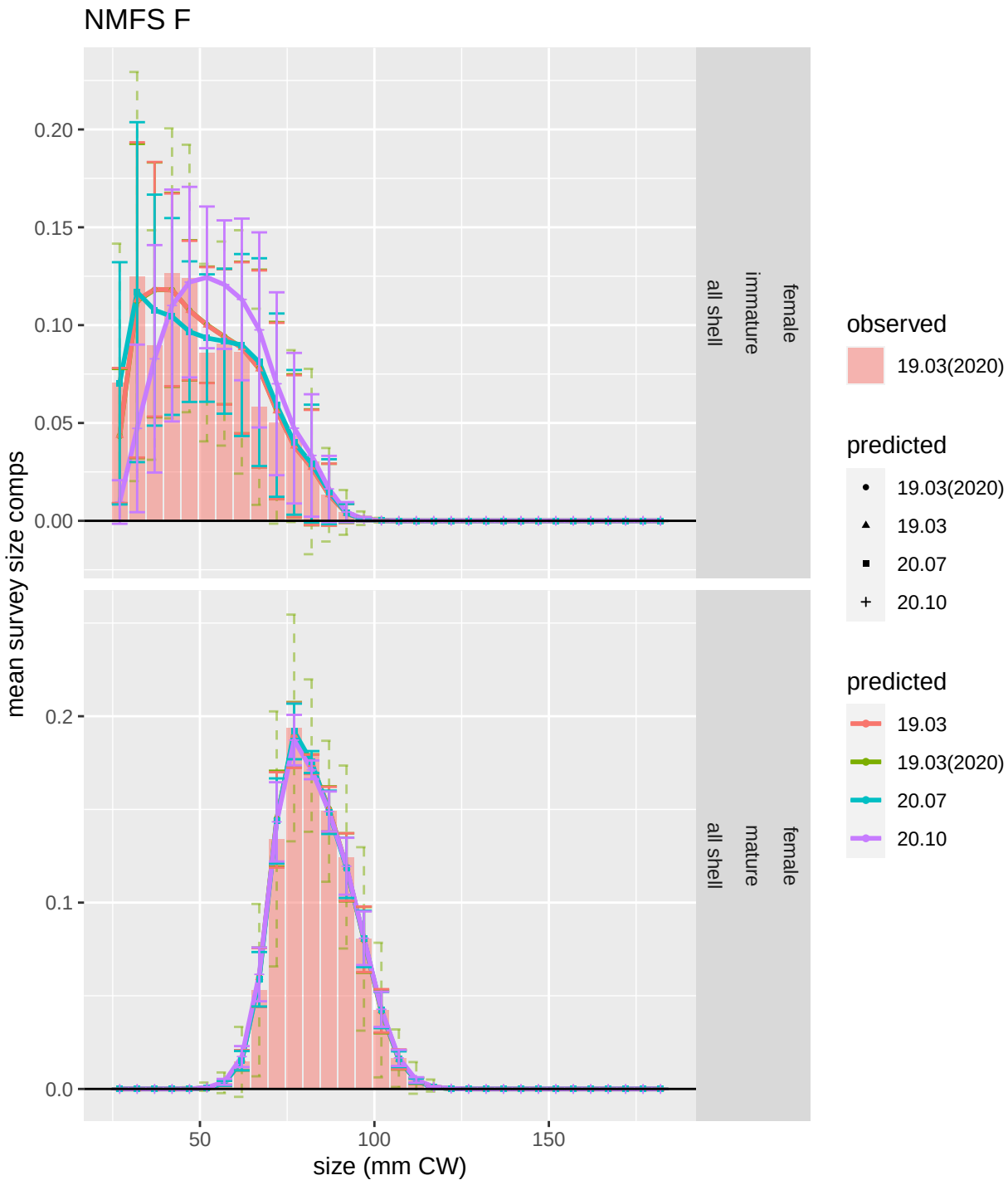

Figure 1: Comparison of observed and predicted mean survey size comps for NMFS F.

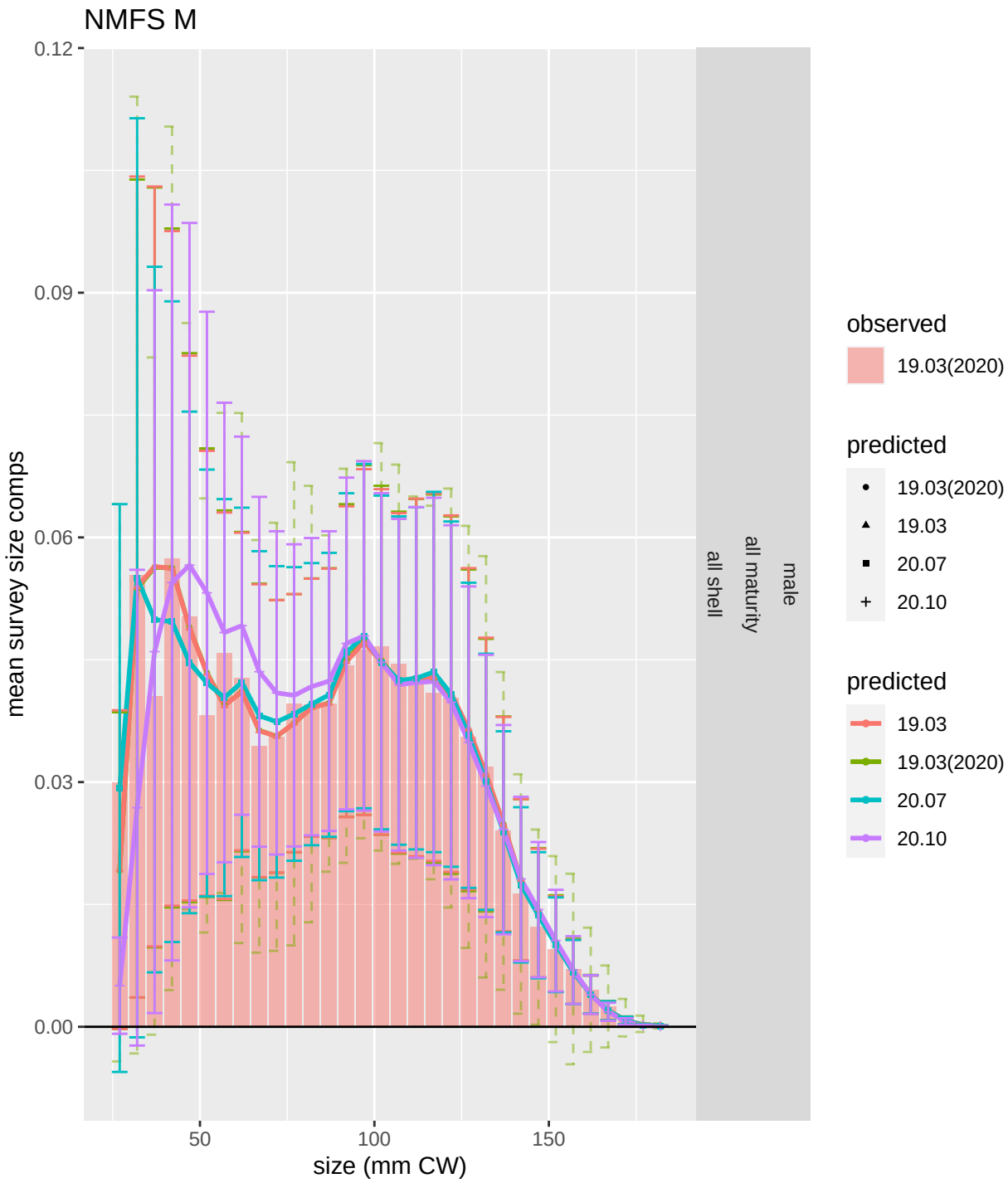

Figure 2: Comparison of observed and predicted mean survey size comps for NMFS M.

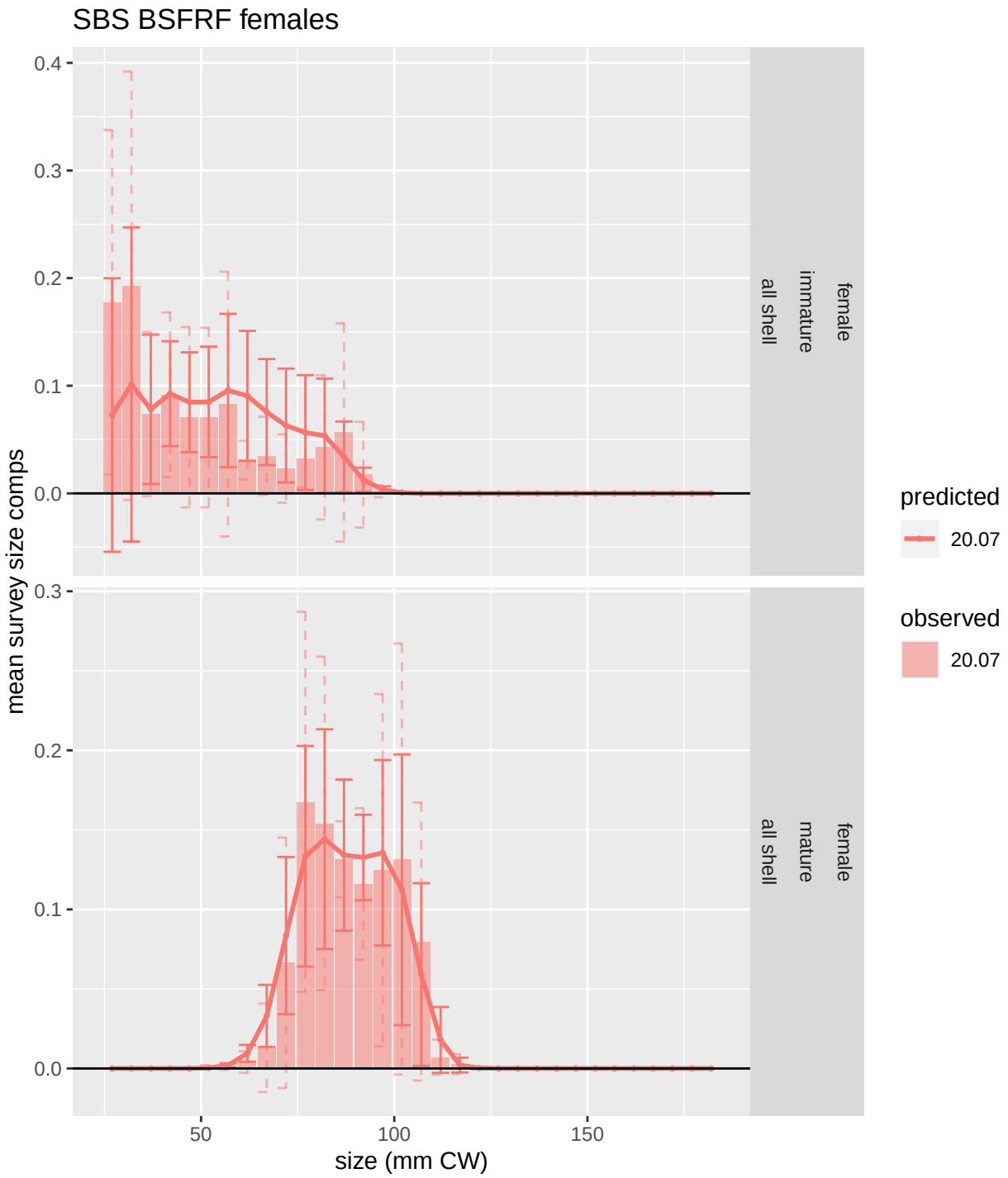

Figure 3: Comparison of observed and predicted mean survey size comps for SBS BSFRF females.

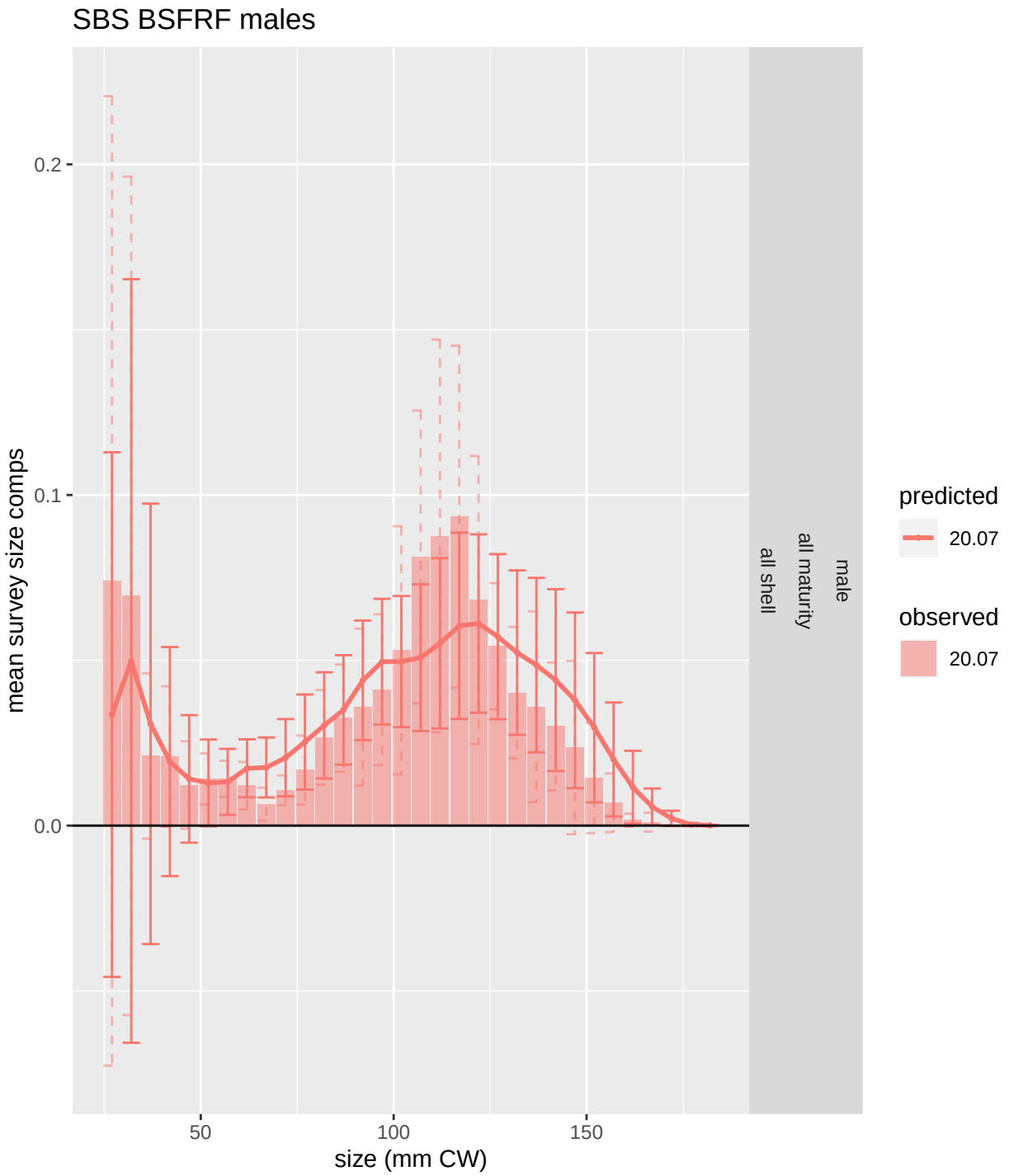

Figure 4: Comparison of observed and predicted mean survey size comps for SBS BSFRF males.

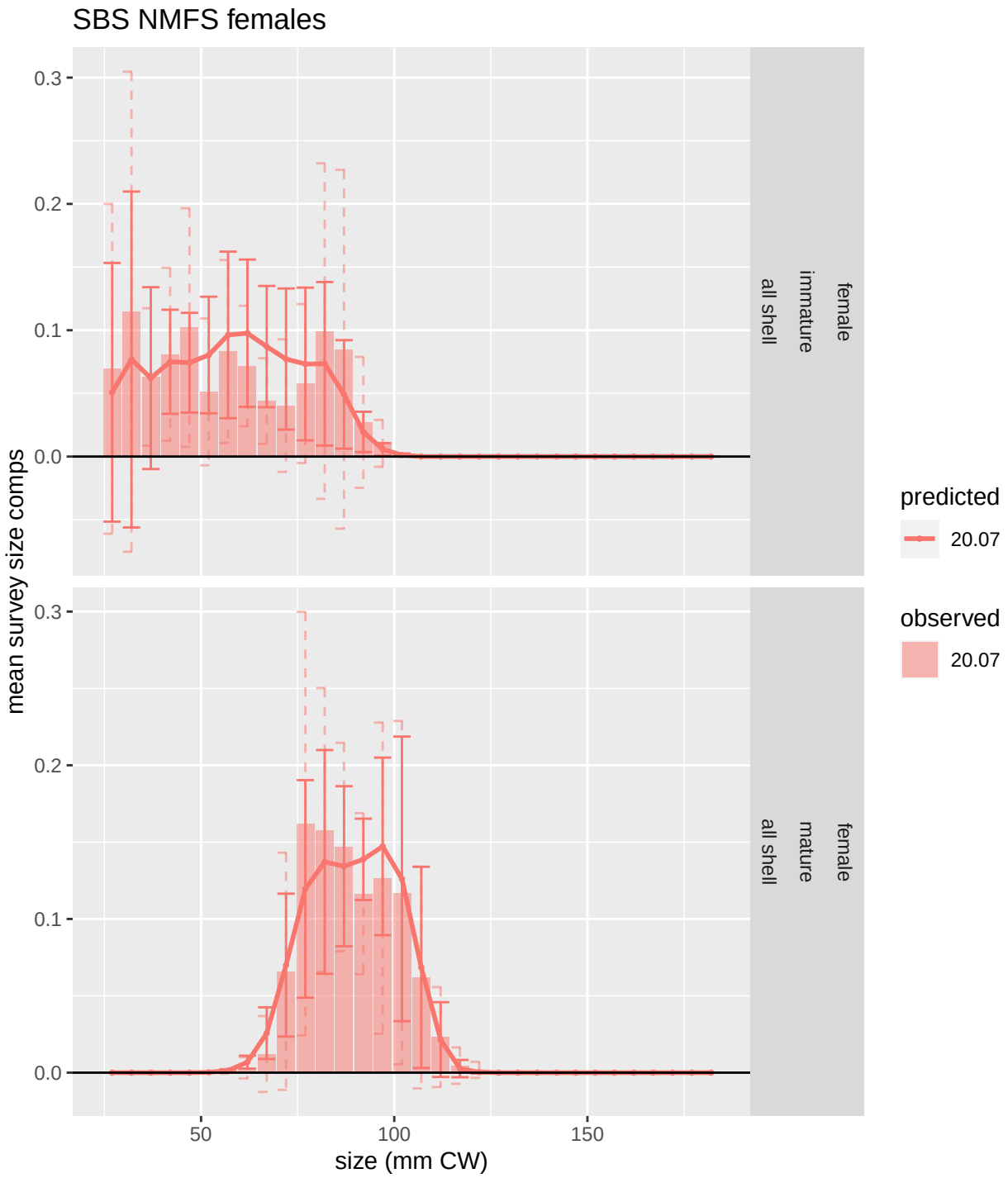

Figure 5: Comparison of observed and predicted mean survey size comps for SBS NMFS females.

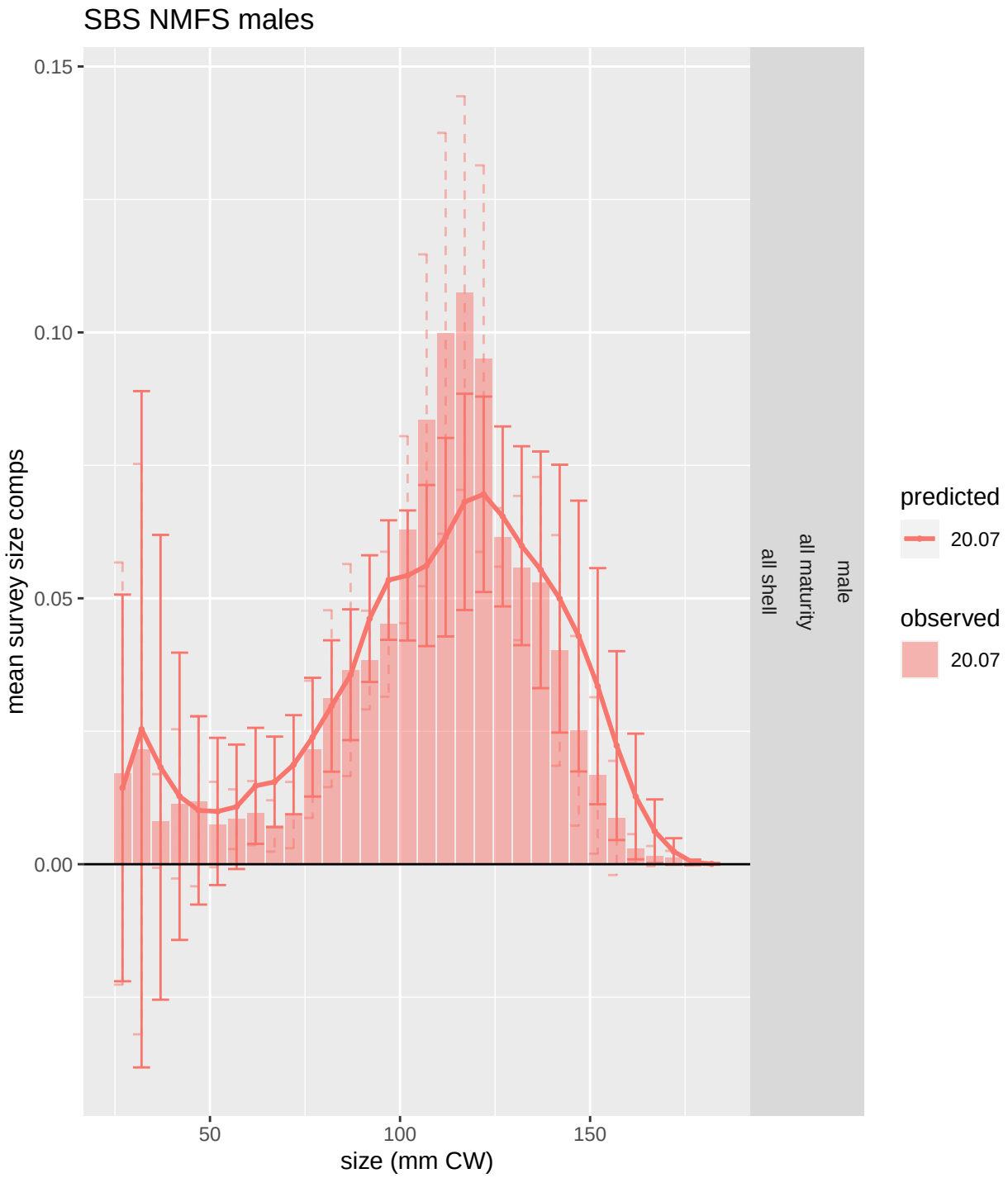

Figure 6: Comparison of observed and predicted mean survey size comps for SBS NMFS males.

Residuals to survey size composition data

Effective sample sizes for survey size compositions

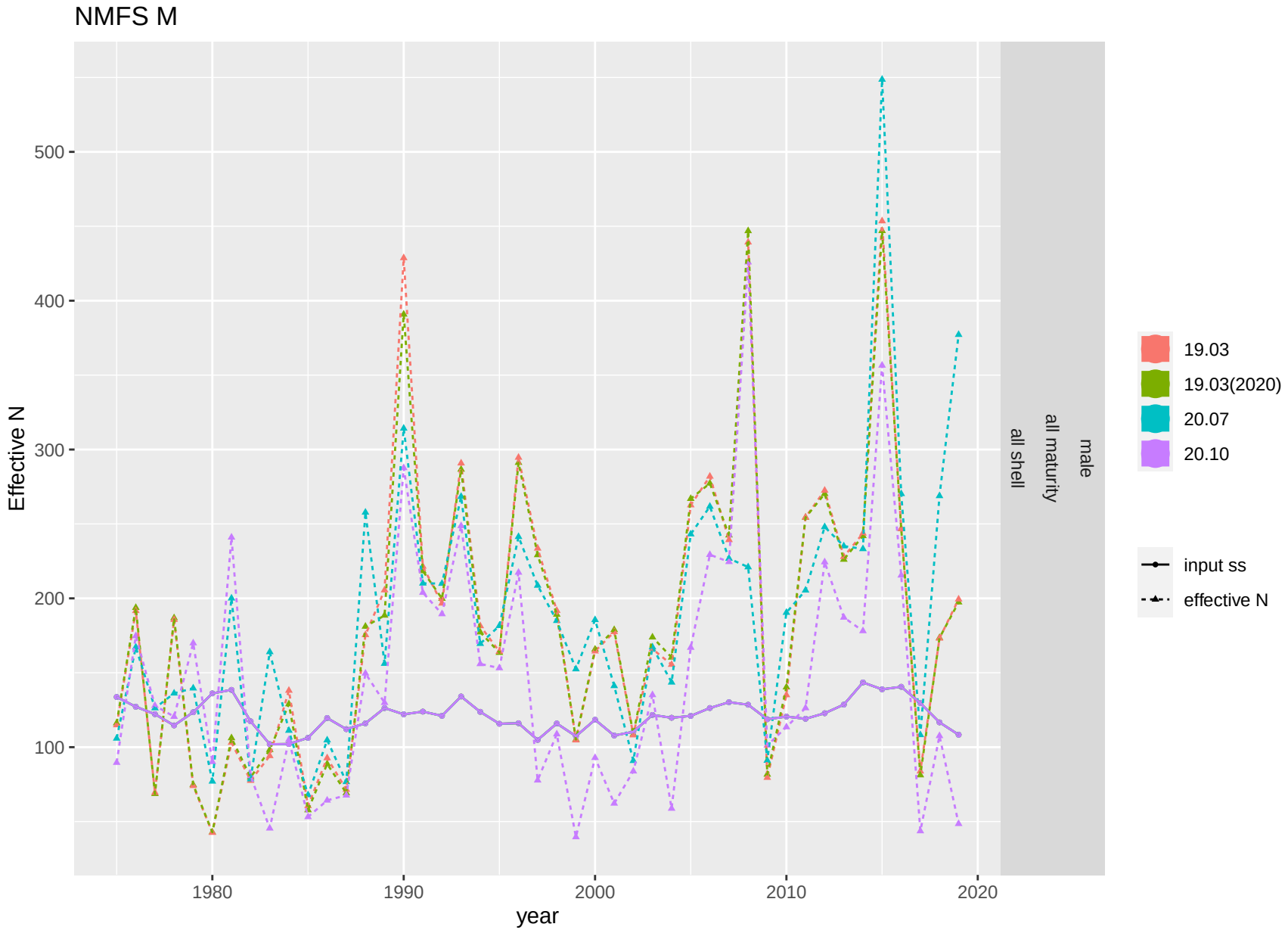

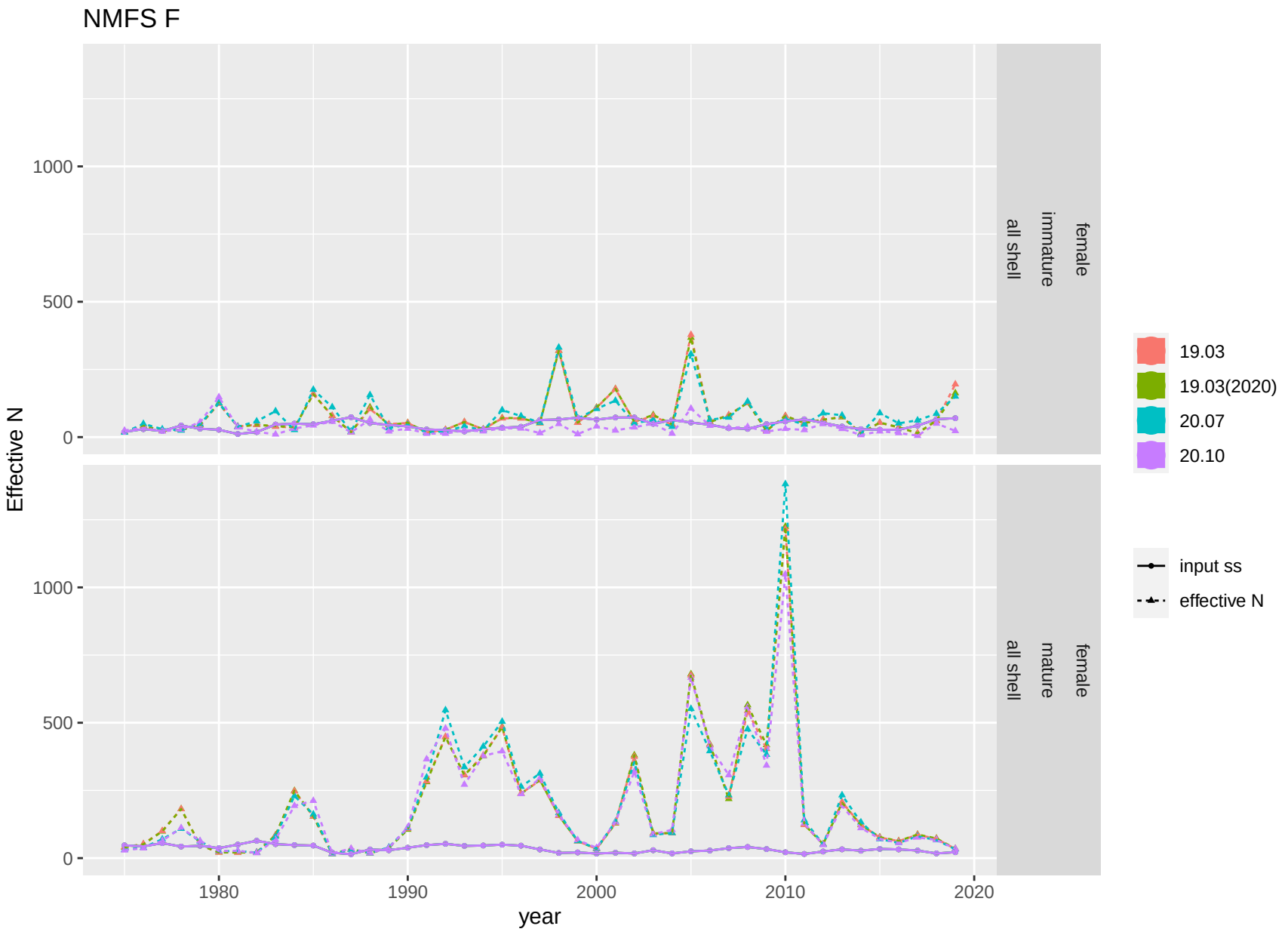

Figure 8: Input and effective sample sizes from retained catch size compositions from the NMFS F.

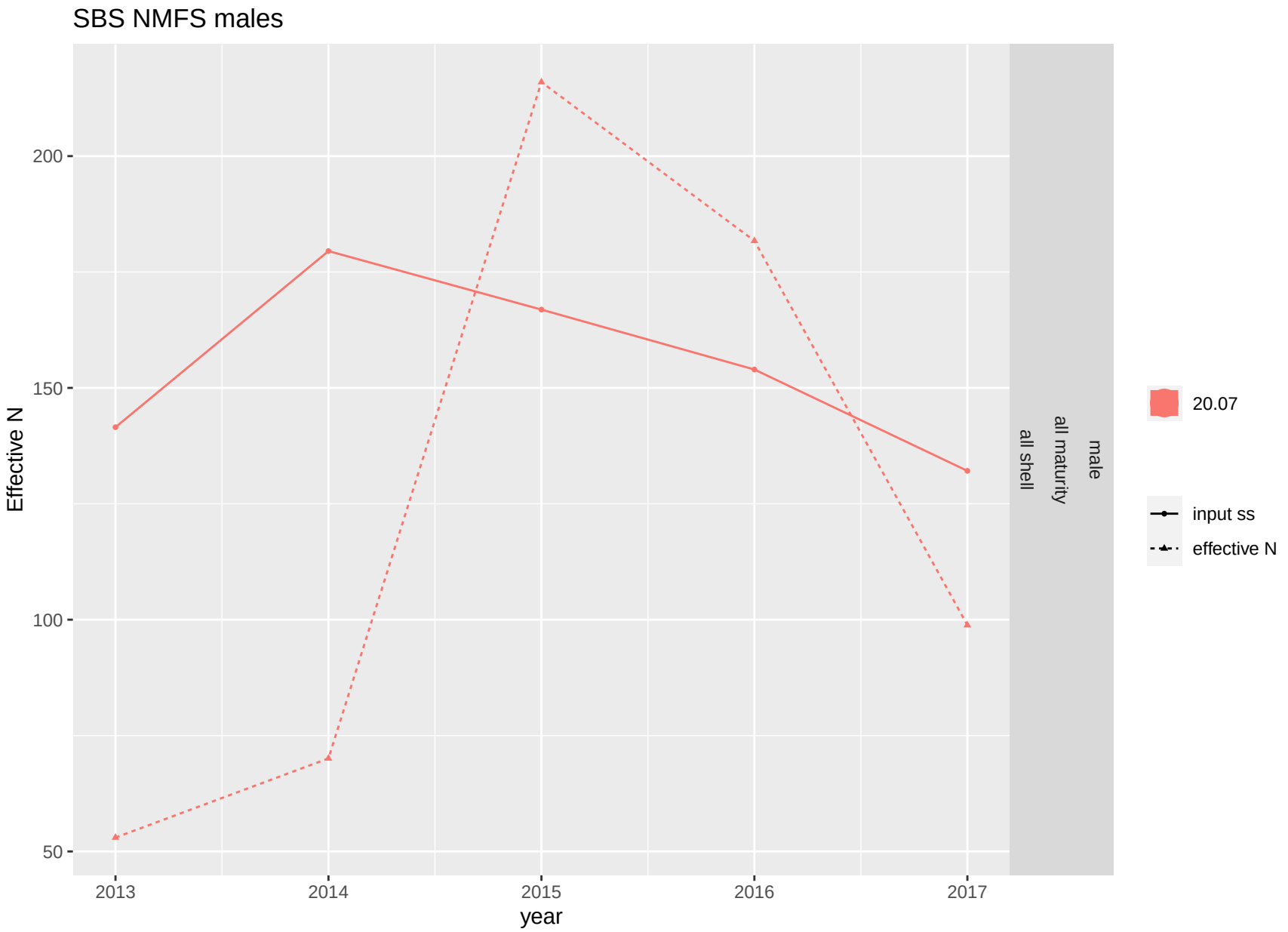

Figure 9: Input and effective sample sizes from retained catch size compositions from the SBS NMFS males.

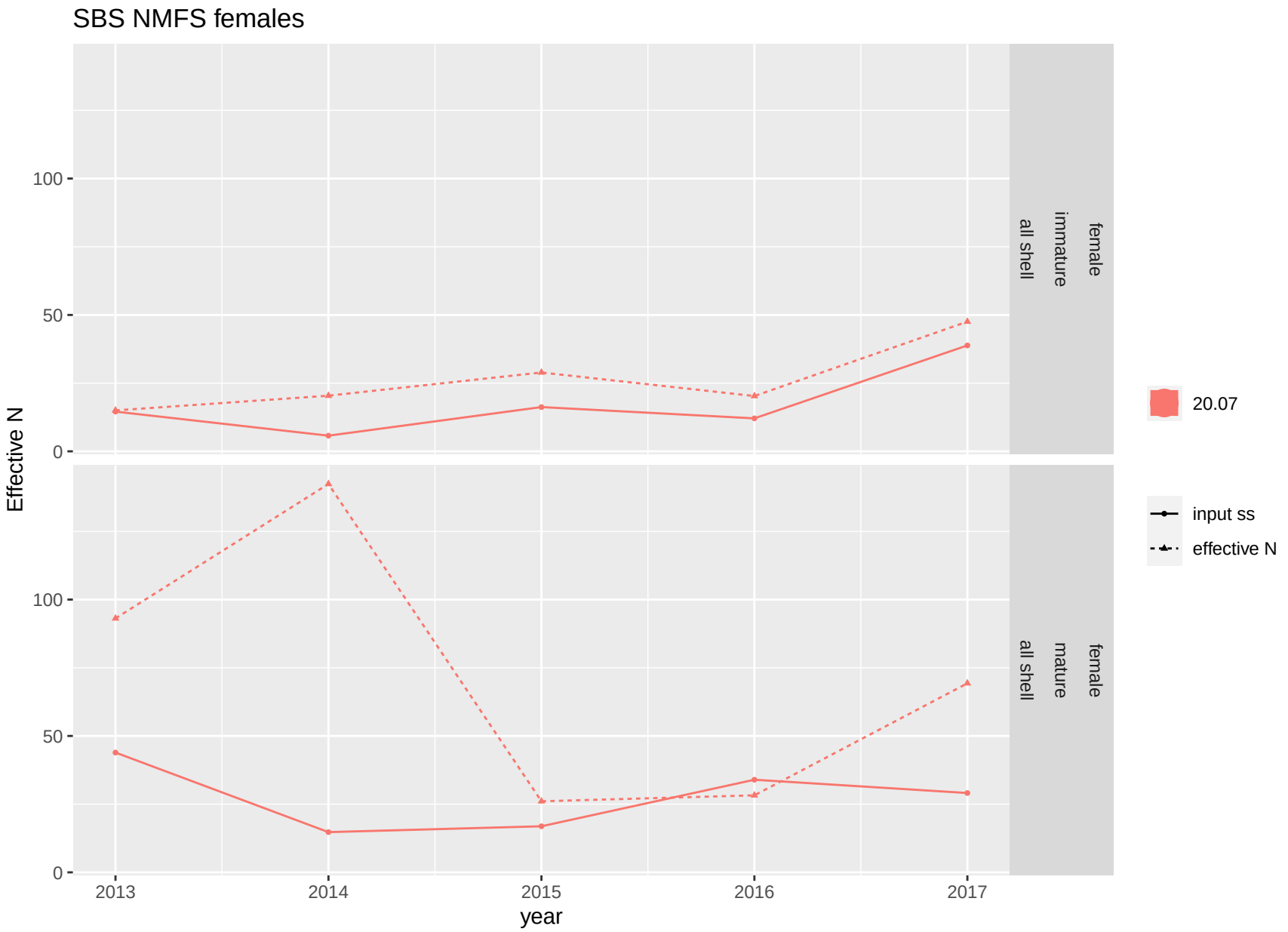

Figure 10: Input and effective sample sizes from retained catch size compositions from the SBS NMFS females.

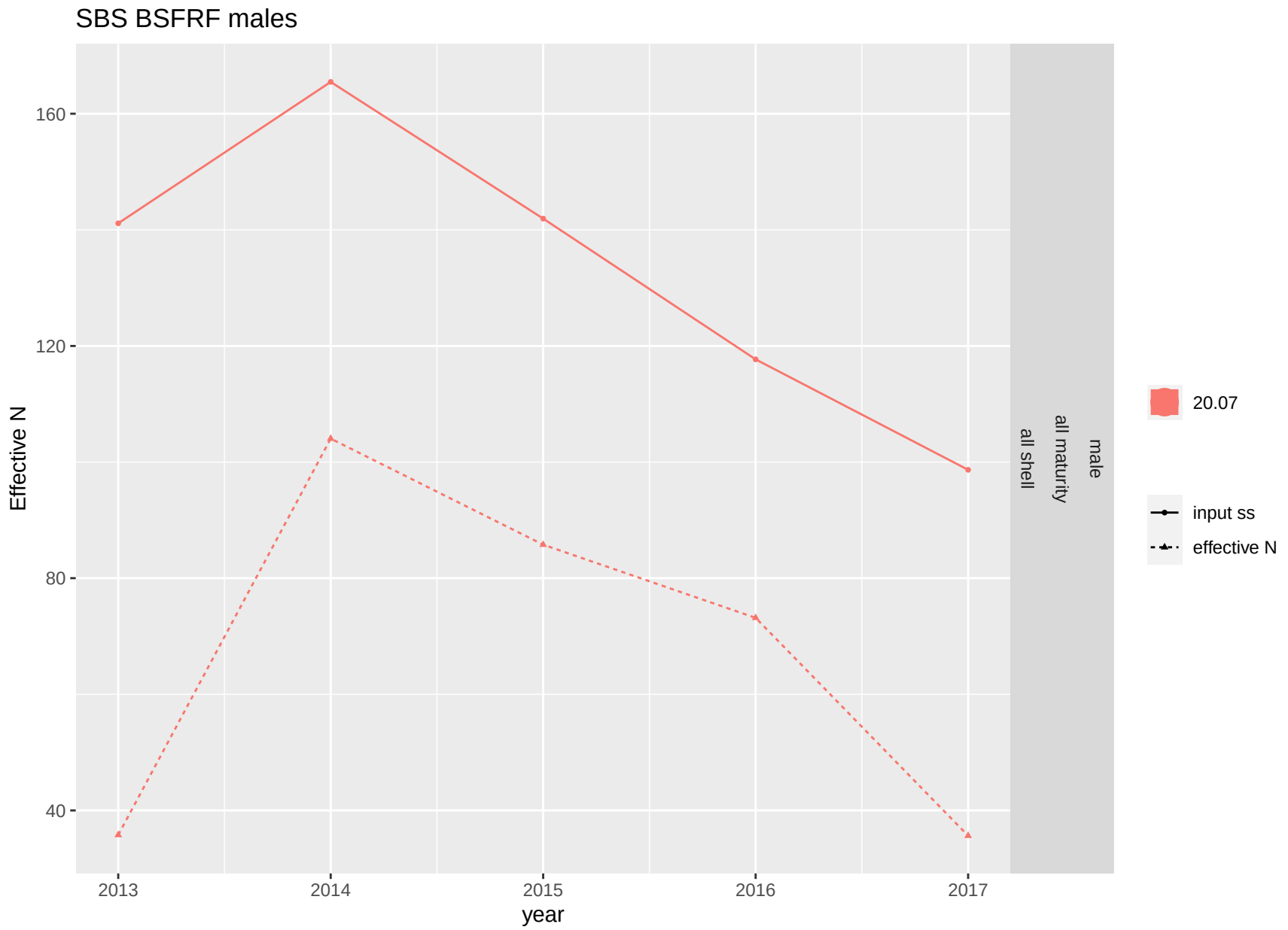

Figure 11: Input and effective sample sizes from retained catch size compositions from the SBS BSFRF males.

Figure 12: Input and effective sample sizes from retained catch size compositions from the SBS BSFRF females.